GEOCHEMISTRY OF INTRUSIVE ROCK SUITES AND RELATED PORPHYRY COPPER MINERALIZATION IN THE PAPUA NEW GUINEA - SOLOMON ISLANDS REGION

by

DOUGLAS ROSS MASON

A thesis submitted for the degree of

DOCTOR OF PHILOSOPHY

in the

AUSTRALIAN NATIONAL UNIVERSITY.

November, 1975.

STATEMENT

Initial field observations and sample collections were made by the author between September 1970 and March 1972 whilst in the employ of International Nickel Australia Limited. The material contained in this thesis is based on work carried out whilst in the Department of Geology, Australian National University between March 1972 and November 1975.

Unless otherwise stated, all data and conclusions in this thesis are the author's own. Assistance rendered by many people is recorded in the acknowledgements.

Signed: .....

Douglas R. Mason

ACKNOWLEDGEMENTS

This study was supported by a Commonwealth Postgraduate Research Award, at the Department of Geology, Australian National University, Canberra.

The author is indebted to the people from many parts of Papua New Guinea. Their cheerful cooperation in the field has greatly facilitated exploration and sample collection programs.

It is a pleasure to acknowledge the guidance of my supervisor, Dr. John A. McDonald, who provided stimulating discussion during all stages of preparation of this thesis.

A number of companies and governmental agencies materially assisted by providing samples, allowing access to prospects and unpublished reports and helping to defray field expenses. Those companies which supported the study are:

Australian Anglo American Limited
Bougainville Copper Pty. Ltd.
Carpentaria Exploration Company Pty. Ltd.
International Nickel Australia Limited
Kennecott Explorations (Australia) Ltd.
Swiss Aluminium Mining Australia Pty. Ltd.
Triako Mines N.L.
Utah Development Company Inc.

Those governmental agencies which supported the study are:

Australian Bureau of Mineral Resources, Geology and Geophysics
British Solomon Islands Department of Geological Surveys
Papua New Guinea Geological Survey

The author wishes to thank the many individuals of these companies and agencies for their assistance and stimulating discussions.

In the laboratory, assistance in X-ray fluorescence analysis was given by Dr. B.W. Chappell and Mr. R.S. Freeman of the Department of Geology, and by Mr. P.H. Beasley of the Research School of Earth Sciences.

Mr. N.G. Ware of the Research School of Earth Sciences instructed the author in the techniques of microprobe analysis. Instruction in wet chemical techniques was given by Mr. Z. Wasik. Computer analysis was performed jointly with Mr. L. Belbin. Technical assistance was rendered by Mr. R. Cliff and his staff.

Thanks are also extended to those who discussed problems and

otherwise assisted during preparation of this thesis. In this context I wish to thank Messers H.-D. Hensel, K.L. Harris, D.E. Mackenzie, R.J. Ryburn, I.E. Smith, and D.J. Whitford.

Finally, for typing and assistance in proof-reading and draughting I thank Mss. N. Blundell, A. Kilner, H. Drury, D. Mason, and J. Heaslip.

ABSTRACT

In the Papua New Guinea-Solomon Islands region of the south-west Pacific, calc-alkaline intrusive complexes and closely associated porphyry-type copper mineralization of Tertiary and younger age occur in three contrasted tectonic settings: in island arcs, in the Australian continental margin (New Guinea Mobile Belt), and in the Australian continental block.

The intrusive complexes of all three settings display a wide range of calc-alkaline mineralogy and chemistry. Geochemical data for the intrusive rocks indicate increasing abundance of 'incompatible' elements from island arc areas, through the continental margin, to the continental block. Regional geochemical variations are also evident in abundance of particular elements in restricted regions, and in overall northwards increase of potassium and related 'incompatible' elements across the Mobile Belt.

Genesis of most of the calc-alkaline intrusive complexes involves hybridism of silicic partial melts and refractory material from igneous source rocks in the base of the crust at depths of 20-40 km. Some mafic suites had their source in the upper mantle. The geochemistry of intrusive suites reflects the composition of their source materials. Partial melting is caused by rise of isotherms during prolonged magmatism, and is aided by decrease in load pressure following rapid uplift and erosion. Partial melting beneath the Mobile Belt in Lower to Middle Miocene times was achieved by such means without the participation of a Benioff zone.

Mineralized intrusive rock suites were slightly more water-rich than non-mineralized suites. They are characterized by the primary mineral assemblage hornblende + magnetite + sphene, stability of increasingly Mg-rich mafic mineral compositions during crystallization, and lack of mafic inclusions. Later intrusion of mineralized suites in intrusive complexes is a consequence of later partial melting of slightly more water-rich source material at higher levels in the base of the crust. The origin of hydrothermal solutions responsible for porphyry-type mineralization is intimately related to final stages of crystallization of relatively water-rich intrusive suites.

TABLE OF CONTENTS

LIST OF TABLES

LIST OF TABLES (Continued)

LIST OF FIGURES

LIST OF FIGURES (Continued

LIST OF FIGURES (Continued)

LIST OF FIGURES (continued)

LIST OF APPENDICES

CHAPTER 1 INTRODUCTION

1.1 PREVIOUS WORK

1.1.1 Regional Geology

Serious investigations of the geology and geophysics of Papua New Guinea and the Solomon Islands commenced as recently as the 1930's. Much of the early impetus arose from the discovery of the Wau-Bulolo goldfields in the southeastern part of the (then) Trust Territory of New Guinea. Initial reports (e.g. Stanley, 1916, 1923; Fisher, 1935, 1936, 1937; Noakes, 1938, 1941) were devoted mainly to aspects of mineralization at particular locations. At an early stage some workers realized the significance of Papua New Guinea as part of the circum-Pacific tectonic zone, and attempts at geologic and tectonic syntheses were made by Carey (1938), and Glaessner (1950).

Systematic regional geologic mapping, undertaken by the Australian Bureau of Mineral Resources and, more recently, by the Papua New Guinea Geological Survey, has been in progress since the 1950's. Much of the current body of knowledge relating to P.N.G. geology can be attributed to the work of the officers of these governmental departments. Some significant contributions on mainland geology include those of Dow & Davies (1964), Dow & Dekker (1964), and Dow et al. (1967, 1968, 1972). Contributions on the geology of P.N.G. islands have come from Thompson (1952) on Manus Island, Blake & Miezitis (1967) on Bougainville and Buka islands, Macnab (1970) and Mackenzie (1971) on New Britain, and Hohnen (1970) on New Ireland. Knowledge of the geology of the British Solomon Islands has been greatly extended by the work of the officers of Her Majesty's Geological Survey.

1.1.2 Geophysics

Geophysical investigations in P.N.G. commenced in the 1920's and 1930's when oil companies began exploration. More recently, further exploration and wide discussion of plate tectonics theory have encouraged subsurface investigations in the P.N.G. region. Important contributions have been made by Denham (1969), who used earthquake data to define plate boundaries and Benioff Zone attitudes; St. John (1970), who used gravimetric data to deduce crustal density distributions; Curtis (1973a, 1973b), who presented further detailed data on spatial seismicity of P.N.G.; and Finlayson and Cull (1973), who used both gravity and seismic data to

deduce crustal structure in the New Britain-New Ireland region.

1.1.3 Geochemistry

Most of the presently-known geochemistry of the P.N.G. region concerns major and trace element distribution in Pleistocene to Recent volcanic rocks. Much of this data has only recently become available. Important contributions have been made by Taylor et al. (1969), Jakes & White (1969), Stanton & Bell (1969), Jakes & Smith (1970), Lowder & Carmichael (1970), Johnson et al. (1971), and Mackenzie & Chappell (1972).

Very little is known of the geochemistry of intrusive igneous rocks from the P.N.G. region. Published data include those of Stanton & Bell (1969), who presented two major element whole-rock analyses of the Limbo River Diorite on New Georgia Island; Macnab (1970), who gave major element analyses of 33 intrusive rocks from the Gazelle Peninsula, New Britain; and Smith (1971), who gave major and trace element analyses of 27 intrusive rocks from the extreme southeast of P.N.G. There is a small quantity of unpublished data known to the writer. This comprises the work of Netzel (1974), who compiled some data on intrusive rocks from Guadalcanal (Solomon Islands); and a small number of analyses procured by the Aust. Bureau of Mineral Resources (6 from New Ireland; 3 from the Western Highlands).

1.1.4 Geochronology

The only major work on the geochronology of intrusive rocks is that of Page (1971, 1975), and Page & MacDougall (1972a, 1972b). These authors have confirmed the relative youthfulness of much of the intrusive activity in Papua New Guinea.

1.2 SCOPE OF THESIS

1.2.1 Aims

The aims of this thesis are twofold:

(i) to determine the geochemical characteristics of a number of intrusive igneous rock suites from the Papua New Guinea region, and

(ii) to assess the occurrence of porphyry-type copper mineralization in the region in the light of the geochemical characteristics of their associated intrusive rock suites.

The greater part of the thesis is devoted to the first aim. As was explained in the previous section, very little is known of the geochemistry of intrusive rocks from Papua New Guinea. This work, then,

can be regarded as a first attempt to arrive at a comprehensive overview of geochemical relationships within and between intrusive rock suites of the region.

In general, the study of intrusive igneous activity can yield valuable insights into the geochemical and geotectonic development of those regions in which it occurs, thus complementing other approaches within the broad subject of geology which bear upon these problems. In particular, geochemical data is useful in clarifying such problems as magma sources, interelationships of rock types within a rock suite, and relationships of rock suites in space and time. The data to be presented in this thesis will be used to attempt to answer questions in the context of magmatism within Papua New Guinea.

The other important aim of this thesis concerns the relationship of intrusive igneous rocks and base metal deposits. The worldwide association of intrusive and extrusive igneous rocks with particular classes of mineral deposits has long been recognized. The association is especially true of the Papua New Guinea region, where mineral deposits of the 'porphyry copper' class are closely associated in space and time with intrusive igneous rock suites. In this thesis, some of the geochemical relationships between porphyry-type copper occurrences and associated intrusive rocks are explored. Clarification of these relationships can yield insights into questions relating to the genesis of such deposits.

1.2.2 Sampling procedures

The distribution of known intrusive rock complexes in Papua New Guinea and the Solomon Islands is shown in Fig. 1. Those complexes studied in this thesis are indicated.

The selection of areas for study was governed mainly by availability of suitable material. In those areas sampled by the writer, outcrop and river float specimens of 1 - 2 kilograms were taken, with smaller amounts of some drill core specimens. Material donated to the study from other sources varied widely in mass (0.5-3 kg).

The complexes studied may be conveniently divided into two geographic categories: those from the Highlands region, and those from the Papua New Guinea islands and Solomon Islands.

(i) Intrusive complexes of the Highlands. The intrusive rocks of Papua New Guinea achieve a wide distribution in the Eastern and

FIG. 1 : DISTRIBUTION OF TERTIARY AND YOUNGER INTRUSIVE COMPLEXES IN THE P.N.G. REGION.
those studied in this thesis are underlined.

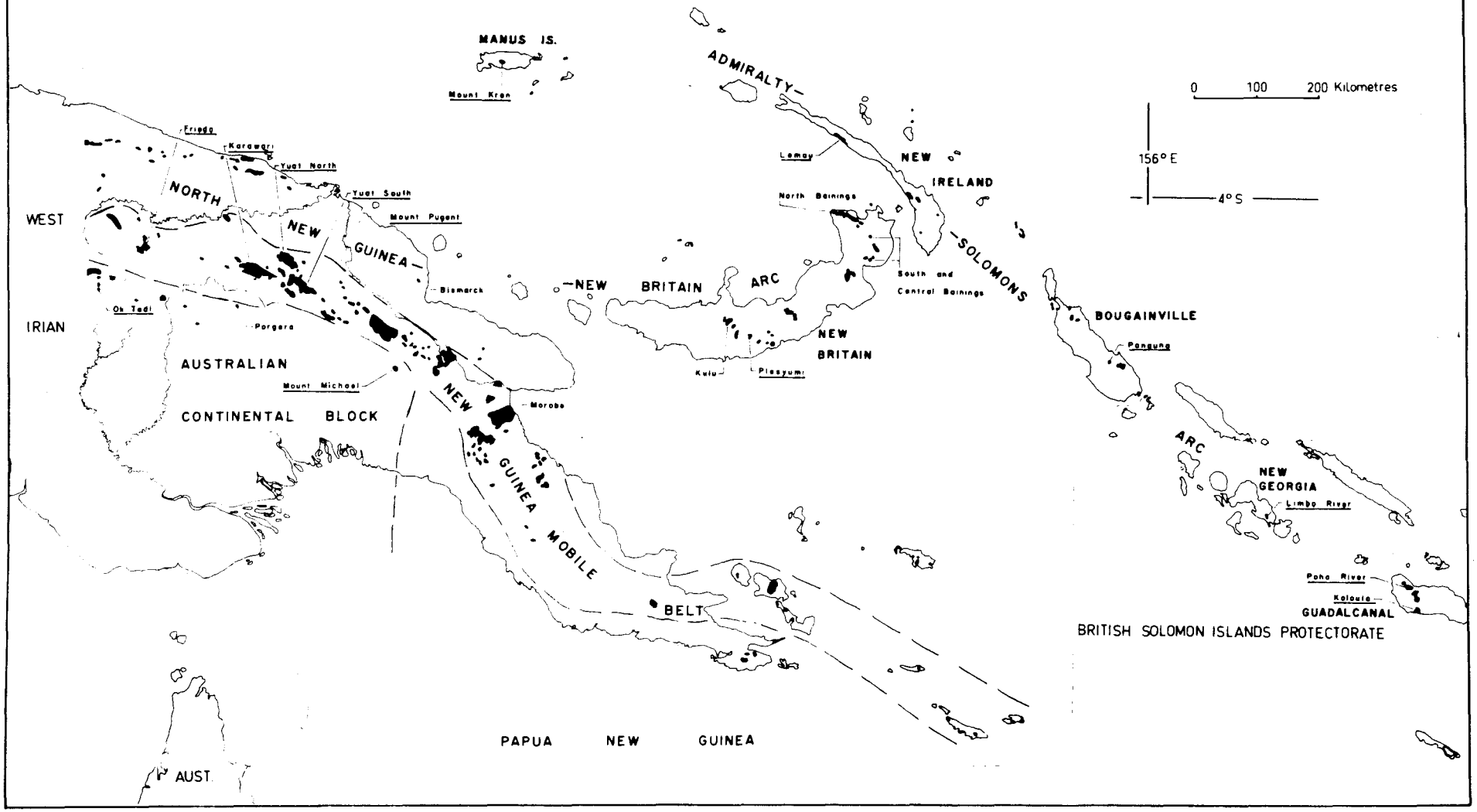

Western Highlands. This fact, together with the writer's familiarity with the area derived from previous fieldwork, made the region a logical point of departure in the study. Supplementary material was obtained from the Frieda River prospect, because of its geotectonic and chronologic similarities with other Western Highlands suites, and from the Ok Tedi prospect, because of its dissimilarities. One complex in the Eastern Highlands (the Mount Michael Stock) was chosen for study because of availability of material and for comparison with the Western Highlands suites. A total of three batholithic masses and seven stocks were chosen for study from the Papua New Guinea Highlands.

(ii) Intrusive complexes of the P.N.G. islands and Solomon Islands. Seven complexes were chosen for study. They are located on New Britain, Manus Island, New Ireland, Bougainville Island, New Georgia Island, and Guadalcanal Island. It was considered that study of these suites from intra-oceanic island arc environments would permit useful comparisons with the suites from the Highlands, a region which may have evolved in a setting more closely related to a continental margin.

From examination of 276 thin sections, 160 specimens were selected for major and trace element whole-rock analysis. Criteria for selection included absence of weathering and hydrothermal alteration effects, and representivity (within the material available) of the range of rock types from each area. In some areas (for example, Ok Tedi and Bougainville) it was impossible to obtain some rock types free of hydrothermal alteration.

In Table 1, the distribution of analyzed rocks among the intrusive complexes is given. The total number of samples which could be processed was dictated mainly by time limitations on the study. A list of analyzed rocks and locations is given in Appendix 1.

Many intrusive complexes remain unrepresented in this study. No material was obtained from the Bismarck Granodiorite, the many intrusive bodies in the Wau-Bulolo area, the smaller intrusive masses of northern Papua New Guinea, or the Permian Kubor complex.

1.2.3 Chemical determinations

(i) Major elements (whole-rocks)

X-ray fluorescence methods were used to determine SiO_2, TiO_2, Al_2O_3, total Fe as Fe_2O_3, MnO, MgO, CaO, K_2O, P_2O_5, and S for 146 whole-rocks (sample numbers DRM001-042, 044-147). For these specimens, Na_2O was determined by flame photometry, and FeO by titration against $K_2Cr_2O_7$.

TABLE 1: DISTRIBUTION OF ANALYZED ROCKS AMONG INTRUSIVE COMPLEXES IN THIS THESIS

Region Name of Intrusive Complex	Location	Number of analyzed rocks	Specimen source(s)
Highlands, P.N.G.			
1. Yuat North Batholith	South Sepik/Western Highlands	8	Author; Bureau Min. Resources
2.* Sekau Stock	" " / " "	6	Author
3.* Yuat South Batholith	Western Highlands	21	Author
4.* Karawari Batholith	" "	21	Author
5. Wale Stock	" "	3	Author
6. Lamant Stock	" "	2	Author
7. Mount Pugent Stock	" "	3	Author
8.* Frieda River Complex	" "	7	Carpent. Explor. Co.; Bureau Min. Resources.
9.* Ok Tedi Complex	" "	10	Kennecott Explor.; Dr R.W.Page
10.* Mount Michael Stock	Eastern Highlands	4	Bureau Min. Resources
P.N.G. Islands and Solomon Islands			
11.* Plesyumi Intrusive Complex	Central New Britain	10	Author
12. *Mount Kren Intrusive Complex	Manus Island	13	Author
Reconnaissance	" "	2	Dr R.W. Page
13. *Lemau Intrusive Complex	Central New Ireland	5	Author
14. *Panguna Intrusive Complex	Bougainville Island	15	Author; Dr R.W. Page
Reconnaissance	" "	3	Bureau Min. Resources
15. Limbo River Diorite	New Georgia Is., B.S.I.P.	3	Geol. Survey, B.S.I.P.
16. *Koloula Igneous Complex	Guadalcanal Is., B.S.I.P.	22	Author
17. Poha River Diorite	" " "	2	Geol. Survey, B.S.I.P.

Note: * indicates presence of mineralization within the complex.

The volatiles H_2O+, H_2O-, and CO_2 were determined by furnace heating and tube collection.

Electron microprobe methods were used to determine SiO_2, TiO_2, Al_2O_3, Cr_2O_3, total Fe as FeO, MnO, MgO, CaO, Na_2O, and K_2O for a further 14 whole-rocks (DRM148-161). For these specimens, total loss on ignition was determined by mass difference after furnace heating.

(ii) Trace elements (whole-rocks)

X-ray fluorescence methods were used to determine Rb, Ba, Sr, La, Ce, Y, Th, U, Zr, Nb, Zn, Cu, Co, Ni, V, Cr, and Pb for all 160 specimens. Ga was determined for 65 specimens (DRM001-042, 044-066). Co was omitted for some specimens because of insufficient sample (DRM070--74, 076-079, 082-083, 085-086, 156-161).

Se and Te were determined for 36 specimens by atomic absorption methods by the staff of Kennecott Exploration Inc. (Geochemical Research and Laboratory Division), Salt Lake City, Utah, U.S.A.

Au and Ag were determined for the same 36 whole-rocks by the staff of Australian Mineral Development Laboratories, Adelaide, South Australia, using atomic absorption techniques.

(iii) Major elements (minerals)

Electron microprobe methods were used to determine SiO_2, TiO_2, Al_2O_3, Cr_2O_3, total Fe and FeO, MnO, MgO, CaO, Na_2O, and K_2O for different mineral species in selected rocks. Specimens were prepared as polished sections or polished thin sections.

Details of all analytical methods employed by the writer are given in Appendix 2.

1.3 FORMAT OF THESIS

This thesis has been organized to lead the reader sequentially through details of petrography, geochemistry and mineralization to consideration of the petrogenesis of intrusive rocks and related porphyry copper systems in the P.N.G. region.

Chapters 2 and 3 are devoted to petrographic description of intrusive rocks from the Highlands and islands regions of P.N.G. The geochemistry of the same intrusive complexes is treated in Chapters 4 and 5.

In Chapter 6, chemical data are presented for different mineral

species mainly from intrusive suites of the Western Highlands. Emphasis is placed upon chemical variation within amphiboles and biotites. The results are used to qualitatively assess changes in magmatic conditions during crystallization.

Different aspects of porphyry-type copper mineralization in the P.N.G. region are examined in Chapter 7. Patterns between intrusive suite chemistry and presence of mineralization are drawn out. The abundances of copper, zinc, lead, silver, gold, selenium, and tellurium are discussed. The geochemical differences of mineralized and non-mineralized rocks are explored using multivariate statistical techniques.

Chapter 8 is devoted to synthesis of the previously-presented data and its bearing upon petrogenesis. Other field data and experimental work are introduced to the discussion. Models for generation of intrusive complexes and porphyry copper systems are developed for the P.N.G. region. The text closes with a summary of conclusions arising from this work.

CHAPTER 2 PETROGRAPHY OF INTRUSIVE ROCK SUITES, HIGHLANDS, PAPUA NEW GUINEA

2.1 ROCK NOMENCLATURE

Nomenclature used here for intrusive igneous rocks will broadly follow the modal scheme of Streckeisen (1967), as modified by the IUGS Subcommission on the Systematics of Igneous Rocks (1973). However, it is unreliable to base a classification scheme entirely on modal abundances for the reason that, with increasing alkali content, less silica becomes available to crystallize as free quartz. The deficiencies of a modal scheme become especially apparent when classification is attempted for rocks of wide alkali range at given silica contents.

Overiding emphasis will be placed on rock chemistry and mineralogy. The chemical classification of calc-alkaline rocks used here is essentially that of Taylor (1969), as applied by Gulson et al. (1972), and is set out below:

	SiO_2 weight %	K_2O weight %
low-K diorites	53-56	<0.7
low-Si diorites	53-56	0.7-2.5
normal diorites	56-62	0.7-2.5
high-K diorites	53-62	>2.5
granodiorites	62-68	>2.5

Gulson et al. (1972) drew attention to the usefulness of this scheme in comparing the chemistries of intrusive and extrusive calc-alkaline igneous rocks of orogenic environments.

The above terms will be qualified where appropriate by using prefixes for abundant mineral species. Thus 'hornblende-biotite granodiorite' refers to a granitic rock with 62-68% SiO_2, >2.5% K_2O, and with hornblende dominant over biotite in its mafic assemblage. A 'porphyritic clinopyroxene-hornblende microdiorite' refers to a relatively fine-grained dioritic rock with 56-62% SiO_2 and with clinopyroxene phenocrysts more abundant than hornblende phenocrysts.

2.2 GEOTECTONIC SETTING AND REGIONAL GEOLOGY OF THE HIGHLANDS

2.2.1 Major Geotectonic Units of the P.N.G. Region

The principal geotectonic units of the P.N.G. region have been defined and described by Thompson & Fisher (1965), Denham (1969), and Bain (1973). Those units which are relevant to this study are shown in Fig. 2. In brief they are:

FIG. 2 : PRINCIPAL GEOTECTONIC UNITS OF THE PAPUA NEW GUINEA - SOLOMON ISLANDS REGION.

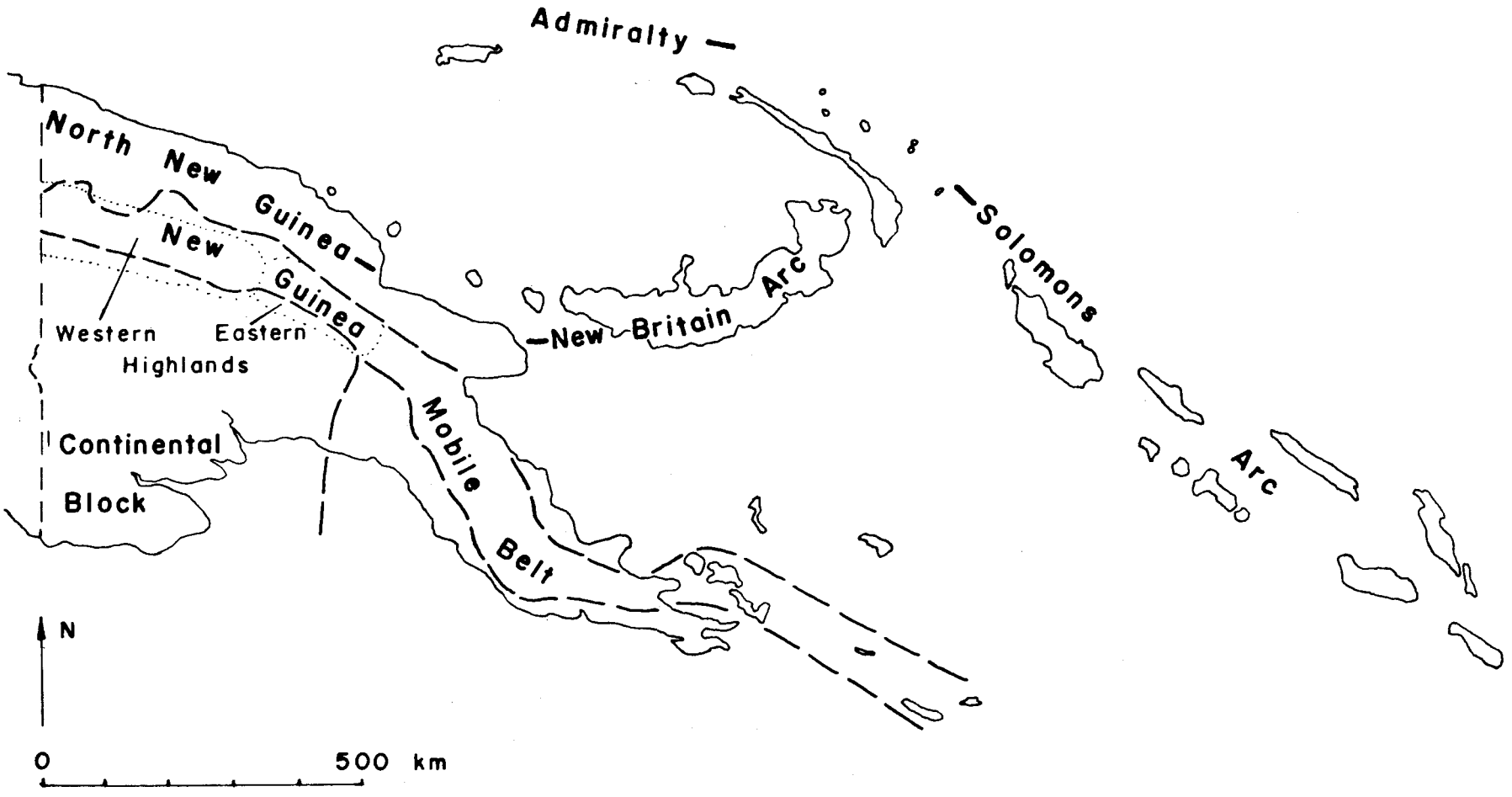

(i) the *Australian continental block*, which occupies the south-western part of the mainland. In includes the Fly Platform and overlying Papuan Fold Belt, and is characterized by the Palaeozoic crystalline basement.

(ii) The *New Guinea Mobile Belt*, which is an elongate feature to the north and east of the Australian continental block. It contains most of the high-angle faults, intrusive, metamorphic, and ultramafic rocks of Mesozoic and younger age of the P.N.G. mainland. The Mobile Belt has been interpreted as part of the zone of interaction between the Indo-Australian and Pacific plates. In this study, attention is confined to that part of the Mobile Belt which lies to the north of the continental block (i.e., the districts of the Western and Eastern Highlands of P.N.G.).

(iii) the *island arcs*, which lie in an oceanic setting to the east of the P.N.G. mainland. The arcs include the *Admiralty-Solomon Islands arc* and the *north New Guinea-New Britain arc*, which form part of the Outer Melanesian Arc system.

2.2.2 Regional Geology of the Highlands, P.N.G.

Principal contributions to knowledge of the regional geology of the Western Highlands have been made by Rickwood (1955), Dow & Dekker (1964), and Dow et al. (1967, 1968, 1972). The latter authors established the stratigraphy in the region (see Table 2), and contrasted the sedimentation and structural histories of the Mobile Belt and continental block.

The crystalline continental block received shelf-type sediments during the Mesozoic and Cenozoic. Deformation mainly by uplift and gravity sliding began in the Tertiary and continues in Recent times. Intrusive rocks of late Miocene to Pleistocene age are known. Calc-alkaline and shoshonitic volcanism began in the Pleistocene and continued into Recent times.

The Mobile Belt to the north was a site of volcanogenic sedimentation from early Mesozoic to early Tertiary times. Faulting, metamorphism and uplift in the early Tertiary was followed by volcanism and emplacement of calc-alkaline intrusive complexes in the Middle and Upper Miocene. Similar styles of sedimentation and deformation have been described in the Eastern Highlands (Bain & Mackenzie, 1974.)

2.3 SUBDIVISION OF INTRUSIVE COMPLEXES

The Tertiary intrusive complexes of the Western Highlands have been collectively referred to as the 'Maramuni Diorite' (Dow et al.

TABLE 2: WESTERN HIGHLANDS STRATIGRAPHY (after Dow *et al.*, 1972)

	South (Australian continental block)			North (New Guinea Mobile Belt)
PLEISTOCENE	Hagen Volcanics			
PLIOCENE				
MIOCENE				Burgers Formation / Wogamush Beds / Karawari Conglomerate
f_{1-2} stage	Yangi Beds (marl, limestone)	Tibinini Limestone Member	LAGAIP	
e stage				Pundugum Formation (tuffaceous siltstone, conglom.)
OLIGOCENE	(Erosion interval)			(Erosion Interval)
EOCENE			FAULT	
PALEOCENE	Lagaip Beds (black shale, siltstone)			Salumei Formation (siltstone, limestone, marine volcanics)
CRETACEOUS			ZONE	
U. JURASSIC				Maril and Sitipa Shales
M. JURASSIC				Mongum Volcanics
L. JURASSIC				(Erosion interval)
U. TRIASSIC				Kana Volcanics
M. TRIASSIC				Yuat Shale

1972). Distinction was made between the 'Yuat Intrusives' in the east and the 'Karawari Intrusives' in the west. Page (1971) showed that the 'South Yuat Intrusives' (11.1-12.6 m.y.) were significantly younger than the 'North Yuat Intrusives' (13.5-14 m.y.), while the 'Karawari Intrusives' (10-15 m.y.) overlapped both periods of intrusion.

Rather than continue with the vague term 'intrusives', it is proposed here to use the terms 'stock' and 'batholith' in the currently accepted sense in which these terms are used. Thus a *'stock'* is an intrusive complex less than 100 km^2 in area, and a *'batholith'* is an intrusive complex greater than 100 km^2 in area. The essential criteria of size and geographic separation are applicable in the distinction of stocks and batholiths in the Western Highlands. Petrographic and geochemical differences, to be described in following sections, support the distinctions.

In Table 3, a scheme for subdivision of the Tertiary intrusive complexes is presented (Mason, 1975). Correlations are made with the nomenclature of Dow et al. and Page (1971). In the proposed scheme, three batholiths are recognized: the Yuat North Batholith, the Yuat South Batholith, and the Karawari Batholith. Newly named stocks are the Wale Stock, Lamant Stock, and the Sekau Stock. Specimen locations in the stocks and batholiths are shown in Fig. 3.

2.4 YUAT NORTH BATHOLITH

2.4.1 Geological Setting

The Yuat North Batholith is elongate northwest-southeast, and underlies an area of approximately 450 km^2. It is a composite body, but the rugged terrain and restricted sampling have prevented the mapping of different phases. Medium grained dioritic to granodioritic rocks predominate, and in places carry more or less ghosted xenoliths several centimetres to 0.5 metre in diameter. Invariably the xenoliths are more mafic than their host rocks.

The batholith and its marginal stocks intrude a variety of sedimentary and volcanic rocks of Lower Jurassic to Upper Triassic age (Yuat Formation and Kana Volcanics of Dow et al., 1972), and the Cretaceous to Eocene Salumei Formation. Unfortunately, no contact relationships have been observed by the writer, but the contact aureole, where developed, appears to be of limited extent.

Large-scale transcurrent faulting, which has dominated the

TABLE 3: SUBDIVISION OF TERTIARY INTRUSIVE COMPLEXES, WESTERN HIGHLANDS, P.N.G.

Dow *et al.*, (1967,1968,1972)	Page (1971)	This author	Approximate Area (km^2).	Remarks
Maramuni Diorite				
Yuat Intrusives	Yuat North Intrusives	Yuat North Batholith	450	Named after Yuat River to east
	Yuat South Intrusives	Yuat South Batholith	600	Named after Yuat River to east
Karawari Intrusives	Karawari Intrusives	Karawari Batholith	650	Named after Karawari River
		Wale Stock	150	to southwest of Yuat South Batholith; named after Wale River in the Maramuni River system.
		Lamant Stock	50	to west of Yuat South Batholith; named after Lamant River in the Maramuni River system.
		Sekau Stock	10	probably equivalent to "Oipo Intrusives" of Dow & Dekker (1964); named after Sekau River in the upper Clay River system.

FIG. 3 : INTRUSIVE COMPLEXES IN PART OF THE WESTERN HIGHLANDS,

showing specimen locations and nomenclature of intrusive complexes.

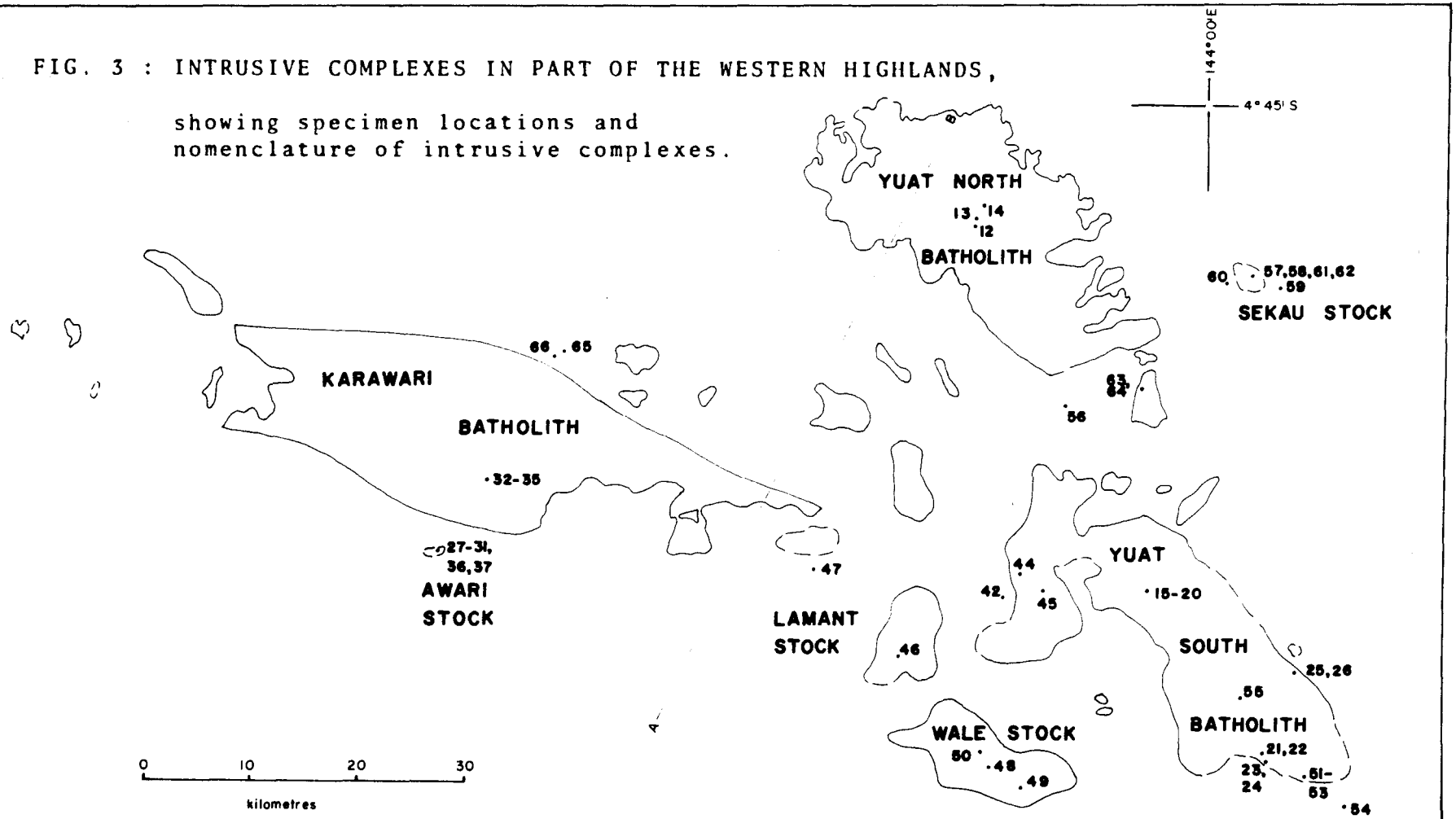

structural style within the Papua New Guinea Mobile Belt, has been important in the location and subsequent exposure of the batholith. Two fault zones, the Jimi Fault Zone in the east and the Maramuni-Bismarck Fault Zone in the west, define a large horst-like structure within which lie the Yuat North and Yuat South batholiths (see Fig. 4).

2.4.2 Petrography

The mineralogy of rock types from the Yuat North Batholith is dominated by the typical calc-alkaline assemblage of zoned plagioclase, alkali feldspar, quartz, green amphibole, and biotite. Lesser amounts of pyroxene and opaque oxide are present, with accessory phases zircon and apatite. Dow et al. (1972) p. 68 report an olivine-bearing pyroxene diorite from the northwestern part of the batholith, but no material was available for analysis.

The bulk of the Yuat North Batholith comprises *high-K hornblende-biotite-quartz diorite*. The rock is medium grained (3-4mm plagioclase prisms), and in thin section displays an hypidiomorphic granular texture with interstitial micrographic intergrowths. Essential mineralogy includes 35-40 volume percent of complexly zoned and twinned andesine plagioclase, 20-25% dusty alkali feldspar, 15-20% angular interstitial quartz, 6-10% biotite (pleochroic light yellowish brown to dark chocolate brown), 6-10% hornblende (pleochroic pale green-brown to dark green-brown), 1-2% pyroxene as cores within hornblende, and 2% titaniferous magnetite. Accessories include zircon, apatite, and minor chlorite alteration of biotite flakes.

Mafic and felsic variants occur as smaller intrusive masses within or adjacent to the batholith. *Orthoclase gabbro* has been found only as float material, the source being a small stock near the southeast margin. It is characterized by large clear plates of K-feldspar poikilitically enclosing buff-coloured euhedral to subhedral clinopyroxene. Large discrete flakes of biotite are pleochroic golden yellow to dark greenish brown, and in places enclose clinopyroxene euhedral and plagioclase laths. Plagioclase forms small laths and hornblende forms small pale green pleochroic subhedra and rims around clinopyroxene. Titaniferous magnetite grains form groups of subhedral crystals, and accessories include apatite prisms and angular sphene crystals.

A felsic phase crops out in the southern part of the Yuat North Batholith. It is a *biotite-hornblende microadamellite*, with twinned and zoned plagioclase laths; clouded K-feldspar anhedra in places forming micrographic intergrowths; abundant interstitial quartz; discrete

FIG. 4 : STRUCTURAL FEATURES OF PART OF THE WESTERN HIGHLANDS, P.N.G.

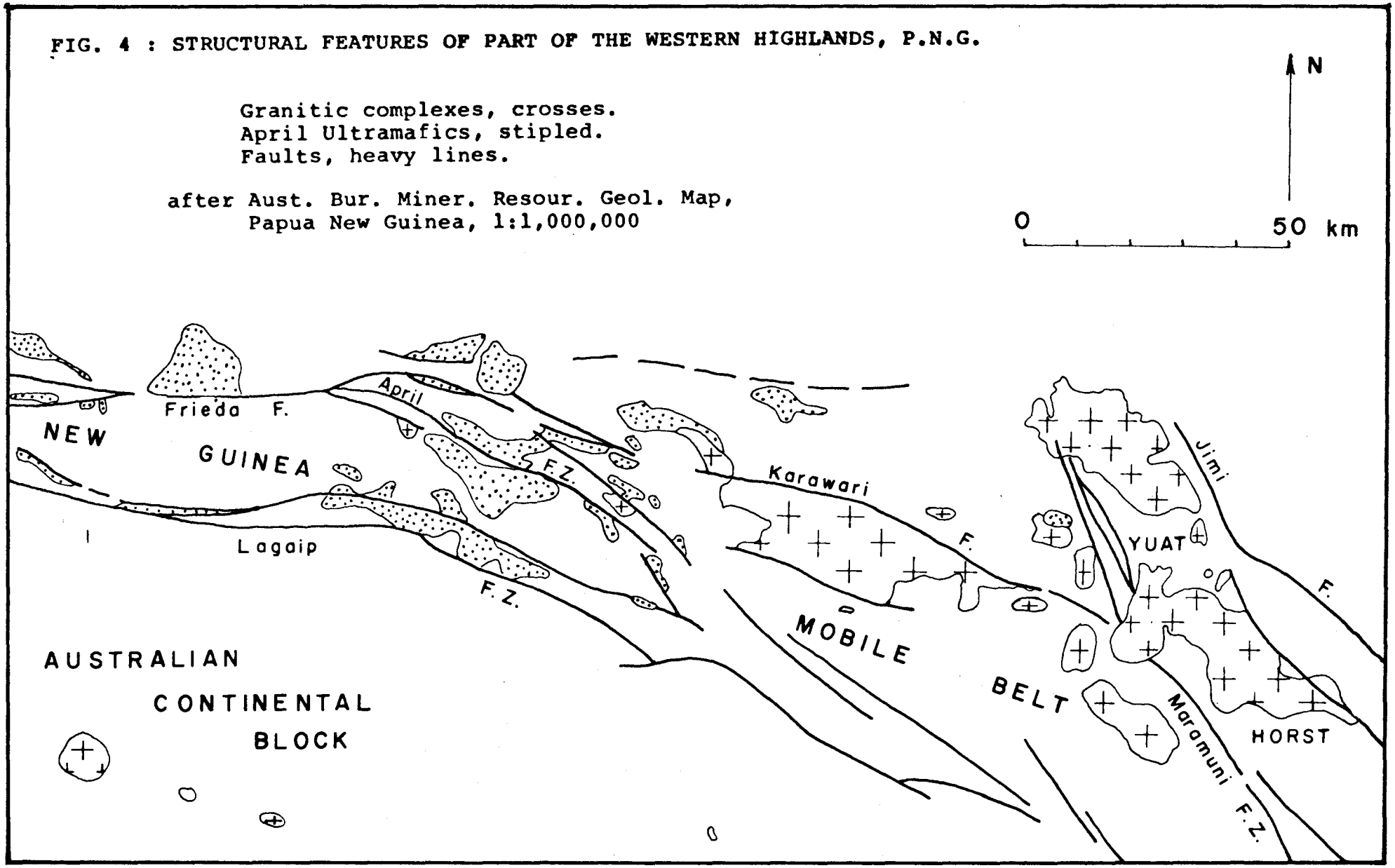

biotite flakes pleochroic yellow-brown to dark brown; small euhedral to subhedral prisms of hornblende pleochroic pale green to dark green or greenish brown; and accessories including zircon, apatite, and minor chlorite.

Optically estimated modes for analyzed specimens are given in Appendix 3, together with modes for all other analyzed rocks.

Some degree of textural variety is present in the high-K diorite of the Yuat North Batholith. Although an hypidiomorphic granular, micrographic texture is dominant, variations in the form of mafic minerals and quartz are observed. Clots of mafic minerals are more common in the slightly more mafic diorites (e.g. DRM012). The clots comprise ragged green amphibole grains with granular clear clinopyroxene cores, poorly-formed reddish-brown biotite flakes replacing the amphibole, subhedral opaque oxide grains, and rare non-pleochroic orthopyroxene grains marginally replaced by finely-twinned cummingtonite. Quartz tends to form subequant, anhedral blebs and micrographic intergrowths with alkali feldspar. In the more felsic diorites (e.g. DRM013) mafic clots are less common, with biotite and green-brown amphibole forming discrete crystals. Quartz tends to form angular interstitial patches.

2.5 YUAT SOUTH BATHOLITH

2.5.1 Geological Setting

Together with the Yuat North Batholith, the Yuat South Batholith lies largely within a horst structure of Mesozoic and early Tertiary sediments and volcanics (see Fig. 4). It is elongate northwest-southeast and underlies an area of approximately 600 km^2. It is a composite body. Intrusive contacts, where seen, are steep and sharp against the volcanic and sedimentary country rocks. A contact aureole approximately 100 metres wide is developed, with recrystallization in the hornblende-hornfels facies. Garnetiferous calc-silicate hornfelses occur adjacent to the western contact in the Tarua River drainage, where country rocks belong to the Cretaceous to Eocene Salumei Formation. At the eastern contact, pelitic rocks of the Triassic to Jurassic Kana Volcanics possess the assemblage biotite-plagioclase-sillimanite-quartz, and basic volcanics have recrystallized to the assemblage plagioclase-epidote-tremolite/actinolite-greenish biotite-sphene-quartz-opaque oxide.

2.5.2 Petrography

The bulk of the Yuat South Batholith consists of normal calc-

alkaline *hornblende-biotite-quartz granodiorite*. The rock is medium grained (2-3 mm. plagioclase prisms), and in thin section displays an hypidiomorphic granular texture. Complexly twinned and zoned plagioclase prisms comprise 40-45 volume percent of the rock; anhedral quartz patches, 25%; larger plates of alkali feldspar, 15%; subhedral hornblende pleochroic green to green-brown, 8%; biotite books pleochroic straw yellow to dark brown, 5-7%; magnetite, 2%; and accessory minerals including large angular sphene grains often associated with hornblende, euhedral apatite prisms, zircon, pyrite, and chlorite sheaves in biotite.

In the western part of the Yuat South Batholith (Baeambo Creek, Tarua River region), the granodiorite contains more hornblende, less biotite, and less K-feldspar. The different modes, the lobate outcrop pattern, and chemical differences (see later section) indicate that this is a distinct intrusive phase of the Yuat South Batholith.

A great variety of rock types occur as marginal stocks and apophyses, and as dykes within the main body of the Batholith. These rock types include hornblende gabbro (pegmatitic in part), pyroxene gabbro, and plagioclase-hronblende diorite porphyries. *Hornblende-clinopyroxene gabbro* forms a narrow discontinuous rim to the batholithic granodiorites at the southern and eastern contacts. Abundant large twinned tablets of plagioclase are slightly sericitized; pale green to dark green-brown hornblende shows some alteration to fibrous tremolite/actinolite, chlorite, and magnetite; rarer clinopyroxene subhedra possess hornblende rims; minor quartz is present as anhedral grains; magnetite subhedra and rare ilmenite prisms are scattered through the rock, and accessory sphene occurs as large anhedral grains. *Plagioclase-hornblende (-quartz) diorite porphyries* form dykes 1-3 metres wide or irregularly shaped apophyses. They comprise variable amounts of complexly twinned and zoned plagioclase phenocrysts and pleochroic prismatic green hornblende phenocrysts in a very fine grained groundmass of plagioclase laths, hornblende prisms, traces of alkali feldspar, interstitial quartz, and scattered magnetite granules. Pyrite and sphene are common accessories, and rounded quartz phenocrysts are rare.

High-K hornblende-biotite (-clinopyroxene) diorite occurs at the southern margin of the Yuat South Batholith. Only found as float material, its distribution suggests that it is of limited extent. The presence of undulatory extinction in polycrystalline quartz patches and also in aggregates of biotite flakes suggests that the rock was one of the earlier phases of the batholith, and has suffered a mild degree of deformation

during intrusion of the main batholithic granodiorites.

2.6 KARAWARI BATHOLITH

2.6.1 Geological Setting

The Karawari Batholith is a large composite body greater than 650 km^2 in area, with marginal stocks and apophyses. It is elongate in a direction west of northwest, and is fault-bounded on its northern and southern margins. It is located in a very rugged part of the Highlands, making access difficult.

The mapping of Dow et al. (1972) indicates that the batholith is intrusive into the Cretaceous to Eocene Salumei Formation and the Upper Oligocene to Lower Miocene Pundugum Formation.

Field relationships of the Awari Stock (see location of Awari Prospect, Fig. 3) reveal that at least some if not all of the peripheral stock-like masses are later than the Alpine-type April Ultramafics.

2.6.2 Petrography

Calc-alkaline intrusive rocks with moderate to low K_2O contents form the bulk of the Karawari Batholith. Medium grained *hornblende-clinopyroxene-quartz diorite* consists of an hypidiomorphic granular assemblage of twinned and zoned plagioclase tablets (60%); large prisms of pleochroic pale brown to dark green hornblende (15%) in places poikilitically enclose plagioclase stumps; equant clinopyroxene (2%) exhibits marginal alteration to pale green amphibole; abundant angular quartz patches (12-15%) and K-feldspar (5%) are interstitial to plagioclase; large ragged blebs of magnetite (2%) and rare ilmenite are associated with mafic minerals; and accessories include euhedral crystals of sphene and apatite.

Hornblende (-biotite) tonalite is a dominant rock type, and carries rounded mafic xenoliths several centimetres in diameter. Plagioclase prisms are abundant (70%); anhedral quartz patches (12%) and minor K-feldspar (5%) occur interstitially; prismatic hornblende (8%) is pleochroic pale brown to dark green; minor biotite flakes (1%) are pleochroic pale brown to dark brown; angular magnetite blebs (2%) and rare ilmenite laths are associated with the mafic minerals; accessories include zircon and sphene.

Less important volumetrically are *hornblende-clinopyroxene basaltic dykes*, and small stocks and dykes of *plagioclase - hornblende (-quartz) diorite porphyries*.

2.7 LAMANT AND WALE STOCKS

2.7.1 Geological Setting

These two stocks are described together because of their proximity and the predominance of mafic rocks in both.

The Lamant and Wale (pronounced 'Wah-le') stocks are composite intrusive masses located to the west and southwest respectively of the Yuat South Batholith (see Fig. 3). The Lamant Stock is approximately 50 km^2, and the Wale stock about 150 km^2. The Wale Stock intrudes the Upper Oligocene to Lower Miocene Pundugum Formation and the Tarua Volcanic Member of the Burgers Formation (Middle to Upper Miocene). The Lamant Stock intrudes these formations and also the Cretaceous to Eocene Salumei Formation.

It is of considerable interest that these two stocks are in close proximity with the Tarua Volcanic Member of the Burgers Formation. Page & McDougall (1970) have shown that K-Ar ages overlap for the Tarua Volcanic Member and the mid-Miocene intrusive rocks. Page (1971) showed that initial $^{87}Sr/^{86}Sr$ ratios were low and indistinguishable for the extrusive and intrusive mid-Miocene igneous rocks. There is sufficient data, then, to allow one to propose that the small Wale and Lamant stocks are the subvolcanic intrusive equivalents of the Tarua Volcanic Member.

2.7.2 Petrography

Rock types represented in these two complex intrusions range from mafic and ultramafic cumulates, through gabbros to granodiorites. The mafic rocks predominate in both complexes.

The core of the Wale Stock comprises *olivine pyroxenite*. It is a coarse-grained, dark green-black rock with reddish brown alteration pseudomorphs. Thin section observations reveal that olivine (8%) has been partly replaced by red-brown iddingsite with associated tiny magnetite granules (2%); clinopyroxene (80%) forms large (5mm) well-cleaved grains and shows some alteration to green-brown hornblende and fibrous green tremolite/actinolite; interstitial plagioclase laths (5%) are twinned but unzoned. The *gabbros* are essentially hornblende-plagioclase rocks with some clinopyroxene, subhedral ilmenite grains, and rare or absent quartz. *Hornblende granodiorite* is an important phase, but unfortunately has not been sampled.

The Lamant Stock also has medium grained *hornblende granodiorite* as an important phase, but neither has this been sampled. A dominant

phase is *porphyritic hornblende-clinopyroxene gabbro*, consisting of large prismatic dark green-brown hornblende with spongy clinopyroxene cores, in a groundmass of plagioclase, ilmenite blebs, accessory sphene and rare or absent interstitial quartz.

2.8 SEKAU STOCK

2.8.1 Geological Setting

Dow et al. (1972, p. 82) infer the presence of an intrusive body in the headwaters of the Clay River. The location of this intrusion has been confirmed through stream prospecting by the author, and it is here named the 'Sekau Stock'. It is a complex intrusive body 3-5 km in diameter, composed principally of low-Si diorites and associated mafic and ultramafic cumulates, but also including a late felsic phase which was too weathered to sample properly. The field relationships of the dioritic and more basic rocks are not clear, but a multiphase intrusive relationship is likely.

The Sekau Stock intrudes the Upper Jurassic Maril Shale (Dow et al., 1972), but nowhere were intrusive contacts observed in the field. The complex could well belong to the Oipo Intrusives of Dow & Dekker (1964), located some 60 km to the southeast.

2.8.2 Petrography

The *low-Si diorites* comprise abundant plagioclase prisms (45-60%) which are twinned and exhibit a moderate degree of normal zoning; deep green pleochroic hornblende (15-20%), in places poikilitically enclosing small plagioclase stumps and associated with discrete flakes of biotite (5-8%), pleochroic yellowish brown to dark chocolate brown, which is in part replaced along cleavages by green chlorite. Higher-K diorites contain a higher proportion of biotite, and also carry clinopyroxene cores in hornblende.

Mafic cumulate rocks are gradational from *hornblende gabbro* to *hornblendite*. Prismatic hornblende is pleochroic pale brown to dark green and exhibits twinning and, more rarely, zoning as evidenced by gradual change in extinction angle from core to rim; small plagioclase tablets fill interstices, and in places are partly or completely replaced by very fine flaky sericite; shpene characteristically forms large angular grains, and apatite forms large prisms; magnetite subhedra and feathery to dendritic sulfides (pyrite, chalcopyrite) are constant accessories.

Serpentinized peridotite, found only as creek float, consists of fresh cuspate clinopyroxene moulded on primary olivine, which is now completely replaced by tremolite and serpentine; large orthopyroxene prisms also are completely serpentinized; accessory opaque oxide blebs are moulded on primary mafic minerals. The peridotite is probably derived from a tectonically emplaced slice similar to the Marum Basic Belt (Dow & Dekker, 1964).

2.9 MOUNT MICHAEL STOCK

2.9.1 Geological Setting

The Mount Michael Stock is located approximately 50 km southeast of the town of Kundiawa in the Eastern Highlands. In its tectonic setting, the stock is located at the eastern end of the Kubor Anticline, with the Bismarck Fault Zone (which marks the southern limit of the New Guinea Mobile Belt) immediately to the north.

The stock is roughly oval in plan, and underlies 60 km^2. It intrudes fine grained clastic marine sedimentary rocks of the Movi Beds (Bain & Mackenzie, 1974). Observations made by the Australian Bureau of Mineral Resources field parties indicate that the upper levels of the stock are presently exposed. These observations include the small size of the stock, the predominance of porphyritic texture among the rock types represented in the stock, and the presence of numerous roof pendants.

Page (1971) gave radiometric ages of 6-7 m.y. for material from the stock. Specimen locations are shown in Fig. 5.

2.9.2 Petrography

A variety of *plagioclase-hornblende diorite porphyries* constitute the bulk of the Mount Michael Stock.

Plagioclase and hornblende are ubiquitous phenocrystic phases. The plagioclase prisms are up to 4 mm long, but more usually 1.5-2 mm. Complex twinning and zoning (frequently oscillatory) are characteristic, and mottled cores are common. Hornblende forms euhedral prisms up to 1.5 mm long, and is pleochroic dark green to greenish brown. Less common but evenly distributed are large angular or euhedral sphene crystals, apatite prisms, and subhedral to anhedral magnetite grains.

The groundmass is exceedingly fine-grained in some specimens, and individual mineral species are difficult to identify. In those specimens where the groundmass is coarser, one can identify plagioclase laths, alkali feldspar tablets, and scattered clear interstitial quartz

FIG. 5 : SPECIMEN LOCATIONS AND STRUCTURAL SETTING,
MOUNT MICHAEL INTRUSIVE COMPLEX.

after Bain & Mackenzie (1974).

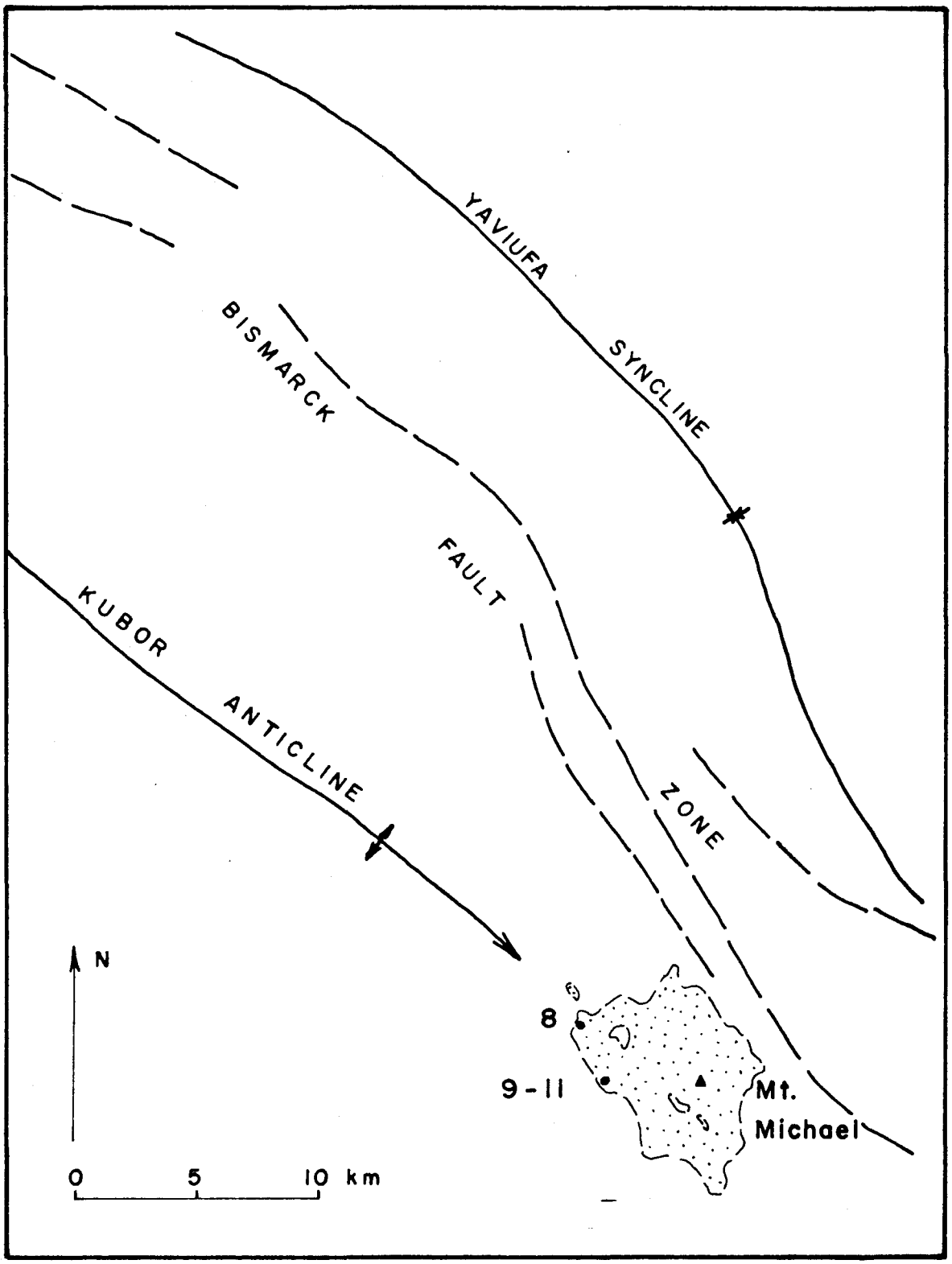

patches. Scattered throughout the groundmass are irregularly-shaped patches of carbonate, in places with associated quartz grains and apatite prisms.

One small xenolith has been observed in thin section. It is a fine-grained microdiorite, somewhat more mafic than the host rock, but with essentially the same mineralogy. Abundant small green-brown hornblende prisms frequently possess a darker core, and plagioclase tablets are heavily mottled and replaced by carbonate. Clear quartz forms rare interstitial patches, and subhedral to anhedral magnetite blebs are present. As in the host rock, sphene is an important accessory phase, but forms smaller angular grains.

Optically estimated modes for the analyzed rocks are given in Appendix 3.

2.10 MOUNT PUGENT STOCK

2.10.1 Geological Setting

The small plug-like body centred on Mount Pugent is located approximately 50 km north-northwest of Mount Hagen township. The intrusive mass is elliptical in plan (1.0 x 1.5 km) and is the most prominent geographic feature in the area. Precipitous cliffs marking the sides of the stock prevent close examination in the field, and only float material has been sampled.

The stock is composed of felsic microsyenite containing abundant, small, fine-grained mafic xenoliths. It intrudes basic pillow lavas, tuffaceous volcanogenic sediments and purple mudstones of the Kondaku Tuff (Dow & Dekker, 1964) of Lower Cretaceous age.

No radiometric dating is available for this particular stock, but it is assumed to be of Tertiary age, most likely Middle or Upper Miocene.

2.10.2 Petrography

Pyroxene (-biotite) microsyenite is the dominant rock type of the Mount Pugent Stock. In thin section it contains up to 80% of interlocking plagioclase laths and alkali feldspar tablets up to 0.5 mm in size. The felsic minerals are heavily dusted. No quartz has been observed. Mafic minerals are represented by small green subidiomorphic crystals of aegerine augite, with closely associated poorly-formed flakes of reddish brown biotite and anhedral magnetite granules.

The lack of quartz and the presence of a sodic pyroxene set this rock type apart from the other Tertiary intrusive rocks of the Highlands.

2.11 FRIEDA RIVER INTRUSIVE COMPLEX

2.11.1 Geological Setting

The complex of porphyritic intrusive rocks in the headwaters of the Frieda River was named the 'Frieda Porphyry' by Dow et al. (1968). These authors described the distribution of the intrusive rocks in the area, their geological setting, petrography, and occurrence of associated mineralization. A major fault zone (Frieda Fault) separates smaller porphyritic stocks to the south which are intrusive into the Cretaceous to Eocene Salumei Formation, from somewhat larger bodies to the north which are intrusive into the Ambunti Metamorphics of probable late Eocene-early Oligocene age (Page, 1971). Hall & Simpson (in press) exclude the Nena Diorite to the north from the 'Frieda Intrusive Complex'.

Page & McDougall (1972a) have shown that stocks of the Frieda Porphyry were emplaced over a period of several million years in the Middle Miocene (13-16 m.y.). Specimen locations are shown in Fig. 6.

2.11.2 Petrography

Dow et al. (1968) were able to distinguish three groups of rock types: hornblende andesite porphyries and altered tuffaceous volcanic rocks which predominated in the southern intrusive bodies, and quartz diorite and monzonite porphyries which formed the stocks to the north.

Thin section studies generally confirm this subdivision. The 'hornblende andesite porphyries' are here called *'hornblende-plagioclase diorite porphyries'*, terminology which emphasizes their shallow intrusive occurrence and phenocrystic mineralogy. In these rocks, phenocrysts of plagioclase up to 5 mm long are strongly zoned (normal and oscillatory) and twinned. Hornblende phenocrysts form euhedral prisms which are pleochroic green to greenish brown. Primary biotite forms large books which are pleochroic dark chocolate brown to pale fawn, and in places are chloritized on margins and along cleavage planes. Magnetite subhedra up to 1 mm in size and rare small ilmenite blades are scattered through the rock. Rounded quartz phenocrysts are rare. The groundmass comprises abundant anhedral quartz, plagioclase laths and irregularly-shaped alkali feldspar patches, with rather less hornblende as small stumps and acicular prisms. Accessory phases include large euhedral apatite prisms, small zircons, and scattered magnetite granules.

FIG. 6 : FRIEDA RIVER INTRUSIVE COMPLEX,

showing intrusive masses (stiple)
faults (heavy lines)
specimen locations

after Page & McDougall (1972a).

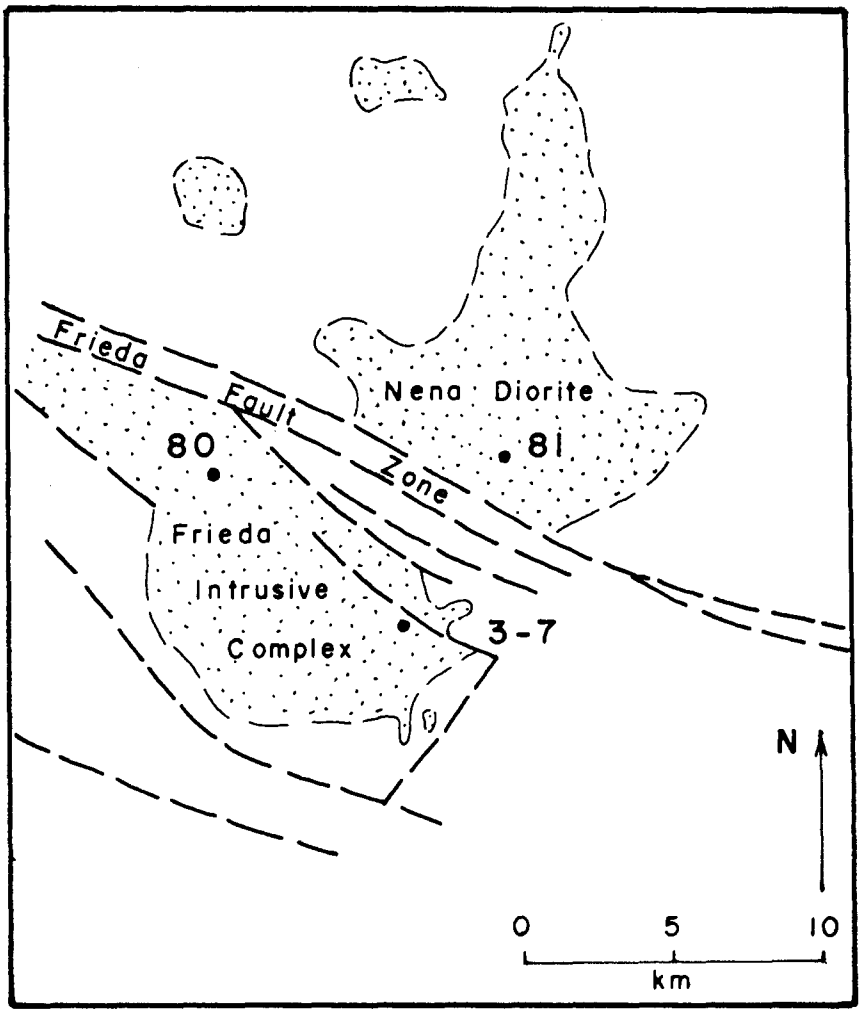

The *'Nena diorite'* is one of the larger stocks to the north of the Frieda River prospect. It is fine-to medium-grained and hypidiomorphic granular in texture, except that larger hornblendes up to 6 mm long lend a sub-porphyritic texture to the rock. Smaller euhedral green hornblende prisms and plagioclase laths and stumps are in places poikilitically enclosed by alkali feldspar plates. Important minor phases are magnetite subhedra and angular pleochroic sphene grains up to 1 mm in size. Accessory phases include small apatite prisms and rare zircon granules.

2.12 OK TEDI (MOUNT FUBILAN) INTRUSIVE COMPLEX

2.12.1 Geological Setting

Bamford (1972) has given an initial account of the geological setting, petrography of rock types, and relationships of mineralization at the Ok Tedi (Mount Fubilan) intrusive complex. He describes the location of a number of stock-like masses to the south of the Lagaip Fault Zone, in an environment which is characterized by Tertiary and older continental shelf-type sedimentation. The sedimentary succession is unaffected by regional metamorphism and has been broadly folded and faulted on a west-northwest axis. The Mount Fubilan stock itself has intruded fine-grained siltstones and limestones, resulting in the doming of these sediments and the formation of a contact metamorphic aureole of limited extent.

Absolute ages for intrusion (1.9 - 2.9 m.y.) and mineralization (approximately 1.2 m.y.) in the Ok Tedi region have been reported by Page (1972a). Specimen locations are shown in Fig. 7.

2.12.2 Petrography

Thin section study of material from the Mount Fubilan stock confirms the presence of intermediate and more silicic rocks within the complex.

The southern part of the stock is composed of *high-K clinopyroxene diorite*. Microphenocrysts of plagioclase and clinopyroxene give a sub-porphyritic texture to the rock. The plagioclase phenocrysts are up to 5 mm in size, and exhibit complex zoning, twinning, and mottling of cores. Greenish clinopyroxene phenocrysts form prisms up to 4 mm long. They are replaced in part by green-blue amphibole and flaky reddish biotite. Large euhedral magnetite and angular sphene grains are scattered through the rock. The groundmass is of variable grain size, and is composed of zoned plagioclase stumps, ragged blue-green amphibole,

FIG. 7 : SPECIMEN LOCATIONS, OK TEDI INTRUSIVE COMPLEX.

Intrusive masses are stipled

Geology after Page & McDougall (1972a).

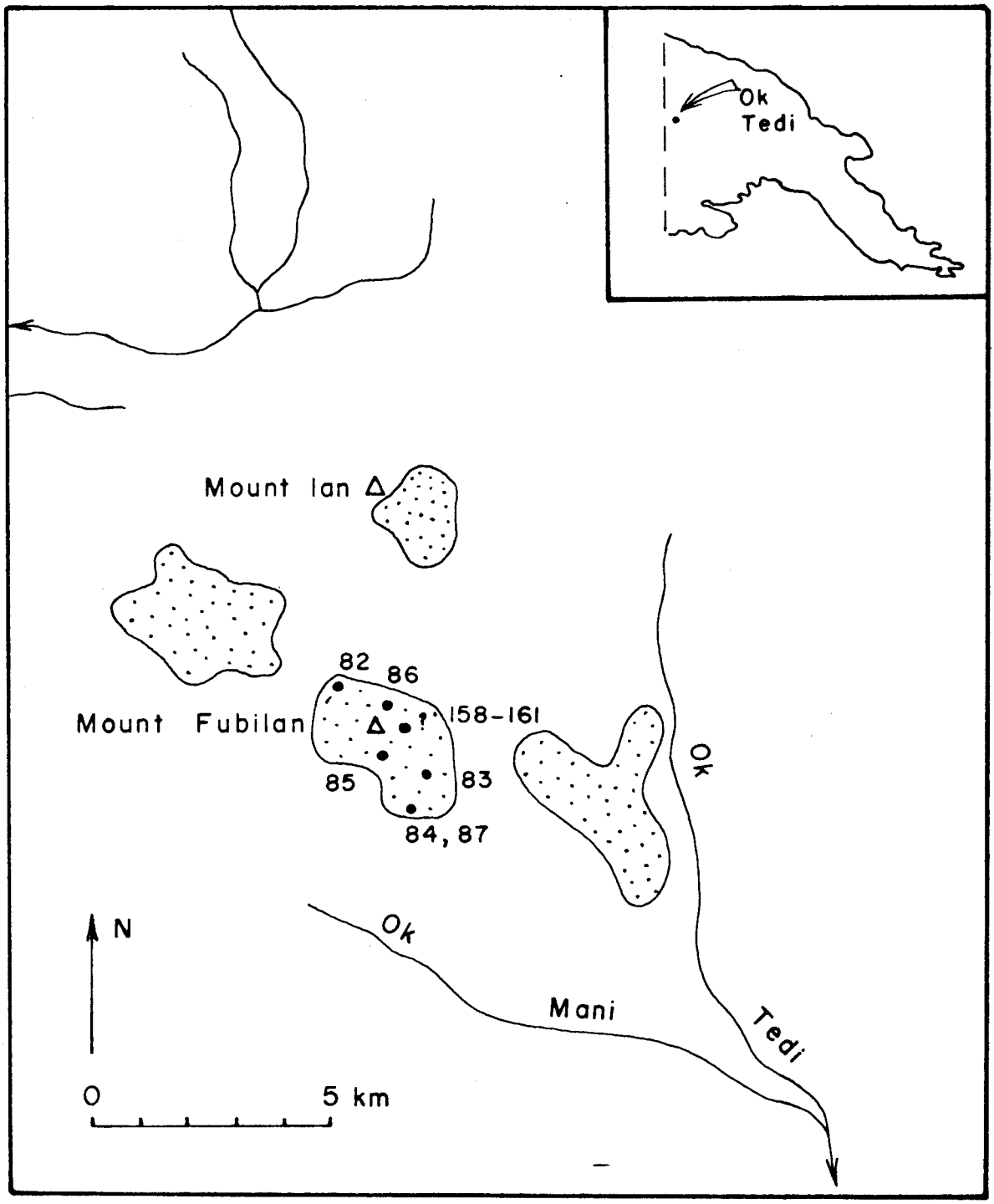

irregular K-feldspar patches, minor interstitial quartz, and pleochroic dark brown to straw yellow biotite flakes. Accessory large apatite prisms are present.

The northern part of the Mount Fubilan stock is composed of *quartz latite porphyry* which shows varying degrees of potassic alteration and mineralization. Large plagioclase phenocrysts up to 6 mm long are twinned and zoned, and show varying degrees of internal mottling. Subhedral to tabular alkali feldspar phenocrysts are microperthitic. Poorly-developed flakes of reddish brown biotite cluster at former mafic mineral (possibly hornblende) sites. The very fine-grained saccharoidal matrix of quartz, alkali feldspar, and biotite flakes contains rare skeletal or prismatic apatite crystals, magnetite granules, zircon grains, and disseminated sulfide blebs. Angular euhedral sphene crystals are completely pseudomorphed by granular opaque oxide.

Although this rock type has been extensively affected by potassic alteration, sufficient of the primary texture remains to indicate that the original rock was felsic and quite alkalic, and may well have approached latite in composition.

2.13 SUMMARY OF MINERALOGY

A summary of the mineralogy of main rock types from intrusive complexes of the Highlands is given in Table 4.

A combined plot of modal variations is presented in Fig. 15b at the end of Chapter 3.

TABLE 4: SUMMARY OF MINERALOGY OF MAIN ROCK TYPES, INTRUSIVE ROCK SUITES, HIGHLANDS

SUITE rock type	QZ	PLAG	KF	HB	BIO	CPX	OPX	OL	MT	ILT	PY	CPY	SPH	APT	ZIRC	Textural features
1. YUAT NORTH BATHOLITH																
orthoclase gabbro	-	+	+	+	+	+	-	-	+	+	+	+	+	+	-	poikilitic Kf
high-K hb-bio-qz diorite	+	+	+	+	+	+	(+)	-	+	-	(+)	(+)	-	+	+	mafic clots
bio-hb microadamellite	+	+	+	+	+	-	-	-	+	+	-	-	-	+	+	fine grained
2. YUAT SOUTH BATHOLITH																
hb-cpx gabbro	+	+	-	+	-	+	-	-	+	+	(+)	(+)	+	+	-	
plag-hb(-qz) diorite porphyry	(+)	+	-	+	(+)	-	-	-	+	-	-	-	-	-	-	phenocrysts
	+	+	+	+	-	-	-	-	+	-	+	(+)	(+)	(+)	-	groundmass
high-K hb-bio(-cpx) diorite	+	+	+	+	+	+	-	-	+	-	-	+	-	+	-	mafic clots
hb-bio-qz granodiorite	+	+	+	+	+	-	-	-	+	-	(+)	(+)	+	+	+	m.g. hypidiomorphic
3. KARAWARI BATHOLITH																
high-Al basalt	-	-	-	-	-	+	-	-	-	-	-	-	-	-	-	phenocrysts
	-	+	-	+	-	-	-	-	+	-	-	-	-	-	-	groundmass
plag-hb(-qz) diorite porphyry	(+)	+	-	+	-	-	-	-	-	-	-	-	-	-	-	phenocrysts
	+	+	+	+	-	-	-	-	(+)	-	+	+	+	+	+	groundmass
hb-cpx-qz-diorite	+	+	+	+	-	+	-	-	+	+	-	-	+	+	-	poikilitic hb
hb (-bio) tonalite	+	+	+	+	+	-	-	-	+	-	-	-	+	-	+	mafic xenoliths
4. WALE STOCK																
olivine pyroxenite	-	(+)	-	(+)	-	+	-	+	+	-	-	-	-	-	-	adcumulate
hb (-cpx) gabbro	(+)	+	-	+	-	+	-	-	-	+	+	+	-	-	-	cumulate
5. LAMANT STOCK																
porphyritic hb-cpx gabbro	-	-	-	+	-	+	-	-	-	+	-	-	-	-	-	phenocrysts
	+	+	-	(+)	(+)	-	-	-	-	+	+	+	+	-	-	groundmass
6. SEKAU STOCK																
hornblendite	-	+	-	+	-	-	-	-	+	-	+	+	+	+	-	adcumulate
hb gabbro	-	+	-	+	-	-	-	-	+	-	+	+	+	-	-	cumulate
low-Si hb-bio diorite	+	+	+	+	(+)	-	-	-	+	-	+	+	+	-	-	mafic clots
high-K hb-bio diorite	+	+	+	+	+	+	-	-	+	-	-	-	+	+	-	mafic clots
7. MOUNT MICHAEL STOCK																
plag-hb diorite porphyry	-	+	-	+	-	-	-	-	-	-	-	-	(+)	(+)	-	phenocrysts
	+	+	+	-	-	-	-	-	(+)	-	+	+	+	+	+	groundmass
8. MOUNT PUGENT STOCK																
cpx (-bio) microsyenite	-	+	+	-	+	+	-	-	+	-	-	-	-	-	-	fine grained, feldspathic
9. FRIEDA RIVER COMPLEX																
hb-plag diorite porphyry	(+)	+	-	+	+	-	-	-	+	+	-	-	-	-	-	phenocrysts
	+	+	+	+	-	-	-	-	-	-	(+)	(+)	-	+	-	groundmass
hb diorite ('Nena Diorite')	+	+	+	+	-	-	-	-	+	-	-	-	+	+	+	poikilitic Kf
10. OK TEDI COMPLEX																
high-K cpx diorite	+	+	+	+	+	+	-	-	+	(+)	+	+	+	+	+	subporphyritic
qz latite porphyry	-	+	+	-	+*	-	-	-	+	-	-	-	-	+	-	phenocrysts
	+	+	+	-	+*	-	-	-	-	-	+	+	+	-	+	groundmass

Note: + = present; (+)=sometimes present; - = absent; * = hydrothermal
silicates observed in transmitted light
oxides and sulfides observed in reflected light

CHAPTER 3 PETROGRAPHY OF INTRUSIVE ROCKS FROM THE P.N.G. ISLANDS AND SOLOMON ISLANDS

3.1 REGIONAL GEOLOGY OF THE P.N.G. ISLANDS AND SOLOMON ISLANDS

In recent years, the geological development of the P.N.G. islands and Solomon Islands has been viewed in the context of plate-boundary interactions between the Indo-Australian and Pacific plates (e.g., Dewey & Bird, 1970; Karig, 1972; Packham, 1973). Regional syntheses have been made possible through studies of the particular island areas.

The oldest rocks in the Solomon Islands are late Mesozoic basaltic lavas, pelagic limestones and gabbroic intrusives (Coleman, 1965, 1970; Hackman, 1973). While basement rocks of similar age have not been described from other parts of the Admiralty-Solomon arc, the ensuing volcanic and related sedimentary sequence of Oligocene to Recent age in the Solomons are also represented in Manus Island (Thompson, 1952), New Ireland (Hohnen, 1970), and Bougainville Island (Blake & Miezitis, 1967). Calc-alkaline intrusive rocks of Oligocene or younger age are known in all these islands.

In the New Britain portion of the north New Guinea-New Britain arc, the oldest recognized rocks are moderately deformed, submarine basaltic volcanic rocks of Eocene age (Macnab, 1970). Sporadic volcanism proceeded to build the arc through the Tertiary, and continues in Recent times. Intrusive calc-alkaline rocks of Oligocene and Miocene age are widespread in New Britain.

3.2 PLESYUMI INTRUSIVE COMPLEX NEW BRITAIN

3.2.1 Geological Setting

The Plesyumi Intrusive Complex in central New Britain invades the Baining Volcanics of Eocene age (Macnab, 1970). The Complex comprises a variety of phaneritic rocks (granodiorites, diorites), later dacite porphyry dykes, and igneous breccias (Titley, 1975). A blanket of tuffaceous detritus (probably the Pliocene Ania Tuff of Mackenzie, 1971) covers the area, and older rocks are exposed only in river-bottom windows.

Page & Ryburn (1973) gave a radiometric age of 22 m.y. for one rock from the Complex, which agrees with the Oligocene to Miocene age as constrained by field relations. The dated specimen has been described as a 'biotite-quartz-hornblende mangerite' (Mackenzie, 1971, p. 8; Page

& Ryburn, 1973, Table 1) and is equated with the high-K diorites to be described below.

The Plesyumi Intrusive Complex at present remains unmapped in detail. Regional mapping indicates that it is approximately 50 km^2 in area. The specimens described in this study come partly from the Plesyumi prospect area, and partly from river float which is confidently correlated with the western part of the Complex. Specimen locations are shown in Fig. 8.

3.2.2 Petrography

The mineralogy of the intrusive rocks of the Plesyumi Intrusive Complex is dominated by the typical calc-alkaline assemblage of zoned plagioclase, green amphibole, biotite, and quartz. In more mafic rock types, clinopyroxene and more rarely orthopyroxene are present. Alkali feldspar becomes more important in the more felsic and higher-K rocks. Opaque oxides (magnetite and ilmenite) are present in all rock types, and small amounts of sulfides (pyrite and chalcopyrite) are observed in hand specimen.

Granodiorites and diorites are most important volumetrically, judging from distribution within outcrop in the Plesyumi area and from abundance of float material in the Lae River. Subordinate rock types include gabbroic cumulates and felsic porphyries.

Hornblende-biotite granodiorite displays an hypidiomorphic generally equigranular texture, but larger plagioclase prisms reach 5 mm in length. Abundant plagioclase prisms and subhedral stumps are twinned and zoned (both normal and oscillatory) and comprise 40-50 volume percent of the rock; clear quartz (20-25%) characteristically forms angular interstitial patches optically continuous over areas of 3-5 mm; euhedral hornblende prisms (15-20%) are pleochroic pale brown to dark greenish brown, and generally achieve a uniform distribution through the rock, except in places where several subhedral crystals aggregate to form poorly-defined clots; alkali feldspar (5-10%) forms small, anhedral interstitial grains; biotite (5%) is pleochroic pale yellowish brown to dark chocolate brown, and mostly forms discrete crystals but in places is in reaction relationship with pale green amphibole; anhedral magnetite blebs and ilmenite blades (2-3%) are intimately associated with the mafic minerals, especially hornblende; accessory phases include zircon prisms, tiny apatite rods, chlorite (which forms as an alteration product of biotite), and sphene (which occurs both as small grains within chlorite-altered biotite and as

FIG. 8 : SPECIMEN LOCATIONS, PLESYUMI INTRUSIVE COMPLEX.

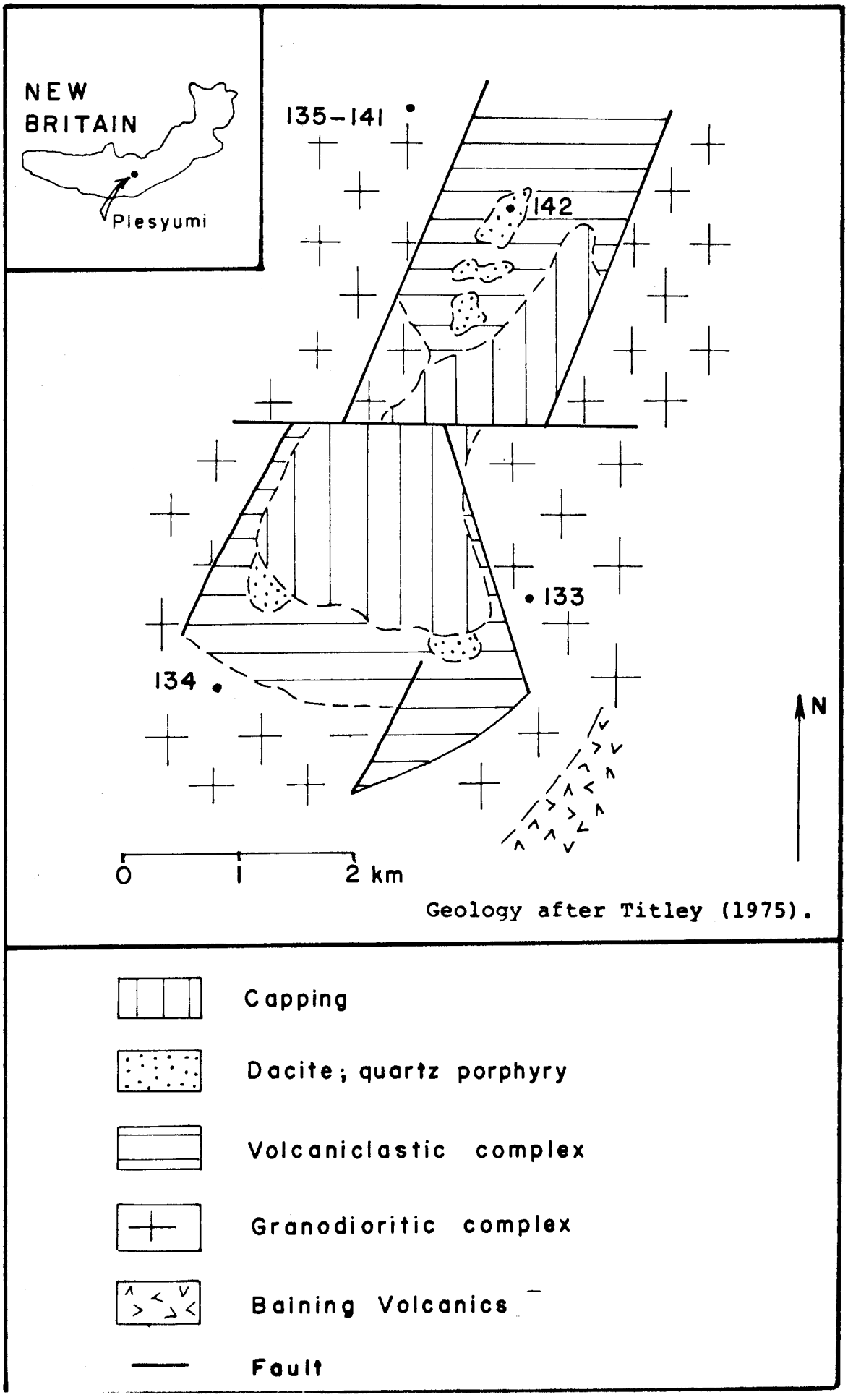

larger angular grains associated with the magnetite).

With decreasing quartz content, the rock grades into *hornblende-biotite-quartz diorite*. The essential mineralogy remains unchanged, and the characteristic optically continuous quartz patches are present. Extensive mottling of pale green amphibole and presence of rare clinopyroxene cores suggest derivation of the amphibole by reaction from pyroxene.

Two pyroxene-hornblende (-biotite) diorite is another mafic variant. Ragged greenish brown hornblende has both clear spongy and pleochroic orthopyroxene cores. The mafic minerals tend to form clots of irregular shape. Biotite flakes are present in the clots, and appear to be derived from the amphibole. A small amount of quartz is present as equant anhedral patches. Accessory apatite occurs as large prisms. Large anhedral magnetite blebs and smaller ilmenite laths are closely associated with the mafic minerals.

Clinopyroxene (-hornblende) -quartz gabbro is characterized by abundant buff-coloured subophitic clinopyroxene which is moulded on moderately zoned plagioclase prisms. Pale green amphibole forms irregularly-shaped patches within the clinopyroxene and also discontinuous reaction rims. Large ilmenite blebs up to 3 mm across are closely associated with the mafic minerals. Quartz is sparsely distributed as small intergranular patches and also as micrographic intergrowths with trace amounts of alkali feldspar.

The most mafic rock obtained from the Plesyumi Intrusive Complex is a *porphyritic olivine-clinopyroxene gabbro.* Large euhedral olivine phenocrysts up to 4 mm long are replaced along crystal margins by very fine-grained talc and magnetite granules. Buff-coloured clinopyroxene phenocrysts are of similar size. The groundmass comprises abundant weakly zoned plagioclase laths, interstitial fibrous pale green amphibole, and minor amounts of opaque oxide (magnetite and ilmenite) and reddish brown biotite.

Two samples of higher-K rocks were obtained from the Plesyumi Intrusive Complex, and these rocks may be similar to the 'mangerite' of Mackenzie (1971) and of Page & Ryburn (1973). These rocks are here called *high-K clinopyroxene-hornblende-biotite diorites.* They contain essentially the same mineralogy as the previously described dioritic rocks, except for much more abundant alkali feldspar and biotite. Textural similarities also occur. The mafic minerals tend to form

irregularly-shaped clots, in which green amphibole extensively replaces clinopyroxene, and orthopyroxene is present as cores within ragged mafic clots. Large subhedral magnetite grains and angular ilmenite blades are closely associated with mafic minerals. Accessory minerals include apatite prisms, zircon grains, and angular sphene crystals which occur in close association with oxides and which are more abundant in the more felsic of the two high-K rocks (DRM139).

A common felsic intrusive rock in the Plesyumi area is *plagioclase-'hornblende'-quartz dacite porphyry*, which occurs as dykes and irregular intrusive masses. These rocks invariably exhibit pervasive propylitic alteration. Large strongly-zoned plagioclase phenocrysts up to 5 mm long are heavily flecked with sericite and are turbid in appearance. Amphibole phenocrysts 1-2 mm in size have been completely replaced by chlorite sheaves, magnetite granules, and calcite. Plagioclase microphenocrysts, small magnetite grains, and whisps of chlorite are scattered through an exceedingly fine-grained turbid felsic groundmass.

Optically estimated modes for analyzed rocks from the Plesyumi Intrusive Complex are presented in Appendix 3.

3.3 MOUNT KREN INTRUSIVE COMPLEX, MANUS ISLAND

3.3.1 Geological Setting

The regional geology of Manus Island was first described by Thompson (1952) and Owen (1954). Mapping by these two authors showed a 'plutonic basement' of possible Palaeozoic age, overlain by Miocene limestone and tuffaceous marine sediments. Pleistocene to Recent tuffs and basaltic to acid lavas occur in the western part of the island, and raised coral reefs of Recent age were described at coastal locations.

More recent work by the P.N.G. Geological Survey has generally confirmed these originally defined untis (L. Jacques, pers. comm.), except for the older 'basement' unit, which has been shown to comprise both intrusive dioritic rocks and extrusive volcanic sequences, and most likely is of early Tertiary age in keeping with the known basement geology of other islands in the Admiralty and New Britain arcs.

The samples used in this study of the intrusive rocks of Manus Island were obtained from the Mount Kren Intrusive Complex in the central southern part of the island. Specimen locations are shown in Fig. 9. The samples are considered to adequately represent the variety of rocks which constitute the Mount Kren Complex, but possibly are not

FIG. 9 : SPECIMEN LOCATIONS, MOUNT KREN INTRUSIVE COMPLEX.

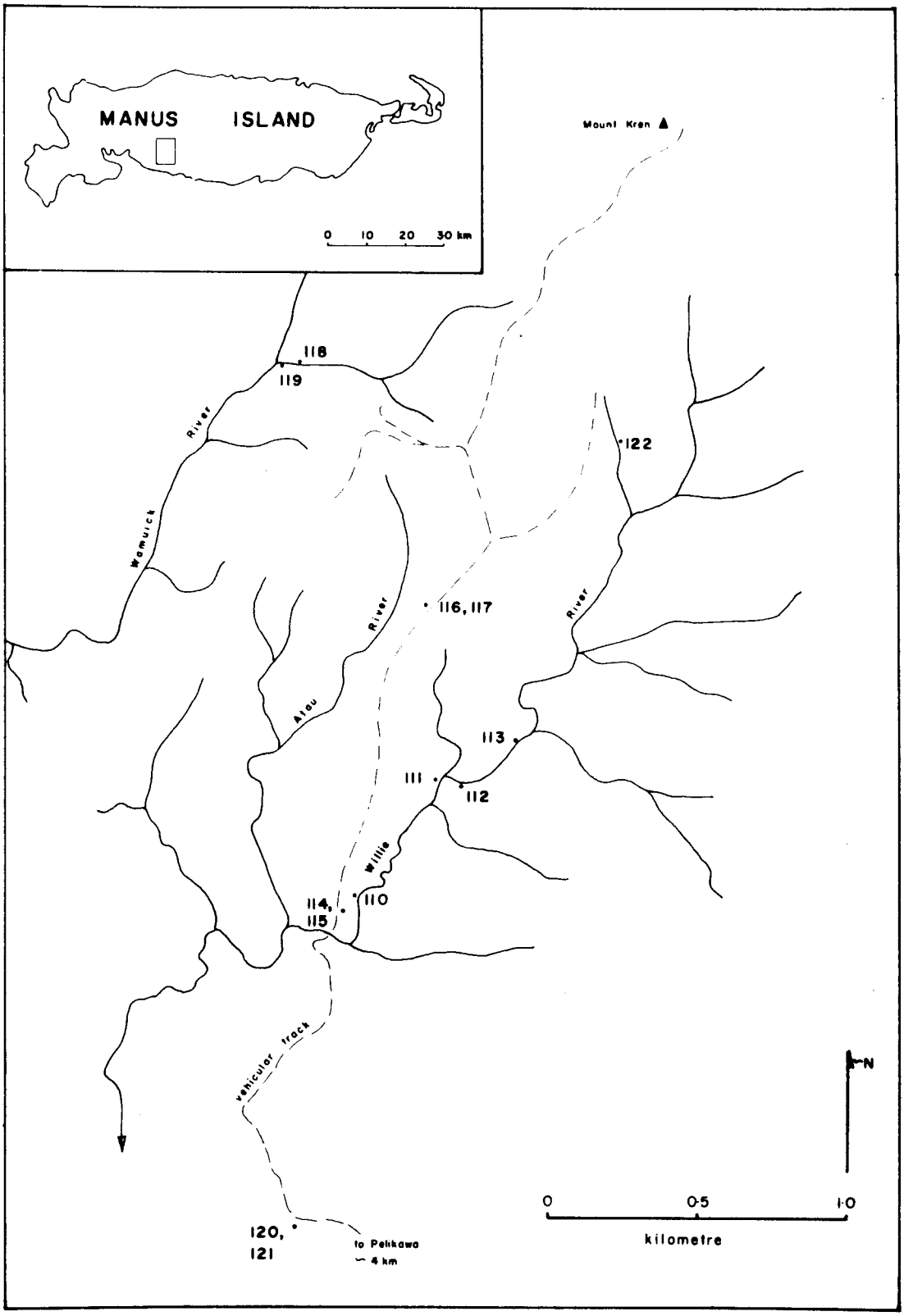

representative of the Tertiary basement as a whole.

3.3.2 Petrography

The most abundant rock types in the Mount Kren Complex are diorites with a restricted silica range. These rocks constitute the stock-like masses which form the complex. Microdiorites and porphyritic microdiorites occur as dykes and small irregularly-shaped intrusive bodies. Small rounded mafic xenoliths are present in the dioritic rocks.

Different abundances of alkali feldspar and biotite permit distinction of high-K rocks and low- to normal-K rocks. Both high- and lower-K suites contain bimodal groupings of dioritic and low-Si dioritic or gabbroic rock types. The subdivisions of rock types from the Mount Kren Intrusive Complex are presented in Table 5.

A variety of *high-K hornblende diorites* constitute the bulk of the Mount Kren Complex. They are massive, and are fine-to medium-grained hypidiomorphic granular in texture. These rocks are characterized by abundant alkali feldspar tablets and interstitial patches. Plagioclase prisms (1-3 mm in length) exhibit strong normal zoning. Core regions of larger plagioclase tablets are mottled and may contain small clinopyroxene inclusions. Angular interstitial quartz patches are optically continuous over areas of 1-2 mm. The mafic mineralogy is quite variable. Amphibole is always dominant, either as euhedral prisms (pleochroic pale yellowish brown to dark greenish brown, with or without small plagioclase inclusions), or as fibrous pale green replacement of clear clinopyroxene. Both forms of amphibole may occur together. Biotite, when present, is pleochroic pale yellowish brown to dark chocolate brown, and mostly occurs as discrete flakes. Subhedral to anhedral magnetite grains are disseminated in amounts up to 3%, and are most abundant in aggregates of mafic minerals. These mafic clots are present to a greater or lesser extent in all of the high-K diorites, and are characterized by green fibrous amphibole with spongy clinopyroxene cores, poorly-formed reddish brown biotite flakes, and magnetite grains. Accessory minerals of the high-K diorites include pleochroic angular sphene grains (either discrete or in close association with magnetite grains), rare zircon granules, and scattered small apatite rods.

Hornblende microgabbro xenoliths are sporadically distributed through the high-K diroites. The xenoliths generally are small (up to several centimetres across) and are subrounded in shape. They comprise

TABLE 5: SUBDIVISION OF ROCK TYPES, MT. KREN INTRUSIVE COMPLEX

K-content	Rock Types	Characteristic Mineralogy	Mode of Occurrence
1. High-K	a) High-K hornblende diorite	abundant K-felds, 20-30%; qtz 8-10% amphibole, ± biotite, ± clinopyroxene	larger stock-like masses
	b) High-K low-Si microdiorite; low-Si porphyritic micro-diorite.	abundant clinopyroxene, less amphibole, ± biotite; groundmass K-feldspar	dykes; small bodies
2. Low- to normal-K	a) Hornblende-quartz diorite	K-feldspar 10%; quartz 12-15%; abundant amphibole.	stock-like masses
	b) Low-Si porphyritic micro-diorite Hornblende micrograbbro	Hb, plag phenocrysts; qtz patches abundant fibrous amphibole; oxide stringers; qtz patches.	dykes ?xenolith in high-K hornblende diorite

abundant green fibrous actinolitic amphibole, magnetite subhedra and stringers, rare clinopyroxene cores, and plagioclase laths. In advanced stages of digestion patches of quartz and alkali feldspar, dark greenish brown hornblende, and ragged biotite appear, and the xenoliths then approach the mafic clots in mineralogy and texture.

Fine-grained high-K rocks are present as dykes and small intrusive bodies. *High-K low-Si microdiorite* is fine-grained and massive, and contains abundant clear clinopyroxene euhedra and granules, subhedral to anhedral magnetite grains, plagioclase laths, and interstitial alkali feldspar and quartz patches. Mafic clots of very fine-grained fibrous amphibole and magnetite grains are present. With the appearance of clouded plagioclase and fresh clinopyroxene phenocrysts, the rock becomes a porphyritic microdiorite.

Low- and normal-K rocks are much less common than the high-K rocks in the Mount Kren Intrusive Complex. *Hornblende-quartz diorite* is similar in mineralogy and texture to the high-K hornblende diorite, except that K-feldspar is rather less abundant (10%), quartz is more abundant (12-15%), and biotite has not been observed. Hornblende prisms may possess a darker greenish brown core. As in the high-K diorites, clots of mafic minerals are common.

Fine-grained low- to normal-K rocks occur as dykes within the dioritic rocks. *Low-Si microdiorite* contains microphenocrysts of greenish brown hornblende and clouded plagioclase prisms up to 3 mm in a groundmass of very fine-grained acicular hornblende, plagioclase laths, magnetite granule and scattered tiny quartz patches. Larger polycrystalline patches of quartz are also present.

In this study, the precise distribution and intrusional relationships between the high-K and low- to normal-K rocks have not been determined.

Optically estimated modes for analyzed rocks from the Mount Kren Intrusive Complex are presented in Appendix 3.

3.4 LEMAU INTRUSIVE COMPLEX, NEW IRELAND

3.4.1 Geological Setting

Hohnen (1970) has outlined the geological development of New Ireland. In the Lower Oligocene, island arc volcanism resulted in the accumulation of a thick pile of mainly volcaniclastic rocks of andesitic composition (Jaulu Volcanics). The volcanic pile was intruded by a wide range of intrusive rock types (Lemau Intrusives), which are older than

basal Miocene but younger than Lower Oligocene according to stratigraphic evidence. Radiometric ages of 30.7 and 31.8 m.y. (AMDEL Report, AN4926/71) indicate a mid-Oligocene age for the intrusive rocks.

Sinistral transcurrent and vertical faulting in Miocene times controlled deposition of tuffaceous sediments and marls in a large graben between the northern and southern parts of the island, while much of the fragmented island subsided and was blanketed by on-lapping limestone reefs until the late Pliocene. Rapid uplift in Pleistocene and Recent times has exposed the biohermal reefs and windows of the igneous basement.

A number of rock types described by Hohnen (1970) such as norite, trondhjemite, and latite have not been included in the small sample of intrusive rocks used in this study, so that only partial coverage of the Lemau Intrusives has been achieved.

The samples used here were obtained from outcrop and stream float near Lemau Village, the type area for the Lemau Intrusives as defined by Hohnen. Specimen locations are shown in Fig. 10. Mapping is currently in progress in this area by an exploration company. Detailed location geology is yet to be published.

The intrusive rocks described here will be referred to as the 'Lemau Intrusive Complex', being that part of the Lemau Intrusives located in the type area.

3.4.2 Petrography

A wide variety of intrusive rock types, ranging from doleritic basic rocks to granodioritic types, were sampled from the Lemau Intrusive Complex. Textures vary from typical subophitic textures in the dolerites and medium-grained hypidiomorphic granular textures in intermediate rocks, to various porphyritic textures in dyke rocks. As reported by Hohnen (1970), hydrothermal alteration is common, and in this study as far as possible only unaltered specimens were chosen for analysis.

The most mafic rock observed is a medium-grained *uralite gabbro*. Subophitic mafic minerals partly enclose abundant fresh plagioclase stumps, which are of variable size (½ - 3 mm) and which possess a moderate degree of normal zoning. A small amount of the primary pyroxene has been replaced by greenish brown hornblende, but most of the mafic minerals have been replaced by fibrous green amphibole ('uralite'), very fine grained chlorite, and granules of magnetite. Large intergranular blebs of magnetite with ilmenite exsolution lamellae are primary

FIG. 10 : SPECIMEN LOCATIONS, LEMAU INTRUSIVE COMPLEX.

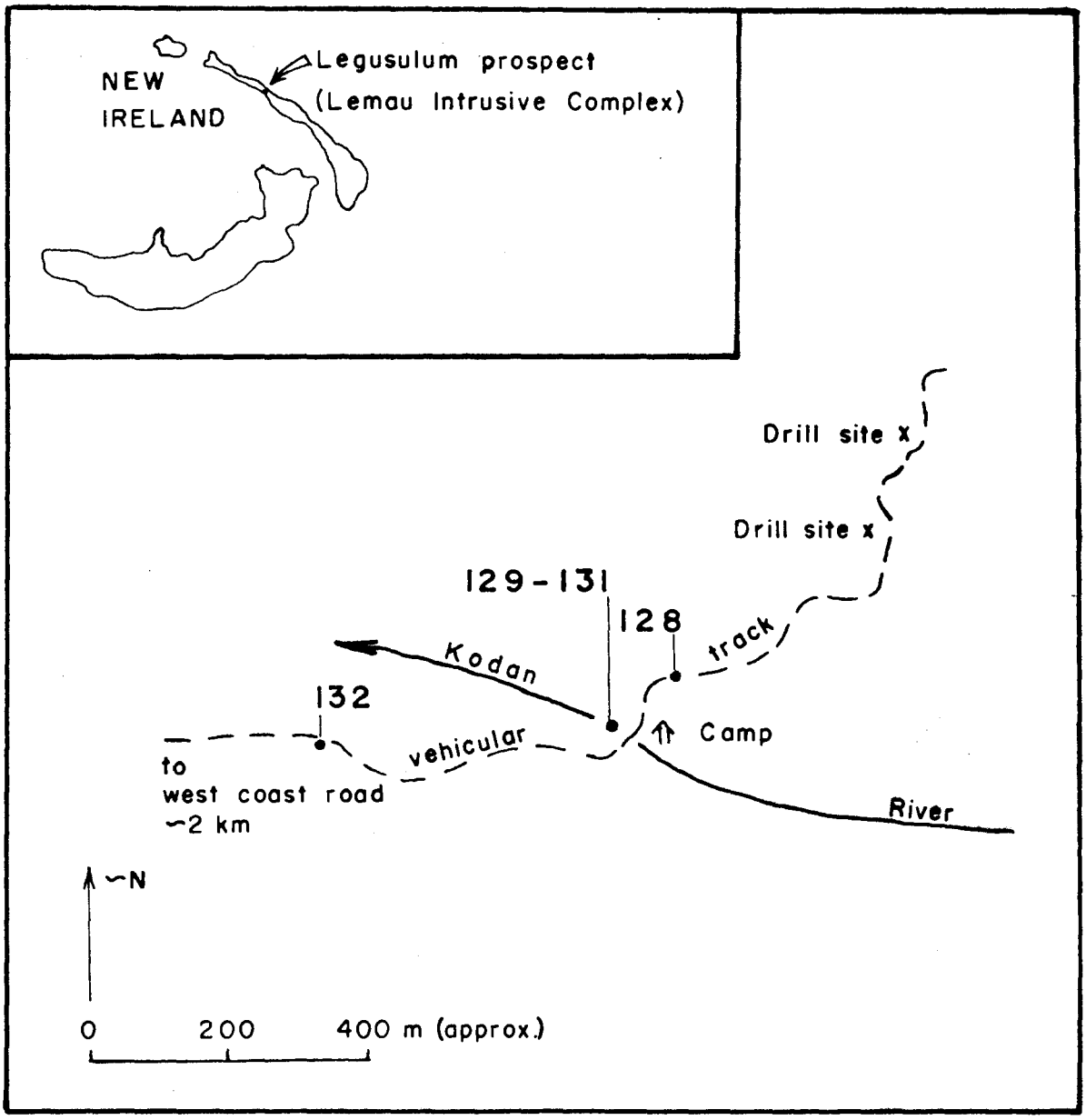

constituents.

Medium-grained intrusive rocks of intermediate composition are more abundant. *Two pyroxene-biotite (-hornblende) -quartz diorite* is characterized by its fresh, hypidiomorphic granular texture, and its varied mafic assemblage. Normal zoning is ubiquitous in the abundant plagioclase prisms, which are 1-2 mm in length and whose mottled cores in places contain inclusions of pyroxene granules. Quartz (20%) and alkali feldspar (5-8%) form angular intergranular patches, the latter in places achieving poikilitic enclosure of smaller plagioclase laths, and quartz in places forming optically continuous patches. Clear subequant clinopyroxene prisms are sieved and marginally replaced by pale green amphibole. Orthopyroxene is less abundant than clinopyroxene, and forms prisms of variable size with only a trace of pleochroism (colourless to pale pink) and with incipient replacement by fibrous amphibole. Large well-cleaved biotite plates are associated with other mafic minerals, and are pleochroic straw yellow to dark reddish brown. Large anhedral blebs of magnetite and smaller subhedral grains of ilmenite are closely associated with mafic minerals. Accessory phases include rare apatite prisms and small zircon granules.

Finer-grained, more mafic clots are present in the diorite. Interlocking pyroxene granules have been almost entirely replaced by green amphibole. Granular magnetite grains are scattered through the mafic phases. Small poorly-developed biotite flakes replace amphibole. Small plagioclase laths and alkali feldspar patches are present.

In a variety of the pyroxene-quartz diorite, coarse grained patches of quartz and larger plagioclase prisms lend a subporphyritic texture to the rock. Small groundmass pyroxene granules are fresh, but larger prisms are almost entirely replaced by green fibrous amphibole and oxide dustings. Anhedral magnetite blebs, in places with associated reddish brown biotite flakes, are disseminated throughout the rock.

The most felsic intrusive rock obtained from the Lemau Intrusive Complex is a *two-pyroxene granodiorite*, which comprises abundant anhedral quartz patches, twinned and zoned plagioclase prisms with mottled cores, interstitial cloudy alkali feldspar patches, clinopyroxene and orthopyroxene partly replaced by fibrous green amphibole and magnetite granules, traces of pleochroic reddish brown biotite in close association with other mafic minerals, and scattered larger magnetite blebs. Ilmenite occurs as exsolution blades in magnetite,

and as discrete grains.

Plagioclase-hornblende diorite porphyry is strongly porphyritic in texture, and differs mineralogically from the more equigranular dioritic rocks in being pyroxene free. Large plagioclase phenocrysts up to 6 mm long show complex zoning patterns (both normal and oscillatory) and have mottled cores. Smaller euhedral hornblende phenocrysts are pleochroic pale brown to dark greenish brown. Small plagioclase and hornblende prisms lie in a very fine-grained (almost isotropic) groundmass of feldspar microlites and patches, and clear quartz patches. Two generations of magnetite are present; an earlier one of subhedral grains (0.2 - 0.3 mm), and a later generation of very tiny granules in the groundmass.

In summary, the Lemau Intrusive Complex appears to comprise two mineralogically distinct suites: a medium-grained suite ranging from gabbro through diorite to granodiorite, in which pyroxenes are the dominant ferromagnesian minerals, and a suite of porphyritic rocks in which greenish brown hornblende is the only ferromagnesian mineral.

3.5 INTRUSIVE ROCKS OF BOUGAINVILLE ISLAND

3.5.1 Geological Setting

Blake & Miezitis (1967) have given a full description of the geological setting of Bougainville and Buka islands. These authors emphasize the importance of igneous activity (especially volcanism) in the development of this group of islands. The oldest recognized unit comprises lavas and volcanogenic sediments (Kieta Volcanics) of probable Oligocene to Lower Miocene age. Small dioritic stocks, some with associated mineralization, intrude the volcanic pile. Page & McDougall (1972b) have shown that intrusive activity continued into the Pleistocene.

Regional uplift and tilting occurred during Middle Miocene to Pliocene times. Renewed andesitic volcanism began in the Pleistocene and continues into Recent times. Reef limestones have been associated with all stages of development.

The distribution of intrusive rocks within Bougainville Island is shown in Fig. 11, and locations of specimens used in this study are shown in Figs. 11 and 12.

3.5.2 Petrography

Blake & Miezitis (1967) report a predominance of porphyritic

FIG. 11 : INTRUSIVE MASSES AND SPECIMEN LOCATIONS, BOUGAINVILLE ISLAND.

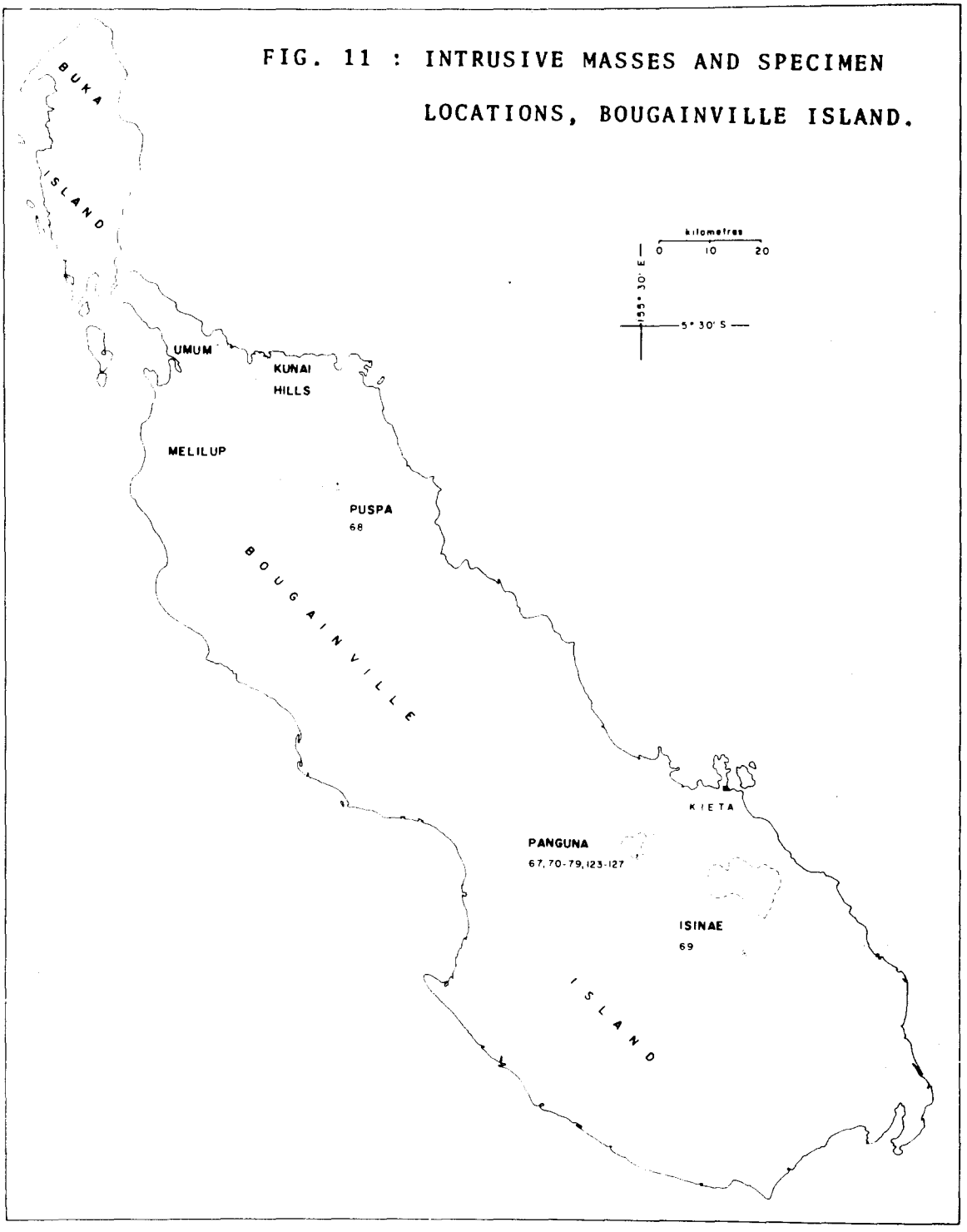

FIG. 12 : PANGUNA INTRUSIVE COMPLEX, showing specimen locations and geology after B.C.P.L. map (1971).

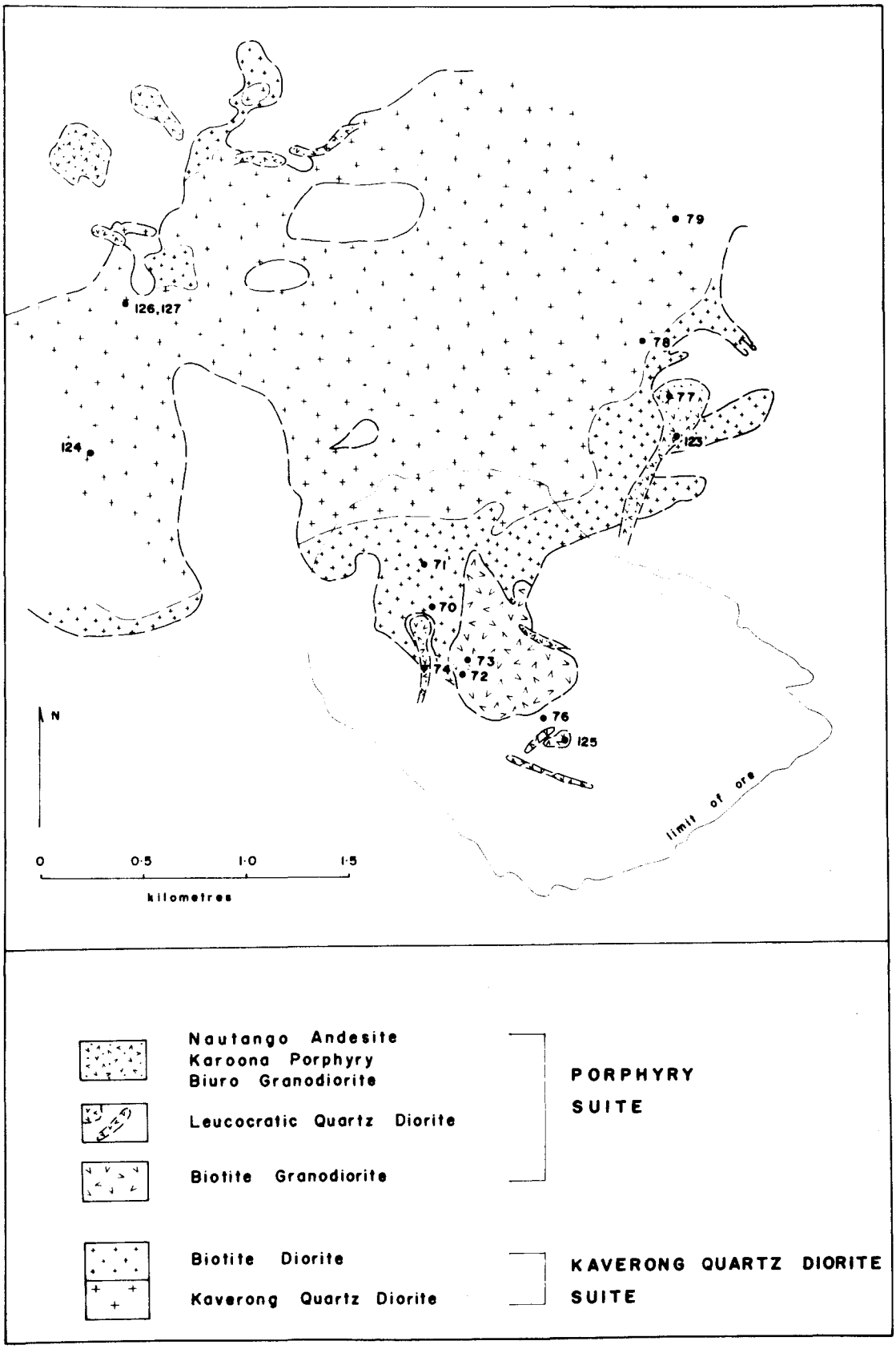

microdiorites in many of the intrusive complexes, particularly in the Umum and Kunai Hills intrusions near the north coast. Both porphyritic and even-grained rocks were reported from the Melilup, Puspa, Panguna, Isinae, and Poenga River intrusions. The Melilup and Puspa intrusions are characterized by the presence of monzonite and syenite respectively. Quartz diorites and granodiorites are reported to be typical of the other intrusive complexes.

Some of the specimens obtained during the regional work of Blake & Miezitis were available for study. Coarse-grained *quartz syenite* from the Puspa intrusion contains abundant microperthitic alkali feldspar as prisms and intergranular patches, normally zoned plagioclase prisms (3-4 mm long), and a small amount (5%) of clear quartz as small anhedral blebs. The mafic mineralogy is dominated by buff or pale greenish clinopyroxene which occurs as small euhedral prisms with corrosion embayments. Half of the pyroxene has been replaced by fibrous pale green amphibole. Also present are small amounts of well-formed dark greenish brown hornblende, and biotite flakes which are pleochroic straw yellow to dark reddish chocolate brown. The mafic minerals tend to form aggregates, and invariably have several magnetite subhedra in close association. Accessory minerals include large angular sphene crystals adjacent to the oxide phase, apatite rods, and rare zircon granules.

Low-Si two-pyroxene-hornblende-biotite microdiorite from a small intrusive body southeast of Mount Takuan in the southern part of Bougainville carries microphenocrysts of clinopyroxene and orthopyroxene and rare plagioclase in a fine-grained groundmass of plagioclase laths, poikilitic K-feldspar patches, pale green amphibole, small biotite plates (pleochroic straw yellow to dark chocolate brown), and minor interstitial quartz. Small magnetite granules are associated with groundmass mafic minerals, and larger oxide blebs possess rims of flaky biotite. The prismatic orthopyroxene microphenocrysts (1 mm long) are pleochroic from colourless to pale pink, and are replaced along margins by fibrous green amphibole and magnetite granules. The plagioclase microphenocrysts are subrounded, exhibit strong normal zoning, and possess mottled cores in places bearing granular clinopyroxene inclusions.

The majority of Bougainville specimens studied in this work come from the *Panguna Intrusive Complex* in the central south of the island. In Table 6 correlations are made between the Panguna intrusive

TABLE 6: SUBDIVISION OF INTRUSIVE ROCKS, PANGUNA INTRUSIVE COMPLEX, BOUGAINVILLE

NOMENCLATURE OF FOUNTAIN (1972)	NOMENCLATURE OF MACNAMARA (1968).	K-Ar AGES OF PAGE & McDOUGALL (1972b)		NUMBER OF ANALYZED SPECIMENS (THIS WORK).	
Nautango Andesite	Nantango Andesite	1.6 m.y.	PLEISTOCENE	2	
Stage III porphyry	Biuro Granodiorite	3.5 m.y.	PLIOCENE	1	
Stage II porphyry	Biotite Granodiorite	3.4 ± 0.3 m.y.	PLIOCENE	2	
Stage I porphyry	Leucocratic Quartz Diorite	3.4 ± 0.3 m.y.	PLIOCENE	1	
	Biotite Diorite	3.4 ± 0.3 m.y.	PLIOCENE	2	
Kaverong Quartz Diorite	Kaverong Quartz Diorite	4-5 m.y.	PLIOCENE	3	
				3	unclassified porphyries
				2	Panguna Andesite
				16	total

nomenclature of Macnamara (1968) and Fountain (1972), ages of intrusion as determined by Page & McDougall (1972b) are given, and distribution of specimens analyzed in this work is indicated. In the petrographic descriptions that follow, reference will be made to the intrusive nomenclature common to Macnamara (1968) and Page & McDougall (1972b).

The largest and earliest intrusive body in the Panguna Intrusive Complex is the *Kaverong Quartz Diorite* which exhibits a moderate degree of textural and compositional variation. The bulk of the body is medium-grained and hypidiomorphic granular in texture, with rock types ranging from low-Si hornblende-clinopyroxene diorite to hornblende-quartz diorite. These rock types contain varying proportions of strongly zoned (normal and oscillatory) plagioclase prisms (1-3 mm), euhedral hornblende prisms pleochroic pale brown to dark greenish brown, spongy clinopyroxene prisms partly replaced by fibrous green amphibole, interstitial quartz and alkali feldspar, traces of poorly-formed biotite flakes, and scattered magnetite subhedra. Accessory minerals include apatite rods, angular sphene grains, zircon granules, and traces of epidote in plagioclase and chlorite in ferromagnesian minerals. Also present in these rocks are mafic clots observable on both outcrop and thin-section scales. They consist of abundant fibrous green amphibole and magnetite granules enclosing small plagioclase grains. The porphyritic variety of the Kaverong Quartz Diorite contains plagioclase and hornblende phenocrysts up to 5 mm long.

The *Biotite Diorite* is considered by Macnamara (1968) and Page & McDougall (1972b) to be a marginal variant of the Kaverong Quartz Diorite. Like the larger body, it varies texturally from equigranular to porphyritic. However, pervasive biotite flakes replace all primary ferromagnesian phases, and other alteration effects such as a recrystallized saccharoidal groundmass are evident.

Peripheral to the Kaverong Quartz Diorite are a number of small porphyritic stocks with which the alteration and mineralization at Panguna are closely associated. The *Leucocratic Quartz Diorite* is the earliest of these stocks (Stage 1 porphyry of Fountain, 1972). The rock retains much of its primary texture, but plagioclase prisms are flecked with sericite and epidote, ferromagnesian minerals have been replaced by biotite (pleochroic pale yellow to reddish brown) and interleaved chlorite, and an equigranular groundmass of quartz, plagioclase, and K-feldspar is developed. The *Biotite Granodiorite* (Stage 2

porphyry of Fountain, 1972) displays a relic porphyritic texture. Plagioclase and quartz phenocrysts lie in a saccharoidal groundmass of quartz, K-feldspar, plagioclase, biotite, chlorite, and magnetite. Sericite flecks are common in the feldspar, and the biotite and chlorite appear to have replaced primary amphibole. The *Biuro Granodiorite* (Stage 3 porphyry of Fountain, 1972) is unaltered and lacks mineralization. It is considered to represent the first post-mineralization intrusive event in the Panguna area. The rock carries large subrounded quartz phenocrysts (up to 3 mm across) and smaller strongly-zoned plagioclase and dark greenish brown hornblende phenocrysts in a fine-grained groundmass of quartz, K-feldspar, and plagioclase. Magnetite occurs as large subhedral grains and smaller groundmass granules. Accessories include apatite prisms, and chlorite sheaves along cleavages of primary biotite flakes (pleochroic yellow to dark brown).

The *Nautango Andesite* is an irregular plug-like body to the northeast of the mineralized stocks, and is the youngest of the post-mineralization stocks (Page & McDougall, 1972b). The rock is essentially a porphyritic andesite, with varying proportions of hornblende, clinopyroxene, and plagioclase phenocrysts in an exceedingly fine-grained groundmass of mostly felsic constituents. The plagioclase phenocrysts are of two generations. The early generation is represented by sparsely distributed corroded prisms with mottled cores, and the later generation is represented by equant grains with clouded cores and fresh, normally zoned rims. Hornblende also occurs as phenocrysts in two generations. The early generation is represented by sparsely distributed large prisms (up to 5 mm long). They are pleochroic pale brown to dark greenish brown, and in places carry clear spongy clinopyroxene cores. The second generation of hornblende phenocrysts occurs as abundant small euhedral grains (½ - 1 mm) which are pleochroic pale brown to greenish brown, and possess oxidation rims of very fine granular magnetite. Clear to buff-coloured clinopyroxene phenocrysts are scattered through the rock, and clinopyroxene also occurs as small prisms in the groundmass. Magnetite grains are disseminated through the groundmass, and occur more rarely as larger anhedral grains.

Other un-named porphyritic intrusive rocks have been sampled to the north of the Panguna area. These rock types include *porphyritic plagioclase-hornblende (-quartz) microdiorite*, and *pyroxene microdiorite*.

In summary, the granodioritic and dioritic intrusive rocks of the Panguna Intrusive Complex are characterized by normal calc-alkaline assemblages of zoned plagioclase, K-feldspar, quartz, hornblende, clinopyroxene, and magnetite. Hydrothermally altered rocks carry reddish brown biotite as the major ferromagnesian phase. Finer-grained intrusive rocks (microdiorites, porphyritic microdiorites) are widely distributed among the intrusive complexes of Bougainville. They consist of the calc-alkaline assemblage described above. In one location (near Mount Takuan) orthopyroxene is present as a phenocrystic phase. An unusual coarse-grained quartz syenite occurs in the Puspa intrusion in northern Bougainville. This intrusion and the nearby Melilup intrusion might define a subprovince of high-K intrusive rock types.

Optically estimated modes for analyzed specimens from Bougainville are given in Appendix 3.

3.6 LIMBO RIVER DIORITE, NEW GEORGIA ISLAND

3.6.1 Geological Setting

The New Georgia group of islands is built of discrete and coalesced volcanic cones of probably late Tertiary to Recent age (Stanton & Bell, 1969). Lavas range from highly mafic picrite basalts to hornblende andesites. Pyroclastic rocks and reef limestones are the main sedimentary rocks represented in the islands. A small dioritic intrusion centred on Mount Kanekolo in the Limbo and Kolo river systems was reported. It was noted that the intrusive body occupies an area of about 15 km^2 near the centre of the volcanic complex of eastern New Georgia (see Fig. 13). Although intrusive relationships of diorite into surrounding lavas have been observed, the contacts in many places are faulted.

Wright (1968a) gave a detailed petrographic description of the Limbo River Diorite.

The material used in this study was kindly provided by the officers of Her Majesty's Geological Survey, B.S.I.P.

3.6.2 Petrography

The three specimens from the Limbo River Diorite examined in this study can not be considered to be fully representative of the intrusion as a whole. However, their petrography is given here.

FIG. 13 : LOCATION OF THE LIMBO RIVER DIORITE, NEW GEORGIA ISLAND, B.S.I.P.

after Stanton & Bell (1969).

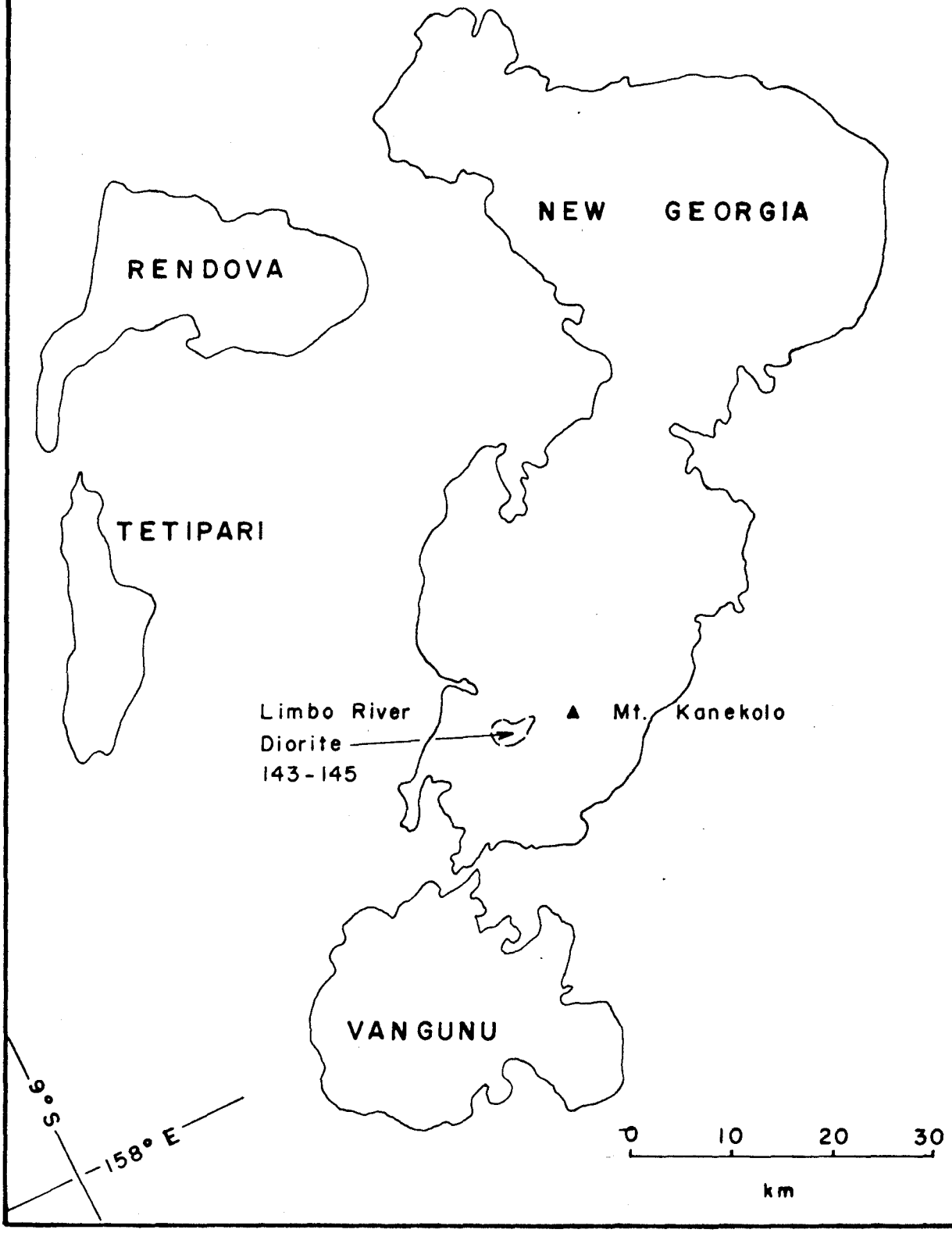

A main rock type is *hornblende-clinopyroxene-biotite microdiorite*. The bulk of the rock consists of fine-grained interlocking zoned plagioclase laths (½ - 1 mm) which exhibit varying degrees of replacement in cores and zones by flaky sericite. Small patches of clear quartz and minor K-feldspar occur interstitially. Larger ferromagnesian minerals lend a subporphyritic texture to the rock. Primary hornblende is pleochroic pale brown to dark greenish brown, and is ragged in form. Prisms of clear clinopyroxene are partly replaced by pale green fibrous amphibole. Large biotite flakes up to 3 mm long are pleochroic yellowish brown to dark chocolate brown. Subhedral grains of titaniferous magnetite are distributed evenly through the rock. Accessory phases include small apatite rods, and traces of sphene associated with fibrous amphibole.

A mafic cumulate rock is present in the complex. *Two pyroxene-biotite (-hornblende) gabbro* contains abundant buff-coloured or clear clinopyroxene which in places enwraps plagioclase stumps. The plagioclase is moderately zoned. A small amount of orthopyroxene is present as large prisms which are pleochroic from light green to pale pink. Pale green hornblende partly replaces some clinopyroxene grains. Biotite mantles other ferromagnesian minerals and is pleochroic pale yellow to reddish brown. Large irregular blebs of titaniferous magnetite are scattered throughout the rock, and in places poikilitically enclose pyroxene and plagioclase.

Orthorhombic pyroxene has previously not been reported from the Limbo River Diorite. Its presence in a mafic cumulate rock of the intrusive complex, and also in some of the nearby lavas (Stanton & Bell, 1969), supports the proposition that the dioritic rocks are the intrusive equivalents of the lavas.

3.7 POHA RIVER DIORITE, GUADALCANAL ISLAND

3.7.1 Geological Setting

A pre-Miocene basement predominantly of gabbroic and dioritic intrusive rocks with basaltic and andesitic volcanic rocks ('Guadalcanal Igneous Complex') is recognized as the oldest formation in Guadalcanal (Coleman et al., 1957). The overlying sedimentary succession ranges from Lower Miocene to Recent, with volcanogenic sediments and limestones as dominant lithologies (Hackman, 1968). Renewed magmatism in Plio-Pleistocene times resulted in emplacement of dioritic intrusive masses (e.g., Koloula Igneous Complex, south-central Guadalcanal) with

contemporaneous volcanic activity in northwest Guadalcanal (Gallego Lavas). The distribution of intrusive masses in Guadalcanal is shown in Fig. 14.

That part of the pre-Miocene basement in the Poha River area of northwestern Guadalcanal is here referred to as the 'Poha River Diorite'. Detailed field and laboratory work is currently being undertaken by the Geological Survey of B.S.I.P.

The material used in this study was kindly provided by the staff of the Geological Survey. The precise geological occurrence of the specimens is not known, but they are considered to represent the dominant intrusive rock types in the Poha River area.

3.7.2 Petrography

The mineralogy of the intrusive rocks of the Poha River Diorite are dominated by plagioclase and amphibole. Medium-grained *hornblende leucogabbro* comprises an hypidiomorphic granular assemblage of plagioclase prisms (½-3 mm) which show only moderate degrees of normal zoning but are commonly mottled and flecked with sericite, and two types of amphibole. Primary hornblende is pleochroic pale greenish brown to dark greenish brown, and forms subhedral grains which in places enclose smaller plagioclase laths. Pale green to pale greenish brown hornblende presumably replaces pyroxene, although no relic cores were observed. Small amounts of clinopyroxene (less than 2%) have been reported in similar rocks to the southeast (Wright, 1968b). Accessory minerals in the leucogabbro include magnetite grains and granules which are closely associated with amphibole, and long apatite rods.

With an increase in abundance of quartz, the rock grades into *hornblende-quartz-biotite diorite*. There are a number of other petrographic features which set this rock type apart from the hornblende leucogabbro. Plagioclase prisms display a greater degree of zoning, both normal and oscillatory. Alkali feldspar is present as interstitial patches and small tablets. Hornblende forms euhedral prisms which are pleochroic pale brown to dark greenish brown. Mafic clots occur irregularly through the rock, and are composed of both dark greenish brown and pale green fibrous amphiboles, and biotite flakes (pleochroic pale brown to dark reddish brown) which are largely replaced by green chlorite, granular sphene, and epidote. Magnetite forms anhedral grains of variable size, and is found chiefly near

FIG. 14 : LOCATION OF INTRUSIVE COMPLEXES,
GUADALCANAL, BRITISH SOLOMON ISLANDS.

Oligocene to Recent intrusive rocks are stipled.

after Hackman (1973),

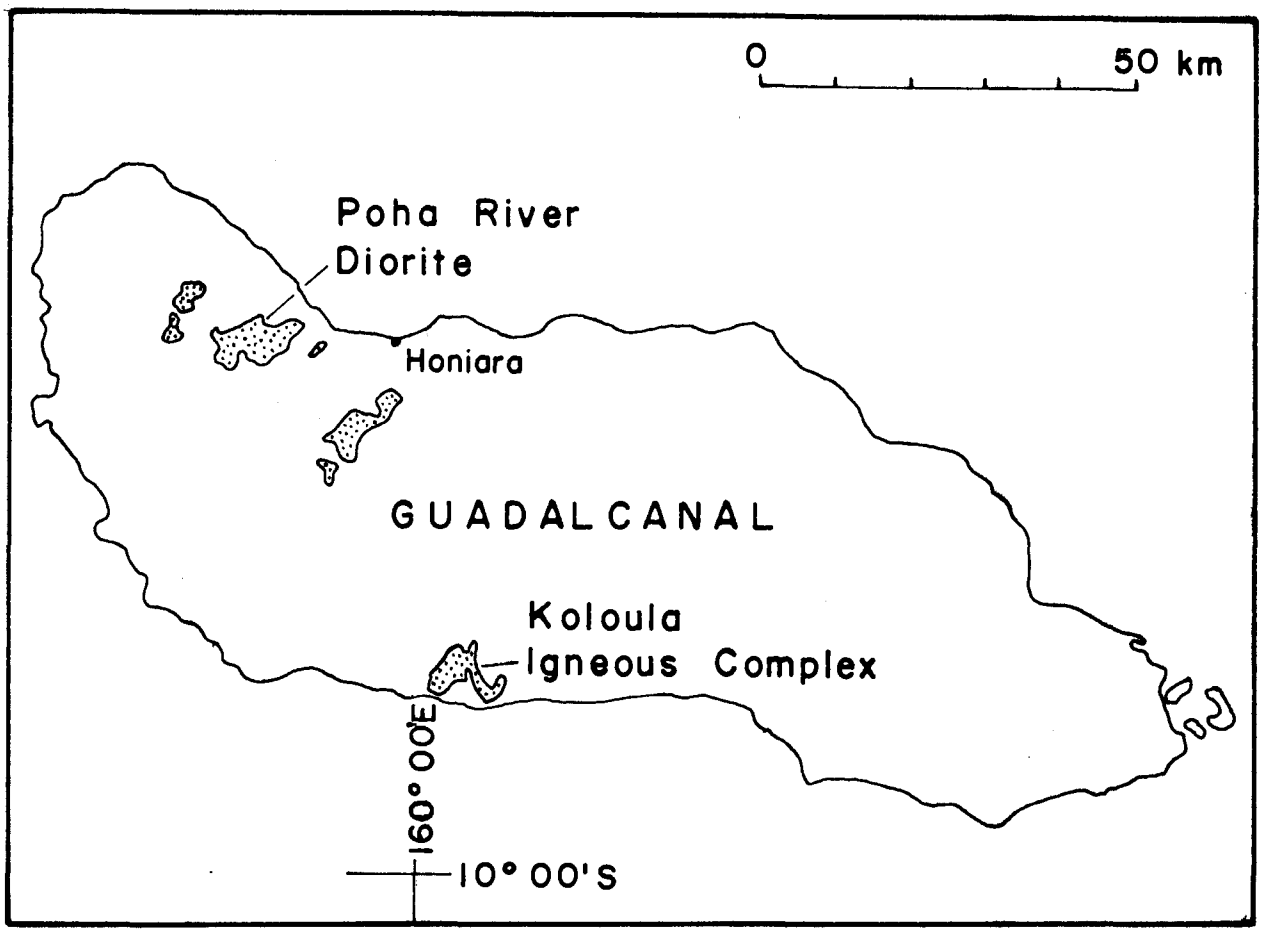

ferromagnesian minerals.

Modes of these rock types are given in Appendix 3.

3.8 KOLOULA IGNEOUS COMPLEX, GUADALCANAL ISLAND

3.8.1 Geological Setting

As noted in the previous section, the intrusive igneous activity on Guadalcanal may be divided into an earlier (pre-Miocene) period, during which the basement Guadalcanal Igneous Complex developed, and a later period (Plio-Pleistocene), during which intrusive complexes such as the Koloula Igneous Complex were emplaced and lavas in north-western Guadalcanal were extruded.

The Koloula Igneous Complex is located near the south coast of central Guadalcanal. A wide range of rock types, from ultramafic cumulates to aplitic dykes, form a complex which covers an area of approximately 60 km^2. Gabbros and granodiorites are the dominant rock types in the complex. Early gabbros have intruded the Suta Volcanics of Oligocene to Lower Miocene age (Hackman, 1968), and later felsic rocks with related copper mineralization intrude the central part of the gabbros to form a roughly annular complex (Chivas, 1975). Preliminary K-Ar dating of the granodiorites give ages of 1-2 m.y. (Chivas, pers. comm.).

The material used in this study was sampled from the Chikora and Ghecha creek areas of the complex (see Fig. 15a). The samples are believed to be representative of the rock types in this part of the complex, but may not fully represent the whole of the complex.

3.8.2 Petrography

The phaneritic intrusive rocks of the Koloula Ingeous Complex can be subdivided into two suites, each containing a variety of rock types. The suites are here called the 'Mafic Suite' and the 'Felsic Suite'. The Mafic Suite comprises the earlier mafic rocks of the complex, including a variety of gabbros, pyroxenitic cumulative rocks, and mafic diorites. The Felsic Suite comprises the later felsic intrusive rocks, including quartz diorites, granodiorites, and aplitic dyke rocks. Petrographically the Felsic Suite is characterized by the mafic minerals hornblende and biotite, and a subporphyritic texture with a groundmass of anhedral quartz blebs, plagioclase prisms, and traces of K-feldspar. The Mafic Suite is characterized by the predominance of clinopyroxene in the ferromagnesian assemblages, and

FIG. 15a : SPECIMEN LOCATIONS, KOLOULA IGNEOUS COMPLEX.

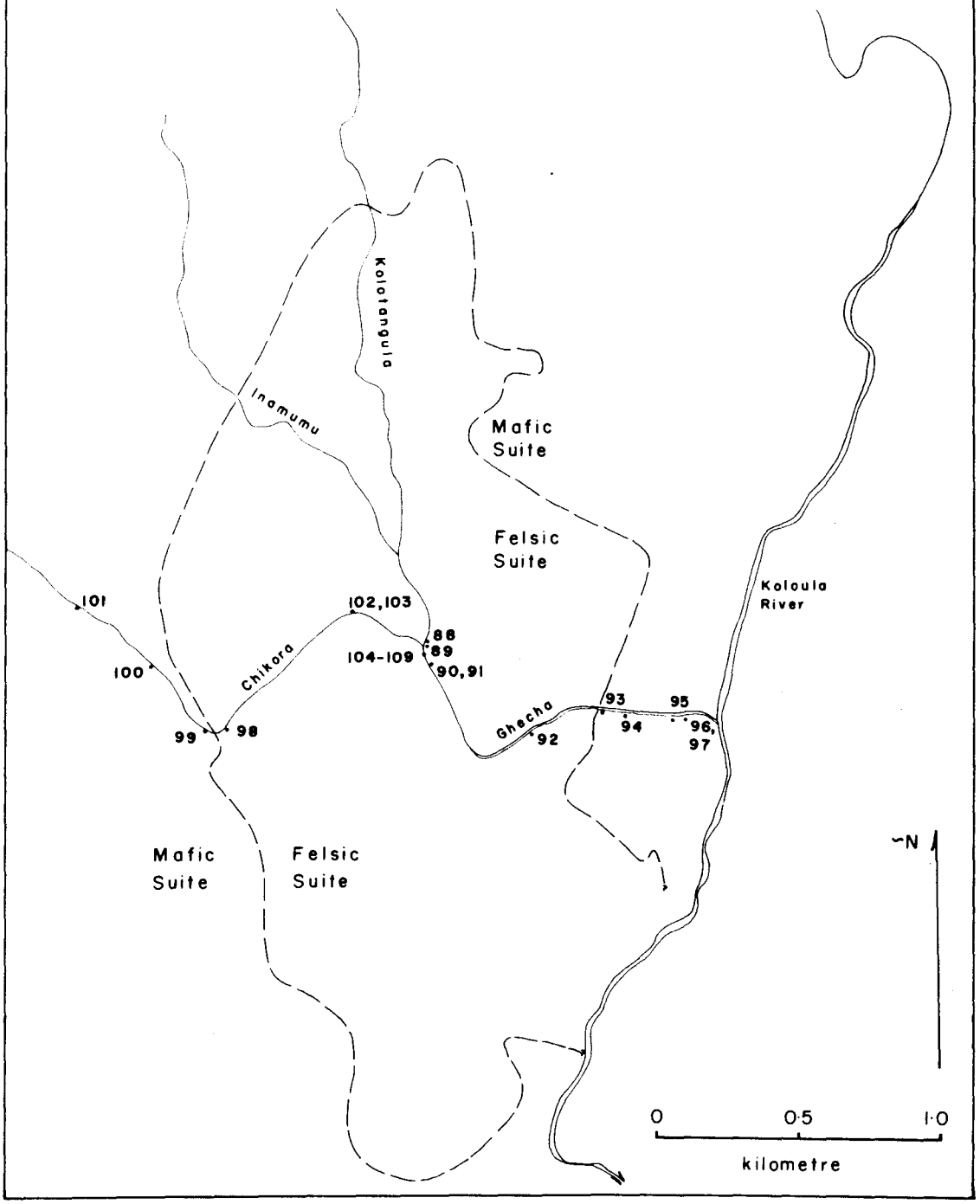

intergranular to subophitic textures. Low-Si porphyritic microdiorites post-date all other intrusional events.

1. The Mafic Suite

The most felsic rock of the Mafic Suite is *two-pyroxene-hornblende-biotite-quartz diorite*, which is quite different in texture and mineralogy from the quartz diorite of the Felsic Suite. The rock is fine- to medium-grained, hypidiomorphic granular in texture. Small (½ - 1½ mm) plagioclase laths, K-feldspar patches and interstitial quartz constitute a felsic groundmass through which are scattered ragged green hornblende prisms with clinopyroxene and orthopyroxene cores, ragged biotite flakes pleochroic golden yellow to dark reddish brown and with traces of chlorite and epidote alteration, and accessory amounts of magnetite, apatite, and zircon.

Gabbroic rocks form a large part of the Mafic Suite. A variety of textures and mineral assemblages are represented among these rocks. Microgabbros are fine-grained, dense rocks. Closely packed plagioclase laths display only a moderate degree of normal zoning. Small granules and larger euhedra of clinopyroxene and orthopyroxene are evenly distributed. In some varieties the pyroxenes are almost entirely replaced by fibrous green amphibole. Larger clinopyroxenes contain small plagioclase laths. Small subhedral magnetite and ilmenite grains are scattered throughout the rock.

Coarser-grained gabbroic rocks are characterized by moderately zoned plagioclase prisms, minor interstitial quartz, and mafic assemblages of clinopyroxene, orthopyroxene, and hornblende. When the two pyroxenes occur alone, they are usually replaced to a greater or lesser extent by pale green fibrous amphibole along margins, and in extreme cases relic pyroxene granules in an amphibole base define former large pyroxene sites. When primary hornblende occurs in the mafic assemblage of the gabbroic rocks, it forms large plates which are pleochroic pale brown to dark greenish brown and which poikilitically enclose small plagioclase prisms. The hornblende in places carries pyroxene cores, and there are small amounts of marginal alteration to poorly-formed reddish brown biotite. Large magnetite and ilmenite blebs are present in the gabbros, and are usually closely associated with the mafic minerals. Smaller magnetite grains occur in close association with hornblende, when present.

Olivine pyroxenite cumulates have only been sampled in river float. These rocks are very dark and coarse-grained in hand specimen, and some primary layering of pyroxenes can be seen. In thin section the rocks display an adcumulate texture, with small unzoned cuspate plagioclase grains interstitial to large euhedral grains of clinopyroxene, orthopyroxene, and minor anhedral olivine.

2. The Felsic Suite

Fine-grained leucocratic *aplite* forms dykes up to 1 metre wide and tens of metres long. The aplitic rock types range from quartz monzonite to potassic granite in composition, and contain varying amounts of anhedral quartz, strongly zoned sodic plagioclase prisms with flecks of sericite in cores, tablets and interstitial patches of K-feldspar, small amounts of biotite mostly replaced by green chlorite and granular sphene, and accessory amounts of magnetite and chalcopyrite.

A dominant rock type in the Felsic Suite is *hornblende-biotite granodiorite*. In hand specimen the rock is medium-grained, but in thin section it is subporphyritic in texture. Plagioclase prisms up to 4 mm long have mottled cores and strongly zoned rims. Quartz grains up to 3 mm across are resorbed and exhibit strain extinction. Large hornblende prisms (1 - 5 mm) are pleochroic pale brown to dark green, enclose small plagioclase prisms, and are partly replaced by small, dark brown biotite flakes. The larger grains of plagioclase, quartz, and hornblende lie in an inequigranular groundmass of quartz, K-feldspar, green hornblende, and biotite flakes which are pleochroic yellowish brown to dark brown and partly chloritized along cleavages. Mafic clots of hornblende, biotite, and magnetite are common. Accessory minerals include zircon and apatite.

With decreasing quartz and more abundant mafic minerals, the rock grades into *hornblende-biotite-quartz diorite*. This rock retains the inequigranular, subporphyritic texture of the granodiorite.

Subrounded xenoliths of *low-Si diorite porphyry* occur within the granodiorite. The diorite porphyry comprises phenocrysts of hornblende and plagioclase with rarer biotite and quartz, in a fine-grained groundmass of amphibole, plagioclase, quartz, and traces of K-feldspar. Magnetite granules are scattered throughout the groundmass, and more rarely occur as large anhedral blebs. The hornblende phenocrysts are pleochroic pale greenish brown to dark green, and enclose small plagioclase prisms. The groundmass amphibole is a poorly-formed,

fibrous pale green variety. Biotite flakes have been almost entirely replaced by chlorite and granular leucoxene. The plagioclase phenocrysts have mottled cores and zoned rims. The large anhedral quartz blebs invariably exhibit strain extinction.

Low-Si porphyritic microdiorites, the latest intrusive rocks in the Complex, carry varied phenocrystic assemblages: plagioclase is always present, with combinations of clinopyroxene, hornblende, and quartz. The plagioclase phenocrysts are up to 4 mm long, and possess mottled cores and zoned rims. Pyroxene phenocrysts exhibit marginal replacement by fibrous green amphibole. Rare large clinopyroxenes (up to 5 mm) contain small plagioclase inclusions. Large hornblende phenocrysts aggregate into clusters with magnetite grains. Quartz phenocrysts are rounded and develop a corona of minute ferromagnesian crystals. The groundmass consists of a felted base of plagioclase laths, with granules of pyroxene mostly replaced by fibrous green amphibole and traces of flaky biotite. Magnetite granules and small amounts of quartz are scattered through the rock.

Optically estimated modes for all analyzed specimens from the Koloula Igneous Complex are given in Appendix 3.

3.9 SUMMARY

A summary of the mineralogy of main rock types for intrusive complexes in the P.N.G. islands and Solomon Islands is given in Table 7.

In Table 8, an attempt is made to estimate relative abundances of the various rock types in intrusive complexes of the P.N.G. region.

Modal variations in island arc and Highlands intrusive suites are compared in Fig. 15b.

TABLE 7: SUMMARY OF MINERALOGY OF MAIN ROCK TYPES, INTRUSIVE ROCK SUITES, P.N.G. ISLANDS AND SOLOMON ISLANDS

SUITE rock type	QZ	PLAG	KF	HB	BIO	CPX	OPX	OL	MT	ILT	PY	CPY	SPH	APT	ZIRC	Textural features
1. PLESYUMI INTRUSIVE COMPLEX																
porphyritic ol-cpx gabbro	-	+	-	+	(+)	+	-	+	+	+	+	+	-	-	-	coarsely porphyritic
cpx(-hb)-qz gabbro	+	+	-	+	-	+	-	-	-	+	-	+	-	-	-	schiller-textured cpx
two px-hb(-bio) diorite	+	+	-	+	+	+	+	-	+	+	+	+	-	+	-	mafic clots
high-K cpx-hb-bio diorite	+	+	+	+	+	+	(+)	-	+	+	-	+	+	+	+	mafic clots
hb-bio-qz diorite	+	+	+	+	+	(+)	-	-	+	+	-	+	+	+	+	optically continuous qz patches
hb-bio granodiorite	+	+	+	+	+	-	-	-	+	+	-	+	+	+	+	optically cts. qz; mafic clots
plag-hb-qz dacite porphyry	+	+	-	+*	-	-	-	-	+	-	-	-	-	-	-	phenocrysts
	+	+	+	-	-	-	-	-	+	-	-	+	+	-	-	groundmass
2. MOUNT KREN INTRUSIVE COMPLEX																
high-K hornblende diorite	+	+	+	+	(+)	(+)	-	-	+	-	-	-	+	+	+	mafic clots
high-K low-Si microdiorite	-	+	-	+	-	+	-	-	-	-	-	-	-	-	-	phenocrysts
	+	+	+	-	-	+	-	-	+	-	+	-	-	-	-	groundmass
hb-qz diorite	+	+	+	+	-	-	-	-	+	-			(+)	+	+	mafic clots
low-Si microdiorite	+	+	-	+	-	-	-	-	+	-	-	-	-	-	-	phenocrysts
	+	+	+	+	-	-	-	-	+	-	-	+	-	-	-	groundmass
3. LEMAU INTRUSIVE COMPLEX																
uralite gabbro	-	+	-	+	-	+	-	-	+	+	+	+	-	-	-	subophitic cpx
two px-bio(hb)-qz diorite	+	+	+	+	+	+	+	-	+	+	-	+	-	+	+	f.g. mafic clots
two px-hb granodiorite	+	+	+	+	(+)	(+)	(+)	-	+	+	-	+	-	-	-	vague mafic clots
plag-hb diorite porphyry	-	+	-	+	-	-	-	-	+	-	-	-	-	-	-	phenocrysts
	+	+	+	-	-	-	-	-	+	-	+	+	-	-	-	groundmass
4. BOUGAINVILLE RECONNAISSANCE																
low-Si two px-hb-bio microdiorite	-	+	-	-	-	+	+	-	+	(+)	-	-	-	-	-	phenocrysts
	+	+	+	+	+	+	-	-	+	-	-	-	-	+	-	groundmass
qz syenite	+	+	+	+	+	+	-	-	+	+	-	+	+	+	-	coarse grained
5. PANGUNA INTRUSIVE COMPLEX																
'Nautango Andesite'	-	+	-	+	-	+	-	-	+	+	-	+	-	-	-	phenocrysts
	+	+	+	-	-	+	-	-	+	-	-	-	-	-	-	groundmass
'Kaverong Quartz Diorite'	+	+	+	+	(+)	(+)	-	-	+	+	-	+	+	+	+	mafic clots
'Biotite Diorite'	+	+	+	-	+*	-	-	-	+	-	-	+	-	-	-	K-altered
'Leucocratic Quartz Diorite'	+	+	+	-	+	-	-	-	+	+	-	+	-	+	-	Mafic clots
'Biotite Granodiorite'	+	+	-	-	-	-	-	-	-		-	-	-	-	-	phenocrysts
	+	+	+	-	+	-	-	-	+		+	+	-	+	-	groundmass
'Biuro Granodiorite'	+	+	-	+	(+)	-	-	-	-		-	-	-	-	-	phenocrysts
	+	+	+	-	-	-	-	-	+		-	-	+	+	-	groundmass
plag-hb (-qz) microdiorite	(+)	+	-	+	-	-	-	-	+		-	-	-	-	-	phenocrysts
	+	+	+	-	-	-	-	-	+		(+)	-	-	(+)	-	groundmass
cpx microdiorite	+	+	+	+	-	+	-	-	+							
6. LIMBO RIVER DIORITE																
two px-bio(-hb)gabbro	-	+	-	+	+	+	+	-	+	+	-	+	-	-	-	cumulate
hb-cpx-bio microdiorite	+	+	(+)	+	+	+	-	-	+	+	-	+	+	+	-	fine grained
7. POHA RIVER DIORITE																
hb leucogabbro	+	+	-	+	-	-	-	-	+	-	+	+	+	+	-	hypidiomorphic granular
hb-qz-bio diorite	+	+	+	+	+	-	-	-	+	-	(+)	+	(+)	-	-	mafic clots
8. KOLOULA IGNEOUS COMPLEX																
i) Mafic Suite																
gabbroic cumulate	-	+	-	(+)	-	+	(+)	+	+		-	-	-	-	-	adcumulate
two px gabbro	-	+	-	(+)	-	+	+	-	+	+	+	+	-	-	-	subidiomorphic
hb-two px gabbro	(+)	+	(+)	+	(+)	+	+	-	+	+	+	+	-	+	-	poikilitic hb
low-Si porphyritic micro-diorite	(+)	+	-	(+)	(+)	(+)	(+)	-	-	-	-	-	-	-	-	phenocrysts
	+	+	+	(+)	(+)	(+)	-	-	+	-	+	-	-	-	-	groundmass
two px-hb-bio-qz diorite	+	+	+	+	+	+	+	-	+	+	-	-	-	+	+	f. to m.g. hypidiomorphic granular
ii) Felsic suite																
hb-bio-qz diorite	+	+	+	+	+	-	-	-	+	-	+	-	-	+	+	mafic clots subporphyritic
hb-bio granodiorite	+	+	+	+	+	-	-	-	+	-	-	(+)	-	+	+	mafic clots subporphyritic
aplite	+	+	+	-	+	-	-	-	+	-	-	(+)	+	+	+	saccharoidal

Note: + = present; (+) = sometimes present; - = absent; * = hydrothermal
silicates observed in transmitted light
oxides and sulfides observed in reflected light.

TABLE 8: RELATIVE ABUNDANCE OF ROCK TYPES IN INTRUSIVE COMPLEXES OF THE P.N.G. REGION

SUITE	LOW- TO NORMAL-K ROCKS				HIGH-K ROCKS				TOTAL AREA (km^2)
	Mafic rocks	Diorite	Granodiorite	Porphyries	Mafic rocks	Diorite	Qz monzonite (Adamellite)	Porphyries	
P.N.G. HIGHLANDS:									
1. Yuat North Batholith	—	—	—	p	5	70	20	5	450
2. Yuat South Batholith	5	5	80	10	—	p	—	—	600
3. Karawari Batholith	5	30	55	10	-	p	—	—	650
4. Wale & Lamant Stocks	90	—	10	p	-	-	-	-	200
5. Sekau Stock	70	20	-	-	-	10	p	-	30
6. Mt Michael Stock	-	-	-	80	-	-	-	20	60
7. Mt Pugent Stock	-	-	-	-	-	-	100*	-	2
8. Frieda River Complex	-	20	-	60	-	20	p	p	200
9. Ok Tedi Complex (Mt Fubilan)	-	-	-	-	-	20	20	60	2
P.N.G. ISLANDS & SOLOMON ISLANDS									
1. Plesyumi Complex	5	40	45	5	-	5	-	-	50
2. Mt Kren Complex	-	10	-	5	-	80	-	5	30
3. Lemau Complex	20	20	60	p	-	-	-	-	60
4. Panguna Complex	-	5	75	20	-	-	-	-	15
5. Limbo River Diorite	-	-	-	-	p	100	-	-	15
6. Poha River Diorite	70	30	-	p	-	-	-	-	55
7. Koloula Complex	60	30	10	p	-	-	-	-	50

Note: abundance figures are percentage of area of complex
p = present in small amounts; * = quartz-poor microsyenite

FIG. 15b : SUMMARY OF MODAL VARIATIONS IN INTRUSIVE ROCK SUITES FROM CONTRASTING SETTINGS.

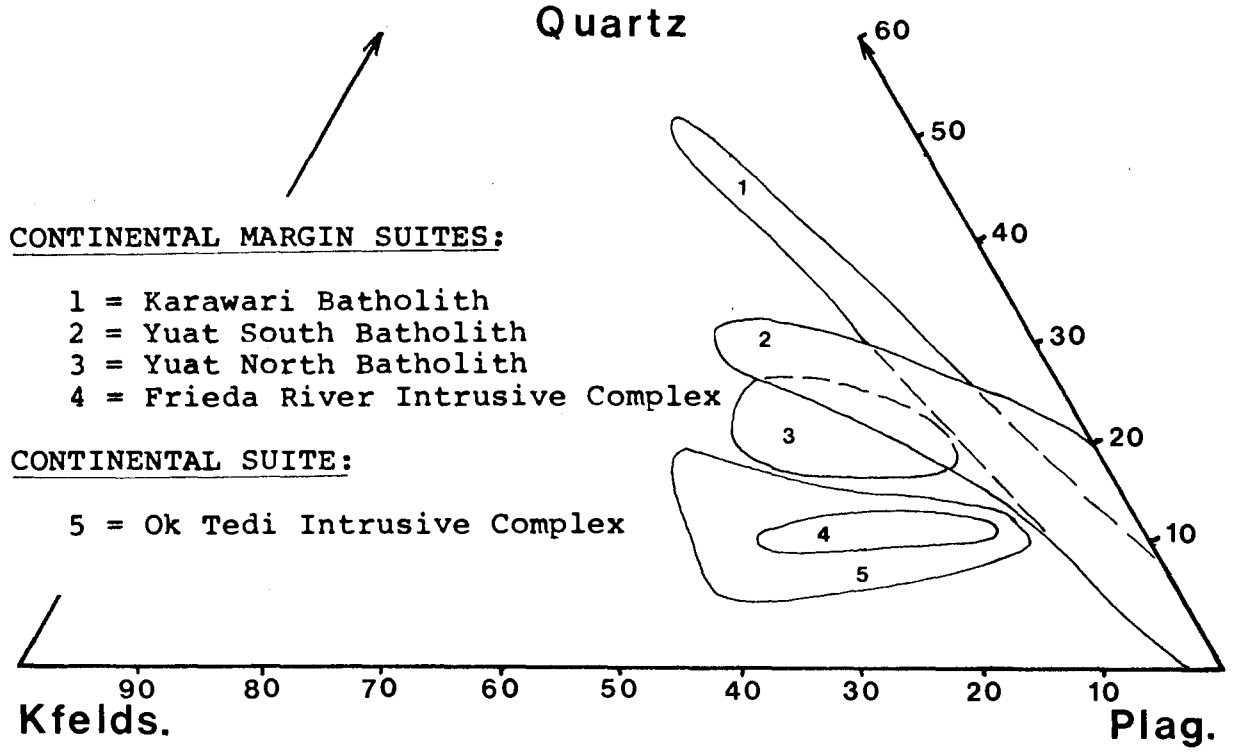

CONTINENTAL MARGIN SUITES:

1 = Karawari Batholith
2 = Yuat South Batholith
3 = Yuat North Batholith
4 = Frieda River Intrusive Complex

CONTINENTAL SUITE:

5 = Ok Tedi Intrusive Complex

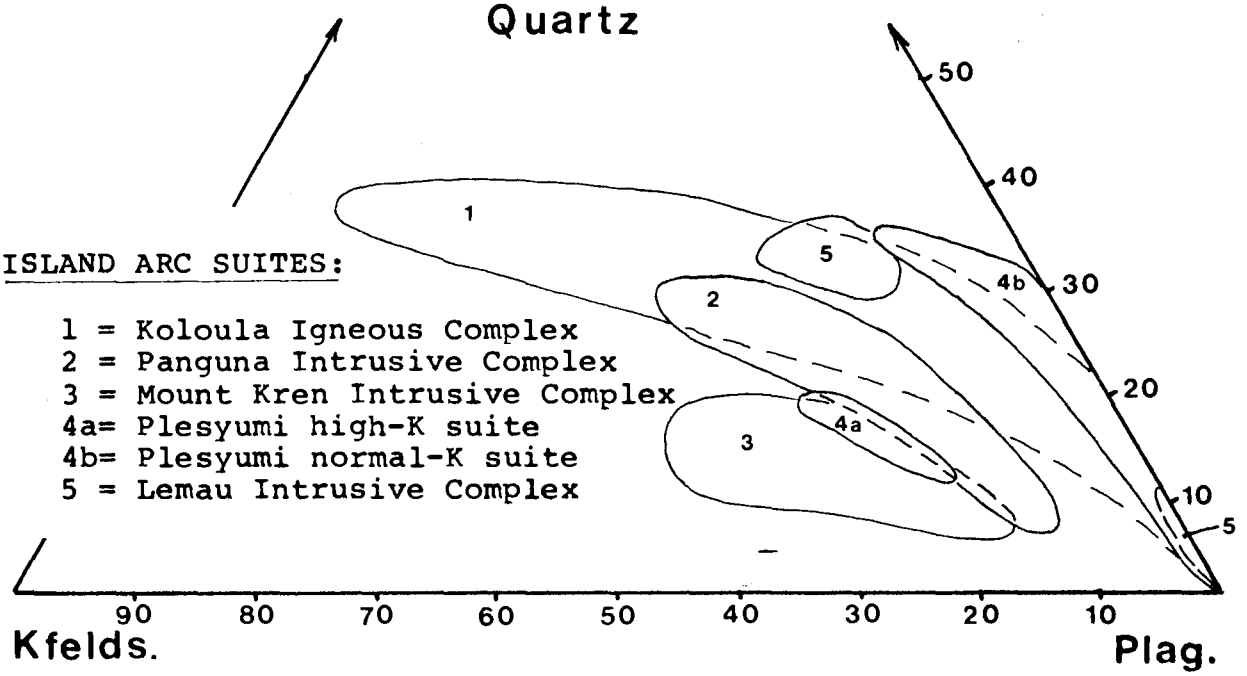

ISLAND ARC SUITES:

1 = Koloula Igneous Complex
2 = Panguna Intrusive Complex
3 = Mount Kren Intrusive Complex
4a= Plesyumi high-K suite
4b= Plesyumi normal-K suite
5 = Lemau Intrusive Complex

CHAPTER 4 GEOCHEMISTRY OF INTRUSIVE ROCK SUITES, HIGHLANDS, PAPUA NEW GUINEA

4.1 DATA PRESENTATION

In Chapters 4 and 5, geochemistry is presented for sixteen intrusive complexes from the Papua New Guinea region. For each complex, major element distributions are discussed with reference to Harker-type variation diagrams (TiO_2, Al_2O_3, total Fe as FeO, MgO, CaO, Na_2O, K_2O, and P_2O_5 *versus* SiO_2, all recalculated on a loss-free basis).

Two calc-alkaline intrusive rock suites from the Gazelle Peninsula, New Britain, have been chosen for comparison with the new data. Macnab (1970) described the petrography and geochemistry of the two Gazelle suites, which are:

1. the *normal-K calc-alkaline plutonic suite from the North Bainings Mountains*, ranging from leucogabbro to granodiorite in composition,

and 2, the *high-K calc-alkaline plutonic suite from the Central and South Bainings Mountains*, ranging in composition from leucogabbro to adamellite and granite.

At the present time, these are the only well-documented intrusive calc-alkaline rock suites from the P.N.G. region. Macnab's data for these two suites are presented in Harker diagram form in Fig. 16, and on MFA (MgO-total Fe as FeO-Na_2O+K_2O) triangular diagrams in Fig. 17. On the MFA diagrams, both suites display the typical flat calc-alkaline trend, showing alkali enrichment and relative iron depletion.

Harker diagrams show that both suites contain most major elements at similar levels of concentration and with similar trends. The two exceptions are K_2O, which is much more abundant and increases much more rapidly with increasing SiO_2 in the high-K suite, and P_2O_5, which shows a regular inverse relationship with SiO_2 in the normal calc-alkaline suite but shows considerable scatter in the high-K suite. The regression lines derived from these Harker diagrams are plotted for comparison on subsequent major element diagrams.

The distribution of selected trace elements within the newly-described complexes are also discussed using Harker-type variation diagrams. Trace elements treated in this way include Rb, Ba, Sr, Zr, Nb, Ni, Co, and V. Concentration levels of the Th, U, and Ga are mentioned

FIG. 16 : MAJOR ELEMENT VARIATIONS, GAZELLE INTRUSIVE SUITES, NEW BRITAIN (data of Macnab, 1970).

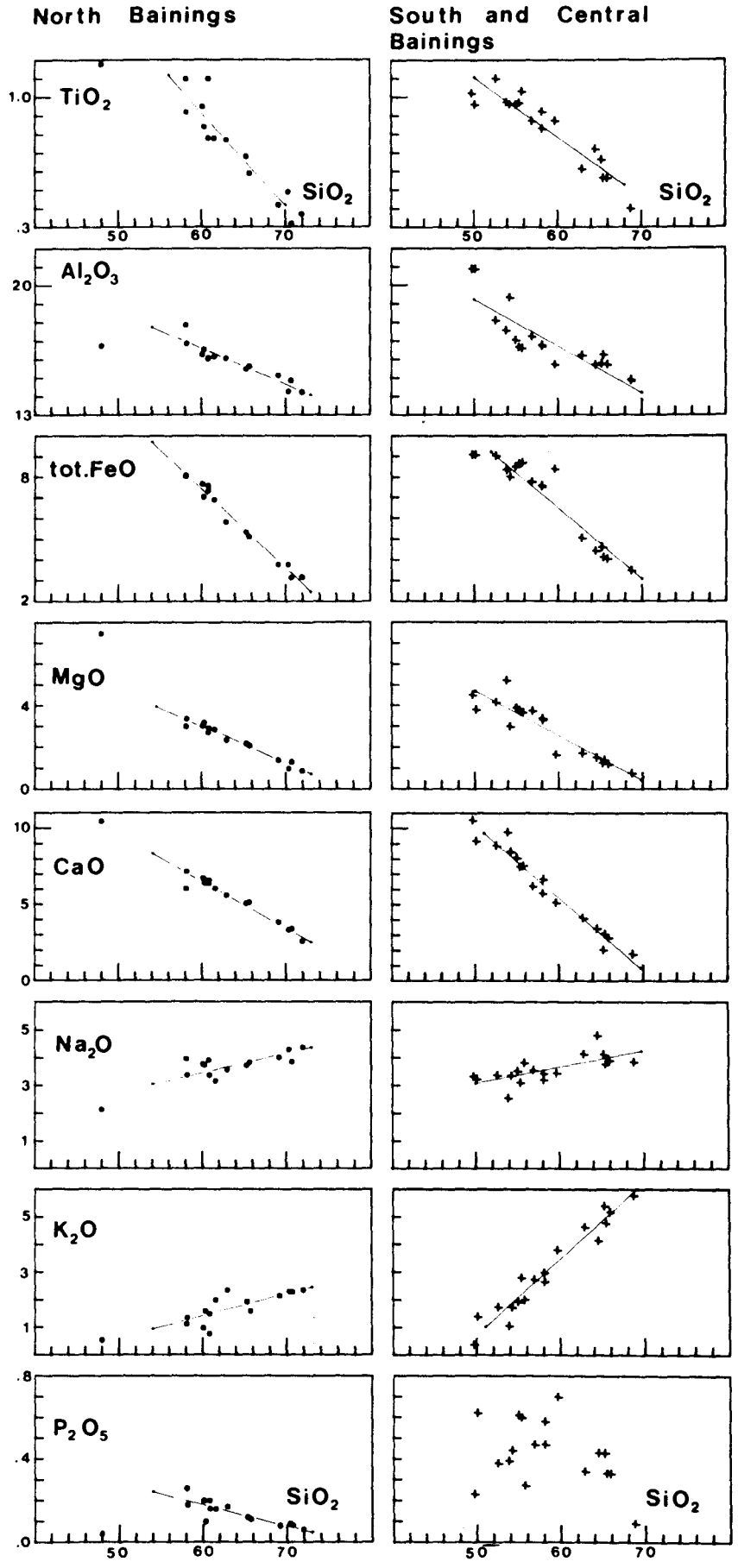

Note: these trends are reproduced on subsequent major element plots for comparison

FIG. 17 : A-M-F DIAGRAMS FOR GAZELLE INTRUSIVE SUITES

(DATA OF MACNAB, 1970).

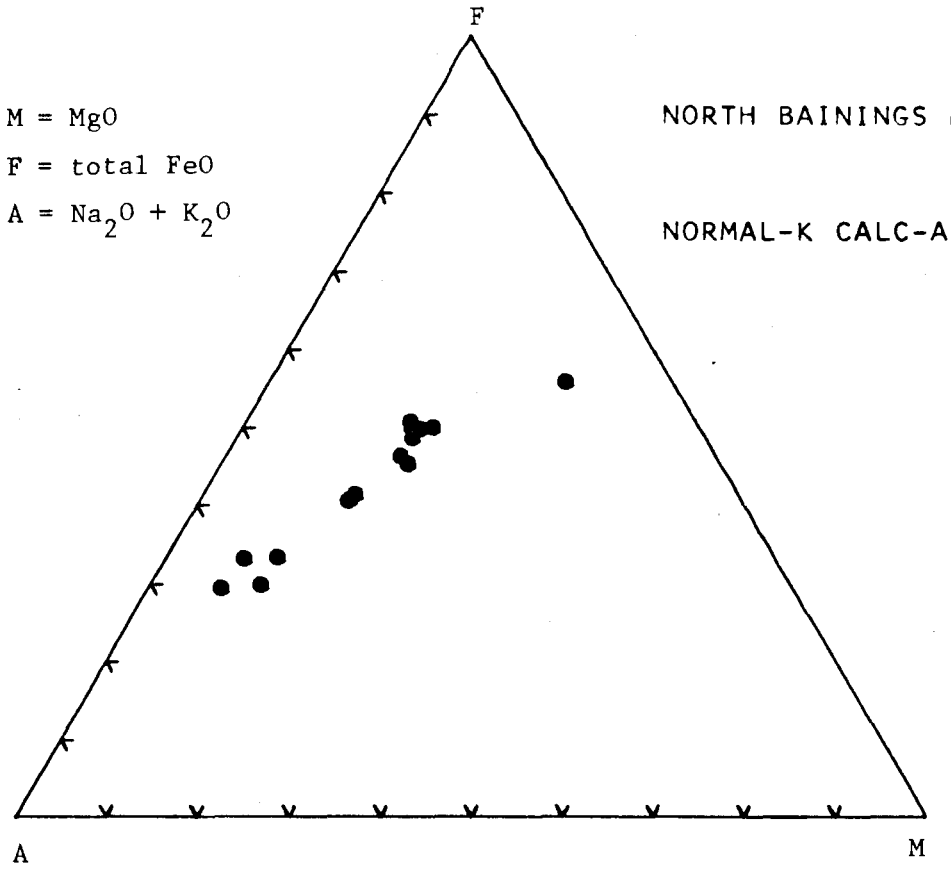

M = MgO

F = total FeO

A = $Na_2O + K_2O$

NORTH BAININGS MOUNTAINS --

NORMAL-K CALC-ALKALINE

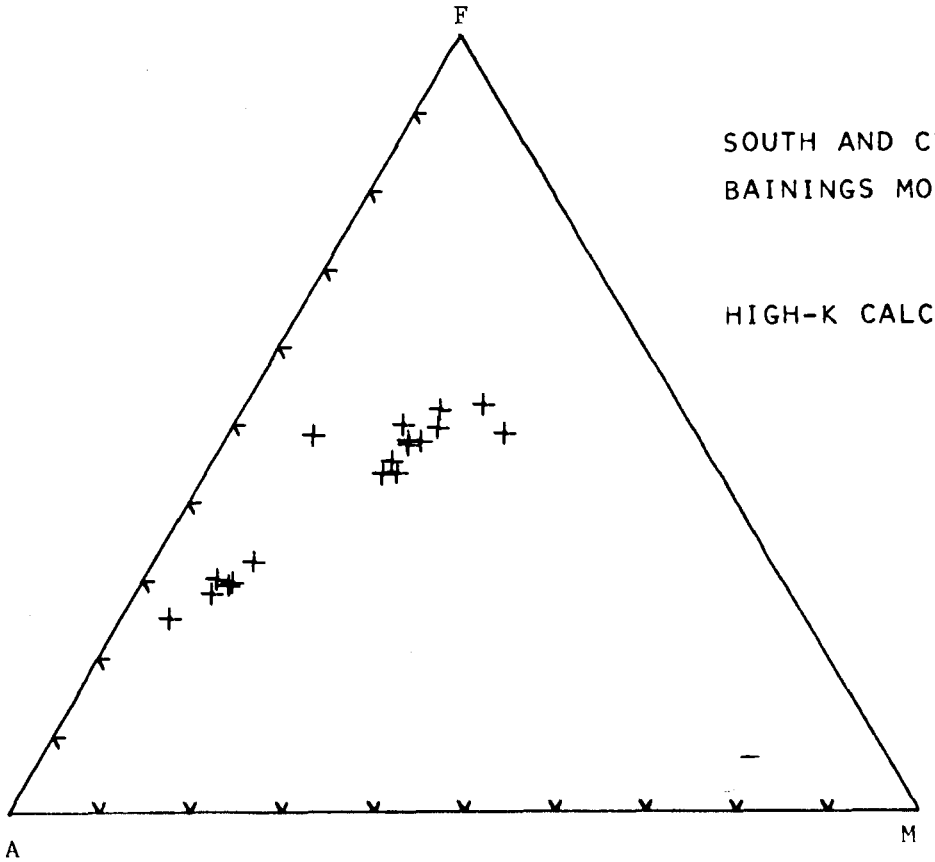

SOUTH AND CENTRAL
BAININGS MOUNTAINS --

HIGH-K CALC-ALKALINE

where data are available. Variations of Nb, Rb, La+Ce+Y, and Sr against K_2O are discussed with reference to the Karawari, Yuat South, and Yuat North suites of the Western Highlands, which are chosen to represent trace element variation in low-to normal-, normal-, and high-K calc-alkaline suites respectively.

The abundances of Cu, Pb, and Zn, together with Ag, Au, Se and Te for selected samples, are discussed in a later chapter on porphyry copper occurrences in the P.N.G. region (see sections 7.4.2 and 7.4.3).

4.2 GEOCHEMISTRY OF THE YUAT NORTH BATHOLITH

Harker-type major element variation diagrams (together with MFA and Quartz-Plagioclase-K-feldspar plots) are given in Fig. 18 for rocks from the Yuat North, Yuat South, and Karawari batholiths. These data are presented together to facilitate comparison. Complete chemical analyses are presented in Appendix 4, Table 1.

Yuat North specimens span a wide silica range from 47 to 69% SiO_2 (see Fig. 18). However, only seven samples have been obtained and there are large gaps in the data between 50 and 60% SiO_2. Five of the specimens define linear trends in the restricted range 62-69% SiO_2. In general the suite displays the usual major element distribution behaviour of positive correlation of Na_2O and K_2O with SiO_2, and negative correlation of TiO_2, Al_2O_3, total FeO, MgO, CaO, and P_2O_5 with SiO_2. Typically calc-alkaline features of the suite are evident in moderate to high Al_2O_3 contents (16.8% Al_2O_3 at 62% SiO_2), moderate TiO_2 contents (0.7% TiO_2 at 62% SiO_2), and a flat trend of alkali enrichment on the MFA diagram.

Two samples (DRM063, 064) possess consistently different major element chemistry. Both have lower TiO_2 and total FeO, and higher MgO and P_2O_5 compared with the other specimens of the suite. In addition, DRM063 has much higher K_2O, and DRM064 has higher Na_2O. These differences are consistent with shoshonitic affinities for these two specimens (Joplin 1965, 1968; Kesson & Smith, 1972) which come from a small stock near the southern margin of the batholith. Their chemistry is in contrast with the high-K calc-alkaline chemistry of the main batholithic mass.

Trace element abundances also confirm differences between the batholith and nearby stock (see Fig. 19). Both barium and strontium at approximately 1000 ppm are twice as abundant in rocks of the stock as in the high-K batholithic suite. Among the ferromagnesian trace elements, nickel is twice as abundant (20-30 ppm) in the shoshonitic rocks as it is in the high-K dioritic rocks (8-10 ppm). Levels of cobalt and vanadium

FIG. 18 : MAJOR ELEMENT VARIATIONS FOR YUAT NORTH, YUAT SOUTH, AND KARAWARI BATHOLITHS.

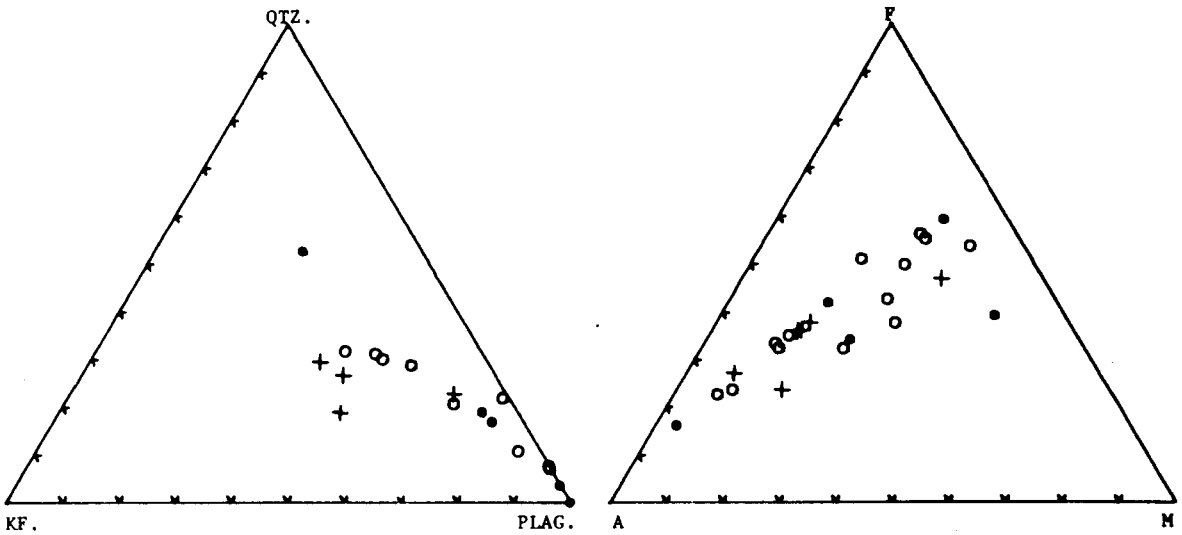

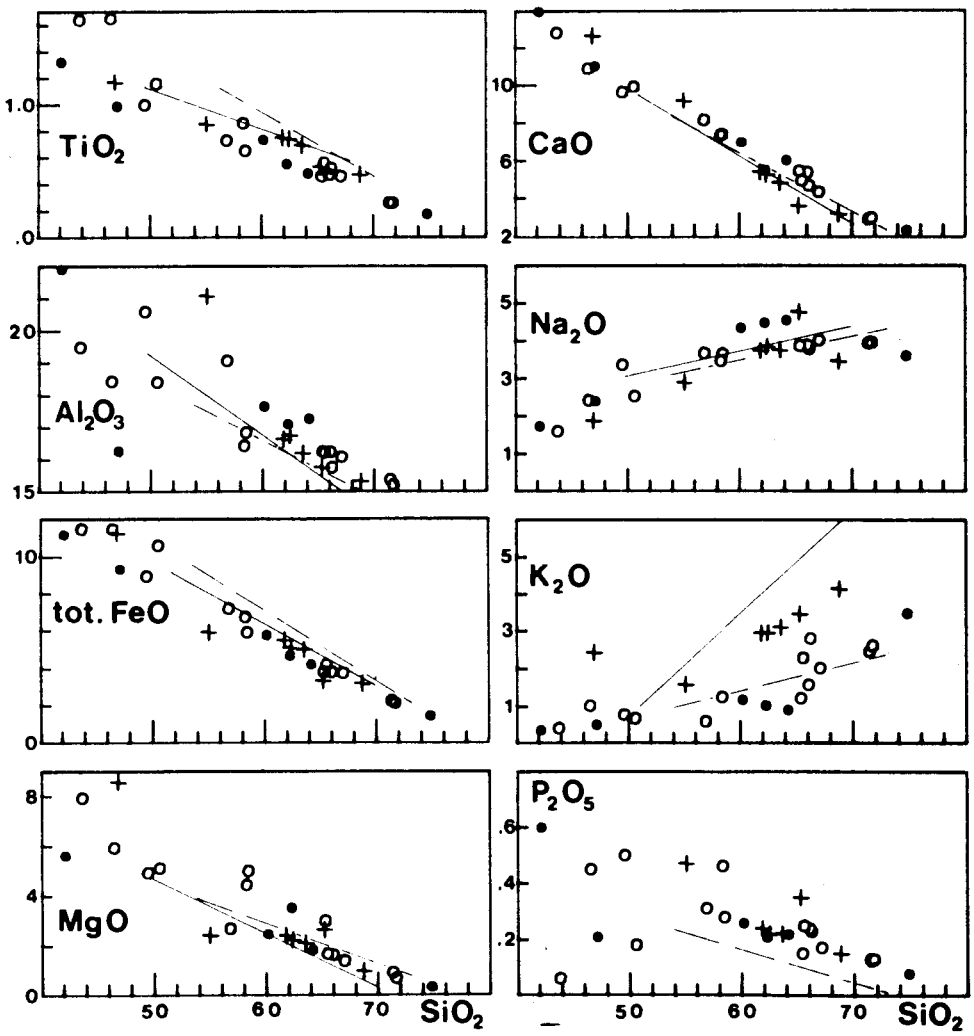

Key: + YUAT NORTH BATHOLITH
o YUAT SOUTH BATHOLITH
• KARAWARI BATHOLITH

FIG. 19 : TRACE ELEMENT VARIATIONS FOR YUAT NORTH, YUAT SOUTH, AND KARAWARI BATHOLITHS.

symbols as in Fig. 18.; trace elements in ppm in this and subsequent similar diagrams.

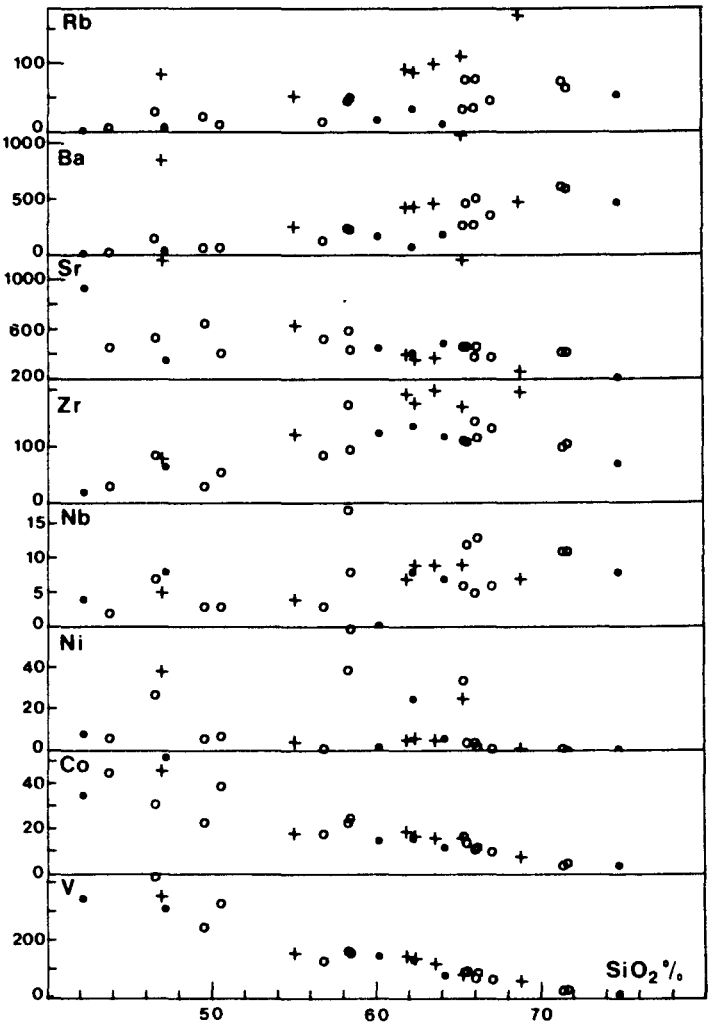

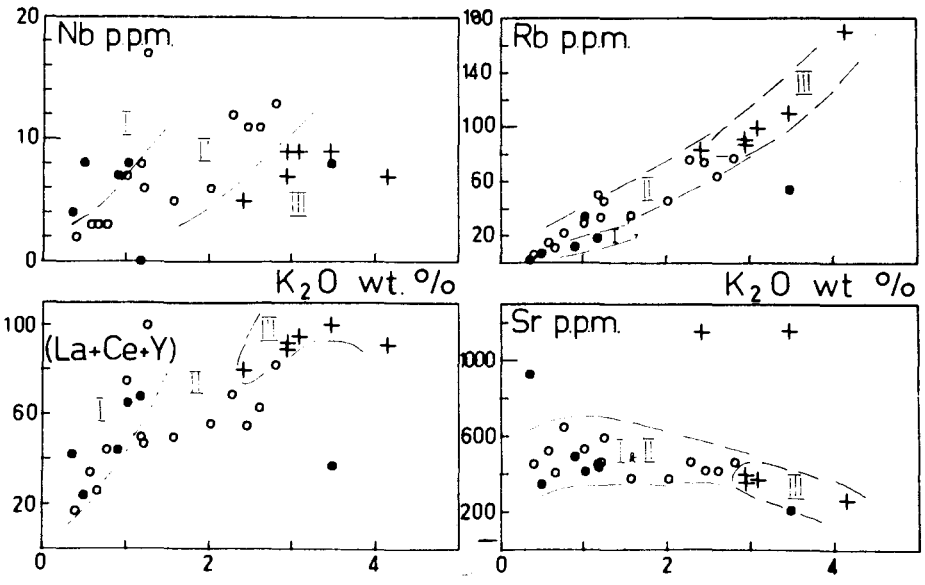

Note: these fields are drawn on later, similar plots for comparison.

are comparable.

More generally, the trends of the trace element contents in the high-K batholithic rocks are quite regular. Both rubidium and barium increase with increasing SiO_2, while strontium, nickel, cobalt, and vanadium gradually decrease. Zirconium and niobium show gentle increases with SiO_2 to reach a maximum at about 60% SiO_2. Both thorium and uranium are positively correlated with SiO_2, and range 5-20 and 2-5 ppm respectively, maintaining a Th/U ratio of approximately 4/1. Gallium is positively correlated with Al_2O_3, but lies within a narrow range of 16-23 ppm.

Variations of Nb, Rb, La+Ce+Y, and Sr *versus* K_2O are plotted in the lower part of Fig. 19. On these diagrams, fields are depicted for the Karawari (low- to normal-K), Yuat South (normal-K), and Yuat North (high-K) batholithic suites. The suites are separated with varying degrees of clarity, as in the major element plots. The best separation is achieved on the plot of Nb *versus* K_2O. The fields are drawn on subsequent similar graphs for comparison purposes.

In conclusion, it is apparent that the abundance of K-feldspar and biotite in the intrusive rocks of the Yuat North Batholith is reflected in moderate to high K_2O contents (3.1% K_2O at 65% SiO_2) and high levels of associated trace elements (Rb, Ba, rare earth elements). Similar but more accentuated patterns are observed in the shoshonitic rocks of the small stock to the south of the batholith. These rocks are more magnesian than the batholithic diorites, and carry higher levels of associated trace elements, especially nickel.

4.3 GEOCHEMISTRY OF THE YUAT SOUTH BATHOLITH

Fig. 18 reveals the wide compositional range and considerable scatter of data for specimens from the Yuat South Batholith. A total of 14 specimens are uniformly distributed through a range of 43-72% SiO_2.

Calc-alkaline features of the suite are apparent on the MFA and Harker-type diagrams. The flat trend toward alkali enrichment on the MFA plot is accompanied by scatter among the more basic rocks of the suite. This scatter of data is also present in the Harker diagrams, although the usual positive correlations of Na_2O and K_2O with SiO_2, and negative correlations of TiO_2, Al_2O_3, total FeO, MgO, CaO, and P_2O_5 with SiO_2, still remain obvious. Straight-line trends are apparent for all major element variations, except for Na_2O which assumes a negative correlation at high levels of SiO_2. The best-defined trends against

SiO_2 are those of total FeO (correlation coefficient (r) =-0.988) and of CaO (r=-0.994).

In comparison with the high-K Yuat North Batholith suite, the normal-K calc-alkaline suite of the Yuat South Batholith displays lower TiO_2 and K_2O, and higher CaO. These differences are consistent with the presence of titaniferous magnetite and higher modal proportions of K-feldspar and biotite in the Yuat North suite.

Most of the Yuat South major element trends closely follow those of the normal-K calc-alkaline North Bainings suite. One exception is P_2O_5, which reaches higher levels of concentration in the Yuat South suite.

Trace element variations are shown in Fig. 19, and the features of distribution are essentially those of the Yuat North Batholith. Significantly lower rubidium and barium correlate with lower K_2O in the suite. Zirconium is impoverished and strontium enriched in the Yuat South suite compared with the Yuat North suite. The zirconium trend achieves a maximum of 140 ppm at approximately 67% SiO_2. The late diorite porphyries, which are relatively Mg-rich, also show enrichment in nickel (20-30 ppm). Thorium ranges 2-14 ppm, while uranium ranges 0-3 ppm. The main batholithic granodiorites have 10 ppm thorium and 2-3 ppm uranium, giving Th/U ratios of approximately 4/1. Gallium correlated positively with Al_2O_3, and varies within the narrow limits of 17-24 ppm.

In the lower part of Fig. 19, the field of normal-K calc-alkaline rocks of the Yuat South Batholith is quite well-defined on the Nb *versus* K_2O plot, while on the other plots of Rb, La+Ce+Y, and Sr *versus* K_2O there is some overlap with the field of low- to normal-K rocks of the Karawari Batholith.

4.4 GEOCHEMISTRY OF THE KARAWARI BATHOLITH

The six specimens from the Karawari Batholith span a silica range of 43-76% SiO_2, but there are wide gaps between 48-60% and 65-75%. Fig. 18 shows that the few specimens available define a calc-alkaline suite with the usual alkali enrichment trend on the MFA diagram, and a low-to normal-K content throughout the silica range. There is overlap with the normal-K calc-alkaline suite of the Yuat South Batholith on many of the major element plots.

However, there are some differences which should be noted. Apart from the somewhat lower K_2O content, the suite possesses higher Al_2O_3 and Na_2O at intermediate SiO_2 levels.

Among the trace elements (see Fig. 19), rubidium and barium are lower in the Karawari suite than in the higher-K suites, but the other trace elements are present in comparable abundances. Both thorium (1-8 ppm) and uranium (less than 2 ppm) are present in low concentrations, but give Th/U ratios of approximately 4/1 at intermediate silica levels. Gallium displays its usual close correlation with Al_2O_3, and ranges 14-25 ppm.

In the lower part of Fig. 19, fields are drawn for the Karawari suite on each of the plots Nb, Rb, La+Ce+Y, and Sr *versus* K_2O. In the plot of Rb *versus* K_2O, low rubidium values give high K/Rb ratios of 550, compared with 300 and 260 for the Yuat South and Yuat North suites respectively (compare Jakes & White, 1970).

4.5 GEOCHEMISTRY OF THE WALE, LAMANT, SEKAU, AND MT. MICHAEL STOCKS

These four stocks are treated together for convenience. All of them have only a limited sample coverage: 5 specimens from the Sekau Stock, 4 from the Mt. Michael Stock, 3 from the Wale Stock, and 2 from the Lamant Stock.

Major element variations are shown in Fig. 20. There is wide scatter of data for the Sekau Stock. The mafic cumulative rocks (hornblende gabbros, hornblendites) are predictably high in MgO and CaO, and low in Al_2O_3. The unusually high K_2O content of these rocks is explained by the presence of fine flakes of sericite within plagioclase. On the K_2O *versus* SiO_2 plot, one dioritic rock with abundant K-feldspar and biotite (DRM058) lies near the high-K trend of the Central and South Bainings suite, while a gabbro and a diorite with hornblende and little or no K-feldspar (DRM062, 059) lie very close to the trend of the normal-K North Bainings suite. This effectively demonstrates the diverse chemical affinities of rocks of the Sekau Stock.

The same plot of K_2O *versus* SiO_2 also demonstrates the presence of both high- and normal-K rocks within the Mt. Michael Stock. However, the relatively high Al_2O_3, CaO, and Na_2O of these rocks indicate that the abundant phenocrystic plagioclase is cumulative in origin.

Little can be said for the few specimens from the Wale and Lamant stocks, except that features such as high MgO and CaO, and low Al_2O_3 point to a cumulative origin for these mafic rocks.

Trace element variations for the four stocks are shown in Fig. 21. Rubidium, barium, zirconium, and niobium closely follow K_2O, with the high-K specimens of the Sekau and Mt. Michael stocks possessing

FIG. 20 : MAJOR ELEMENT VARIATIONS FOR WALE, LAMANT, SEKAU, AND MOUNT MICHAEL STOCKS.

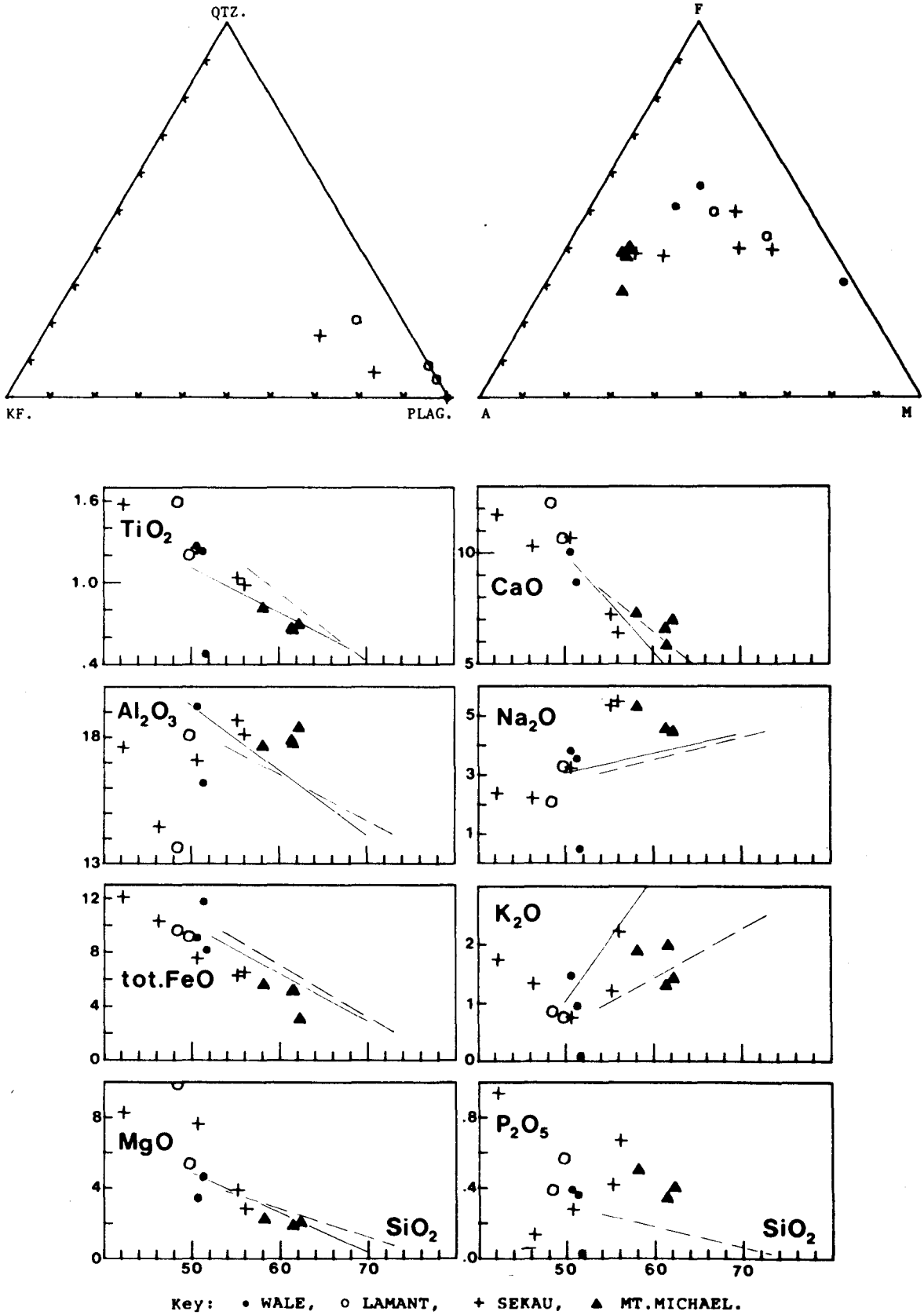

FIG. 21 : TRACE ELEMENT VARIATIONS FOR WALE, LAMANT, SEKAU, AND MOUNT MICHAEL STOCKS.

symbols as in Fig. 20.

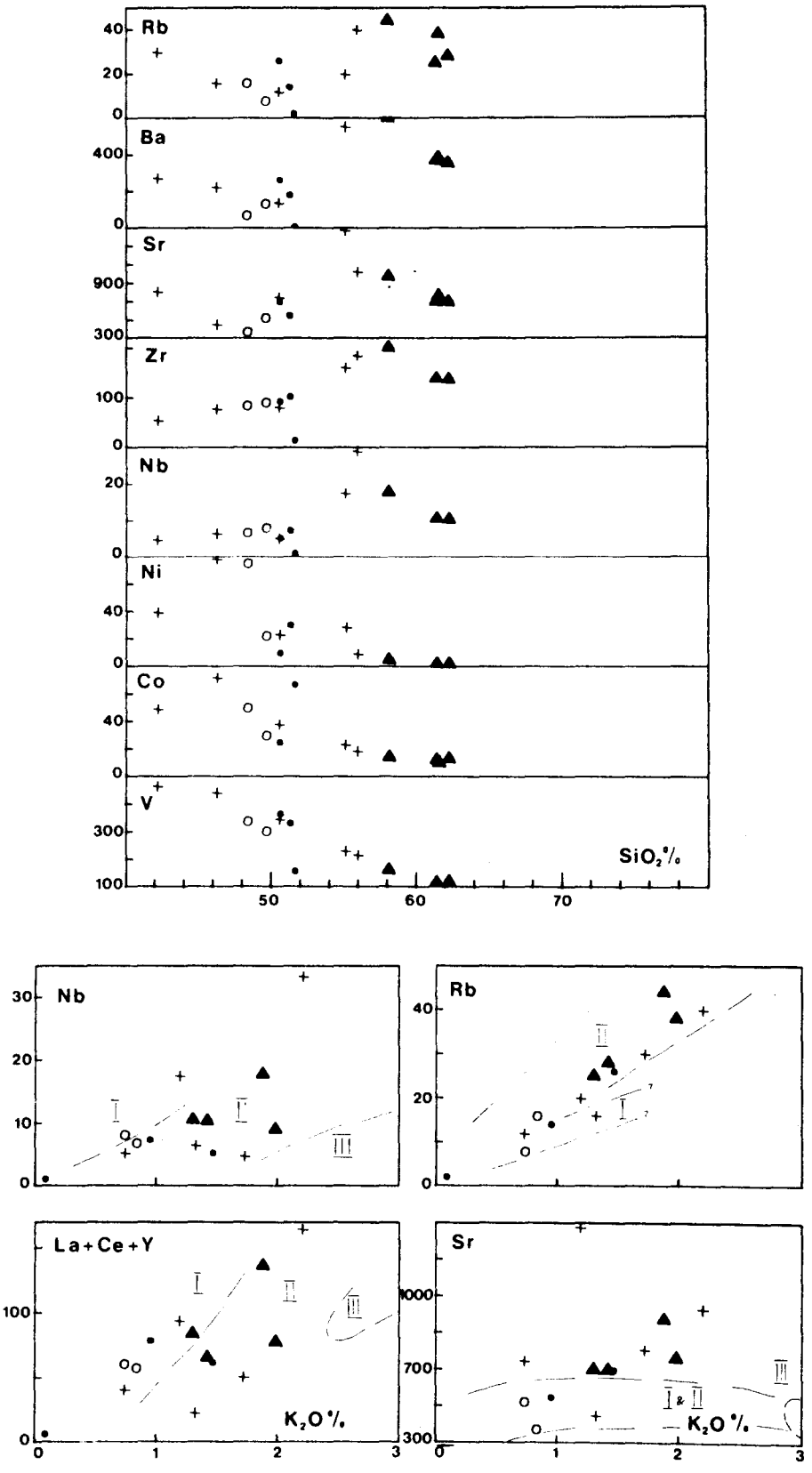

Note: fields from Fig. 19.

higher levels of these elements than the lower-K rocks of those suites. The mafic cumulative rocks of the Wale, Lamant, and Sekau stocks predictably display high but variable concentrations of the ferromagnesian trace elements (nickel, cobalt, and vanadium).

In the lower part of Fig. 21, variations of Nb, La+Ce+Y, Rb, and Sr *versus* K_2O are depicted. However, the cumulative origin of many of the mafic rocks and of the prophyritic rocks of Mt. Michael render comparison difficult with the superimposed fields of low-, normal- and high-K suites. The abundance of plagioclase phenocrysts in the Mt. Michael suite is reflected in high Sr/K_2O.

Both thorium (12 ppm) and uranium (3 ppm) are highest in the higher-K rocks of the Sekau and Mt. Michael stocks. Elsewhere, these elements are present in only small amounts. Gallium also tends to be slightly higher in the higher-K rocks, but generally maintains a uniform concentration of approximately 20 ppm.

4.6 GEOCHEMISTRY OF THE MOUNT PUGENT STOCK

Only two specimens are available from the Mount Pugent Stock. In Table 9, an average major and trace element analysis is given for the microsyenite, together with mineralogical and C.I.P.W. normative characteristics. Comparative data is provided for the high-K diorite of the Yuat North Batholith, and for a syenite from southeastern Papua (Smith, 1971).

In both major and trace element composition, the quartz-free microsyenites of the Mount Pugent Stock differ markedly from the other intrusive rocks of the Western Highlands. Compared with the high-K diorites of the Yuat North Batholith, the microsyenites are characterized by:

1. very high total alkalis (11.8%, compare 6.7%)
2. low TiO_2 (0.3%, cf. 0.7%); MgO (0.3%, cf. 2.3%); CaO (0.3%, cf. 5.1%)
3. very much higher levels of La+Ce+Y (320 ppm, cf. 95 ppm); and La, Ce, and Y individually.

The mineralogy and major element chemistry of the Mount Pugent microsyenites compare favourably with a syenite from a near-saturated suite of mid-Miocene intrusive rocks in southeastern Papua (Smith, 1971). Both syenites contain normative nepheline, hypersthene, and olivine. However, the Mount Pugent rocks are much lower in strontium and barium, and lower in copper, nickel, and vanadium.

TABLE 9: COMPARISON OF MT PUGENT MICROSYENITE WITH OTHER INTRUSIVE ROCKS OF P.N.G.

	Microsyenite, Mt Pugent (Ave of 2 ± 1SD)	Syenite, southeast Papua (Smith, 1971)	High-K diorite, Yuat North batholith (Ave of 3, ± 1SD)
Major Element Chemistry:			
SiO_2	61.8 ± .1	64.2	62.1 ± .7
TiO_2	.37 ± .00	.25	.72 ± .04
Al_2O_3	17.9 ± .1	17.3	16.4 ± .3
Fe_2O_3	2.37 ± .04	.85	2.4 ± .1
FeO	2.79 ± .04	1.5	3.0 ± .2
MnO	.18 ± .01	.03	.10 ± .00
MgO	.32 ± .02	.95	2.3 ± .2
CaO	1.98 ± .01	1.4	5.1 ± .3
Na_2O	6.66 ± .01	7.25	3.74 ± .05
K_2O	5.10 ± .01	5.55	2.97 ± .08
P_2O_5	.20 ± .01	.1	.23 ± .01
S	.05 ± .01	-	.07 ± .01
H_2O+	.70 ± .03	.2	.7 ± .1
H_2O-	.29 ± .01	1.14	.2 ± .1
CO_2	.14 ± .06	.03	.2 ± .1
Total	100.85	99.75	100.23
Trace Element Chemistry:			
Sr	194 ± 2	>1000	376 ± 20
Ba	557 ± 21	>2000	440 ± 18
La	96 ± 3	< 100	21 ± 2
Y	49 ± 2	< 40	27 ± 2
Zr	814 ± 107	150	190 ± 11
Cu	4 ± 1	24	67 ± 26
Ni	<2	18	5 ± 1
V	6 ± 1	105	135 ± 13
Mineralogy:			
	K-feldspar plagioclase aegerine augite biotite oxides zircon	K-feldspar aegerine augite hornblende (pale green) oxides zircon ± plagioclase ± nepheline	quartz K-feldspar plagioclase hornblende biotite oxides zircon, apatite ± clinopyroxene, orthopyroxene
CIPW Norm Characteristics:			
	Ne, Di, Ol	Ne, Di, Ol	Q, Di, Hy

With high levels of thorium (20 ppm), uranium (4 ppm), and gallium (34 ppm), the Mount Pugent microsyenites again differ markedly from the other Miocene intrusive rocks of the New Guinea Mobile Belt.

4.7 GEOCHEMISTRY OF THE FRIEDA RIVER AND OK TEDI INTRUSIVE COMPLEXES

Major element variations for the Frieda River and Ok Tedi intrusive complexes are presented in Fig. 22. From the K_2O *versus* SiO_2 plot it can be seen that the Frieda River suite closely follows the normal-K trend of the North Bainings suite, while unaltered dioritic rocks from Ok Tedi lie very near the high-K trend of the South and Central Bainings suite. Unfortunately, fresh rocks from both complexes span only small silica ranges. One specimen from Frieda River (DRM003) contains abundant phenocrystic and groundmass hornblende, and consequently is MgO-rich and Al_2O_3-poor relative to the main Frieda trend.

The major element variation diagrams reveal that the Frieda River and Ok Tedi suites are similar to the extent that both suites possess higher Al_2O_3, Na_2O, and P_2O_5, and lower TiO_2 and total FeO, when compared with the Bainings calc-alkaline trends. At higher silica levels, anomalous trends occur in the Ok Tedi altered specimens.

Hydrothermal alteration in both suites has resulted in a variety of major element changes. In altered rocks of the Frieda suite, lower CaO and Na_2O correspond with destruction of plagioclase, while higher K_2O corresponds with the formation of hydrothermal biotite in areas of potassic alteration. The effects of potassic alteration in the Ok Tedi suite are more variable and pronounced. Several altered specimens, however, lie on continuations of variation trend lines originating from the fresh, high-K dioritic rocks. The more heavily altered specimens plot away from the trend lines. At higher silica levels (>70% SiO_2), anomalous trends include increasing TiO_2, total FeO, and MgO, and rapidly decreasing Al_2O_3 and Na_2O.

Trace element variations are presented in Fig. 23. Much higher rubidium, barium, and strontium in the Ok Tedi suite compared with the Frieda suite is in accord with the high-K character of the former. However, trend differences are apparent. While rubidium increases with SiO_2 in the Ok Tedi suite, it is present in lower, more uniform concentrations in the Frieda suite (except for one specimen displaying potassic alteration). Barium is uniformly high in the Ok Tedi rocks, but increases with SiO_2 in the Frieda suite. While strontium increases slowly with SiO_2 in the Frieda suite, it decreases rapidly in the Ok Tedi suite, especially

FIG. 22 : MAJOR ELEMENT VARIATIONS FOR FRIEDA RIVER AND OK TEDI INTRUSIVE COMPLEXES.

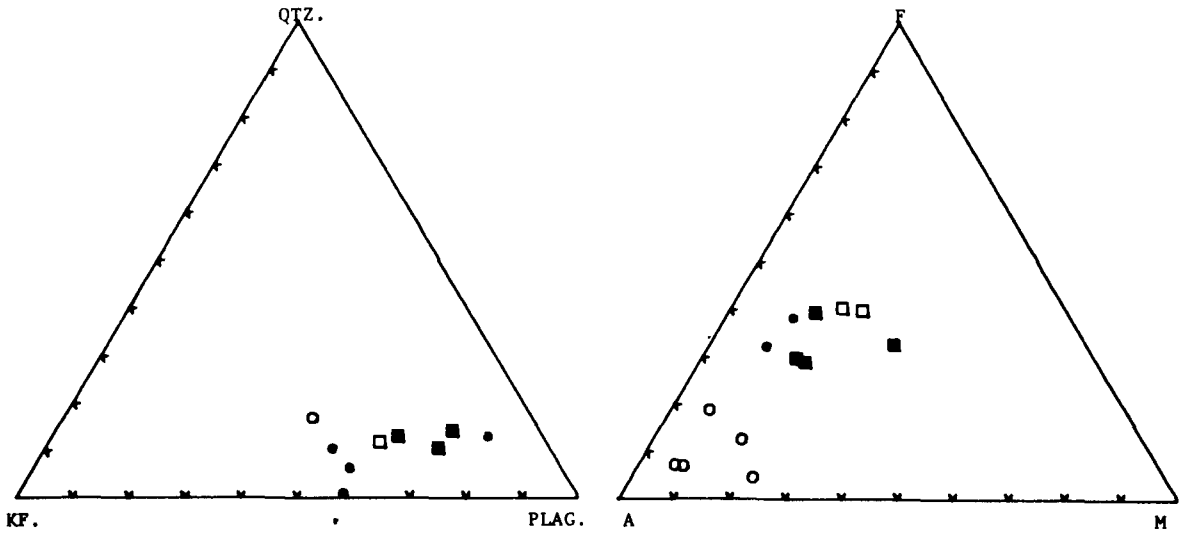

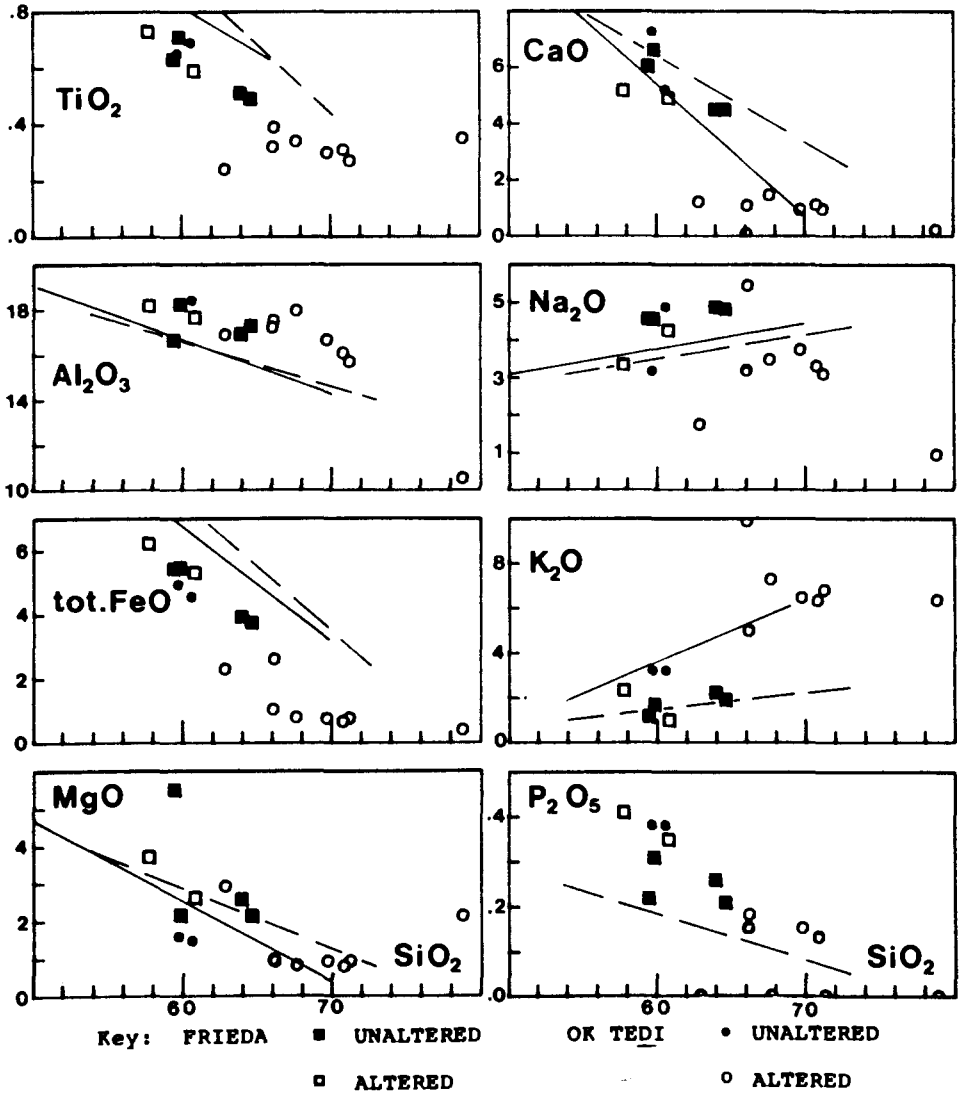

FIG. 23 : TRACE ELEMENT VARIATIONS FOR FRIEDA RIVER AND OK TEDI INTRUSIVE COMPLEXES.

symbols as in Fig. 22.

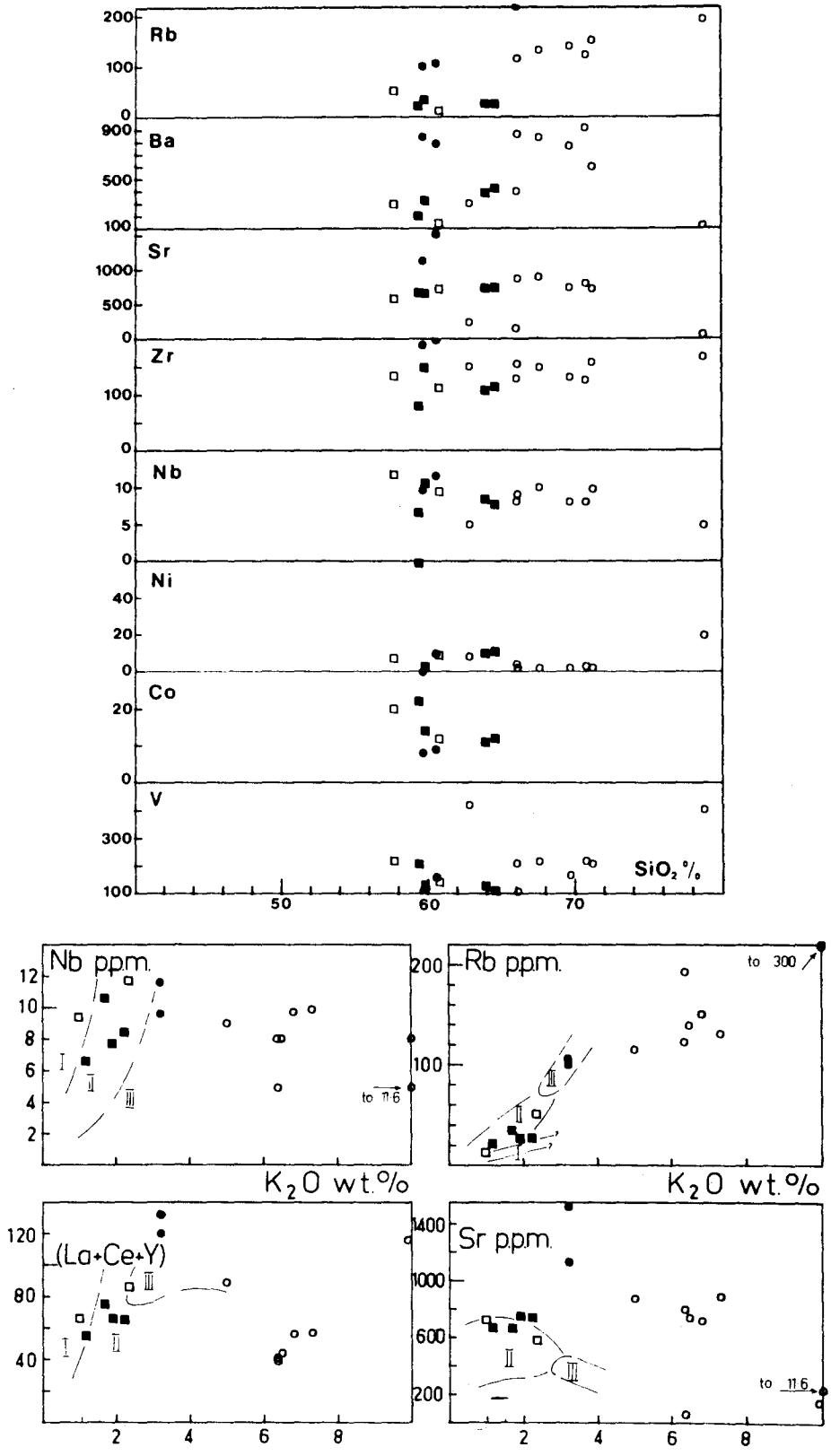

Note: fields from Fig. 19.

in the altered rocks.

Zirconium is consistently higher in the Ok Tedi suite, but niobium occurs at similar levels in both suites. The ferromagnesian trace elements (nickel, cobalt, and vanadium) are uniformly low in both suites. Predictably, the more mafic diorite porphyry from Frieda River possesses high nickel and slightly higher cobalt. Insufficient material was available to determine cobalt for the altered Ok Tedi specimens, but it would be present in only very small amounts. Vanadium decreases regularly in the Frieda suite, but increases markedly in the altered high-SiO_2 rocks from Ok Tedi.

For both suites, thorium ranges up to 11 ppm, while uranium is low at 1-3 ppm. Fresh specimens have Th/U ratios of 5/1 (Frieda) to 11/1 (Ok Tedi). Data for gallium are only available for the Frieda suite, in which there is a uniform concentration of 22 ppm.

CHAPTER 5 GEOCHEMISTRY OF INTRUSIVE ROCK SUITES, P.N.G. ISLANDS AND SOLOMON ISLANDS

5.1 GEOCHEMISTRY OF THE PLESYUMI INTRUSIVE COMPLEX, NEW BRITAIN

Major element variations for the Plesyumi Intrusive Complex are shown in Fig. 24. The ten specimens from the complex are distributed regularly through the range 50-70% SiO_2. The plot of K_2O *versus* SiO_2 shows that the majority of the specimens closely follow the normal-K trend of the North Bainings suite, while two specimens (DRM137,139) straddle the high-K trend of the Central and South Bainings suite. These two rocks are high-K diorites, with more abundant K-feldspar and biotite compared with the normal-K diorites and granodiorites. On the other major element plots, the high-K Plesyumi rocks show consistent differences compared with the normal-K rocks: lower Al_2O_3, MgO, and CaO, and higher Na_2O and P_2O_5.

The rocks belonging to the normal-K Plesyumi suite define straight line trends on all of the major element variation diagrams. Two groups of rocks, however, introduce scatter into the suite. At the mafic end, coarse-grained gabbroic rocks with variable TiO_2, lower Al_2O_3, Na_2O, and P_2O_5, and higher MgO, are probably of cumulative origin. At the felsic end of the normal-K trend, hydrothermal alteration has resulted in certain changes in the granodiorite (DRM133) and dacite porphyry (DRM142) from the Plesyumi prospect area. Both of these rocks have suffered propylitic alteration, resulting in higher Al_2O_3 and Na_2O, and lower K_2O. Other major elements such as TiO_2 and P_2O_5 appear to be little affected. In addition to the gross effects noted above, the altered granodiorite contains lower MgO and slightly higher CaO compared with the Plesyumi normal-K trend.

There are striking similarities in major element trends of the high-K and normal-K calc-alkaline suites from Plesyumi and the Bainings Mountains (see Fig. 24). The high-K suites from these two regions of New Britain possess similar levels of TiO_2, Al_2O_3, total FeO, MgO, CaO, K_2O, and P_2O_5. The normal-K suites display identical levels of TiO_2, MgO, CaO and K_2O, but the Plesyumi normal-K suite possesses higher Al_2O_3, Na_2O, and P_2O_5, and lower total FeO, compared with the North Bainings normal-K suite. Although the Gazelle Peninsula is approximately 250 km distant from the Plesyumi region of central New Britain, and although there may be an 8 m.y. interval between emplacement of the intrusive masses in the two regions (Page & Ryburn, 1973), the remarkably similar major element trends imply

FIG. 24 : MAJOR ELEMENT VARIATIONS FOR PLESYUMI INTRUSIVE COMPLEX.

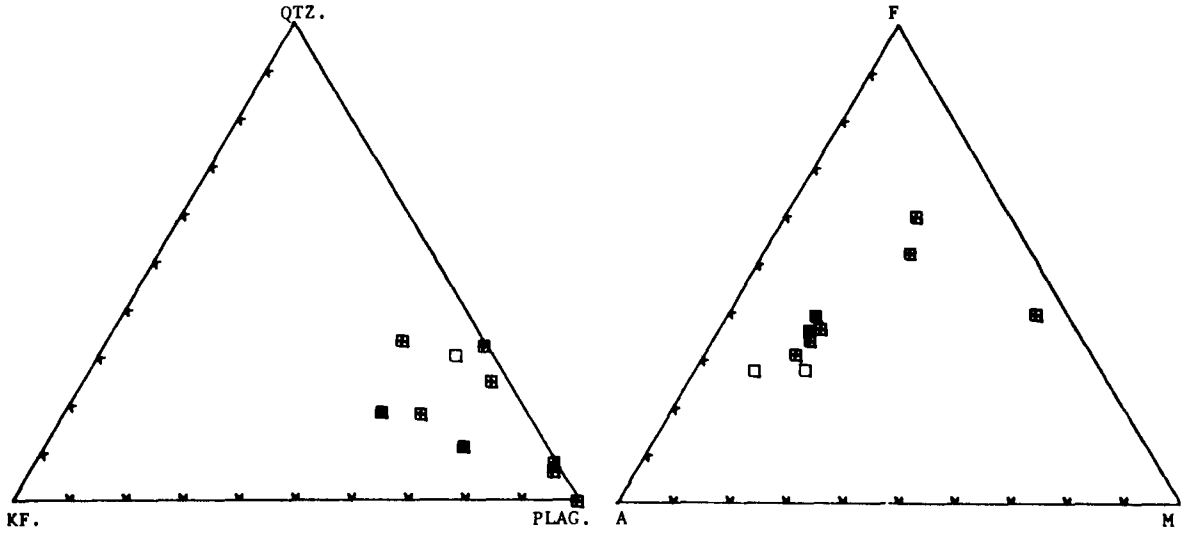

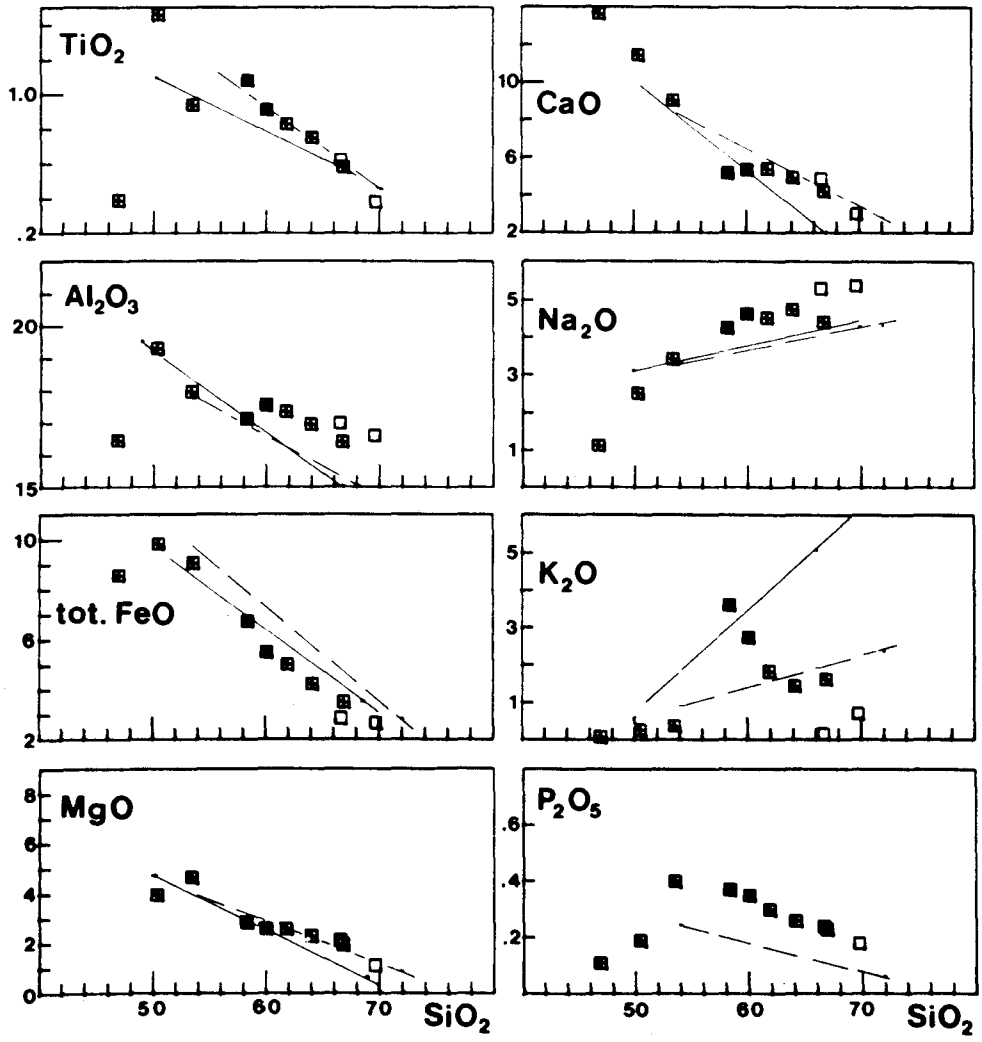

Key: ⊞ Normal-K suite

■ High-K suite

□ Altered

that: 1. source regions of similar composition existed beneath much of New Britain in Tertiary times, and

2. similar processes were operative during evolution of these calc-alkaline rock suites.

Some unpublished major element analyses of New Britain intrusive rocks are available (Aust. Bur. Min. Res., unpub. data; R. Hine, pers. commun.), and these data are compared with the new data from Plesyumi and the Bainings trends in Fig. 25. The plot of K_2O *versus* SiO_2 reveals that the majority of New Britain intrusive rocks are less potassic than the normal-K North Bainings trend. Two analyses from the Plesyumi area and one from the Sai River intrusive body (east central New Britain) lie near the high-K Bainings trend and the new Plesyumi data. In the plot of CaO *versus* SiO_2, the higher-K rocks are consistently less calcic and plot near the high-K Bainings trend, while the majority plot on a trend which is a little more calcic than the North Bainings trend.

These plots illustrate two points:

1. intrusive complexes possess unique elemental variation trends (e.g., Plesyumi Intrusive Complex), and

2. the unique trends of different intrusive complexes from New Britain vary within a limited range.

Trace element variations within the Plesyumi rocks are given in Fig. 26. The high-K specimens are higher in rubidium, barium, zirconium, and niobium compared with the normal-K suite, and are lower in strontium and nickel. Cobalt and vanadium occur in similar concentrations in the high-K and normal-K suites, and are negatively correlated with silica.

Also plotted on Fig. 26 are unpublished trace element data for intrusive rocks from the Kulu River area of west central New Britain (R. Hine, pers. commun., 1975). Other than the present study, these are the only available trace element data for New Britain intrusive rocks. The Kulu granitic rocks, being somewhat less potassic than the normal-K Plesyumi trend, are slightly lower in rubidium and niobium, and much lower in strontium. Zirconium and nickel are present in similar concentrations in the Plesyumi normal-K suite and Kulu suite.

The comparison of major element data for various New Britain intrusive rock suites showed that K_2O and CaO were most effective discriminators between suites. However, strontium discriminates even more effectively, being approximately 400 ppm higher at 60% SiO_2 in the

Fig. 25 : Combined New Britain data

□ Plesyumi normal-K suite

■ Plesyumi high-K suite

\+ Other data (unpub.)

Gazelle regressions for comparison.

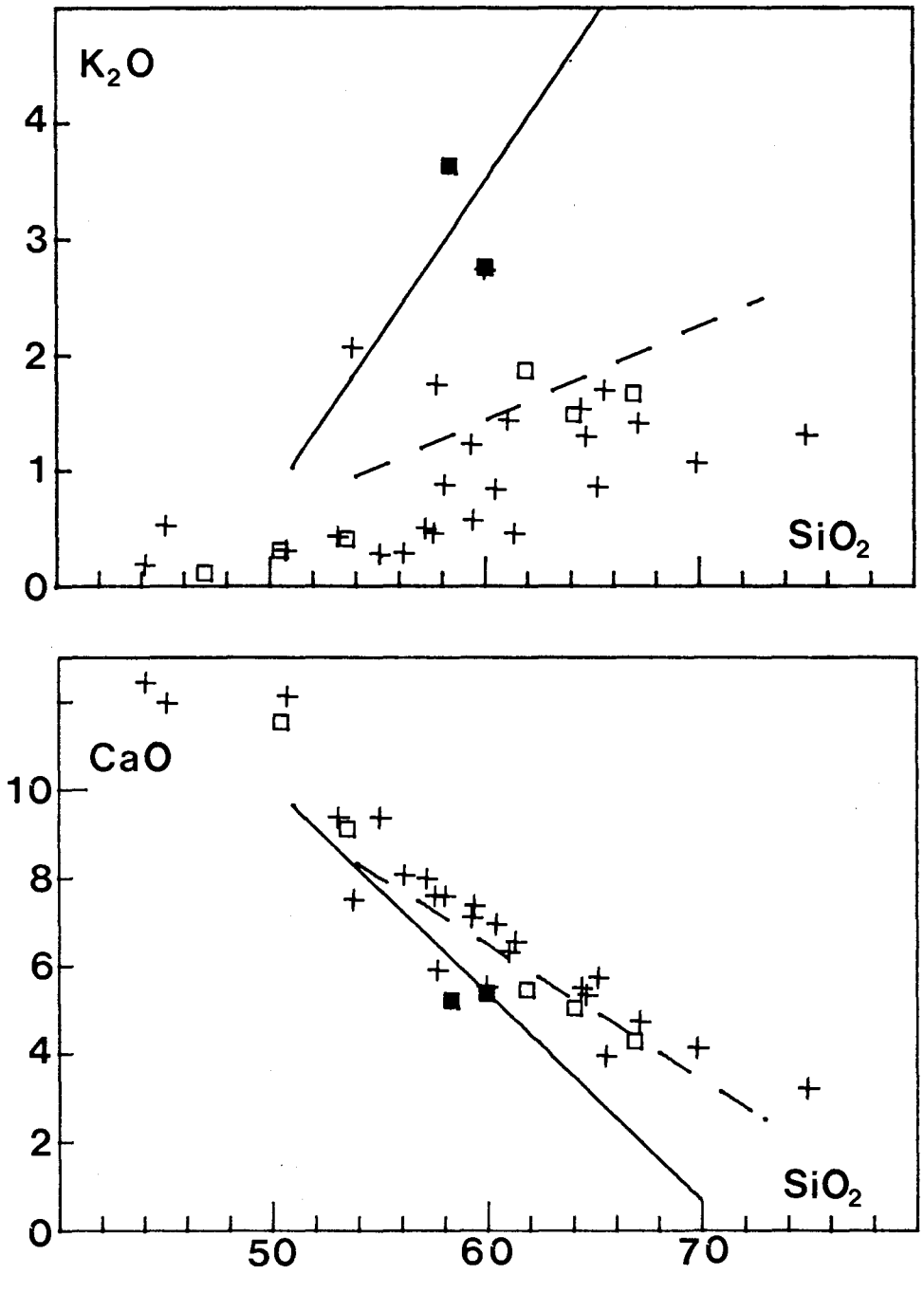

FIG. 26 : TRACE ELEMENT VARIATIONS FOR NEW BRITAIN INTRUSIVE ROCKS.
Filled squares, Plesyumi normal-K; crossed squares, Plesyumi high-K; open squares, Plesyumi altered rocks; crosses, Kulu low- to normal-K intrusive rocks (data of R.Hine, unpub.).

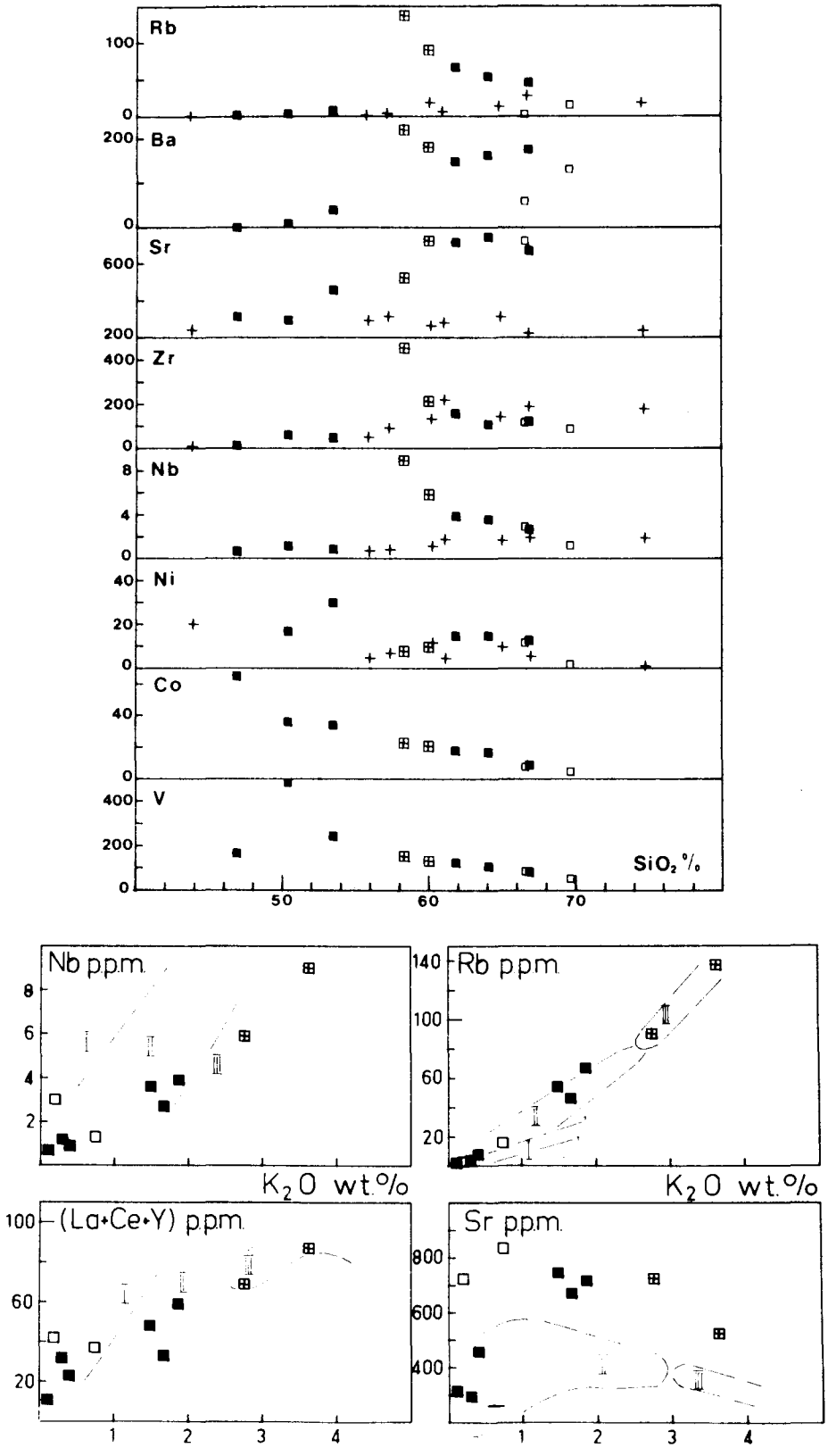

Note: fields from Fig. 19.

Plesyumi normal-K suite compared with the Kulu granitic suite.

New data for thorium and uranium for the Plesyumi suites reveal that both vary within small ranges and maintain Th/U ratios of between 3/1 and 5/1. Thorium is low and ranges 1-5 ppm, and is highest in higher-K and silicic rocks. Uranium maintains low concentrations of less than 2 ppm.

5.2 GEOCHEMISTRY OF THE MOUNT KREN INTRUSIVE COMPLEX, MANUS ISLAND

Major element variation diagrams for 13 specimens from the Mount Kren Intrusive Complex are presented in Fig. 27. Three mafic rocks cluster within a silica range of 52-55% SiO_2, while the dioritic rocks span a range of 59-63% SiO_2.

One of the mafic specimens (DRM116) is a hornblende micrograbbro xenolith from a high-K diorite host. The xenolith falls close to an extension of the dioritic trend on most of the major element plots, implying a genetic relationship between the xenolith and the dioritic rocks. The other two mafic specimens (DRM120, 113) are low-Si porphyritic microdiorites and are clearly different in origin. They both possess low Al_2O_3 and high MgO, due to the abundance of ferromagnesian minerals. Phenocrystic pyroxene in DRM113 is probably cumulative. On the plot of K_2O *versus* SiO_2, the rock displays the highest K-content of all the Mount Kren intrusive rocks.

The dioritic rocks from Mount Kren fall between the normal-K and high-K Bainings trends on the K_2O *versus* SiO_2 plot. The single specimen of hornblende-quartz diorite (DRM112) is distinct from the high-K diorites in containing much lower K_2O and higher CaO. These differences are consistent with less modal K-feldspar and absence of biotite in the hornblende-quartz diorite.

The Mount Kren high-K suite has K_2O and CaO trends intermediate between the two Bainings suites. However, Fig. 27 reveals that the Mount Kren rocks possess lower TiO_2, total FeO, and higher Al_2O_3, MgO, and Na_2O than the Bainings suites. Levels of P_2O_5 in the Mount Kren rocks are comparable with those in the high-K Bainings suite.

All of the major element trends for the dioritic rocks show the usual positive correlations of Na_2O and K_2O with SiO_2, and negative correlations of TiO_2, Al_2O_3, total FeO, MgO, CaO, and P_2O_5 with SiO_2. However, there is some evidence for a change in the Na_2O trend, with Na_2O decreasing with increasing SiO_2 at higher silica levels.

Trace element variations are shown in Fig. 28. The high-K porphyritic microdiorite has appropriately high levels or rubidium and

FIG. 27 : MAJOR ELEMENT VARIATIONS FOR MOUNT KREN INTRUSIVE COMPLEX.

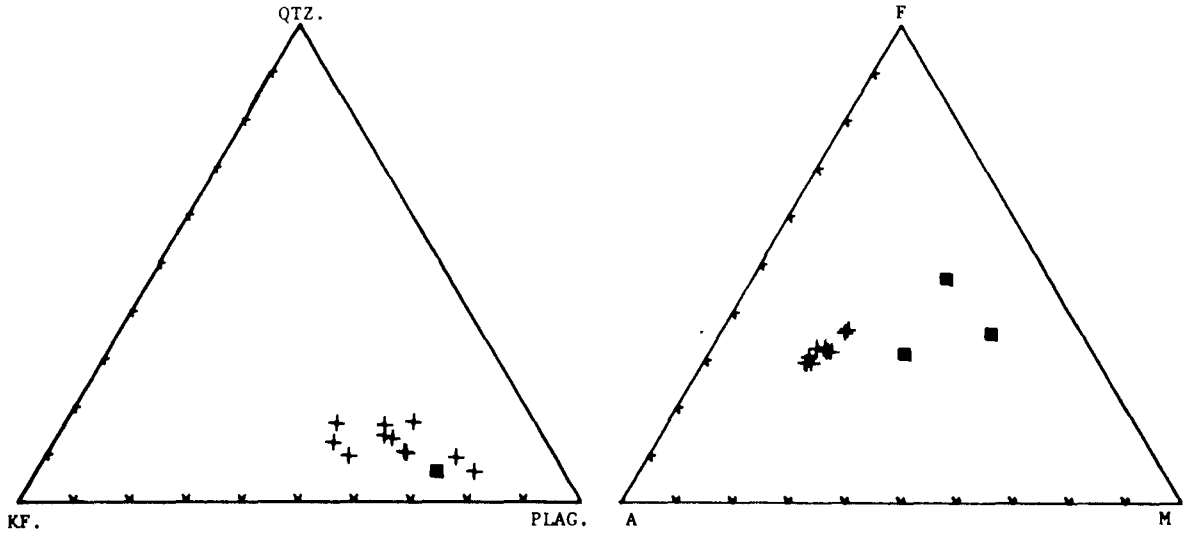

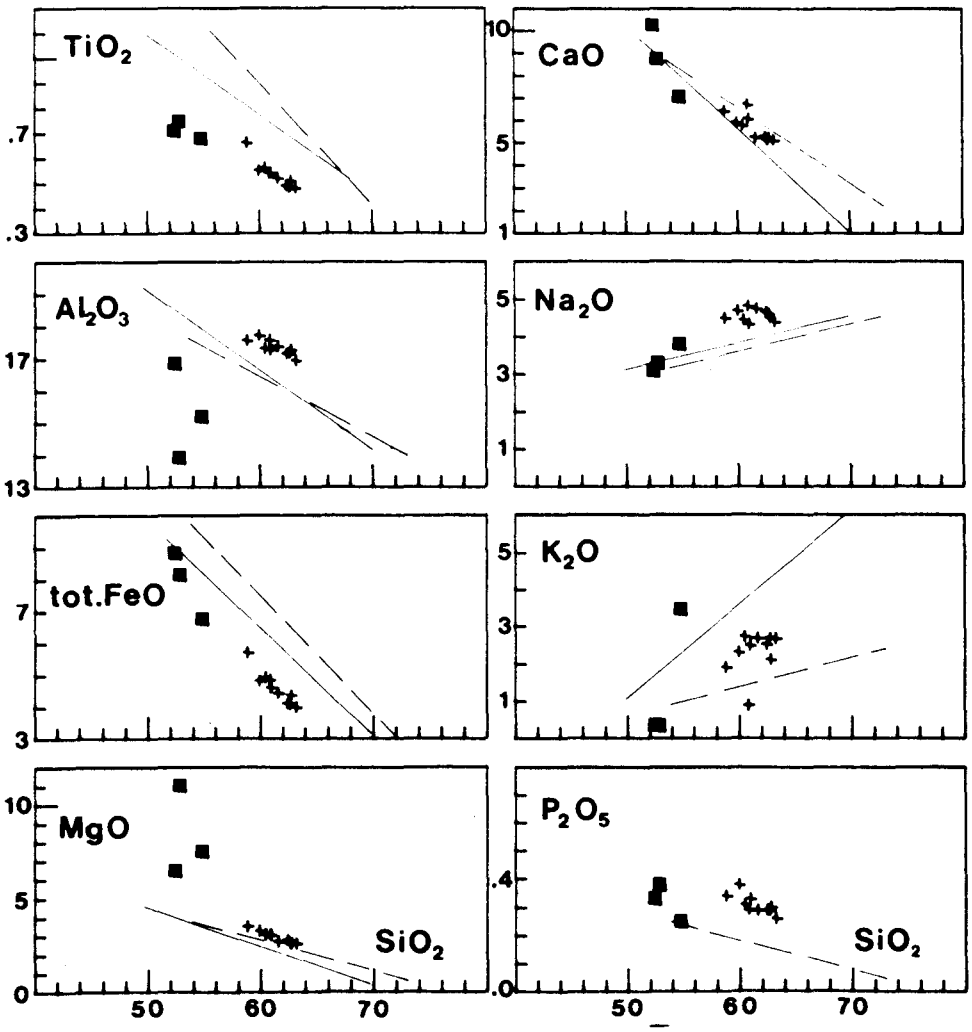

Key: + Dioritic rocks

■ Mafic rocks (dykes, xenoliths).

FIG. 28 : TRACE ELEMENT VARIATIONS FOR MOUNT KREN INTRUSIVE COMPLEX.

symbols as in Fig. 27.

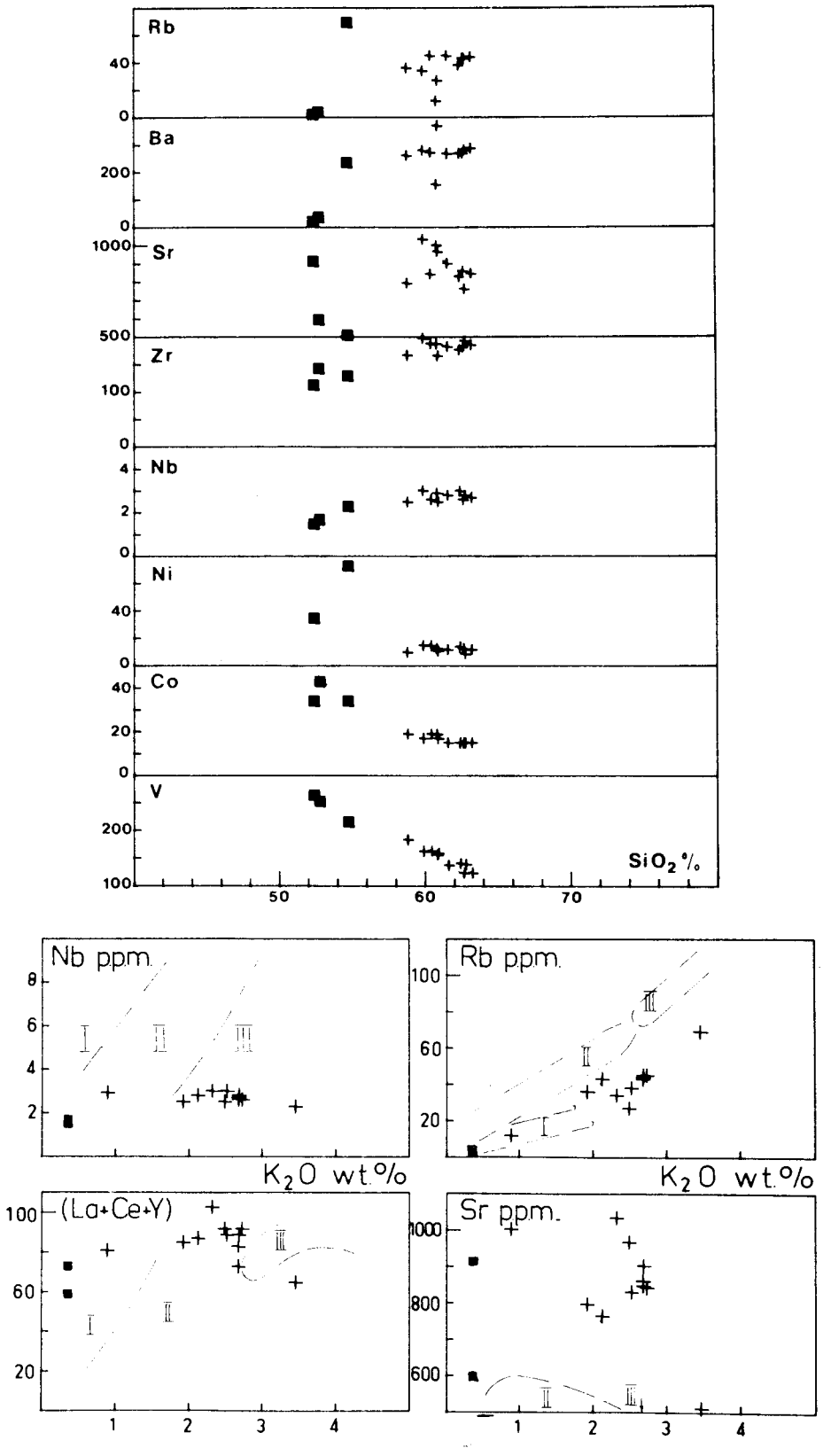

Note: fields from Fig. 19.

nickel, and very low strontium. The high-K dioritic rocks display constant levels of moderate rubidium and high barium, and very high strontium which decreases rapidly with increasing SiO_2. Zirconium maintains constant high values, whereas niobium is low. Nickel and cobalt also maintain low levels of concentration, but vanadium is high and decreases with increasing SiO_2.

Thorium ranges from 2 to 6 ppm, while uranium remains low at less than 2 ppm, giving Th/U ratios of 2/1 to 5/1.

In the lower part of Fig. 28, the moderate rubidium concentrations result in high K/Rb ratios of approximately 550, with the dioritic rocks falling below the normal- and high-K fields of the Western Highlands on the plot of Rb *versus* K_2O. On the plot of Nb *versus* K_2O, the Mount Kren suites fall within the appropriate Western Highlands fields, but at much lower levels of Nb. Similar levels of La+Ce+Y in the Mount Kren high-K suite are achieved at lower K_2O contents than for the high-K suite of the Western Highlands. On the plot of Sr *versus* K_2O, the very high levels of strontium in the Mount Kren suites distinguish them from the Western Highlands suites.

5.3 GEOCHEMISTRY OF THE LEMAU INTRUSIVE COMPLEX, NEW IRELAND

New major element data for 5 rocks from the Lemau Intrusive Complex are presented on Harker diagrams in Fig. 29, together with earlier data of Hohnen (1970), and Bainings regression lines for comparison. The available data covers a range of 48-68% SiO_2.

On first inspection, there appears to be considerable scatter in the data. The most mafic rocks (uralite gabbros) are low in TiO_2 and total FeO, and high in Al_2O_3, MgO, and CaO. These features are accounted for by the presence of cumulative mafic minerals and, in some cases, cumulative plagioclase.

The plot of K_2O *versus* SiO_2 reveals that the Lemau suite contains potassium in concentrations comparable with the normal-K North Bainings suite. Similar levels of the other major elements are also observed in the Lemau suite. One specimen at 65% SiO_2 (DRM131) is a microdiorite which is porphyritic in plagioclase and hornblende. The rock possesses lower TiO_2, total FeO, and K_2O, and higher Al_2O_3 compared with the other rocks of the Lemau suite in which pyroxene dominates the mafic mineral assemblage.

Differences between the porphyritic microdiorite and the pyroxene-bearing rocks are more apparent in a comparison of trace element abundances (see Fig. 30). Rubidium, barium, zirconium, and niobium are much lower in

FIG. 29 : MAJOR ELEMENT VARIATIONS FOR LEMAU INTRUSIVE COMPLEX.

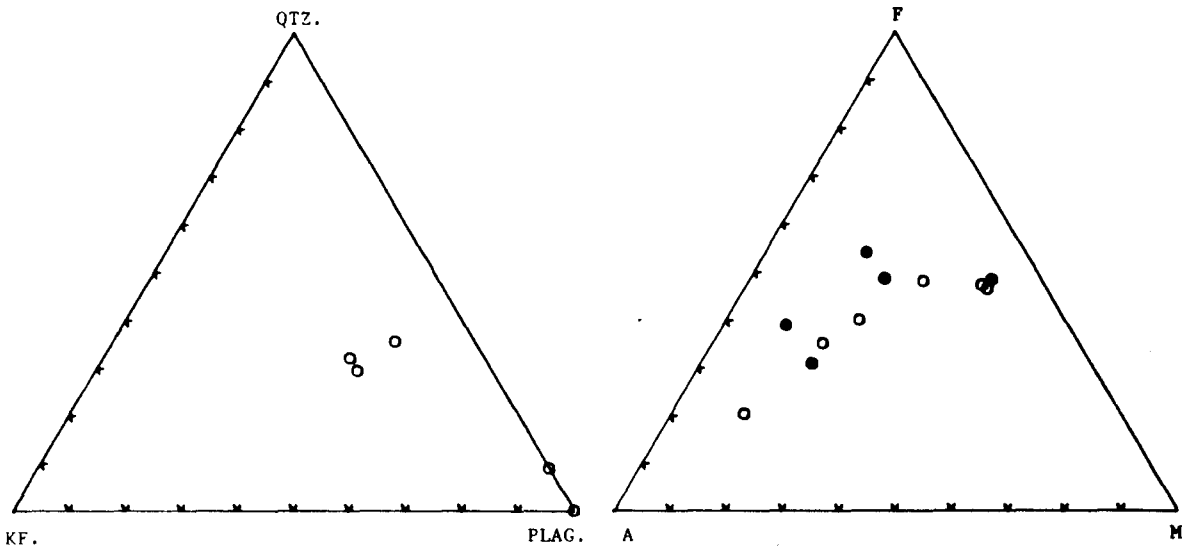

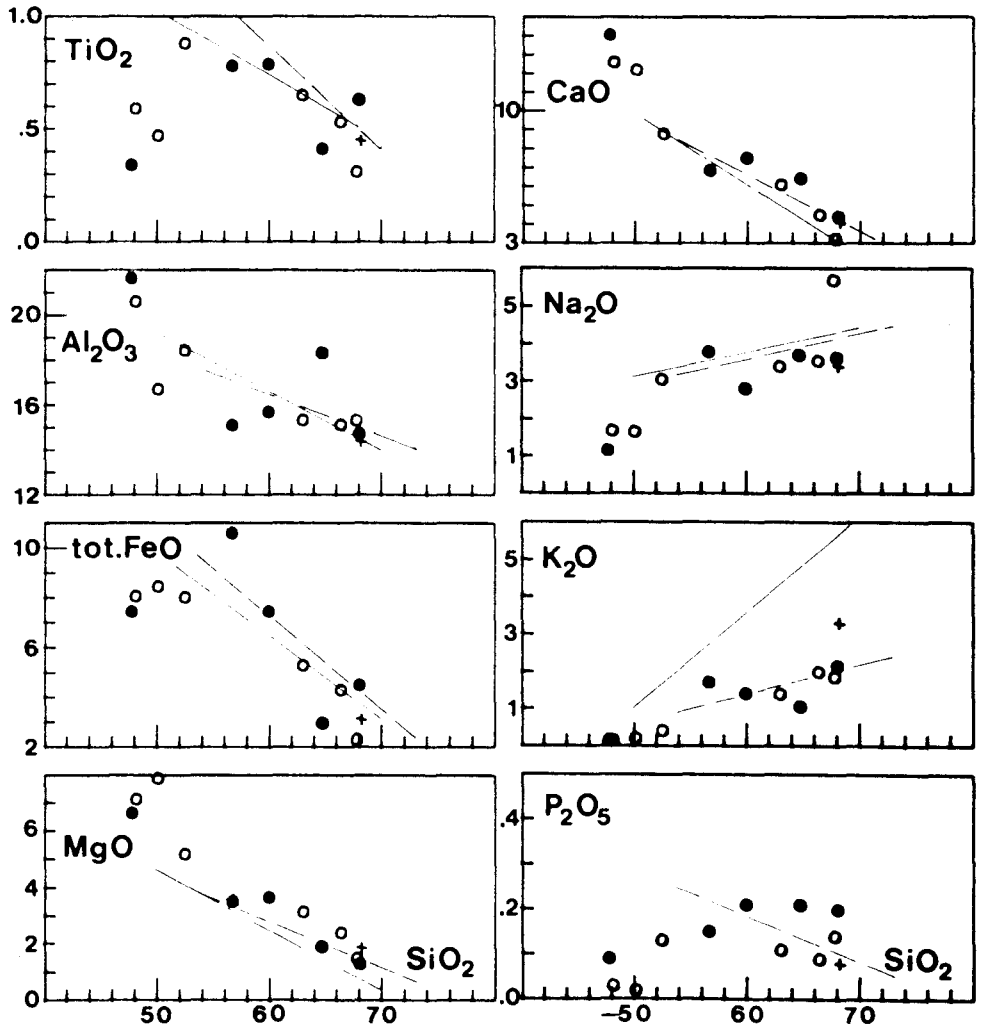

Key: ● data of this study
o data of Hohnen (1970; + = xenolith).

FIG. 30 : TRACE ELEMENT VARIATIONS FOR LEMAU INTRUSIVE COMPLEX.

Filled circles, rocks of pyroxene-bearing series; open circle, hornblende-bearing diorite porphyry.

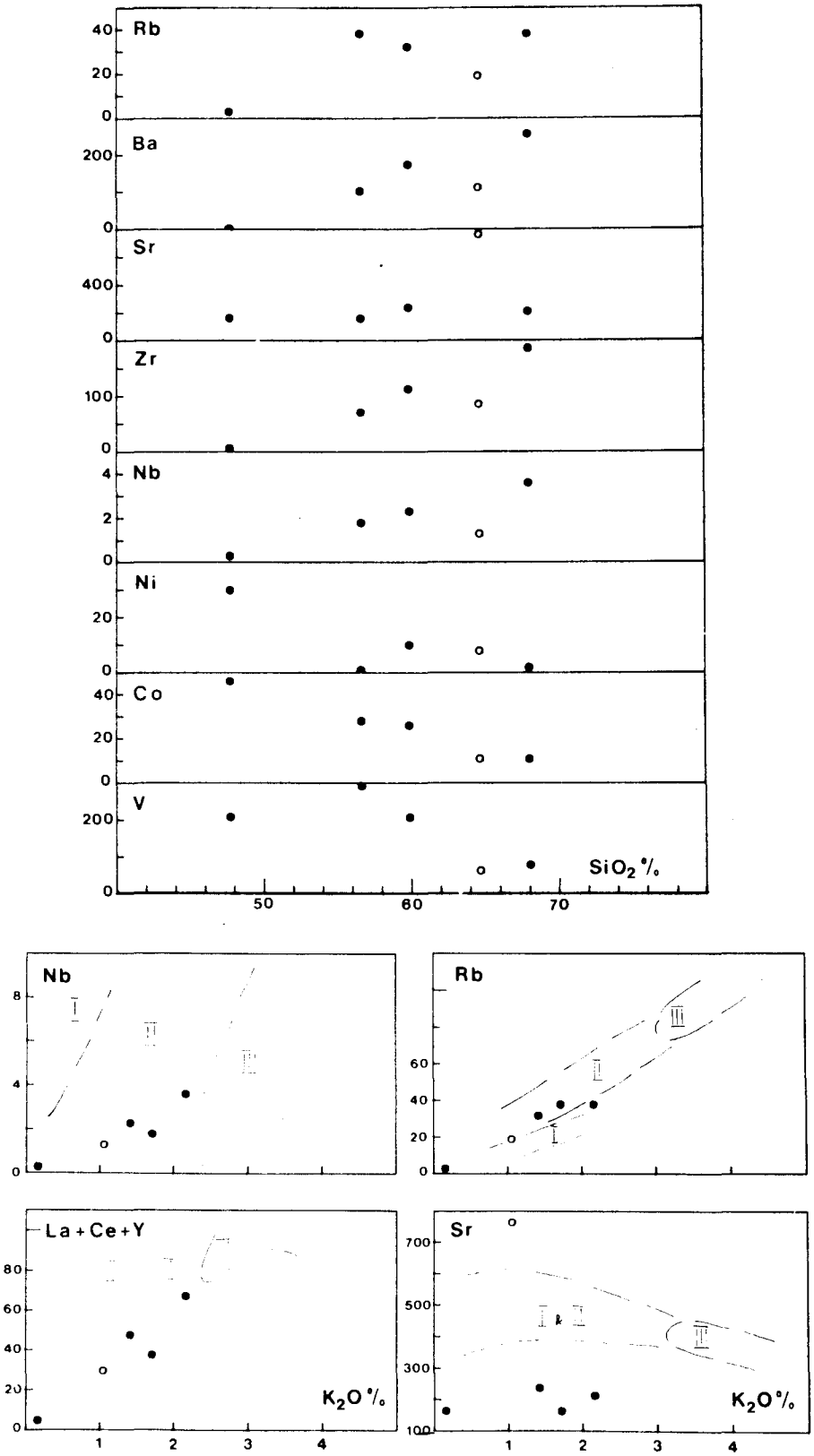

Note: fields from Fig. 19.

the porphyry; cobalt and vanadium are somewhat lower; while strontium is much higher.

In the pyroxene-bearing series, rubidium reaches moderate concentrations, while strontium remains low at 200 ppm. Barium increases with SiO_2 throughout the series but remains low (less than 300 ppm). Both zirconium and niobium increase steadily with SiO_2, with zirconium reaching quite high values (180 ppm). Niobium remains low (less than 4 ppm). Nickel, cobalt, and vanadium gradually decrease with increasing SiO_2. Cobalt is present in moderate amounts (30 ppm at 60% SiO_2), while vanadium is quite high at 200-300 ppm.

Both thorium (up to 3 ppm) and uranium (less than 2 ppm) are very low in rocks of the Lemau Intrusive Complex.

In the lower part of Fig. 30, the data for the New Ireland suite plot within the fields for the normal-K suite from the Western Highlands. Differences lie in lower niobium and much lower strontium contents in the Lemau rocks.

5.4 GEOCHEMISTRY OF THE PANGUNA INTRUSIVE COMPLEX, BOUGAINVILLE ISLAND

In Fig. 31, major element variations are shown for 15 specimens from the Panguna Intrusive Complex (both fresh and altered rocks), together with one specimen from the Puspa intrusion in northern Bougainville.

The Panguna specimens are distributed uniformly through a range of 55-70% SiO_2. On all the major element variation diagrams, they plot on straight-line trends, with some scatter being introduced by alteration. The plot of K_2O *versus* SiO_2 shows that the fresh Panguna samples fall across the normal-K trend of the North Bainings suite. The other major element plots reveal that the Panguna rocks contain similar levels of MgO, CaO, and Na_2O, but lower TiO_2 and total FeO, and higher Al_2O_3 compared with the Bainings suites.

In order to more closely examine the relationships between the various intrusive bodies of the Panguna Intrusive Complex, the different rock types have been plotted on K_2O and CaO *versus* SiO_2 diagrams (see Fig. 32). On the plot of K_2O *versus* SiO_2 (and less clearly on the plot of CaO *versus* SiO_2) two groupings are apparent. The first group defines a higher-K trend, and comprises the earlier intrusive rocks of the Panguna Complex (i.e., Kaverong Quartz Diorite and associated Biotite Diorite). The second group defines a normal-K trend, and comprises the various porphyries of the Complex (i.e., Leucocratic Quartz Diorite, Biotite Granodiorite, Biuro Granodiorite, various un-named porphyries,

FIG. 31 : MAJOR ELEMENT VARIATIONS FOR PANGUNA INTRUSIVE COMPLEX.

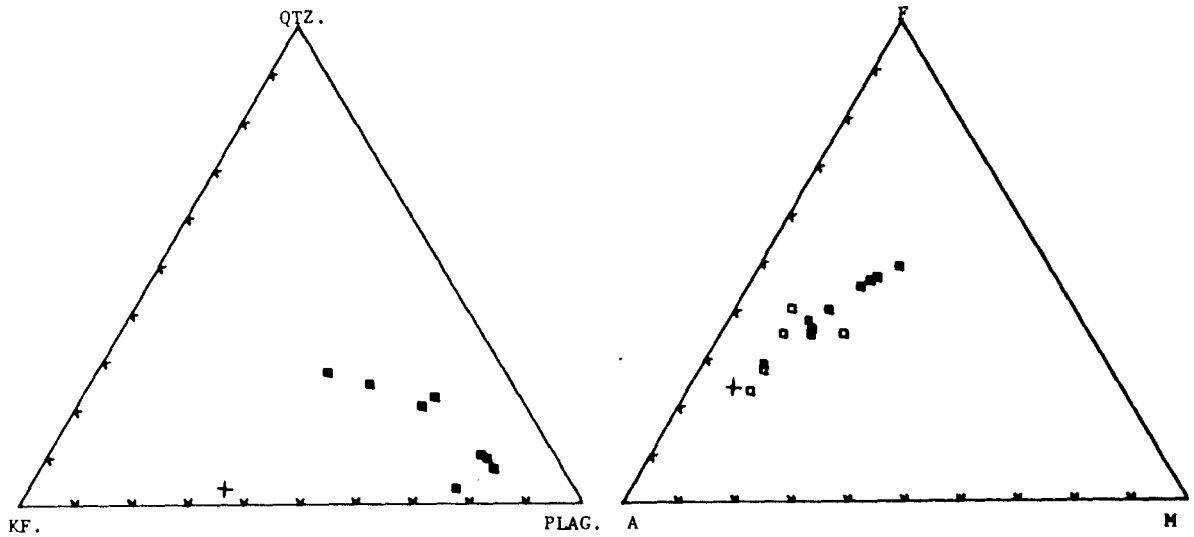

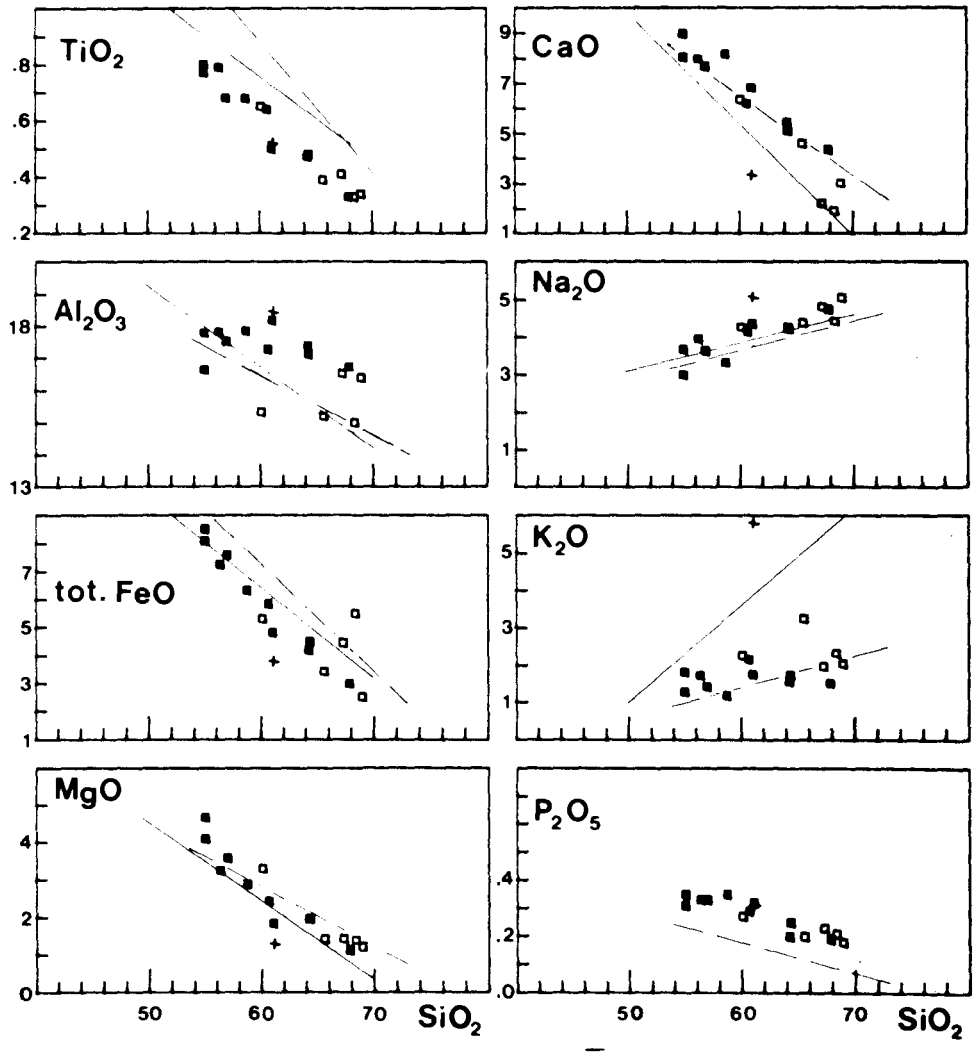

Key: ■ unaltered intrusive rocks
□ altered intrusive rocks
+ Pusapa syenite

Fig. 32: Panguna suites

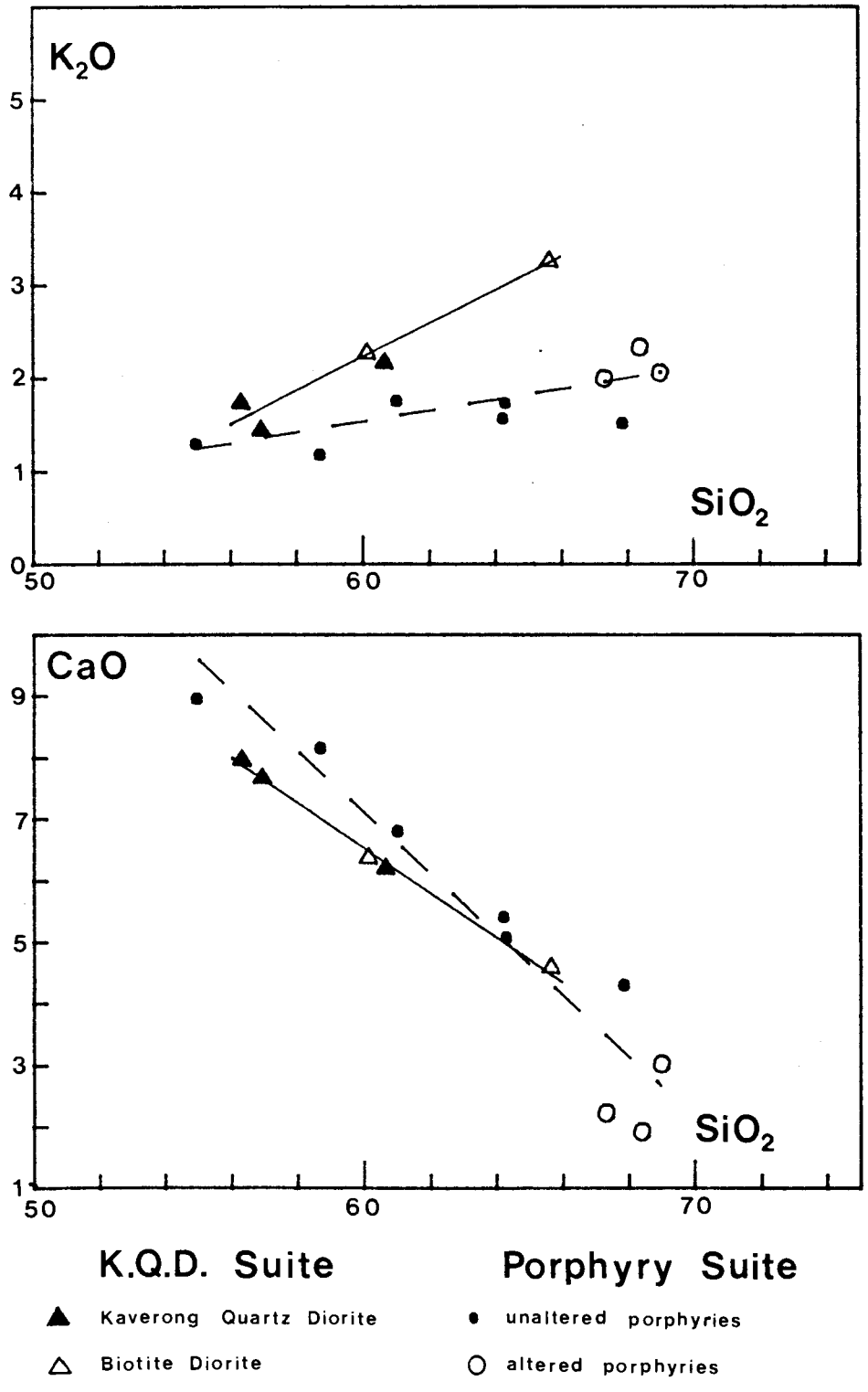

Nautango Andesite). The two suites are here called the *Kaverong Quartz Diorite Suite*, and the *Porphyry Suite*.

All of the major element data has been tested to determine the validity of the two-suite hypothesis. In Table 10, correlation coefficients for major element variations with silica are given separately for the Kaverong Quartz Diorite Suite and the Porphyry Suite, and also for all fresh rocks of the Panguna Complex. In all cases except total FeO and MgO *versus* SiO_2, an improvement results from treatment of the Panguna samples in separate suites. Greatest improvements are evident in the regressions of Al_2O_3, K_2O, and P_2O_5. The fact that improvements in data correlation are effected by separate treatment supports the contention that two geochemically distinct suites are present in the Panguna Complex.

Field evidence for the distinction of at least two intrusive suites has been provided by Macnamara (1968) and Fountain (1972), who note the occurrence of Biotite Diorite at the margin of the larger and earlier Kaverong Quartz Diorite intrusion, and the presence of demonstrably later porphyritic bodies, some of which are closely associated with mineralization. Age determinations of Page & McDougall (1972b) confirm an earlier intrusive age for the Kaverong Quartz Diorite (4-5 m.y.) and slightly later ages for the porphyritic mineralized rocks (3.4 ± 0.3 m.y.), followed by much later post-mineralization Nautango Andesite (1.6 m.y.).

Trace element variations within the Panguna samples, together with a microdiorite from near Mount Takuan and a syenite from the Puspa intrusion, are shown in Fig. 33. The syenite displays grossly different trace element distributions compared with the dioritic, frequently porphyritic, rocks of Bougainville. Very high rubidium in the syenite is accompanied by high levels of barium, zirconium, and niobium, and low levels of nickel, cobalt and vanadium.

As a group, the Panguna specimens display only limited variation of trace element contents. Rubidium (25 ppm) and strontium (650 ppm) are present in constant moderate amounts, while zirconium (100 ppm), niobium (5 ppm), nickel (5 ppm), cobalt (10-20 ppm) occur in quite low concentrations. Barium (200-400 ppm) increases with SiO_2, and moderate levels of vanadium (200-100 ppm) decrease with SiO_2.

Altered specimens generally possess higher rubidium and vanadium, which one would expect to be located in the potassic and oxide phases

TABLE 10: CORRELATION COEFFICIENTS FOR PANGUNA SUITES

showing improved correlations when two suites are considered

	Correlation for all fresh rocks	Correlation for Kaverong Quartz Diorite Suite	Correlation for Porphyry Suite	Remarks
TiO_2 vs SiO_2	-.968	-.957	-.977	marginally improved correlation
Al_2O_3 vs SiO_2	-.715	-.795	-.777	improved
total FeO vs SiO_2	-.981	-.975	-.834	marginally worse
MgO vs SiO_2	-.951	-.921	-.946	marginally worse
CaO vs SiO_2	-.967	-.997	-.951	improved
Na_2O vs SiO_2	+.843	+.836	+.928	marginally improved
K_2O vs SiO_2	+.253	+.971	+.768	greatly improved
P_2O_5 vs SiO_2	-.861	-.980	-.868	improved

FIG. 33 : TRACE ELEMENT VARIATIONS FOR PANGUNA INTRUSIVE COMPLEX.

symbols as in Fig. 31.

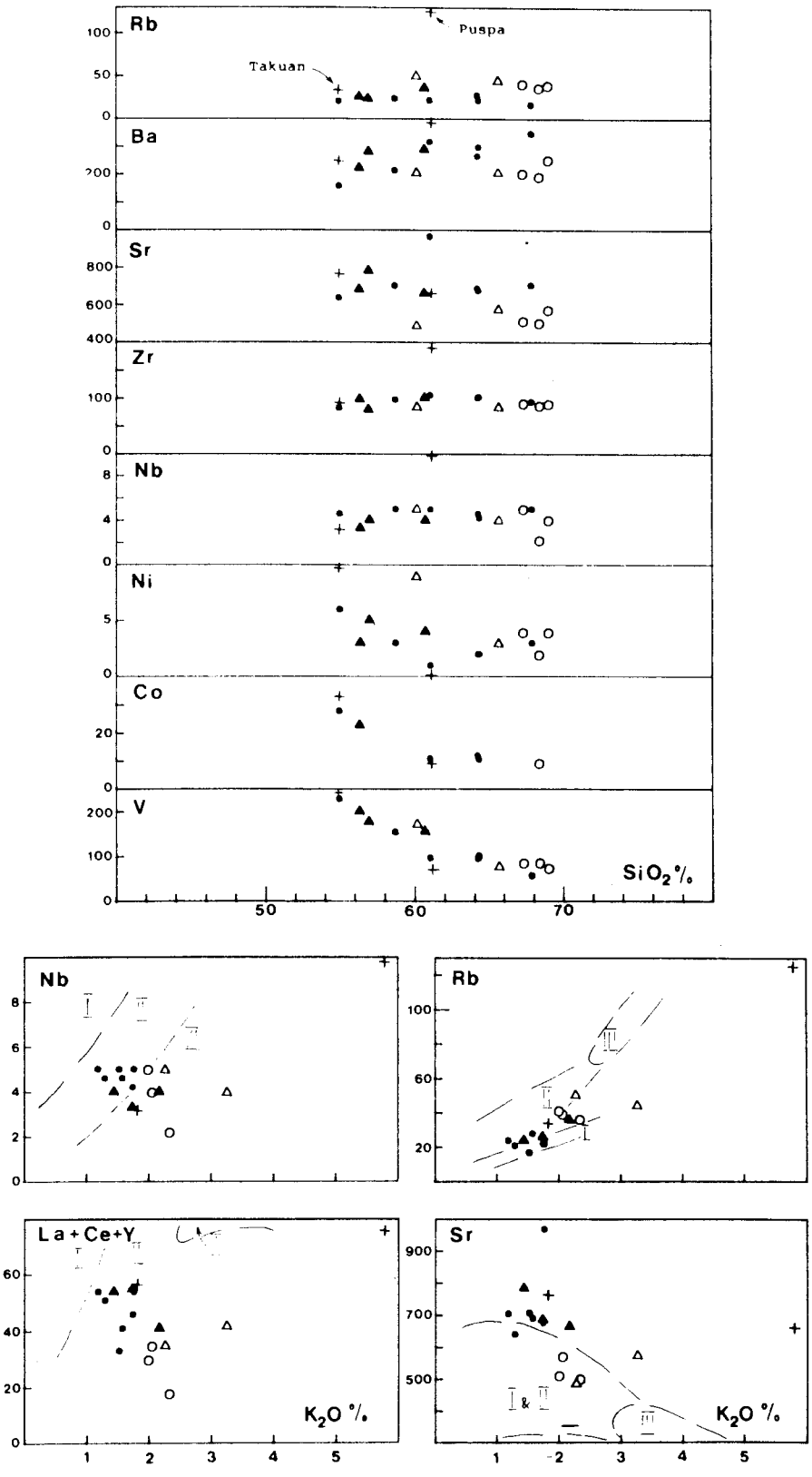

Note: fields as in Fig. 19

respectively. Barium and strontium are a little lower in the altered rocks, while zirconium, niobium, and cobalt remain relatively unaffected. Nickel is slightly higher in the altered specimens.

Some trace element evidence for the presence of two intrusive suites at Panguna is found in the distribution of rubidium. In rocks of the somewhat more potassic Kaverong Quartz Diorite Suite, rubidium is a little higher (30-50 ppm) than in the Porphyry Suite (20-40 ppm). Apart from this, other trace elements are present at similar levels of concentration in both suites. On plots of Nb and La+Ce+Y *versus* K_2O (see lower part of Fig. 33), the Kaverong Quartz Diorite Suite displays similar or lower niobium contents at higher K_2O levels compared with the Porphyry Suite, and contains higher total rare earth abundances for a given K_2O content.

Thorium (1-3 ppm) and uranium (less than 2 ppm) are present in only very small amounts in the Panguna rocks, but reach 8 ppm and 3 ppm respectively in the Puspa syenite.

5.5 GEOCHEMISTRY OF THE LIMBO RIVER DIORITE, NEW GEORGIA ISLAND

The available major element data for the Limbo River Diorite are presented on Harker-type diagrams in Fig. 34. Three whole-rock analyses were made in this study, and together with two analyses by Stanton and Bell (1969), the data cover a range of 44-62% SiO_2. On the MFA diagram, the rocks define a trend of relative iron depletion and alkali enrichment typical of calc-alkaline associations.

The major element variation diagrams clearly show the cumulative nature of the mafic pyroxene gabbro (DRM145). This rock is depleted in SiO_2, Al_2O_3, Na_2O, and K_2O, and enriched in total FeO, MgO, and CaO. The plot of K_2O *versus* SiO_2 reveals that the intermediate rocks of the Limbo suite contain K_2O at concentrations approaching those of the high-K Bainings suite. Levels of MgO and CaO are closely comparable with the high-K Bainings suite. However, total FeO and TiO_2 are lower, Na_2O and Al_2O_3 are higher, and P_2O_5 is progressively enriched through the suite.

Trace element data are available only for the three Limbo specimens studied in this work. As for the major elements, smooth variations are observed (see Fig. 35). Rubidium, barium, zirconium, and niobium are all positively correlated with SiO_2, while strontium, nickel, cobalt, and vanadium are all negatively correlated with SiO_2. Zirconium (100 ppm) and niobium (5 ppm increasing to 8 ppm) are quite low. Barium

FIG. 34 : MAJOR ELEMENT VARIATIONS FOR POHA RIVER DIORITE AND LIMBO RIVER DIORITE.

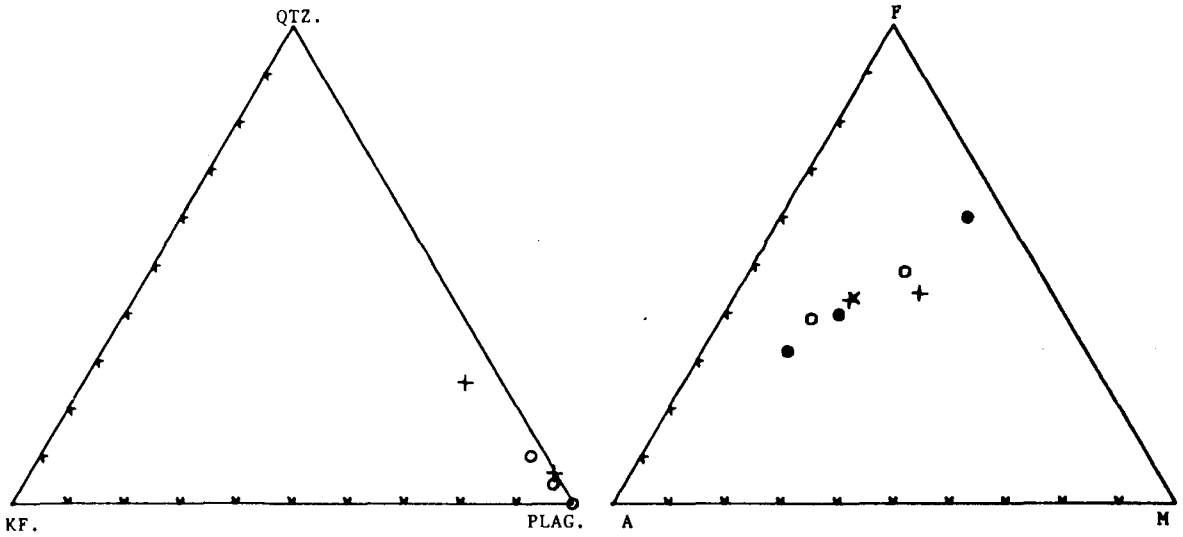

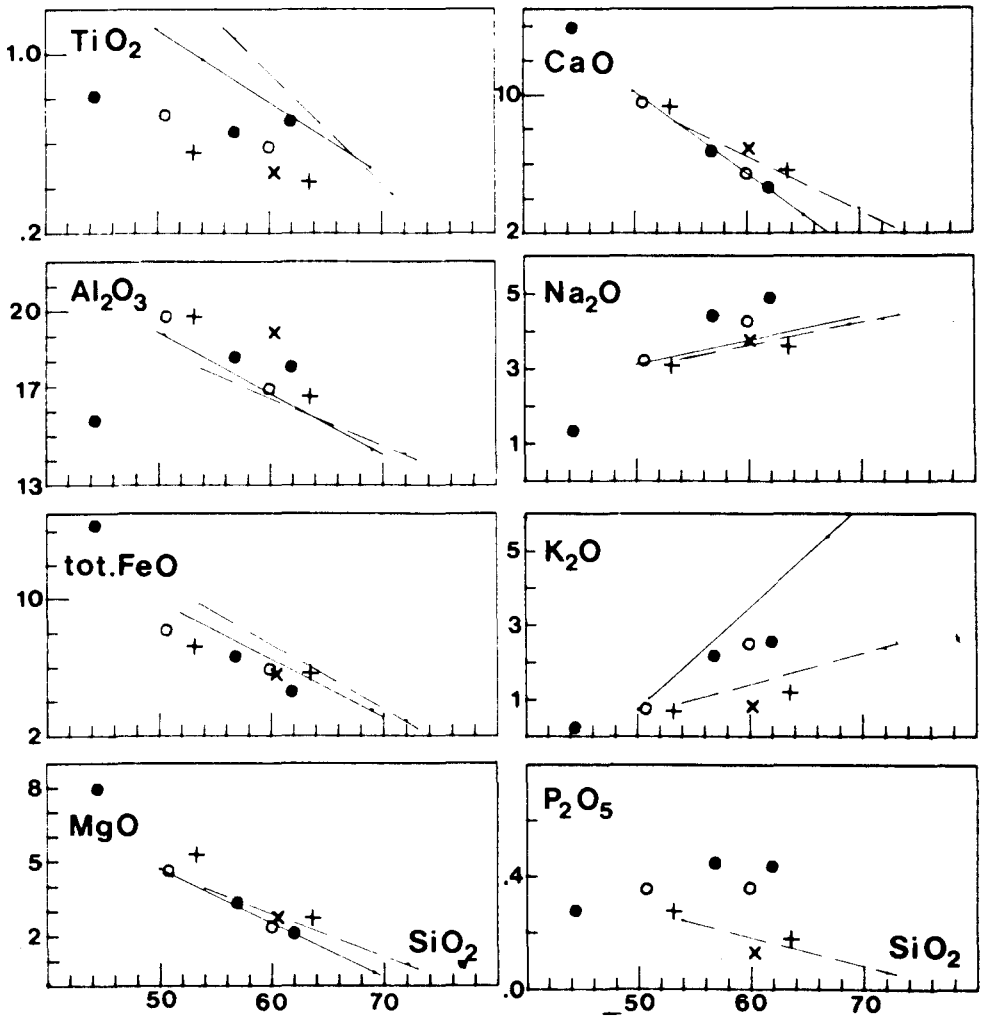

Key: POHA + this study LIMBO • this study

× Hackman(1971) ○ Stanton & Bell(1969)

FIG. 35 : TRACE ELEMENT VARIATIONS FOR POHA RIVER DIORITE AND LIMBO RIVER DIORITE.

squares, Limbo; crosses, Poha.

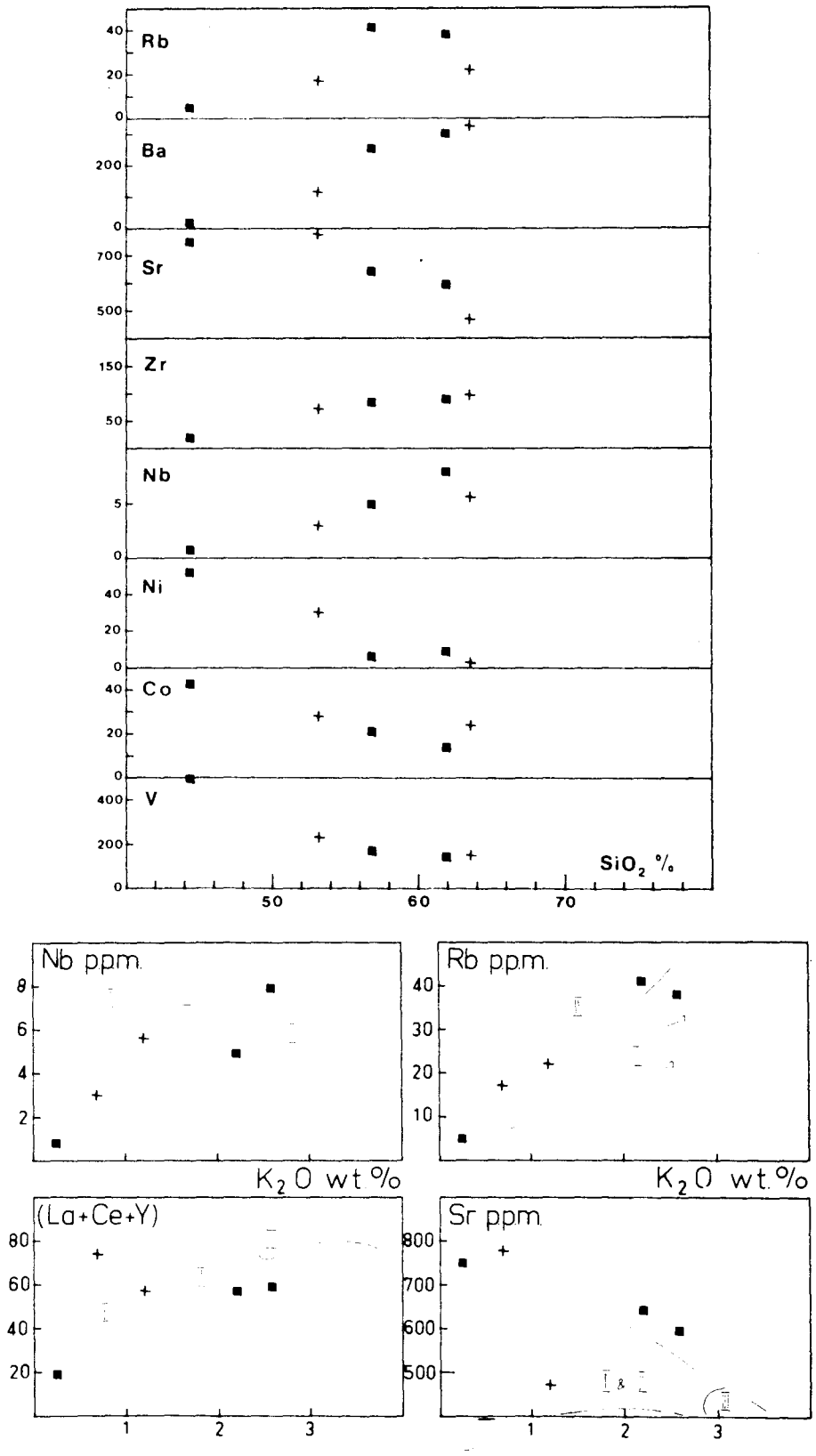

Note: fields from Fig 19.

and strontium are present in moderate amounts. Nickel and cobalt are low in the microdiorites, but vanadium (200 ppm) is high.

In the lower part of Fig. 35, the Limbo suite plots within or near the fields of the normal-K suite of the Western Highlands on the plots of K_2O *versus* Nb, Rb, La+Ce+Y, and Sr.

Thorium (1-3 ppm) and uranium (less than 2 ppm) are present in very low amounts in rocks of the Limbo River Diorite suite.

5.6 GEOCHEMISTRY OF THE POHA RIVER DIORITE, GUADALCANAL ISLAND

The available major element data for the Poha River Diorite are presented in Fig. 34. Two whole-rock analyses were made in this study, and one is from Hackman (1971). Differences between the Poha and Limbo suites are readily apparent, and in fact the Poha River Diorite can be compared more closely with the Koloula Igneous Complex to be described in the next section.

There are similarities in major element variations between the Poha River Diorite and the normal-K North Bainings suite. On the plot of K_2O *versus* SiO_2, the Poha rocks plot a little below the North Bainings normal-K trend (i.e. they are a little less potassic). All of total FeO, MgO, CaO, Na_2O, and P_2O_5 are present in similar amounts in both suites. The Poha suite contains more Al_2O_3 and less TiO_2 compared with the North Bainings suite.

Trace element data for the two specimens of this study are plotted with the data from the Limbo River Diorite in Fig. 35. Similar trends in trace element variation are observed, and most elements occur in both suites at similar levels of concentration. However, rubidium (20 ppm) is much lower in the Poha rocks due to lower K_2O. In the lower part of Fig. 35, the Poha rocks fall in the field of the low- to normal-K suite of the Western Highlands on the plot of La+Ce+Y *versus* K_2O. On the plot of Sr *versus* K_2O, strontium enrichment in the leuco-gabbro is obvious, and can be correlated with abundant calcic plagioclase.

Thorium (3-4 ppm) and uranium (1-2 ppm) are quite low, but are twice as abundant as in the Limbo River suite.

5.7 GEOCHEMISTRY OF THE KOLOULA IGNEOUS COMPLEX, GUADALCANAL

New major element data for 20 intrusive rocks from the Koloula Igneous Complex are plotted in Fig. 36. On the MFA diagram, there is much scatter among the mafic rocks whereas rocks of more silicic composition define a flat calc-alkaline trend of relative iron depletion and alkali enrichment. These two groups of rocks belong respectively to the Mafic and

FIG. 36 : MAJOR ELEMENT VARIATIONS FOR KOLOULA IGNEOUS COMPLEX.

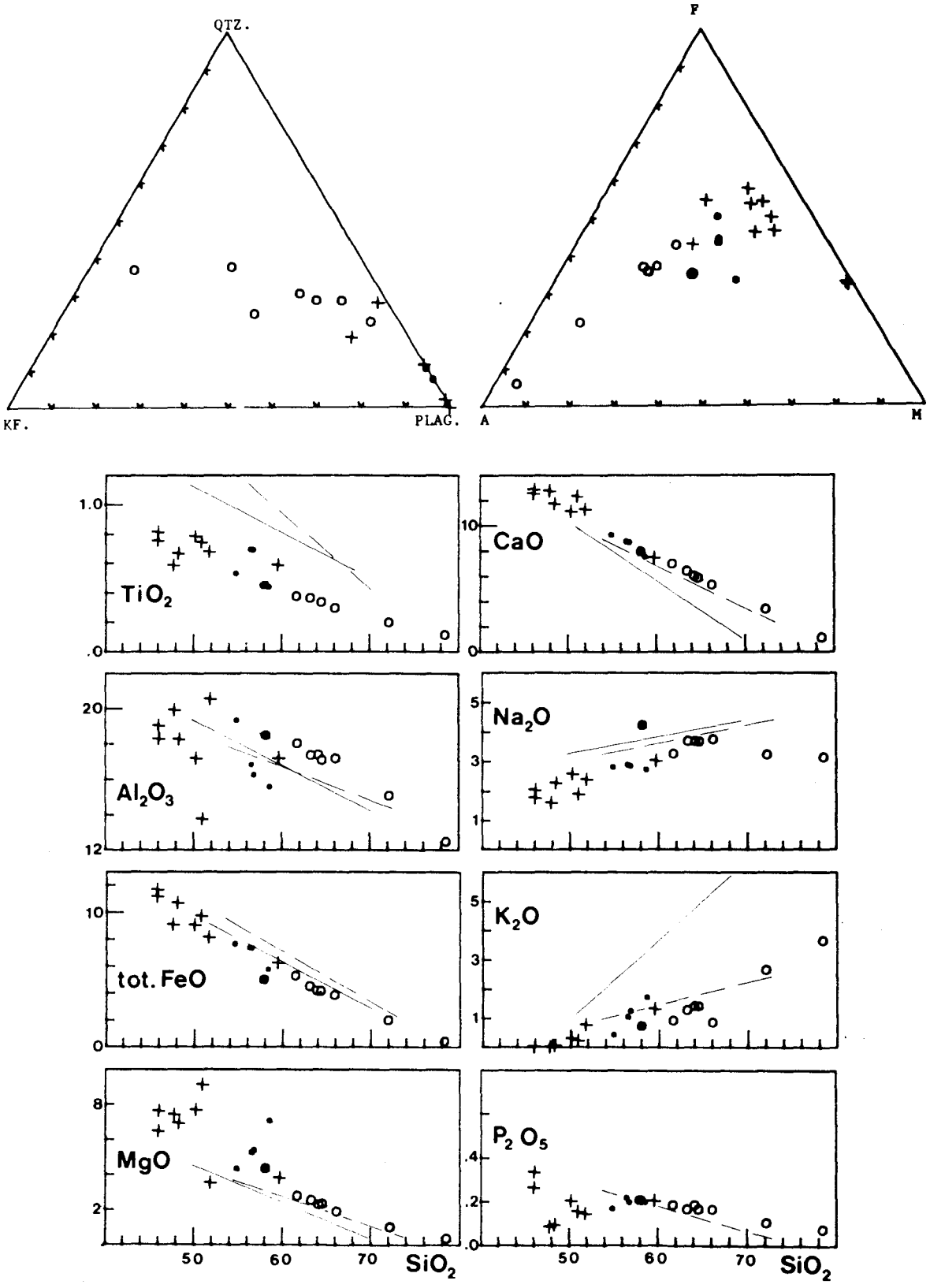

Felsic Suite described in the section on petrography (see Chapter 3, section 3.8.2).

Major element variation diagrams reveal the wide silica range of the Koloula rocks (46-78% SiO_2). On all plots of major element oxides against silica, rocks of the Mafic Suite together with the andesitic porphyries display gross scatter. On the other hand, rocks of the Felsic Suite define linear trends. For both suites there is a decrease of Al_2O_3, TiO_2, total FeO, MgO, CaO with increasing SiO_2. In the Mafic Suite, both Na_2O and P_2O_5 increase with SiO_2, but decrease in the Felsic Suite.

Relative to the Bainings suites, the Koloula suites tend to be higher in Al_2O_3, MgO and CaO, and lower in TiO_2, total FeO, Na_2O and K_2O.

On the plot of K_2O *versus* SiO_2, some of the andesitic porphyries and the more silicic rocks of the mafic suite display higher K_2O values than do the more mafic rocks of the Felsic Suite. Other differences between the Mafic Suite and Felsic Suite are apparent: compared with the Mafic Suite, the Felsic Suite possesses higher Al_2O_5, lower TiO_2, and lower K_2O. The diorite porphyry xenolith (DRM091) from a granodiorite of the Felsic Suite possesses characteristics more like those of the Felsic Suite thanthe Mafic Suite. On all of the major element variation diagrams (except total FeO *versus* SiO_2) the xenolith lies near a projection of the Felsic trend.

In order to further examine the possibility of the presence of separate intrusive suites within the Koloula Igneous Complex, previous data of Netzel (1974) and Chivas (pers. commun., 1975) have been combined with the new data. Plots of K_2O, TiO_2, and Al_2O_3 *versus* SiO_2 (see Fig. 37) indicate that the combined data fall into the fields of the Mafic Suite and the Felsic Suite of the present study. Three specimens of Netzel (numbers 362, 364, 372), which were described as 'hornblende quartz diorite' of 'Unit 1.4' (Netzel, 1974, Table D), differ from the other specimens of that Unit in having lower K_2O, lower TiO_2, and higher Al_2O_3. These are characteristics of rocks ofthe Felsic Suite, and in fact the rocks plot in the field of the Felsic Suite. Two specimens of Chivas (specimens CH3, CH7), described as 'diorite', also plot near the mafic end of the Felsic Suite trend. The 'biotite granodiorite' (specimen A524) of Chivas has relatively high TiO_2, high K_2O, and low Al_2O_3, and plots toward the felsic end of the Mafic Suite trend. A 'hornblende quartz diorite' of Netzel (specimen 352) has similar chemical characteristics.

Fig. 37: Combined Koloula data

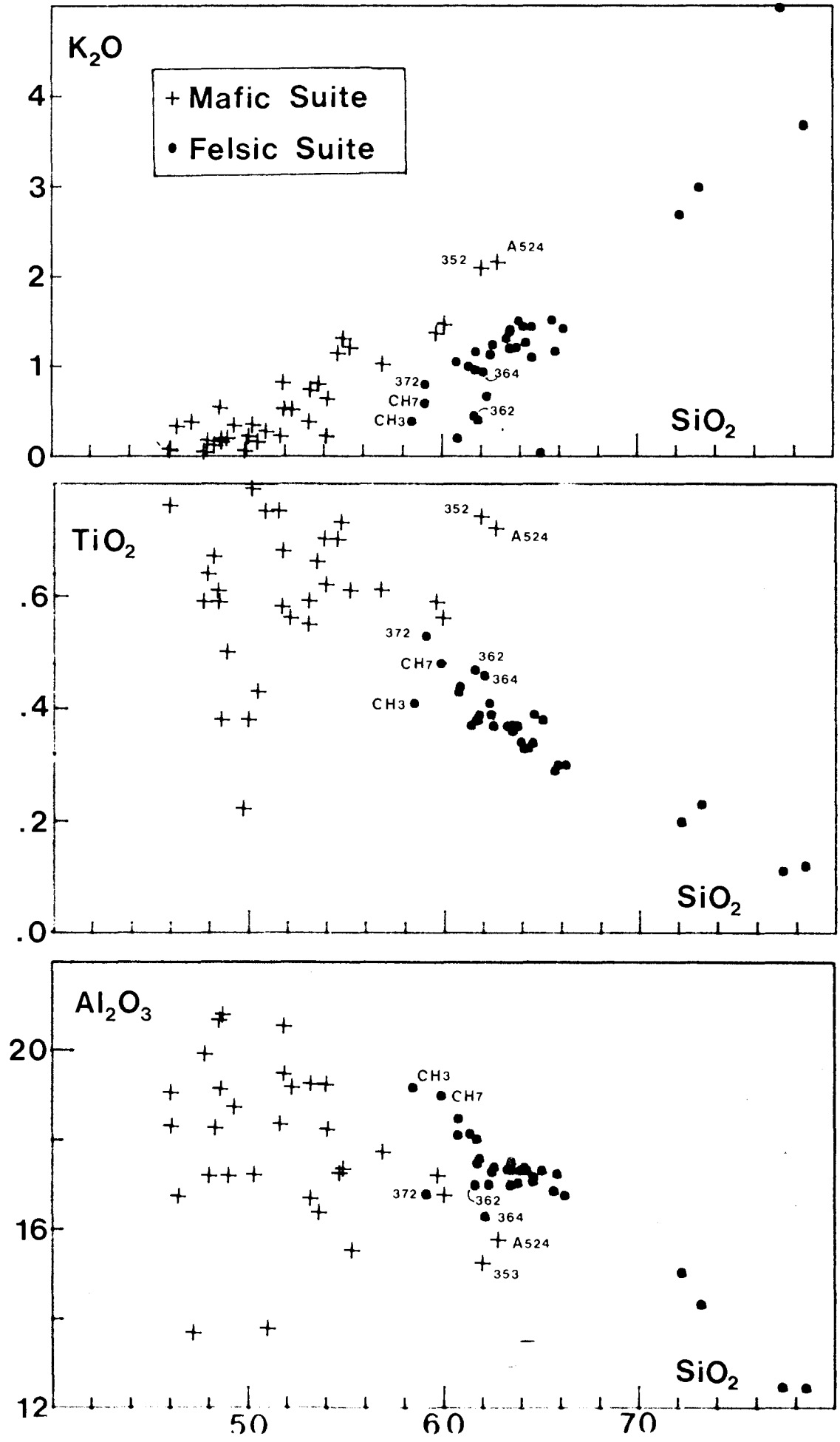

The multivariate analytical technique of discriminant analysis (Lohnes, 1961; Cooley & Lohnes, 1962) has been applied to the Koloula major element data to assess the validity of the hypothesis that at least two distinct intrusive suites are present. On the basis of distribution on the K_2O *versus* SiO_2 plot, specimens were assigned to one of four suites:

1. the *Mafic Suite*, comprising gabbros and a two pyroxene-hornblende-biotite-quartz diorite of this study; a pyroxenite, gabbros, basic diorites, diorites, quartz diorites, and a biotite granodiorite of Chivas; and gabbros, leucogabbros, and hornblende-quartz diorites of Netzel. A total of 34 specimens were allocated to this suite.

2. the *Felsic Suite*, comprising a hornblende-biotite-quartz diorite, hornblende-biotite granodiorites, a diorite porphyry xenolith, and aplitic dykes of this study; quartz diorites, tonalites, granodiorites, and aplitic dykes of Chivas; and hornblende-quartz diorites and quartz-hornblende (-biotite) diorites of Netzel. A total of 34 rocks were allocated to this suite.

3. the *Andesite Porphyry Suite*, comprising various porphyritic microdiorites of this study; porphyritic andesites of Netzel; and andesitic dykes of Chivas. A total of 8 samples were allocated to this suite.

4. the *Tonalite Porphyry Suite*, comprising tonalite porphyries of Chivas (3 specimens.)

To preserve clarity, specimens belonging to the latter two groups have been omitted from Fig. 37.

The results of the discriminant analysis are as follows:

(i) The major element oxides which best discriminate between the suites are, in order of decreasing discriminatory power, K_2O, CaO, TiO_2, and Fe_2O_3. The usefulness of K_2O and TiO_2 has been seen in plots of those oxides against SiO_2. It is to be expected that CaO will vary inversely as K_2O, and so will possess discriminatory ability. In addition, CaO is less abundant in the Felsic Suite. Both Fe_2O_3 and total FeO are more abundant in the Mafic Suite, and so serve to distinguish between the suites.

(ii) Of the 79 samples, 73 (or 92%) were allocated to their original suite, while the remaining 6 were re-allocated because of closer geochemical affinity with another suite. Only 2 of the re-allocated

specimens possessed a fair probability for re-allocation. These were a 'diorite' of Chivas (CH7) which was removed from the Felsic Suite and re-allocated to the Andesite Porphyry Suite, and a hornblende-biotite granodiorite of this study (DRM106) which was removed from the Felsic Suite and re-allocated to the Tonalite Porphyry Suite. There were no re-allocations from the Mafic Suite to the Felsic Suite, or vice versa, indicating that rocks of these two suites are readily distinguished.

On the basis of this study of major element variation in a large body of data from three different workers, it is concluded that the Koloula Igneous Complex comprises two readily distinguished suites which are here called the Mafic Suite and the Felsic Suite, and at least two less widespread, but distinguishable suites which are referred to as the Andesite Porphyry Suite and the Tonalite Porphyry Suite.

Trace element variations in the Koloula specimens of the present study are shown in Fig. 38. As in the major element plots, there is considerable scatter in the Mafic Suite whereas the Felsic Suite displays smooth variations. Rubidium is low and increases with SiO_2. It is relatively more abundant in the andesitic dykes and the more silicic members of the Mafic Suite. Barium increases steadily through the Mafic and Felsic suites. Strontium is moderately abundant in the Mafic Suite and the earlier members of the Felsic Suite, but drops to very low levels in the K-feldspar-rich quartz monzonite and aplitic dykes. Zirconium and niobium are present in very low concentrations in both the Mafic and Felsic suites. Some of the andesitic dykes and more silicic members of the Mafic Suite possess higher values. Nickel is high in the cumulative pyroxenites of the Mafic Suite, and is very low in the Felsic Suite. Cobalt and vanadium decrease steadily with increasing SiO_2, and are present in moderate to low amounts in rocks of the Felsic Suite. Trace element abundances within the diorite porphyry xenolith suggest close affinity with its host rock of the Felsic Suite. Both thorium and uranium are present in only very small amounts in the Mafic and Felsic suites. Thorium is generally low at 0-2 ppm, and reaches 6 ppm in aplitic dykes. Uranium mostly ranges 0-1 ppm, and reaches 2 ppm in the aplites.

The limited trace element data tend to support the distinction of separate intrusive rock suites at the Koloula Igneous Complex.

FIG. 38 : TRACE ELEMENT VARIATIONS FOR KOLOULA IGNEOUS COMPLEX.

symbols as in Fig. 36.

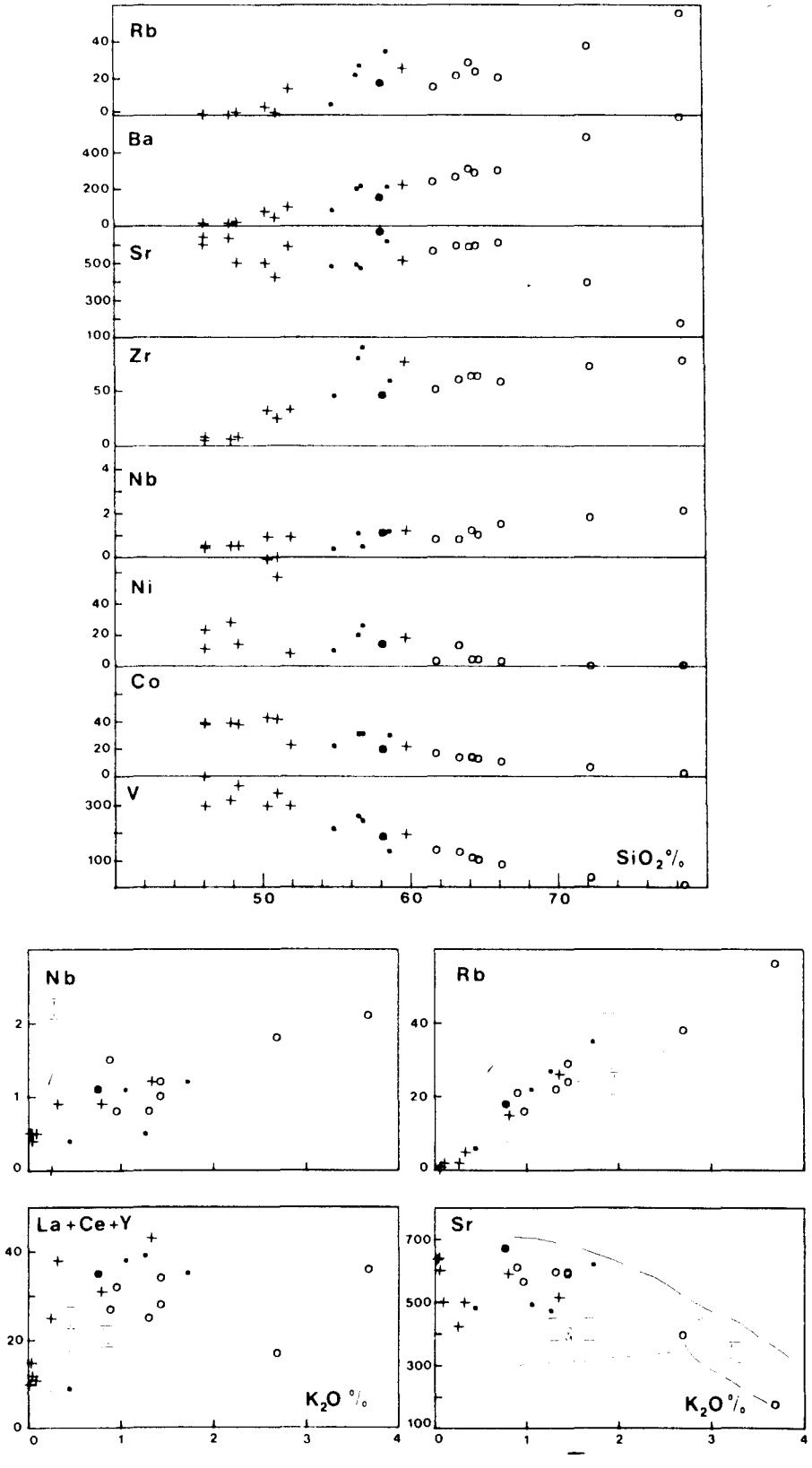

Note: fields from Fig. 19.

CHAPTER 6 MINERAL CHEMISTRY IN MINERALIZED AND NON-MINERALIZED INTRUSIVE ROCK SUITES

6.1 INTRODUCTION

Compositional variations of different mineral species have been determined in a variety of intrusive rocks. These have proven useful in distinguishing different conditions of crystallization in mineralized and non-mineralized intrusive suites.

Samples studied were restricted to 25 specimens from the Western Highlands, and 3 specimens from the Limbo River Diorite, Solomon Islands. Where possible, compositions were determined for all essential minerals in each specimen (see Table 11). Compositions were determined for plagioclase feldspars, alkali (K-) feldspars, amphiboles, biotites, Fe-Ti oxides, and pyroxenes. Olivine and chromite compositions were obtained from Alpine-type ultramafic rocks of the Western Highlands, and are reported separately in Appendix 6.

All mineral compositions were determined using electron microprobe facilities at the Research School of Earth Sciences, Australian National University (see Appendix 2 for techniques).

6.2 FELDSPAR COMPOSITIONS

6.2.1 Plagioclase Feldspar

Plagioclase is abundant in practically all intrusive rock types from the Western Highlands. The recorded range of composition is from An(90) in gabbroic rocks of the Yuat South Batholith, to An(7) in granodiorites of the same batholith. Zoned plagioclase is common in most rock types, but less so in gabbroic rocks. Although normal zoning is dominant, oscillatory zoning is often present especially in more silicic rock types.

Composition ranges for zoned plagioclase from individual specimens are given in Table 12. Compositions observed for Western Highlands rocks are generally in accord with those recorded in granitic rocks elsewhere. Gabbroic rocks contain calcic plagioclase, while diorites and granodiorites typically contain andesine and oligoclase. In Fig. 39, the plagioclase compositional range has been plotted for individual specimens from particular regions of the Western Highlands. Plagioclase from the Yuat South Batholith (see Fig. 39b) shows a regular decrease in An-content with increasing SiO_2 content of the host-rock. This simple relationship is not observed in the Yuat North Batholith (see Fig. 39a),

TABLE 11: MINERALS ANALYZED BY ELECTRON MICROPROBE, indicating number of spot analyses.

LABORATORY SPECIMEN NO.	H'B	BIO	OX	CPX	OPX	PLAG	KF	OTHERS
DRM.004	-	2	-	-	-	-	-	
DRM.006	4	6	-	-	-	4	-	
DRM.012	4	5	5	2	-	7	4	
DRM.013	8	5	5	-	-	2	5	
DRM.019	14	22	4	-	-	15	2	
DRM.025	41	34	3	-	-	8	2	
DRM.027	-	3	-	-	-	5	-	3 chlorites
DRM.029	8	-	-	-	-	1	-	
DRM.034	2	-	-	-	-	1	-	
DRM.035	3	-	1	5	-	3	1	
DRM.036	7	-	-	-	-	9	-	3 chlorites
DRM.044	8	6	5	-	-	4	-	
DRM.051	2	3	-	-	-	10	1	
DRM.052	10	-	4	-	-	3	-	
DRM.054	16	-	7	-	-	4	-	1 sphene
DRM.056	7	4	-	-	-	8	2	
DRM.063	-	11	2	2	-	2	3	
DRM.065	6	-	3	9	-	4	-	
DRM.080	25	11	8	-	-	6	3	
DRM.081	12	-	2	-	-	11	-	4 sphenes
DRM.084	-	-	-	-	-	4	-	
DRM.087	-	-	-	8	-	6	-	5 sphenes
DRM.143	1	4	-	2	-	4	2	
DRM.144	6	3	6	8	-	5	2	1 chlorite
DRM.145	-	4	2	7	2	2	-	
DRM.149	4	-	-	-	-	3	-	
DRM.155	-	-	5	-	-	-	-	5 olivines
DRM.160	-	5	-	-	-	8	8	

TABLE 12: SUMMARY OF PLAGIOCLASE COMPOSITIONS

SPECIMEN NUMBER	ROCK NAME	An.RANGE	NO OF SPOT ANALYSES	NOTES
DRM.006	K-altered plag-bio.diorite porphyry	37-31	4	Av.core An (37)
DRM.012	High-K hb-bio-qtz diorite	49-24	7	
DRM.013	High-K hb-bio-qtz diorite	46-27	2	
DRM.019	hb-bio-qtz granodiorite	39-7	15	Small grain An(20); larger part of most grains is sodic oligoclase
DRM.025	hb-bio-qtz granodiorite	48-17	8	larger part of most grains is calcic oligoclase
DRM.027	K-altered plag-hb. diorite porphyry	50-26	5	Mottled phenocryst core An(50); zoned rims are calcic andesine; smaller pheno. core An(26).
DRM.029	Uralite gabbro	86	1	core
DRM.034	hb(-bio) tonalite	33	1	Rim
DRM.035	hb(-cpx)-qtz diorite	35-33	3	
DRM.036	Plag-hb-qtz diorite porphyry	55-36	8	Oscillatory zoning
DRM.044	hb-bio-qtz grano-diorite	33-30	4	Limited normal zoning
DRM.051	High-K hb-bio-qtz diorite	40-34	10	Limited normal zoning, dominant calcic andesine
DRM.052	hb(-cpx-qtz) gabbro	56-44	3	Normal zoning
DRM.054	hb(-cpx-qtz) gabbro	90-50	4	
DRM.056	Bio-hb microadamellite	55-15	8	Larger grains calcic andesine to sodic labra-dorite; smaller grains calcic oligoclase.
DRM.063	Orthoclase gabbro	50-46	2	Lath in biotite An(46)
DRM.065	hb(-cpx) gabbro	88-85	4	Granoblastic texture
DRM.080	'Qtz diorite porphyry'	46-23	6	Phenocryst core An(32); small groundmass grains An(23-33)
DRM.081	'Nena Diorite'	35-22	8	Large grains An(35-26); smaller grains An(30-26)

TABLE 12 continued.

SPECIMEN NUMBER	ROCK NAME	An.RANGE	NO OF SPOT ANALYSES	NOTES
DRM.084	High-K hb(-bio) diorite	72-43	4	Cores sodic bytownite; rims outside zone of inclusions are calcic andesine
DRM.087	High-K cpx-hb diorite	43-23	6	Some reverse zoning. Oligoclase groundmass laths.
DRM.143	hb-bio (-cpx) microdiorite	52-38	3	normal zoning
DRM.144	hb-bio-cpx microdiorite	54-19	5	Sodic labradorite cores of large prisms; oligoclase groundmass grains.
DRM.145	Two pyroxene-bio(-hb) gabbro	76-75	2	
DRM.160	K-altered plag-Kf. latite porphyry	42-14	8	Large phenocrysts have cores An(42); groundmass grains are oligoclase

Fig. 39 : VARIATION OF PLAGIOCLASE COMPOSITIONS FOR WESTERN HIGHLANDS ROCKS.

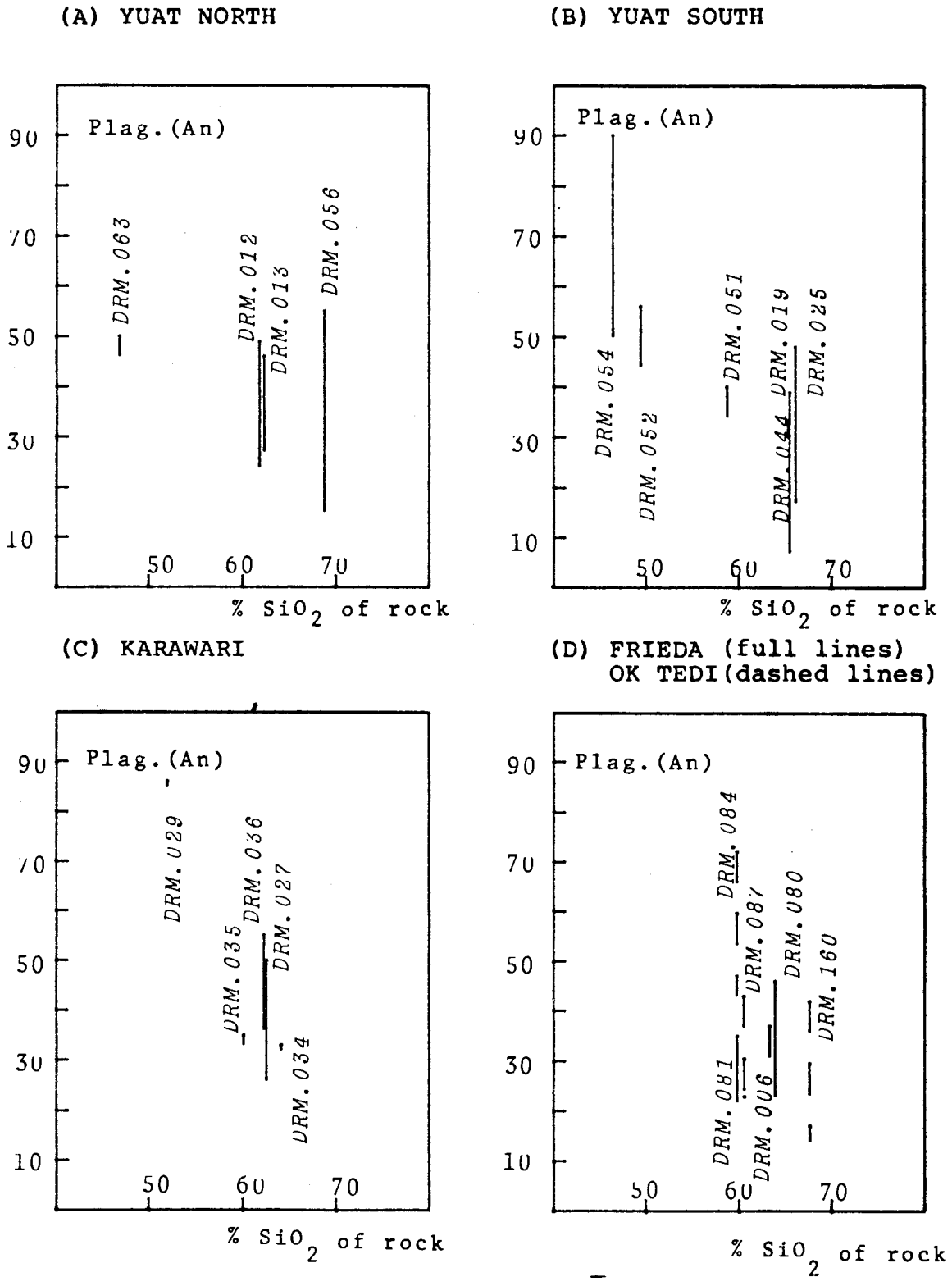

where plagioclase in the silicic microadamellite (DRM056) spans a wider range than does plagioclase from the high-K diorites (DRM012, 013).

Similarly, limited data for the Frieda River Intrusive Complex (see Fig. 39d, full lines) indicate that plagioclase compositions actually become more calcic with increasing SiO_2 content of the host rock. This may be an artifact of inadequate sampling, or alternatively (and more likely, in the writer's opinion) it may imply that the Frieda River specimens are not related in any simple way, but represent suites of quite different origin.

Ok Tedi plagioclase compositions (dashed lines) are plotted together with the Frieda River data in Fig. 39d. The high-K dioritic rocks (DRM084, 087) display a wide range in composition (An(70-25)), while the silicic altered latite porphyry (DRM160) has less-calcic plagioclase phenocrysts (An(40-15)).

Data from the Yuat North and Yuat South batholiths indicate a wider range in composition of plagioclase from the dominant rock type (granodiorite) of the Yuat South Batholith. Plagioclase cores in the high-K diorite of the Yuat North Batholith and in the Yuat South granodiorite are calcic andesine (approximately An(48)). Conditions during later stages of crystallization of the granodiorite were such that plagioclase continued to precipitate to compositions of calcic albite (approximately An(7)). However, the plagioclase of the high-K diorite ceased crystallizing at compositions of intermediate oligoclase (An(24)). Both the high-K diorite and the granodiorite have comparable SiO_2 contents (61-65%) and possess similar normative plagioclase compositions (approximately An(35)), but it is apparent that the plagioclase in the Yuat South granodiorite remained in reaction relationship with residual silicic liquids for a longer period of time than plagioclase in the Yuat North high-K diorites. Prolonged crystallization in the Yuat South body relative to the Yuat North body would have been a suitable mechanism to produce a fractionated, silicic liquid capable of exsolving a hydrothermal phase. The occurrence of porphyry-type copper mineralization in and adjacent to the Yuat South body supports that contention.

6.2.2 Alkali Feldspar

Alkali (K-) feldspar is present as interstitial patches in most rocks of intermediate and more silicic composition. In the potassic rocks of Ok Tedi, K-feldspar is also present as a phenocrystic

phase.

There are limited but measurable variations in K-feldspar compositions from these different occurrences in the Western Highlands (see Table 13). The variations may be summarized as follows:

(i) The anorthite molecule is present in only small amounts, reaching 5% in K-feldspar of the orthoclase gabbro (DRM063) of the Yuat North Batholith.

(ii) The high-K diorites of the Yuat North Batholith contain a less potassic K-feldspar (Or(72) than the granodiorites of the Yuat South Batholith (Or(88)).

(iii) K-feldspars from the Karawari Batholith (e.g. specimen DRM035) are comparable to those from the Yuat South Batholith.

(iv) The 'Nena Diorite' (DRM080) from Frieda River contains K-feldspars of variable composition (Or(76) to Or(66)), that are comparable to K-feldspars of the Yuat North Batholith.

(v) Rims (Or(84)) of K-feldspar phenocrysts from Ok Tedi are more potassic than cores (Or(75)).

Within the high-K Yuat North suite, K-feldspar becomes more potassic with increasing SiO_2 content of the host rock (compare DRM012, 013, and 056). However, in the normal-K Yuat South suite, K-feldspars are more potassic than K-feldspars of higher-K, less silicic diorites of the Yuat North suite. This suggests that a complex relationship exists between K-content of alkali fledspars and other rock parameters (e.g. K-content of residual liquids; amount of K-feldspar formed from the liquid; abundance of coexisting K-bearing phases).

6.3 AMPHIBOLE COMPOSITIONS

6.3.1 Introduction

Amphibole is the dominant ferromagnesian mineral in most calc-alkaline intrusive rock types of the Papua New Guinea region. In least silicic rocks, its place may be taken by pyroxenes and, more rarely, by olivine. In intermediate and more silicic rocks, amphibole may be accompanied by biotite and, more rarely, by pyroxene.

In the relevant sections on petrography, various habits and optical properties of amphiboles were noted. A broad distinction can be made between fibrous pale green amphibole ('tremolite/actinolite' or 'uralite' of some authors), and better-formed, frequently euhedral greenish brown amphibole. The former is observed as a replacement of pyroxene in mafic rocks, and also in ragged clots of mafic minerals

TABLE 13: K-FELDSPAR COMPOSITIONS

Specimen no/ no. of spot analyses.	SiO_2(wt%)	Al_2O_3	FeO**	CaO	Na_2O	K_2O	Total	Composition (Na:Ca:K)
DRM.012/4	66.3(0.6)*	18.7(0.1)	-	0.27(0.03)	2.94(0.06)	11.57(0.09)	99.70	28:1:71
DRM.013/5	65.6(0.3)	18.6(0.1)	-	0.24(0.06)	2.9 (0.2)	11.9 (0.4)	99.29	27:1:72
DRM.019/2	65.6(0.2)	18.6(0.1)	-	-	1.2 (0.3)	14.5 (0.4)	99.90	11:0:89
DRM.025/2	65.3(0.2)	18.4(0.1)	-	-	1.41(0.01)	13.86(0.02)	98.93	13:0:87
DRM.035/1	65.0	18.6	0.7	0.09	1.91	13.03	99.34	18:1:81
DRM.051/1	66.1	18.8	-	0.35	0.90	14.41	100.56	9:2:90
DRM.056/2	63.6(0.5)	18.5(0.7)	-	-	1.3 (0.1)	13.9(1.4)	97.40	13:0:87
DRM.063/3	65.3(0.6)	19.3(0.3)	-	0.94(0.05)	2.53(0.07)	11.6(0.1)	99.81	24:5:71
DRM.080/3	66.2(0.4)	18.3(0.3)	-	0.4(0.3)	2.7(0.3)	11.7(1.2)	99.29	23:1:76 to 30:4:66
DRM.143/2	65.5(1.3)	18.6(0.3)	-	0.19(0.01)	2.3(0.5)	12.8(0.9)	99.29	21:1:78
DRM.144/2	65.5(0.4)	18.2(0.1)	0.3(0.1)	0.3(0.1)	2.4(0.2)	12.4(0.4)	99.10	22:2:76
DRM.160/5	65.7(0.6)	18.7(0.4)	-	0.20(0.06)	2.6(0.2)	12.2(0.4)	99.32	24:1:75 (phenocrysts)
DRM.160/2	66.1(0.2)	18.4(0.1)	-	-	1.7(0.3)	13.6(0.2)	99.80	16:0:84 (rim of phenocrysts)
DRM.160/1	66.0	18.7	-	0.30	3.99	10.04	99.07	37:2:61 (rim of plag. pheno.)

Note: * = one standard deviation
** = total Fe as FeO

in more silicic rocks where presumably (and in some cases, demonstrably) it has replaced monoclinic pyroxene. The latter, better-formed amphibole has every appearance of a freely-crystallizing primary phase in that it displays well-formed crystal margins, good cleavages, and uniform colouring (although patchy absorption is not uncommon).

The major element data obtained for amphiboles by electron microprobe in this study pertain largely to amphiboles belonging to the latter variety, although limited data have been collected for replacement-type amphiboles in mafic rocks. The data also have a bias toward Western Highlands (continental margin) rocks rather than rocks of present island arc regions (see section (6.1) Introduction). A total of 178 spot analyses of amphiboles, together with structural formulae based on 23 oxygens, are set out in Appendix 4, Table 2.

6.3.2 Amphibole classification

The classification of calcic amphiboles used here is that of Leake (1968), in which three subdivisions are recognized:

(i) the tschermakite - actinolite series, in which Ca+Na+K is less than 2.5, and Ti is less than 0.5 (atoms in half unit cell),

(ii) the pargasite/hastingsite - richterite series, in which Ca+Na+K is greater than 2.5, and Ti is less than 0.5,

and (iii) the kaersutites, in which Ti is greater than 0.5.

The great majority of amphiboles from intrusive rocks of the Western Highlands belong to the tschermakite - actinolite series (see Fig. 40), and range from magnesio-hornblendes through actinolitic hornblendes to actinolite with increasing Si in the unit cell. In contrast, amphiboles from the Limbo River Diorite belong to the pargasite/hastingsite - richterite series, and range narrowly from ferroan pargasitic hornblende to edenitic hornblende with increasing Si in the unit cell. One sample from the Western Highlands (DRM065, a gabbro with granulitic texture from the Karawari Batholith) has amphibole compositions ranging from ferroan pargasite to ferroan pargasitic hornblende.

6.3.3 Compositional Variation in Amphiboles

The available data indicate a wide range of amphibole compositions, not only between those from different rock types, but also within individual amphibole crystals from a single specimen. The former type of variation has been widely discussed by many authors (Deer, 1938;

Fig. 40 : NOMENCLATURE OF AMPHIBOLES after LEAKE(1968), with fields of some amphiboles from Papua New Guinea.

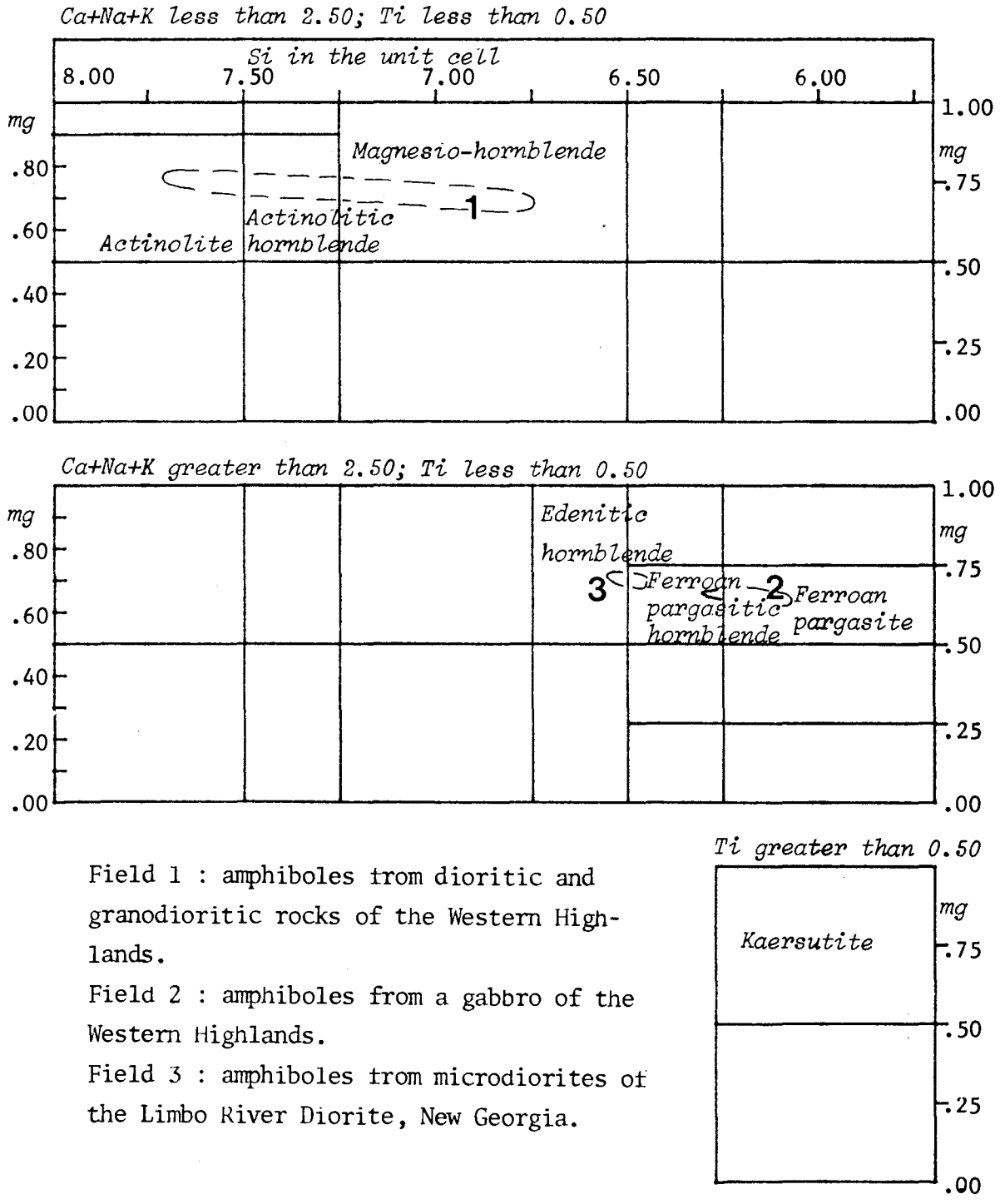

Field 1 : amphiboles from dioritic and granodioritic rocks of the Western Highlands.

Field 2 : amphiboles from a gabbro of the Western Highlands.

Field 3 : amphiboles from microdiorites of the Limbo River Diorite, New Georgia.

Deer, et al., 1963; Larsen & Draisin, 1950; Nockolds & Mitchell, 1948; Dodge, et al., 1968), but only recently has the latter (within-crystal) type of variation been discussed in relation to amphiboles in metamorphic rocks (Grapes, 1974; Vejnar, 1975) and intrusive rocks (Czamanske & Wones, 1973).

Ranges of amphibole compositions for selected intrusive rocks from the Western Highlands are presented in Table 14. For each of four intrusive complexes (Yuat North Batholith, Yuat South Batholith, Karawari Batholith, Frieda River Intrusive Complex), amphibole compositions are given for a range of rock types. In general, amphiboles from more mafic rocks are lower in SiO_2, and higher in TiO_2, Al_2O_3, and alkalis. This is in accord with previous findings (Nockolds & Mitchell, 1948; Dodge, et al., 1968). However, the wide range of composition displayed by Western Highlands amphiboles precludes closer comparison with those from other regions, and casts doubt on the validity of analysis of amphibole separates, a technique commonly used prior to the advent of the electron microprobe, and still used in some recent studies (e.g., Dodge, et al., 1968; Graybeal, 1973). Study of mineral separates is useful to the extent that it yields information on bulk mineral compositions, but may conceal important within-crystal compositional variations.

Fig. 41 displays extremes of Al(4) variation with SiO_2 content of the host rock for all analyzed amphiboles. Because Si and Al(4) vary antipathetically in the Z site, the demonstrated decrease in Al(4) with increasing rock SiO_2 corresponds to an increase in Si in the Z site. All Western Highlands amphiboles (mainly magnesio-hornblendes and actinolitic hornblendes) fall near or below the field of continental ('Andean'-type) calc-alkaline volcanic hornblendes of Jakes & White (1972) (field 2). The ferroan pargasitic hornblendes and edenitic hornblendes of the microdiorites of the Limbo River Diorite (Solomon Islands) plot appropriately near the field of island arc calc-alkaline volcanic hornblendes (field 1) which sets them apart from the Western Highlands hornblendes.

Significant differences between amphiboles of mineralized and non-mineralized suites from the Western Highlands are apparent on plots of Al(4) *versus* total Fe atoms in structural formulae. In Fig. 42, all available hornblende spot analyses for two granodiorites of the mineralized Yuat South Batholith have been plotted. The analyses fall on a well-defined trend of decreasing total Fe with decreasing Al(4). The absence

TABLE 14: RANGES OF AMPHIBOLE COMPOSITIONS FOR SELECTED INTRUSIVE ROCKS, WESTERN HIGHLANDS OF P.N.G.

	1	2	3	4	5	6	7	8	9	10
SiO_2(wt%)	43.2-50.2	48.2-51.1	46.1-53.8	47.9-53.9	46.9-54.8	41.6-43.5	49.6-49.2	47.7-54.6	44.9-50.3	42.8-53.0
TiO_2	3.2- 0.9	1.9- 0.6	1.7- 0.2	1.4- 0.2	1.8- 0.3	2.6- 2.1	1.6- 1.2	0.9- 0.0	2.0- 0.8	2.0- 0.5
Al_2O_3	10.4- 5.4	7.8- 4.9	8.2- 2.6	6.0- 1.2	7.1- 1.9	13.0-11.4	6.2- 6.1	8.1- 1.7	7.9- 5.2	11.1- 2.8
total FeO	14.4-14.1	14.9-12.8	14.1-11.5	14.5-17.2	17.9-14.0	14.1-13.7	13.2-13.0	13.8-11.4	16.4-13.9	15.0- 9.2
MnO	0.4- 0.3	0.4- 0.4	0.5- 0.8	0.4- 0.5	0.2- 0.4	0.4- 0.3	0.7- 0.6	0.6- 0.0	0.6- 0.7	0.4- 0.6
MgO	12.4-14.1	13.8-15.3	13.5-16.6	14.2-13.7	11.8-16.4	12.5-13.1	14.7-14.9	14.4-16.9	12.5-14.1	12.4-17.9
CaO	11.5-12.2	11.5-12.1	11.5-12.1	11.3-12.1	11.2-11.3	12.0-12.3	11.7-11.7	10.8-12.6	11.2-12.0	11.4-11.5
Na_2O	1.5- 0.5	1.0- 0.4	1.4- 0.2	1.2- 0.0	1.5- 0.4	2.2- 1.7	1.3- 1.2	1.1- 0.0	1.4- 0.6	2.2- 0.6
K_2O	0.6- 0.5	0.5- 0.2	0.6- 0.2	0.5- 0.1	0.7- 0.2	0.8- 0.7	0.3- 0.4	0.2- 0.0	0.6- 0.4	0.7- 0.2
100 Mg/Mg + tot. Fe (at propns).	61 - 64	62 - 68	63 - 72	64 - 59	54 - 68	61 - 63	66 - 67	65 - 73	58 - 64	60 - 78

1 = DRM.054, h'b (-cpx-qtz) gabbro, Yuat South Batholith; analysis numbers 2 and 16.

2 = DRM.052, h'b (-cpx-qtz) gabbro, Yuat South Batholith; analysis numbers 8 and 10.

3 = DRM.025, h'b-bio-qtz granodiorite, Yuat South Batholith; analysis numbers 12 and 36.

4 = DRM.013, high-K h'b-bio-qtz diorite, Yuat North Batholith; analysis numbers 6 and 1.

5 = DRM.056, microadamellite, Yuat North Batholith; analysis numbers 5 and 7.

6 = DRM.065, h'b (-cpx) gabbro, Karawari Batholith; analysis numbers 1 and 6.

7 = DRM.035, h'b (-cpx)-qtz diorite, Karawari Batholith; analysis numbers 1 and 3.

8 = DRM.036, plag.-h'b-qtz diorite porphyry, Karawari Batholith; analysis numbers 4 and 6.

9 = DRM.081, "Nena Diorite", Frieda River Intrusive Complex; analysis numbers 10 and 8.

10 = DRM.080, "Quartz Diorite Porphyry", Frieda River Intrusive Complex; analysis numbers 12 and 9.

FIG. 41 : VARIATION OF HORNBLENDE Al(4) AND ROCK SiO_2.

Field 1 = island arc calc-alkaline volcanic hornblendes
Field 2 = continental margin hornblendes (Jakes & White,1972).

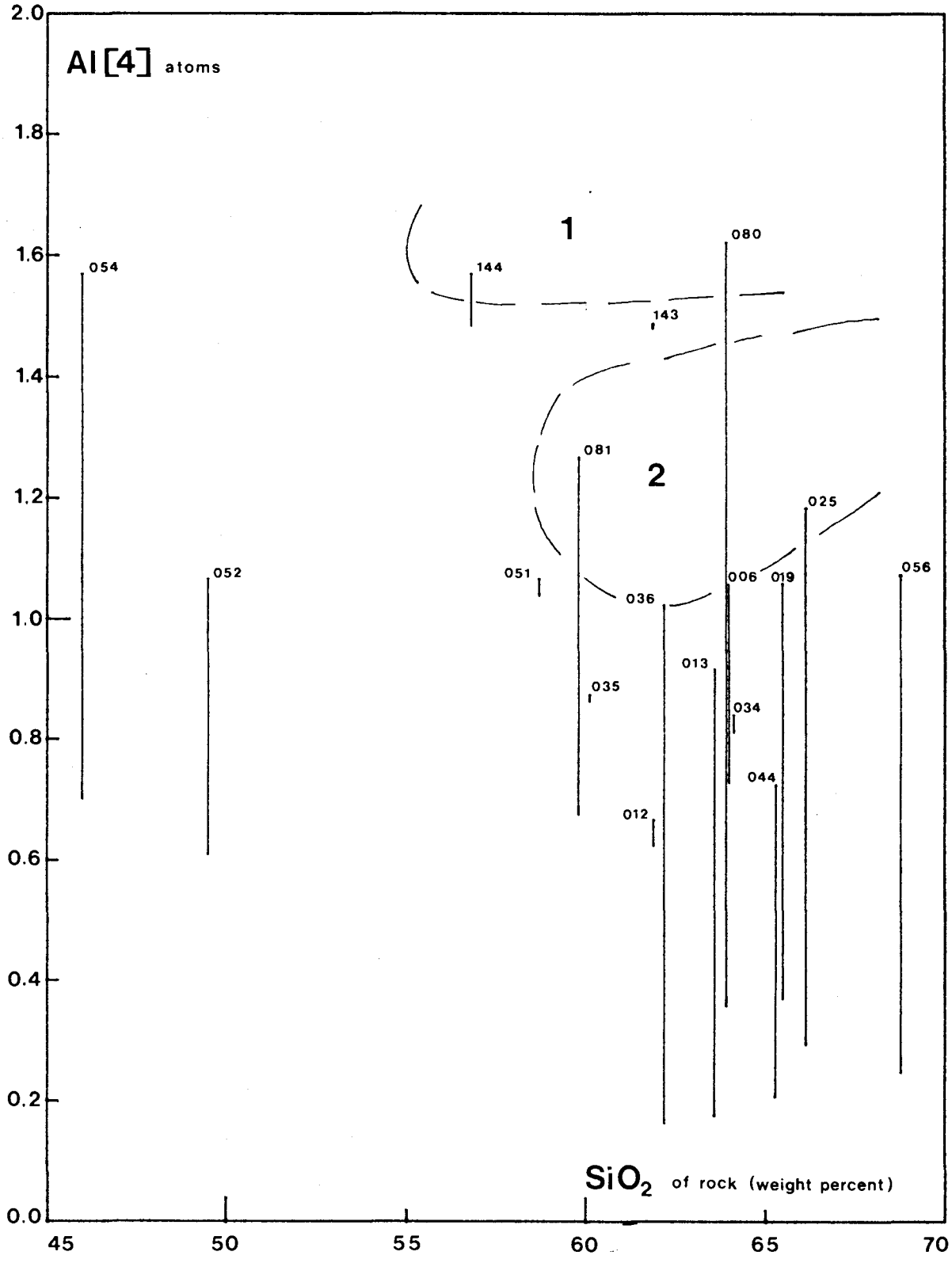

Fig. 42: Al(4) versus tot.Fe atoms, hornblendes from granodiorites, Yuat South Batholith.

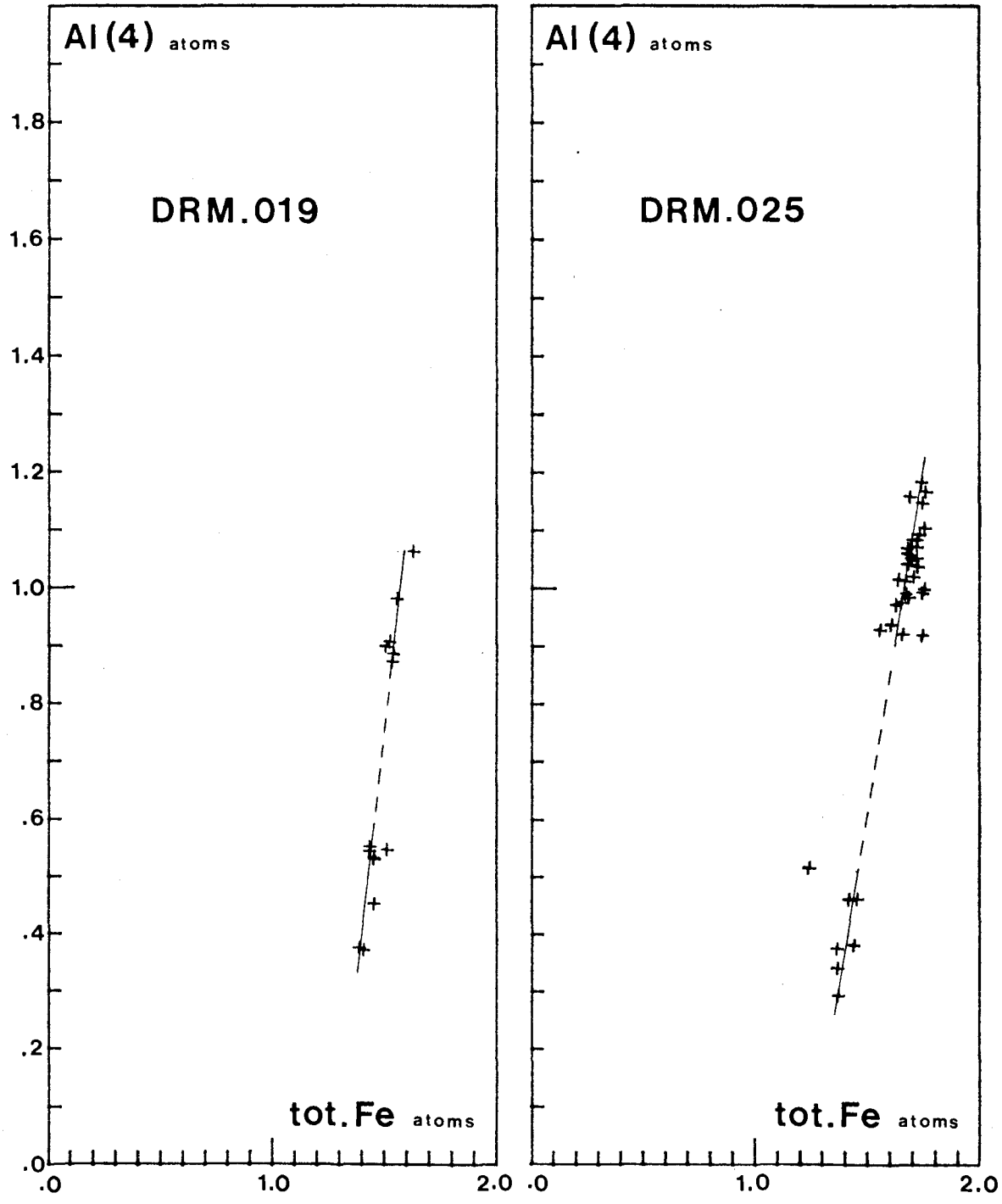

of analyses between Al(4) = 0.85-0.55 is considered to be real, and reflects a sudden change of conditions during crystallization of the hornblendes. Similar trends are observed for other Western Highlands hornblende-bearing intrusive rocks associated with porphyry-type copper mineralization (see Fig. 43: diorite porphyry of the Awari Stock, Karawari Batholith; granodiorite of the western part of the Yuat South Batholith; diorite porphyry and Nena Diorite of the Frieda River Intrusive Complex).

In contrast, hornblendes from the high-K diorites of the non-mineralized Yuat North Batholith show the reverse trend, namely *in*creasing total Fe with decreasing Al(4). Only the highly differentiated microadamellite displays a trend of decreasing total Fe with decreasing Al(4).

In an endeavour to spatially relate the observed hornblende chemical variations, spot analyses were made on traverses from core to rim across individual hornblende crystals. The results of traverses selected to show all observed variations are presented in Figs. 44 to 46. Each traverse spans a distance of 0.5-1.0 mm., and spot analyses are located relative to distance from the crystal core. In Figs. 44 and 45, it is readily apparent that there are systematic changes in hornblende composition from core to rim: SiO_2 and MgO increase, while TiO_2, Al_2O_3, and total FeO decrease. This is true for the majority of amphibole crystals from intrusive rocks closely associated with mineralization. Other regular changes not plotted include increase of MnO and CaO,and decrease of Na_2O and K_2O, from core to rim. Some crystals (e.g. DRM025, crystal 4) display little or no change in composition. One crystal (DRM025, crystal 6) displays anomalous changes for its two traverses.

It is stressed that, in transmitted light, the hornblendes under discussion exhibit little evidence of the considerable chemical variations they contain. Most of the crystals are evenly coloured, but under crossed polarizers a small change in extinction angle can be observed toward rims. There is no evidence that dueteric alteration has been responsible for affecting the hornblende rims.

Even hornblendes from gabbroic rocks of the Yuat South Batholith display the same type of chemical variations (see Fig. 46). Traverses across three crystals from DRM054, a hornblende (-clinopyroxene-quartz) gabbro, reveal complex core chemistry resulting from growth of primary hornblende (crystal 1, with low SiO_2 and high TiO_2 and Al_2O_3),

Fig. 43: Al(4) versus total Fe atoms for Western Highlands hornblendes.

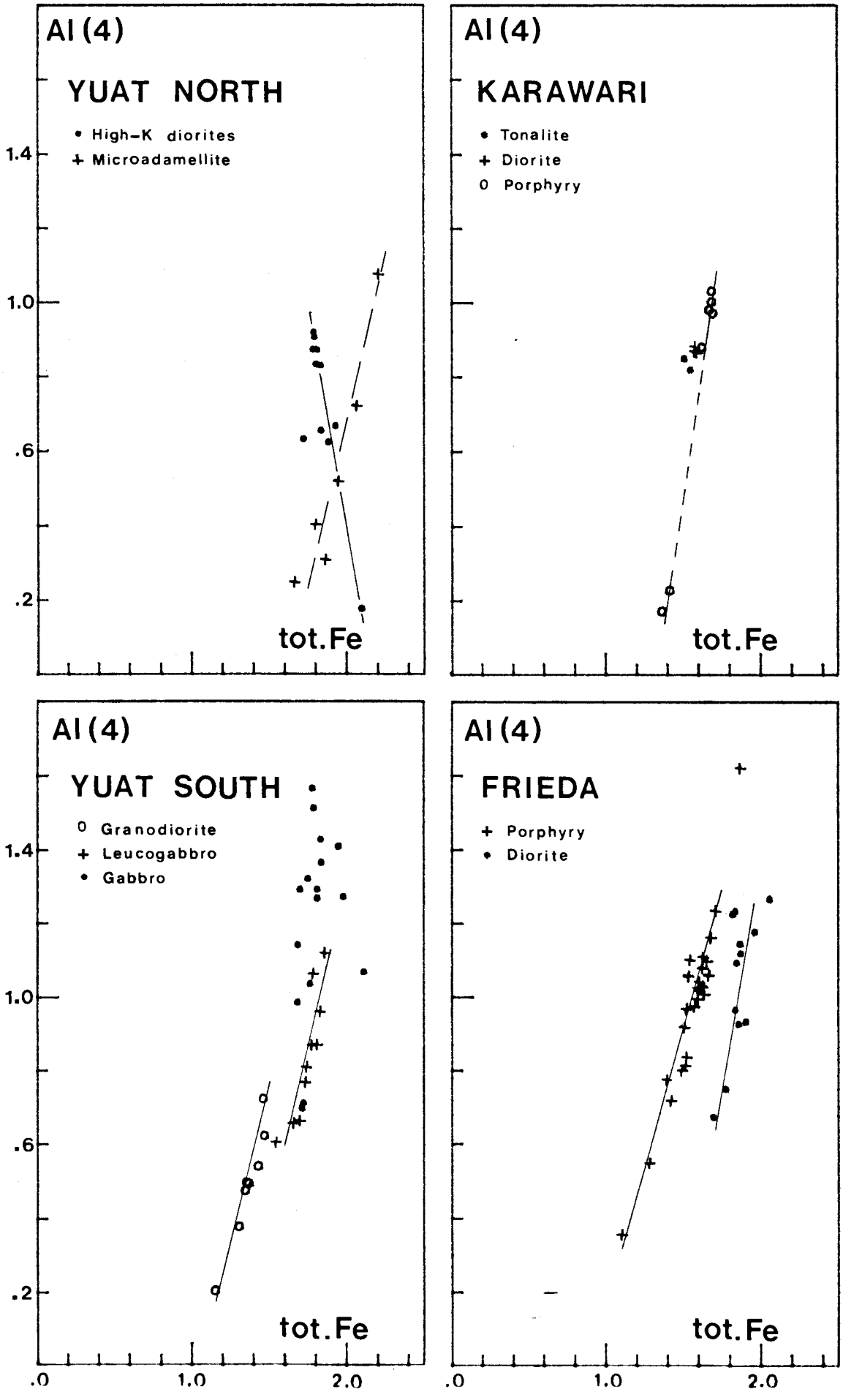

Fig. 44: Hornblende traverses

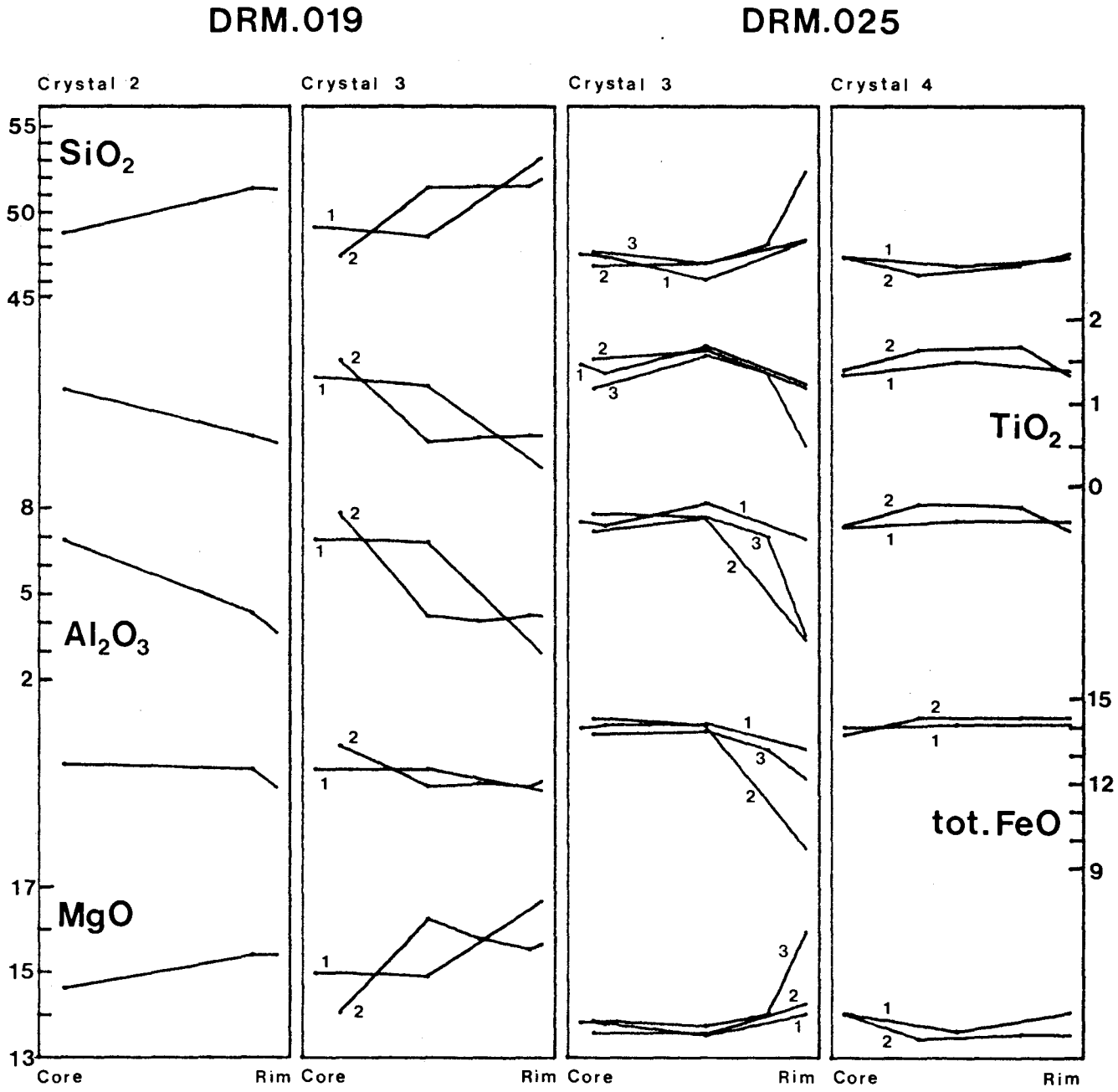

Fig. 45: Hornblende traverses

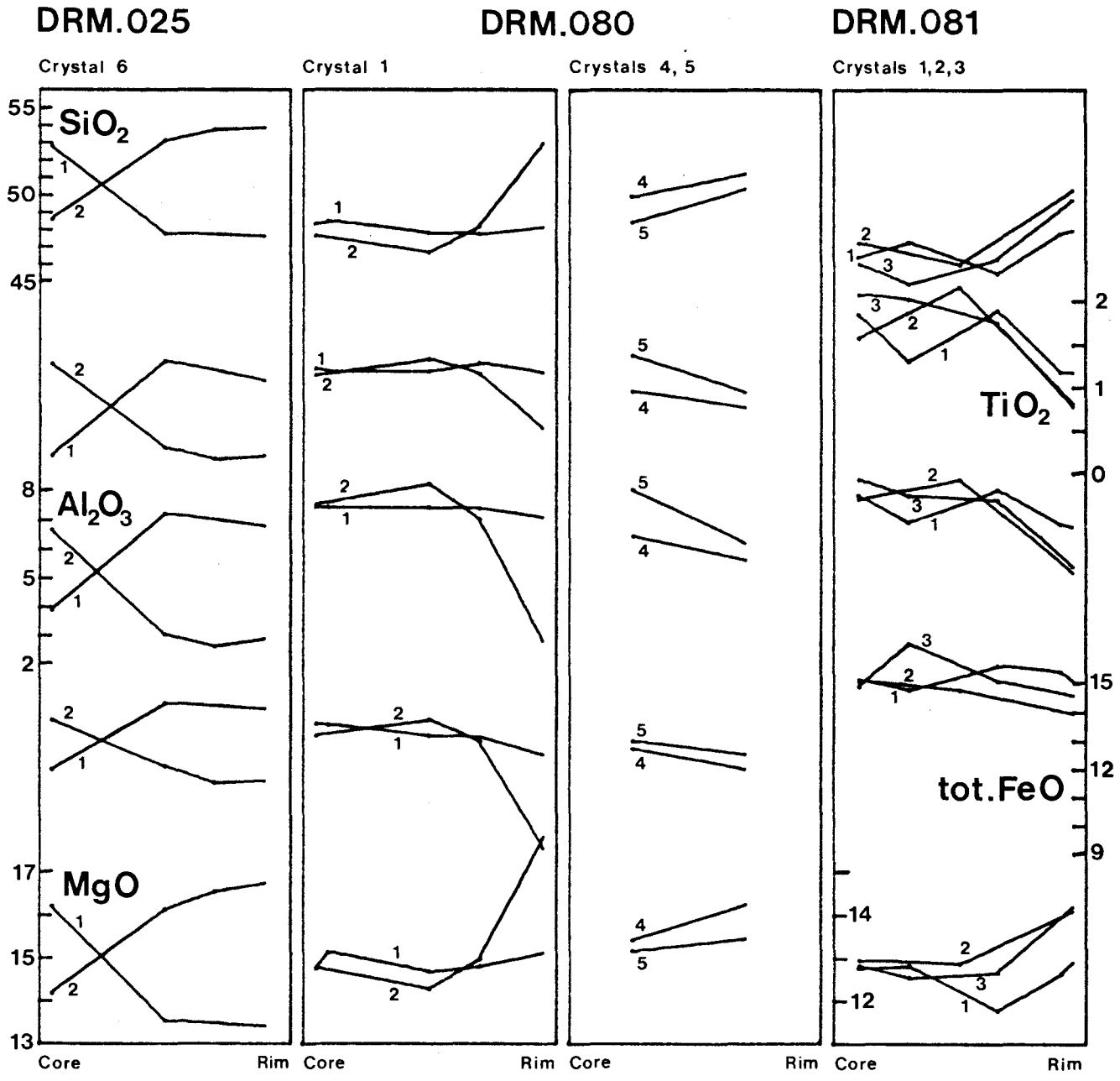

Fig. 46: Hornblende traverses

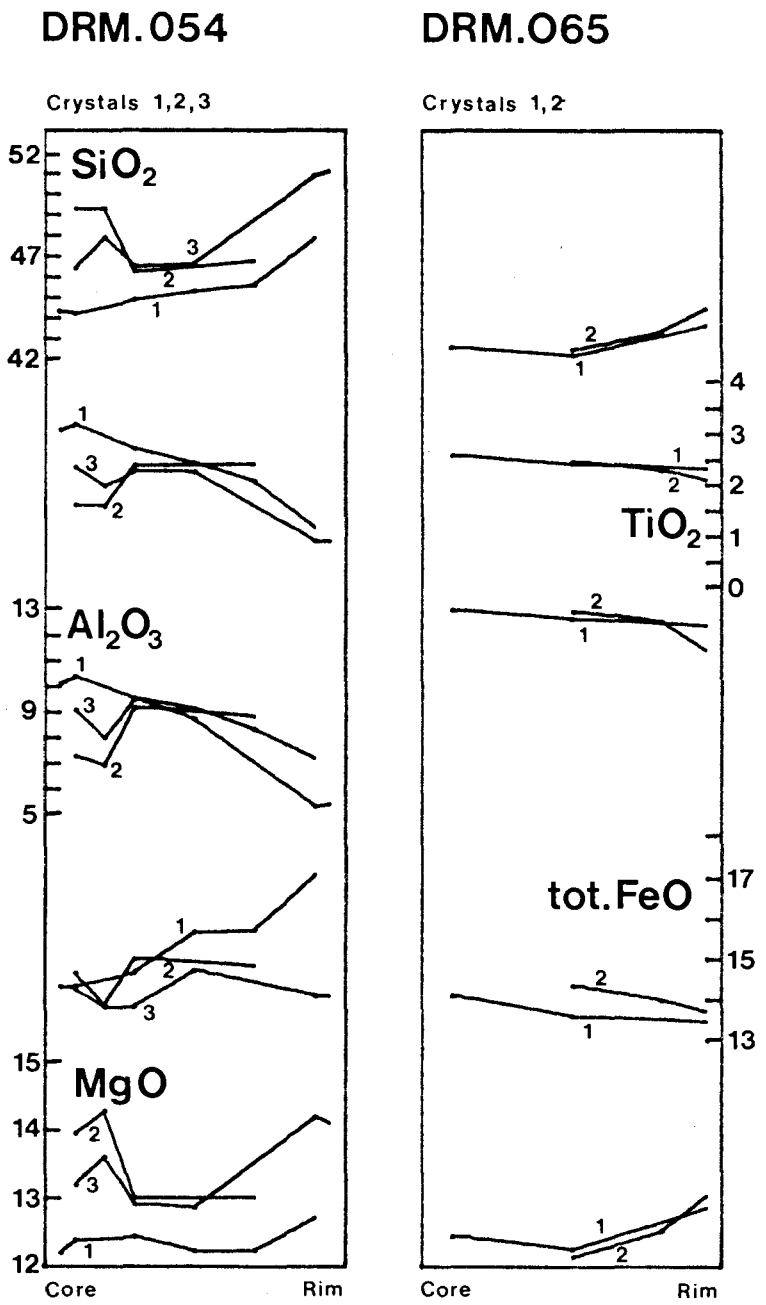

and from replacement of clinopyroxene (crystal 2, with high SiO_2 and lower TiO_2 and Al_2O_3 in the core). However, in central and outer parts of crystals, all three traverses display changes which are similar qualitatively to those observed in the dominant granodiorites of the Batholith (i.e. increasing SiO_2 and MgO, with decreasing TiO_2, Al_2O_3, total FeO, and alkalis toward rims).

Changes in amphibole composition similar to those described above have been reported by Czamanske & Wones (1973) from the shallow-level Finnmarka Complex, Oslo Area, Norway. The data for amphiboles of Finnmarka granodiorite are plotted on Fig. 47 with some amphibole data from Yuat South granodiorite. Those authors appealed to conditions of increasing oxygen fugacity during crystallization to produce the observed changes in amphibole chemistry. Their rationale (Czamanske & Wones, 1973, pp. 376-378), equally applicable to the Western Highlands rocks, is: progressive oxidation encourages precipitation of magnetite, thus lowering the activity of FeO in the melt and, as a consequence, the FeO content of the crystallizing amphibole; the activity of SiO_2 increases during crystallization, resulting in higher SiO_2 contents of the amphibole and lower Al(4); because Al(4) is involved in a number of different coupled substitutions in the amphibole structure, its decrease will affect the contents of other elements (Mg, Si, Ca, Na); because of possible reactions such as

ferrotremolite + ilmenite + oxygen
= magnetite + quartz + sphene + water

and

titanoferropargasite + quartz + oxygen
= magnetite + plagioclase + sphene + water,

it is likely that magnetite and sphene will be accessory phases in rocks which have evolved under these conditions.

The following textural features of Western Highlands rocks support the above rationale:

(i) the studied amphiboles are subhedral in form, are well cleaved, and display even colouring, suggesting that they have crystallized freely from a melt.

(ii) subhedral magnetite and associated sphene are constant accessories in the Yuat South granodiorites and related gabbroic rocks. In contrast, the high-K diorites of the Yuat North Batholith possess a titaniferous magnetite and lack sphene.

Fig. 47: Comparison of hornblende variation in granodiorites from Yuat South and Finnmarka

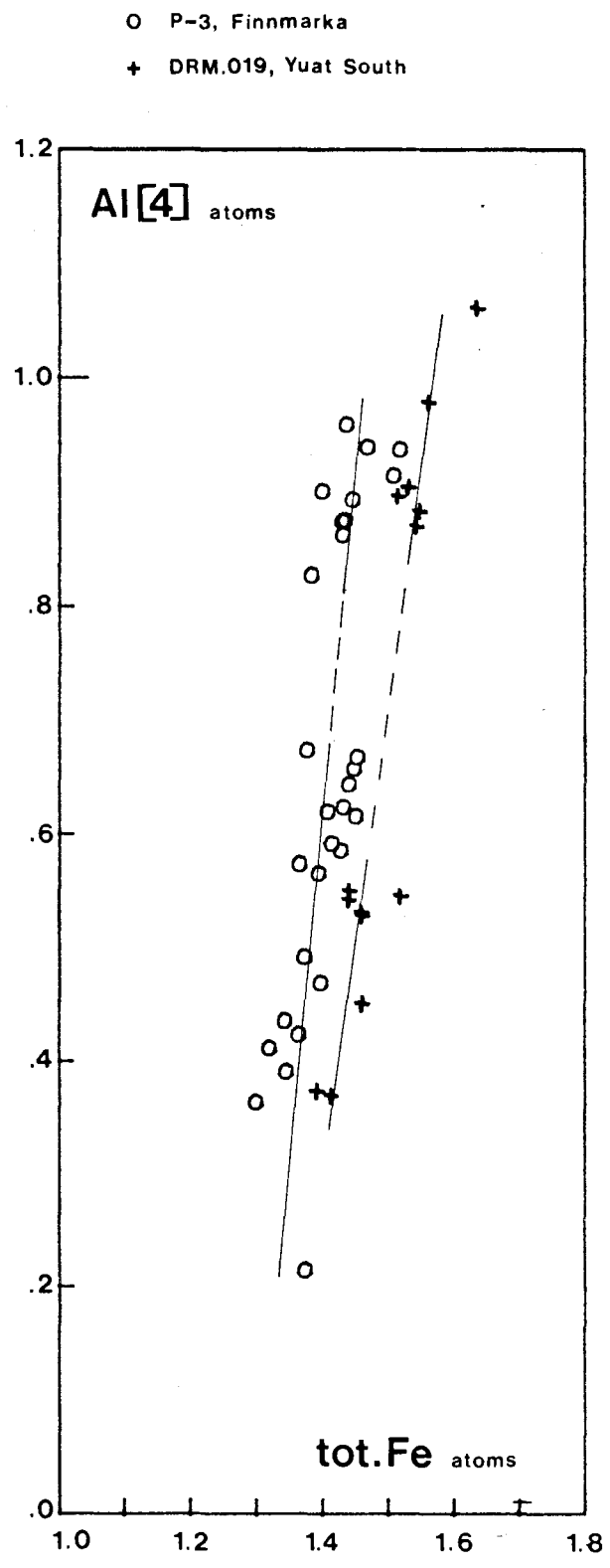

(iii) the presence of late-forming interstitial quartz in the granodiorites and gabbros of the Yuat South Batholith implies that the melt became saturated with quartz at the final stages of crystallization, allowing continuous SiO_2-enrichment in amphiboles during their crystallization.

(iv) the consistent variations in amphibole composition from core to rim (a feature not found, and remarked upon, by Czamanske & Wones) can logically be attributed to the response of the growing crystals to the changing conditions in, and composition of, the residual melt immediately adjacent.

(v) the requirement of increasingly oxidizing conditions, possibly leading to separation of a hydrothermal metal-rich phase, is in accord with the association in the Western Highlands of porphyry-type copper mineralization and intrusive rocks displaying the amphibole variations described above.

6.4 BIOTITE COMPOSITIONS

6.4.1 Introduction

Biotite is the next most abundant ferromagnesian mineral after amphibole in the Western Highlands intrusive rocks. It is usually lacking in mafic rocks, although the orthoclase gabbro (DRM063) of the Yuat North region is a notable exception. In dioritic and granodioritic rocks, biotite forms discrete well-cleaved plates ('primary' biotite), but may also be observed as rims developed on amphibole grains and as ragged flakes associated with clots of mafic minerals ('secondary' biotite). Both of these biotites are usually pleochroic in shades of yellow and dark brown. In rocks closely associated with mineralization (e.g., Awari Stock of Karawari Batholith; Frieda River Intrusive Complex; Ok Tedi Intrusive Complex), fine-grained flaky biotite occurs as mafic mineral pseudomorphs and groundmass aggregates ('hydrothermal' biotite). This biotite is pleochroic from pale yellow to reddish brown.

Major element electron microprobe data for Western Highlands biotites (and some Solomon Islands biotites) pertain mainly to primary biotites. In some specimens primary and secondary biotites are present (e.g. DRM012), but distinction between the two forms could not always be made under the reflected light conditions in which much of the electron microprobe data was collected. Hydrothermal biotites were analyzed in rocks from three Western Highlands locations: Awari, Frieda and Ok Tedi. In Appendix 4, Table 3, 125 spot biotite analyses and structural formulae based on 22 oxygens are presented. The data come from a total

of 13 Western Highlands rocks and 3 Solomon Islands rocks.

6.4.2 Compositional Variation in Biotites

Average biotite compositions for selected Western Highlands rocks are presented in Table 15. Generally, TiO_2 decreases and MgO increases from primary biotite through secondary biotite to hydrothermal biotite. Mg/Mg+tot.Fe for hydrothermal biotites is much higher (0.7-0.8) than for primary and secondary biotites (0.5-0.7). These findings are in accord with recent work on biotites from the Bingham district, Utah (Moore & Czamanske, 1973).

Fields of biotite compositions for the 16 analyzed rocks are shown in Fig. 48, which is based on the extreme ideal trioctahedral mica compositions of phlogopite, K_2Mg_6 $(Si_6Al_2O_{20})$ $(OH)_4$: eastonite, K_2Mg_5 $Al(Si_5Al_3O_{20})$ $(OH)_4$: siderophyllite, $K_2Fe_5Al(Si_5Al_3O_{20})(OH)_4$: and annite, $K_2Fe_5(Si_6Al_6O_{20})(OH)_4$ after Deer et al. (1963). The abscissa represents increasing Al(6) and the ordinate represents increasing Fe/Fe+Mg.*

Most of the biotite fields cluster near the phlogopite-annite join, in the region Fe/Fe+Mg = 0.35-0.50. The biotites of the Yuat North microadamellite (DRM056) have higher Fe/Fe+Mg than the biotites of associated high-K diorites (DRM012,013). This has been considered the usual trend in calc-alkaline rocks (Nockolds, 1947; Larsen and Draisin, 1950). Biotites of the Limbo River Diorite (DRM143, 144, 145) are more Mg-rich than and have the lowest Fe/Fe=Mg of, all other primary biotites. Hydrothermal biotites display lowest Fe/Fe+Mg and highest MgO, and both secondary and hydrothermal biotites display considerable variation in Al(6).

The primary biotite fields show limited but measurable variation in Al(6). There are two types of variation: *in*creasing Fe/Fe+Mg with increasing Al(6) (e.g. DRM012, 056, 145), and *de*creasing

---

*Variations in Al(6) are small for biotites from most Western Highlands and Solomon Islands occurrences. However, the variations are much greater than errors related to measurement of Al_2O_3 and SiO_2, upon which the calculation of octahedral aluminium is strongly dependent. For example, the combined effect of +0.1% SiO_2 and +0.1% Al_2O_3 is to increase Al(6) by only 0.02 atoms, which is to be compared with the range of 0.25 atoms of Al(6) in biotites of some specimens. The assumptions of charge balance implicit in the structural formula calculation are accepted here. Further, it is considered that there is sufficient evidence to confirm the presence of octahedral aluminium in natural and some synthetic micas (Foster, 1960; Hazen & Wones, 1972).

TABLE 15: AVERAGE BIOTITE COMPOSITIONS FOR SELECTED WESTERN HIGHLANDS ROCKS

No.	1	2	3	4	5	6	7	8	9	10	11
type/no. of anals.	P/3	S/2	P/4	P/19	S/1	P/6	H/3	P/3	**H/4	P/11	H/5
SiO_2	42.5(4.0)*	42.3(0.7)	37.1(0.3)	37.2(0.5)	37.0	37.7(0.3)	39.3(1.6)	35.9(0.8)	31.9(1.3)	38.1(0.4)	42.7(0.3)
TiO_2	4.8(0.4)	4.1(0.1)	5.2(0.1)	4.4(0.4)	3.2	3.6(0.2)	1.7(0.1)	3.7(0.2)	0.1(0.1)	4.3(0.3)	2.3(0.2)
Al_2O_3	13.5(1.4)	12.8(1.6)	13.9(0.2)	14.2(0.4)	14.5	14.0(0.2)	15.7(0.1)	16.0(0.2)	20.1(0.7)	13.9(0.3)	11.6(0.4)
tot.FeO	17.2(2.1)	17.2(1.0)	21.6(0.4)	18.2(0.5)	17.8	16.3(0.4)	11.6(0.7)	16.8(0.4)	22.7(0.7)	14.5(0.3)	8.1(0.4)
MnO	0.0	0.0	0.0	0.4(0.1)	0.5	0.0	0.0	0.1(0.1)	0.3(0.1)	0.0	0.0
MgO	11.5(1.7)	12.6(0.1)	10.7(0.2)	13.0(0.4)	12.7	14.9(0.2)	17.9(0.4)	17.8(0.1)	20.8(0.4)	15.9(0.4)	20.9(0.5)
CaO	0.5(0.4)	2.4(1.6)	0.0	0.2(0.1)	1.1	0.2(0.1)	0.3(0.1)	0.2(0.1)	0.2(0.1)	0.1(0.1)	0.1(0.1)
Na_2O	0.0	0.0	0.0	0.0	0.0	0.0	0.0	0.0	0.0	0.0	0.0
K_2O	8.3(0.7)	6.4(1.5)	9.1(0.1)	8.9(0.5)	8.1	8.9(0.1)	7.0(1.3)	5.1(0.5)	0.1(0.1)	8.9(0.2)	9.8(0.2)
total	98.3	97.8	97.6	96.5	94.9	95.6	93.5	95.6	96.2	95.7	95.5
Mg/Mg+Fe (at propns)	.54	.57	.47	.56	.56	.62	.73	.65	.62	.66	.82
MgO/MgO+tot.FeO (rock)	.31	.31	.24	.29	.29	.44	.44	.39	.39	.40	.50

Key: P = primary
S = secondary
H = hydrothermal
* = one standard deviation
** = greenish brown mica after hornblende

Yuat North Batholith: 1,2 = DRM.012
3 = DRM.056

Yuat South Batholith: 4,5 = DRM.019
6 = DRM.044

Karawari Batholith (Awari Stock): 7 = DRM.027

Frieda River Intrusive Complex: 8,9 = DRM.006
10 = DRM.080

Ok Tedi Intrusive Complex: 11 = DRM.160

Fig. 48: Fields of biotite compositions

h = hydrothermal

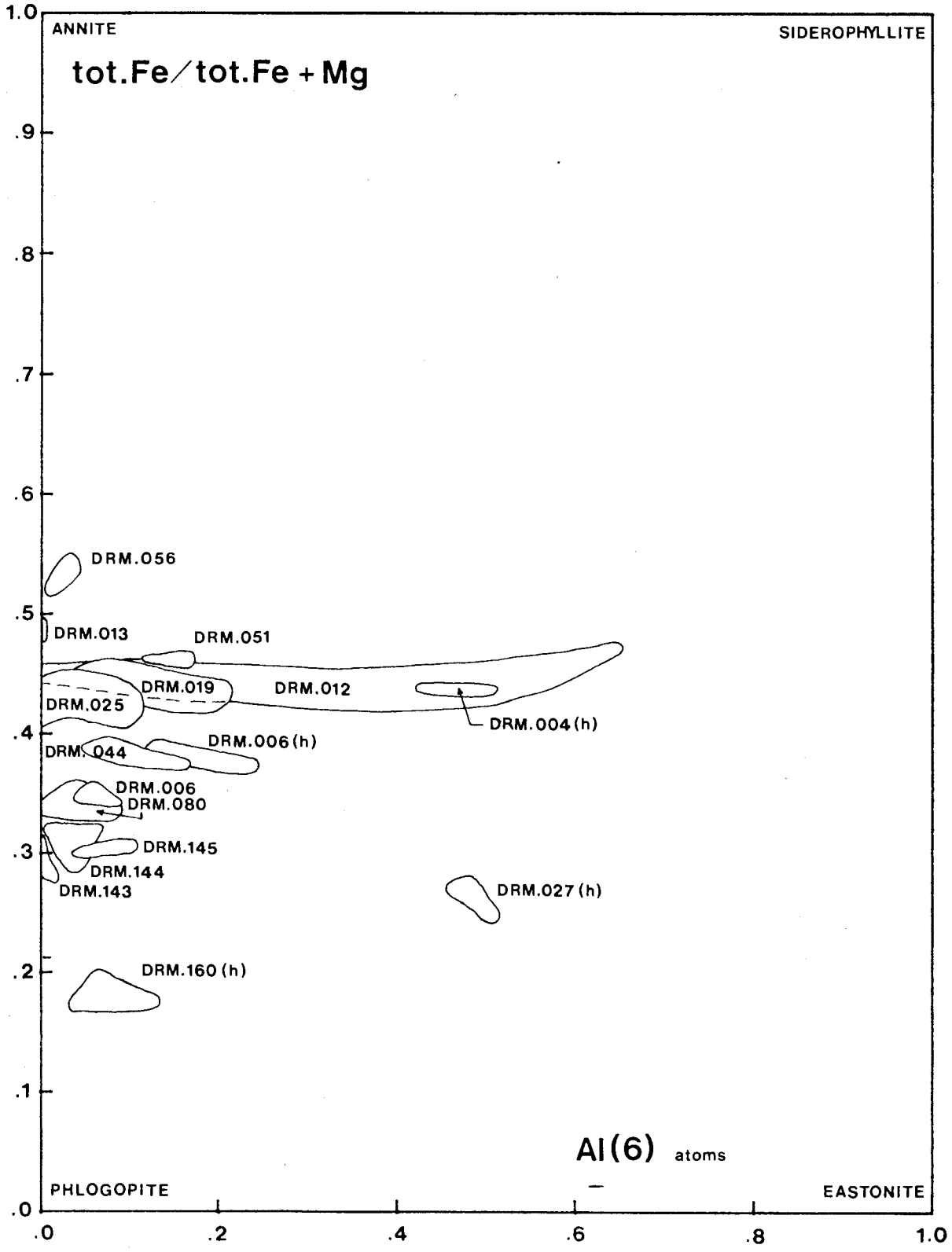

Fe/Fe+Mg with increasing Al(6) (e.g. DRM019, 025, 044, 006, 080). These two types of variation correspond to non-mineralized and mineralized suites respectively. The latter type of variation is further illustrated in Fig. 49, where all available analyses for the mentioned specimens are plotted, together with 3 biotite analyses from Finnmarka granodiorite (Czamanske & Wones, 1973) for comparison. Those authors concluded that oxygen fugacity increased during crystallization of the Finnmarka Complex, and it would appear that similar conditions prevailed in intrusive rocks associated with mineralization in the Western Highlands.

Much of the Western Highlands biotite data was collected along crystal traverses (core to rim). In Fig. 50, variation of TiO_2 and Mg/Mg+Fe are depicted for traverses across biotites from Yuat South granodiorites (DRM019, 025). Most traverses reveal decreasing TiO_2 and increasing Mg/Mg+Fe toward rims. Some crystals display little variation (e.g. DRM019, crystal 3; DRM025, crystal 2). The variations are considered to be real ($TiO_2 \pm 0.3\%$ at 95% confidence; Mg/Mg+Fe $\pm$ 0.7 at 95% confidence). In Fig. 51, similar plots are presented for biotites from another Yuat South granodiorite (DRM044) and a diorite porphyry from Frieda River (DRM080). Variations for DRM044 are equivocal, while the Frieda specimen displays trends which are opposite those of the Yuat South rocks (i.e., increasing TiO_2 and decreasing Mg/Mg+Fe toward rims).

It is stressed that in thin section these biotites appear to be quite unaffected by alteration. The dominant type of variation (decreasing TiO_2 and increasing Mg/Mg+Fe toward rims) is qualitatively similar to that observed in amphiboles from the same rocks (see previous section). It is concluded, therefore, that there has been some degree of disequilibrium between crystallizing biotites and residual melts. In rocks associated with mineralization, the disequilibrium has arisen from increasingly oxidizing conditions in the melt, resulting in successively different compositions of crystallizing mafic minerals. Biotites appear not to reflect these conditions as readily as amphiboles. This may be a function of paragenesis (amphiboles crystallizing to a later stage), which is unsupported petrographically, or it may reflect more rapid diffusion (and hence more rapid reaction of biotites with residual melts) in the sheet lattice of the micas compared with the chain lattice of the amphiboles.

6.5 PYROXENE COMPOSITIONS

In the intrusive calc-alkaline rocks of the Papua New Guinea region, pyroxenes are generally less abundant than amphiboles and

Fig. 49: Biotite compositional variations

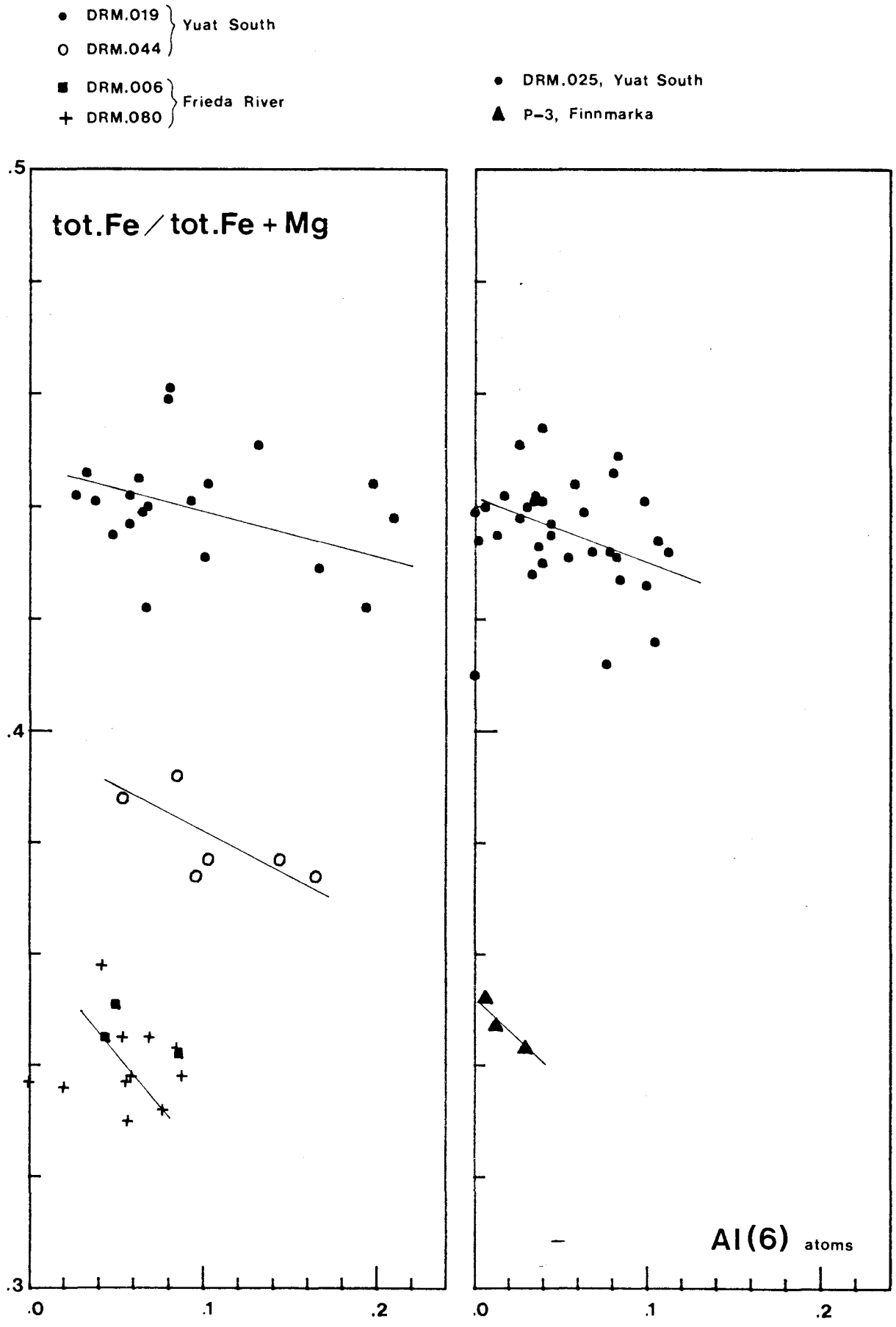

Fig. 50: Biotite traverses

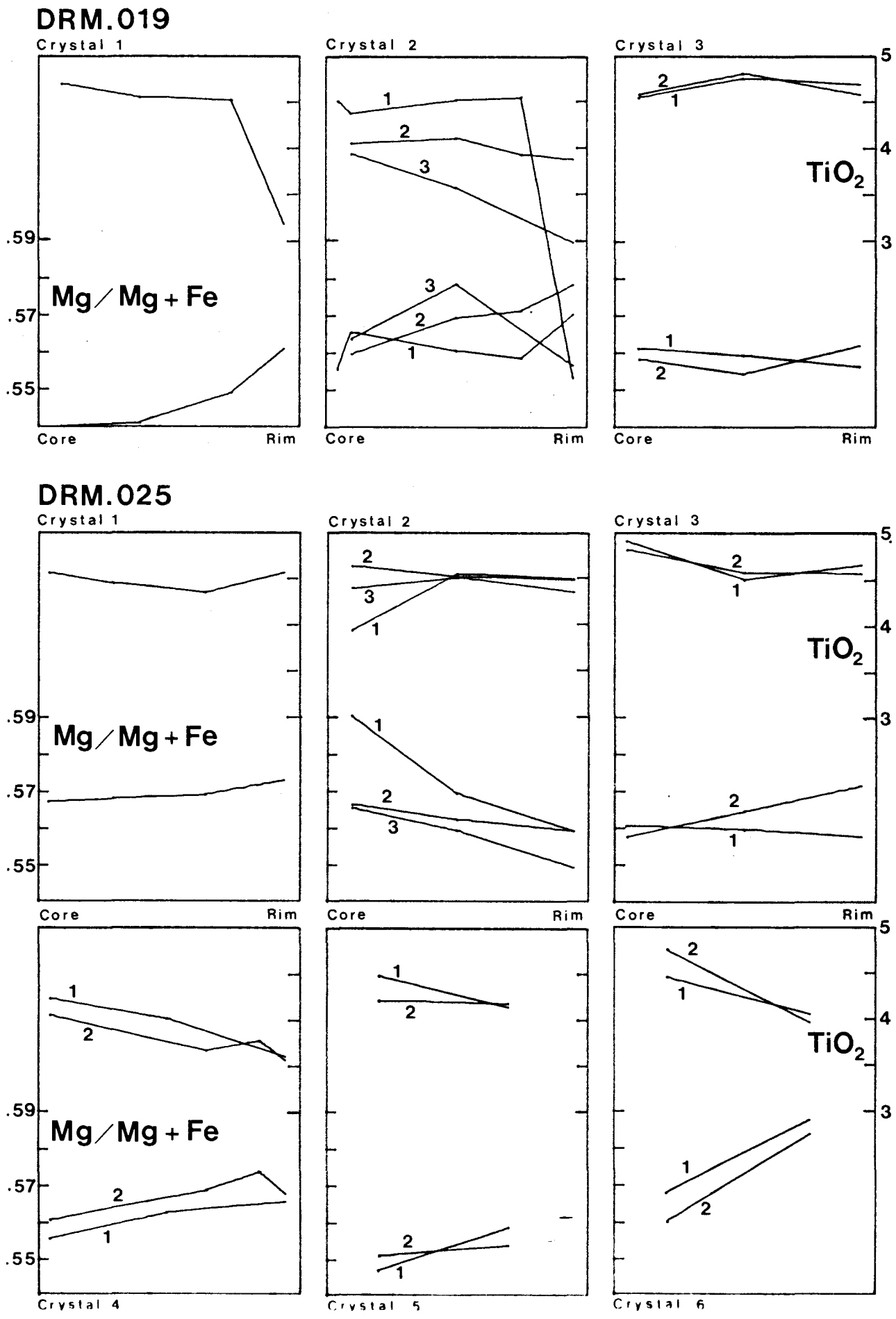

Fig. 51: Biotite traverses

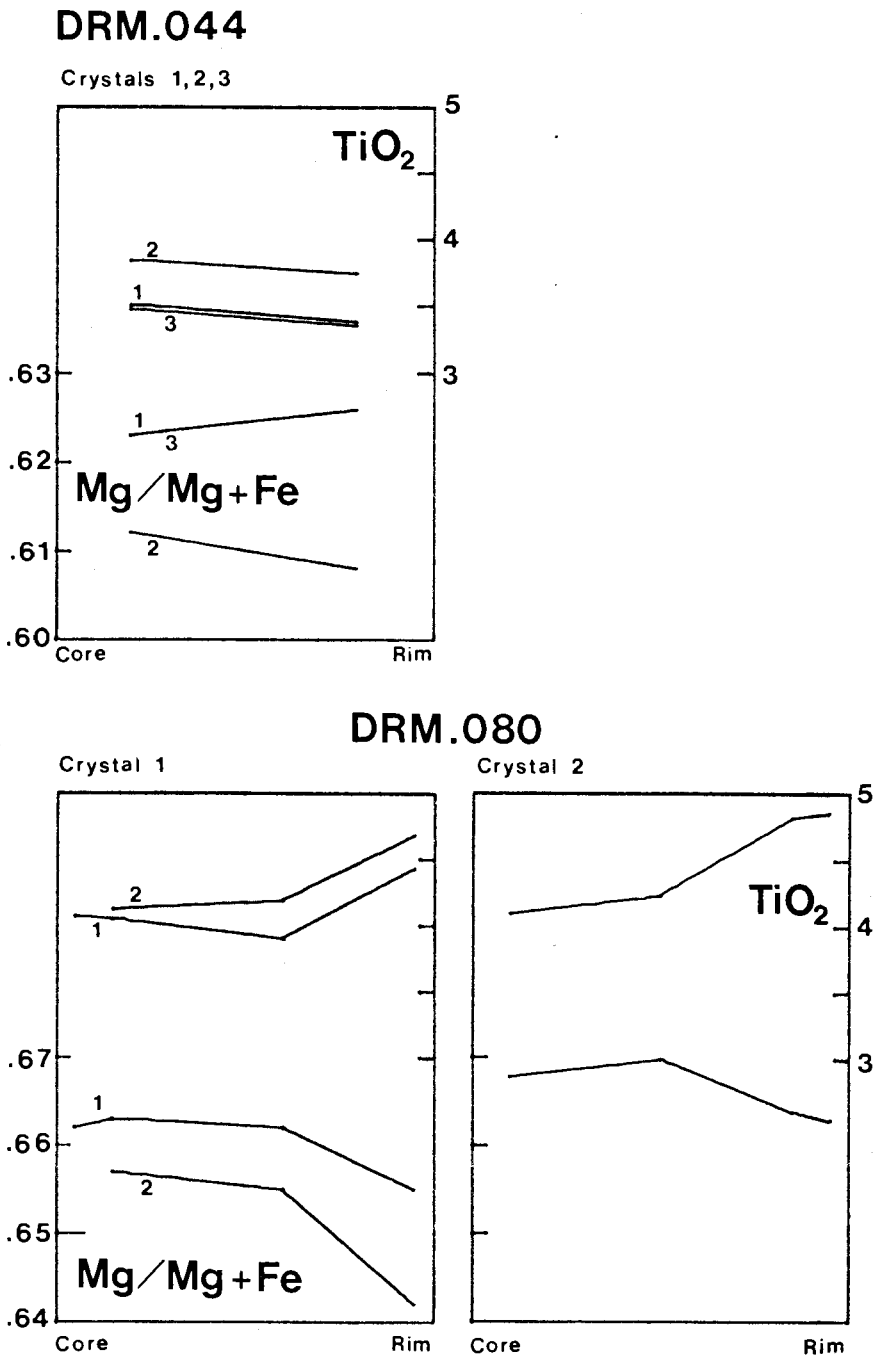

biotites. This conforms to the known distribution of mafic minerals in other calc-alkaline intrusive rocks. In the P.N.G. rocks, clinopyroxenes of gabbroic rocks frequently possess rim alteration to an amphibole. In dioritic rocks, clinopyroxene may occur as cores within amphibole grains. More rarely, clinopyroxene becomes dominant in the mafic assemblage (e.g. Ok Tedi Intrusive Complex of the Western Highlands; the Lemau Intrusive Complex of New Ireland; the Mafic Suite of the Koloula Igneous Complex, Guadalcanal).

Orthopyroxene is rare in the intrusive rocks studied here. In rocks of the Western Highlands, it has been observed only as rare relic cores within amphibole in high-K diorite of the Yuat North Batholith. Bastite pseudomorphs after orthopyroxene occur in parts of the Alpine-type ultramafic bodies forming the April Ultramafics (Dow, et al., 1968) of the Western Highlands. Orthopyroxene-bearing intrusive rocks are relatively more common in the island regions of Papua New Guinea and the Solomon Islands (e.g., Plesyumi Intrusive Complex; Lemau Intrusive Complex; Limbo River Diorite; Mafic Suite of Koloula Igneous Complex).

Major element electron microprobe data have been collected for pyroxenes from 5 intrusive rocks of the Western Highlands (Yuat North and Karawari batholiths; Ok Tedi Intrusive Complex), and for pyroxenes from 3 intrusive rocks of the Limbo River Diorite. Average compositions for these pyroxenes are presented in Table 16.

The relic clinopyroxene of the Yuat North high-K diorite is a calcic augite with Ca:Mg:Fe = 44:38:18 (see Fig. 52). Clinopyroxenes from the low- to normal-K Karawari Batholith are even more calcic (Ca:Mg:Fe = 48:39:13), and fall within the salite field on the pyroxene quadrilateral. The greenish clinopyroxene from high-K diorite of the Ok Tedi Complex also plots in the salite field (Ca:Mg:Fe = 48:35:17).

The more mafic rocks of the Limbo River Diorite carry two pyroxenes. The gabbroic cumulate (DRM145) has a diopsidic augite (Ca:Mg:Fe = 44:45:11) and coexisting bronzite (approximately En(75)), while the microdiorites possess salite (Ca:Mg:Fe = 45:42:13) and a subcalcic augite (Ca:Mg:Fe = 26:54:20).

TABLE 16: PYROXENE COMPOSITIONS

SPEC. NO.	DRM.012	DRM.035	DRM.063	DRM.065	DRM.087	DRM.143	DRM.144	DRM.144	DRM.145	DRM.145
no of anal.	2	4	2	6	8	2	4	4	5	2
Pyroxene	calcic augite	salite	salite	salite	salite	salite	subcalcic augite	salite	calcic augite	bronzite
SiO_2	51.6 (2.1)*	53.6(0.6)	51.6 (0.3)	52.37(0.3)	52.0 (0.6)	54.3 (0.5)	56.6 (0.7)	53.6 (0.5)	53.2 (0.7)	55.2 (0.2)
TiO_2	0.8 (1.0)	0.0	0.55(0.04)	0.18(0.04)	0.1 (0.1)	0.0	0.0	0.0	0.3 (0.1)	0.0
Al_2O_3	0.9 (0.2)	0.6(0.1)	3.26(0.04)	1.9 (0.2)	1.5 (0.4)	0.44(0.04)	1.4 (0.2)	0.7 (0.2)	1.5 (0.5)	0.99(0.04)
FeO**	11.1 (0.2)	8.6(0.2)	8.2 (0.3)	7.2 (0.1)	10.6 (0.9)	7.28(0.06)	11.2 (0.6)	8.0 (0.2)	7.0 (0.5)	14.8 (0.2)
MnO	0.42(0.04)	0.8(0.1)	0.17(0.05)	0.37(0.04)	0.81(0.07)	0.9 (0.2)	0.81(0.07)	0.8 (0.1)	0.30(0.06)	0.68(0.08)
MgO	13.5 (0.5)	13.5(0.3)	14.11(0.03)	14.0 (0.2)	11.7 (0.6)	15.0 (0.4)	17.5 (0.3)	14.7 (0.2)	15.8 (0.2)	27.7 (0.2)
CaO	21.54(0.06)	22.8(0.2)	21.4 (0.5)	23.5 (0.1)	22.6 (0.3)	22.1 (0.2)	11.8 (0.2)	21.5 (0.2)	21.7 (0.6)	1.37(0.06)
Na_2O	0.0	0.0	0.0	0.0	0.5 (0.1)	0.0	0.3 (0.2)	0.0	0.0	0.0
K_2O	0.0	0.0	0.0	0.0	0.0	0.0	0.0	0.0	0.0	0.0
Total	99.86	99.9	99.29	99.52	99.8	100.02	99.61	99.30	99.80	100.71
100 Mg/Mg+Fe	68.4	74.8	75.4	77.6	66.3	78.6	73.6	76.6	80.1	76.9
Ca/Mg/Fe	44/38/18	48/39/13	45/41/14	48/40/12	48/35/17	45/43/12	26/54/20	45/42/13	44/45/11	3/75/22

Note: * (one standard deviation); ** (total Fe as FeO).

Fig. 52: Pyroxene compositions

● Western Highlands, P.N.G.

\+ Limbo River, Solomon Islands

Lines join coexisting pyroxenes

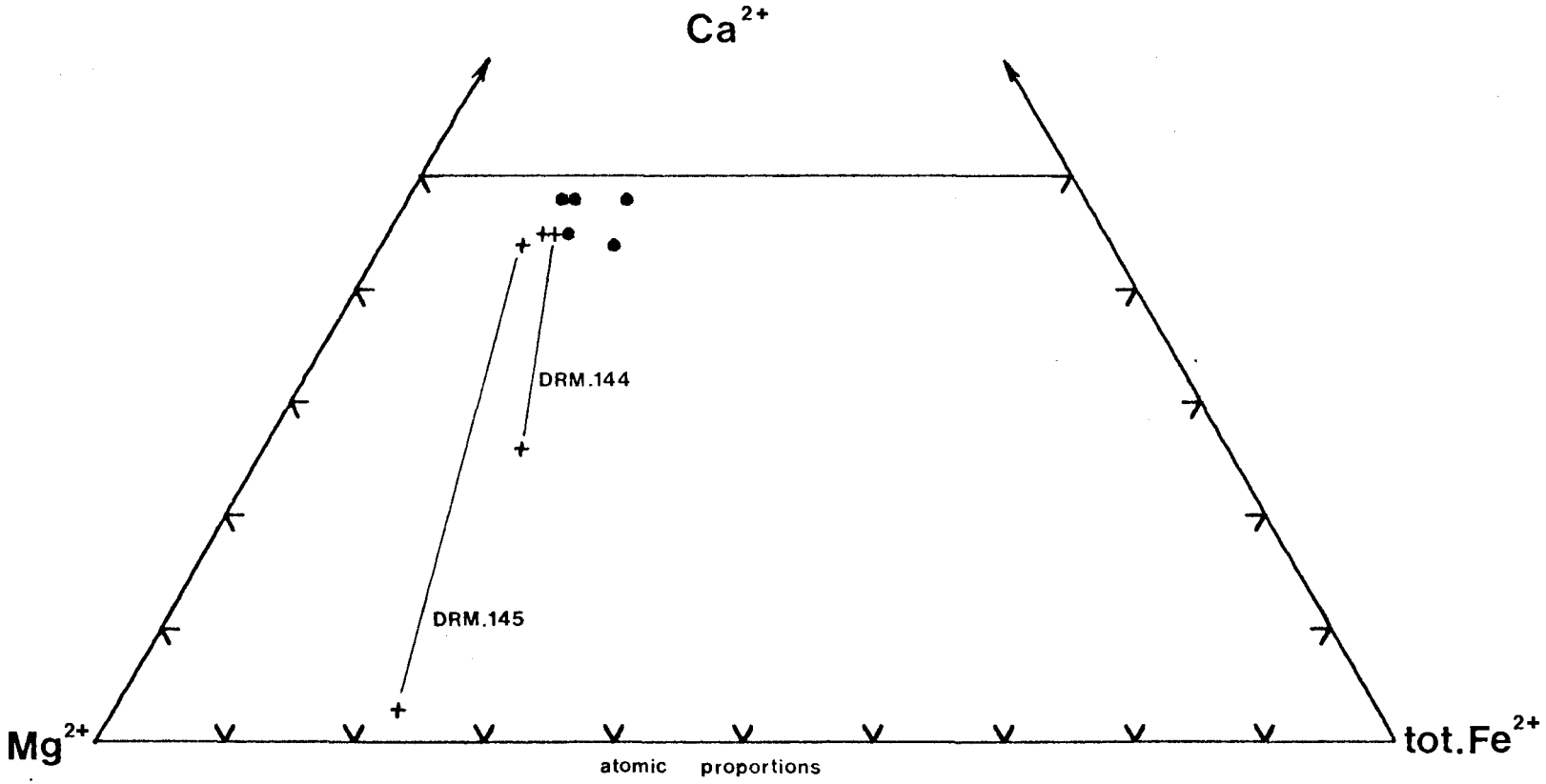

6.6 IRON-TITANIUM OXIDE COMPOSITIONS

6.6.1 Introduction

The limited data obtained in this study for iron-titanium (Fe-Ti) oxide phases is in contrast to their importance as indicators of magmatic conditions during crystallization and of sub-solidus conditions after crystallization. Nevertheless, preliminary studies have revealed consistencies in the distribution of Fe-Ti oxides in Papua New Guinea intrusive rocks.

Nomenclature used here for the Fe-Ti oxide minerals is essentially that of Buddington & Lindsley (1964). Thus, within the ternary system FeO-Fe_2O_3-TiO_2, minerals of the 'spinel series' are considered to lie on the join magnetite (Fe_3O_4) - ulvöspinel (Fe_2TiO_4) and are referred to as 'magnetite' or 'titaniferous magnetite'. Minerals of the 'rhombohedral series' lie on the join haematite (Fe_2O_3) - ilmenite ($FeTiO_3$), and are referred to as 'ilmenite'.

Fe-Ti oxide phases are constant accessory minerals in calc-alklaine intrusive rocks of the Papua New Guinea region. In dioritic and granodioritic rocks, they usually constitute 1-2% by volume of the rock, and in mafic rocks up to 5% or more.

Magnetites and titaniferous magnetites are the most abundant Fe-Ti oxide phases of Western Highlands intrusive rocks. Optically, the discrete grains and aggregates of grains are uniform to magnifications x 1000. Rare ilmenite exsolution lamellae are observed in magnetite of granodiorite (DRM044) from the western part of the Yuat South Batholith. Ilmenite has been observed as a discrete phase in a gabbro (DRM054) from the Yuat South Batholith, in the Yuat North microadamellite (DRM056), and in a diorite porphyry (DRM080) of the Frieda River Intrusive Complex. In all three occurrences, the rhombohedral phase is less abundant than the associated spinel phase.

Ilmenite is much more common in the intrusive rocks of the island regions. Both magnetite and ilmenite have been observed in varying proportions in all studied intrusive rock suites of these regions, except the Mount Kren Intrusive Complex (Manus Island) and the Felsic Suite of the Koloula Igneous Complex (Guadalcanal), in which only an Fe-Ti oxide of the spinel series is present. Mafic rocks of the Plesyumi Intrusive Complex (New Britain) are characterized by (titaniferous?) magnetite containing abundant exsolution lamellae of ilmenite, in addition to discrete ilmenite grains. The persistence of

ilmenite with an associated spinel in more felsic rocks of the suite results in high whole-rock TiO_2 contents which characterize the New Britain suites relative to other calc-alkaline intrusive suites of the P.N.G. region.

6.6.2 Fe-Ti Oxide Compositions

Microprobe data have been collected for Fe-Ti oxides for 12 intrusive rocks from the Western Highlands and for 2 rocks from the Limbo River Diorite (Solomon Islands). The data are presented in Table 17. For Fe-Ti oxides of the spinel series, values have been calculated for Fe_2O_3, FeO, revised total, and molecular percent of ulvöspinel (mol.% Usp), using the method of Carmichael (1967). For Fe-Ti oxides of the rhombohedral series, values have been calculated for the sum of the trivalent ions (R_2O_3) and revised totals. The revised totals are high (100-105%) for all the analyzed Fe-Ti oxides. This is attributed to failure to standardize on oxide phases during analysis. However, this does not affect the qualitative conclusions arising from the data.

Most of the spinels from the Western Highlands rocks are magnetites which are poor in titanium (TiO_2 less than 0.5%; mol.% Usp less than 1.0). In contrast, titaniferous magnetites of the Yuat North high-K diorites have TiO_2 = 6-7% (mol.% Usp = 16-19). Titaniferous magnetites are also characteristic of the Limbo River Diorite.

All of the spinels fall along the join magnetite-ulvöspinel on a ternary plot of TiO_2-FeO-Fe_2O_3 (see Fig. 53), with a concentration of compositions close to the magnetite end.

6.7 SUMMARY

Mineral assemblage and mineral compositional variations in mineralized and non-mineralized intrusive suites indicate different conditions of crystallization.

In intrusive rock suites associated with mineralization, the presence of the mafic mineral assemblage hornblende + magnetite + sphene indicates relatively high P_{O_2} during crystallization (Verhoogen, 1962; Wones, 1966). Compositional variations in amphiboles and biotites of this assemblage can also be attributed to relatively high P_{O_2} (Czamanske & Wones, 1973). These conditions are appropriate for evolution of hydrothermal solutions in final stages of crystallization, leading to formation of porphyry-type mineralization.

In contrast, non-mineralized suites possess the mafic assemblage hornblende $\pm$ pyroxene + Ti-magnetite $\pm$ ilmenite, indicating lower P_{O_2}

TABLE 17: AVERAGE Fe-Ti OXIDE COMPOSITIONS FOR INTRUSIVE ROCKS FROM P.N.G. AND B.S.I.P.

SPEC. NO.	DRM.012	DRM.013	DRM.019	DRM.025	DRM.035	DRM.044	DRM.044	DRM.052	DRM.054	DRM.054
No of anals.	5	5	3	3	1	3	1	4	6	1
SiO_2	0.0	0.0	0.0	0.0	0.6	0.0	0.0	0.0	0.0	0.0
TiO_2	7.0(1.4)	5.6(0.5)	0.3(0.1)	0.2(0.1)	0.2	0.3(0.2)	24.1	0.4(0.1)	0.2(0.1)	52.3
Al_2O_3	1.7(1.0)	1.2(0.6)	0.3(0.1)	0.3(0.1)	0.2	0.3(0.1)	0.1	0.4(0.1)	0.3(0.1)	0.3
Cr_2O_3	0.3(0.1)	0.3(0.1)	0.2(0.1)	0.2(0.1)	0.2	1.0(0.2)	1.1	0.3(0.1)	0.4(0.1)	0.2
tot.FeO	89.3(1.7)	89.0(3.7)	98.5(0.6)	98.6(0.3)	97.7	98.0(0.3)	76.0	98.9(0.7)	98.4(0.4)	49.3
MnO	0.5(0.1)	0.5(0.1)	0.2(0.1)	0.2(0.1)	0.0	0.0	0.2	0.0	0.0	3.7
MgO	0.1(0.1)	0.6(0.7)	0.1(0.1)	0.2(0.1)	0.2	0.2(0.1)	0.0	0.0	0.0	0.2
CaO	0.6(0.8)	0.9(0.6)	0.1(0.1)	0.0	0.1	0.1(0.1)	0.0	0.0	0.2(0.1)	0.3
Na_2O	0.0	0.0	0.0	0.0	0.0	0.0	0.0	0.0	0.0	0.0
K_2O	0.0	0.0	0.0	0.0	0.0	0.0	0.0	0.0	0.0	0.0
total	99.5	98.1	99.7	99.7	99.2	99.9	101.5	100.0	99.5	106.3
$\%Fe_2O_3$	56.9	59.8	72.7	73.0	71.3	72.1	23.9	72.4	72.5	7.5
%FeO	38.1	35.2	33.1	32.9	33.6	33.2	54.5	33.7	33.1	42.5
total	105.2	104.2	107.0	107.0	106.4	107.1	103.9	107.2	106.7	107.0
mol % Usp	19.2	15.5	0.8	0.5	2.7	0.8	66.0	1.1	0.5	-
mol % R_2O_3	-	-	-	-	-	-	-	-	-	7.0

TABLE 17 (continued)

SPEC. NO.	DRM.063	DRM.065	DRM.080	DRM.080	DRM.081	DRM.144	DRM.144	DRM.145
No of anals.	2	3	4	3	2	3	1	2
SiO_2	0.0	0.0	0.0	0.0	0.5(0.1)	0.3(0.1)	0.3	0.6(0.0)
TiO_2	0.8(0.3)	0.2(0.1)	1.3(0.2)	34.5(1.7)	0.3(0.1)	0.6(0.2)	6.4	4.1(1.0)
Al_2O_3	0.8(0.7)	0.5(0.3)	0.7(0.1)	0.0	0.4(0.1)	0.6(0.1)	0.7	1.3(0.7)
Cr_2O_3	0.6(0.1)	0.2(0.1)	0.3(0.1)	0.0	0.2(0.0)	0.2(0.1)	0.3	0.3(0.1)
tot.FeO	92.5(0.7)	98.7(0.4)	96.9(0.5)	60.8(0.9)	97.1(0.4)	97.0(0.7)	89.6	91.9(1.8)
MnO	0.0	0.0	0.3(0.1)	4.2(0.5)	0.3(0.1)	0.0	2.6	0.7(0.2)
MgO	0.2(0.1)	0.0	0.3(0.1)	0.0	0.2(0.1)	0.0	0.4	0.6(0.1)
CaO	0.0	0.3(0.1)	0.0	0.0	0.2(0.1)	0.0	0.1	0.2(0.1)
Na_2O	0.0	0.0	0.0	0.0	0.0	0.0	0.0	0.0
K_2O	0.0	0.0	0.0	0.0	0.0	0.0	0.0	0.0
total	94.9	99.9	99.80	99.5	99.2	98.7	100.4	99.7
$\%Fe_2O_3$	67.1	72.8	70.2	37.8	71.1	70.2	59.4	62.3
%FeO	32.1	33.2	33.7	26.8	33.2	33.9	36.1	35.9
total	101.6	107.2	106.8	103.3	106.4	105.8	106.3	106.0
mol % Usp	2.3	0.5	3.5	-	2.6	2.7	18.4	13.3
mol % R_2O_3	-	-	-	35.4	-	-	-	-

Fig. 53: Ternary plot of Fe–Ti oxide compositions – TiO_2 includes SiO_2
R^{2+} " Fe^2,Mn, Mg, Ca
R^{3+} " Fe^3, Al, Cr

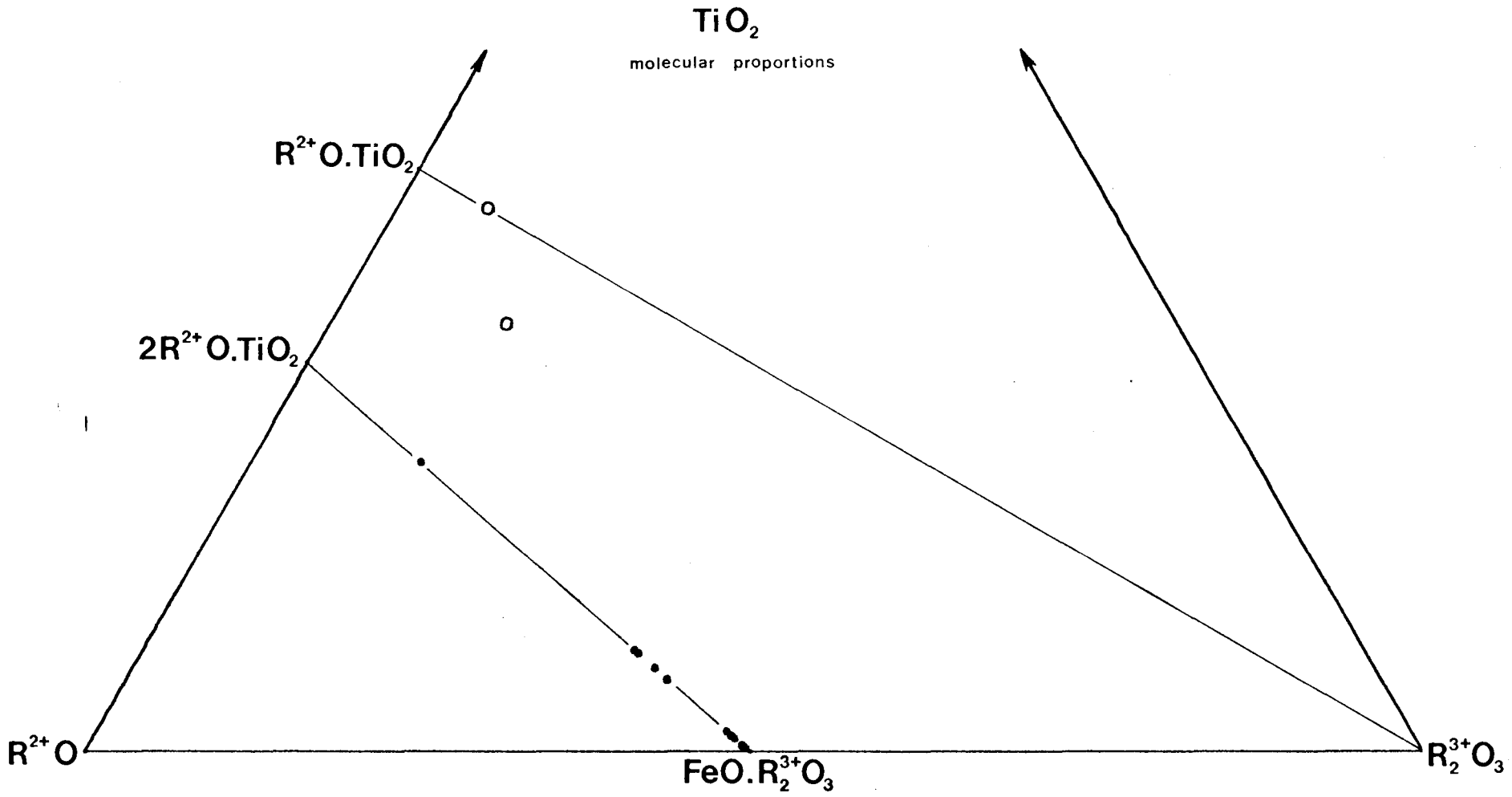

during crystallization. Compositional variations in amphiboles and biotites of this assemblage also indicate conditions of lower P_{O_2}. Residual silicate melts of these rocks were not sufficiently water-rich to exsolve a substantial hydrothermal fraction.

CHAPTER 7 ASPECTS OF PORPHYRY-TYPE COPPER MINERALIZATION IN THE PAPUA NEW GUINEA REGION

7.1 INTRODUCTION

In previous Chapters (4 and 5), emphasis was placed upon geochemical variations within suites of intrusive rocks from various parts of Papua New Guinea and the Solomon Islands. Whole-rock abundances of major and trace elements were shown to be characteristic for each suite, permitting distinction even between those suites in close proximity. Only rocks free of alteration and mineralization were used to determine the geochemical characteristics of each suite. Where data were available for mineralized rocks from a particular suite, reference was made to departure from (or conformity with) the established trends of that suite.

In Chapter 6, chemical variations in particular minerals were reported, and in some cases (e.g., amphiboles; biotites) the variations were related to the presence or absence of porphyry-type copper mineralization.

In this Chapter, aspects of porphyry-type copper mineralization in the Papua New Guinea region are considered. After a brief review of definition and classification of porphyry-type copper mineralization, consideration is given to the distribution and age of porphyry mineralization in the P.N.G. region. Geochemical relationships of mineralized and non-mineralized rocks are then further investigated. Two approaches are made:

(i) firstly, patterns between suite chemistry and presence or absence of closely associated mineralization are elicited. In addition, the abundance and distribution of those elements typically concentrated in hydrothermal systems (base metals; precious metals; selenium and tellurium) are examined.

(ii) secondly, geochemical comparisons are made between mineralized and non-mineralized rocks as two separate groups. In this approach, the alteration/mineralization characteristics of different occurrences are overlooked, and all mineralized rocks are treated together as a single group.

7.2 DEFINITION AND CLASSIFICATION OF PORPHYRY-TYPE COPPER MINERALIZATION

7.2.1 Definition

With the early, intensive search for, and study of, porphyry-

type copper deposits in the southwestern United States of America, initial understanding of this class of ore deposit reflected the observations made in that part of the world. Thus Parsons (1933, 1957) emphasized the association of igneous rocks with porphyry coppers, and the presence of a blanket of supergene enriched material, as well as the characteristics of large size and low grade. In some cases, relationships with igneous rocks are unclear (White, 1968), and particular climatic environments may preclude the formation of a thick supergene capping (Titley, 1973). Hence the essential characteristics of large size and low grade have persisted in definitions, while locational features have become less widely used. One such definition which has wide applicability is modified from Sillitoe (1972a), and is as follows:

'*Porphyry copper deposits* are large tonnage (commonly exceeding 500 million tons), low grade (hypogene ore commonly less than 0.5% Cu), roughly equidimensional deposits of disseminated and stockwork-veinlet, pyrite-chalcopyrite mineralization, carrying at least trace amounts of molybdenum, gold and silver'.

7.2.2 Classification

Various characteristics of porphyry copper deposits have been used by different authors as aids to classification. Thus Stringham (1960) used structural features of country rocks in distinguishing between 'forceful', 'passive', and 'permissive' intrusive stocks. From a study of the deposits of the western United States, he concluded that passively emplaced stocks were more likely to be associated with mineralization than those which had been forcefully emplaced.

Titley (1966) based discussion on locus of mineralization in the intrusive/country rock system. 'Simple' porphyry copper deposits were defined as those in which the mineralization was restricted to either the intrusive host rocks or the adjacent wall rocks (which may be sedimentary, metamorphic, or earlier intrusive rocks). 'Complex' porphyry copper deposits were regarded as those in which mineralization occurred in both the country rocks and the intrusive body apparently parental to the mineralization. Titley (1972a) formally recognized two types of 'simple' deposits, *viz* 'intrusion' and 'wall rock' porphyry copper deposits, and recognized that "...most porphyry copper deposits are composites of the intrusion and wall rock types".

Sutherland Brown (1969) recognized the porphyry deposits of British Columbia as lying within a spectrum ranging from deposits

least related to magmatic activity ('syngenetic Cu-Mo deposits') to those most obviously related to magmatism ('magmatic Cu-Mo deposits'). Further, he distinguished 'simple', 'elaborate', 'complex', and 'plutonic' porphyry Cu-Mo deposits according to depth of intrusion and complexity of mineralization.

Following the proposal of Sillitoe (1973) that porphyry systems extend upward from plutonic environments into stratovolcanoes, Linder (1975) suggested distinction of 'volcanic', 'conduit', and 'plutonic' porphyry deposits. Further, he proposed a broader recognition of 'arc' and 'cratonic' environments of emplacement of calc-alkaline igneous rocks and associated mineralization. Hollister et al. (1975) also recognized two crustal environments in a study of porphyry copper distribution in the Alaskan region: an 'interior porphyry belt' and a 'continental margin porphyry belt'. On the bases of petrography and alteration patterns, they further recognized 'quartz monzonite'-type and 'diorite'-type porphyry copper deposits, the latter occurring only in the continental margin belt.

In a broader attempt to define world-wide distribution of porphyry copper deposits in terms of plate tectonic theory, Sillitoe (1972a) defined three belts which contained the known distribution of post-Palaeozoic porphyry copper deposits: the 'Western Americas belt', the 'southwest Pacific belt', and the 'Alpide belt'. The limited applicability of such a broad analysis of porphyry copper distribution is apparent in the light of closer analysis of geotectonic environments of emplacement (e.g., Linder, 1975; Hollister et al., 1975; this work). Nevertheless, the important relationship between porphyry copper deposits and calc-alkaline magmatism of orogenic belts (particularly Mesozoic-Cenozoic belts) is emphasized in the earlier work of Sillitoe.

In a similar way, syntheses of porphyry characteristics to yield general models also face the same problem of limited applicability. The work of Rose (1970), Lowell & Guilbert (1970) and James (1971), must all be assessed with the fact in mind that their syntheses were formulated from data drawn from the restricted environment of the south-western United States. Although their generalized models are useful in understanding the porphyry systems of that region, they are of more limited use in assessing porphyry systems of other regions (e.g. Titley, 1973, 1975).

7.3 DISTRIBUTION AND AGE OF PORPHYRY-TYPE COPPER MINERALIZATION IN THE PAPUA NEW GUINEA REGION

7.3.1 Distribution

Locations of known porphyry copper mineralization in the Papua New Guinea region are shown in Fig. 54. The distribution closely follows that of the calc-alkaline intrusive masses of the region.

While the porphyry copper occurrences of Papua New Guinea and environs may be considered part of the 'southwest Pacific porphyry copper belt' of Sillitoe (1972a), closer examination reveals distribution in three contrasted geotectonic environments. These environments, and contained porphyry occurrences, are as follows:

(i) *Island arc porphyry copper occurrences.* The island arc structures of the southwest Pacific have been considered by numerous authors to represent intra-oceanic arcs resulting from post-Mesozoic lithospheric plate interactions. (e.g. Dewey & Bird, 1970; Coleman, 1967, 1970: Karig, 1971, 1972). Porphyry copper occurrences are known from most parts of the southwest Pacific arcs.

In the Admiralty-Solomons arc, porphyry copper occurrences are known on Manus Island (Mount Kren prospect), and on New Ireland (Legusulum, Kaluan, and Sinelu prospects). In the Solomons chain, the only present porphyry copper producer in the P.N.G. region is located on Bougainville Island, and other occurrences are known on Guadalcanal Island (Chikora prospect in the Koloula Igneous Complex).

In the New Britain arc, porphyry copper occurrences are known at Kulu, Plesyumi, Yau Yau-Uasilau, Pelapuna, and Esis.

No occurrences are known from the Finisterre-Saruwaged ranges, which appear to be structurally related to the New Britain arc (Robinson, 1974), nor are porphyry occurrences known in the Torricelli Ranges of the northern New Guinea arc (Hutchison, 1974).

(ii) *Continental margin porphyry copper occurrences.* The structural history and palaeotectonic development of the New Guinea Mobile Belt remains poorly understood, but it appears to have developed at least in part adjacent to or on the Australian continental margin (Dow, et al., 1972; Dow, 1973; compare Mason, 1975). Porphyry copper occurrences are known from many locations throughout the Belt.

In the Western Highlands, occurrences are known (from west to

FIG. 54 : LOCATION OF PORPHYRY COPPER OCCURRENCES IN THE P.N.G. REGION.
those studied in this thesis are underlined.

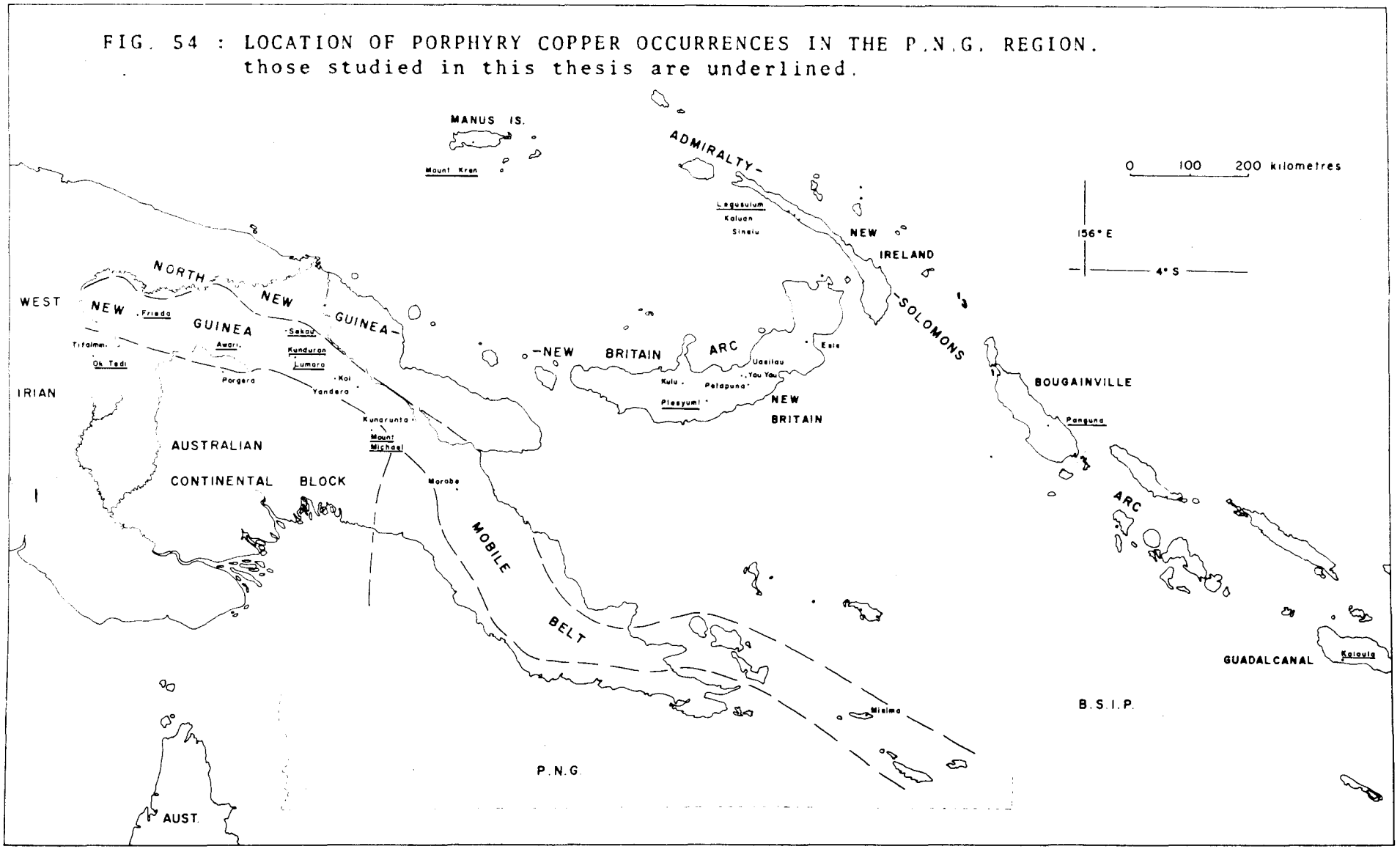

east) at Frieda River, Awari, Kunduron-Lumoro, and Sekau Valley; in the Eastern Highlands at Kol, Yandera, and Kunarunta prospects; in the Morobe district; and in southeastern Papua (Misima Island).

It is possible that the Ertsberg deposit (Flint, 1972) in Irian Barat may belong to this geotectonic region.

(iii) *Cratonic porphyry copper occurrences*. The Australian continental block and related shelf-type sediments have developed in a structural style dominated by broad arching of Palaeozoic metamorphic and granitic basement rocks, and by development of *en echelon* folds, faults and décollement structures in overlying Mesozoic to Tertiary sedimentary sequences (Bain, 1973; Jenkins, 1974). Porphyry copper occurrences are known at the Ok Tedi (Mount Fubilan) deposit, and Tifalmin and Porgera prospects in the Western Highlands, and at Mount Michael in the Eastern Highlands.

7.3.2 Age

Apart from direct geologic evidence giving stratigraphic controls on ages of intrusive events, much of the knowledge concerning intrusive and mineralizational ages in the Papua New Guinea region comes from the systematic radiometric work of Page (1971; in prep.), Page & McDougall (1970, 1972a, 1972b), and Page & Ryburn (1973). It is from these sources that the ages discussed in this section are taken.

In Table 18, known ages of intrusion and (where applicable) of mineralization are summarized for different tectonic units of the P.N.G. region.

Ages of intrusion fall broadly into three groups (Page & Ryburn, 1973):

(i) Eocene-Oligocene (40-30 m.y. b.p.). This group includes intrusive rocks from the northern New Guinea arc, from New Ireland, and possibly from the 'pre-Miocene' basement of Guadalcanal (Coleman, 1957; Hackman, 1971).

(ii) Miocene (22.5 - 5.5 m.y. b.p.). Many of the intrusive bodies of the New Guinea Mobile Belt fall into this group. A large number range narrowly 15-12 m.y. in age.

Some ages from New Britain intrusive rocks lie between the ranges of these first two major age groupings.

(iii) Pliocene-Pleistocene (5.5 - 1.0 m.y. b.p.). Intrusive rocks of this age are known from the Ok Tedi and nearby areas, from

TABLE 18: AGES OF INTRUSION AND MINERALIZATION IN THE P.N.G. REGION

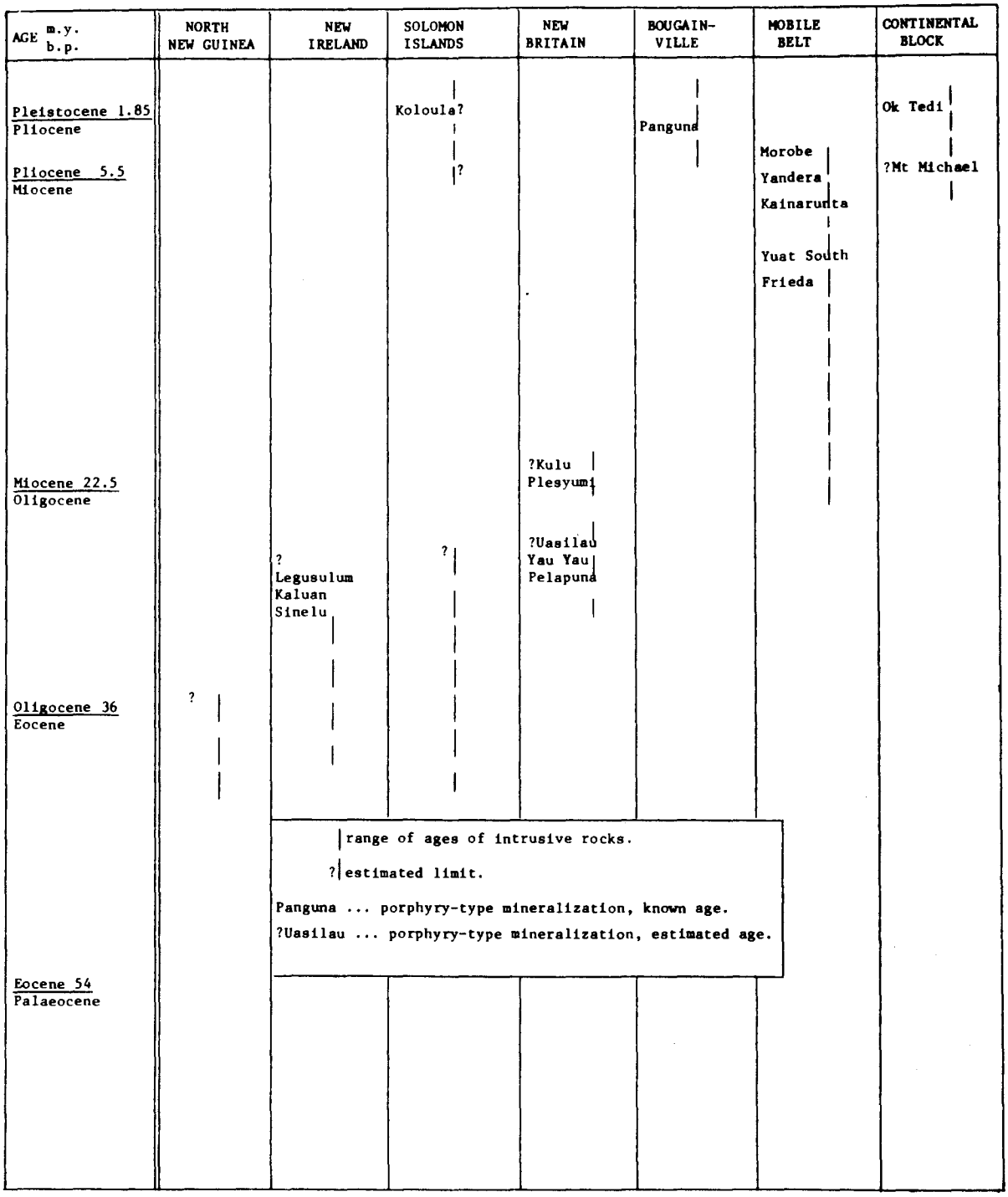

Bougainville island and from the Solomon Islands (at least part of the Koloula Igneous Complex; possibly also the Limbo River Diorite).

Ages of mineralization in many areas are younger by a few million years than the age of initiation of intrusive igneous activity. For example, ages of commencement of intrusion and later mineralization at the Yandera prospect within the Bismarck Granodiorite are 12.5 and 7 m.y. respectively; at the Panguna mine, 4.2 and 3.5 m.y.; at the Ok Tedi (Mount Fubilan) deposit, 4? and 1.1 m.y. This sort of intrusion/mineralization pattern is observed in porphyry deposits in other parts of the world (e.g., Moore & Lanphere, 1971; Moore, 1973; Banks & Stuckless, 1973; Waterman & Hamilton, 1975).

From the available data, it is apparent that most of the known porphyry occurrences in P.N.G. are located within the New Guinea Mobile Belt, and range from Miocene to Pliocene in age. The only producing deposit (Panguna) and proven prospect (Ok Tedi) are both Pliocene-Pleistocene in age, but occur in different tectonic settings.

7.4 GEOCHEMICAL CHARACTERISTICS OF INTRUSIVE ROCKS AND ASSOCIATED PORPHYRY-TYPE COPPER MINERALIZATION

7.4.1 Patterns of Intrusion, Mineralization, and Intrusive Suite Chemistry

In the course of this study, petrographic, mineralogical, and geochemical data acquired for a large number of intrusive rock complexes in the Papua New Guinea region have permitted the distinction of different intrusive suites even within complexes of limited areal extent. Field evidence, where available, confirm the laboratory data. It is appropriate here to summarize the diverse suite chemistries, and to point out persistent patterns relating timing of intrusion, presence of mineralization, and nature of intrusive suite chemistry.

Table 19 summarizes geochemical and chronological data for the studied mineralized intrusive complexes. K-content has been chosen to distinguish between suites because, of all the major elemental oxides, K_2O provides the clearest distinction between suites and is entrenched in the literature as a discriminating parameter for volcanic and plutonic calc-alkaline suites (Kuno, 1966; Taylor, 1969; Dickinson, 1968, 1975; Gulson et al., 1972).

It is apparent that, at all studied mineralized complexes, one may distinguish higher- and lower-K calc-alkaline suites. The levels of K_2O in each suite, and the difference in K_2O between the suites, varies

TABLE 19: GEOCHEMICAL AND CHRONOLOGICAL RELATIONSHIPS IN MINERALIZED INTRUSIVE COMPLEXES OF THE PAPUA NEW GUINEA AND SOLOMON ISLANDS REGION

Intrusive Complex, Location	Higher-K* suite (age, m.y.)	Lower-K suite (age, m.y.)	Remarks	Data sources (chemical; chronological)
(A) ISLAND ARC ENVIRONMENT:				
Mount Kren, Manus Is.	Present	Present	Limited chemical data for lower-K rocks; higher-K suite mineralized?	1
Legusulum, New Ireland	Earlier (30.1)	Later	Limited chemical data; later suite mineralized	1, 2; 2
Plesyumi, New Britain	Earlier (22)	Later	Later, lower-K suite mineralized	1; 3
Kulu, New Britain	Earlier (22)	Later	Later 'porphyry' suite mineralized	4; 3
Panguna, Bougainville Is.	Earlier (4.2)	Later (3.5-1.6)	Later, lower-K 'Porphyry Suite' mineralized	1; 5
Koloula, Guadalcanal Is.	Earlier	Later (?2)	Later, lower-K suite 'Felsic Suite' mineralized	1, 6, 7; 6
(B) CONTINENTAL MARGIN ENVIRONMENT:				
Frieda, Western Highlands	?Present (16-13)	?Present (16-13)	Limited chemical data; later porphyries mineralized	1; 8
Karawari, Western Highlands	Present	Present (15-10)	Limited chemical data; mineralization with later porphyries (lower-K suite)	1; 9
Yuat South, Western Highlands	Earlier (14.0-13.5)	Later (12.6-11.1)	Later, lower-K suite mineralized. Higher-K suite age inferred from Yuat North	1; 9
Sekau, West.H'lands/Sth Sepik	Present	Present	Lower-K suite mineralized?	1.
(C) CRATONIC ENVIRONMENT:				
Ok Tedi (Mt Fubilan), West.Highlands	Present (4-1)	Present	Later rocks mineralized at Ok Tedi; lower-K rocks in nearby stocks	1, 10; 8
Mount Michael, East.H'lands	Present	Present	Limited chemical data; extent and degree of mineralization unknown	1; 9

Note:

* Levels of K_2O, and difference in K_2O between suites, vary between locations.

Key to data sources: 1 = author, this study; 2 = Hohnen (1970); 3 = Page and Ryburn (1973); 4 = R. Hine (pers. commun., 1975); 5 = Page and McDougall (1972); 6 = A. Chivas (pers. commun., 1975); 7 = Netzel (1974); 8 = Page and McDougall (1972); 9 = Page (1971); 10 = Ayres and Bamford (in press).

from complex to complex. For example, in the Plesyumi Intrusive Complex, the high-K suite differs from the normal-K suite by approximately 2% K_2O at 60% SiO_2. Within the Panguna Intrusive Complex, both the Kaverong Quartz Diorite Suite and the Porphyry Suite have levels of K_2O which are appropriate to normal-K calc-alkaline rocks, but the Kaverong Quartz Diorite Suite differs from the lower-K Porphyry Suite by 0.8% K_2O at 60% SiO_2. Similarly, the intrusive rocks from the Ok Tedi region are all high-K calc-alkaline in their affinities, but those from the Mount Fubilan stock are more K-rich at a given silica level than the rocks from some nearby stocks (e.g., Mount Frew, data of Ayres & Bamford, in press). On the other hand, the igneous rocks of the Koloula Intrusive Complex are low- to normal-K calc-alkaline in character, but the Mafic Suite reaches 1.5% K_2O at 60% SiO_2 while the lower-K Felsic Suite only reaches 0.5% K_2O at that silica level.

There are, then, measurable differences in K_2O between different intrusive suites within single intrusive complexes. With varying degrees of clarity, other major and trace elements also reflect the characters of the different suites. Thus calcium varies antipathetically with potassium, while the trace elements rubidium, barium, zirconium, niobium and rare earth elements are strongly correlated with potassium.

Of further interest is the frequent association of porphyry copper mineralization with later, less-potassic suites. In at least three locations (Yuat South; Panguna; Koloula) it is firmly established that intrusion of an earlier, higher-K suite was followed after an interval of up to several million years by a later, lower-K intrusive suite. At all three locations, porphyry copper mineralization is closely associated with the later, less-potassic suite.

At other porphyry occurrences, suites of differing chemistry have been established, but paucity of chemical data and lack of chronologic controls render it difficult to assess whether the tendency for mineralization to occur with later, lower-K suites holds true for those occurrences.

7.4.2 Abundance of Copper, Zinc, and Lead in Intrusive Suites

Copper, zinc, and lead are the base metals commonly concentrated in, or in the vicinity of, porphyry-type copper deposits. For this reason it is of interest to examine the abundance of these elements in calc-alkaline intrusive rock suites of the Papua New Guinea region, some of which are closely associated with porphyry mineralization and possibly represent suitable sources for at least some, if not all, of the

concentrated ore material.

Because of wide sample coverage in the *Yuat North*, *Yuat South*, and *Karawari batholiths* of the Western Highlands, these three calc-alkaline intrusive suites have been selected for close examination. The suites are particularly well-suited for comparison of base metal distribution because they lie within the same geotectonic environment (the New Guinea Mobile Belt), they are of similar age (Middle Miocene), they span a wide range of rock types and chemical characteristics (from high-K, through normal-K, to low- to normal-K), and one of the suites Yuat South) is associated with mineralization while the other two (Yuat North and Karawari) are apparently barren. However, mineralization is known in the Awari Stock to the south of the Karawari Batholith.

For all three suites, strongly altered and mineralized samples were excluded from the plots of copper, zinc, and lead against SiO_2 content (see Figs. 55 to 57). Some samples showing mild degrees of alteration were included, but the majority are fresh, unaltered rocks representative of the main rock types of each suite. In the plots of copper and lead, the average abundances for orogenic rock types (Taylor, 1969) are also plotted for comparison.

In Fig. 55, abundance of copper is plotted against SiO_2 content of each specimen from the three suites. In the Karawari low- to normal-K suite, the more mafic rocks of the suite have copper levels comparable with those of the average orogenic rocks. At approximately 62% SiO_2 there is a great increase in copper content (specimen from Awari prospect) immediately followed by a steep decrease. There is only a small increase in copper toward the end of the silica range.

In the Yuat South normal-K suite, copper levels are generally lower than average among the more mafic rocks, except for one specimen at 46.5% SiO_2 which is a gabbroic marginal phase associated with mineralization. Between 58 and 66% SiO_2 there is a marked increase in copper contents to over 300 ppm, followed by a rapid drop in the later, more felsic rocks. These lower copper levels (less than 10 ppm) are recorded in two specimens (DRM019, 025) which represent the dominant intrusive phases of the batholith, and both of which are closely associated with mineralization (Kunduron-Lumoro prospects).

The specimens from the Yuat North Batholith include dominant high-K calc-alkaline rocks and rarer shoshonitic types. The calc-alkaline rocks possess copper levels comparable with the average rocks of Taylor, but there is a modest enrichment (to approximately 100 ppm) at 62.5% SiO_2.

FIG. 55 : Cu versus SiO_2

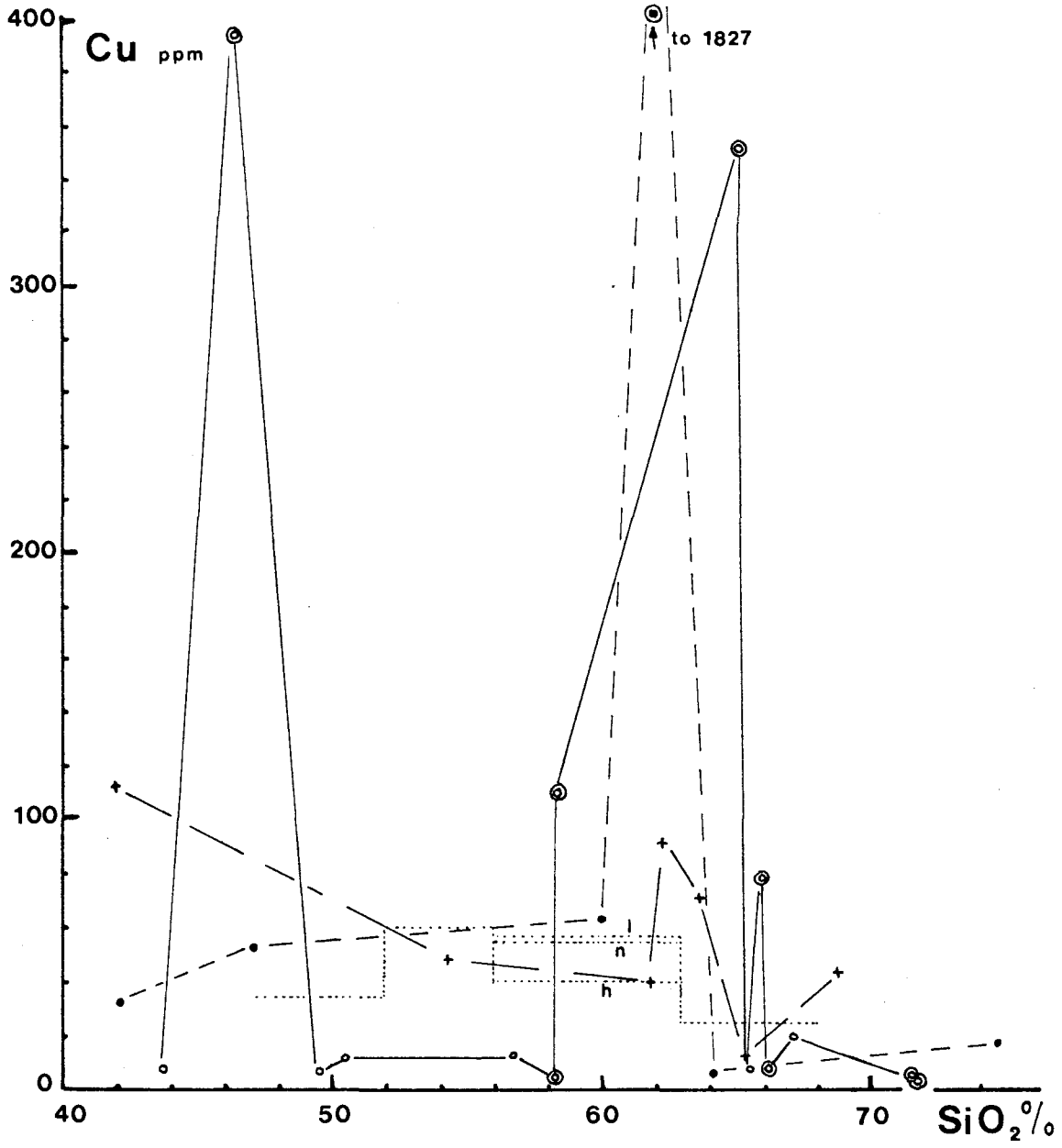

+—— ——+ Yuat North Batholith

o———— o Yuat South Batholith

•— — — —• Karawari Batholith

Specimens associated with mineralization are circled.

Average abundances of Taylor(1969) are dotted (l=low-K, n=normal-K, h=high-K).

FIG. 56 : Zn versus SiO_2

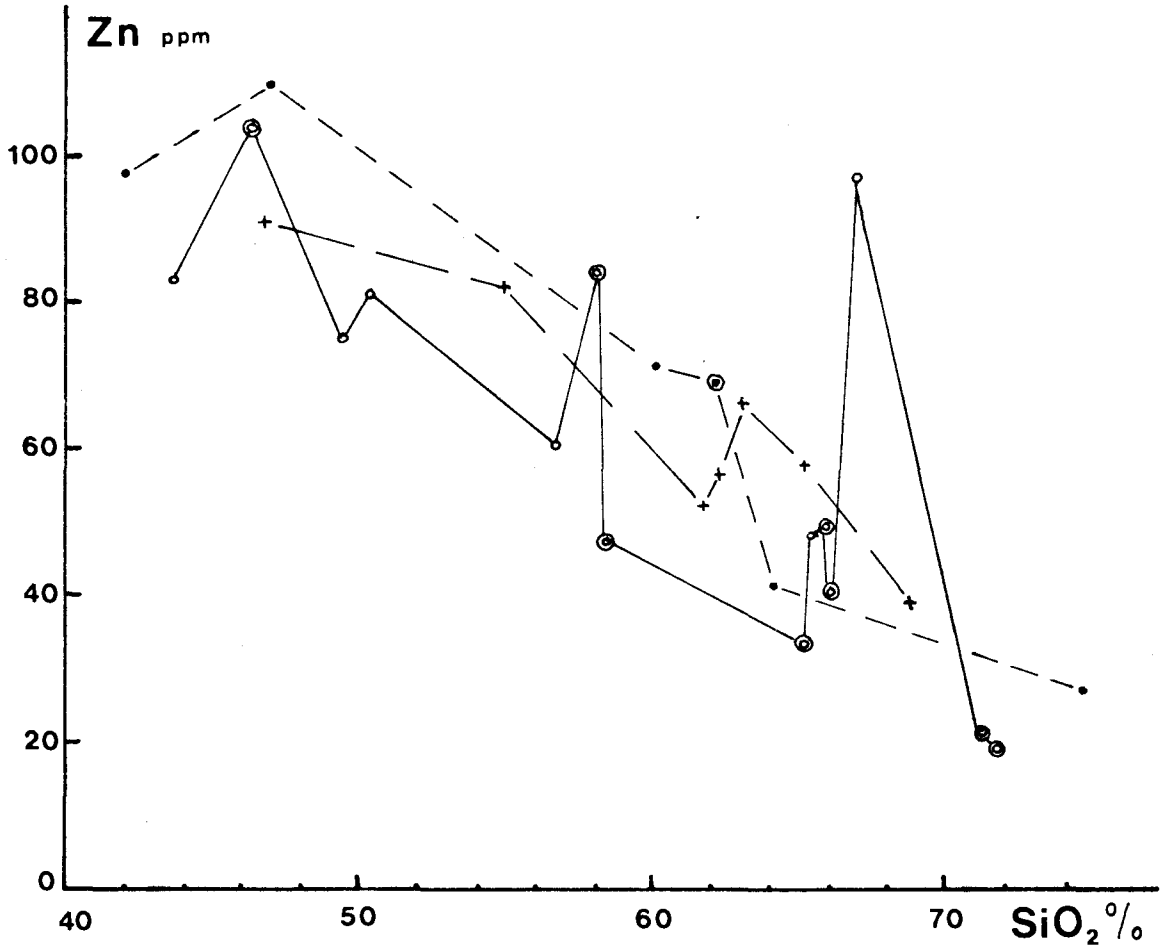

Symbols as in Fig. 55.

FIG. 57 : Pb versus SiO_2

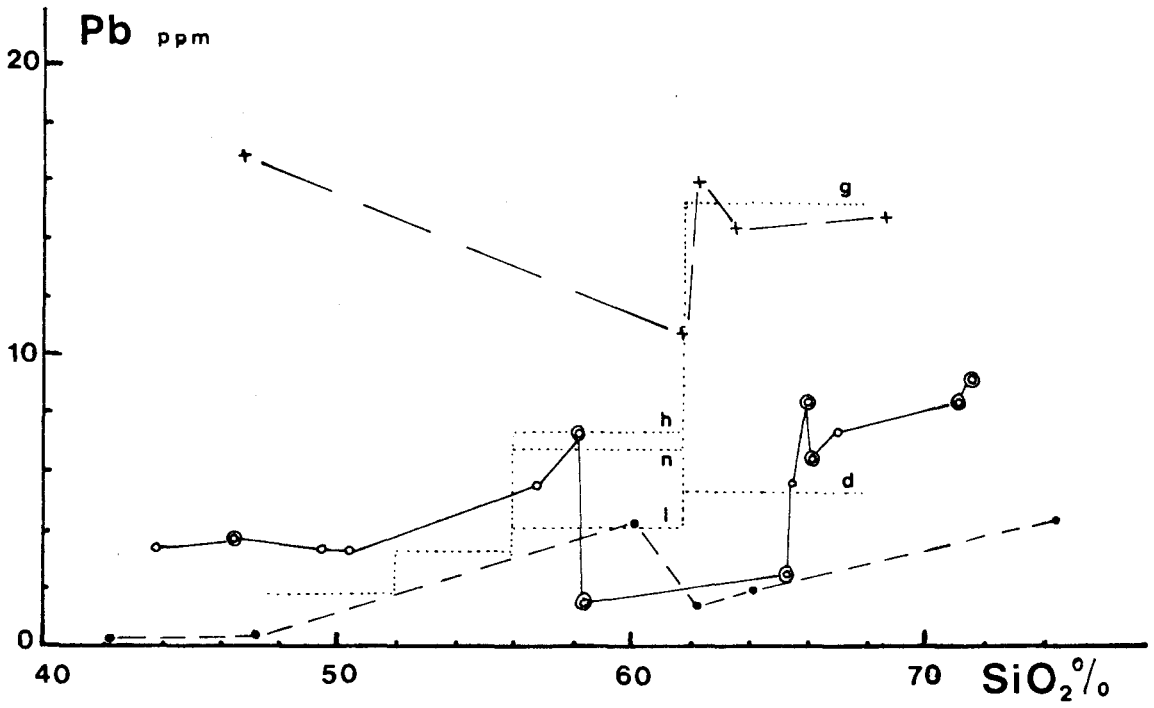

Symbols as in Fig. 55.

Taylor's(1969) average abundances are dotted (l=low-K, n=normal-K, h=high-K, g=granodiorites, d=dacites).

There are no dramatic depletions of copper in the trend, although the relatively few samples may not display all features.

In summary, a study of the copper distribution in three calc-alkaline intrusive rock suites from the Western Highlands reveals that:

(i) all three suites generally have copper levels comparable with Taylor's (1969) averages, except for the normal-K suite of the Yuat South Batholith which shows copper depletion in the silica ranges less than 58% SiO_2 and greater than 66% SiO_2.

(ii) all three suites exhibit a marked copper peak within the range 58-66% SiO_2. The peak intensities range from 1830 ppm in the lower-K suite, through 300 ppm in the normal-K suite, to 100 ppm in the high-K suite. This takes no account of localized concentrations which are known to occur, so that peak intensities mentioned here should not be taken as upper limits for any suite.

Fig. 56 displays variation of zinc with SiO_2. In general, all three suites show a negative correlation of zinc with SiO_2. Concentrations range from 120 ppm in mafic rocks from the Karawari suite to 20 ppm in felsic rocks of the Yuat South suite. In all suites there is a significant depletion of zinc within the range 58-66% SiO_2. This depletion correlates with the copper enrichment described above.

Fig. 57 shows variation of lead with SiO_2, and also the average values of orogenic rocks (Taylor, 1969). All three suites can be clearly distinguished. The high-K Yuat North suite has high levels of lead (15 ppm) and compares favourably with the average granodiorite value of Taylor. The two shoshonitic rocks have even higher levels of lead. In general, lead correlates positively with SiO_2 in all suites, but for any given SiO_2 level, lead increases from the lower-K suites through to the high-K calc-alkaline and shoshonitic rocks. In this sense, lead follows potassium and displays its lithophilic character. In all three suites the normal increase of lead with SiO_2 is interrupted in the region 58-66% SiO_2. Depletion of lead in this silica range correlates with the zinc depletion and copper enrichment described above.

Thus the variation of copper, zinc, and lead in the three calc-alkaline suites is complex in detail, but broad trends are apparent.

Of the metals, lead is most useful as a discriminant between the three suites, correlating positively with SiO_2 but increasing from the lower-K suites through to the higher-K suites. There is good agreement with Taylor's average lead abundances.

Zinc generally shows a negative correlation with SiO_2, but is not as useful as lead in distinguishing between the suites.

The behaviour of copper is more irregular, but all suites show a marked concentration in the silica range 58-66% SiO_2. The normal-K suite shows copper depletion in the more mafic and felsic rocks relative to the respective averages of Taylor (1969). Perturbations in the zinc and lead trends correlate with the copper enrichment. In most instances, zinc and lead levels fall as copper levels rise.

The precise location of the base metals within the rock-forming minerals of these calc-alkaline suites is beyond the scope of this study. However, polished section studies reveal the presence of accessory (apparently primary) chalcopyrite in many rock types. The small sulfide grains are frequently in close association with, and may occur completely within, accessory Fe-Ti oxide grains. Copper may also be expected to occur as Cu^{2+} in biotite up to concentrations of several hundred parts per million or greater (Graybeal, 1973; Kesler, et al., 1975b). In amphiboles, copper levels of several tens to 100 ppm may be expected (Dodge, et al., 1968; Graybeal, 1973). In those amphiboles showing Mg-enrichment toward rims, one would expect higher copper levels in the marginal actinolitic portions (Dodge, et al., 1968). An attempt was made to measure copper abundances across amphibole grains using an ARL microprobe. However, the detection limit of the instrument (80-100 ppm Cu) was at the upper limit of the expected range of concentrations, and no reliable measurements could be made.

Lead and zinc behave more regularly in the suites under discussion than does copper. The camouflaging of Zn^{2+} by Fe^{2+} in ferromagnesian minerals (Mason, 1966; Ringwood, 1955a) results in the observed gradual depletion of zinc in felsic rocks of all three suites. On the other hand, Pb^{2+} is diadochic with K^{+} and consequently becomes enriched with potassium in residual melts and is captured by K-bearing minerals. This results in the observed positive correlation of lead with silica content of rocks of all three suites.

The distribution of copper, zinc, and lead has also been examined in other calc-alkaline intrusive rock suites from the P.N.G. region. The suites include those from Frieda River and Ok Tedi in the Western Highlands, and from Plesyumi, Mount Kren, Lemau, Panguna, Koloula, Poha River, and Limbo River in the island arc regions. Conclusions concerning base metal distribution in these suites are rendered more difficult for the following reasons:

(i) few samples were available from some areas (e.g., Frieda; Lemau).

(ii) despite sufficient samples, some suites display limited silica variation (e.g. Mount Kren; Frieda River).

(iii) some suites are dominanted by strongly mineralized samples (e.g., Panguna; Ok Tedi).

Nevertheless, with these limitations in mind, some observations can be made on base metal distribution in these suites.

In the *Frieda River suite*, there is a dominance of high copper values even in unaltered rocks, but also some very low values (20 ppm). Zinc is generally low (approximately 30 ppm) relative to the normal-K Yuat South suite. Lead (2-3 ppm) is comparable with the low- to normal-K Karawari suite with which the Frieda rocks are more closely related geographically. It should be noted that the restricted silica range of the Frieda specimens (57-64% SiO_2) falls within the silica range of other Western Highlands suites within which major copper fluctuations have been noted above.

Of the *Ok Tedi* specimens, only two are unaltered and the balance display varying degrees of potassic alteration and mineralization. Copper is very high in all specimens. The unaltered high-K dioritic rocks have very high copper contents (700-1400 ppm) compared with average values for high-K orogenic rocks. The highest copper peak in the available data from Ok Tedi occurs at 62% SiO_2, which lies within the silica range in which other Western Highlands suites also achieve copper peaks.

Zinc generally decreases with increasing SiO_2. Values in the unaltered, more mafic rocks (51, 67 ppm) compare favourably with zinc levels in the high-K calc-alkaline suite of the Western Highlands. A rapid decrease in zinc to 5 ppm at 62% SiO_2 correlates with the highest copper peak. Concentrations of zinc tend to decrease from 12 to 10 ppm.

Lead fluctuates widely between 1 and 15 ppm. Values for the unaltered specimens (7-10 ppm) are comparable with Taylor's averages for high-K rocks. Apart from lower lead levels in strongly mineralized rocks, there is a tendency for highly siliceous rocks to be lowest in lead.

In the intrusive rocks from the *Plesyumi Intrusive Complex*, copper shows a steady decrease from 120 ppm at 50% SiO_2 to 40 ppm at 62% SiO_2. There is sudden enrichment in the more siliceous rocks

(especially the 'dacite porphyry'). Zinc shows a fair correlation with copper, decreasing from 100 to 55 ppm, and then increasing to 80 ppm. Lead, however, is constant at 3-4 ppm throughout, except for slightly higher levels in the two high-K specimens and lower values (1-2 ppm) in copper-rich siliceous rocks.

Within the rather limited silica range of the specimens from the *Mount Kren Intrusive Complex*, copper displays rapid fluctuations with a peak of 640 ppm at 57% SiO_2. Zinc generally decreases from 100 to 40 ppm with decreasing SiO_2 content. Lead is fairly constant at 5 ppm which is much lower than for the high-K suite of the Western Highlands (10-15 ppm), but comparable with the high-K rocks of the Plesyumi area.

For the few specimens available from the *Lemau Intrusive Complex*, there is fair correlation between copper, zinc, and lead, all of which increase to 60% SiO_2, decrease to 65% SiO_2, and show slight increases in more siliceous rocks. Copper reaches 95 ppm in dioritic rocks. These concentrations are significantly greater than Taylor's averages in the appropriate silica range. Levels of lead (2-5 ppm) are comparable with Taylor's averages.

Specimens from the *Panguna Intrusive Complex* span a wide silica range (54-68% SiO_2), but many of the specimens are strongly mineralized. Thus copper shows rapid fluctuations throughout the range. Zinc generally decreases with increasing SiO_2, and displays similar levels of concentration to the Western Highlands suites (80-100 ppm at 55% SiO_2; 30-40 ppm at 68% SiO_2). Lead generally decreases with increasing SiO_2, and compares favourably with 'normal-K' calc-alkaline lead values (2-4 ppm).

There are marked fluctuations in copper content in rocks from the *Koloula Igneous Complex*. Gabbroic rocks of the Mafic Suite have uniformly high values (100-200 ppm). An early depletion of copper in the Felsic Suite is followed by occasional peaks and late enrichment in aplitic dyke rocks. The characteristics of copper depletion and enrichment in the region of 58-65% SiO_2 are rather similar to behaviour of copper in the mineralized suite of the Yuat South Batholith, Western Highlands.

Zinc is high but variable in rocks of the Mafic Suite (80-130 ppm) whilst it decreases smoothly from 50 to 15 ppm in the Felsic Suite. Levels of zinc in the Felsic Suite are comparable with the lower-K suite

of the Western Highlands. Lead is quite uniform in abundance (2-5 ppm) in the Mafic and Felsic suites, with a tendency to be slightly higher in the former.

Only two specimens are available from the *Poha River Diorite* on Guadalcanal Island. The more mafic of the two rocks has low abundances of copper and zinc and falls away from the Koloula plots of those elements. The more felsic specimen (64% SiO_2) plots near a copper peak for the Koloula Felsic Suite. Lead levels for both specimens plot close to the Koloula trend.

The three specimens from the *Limbo River Diorite* show uniformly decreasing zinc (80-45 ppm) and lead (7-1 ppm) with increasing SiO_2. Copper, however, has a maximum value of greater than 200 ppm at 75% SiO_2, which correlates with a copper peak in the silicic rocks of the Mafic Suite at Koloula.

7.4.3 Abundance of Gold, Silver, Selenium, and Tellurium in Mineralized and Non-mineralized Intrusive Rocks

Gold, silver, and molybdenum are frequently recovered as by-products from porphyry copper deposits. The predominance of molybdenum over copper in some porphyry deposits has lead to the distinction of 'porphyry molybdenum' deposits (Sutherland Brown, 1969; Clark, 1972), and to the concept of a range of porphyry-type deposits from porphyry copper deposits, through porphyry copper-molybdenum deposits, to porphyry molybdenum deposits (Ayres et al., 1973; Soregaroli, 1974). While molybdenum occurs as its sulfide in veins and more rarely as disseminations, gold and silver are present as the native metal or in solid solution in other metal sulfides.

Limited data have been obtained from other laboratories for *gold and silver abundances* in mineralized and non-mineralized intrusive rocks from the P.N.G. region (see Table 20). Although both metals are highest in mineralized rocks, the Panguna rocks tend to be silver-rich (Au/Ag<1) while the Ok Tedi rocks tend to be gold-rich (Au/Ag>1). These characteristics are also displayed by non-mineralized rocks associated with mineralization at both locations. Gold is also the dominant precious metal associated with the intrusive rocks at Porgera (Dow, et al., 1972), which, like the Ok Tedi occurrence, is located within the Australian continental block. Although small amounts of gold are won from many locations within the New Guinea Mobile Belt (Thompson & Fisher, 1965), the limited data of this study indicate that at least some of the porphyry

TABLE 20: GOLD, SILVER, SELENIUM, AND TELLURIUM ABUNDANCES IN SOME MINERALIZED AND NON-MINERALIZED INTRUSIVE ROCKS FROM THE PAPUA NEW GUINEA REGION

Specimen Number	Au ppb	Ag ppb	Se ppm	Te ppm	Sulfides	Rock type; Location
(A) MINERALIZED ROCKS:						
DRM.015	4	< 50	1.10	1.1	5% Py, Cpy, Mo	Microgranodiorite, Yuat South
DRM.156	12	3750	1.00	<.5	3% Cpy	granodiorite; Yuat South
DRM.157	< 4	490	<.50	<.5	tr. Cpy	granodiorite; Yuat South
DRM.027	28	60	1.86	0.9	4% Py, Cpy	diorite porphyry; Awari stock, Karawari
DRM.125	1040	4400	3.82	< .5	4% Cpy	'Leucocratic Quartz Diorite'; Panguna
DRM.158	100	100	1.05	< .5	<1% Cpy	latite porphyry; Ok Tedi
DRM.159	52	90	0.90	< .5	tr. Cpy	latite porphyry; Ok Tedi
DRM.160	1280	180	3.89	< .5	1% Cpy	latite porphyry; Ok Tedi
DRM.161	720	750	10.31	< .5	1% Cpy	latite porphyry; Ok Tedi
(B) NON-MINERALIZED ROCKS, ASSOCIATED WITH MINERALIZATION						
DRM. 016	< 4	< 50	<.50	0.5	2% Py	microgranodiorite; Yuat South
DRM.017	< 4	< 50	<.50	1.0	-	granodiorite; Yuat South
DRM.019	4	< 50	<.50	<.5	tr. Cpy	granodiorite; Yuat South
DRM.025	< 4	< 50	<.50	<.5	tr. Cpy	granodiorite; Yuat South
DRM.044	4	50	1.28	< .5	1% Py, Cpy	granodiorite; Yuat South
DRM.045	4	< 50	<.50	<.5	1% Py	granodiorite; Yuat South
DRM.005	8	< 50	< .50	0.5	-	diorite porphyry; Frieda River
DRM.080	4	< 50	< .50	<.5	-	diorite porphyry; Frieda River
DRM.084	56	270	<.50	<.5	2% Py, Cpy	high-K diorite; Ok Tedi
DRM.087	116	120	2.09	< .5	1% Cpy	high-K diorite; Ok Tedi
DRM.088	< 4	< 50	<.50	<.5	-	granodiorite; Koloula
DRM.090	< 4	< 50	< .50	< .5	-	granodiorite; Koloula
DRM.092	< 4	< 50	<.50	<.5	tr. Cpy	granodiorite; Koloula
DRM.110	< 4	50	< .50	< .5	-	high-K diorite; Mt Kren
DRM.112	4	50	< .50	< .5	-	diorite; Mt Kren
DRM.115	< 4	120	< .50	0.5	-	high-K diorite; Mt Kren
DRM.118	4	120	< .50	<.5	-	high-K diorite; Mt Kren
DRM.124	24	230	<.50	<.5	-	'Kaverong Quartz Diorite'; Panguna
DRM.127	8	150	< .50	1.0	-	microdiorite; Panguna
(C) NON-MINERALIZED ROCKS, NOT ASSOCIATED WITH MINERALIZATION						
DRM.012	< 4	< 50	< .50	1.8	tr. Cpy	high-K diorite; Yuat North
DRM.014	< 4	< 50	< .50	0.9	tr. Cpy	high-K diorite; Yuat North
DRM.018	4	< 50	< .50	< .5		diorite porphyry; Yuat South
DRM.034	< 4	< 50	< .50	< .5	-	tonalite; Karawari
DRM.035	< 4	520	< .50	< .5	-	diorite; Karawari
DRM.081	< 4	< 50	< .50	<.5	-	'Nena Diorite'; Frieda River
DRM.094	< 4	60	< .50	<.5	tr. Py	gabbro, Koloula
DRM.123	< 4	50	< .50	<.5	-	'Nautango Andesite'; Panguna

Analysts: Au, Ag: Australian Mineral Development Laboratories, Adelaide, Sth Australia
Se, Te: Kennecott Explor. Inc., Salt Lake City, Utah, U.S.A.

occurrences from this tectonic unit are silver-rich (e.g., Kunduron-Lumoro prospects of the Yuat South Batholith), and in this sense are more comparable with the porphyry deposits of the island arc realms. Non-mineralized rocks from other island arc locations (Mount Kren and Koloula, this study; Uasilau and Legusulum, unpub. company data) also tend to show slight silver enrichment over gold.

Selenium and tellurium may achieve marked concentration in porphyry copper systems, but for different reasons. Selenium tends to substitute for sulfur in, or form isomorphous solid solutions in, the various sulfide species because of similar ionic size and charge of Se^{2-} and S^{2-} (Goldschmidt, 1954). Tellurium, even though positioned in Group 6 with sulfur and selenium in the Periodic Table, has sufficiently different ionic radii and bonding characteristics to result in quite different geochemical behaviour (Sindeeva, 1964). Consequently tellurium tends to be partitioned out of the rock-forming minerals even more so than selenium. It is relatively enriched in more felsic igneous rocks (Beaty & Manuel, 1973), and achieves its greatest concentration in the volcanic precious metal telluride ore association (Stanton, 1972).

The limited data obtained here for selenium and tellurium (see Table 20) generally substantiate the earlier findings of Sindeeva (1964) and Beaty & Manuel (1973). Selenium reaches 10 ppm in the sulfide-rich mineralized rocks from Ok Tedi, but in most non-mineralized rocks is below the detection limit (less than 0.5 ppm). Tellurium is also present in amounts less than 0.5 ppm for most rocks, but reaches 1-2 ppm in the more felsic and alkalic rocks.

7.5 STATISTICAL ANALYSIS OF MINERALIZED AND NON-MINERALIZED ROCKS

7.5.1 Application of Statistical Techniques

Multivariate statistical techniques are here used to compare and contrast the geochemistry of mineralized and non-mineralized rocks from porphyry copper occurrences in the P.N.G. region. The three techniques used, and the sequence in which they are applied, are:

(i) factor analysis in the Q-mode

(ii) factor analysis in the R-mode

and (iii) discriminant analysis.

Rock groups established in Q-mode analysis are subjected to separate R-mode analysis to evaluate their geochemical variations, and are further tested for distinctiveness by discriminant analysis. In

this way, objectivity is preserved in the analysis of the geochemical data.

A detailed description of the methods and interpretation employed is in preparation (Mason & Belbin, in prep.). It is sufficient here to provide the following brief definitions which apply throughout this section.

1. a *'sample'* refers to a single whole-rock sample which has been analyzed for major and trace element abundances.

2. a *'variable'* refers to a major or trace element whose abundance has been determined for the number of samples. Values of variables constitute a *'dataset'*.

3. *'factor analysis in the Q-mode'* involves comparison of samples by way of their variables, and results in the subsequent ordering of like-samples into internally similar groups. The technique yields information on whole-rock compositional variability.

4. *'factor analysis in the R-mode'* involves comparison of variables within samples, and the subsequent ordering of variables into similar groups by way of factors. The technique yields insights into possible processes producing elemental variations within the dataset.

5. a *'factor' in Q-mode analysis* is a variable (or, more usually, a combination of variables) which characterizes a group of samples, and which accounts for a proportion of the variance within the dataset. Each sample achieves a certain *'factor score'* between -1.0 and 1.0 on each factor.

6. a *'factor' in R-mode analysis* is a combination of variables with positive and/or negative loadings which account for a proportion of the variance within the dataset. Each variable achieves a certain *'factor loading'* on each factor.

7. a *'rotation'* in Q- or R-mode analysis is a mathematical procedure resulting in a different 'view' of the variance within the dataset. In this study, rotations have assisted interpretation by highlighting subtleties in the dataset variance. In a series of analyses, the first is referred to as 'Version 1', and subsequent rotations are referred to as 'Version 2' and 'Version 3'.

8. *'Discriminant analysis'* involves comparison of pre-assigned groups of samples by way of analysis of variance of the variables, testing the distinctiveness of the groups, and re-allocation of samples (if

necessary) to one or other of the pre-assigned groups. Thus the technique can be used to test rock subdivisions which have been based upon arbitrarily chosen parameters or upon more objective analytical techniques (e.g. Q-mode analysis). Output from the discriminant analyses includes:

(i) average of each variable for each group, giving, in this work, *'average chemical analyses'* for the mineralized and non-mineralized groups.

(ii) *'univariate F ratios'* and *'univariate probabilities'* for each variable. The former refers to a value derived by dividing the between-group variance of a variable by the within-group variance of that variable. Thus variables which differ markedly between groups (e.g. in this case, sulfur) will have large univariate F ratios. The univariate probability of a variable (range 0.0 - 1.0) is a function of that variable's ability to distinguish between groups. Small values (0.0 - 0.01, equivalent at worst to a 1% chance of misallocation) indicate that the variable readily distinguishes between the established groups. Similarly, *'multivariate F ratios'* and *'multivariate probabilities'* are also given for each variable, the former derived by a comparison of variance of each variable with the combined variance of all variables, and the latter indicating the ability of each variable to distinguish between the groups considering the variability of all variables.

(iii) *'discriminant functions'* for each variable and for each group. These are constants by which the variables of each sample are multiplied, and the products summed, to give a *'multiple discriminant score'* for each sample for each group. A sample is assigned to the group for which it achieves the highest multiple discriminant score. Discriminant functions for each group are derived from the input variables of the samples of each group, but have wider application in that they can be used to assign other samples not included in the input data.

A total of 149 chemically analyzed rock samples were selected for statistical analysis. The rejected samples were volcanic and metamorphic country rocks, and intrusive rocks for which closely similar analyses were available from individual locations. Only rocks of undoubted intrusive origin have been included in the statistical study. Although a variety of sedimentary and metamorphic rocks peripheral to mineralized intrusive masses may carry significant amounts of porphyry copper mineralization (e.g. Panguna; Ok Tedi), these rocks have been

excluded because it is considered that they are not relevant to the thrust of this thesis, *viz.* geochemical relationships between intrusive rocks and closely associated porphyry copper mineralization.

The studied samples cover a wide range of calc-alkaline rock types, of suite chemistry, and of degree of mineralization and alteration. They come from widely scattered locations in the island arc, continental margin, and cratonic structural units of the Papua New Guinea and Solomon Islands region. Thus they are considered to be representative of the mineralized and non-mineralized intrusive rocks of this part of the southwest Pacific.

All computations were performed using programs on file at the U1108 Computer Suite, Australian National University.

7.5.2 Factor Analysis in the Q-mode

The aim of Q-mode factor analysis, as applied here, is to distinguish groups of rocks of similar geochemical affinity. Rocks might not only be distinguished by absolute abundances of particular elements (e.g., high-Cu rocks from low-Cu rocks) but also might be distinguished by the quality and magnitude of chemical variation between them (e.g., calc-alkaline ultramafic cumulates from Alpine-type ultramafic rocks).

The Q-mode factor analyses were conducted using the 149 samples for which values of 30 major and trace elements had been determined. The variables were:

(i) Major elements - SiO_2, TiO_2, Al_2O_3, Fe_2O_3, FeO, MnO, MgO, CaO, Na_2O, K_2O, P_2O_5, S.

(ii) Trace elements - Rb, Ba, Sr, La, Ce, Y, Th, U, Zr, Nb, Zn, Cu, Co, Ni, V, Cr, Ga, Pb.

The results of the two Q-mode analyses are summarized in Table 21, and the relationships between factors of the two versions are indicated. The factors of the two versions are readily correlated. While the five significant factors cover practically all (98.4%) of the variance, the first two factors in the first version (which correlate with the first three factors in the rotated version) account for approximately 85% of the variance. These factors cover the range of geochemical variation in the calc-alkaline rocks of intermediate and more silicic composition, and also include mineralized rocks.

Important results from the Q-mode analyses are:

(i) The wide compositional range is explained by a small number

TABLE 21: SUMMARY OF Q-MODE FACTOR ANALYSES

Number of samples = 149 whole-rock analyses

Number of variables = 12 major elements + 18 trace elements

VERSION 1			VERSION 2			
Factor characteristics	Factor	Factor relationship	Factor	Percent of variance	Cumulative percent of variance	Factor characteristics
Large group (~100 samples), all with large negative scores ↓ increasing SiO_2, K_2O, Cu ↓ decreasing island arc setting ↓ increasing continental margin setting	1		1	45.1	45.1	Low-K, low-Si rocks
All negative scores Very high negative scores indicate strongly mineralized samples	2		2	23.0	68.1	High-K, high-Si rocks
Positive or negative scores Correlates with addition of ferromagnesian minerals to form mafic cumulate rocks (positive score) or felsic derivatives (weak negative score)	3		3	16.8	84.9	High-Cu rocks
Positive scores only Correlates with addition of pyroxene and olivine to form Alpine-type ultramafic rocks	4		4	7.1	92.0	High Mg, Ni, Cr rocks
Positive scores only Correlates with addition of Fe-Ti oxides	5		5	6.4	98.4	High V, Ti rocks

of factors (i.e. five factors).

(ii) In decreasing order of importance, the factors correspond to calc-alkaline intermediate and more silicic rocks, copper-mineralized rocks, mafic and ultramafic rocks, and Fe-Ti oxide-rich rocks.

(iii) The copper-mineralized rocks form a distinct group which accounts for 16.8% of the variance within the dataset.

(iv) Within Factor 1 of Version 1, the ordering of rocks according to factor score reveals a gradation from island arc rocks which score high in the factor, through mixed island arc and continental margin rocks, to continental margin and cratonic rocks which score low in the factor. This gradation involves increasing SiO_2, K_2O, and Cu, but is interpreted more generally as indicating broad changes in intrusive whole-rock chemistry from the island arc environments, through the continental margin environment (New Guinea Mobile Belt), to the Australian continental block. A similar gradation is observed in the mineralized rocks (Factor 3) of Version 2, which implies that there are compositional differences in mineralization between the contrasted environments, and/or that there are gross whole-rock compositional differences such as those referred to above. Certainly the latter has been established above for non-mineralized rocks, and would be expected to persist to a certain extent in mineralized rocks (e.g. relative immobility of Ti, Zr, etc. (Pearce & Cann, 1971; this study)). In relation to the former implication that there may be compositional differences in mineralization, it remains to be determined whether copper enrichment is greater in any of the tectonic environments, but it has been shown above (see section 7.4.3) that precious metal abundances differ in both mineralized and non-mineralized rocks from the different tectonic environments).

(v) Although the factors relating to mafic and ultramafic rocks account for only small proportions of the variance, they highlight important features of the samples studied. Petrographic and mineral chemical data have indicated that Fe-Ti oxides were important early phases in some of the suites, and this is reflected in Factor 5 (of both versions) which accounts for Fe-Ti oxide-rich rocks. Factors 3 and 4 of Version 1 (which correlate with Factor 4 of Version 2) distinguish between ultramafic rocks of calc-alkaline character and those of Alpine-type origin.

In summary, factor analysis in the Q-mode has proved to be a powerful technique in distinguishing between rocks of grossly and

subtely different chemical composition. The grossly different copper-mineralized rocks are recognized as a distinct group. More subtle differences in rock chemistry arising from magma generation in different environments (island arc *versus* continental margin; calc-alkaline ultramafic *versus* Alpine-type associations) are also recognized.

7.5.3 R-mode Factor Analysis for Non-mineralized Rocks

Separate R-mode factor analyses have been performed on mineralized and non-mineralized groups of rocks as distinguished by Q-mode analysis. Of the 149 samples, 120 fell into the non-mineralized group, and 29 fell into the mineralized group. A sample was considered to be 'mineralized' if it scored in the range 40-100 on Factor 2 of Version 1 or Factor 3 of Version 2 in the Q-mode analyses. This range of factor scores correlates with a range of 200-8000 ppm Cu, and a correspondingly wide range of alteration types.

The same 30 major and trace element variables were used in R-mode analysis as were used in Q-mode analysis. Because R-mode factor analysis groups variables into positive and negative correlations, any differences in correlations between the separate analyses of mineralized and non-mineralized rocks will have implications for the genesis of the two rock groups.

The results of the R-mode analyses on the non-mineralized rocks are summarized in Table 22. The major and trace element correlations (positive and negative) are shown for each factor of each version. For each factor, the major and trace elements are arranged in order of decreasing factor loading. Thus in Factor 1 of Version 1, the major element oxides Na_2O, K_2O, and SiO_2, together with the trace elements Th, Rb, La, Ce, Zr, and Ba are in sympathetic correlation with each other, but are in antipathetic correlation with CaO, MgO, FeO, Co, and V. All have factor loadings between $\pm$0.6 - $\pm$1.0. Variables in parentheses are less well-correlated (i.e. they have factor loadings between 0.4 - 0.6 or between -0.4 - -0.6. Only factor loadings between 0.4 - 1.0 and between -0.4 - 01.0 have been accepted as indicative of significant correlation).

Inter-relationships of factors between the three versions are also depicted in Table 22. Two examples will suffice to illustrate types of factor relationships.

Comparison of Factor 4 in Versions 1 and 2 reveals that the elemental correlations are closely similar in both versions. Whilst Ga

TABLE 22: SUMMARY OF R-MODE FACTOR ANALYSES FOR NON-MINERALIZED ROCKS

Number of samples = 120

Number of variables = 12 major elements + 18 trace elements

Cumulative percent of variance	Percent of variance	Factor	Major Elements	Trace Elements	Factor relat-ions	Major Elements	Trace Elements	Factor relat-ions	Major Elements	Trace Elements
23.3	23.3	1	+Na_2O,K_2O,SiO_2	Th,Rb,La,Ce,Zr, Ba,(U,Nb,Ga)		+FeO,MnO,CaO,TiO_2 Fe_2O_3,(MgO)	V,(Co,Zn)		+Na_2O,K_2O,SiO_2	Th,Rb,La,Ce,Zr Ba,(U,Nb,Ga)
			-CaO,MgO,FeO, (Fe_2O_3,MnO)	Co,V,(Cr,Ni)		-SiO_2,K_2O,Na_2O	none		-CaO,MgO,FeO (Fe_2O_3,TiO_2–	Co,V,(Cr)
			broad geochemical fractionation			*addition of Fe-Ti oxides, ferromagnesians; relative depletion in silica, alkalies*			*broad geochemical fractionation; note inclusion of TiO_2*	
46.3	23.0	2	+(SiO_2)	none	↔	+(K_2O,Na_2O)	Zr,La,Ce,Nb (Th,U,Y,Ga)	↔	+(SiO_2)	none
			-MnO,FeO,(TiO_2, P_2O_5)	Y,Zn,Ce,La,(Nb, Ga,Zr)		- none	none		-MnO,(FeO,TiO_2)	(Ga,Nb,La,Ce,Y,Zn, Zr)
			removal of Fe-Ti oxides, apatites; relative silica enrichment of residua			*formation of late felsic rocks*			*removal of Fe-Ti oxides; relative silica enrichment*	
59.9	13.6	3	+(MgO)	Cr,Ni		+MgO,(FeO)	Cr,Ni,(Co)		+MgO	Cr,Ni,(Co)
			-Al_2O_3	(Ga,Sr)	↔	-Al_2O_3,(Na_2O)	(Ga)	↔	-Al_2O_3	(Ga,Sr)
			addition of olivine, pyroxene; removal of plagioclase			*addition of pyroxene, olivine; removal of plagioclase*			*removal of plagioclase; addition of ferromagnesians*	
67.7	7.8	4	+(P_2O_5)	(Ba,Sr)		+(P_2O_5,K_2O)	Ba(Rb,Sr,Pb)		+(P_2O_5)	(Ba,Sr)
			- none	(Ga)	↔	- none	none	↔	- none	none
			addition of apatite			*addition of apatite; concentration of K,Rb,Ba,Pb in late liquids*			*addition of apatite*	

Note: *Italics* is genetic interpretation of elemental correlations

is not included in Factor 4 of Version 2, and K_2O, Rb, and Pb are not included in Factor 4 of Version 1, both factors can be interpreted as representing apatite crystallization in late felsic rocks with removal of Ga in earlier-formed plagioclase.

A different type of factor relationship is revealed in comparison of Factors 1 and 2 of all three versions. Inspection of the elemental correlations shows very close similarities in these two Factors between Version 1 and Version 3. In each of these two versions, Factor 1 can be interpreted as covering the elemental correlations expected in magmatic fractionation processes in the broad sense, and Factor 2 can be interpreted as indicating removal of Fe-Ti oxides with consequent silica enrichment in the residual melts. However, in Version 2 the first two factors are more specific in covering the same geochemical correlations. Thus, Factor 1 accentuates the addition of ferromagnesian and Fe-Ti oxide minerals to form mafic cumulate rocks, while Factor 2 accentuates the complementary process (i.e. formation of alkalic liquids rich in the large, highly-charged cations).

Considered together, the three R-mode versions provide the following insights into possible processes responsible for the dataset variance:

(i) Removal of TiO_2, MnO, FeO, and V is important in Factors 1 and 2, and can be accounted for by precipitation of Fe-Ti oxides.

(ii) Removal of the ferromagnesian major and trace elements can be accounted for either by crystallization and removal of ferromagnesian minerals, or by wholesale removal of mafic material from a solid-liquid mush.

(iii) Addition of mafic minerals and removal of plagioclase are suitable mechanisms to form mafic and ultramafic cumulative rocks. This interpretation is applied to Factor 3, which is less important than the first two factors in accounting for the dataset variance.

(iv) Factor 4 can be interpreted as representing crystallization of apatite in late silicic rocks. The presence of P_2O_5 in Factors 2 and 4 of Version 1, and its associated correlated elements, indicate that apatite was available for crystallization in a wide variety of rocks. This is supported by observations of apatite in gabbroic, dioritic, and aplitic rocks.

(v) Copper does not achieve any significant factor loadings

in this analysis of non-mineralized rocks. This reflects the element's variable chalcophilic and lithophilic character.

7.5.4 R-mode Factor Analysis of Mineralized Rocks

The results of R-mode factor analysis upon a group of 29 copper-mineralized rocks are presented in Table 23. The same 30 major and trace element variables were used as in R-mode analysis of the non-mineralized rocks.

Important points arising from study of the results are:

(i) In comparison with the non-mineralized rocks, the mineralized rocks require more factors to explain the dataset variance. Further, the first three factors (which account for 65.4% of the variance) contain similar geochemical correlations as do the four factors (which account for 67.7% of the variance) of the non-mineralized R-mode analyses. The remaining three factors of the mineralized R-mode analyses reflect processes closely related to alteration and mineralization, which have acted upon rocks whose chemistry was initially determined by earlier magmatic processes.

(ii) The presence of copper in Factor 2 of Version 1 (where it is in positive correlation with SiO_2, K_2O, and Rb, and in negative correlation with V) and also in Factor 4 (where it is in positive correlation with S and V, and in negative correlation with Sr), displays the variable geochemical behaviour of copper. In Factor 2, copper can be interpreted as behaving in a lithophilic manner and is enriched in late silicic, alkaline liquids due to only limited substitution in silicate crystal lattices. The true extent of this process (and, more generally, the partition of copper between silicate and oxide minerals) remains unevaluated for the rocks under discussion. In many of the non-mineralized intrusive rocks, small amounts of presumably primary chalcopyrite are present as small interstitial grains or occur within early-formed Fe-Ti oxide grains. Hence some degree of chalcophilic behaviour can be deduced for copper throughout crystallization of the host rocks. Nevertheless, other studies (Dodge et al., 1968; Putnam, 1972; Graybeal, 1973) have demonstrated extensive lithophilic behaviour of copper in granitic rocks with and without accessory sulfides. The elemental correlations of Cu in Factor 2 of Version 1 are in accord with those studies, and it is tentatively concluded that they indicate lithophilic behaviour of copper. In Factor 4, copper displays its strong chalcophilic character under the conditions prevailing during alteration and mineralization.

TABLE 23: SUMMARY OF R-MODE FACTOR ANALYSES FOR COPPER-MINERALIZED ROCKS

Number of samples = 29 whole-rock analyses

Number of variables = 12 major elements + 18 trace elements

Factor	Percent of variance	Cum. % of variance	Major Elements	Trace Elements	Factor relations	Major Elements	Trace Elements	Factor relations	Major Elements	Trace Elements
1	24.0	24.0	+Al_2O_3,Na_2O,(SiO_2 K_2O) -MgO,(FeO,CaO, MnO) *enrichment of felsic rocks in sodic plag., alkalis, and large cations; relative depletion in ferromagnesian components*	Ga,La,Ba,Ce,Th,Zr, Sr,U,(Rb,Nb) Co,Cr,Ni	←→	+Al_2O_3,Na_2O(SiO_2) -MgO *enrichment of felsic rocks in sodic plag.; relative depletion ferromagnesian components*	Ga,(Sr,Zr) (Co,Ni,Cr)	←→	+Al_2O_3,Na_2O(SiO_2, K_2O,P_2O_5) -MgO,(FeO,CaO) *enrichment of felsic rocks in sodic plag., apatite, K,Rb,Sio_2; depletion of ferromagnesians.*	Ga,Zr,La,Sr, Ba,Ce,Th,U, (Rb,Nb) Co,Cr,Ni
2	21.1	45.1	+(SiO_2,K_2O) -TiO_2,P_2O_5, (Fe_2O_3,MnO, CaO,FeO) *enrichment of K, Cu,Rb in felsic rocks; depletion of Fe-Ti oxides, apatite, calcic plag.*	(Cu,Rb) Zn,Y,V,(Ga,Pb, Nb,Zr)	←—	+TiO_2,FeO,(Fe_2O_3, P_2O_5,MnO) -(SiO_2) *addition of Fe-Ti oxides, apatite relative depletion of silica*	V,Y,Zn,(Pb) none	←—	+(SiO_2) -TiO_2,P_2O_5, (Fe_2O_3,FeO,MnO) *removal of Fe-Ti oxides, apatite; relative silica enrichment*	none Y,V,Zn,(Ga, Pb,Zr)
3	20.3	65.4	+ none - (MgO) *depletion of ferromagnesian components*	none (Ni,Nb,Co,Cr)	←— →	+P_2O_5 - none *addition of apatite, zircon, including large cations.*	Ce,La,Nb,(Zr, Th,U,Ba,Sr, Ga) none	←— →	+(Na_2O) - (MgO) *alkali enrichment in felsic rocks relative depletion of ferromagnesian components*	none (Ni,Nb,Co, La,Ce,Sr)
4	10.0	75.4	+ (S) - none *addition of sulfides; stability of V in mineralised rocks; relative loss of Sr by destruction of plagioclase*	Cu(V) (Sr)	←— →	+ K_2O - (Fe_2O_3) *enrichment of K,Rb,Cu in felsic rocks; relative loss of Fe^{3+},Sr.*	Rb,(Cu) (Sr)	←— →	+ S - none *Addition of sulfides; stability of V in mineralised rocks; destruction of calcic plag.*	Cu,(V) (Sr)
5	6.2	81.6	+ (S) - none *depletion of Pb,Rb in mineralised rocks; base metal zoning*	none Pb,(Rb)	←—	+ none - S *enrichment of Pb in low-S, low-Cu zones; base metal zoning*	Pb (Cu)	←—	+ S - none *depletion of Pb in sulfide-rich rocks; base metal zoning*	none Pb
6	6.1	87.7	+ none - CaO *loss of Ca in mineralised rocks by destruction of calcic plagioclase*	none none	←—	+ none - CaO *destruction of calcic plagioclase in altered/mineralised rocks*	(Ga) none	←—	+ none - CaO *destruction of calcic plagioclase in altered/mineralised rocks*	(Ga) none

Note: *Italics* is genetic interpretation of elemental correlations.

(iii) Aspects of alteration and mineralization are brought out in Factors 5 and 6. Factor 5 refers to the antipathetic correlation of Pb with S and Cu, and thus represents the tendency towards base metal zoning in porphyry-type copper deposits (Rose, 1970; Fisher, 1972; Jambor, 1974). Factor 6 represents the destruction of calcic plagioclase in altered, mineralized rocks.

In summary, R-mode factor analysis of mineralized and non-mineralized rocks has proved fruitful in establishing dominant elemental correlations. In non-mineralized rocks, the elemental correlations can be interpreted as representing fractionation processes involving discrete mineral species (Fe-Ti oxides; ferromagnesian minerals; apatite), but do not distinguish between these crystal-liquid processes and other possible fractionation processes involving wholesale removal of mafic material from a silicic liquid. In mineralized rocks, much of the geochemical variation is accounted for by correlations which are closely similar to those determined for non-mineralized rocks. Factors attributable to alteration/mineralization processes account for a relatively small proportion of the total variance. However, these factors confirm the variable geochemical behaviour of copper and vanadium, reveal the tendency towards base metal zoning, and show that destruction of calcic plagioclase is an important alteration feature.

7.5.5 Discriminant Analysis of Mineralized and Non-mineralized Rocks.

Discriminant analyses have been performed on mineralized and non-mineralized rock groups, firstly using the 12 major element variables, and secondly using 28 major and trace element variables (the same variables as were used for Q- and R-mode factor analysis, except for cobalt and gallium which had not been determined for some samples).

The function of the discriminant analysis is essentially to determine the distinctiveness of the mineralized and non-mineralized rock groups. Indirectly, it is a check on the Q-mode analysis, upon which the allocation of samples to mineralized and non-mineralized groups was based.

For the *major element discriminant analysis*, 113 rocks were allocated to the non-mineralized group and 24 were allocated to the mineralized group. The results of the analysis are summarized below:

(i) Comparison of the average rock analysis for each group (see Table 24) shows that SiO_2, Na_2O, K_2O, and S are higher in the mineralized group, while CaO, TiO_2, MnO, and MgO are much lower. The average SiO_2

TABLE 24: SUMMARY OF DISCRIMINANT ANALYSIS (major element variables)

Variable	Avge Group Analysis (wt.%) non-min'z'd (113 samples)	Avge Group Analysis (wt.%) Cu-min'z'd (24 samples)	Univariate F	Univariate prob.	Multivariate F	Multivariate prob.	Discriminant functions non-min'z'd	Discriminant functions Cu-min'z'd
SiO_2	57.24	61.32	6.10	.015	1.30	0.256	93.629	93.272
TiO_2	0.68	0.56	3.14	.079	0.01	0.941	107.520	107.372
Al_2O_3	16.61	16.42	0.11	.741	0.73	0.395	105.365	105.036
Fe_2O_3	3.03	2.30	5.97	.016	0.21	0.645	80.725	80.930
FeO	3.49	2.56	9.78	.002*	0.12	0.735	121.190	120.972
MnO	0.11	0.04	29.50	.000*	7.76	0.006*	-389.976	-416.816
MgO	4.34	2.59	4.93	.028	0.20	0.652	123.429	123.224
CaO	7.38	4.63	15.97	.000*	0.39	0.531	69.529	69.317
Na_2O	3.44	4.04	6.29	.013	1.49	0.225	99.358	100.188
K_2O	1.54	2.53	11.24	.001*	1.32	0.253	86.752	87.264
P_2O_5	0.27	0.24	1.00	.318	2.24	0.137*	276.279	271.859
S	0.11	0.68	60.80	.000*	36.53	0.000*	138.133	144.143
CONSTANT	-	-	-	-	-	-	-4711.649	-4686.242

* variable is good discriminator

content of the mineralized group (61.3% SiO_2) closely approximates the SiO_2 level at which the Yuat South and Karawari batholiths achieve their copper peaks (compare Fig. 55).

(ii) Comparison of univariate and multivariate F ratios and probabilities (see Table 24) reveals that S, MnO, CaO, FeO, and K_2O as univariant elements distinguish quite well between the two groups, while S, MnO, and P_2O_5 distinguish best when multivariate data are considered.

(iii) Of the 113 rocks initially allocated to the non-mineralized group, only one sample (DRM015) was re-allocated (to the copper-mineralized group). This re-allocation is appropriate, because the rock is an orbicular microgranodiorite carrying 5% total sulfides (pyrite > chalcopyrite ≈ molybdenite.) While the rock was considered 'non-mineralized' by the Q-mode analysis because of its low copper content (95 ppm Cu) relative to other copper-mineralized rocks, its whole-rock chemistry has been correctly evaluated by the discriminant analysis to be more like the mineralized group. The high discriminating power of sulfur, and the large amount of sulfur in the rock (1.02%), were instrumental in effecting the re-allocation. Of the 24 rocks initially allocated to the mineralized group, 7 were re-allocated (to the non-mineralized group). Probability for re-assignment was high for 5 of the rocks (DRM003, 054, 076, 080, 122), all of which are closely associated with mineralization but are not strongly mineralized themselves. Probability for re-assignment was low for the two other samples (DRM087, 142), both of which are closely associated with mineralization but only weakly mineralized. Thus 129 out of 137 samples were assigned to their original group, representing a success rate of 94.2%. It must be appreciated that, whilst the re-allocated samples were considered to be 'mineralized' by the Q-mode analysis on the basis of copper content, their major element chemistry has been evaluated by the discriminant analysis to be more like the non-mineralized group.

(iv) The discriminant functions of the major element variables (see Table 24) can be used to calculate multiple discriminant scores in order to assign other analyzed rocks to one or other of the two established groups. For example, the 6 samples DRM039, 040, 100, 104, 108, and 119 (which were all excluded from the statistical analyses because of close similarity with other analyses from their respective areas) all fall into the non-mineralized group (see Table 26). From other observations, these rocks are known to be non-mineralized. Similarly, of the 6 specimens DRM156, 157, 159, 158, 160, and 161 (all of which are

known to be mineralized and which could not be included in the statistical analyses due to lack of S, P_2O_5, and FeO data), the last three fall into the correct (mineralized) group despite lack of data for the best elemental discriminators.

It could be argued that it is not valid to apply this major element discriminant analysis to groups of rocks which have been distinguished by Q-mode factor analysis using both major and trace element variables. However, it is reasonable to inquire whether major elements alone are able to distinguish copper-mineralized and non-mineralized rocks, not only because of intrinsic academic interest but also because of the prevalence of major element whole-rock analyses and general lack of trace element data. It has been shown above that major elements alone do, in fact, distinguish copper-mineralized and non-mineralized rocks with considerable success. One can conclude that the processes leading to mineralization also result in development of certain major element characteristics in mineralized rocks. Failure of a 'copper-mineralized' sample (as defined by Q-mode analysis) to acquire those major element characteristics (either because of very weak mineralization and negligible alteration, or because of higher amounts of primary copper sulfides and lack of alteration) will result in the discriminant analysis re-allocation of such rocks to the 'non-mineralized' group.

For the *major and trace element discriminant analysis*, 110 rocks were allocated to the non-mineralized group, and 23 rocks to the mineralized group. The results of the analysis are summarized as follows:

(i) Average major element abundances for the two groups (see Table 25) are comparable with those obtained in the previous discriminant analysis. Small differences are due to the slightly different number of samples involved. Average trace element abundances are in accord with the more felsic character of the mineralized group compared with the non-mineralized group. Thus Rb, Ba, La, and Ce are markedly higher in the mineralized group, while Zn, Ni, V, Cr, and Pb are lower. Average copper abundance in the mineralized group is, of course, much greater than the non-mineralized group (1456 and 85 ppm respectively).

(ii) Under univariate conditions the best elemental and elemental oxide discriminators are, in order of discriminating power, Cu, S, MnO, CaO, K_2O, Zn, Rb, and FeO. The best multivariate discriminators are Cu, S, Rb, and MgO.

TABLE 25: SUMMARY OF DISCRIMINANT ANALYSIS (major and trace element variables)

Variable	Avge group analysis (majors,wt.%; traces,ppm)		Univariate	Univariate	Multi-variate	Multi-variate	Discriminant functions	
	non-min'z'd	Cu-min'z'd	F	prob.	F	prob.	non-min'z'd	Cu-min'z'd
SiO_2	57.34%	61.22%	5.23	0.024	3.09	0.082	143.23	144.20
TiO_2	0.67	0.55	2.96	0.088	0.76	0.384	413.30	417.16
Al_2O_3	16.61	16.40	0.12	0.725	2.08	0.152	153.13	154.09
Fe_2O_3	3.02	2.33	4.98	0.027	0.41	0.522	132.97	133.51
FeO	3.47	2.29	8.58	0.004*	2.31	0.132	114.33	112.78
MnO	0.11	0.04	28.01	0.000*	0.30	0.588	-572.15	-582.86
MgO	4.31	2.61	4.40	0.038	6.88	0.010*	183.83	186.24
CaO	7.33	4.52	15.92	0.000*	0.47	0.493	131.21	131.76
Na_2O	3.45	4.05	6.07	0.015	3.62	0.060	164.27	166.96
K_2O	1.56	2.62	12.35	0.001*	2.17	0.143	124.89	123.01
P_2O_5	0.27	0.24	0.77	0.382	1.37	0.244	143.76	137.46
S	0.11	0.66	56.06	0.000*	28.27	0.000*	285.45	295.12
Rb	35 ppm	59 ppm	8.81	0.004*	8.72	0.004*	0.48	0.61
Ba	261	329	1.68	0.197	1.13	0.290	0.31	0.32
Sr	593	629	0.38	0.540	0.09	0.763	0.05	0.05
La	12	15	2.54	0.113	2.02	0.159	-3.53	-3.84
Ce	25	30	1.32	0.252	4.74	0.032	3.93	4.18
Y	18	16	1.53	0.219	1.42	0.236	1.20	1.36
Th	4.6	4.8	0.07	0.788	0.81	0.369	-1.90	-2.19
U	1.1	1.0	0.24	0.626	5.00	0.027	-11.57	-12.97
Zr	107	115	0.36	0.550	3.82	0.054	-0.64	-0.67
Nb	5.2	6.6	1.50	0.223	0.01	0.942	-12.94	-12.96
Zn	67	44	8.88	0.003*	0.23	0.635	2.20	2.21
Cu	85	1455	119.59	0.000*	38.93	0.000*	0.10	0.11
Ni	32	14	0.80	0.372	0.03	0.858	0.54	0.54
V	183	159	1.03	0.312	2.94	0.089	-0.25	-0.23
Cr	73	46	0.34	0.560	3.74	0.056	-0.05	-0.05
Pb	5.8	3.8	1.79	0.183	0.02	0.896	-1.80	-1.81
CONSTANT	-	-	-	-	-	-	-7260.71	-7368.52

* variable is good discriminator

TABLE 26: APPLICATION OF DISCRIMINANT FUNCTIONS

Specimen No.	Major element discriminant analysis		Majors + trace elements discriminant analysis	
	Score for Non-mineralized Group	Score for Mineralized Group	Score for Non-mineralized Group	Score for Mineralized Group
DRM.039	4808.01^{+-}	4807.80	5914.66^{+-}	5900.88
DRM.040	4791.01^{+-}	4790.58	5536.89^{+-}	5518.46
DRM.100	4765.40^{+-}	4761.77	7374.19^{+-}	7369.90
DRM.104	4746.76^{+-}	4741.18	7331.69^{+-}	7328.39
DRM.108	4720.01^{+-}	4716.23	7250.41^{+-}	7240.09
DRM.119	4710.25^{+-}	4709.18	7323.76^{+-}	7319.81
DRM.156*	4774.93^{-}	4774.56^{+}	7500.70	7532.15^{+-}
DRM.157*	4850.05^{-}	4849.63^{+}	7269.69^{-}	7264.54^{+}
DRM.158*	4796.12	4796.48^{+-}	7298.68	7303.90^{+-}
DRM.159*	4765.73^{-}	4763.09^{+}	7135.39	7146.04^{+-}
DRM.160*	4779.81	4781.25^{+-}	7489.25	7508.44^{+-}
DRM.161*	4801.23	4804.86^{+-}	8173.97	8289.81^{+-}

Note:

* = discriminant scores calculated with no S, P_2O_5, or FeO determinations

$^{+}$ = expected group

$^{-}$ = assigned group

(iii) Of the 133 samples, 129 were assigned to their original group. This represents a success rate of 97.0%. All 110 non-mineralized rocks were assigned to their initial group, while 4 of the 23 mineralized samples were re-assigned to the non-mineralized group. These four samples (DRM054, 076, 080, 122) were also re-assigned in the previously-described major element discriminant analysis.

(iv) The discriminant functions (see Table 25) can be used to assign other analyzed rocks. Thus, the 6 samples DRM039, 040, 100, 104, 108 and 119 all fall into their correct (non-mineralized) group (see Table 26). Similarly, all of the samples DRM156-161 fall into their correct (mineralized) group, except for DRM157 which is only very weakly mineralized. This latter success is achieved despite lack of S, P_2O_5, and FeO determinations for these 6 samples.

In summary, discriminant analysis has proved successful in confirming the distinctiveness of mineralized and non-mineralized rock groups in the P.N.G. region. Discriminant functions can be successfully applied to other rock analyses to confirm whether mineralized or not. This procedure, of course, is of doubtful practical value since mineralized samples can usually be distinguished in the field. However, the principle has been established that different rock groups can be distinguished using this technique. A more fruitful area for future work will be to determine discriminant functions for those two groups of rocks which are much more difficult to distinguish in the field, namely non-mineralized intrusive rocks which are, and which are not, closely associated with porphyry-type copper mineralization.

CHAPTER 8 GENESIS OF CALC-ALKALINE INTRUSIVE ROCK SUITES AND ASSOCIATED PORPHYRY COPPER MINERALIZATION, WITH PARTICULAR REFERENCE TO THE PAPUA NEW GUINEA-SOLOMON ISLANDS REGION.

8.1 INTRODUCTION

The geological fraternity has long been occupied with problems relating to the origin of calc-alkaline magmas and the rock suites which now represent those magmas. Focal points of investigation have centred on possible source materials for the magmas, and magmatic processes consequent upon magma generation. The frequent occurrence of a variety of ores in association with calc-alkaline rocks has given added impetus to the search for patterns in rock/ore distributions as aids to mineral exploration, and to the more academic but intimately related questions concerning origin and evolution of these geochemical systems.

In this chapter, an attempt will be made to synthesize certain data from calc-alkaline intrusive rocks and associated porphyry-type copper mineralization in the P.N.G.-Solomon Islands region, and to bring the synthesized data to bear upon the problems relating to their genesis in particular, and the genesis of intrusive rock/porphyry copper systems in general. Such systems in the southwest Pacific occur in geotectonic settings ranging from active island arcs, through continental margin, to continental locations. Results of studies upon granitic rocks and porphyry systems in these relatively youthful settings might well have further application to the understanding of similar systems located in older, inactive structural units of the Earth's crust.

8.2 COMPARATIVE GEOCHEMISTRY OF INTRUSIVE ROCK SUITES OF THE P.N.G. - SOLOMON ISLANDS REGION

8.2.1 Major Element Chemistry

Major element trends for fifteen geochemically distinct suites from thirteen intrusive complexes are summarized in Harker-type diagram form in Fig. 58. Only those suites have been depicted for which sufficient samples were available to define trends, and only those trends have been drawn which possess correlation coefficients (r) between 0.7 and 1.0, or between -0.7 and -1.0. Of the 111 trends drawn, 47 have r better than 0.95, 76 have r better than 0.91, and only 5 have r worse than 0.71 (see Appendix 4, Table 4). It is considered significant that the majority of major element trends for each suite closely approximate to straight lines.

Fig.58 Major element trends for intrusive rock suites.

(Red, high-K suites; blue, low- and normal-K suites)

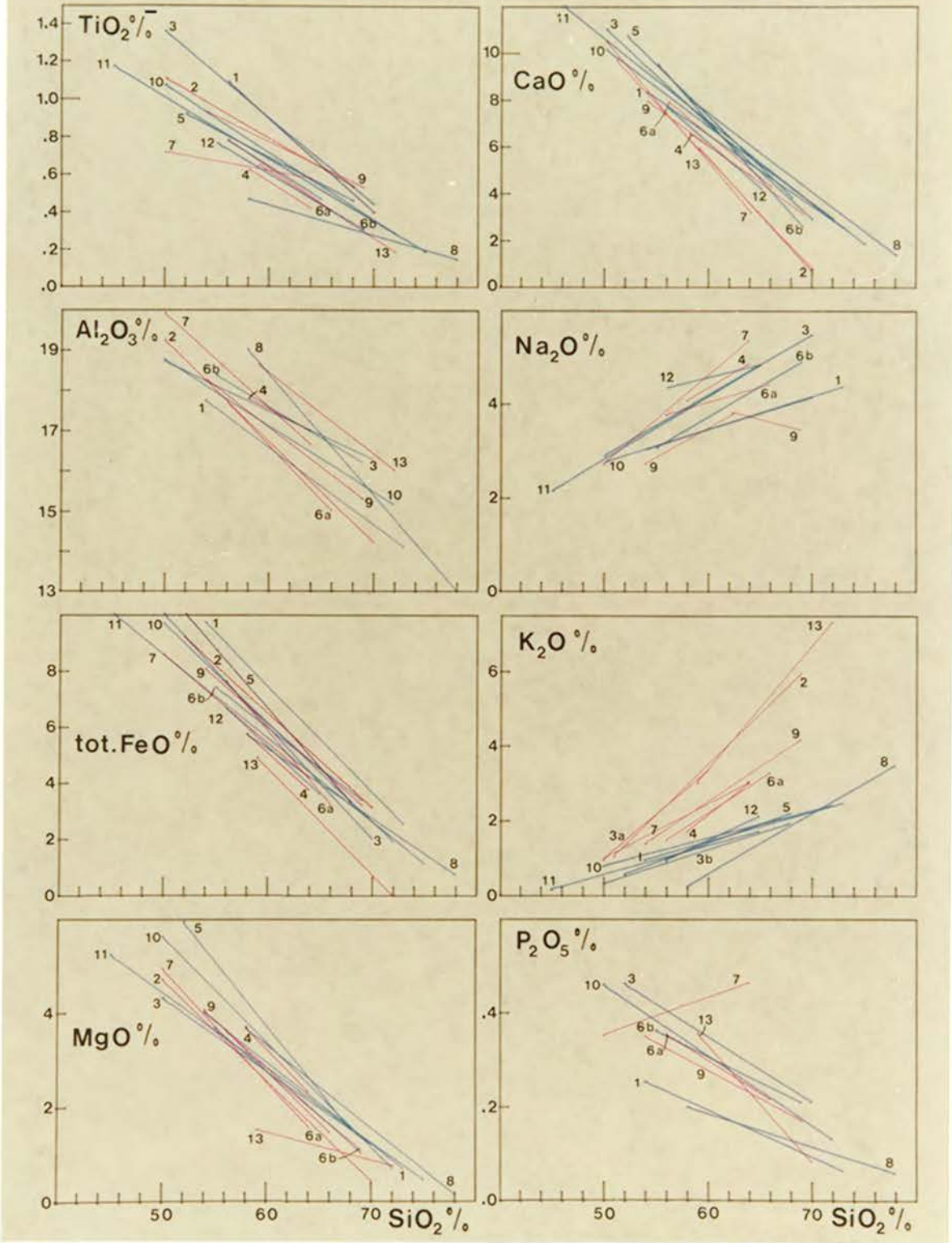

KEY TO SUITE NUMBERS IN FIG. 58 :

ISLAND ARC SUITES

1 = North Bainings normal-K suite

2 = South and Central Bainings high-K suite

3a= Plesyumi high-K suite

3b= Plesyumi normal-K suite

4 = Mount Kren high-K suite

5 = Lemau normal-K suite

6a= Panguna higher-K suite (Kaverong Quartz Diorite Suite)

6b= Panguna lower-K suite (Porphyry Suite)

7 = Limbo River high-K suite

8 = Koloula low- to normal-K suite

CONTINENTAL MARGIN SUITES

9 = Yuat North high-K suite

10= Yuat South normal-K suite

11= Karawari low- to normal-K suite

12= Frieda River normal-K suite

CONTINENTAL SUITE

13= Ok Tedi (Mount Fubilan) high-K suite

Note: Correlation coefficients for the trends displayed by these suites are provided in Appendix 4, Table 4.

An initial constraint, then, upon the genesis of progressively more silicic rocks within an individual rock suite is that the process or processes involved must be capable of producing the approximately linear elemental variations observed to be characteristic for each intrusive rock suite. Those samples which depart from suite trends can be shown petrographically and chemically to be mafic, cumulative rocks, or are felsic and can be shown to have suffered hydrothermal alteration.

Linear geochemical variations have long been observed to be a feature of calc-alkaline intrusive rock suites from many parts of the world (e.g., Nockolds, 1941; Nockolds & Mitchell, 1948; Larsen, 1948; Nockolds & Allen, 1953; Bateman et al., 1963; Chappell, 1966). The new P.N.G. data confirm the prevalence of these variations in such suites. Various processes have been proposed by different workers to account for the observed regular variations. These range from forms of hybridism (Nockolds, 1934; Wilkinson et al., 1964; Wilkinson, 1966) and crystal fractionation (Bowen, 1928; Nockolds, 1941; Ragland & Butler, 1972), to fractionation of mafic refractory source material from a low-melting silicic liquid (Chappell, 1966; Presnall & Bateman, 1973; Chappell & White, 1974). In any suite, geochemical data alone are usually insufficient to distinguish between those mechanisms which can account for the geochemical variation; data must be integrated with field, petrographic, and other laboratory data to establish with any certainty the mechanisms responsible for the observed variations.

The best distinction of the studied suites is achieved on plots of K_2O and CaO *versus* SiO_2 (see Fig. 58). The gradational nature of the suite chemistries is apparent on the plot of K_2O *versus* SiO_2, although there is a predominance of normal-K suites (compare Gill, 1970, fig. 8). The suites cover a wide range of calc-alkaline chemistry, from the low- to normal-K Felsic Suite of theKoloula Igneous Complex to the high-K Ok Tedi suite. While the whole range of major element chemistries may occur in the island arc and continental margin environments, only normal- and high-K suites have been found in the cratonic setting. It is also true that the lowest-K suite of this study lies in an island arc setting (Koloula Felsic Suite, Guadalcanal), and the highest-K suite lies in the cratonic environment (Ok Tedi Intrusive Complex). In a broad sense, this direction of increase of K-content from island arc to cratonic environments can be compared with the landward increase in K-content observed in batholithic rocks in other parts of the world (e.g. Moore,

1962; Bateman & Dodge, 1970). Another constraint, then, upon the genesis of the P.N.G. intrusive suites is that the process or processes responsible for magma generation must be capable of producing a wide compositional range of calc-alkaline magmas in a variety of environments, but with the added constraint that the most primitive (K-poor, Ca-rich) magmas be produced in island arc settings and the most evolved (K-rich, Ca-poor) magmas in the cratonic environment.

8.2.2. Trace Element Chemistry

Trends of trace element variations in the studied intrusive suites (see figures of Chapters 4 and 5) conform to the approximately linear trends observed in major element variations. This is especially true for the ferromagnesian trace elements (Ni, Co, V), which decrease regularly with increasing silica and which are all successively lower in island arc, continental margin, and cratonic rocks throughout most of the silica range (see Table 27). All of Ni, Co, and V span narrow ranges at a given silica content. In general, nickel and cobalt are low and vanadium is high. These features are characteristic of calc-alkaline geochemistry (Taylor et al., 1969a). The high levels of vanadium in rocks of intermediate silica content preclude derivation of those rocks by schemes involving fractional crystallization of Fe-Ti oxides (or much pyroxene and amphibole) from melts of basaltic compositions (Taylor et al., 1969b; compare Osborn, 1969).

Of the alkaline earth metals, the behaviour of barium is quite regular, and closely follows potassium in being more abundant in more potassic suites. Barium increases steadily with increasing silica in all suites. At intermediate silica contents, barium spans a narrow range in island arc suites, ranges higher in the continental margin suites, and reaches its highest levels in suites from the cratonic environment. Strontium, on the other hand, does not display such regular distribution. In some suites it decreases with increasing silica, and in other suites it increases. Levels of abundances of strontium also vary widely. However, the lowest strontium abundances occur in island arc suites, and highest strontium levels are present in cratonic suites and late porphyries in the island arcs.

On plots of zirconium and niobium against silica, good separation is achieved between island arc suites, and continental margin and cratonic suites. There is gradual increase in both elements with increasing silica in suites from all environments.

TABLE 27: COMPARISONS* OF SELECTED TRACE ELEMENTS FOR INTRUSIVE SUITES FROM VARIOUS GEOTECTONIC SETTINGS, P.N.G. REGION

	Island arc suites	Continental margin suites	Cratonic suites	Variation with increasing SiO_2	Remarks
Ba	moderate 120-280+	moderate-high 100-400	high 400-800	increases	higher in higher-K suites
Sr	variable 220-900	moderate 400-600	high 700-1100	increases or decreases	decreases rapidly at higher silica levels in some suites
Zr	low-moderate 80-110(180)	moderate-high 150-180	moderate-high 150-200	increases	decreases at higher silica levels in some suites; high in Mt Kren (island arc) high-K suite
Nb	very low <5	low-moderate 8-10	moderate-high >10	increases	ditto
Ni	low-moderate 5-20	low 10	low <10	decreases	most island arc suites have moderate (10-20) levels of Ni
Co	moderate 15-25	moderate 15-20	low <15	decreases	cratonic suites lower than other suites
V	high 150-220	moderate-high 140-160	moderate 100-140	decreases	small range covers most suites

* Elemental abundances are compared at 60% SiO_2

\+ all values in p.p.m.

Abundances of uranium and thorium also differ between the island arc suites and suites from the continental margin and cratonic settings (see Fig. 59). Even in high-K island arc intrusive suites, U ranges to only 2 ppm, and Th to 6 ppm. In contrast, continental margin and cratonic suites range to 5 ppm of U, and 15 ppm of Th.

Rare earth elemental abundances also differ according to suite chemistry and tectonic setting (see Fig. 60). Abundances of lanthanum, cerium, and yttrium increase from low- to normal-K suites, through normal-K suites to high-K suites. Within the fields defined by suite chemistry, there is increasing abundance of REE from island arc suites, through continental margin to cratonic suites.

8.3 GENETIC IMPLICATIONS OF REGIONAL GEOCHEMICAL VARIATIONS

8.3.1 Geochemical Variations Between Tectonic Settings

The major and trace element chemistry summarized above reveal consistent geochemical differences between calc-alkaline intrusive rock suites from island arc, continental margin, and cratonic settings in the P.N.G. region. These differences involve increasing abundances of those elements (the 'incompatible' elements) typically fractionated in the continental environment, and confirm the relatively primitive character of the island arc suites compared with suites from the other environments. The gradational nature of these changes in geochemical character was assessed by Q-mode factor analysis (see Chapter 7, section 7.5.2) as constituting part of the most important factor accounting for geochemical variation in the P.N.G. intrusive rocks.

In attempting to explain similar regional variations elsewhere, most workers have appealed to some degree of involvement of continental crustal material in magma generation, or post-magma generation processes. Bateman & Dodge (1970) and Presnall & Bateman (1973) appeal to crustal compositional differences to account for the observed major element variations across the Sierra Nevada Batholith. Moore (1962) and Moore et al. (1962) applied the concept to the granitic rocks of the entire North American western cordillera. It seems reasonable to assume the working hypothesis that compositional differences of the lower crust have caused the progressively more evolved granitic compositions described here in the P.N.G. region.

8.3.2 Geochemical Variations Across the New Guinea Mobile Belt

Regional geochemical variations are also apparent on a more

FIG. 59 : U versus Th for intrusive rocks from different tectonic settings, P.N.G. region.

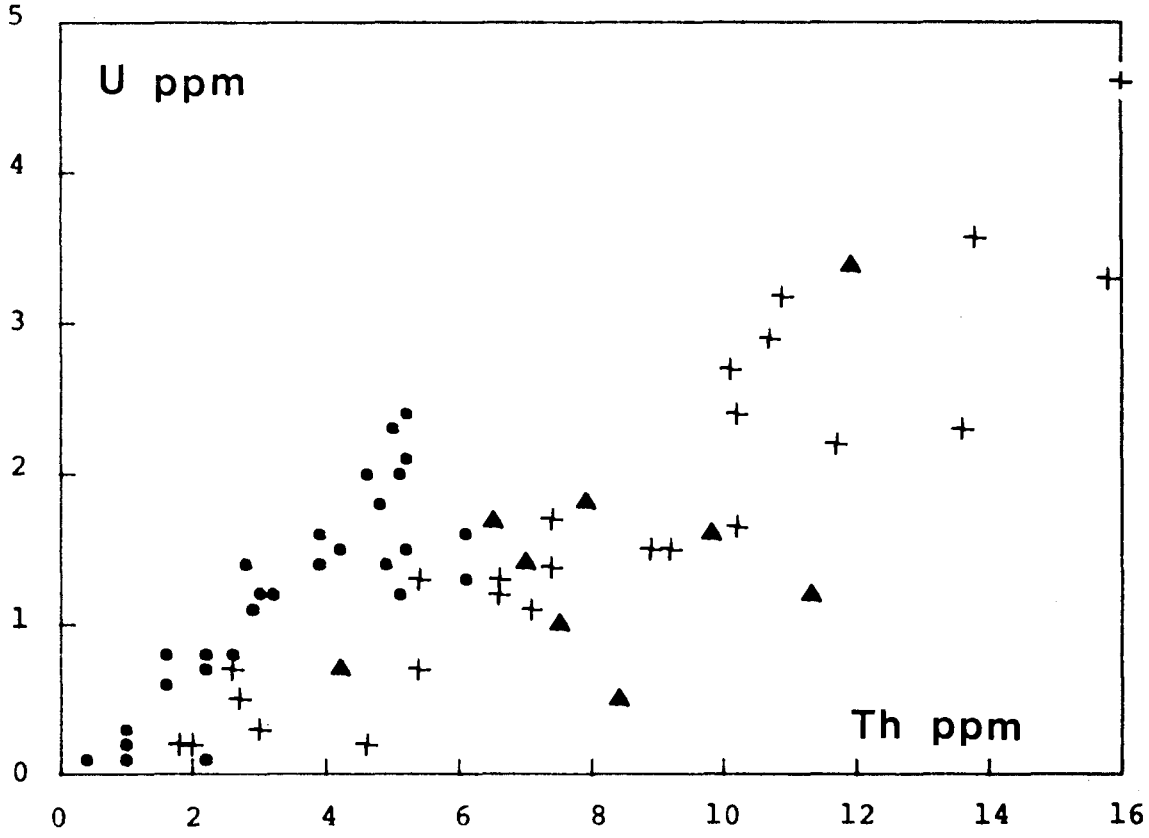

KEY : Intrusive rocks from ● island arcs
+ continental margin
▲ continental block

FIG. 60 : VARIATION OF REE FOR INTRUSIVE ROCK SUITES, PAPUA NEW GUINEA - SOLOMON ISLANDS REGION.

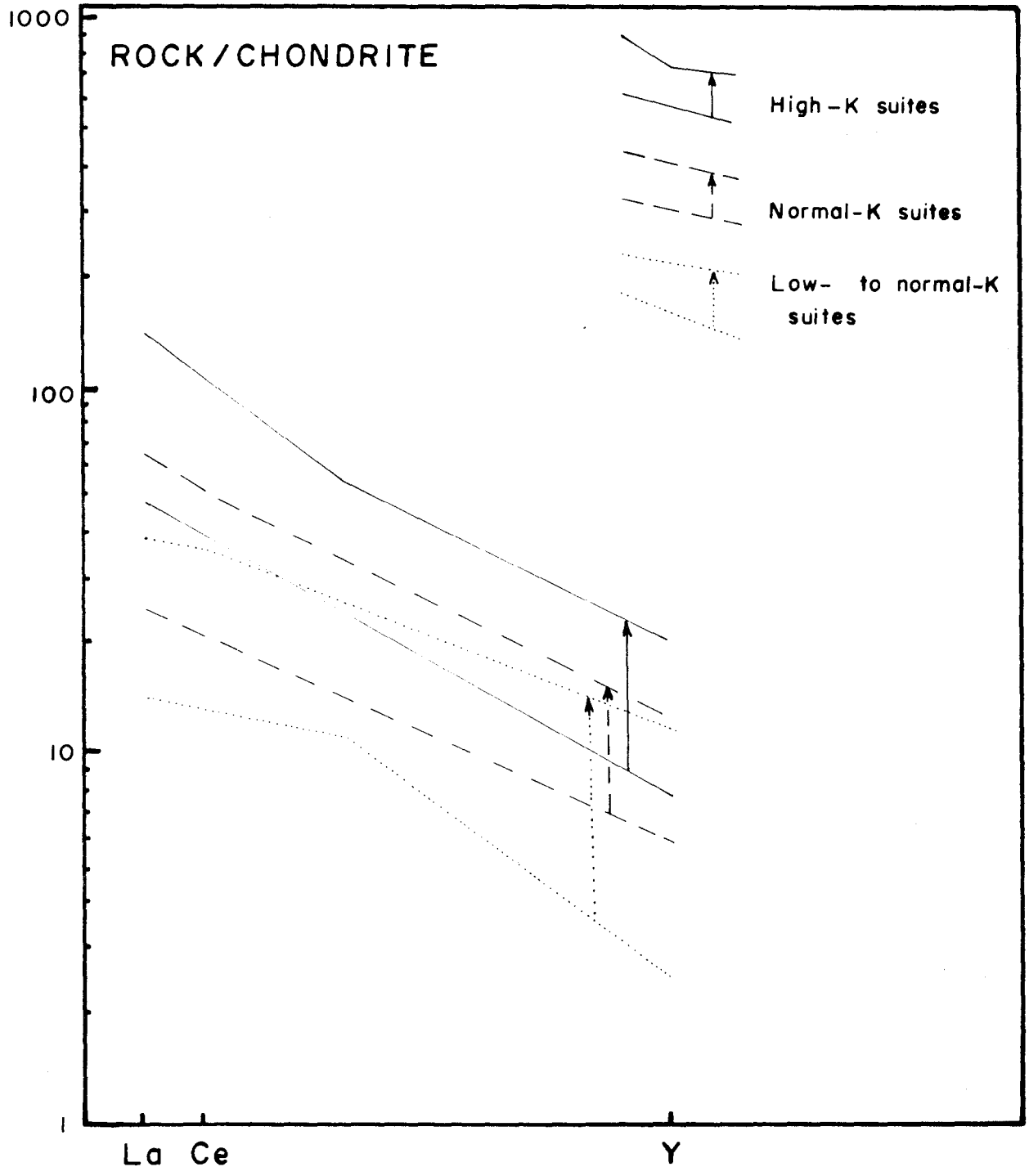

NOTE : Yttrium plotted in place of dysprosium.

Arrows indicate direction of increase of REE from island arc, through continental margin, to continental rocks.

restricted scale. Within the New Guinea Mobile Belt, mineralogical and geochemical comparison of dominant suites of the Middle Miocene Yuat North, Yuat South, and Karawari batholiths indicate a regional geochemical polarity of increasing K_2O (and related elements) northwards across the Mobile Belt (Mason, 1975; see Fig. 61). Applying the working hypothesis of 8.3.1 above, the regional polarity can be interpreted as indicating a regional variation in composition of the basal crust regions beneath the Mobile Belt.

If interpreted in terms of current plate theory concerning geochemical polarity across island arcs and continental margins (Dickinson, 1968, 1975; Dewey & Bird, 1970), the polarity requires the presence of a pre-Miocene trench on the southern margin of the Mobile Belt with a northward-dipping Benioff zone beneath the Belt. This model demands that the New Guinea Mobile Belt developed as an island arc structure remote from the Australian continental block (Mason, 1975). However, the model has three major deficiencies:

(i) it does not explain the correlation of time-stratigraphic units between this portion of the Mobile Belt and the continental block (Dow et al., 1972). The correlation strongly suggests contiguous development of the two structural settings since at least Middle Jurassic times.

(ii) it does not explain the earlier emplacement of the high-K Yuat North Batholith (13.5 - 14.0 m.y. b.p.) and the later emplacement of the normal-K Yuat South Batholith (11.1 - 12.6 m.y. b.p.; Page, 1971).

(iii) it does not readily explain the presence of minor normal-K rocks in the high-K Yuat North Batholith (specimens DRM041, 042), minor high-K rocks in the normal-K Yuat South Batholith (specimen DRM051), and minor high-K rocks in the low-to normal-K Karawari Batholith (specimen DRM066).

These difficulties are sufficiently serious to force a reconsideration of the model. One might consider the possibility of a southward-dipping Benioff zone with the corresponding trench on the northern margin of the Belt. Whilst this model permits contiguous development of the Mobile Belt and continental block, it does not account for the observed northward geochemical polarity across the Belt. These sorts of anomalies in simplified 'plate tectonic' models lead one to consider the possibility that other types of tectonic styles might have

FIG. 61 : GEOCHEMICAL POLARITY ACROSS THE NEW GUINEA MOBILE BELT.

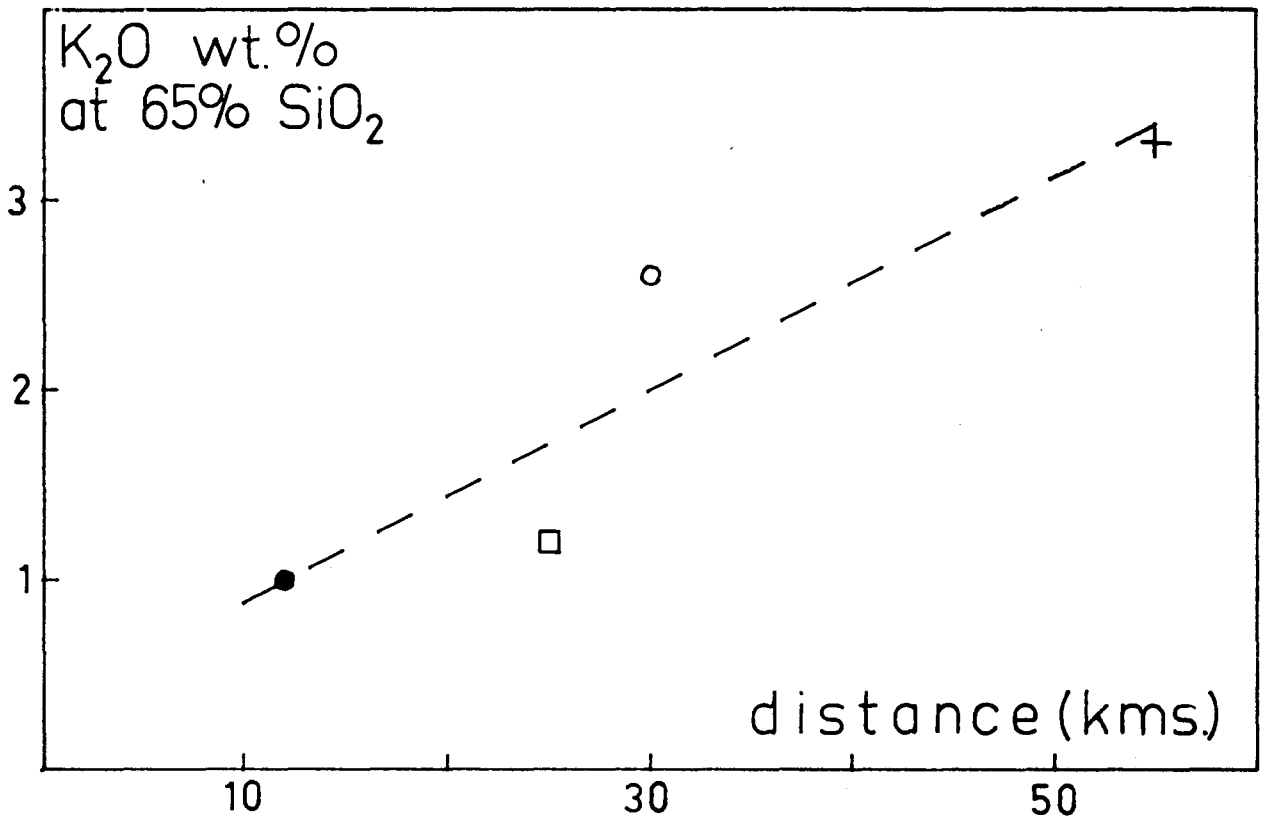

KEY :
- ● Karawari Batholith
- □ Yuat South Batholith (western region)
- o Yuat South Batholith (eastern region)
- \+ Yuat North Batholith

Distance is measured along AB in Fig. 3.
Data represents dominant compositions from each region.

been responsible for the deformation, uplift, and development of the geochemical 'polarity' in the New Guinea Mobile Belt. A model compatible with the geology and geochemistry will be developed in the ensuing sections.

8.3.3 Geochemical Characteristics of Particular Regions

Regional geochemical characteristics of calc-alkaline intrusive rocks are evident in other parts of the P.N.G. region. For example, the intrusive rock suites of New Britain contain the highest levels of TiO_2 of all the studied suites. The Plesyumi suites of this study, the Gazelle suites of Macnab (1970), and suites from other locations in New Britain (data of Aust. Bur. Min. Resources; and R. Hine, pers. commun.) all possess 0.8 - 0.9% TiO_2 at 60% SiO_2 compared with levels of 0.4 - 0.7% TiO_2 for other studied calc-alkaline suites in the P.N.G.region. In the Plesyumi rocks, the relatively high titanium abundance is distributed between abundant titaniferous magnetite and ilmenite, and also abundant amphibole. Later intrusive porphyries from various parts of New Britain may possess lower TiO_2 abundances (R. Hine, pers. commun.). It appears, however, that many of the phaneritic calc-alkaline intrusive rocks throughout New Britain were generated under similar conditions from similar source material, resulting in the observed close similarity of geochemical characteristics and of ages of emplacement.

Similar conclusions can be drawn from comparison of calc-alkaline intrusive rocks from Guadalcanal, Solomon Islands, where the Poha River Diorite of (?)pre-Miocene age and the (?)Miocene-Pleistocene Koloula Igneous Complex display similar trace element abundances. It would seem that calc-alkaline magmas of similar composition were capable of being generated beneath Guadalcanal over a considerable period of time, during which interval the tectonic regime changed markedly (Coleman, 1970; Karig, 1972; Hackman, 1973). The implication of constant source composition in turn suggests derivation from a constant source beneath Guadalcanal. Possible sources include crustal volcanic rocks (either early members of the island arc, or pre-existing ocean-floor basalts), and upper mantle ultramafic material.

8.4 CONSTRAINTS ON SOURCE MATERIALS FOR CALC-ALKALINE INTRUSIVE ROCK SUITES

8.4.1 Location in Orogenic Belts

The characteristic occurrence of large granitic batholiths in long, narrow, strongly deformed belts of widely ranging geologic age has long been remarked upon by many field workers,-and the emplacement of

the granitic rocks has been interpreted as part of the intermediate and final stages of development of these 'orogenic' or 'mobile' belts of the Earth's crust. Recognition of differences in metamorphic grades of enveloping country rocks, differences in internal structure of granitic masses, and differences in contact metamorphic effects lead to Read's (1949, 1955) concept of a 'granitic series'; distinction of Buddington's (1959) 'katazonal', 'mesozonal', and 'epizonal' granites; and to the 'regional-aureole granites', 'contact-aureole granites', and 'subvolcanic granites' of White et al. (1964). All of the post-Palaeozoic granitic rocks so far observed in the P.N.G. region would be classified as 'mesozonal' or 'epizonal'according to Buddington (1959), or 'contact-aureole' or 'subvolcanic' granites according to White et al. (1964).

The same belt-like distribution of granitic rocks is observed in the P.N.G. region, with abundant intrusive masses in the New Guinea Mobile Belt, rather fewer in the adjacent parts of the Australian continental block, and also in the island arcs fringing the New Guinea mainland. Because all these tectonic belts are still active, it is inviting to speculate that they represent youthful, developing counterparts of the older tectonic belts located within, and on the margins of, continental blocks.

It is pertinent here to examine the time-relationships of emplacement of the granitic masses in the development of the various tectonic belts in the P.N.G. region. In the island arc structures, emplacement of granitic rocks did not occur until the arcs were in an advanced stage of development. Thus in the northern New Guinea arc, the earlier Cretaceous-Eocene volcanic and volcanogenic rocks were intruded by late Eocene (-?Miocene) calc-alkaline diorites and related rocks (Hutchison, 1974). In New Britain, the Eocene 'basement' volcanic rocks were intruded by Oligocene-Miocene complexes (Macnab, 1970; Page & Ryburn, 1973). In New Ireland, the (?pre-) Lower Oligocene Jaulu Volcanics were intruded by Oligocene calc-alkaline intrusive complexes (Hohnen, 1970). In Bougainville, the oldest exposed volcanic rocks (Kieta Volcanics) of Upper Oligocene-Lower Miocene age were intruded by Pliocene-Pleistocene dioritic complexes (Blake & Miezitis, 1967; Page & McDougall, 1972b). In Guadalcanal, gabbroic rocks intrude the late Mesozoic basement but more felsic intrusive complexes were not intruded until Pliocene times (Hackman, 1973; Chivas, 1975).

It is considered significant that dioritic and more felsic calc-alkaline intrusive complexes did not appear in the above-mentioned island arc strcutures until the arcs became well-established. The time interval between commencement of arc volcanic activity and intrusion of calc-alkaline complexes is of the order of several tens to perhaps seventy million years. In this time, island arc volcanism was responsible for development of arc structures with thicknesses of the order of 25-40 km. (e.g., New Britain and New Ireland, 30-40 km, Finlayson & Cull, 1973). It appears that generation and emplacement of calc-alkaline intrusive complexes in the island arc structures is in some way dependent upon the presence of thickened island arc and subjacent oceanic crust (compare Fiji, Gill, 1970; Caribbean occurrences, Kesler et al., 1975a). It might reasonably be inferred that likely sources for intrusive calc-alkaline magmas lie in the basal portions of thickened island arc crust and in immediately underlying oceanic crust.

A similar delayed time-relationship between commencement of belt development and emplacement of granitic magmas occurs in the New Guinea Mobile Belt. Dow et al. (1972) document Upper Triassic and Middle Jurassic volcanism in the Belt, followed by a break in sedimentation, then renewed volcanogenic sedimentation in the Lower Miocene. It was not until after an episode of regional greenschist metamorphism accompanied by continued faulting and uplift of the Mobile Belt that the widespread granitic masses were emplaced. Much of the intrusive activity took place over a relatively short period of time between 15-12 m.y. b.p., although there is evidence of earlier (approximately 20 m.y.) and later (12-7 m.y.) intrusive activity within the Mobile Belt (Page, 1971). Attention is here drawn to the widespread generation and emplacement of calc-alkaline intrusive complexes over a limited period of time, at a time when volcanogenic sedimentation in the Mobile Belt had attained considerable thicknesses, and at a time when rapid uplift and associated faulting were occurring. Vertical displacements of up to 6 km (with suspected but unknown amount of transcurrent movement) are recorded for some of the major fault zones of the Mobile Belt (Dow et al., 1972, p. 72-77). Continued faulting and uplift into Recent times is evident in fault-bounded intrusive complexes (e.g. Karawari Batholith), décollement folding and thrust faulting of the continental sediments to the south, and in the physiographic expression of the uplifted Highlands region. There appears, then, to be a close correlation between the deformation and rapid uplift of the Mobile Belt in Upper Oligocene to Lower Miocene times, and the

subsequent widespread intrusion of the calc-alkaline complexes over a short period of time in the Middle Miocene. It is suggested that the rapid uplift of the Mobile Belt may have caused initiation of partial melting in the basal parts of the Belt or in immediately underlying oceanic crust (presuming that the Belt had developed at least partly on oceanic crust marginal to the Australian continental crust). Thus andesitic and/or basaltic volcanic rocks would be the source rocks involved in such processes. This simpler model for generation of the Middle Miocene calc-alkaline magmas is preferred to currently popular Benioff zone models in view of the difficulties previously described in attempting to apply the latter type of model to the Mobile Belt. The preferred model will be pursued in following sections.

8.4.2 Igneous Activity associated with Intrusive Complexes

It is beyond the scope of this work to compare the batholithic intrusive complexes of orogenic belts with supposedly contemporaneous and comagmatic volcanic rocks which have been described for many parts of the world (e.g. Hamilton & Myers, 1967, on western U.S. examples; Hamilton, 1969, on South American and North American comparisons; Ustiyev, 1970, on Russian and Asian examples). It is recognized, however, that the problem of the association of batholithic rocks and volcanic fields is one which requires close study.

The problem is relevant to magmatism in the P.N.G. region, not only in the island arc structures where relative youthfulness and lack of erosion combine to preserve such relationships (e.g. Limbo River Diorite, Stanton & Bell, 1969), but also in the Mobile Belt where widespread Middle to Upper Miocene volcanic sequences have been interpreted as comagmatic correlatives of the Middle Miocene calc-alkaline intrusive complexes (Page & McDougall, 1970; Dow et al., 1972). While it has been demonstrated in this work that many of the felsic intrusive complexes of the Mobile Belt are variably calc-alkaline in their mineralogy and chemistry, it has yet to be demonstrated what geochemical relationships exist between these and the volcanic rocks. A small amount of data from the Daulo Volcanics in the Eastern Highlands indicate the dominance of mafic, undersaturated volcanic rocks in the Miocene of that area (D. Mackenzie, pers. commun.). The nearest Miocene intrusive complexes are the Bismarck Granodiorite to the north, which, according to limited petrographic observations (this author; and G. Watmuff, pers. commun.), is similar to the normal-K Yuat South Batholith of this study, and the Mount Michael Stock to the south, which, as shown in this study, has mineralogy and chemistry appropriate to normal- and higher-K calc-

alkaline rocks. Thus presently available data from the Eastern Highlands reveal geochemical dissimilarities between the Miocene intrusive and extrusive rocks of the area, implying that no direct genetic relationship exists between them. While an upper mantle source would be appropriate for the undersaturated mafic volcanic rocks (Green, 1969; Green et al., 1967), it is not at all clear that this is so for the nearby felsic calc-alkaline intrusive rocks, and in fact a source in basal crustal regions might well be preferred.

In the Western Highlands, however, it has been suggested above (see Chapter 2, section 2.7.1) that the mafic cumulate rocks of the Wale and Lamant Stocks might represent subvolcanic equivalents of the Tarua Volcanic Member of the Middle Miocene Burgers Formation.

It is evident that no simple relationship exists between the Miocene intrusive and extrusive igneous rocks within the New Guinea Mobile Belt, and further evaluation must await accumulation of more data, especially for the volcanic rocks.

8.4.3 Mafic Inclusions in Granitic Rocks

Important constraints upon possible source rocks for calc-alkaline batholithic rocks may be deduced from studies of the megascopic and microscopic textures of the rocks in question. In particular, past workers have applied themselves to ascertaining possible genetic implications of the frequently-observed mafic inclusions (as distinct from accidental metasedimentary xenoliths) in granitic rocks, and the geochemical consequences of their disintegration and reaction with enclosing melts. It is believed that the final stages of these processes can be recognized in the abundant clots or aggregates of dominantly mafic minerals which are texturally characteristic of many batholithic granitic rocks.

Accounts of mafic inclusions in granitic rocks are numerous in the literature. Well-documented occurrences have been presented by Deer (1935) on the Scottish Cairnsmore of Carsphairn complex, by Nockolds (1941) on the Garrabal Hill-Glen Fyne intrusive complex, by Larsen (1948) on the northern part of the Southern California Batholith, and by Bateman et al. (1963) on the central part of the Sierra Nevada Batholith. The widespread distribution of mafic inclusions in many granites, the frequent absence of suitable exposed source materials, and the common occurrence of similar mineralogy in inclusions and enclosing granite have lead to a consensus that the mafic inclusions are cognate with the enclosing granitic material, and that they are derived from a source at considerable depth.

Earlier explanations accounting for the origin of mafic inclusions in granitic rocks appealed to processes involving hybridism (Nockolds, 1934; Joplin, 1959), crystal fractionation, and combinations of both (Nockolds, 1941). More recent work on inclusion-bearing intrusions from the southern part of the New England Batholith, New South Wales, has revealed close geochemical relationships between inclusions and enclosing granitic rocks, such that each intrusion (or group of intrusions) and contained inclusions display their own geochemical characteristics (Chappell, 1966). The interpretation was made that hybridism had occurred between silicic partial melts from mafic igneous material in the lower crust and relic mafic material from the source rocks. Such granitic rocks have been termed 'I-type' granites by Chappell & White (1974), and, together with field and chemical criteria, may be distinguished from 'S-type' granites carrying reconstituted sedimentary xenoliths which are believed to represent relic material from a partially melted sedimentary source (Joyce, 1970; 1973). Whilst both 'S-type' and 'I-type' granites may occur as 'contact-aureole' and 'subvolcanic' granites, only 'S-types' occur as 'regional-aureole' granites (White et al., 1974).

Features of granitic rocks from P.N.G. such as shallow levels of emplacement, narrow contact aureoles, and association with volcanic rocks indicate that all of the observed intrusive rocks are 'contact-aureole' or 'subvolcanic' types. Further, their mineralogy, chemistry, and contained mafic inclusions suggest that they are all 'I-type' in origin.

In endeavouring to apply current ideas concerning granitic rocks and their inclusions to the P.N.G. region, one is faced with a lack of descriptive petrography in the literature and a complete lack of geochemical data for such phenomena in the region. Some authors, however, have made passing mention of mafic inclusions in studies of granitic rocks of the region.

Hohnen (1970) recognized considerable textural heterogeneity in the 'Lemau Intrusives' of New Ireland. He describes (p. 22) "... what appears to be normal gabbroic mineral composition modified by late crystallization of silica and alkali-rich mineral phases". His description of "... later minerals ... commonly peripheral to earlier formed minerals such as pyroxene and calcic plagioclase ..." is reminiscent of mafic clots observed by the writer in specimens from the Lemau Intrusive Complex. Hohnen (1970, p. 22) goes on to make the observation that "...The more acid plutonics in the type area commonly contain fine-grained melanocratic

xenoliths 10-15 cm. in diameter and with ill-defined boundaries". Although Hohnen concludes that "... these patches or clusters of mafic minerals may represent relic fragments of the Jaulu Volcanics" (nearby country rocks), it is more likely that he has described the widespread phenomenon of cognate mafic inclusions and their disintegration to form mafic clots in silicic melts.

Macnab (1970) notes that the calc-alkaline intrusive rocks of the Gazelle Peninsula "... show no evidence of large-scale stoping of country rock, and little evidence of crustal contamination". From this it must be assumed that the Gazelle intrusive rocks are relatively free of mafic inclusions. However, in reference to the normal-K North Bainings Mountains suite, Macnab (1970 , p. 70) states: "Where igneous xenoliths are present, they are invariably more basic than the host". In describing a coarse-grained adamellite from the high-K South and Central Bainings Mountains suite, Macnab (1970, p. 77) refers to "... unaltered xenoliths of slightly porphyritic hornblende microdiorite". In a leucocratic monzonite, he describes the presence of "... ferromagnesian aggregates". Although Macnab (1970, p. 82) concludes that the magmas responsible for the Gazelle suites were "... presumably generated in the mantle", his references to mafic xenoliths and ferromagnesian aggregates, together with the writer's observations of mafic clots in intrusive rocks from the Plesyumi Intrusive Complex, can be re-interpreted to indicate that at least the felsic intrusive rocks of New Britain were derived by partial melting of mafic material at the base of the island arc crust,and that these rocks now contain dissaggregated relic mafic source material in the form of occasional xenoliths and more abundant mafic clots.

Dow et al. (1972, p. 69), in reference to the 'Maramuni Diorite', claim that "... the effects of assimilation can be seen along the border of the batholith..." where "... the border zone is rich in xenoliths". It is not clear to which batholithic mass of the 'Maramuni Diorite' this comment is directed, nor is it stated whether the xenoliths are mafic inclusions or of metasedimentary origin.

Field observations by the writer in the Yuat South, Yuat North, and Karawari batholiths indicate that mafic inclusions are present in all three masses, and that the abundance varies between the batholiths. In the dominant hornblende (-biotite) tonalite of the low- to normal-K Karawari Batholith, mafic inclusions are common and occur together with rare, biotite-rich metasedimentary xenoliths of accidental origin. In the high-K diorites of the Yuat North Batholith, mafic inclusions are

very common and all degrees of partial disintegration and 'ghosting' can be seen. Mafic clots are common in thin section (see Chapter 2, section 2.4.2). It is interesting to note that neither the Yuat North nor the Karawari Batholith* is host to porphyry-type copper mineralization.

On the other hand, in the mineralized Yuat South Batholith the hornblende-biotite granodiorites carry few mafic inclusions, and those present are observed to be fine-grained, dark grey dioritic rocks with occasional plagioclase phenocrysts and, although rounded in form, display quite sharp contacts with the enclosing granodiorite. Despite the fact that mafic inclusions are few and ferromagnesian minerals tend to form euhedral crystals, mafic clots are observed in thin section.

Thus there appears to be a correlation between lack of mafic inclusions and presence of porphyry copper mineralization. This generalization at least applies to this group of batholiths in the Western Highlands. If it is accepted that mafic inclusions represent relic material from partial melting of basal crustal source rocks, it would appear that the ability of an intrusive mass to generate porphyry copper mineralization is in some way related to the ability of the silicate melt to segregate from the accompanying mafic inclusions. Burnham (1967, p. 46 and figure) has shown that viscosities of low-melting granitic liquids decrease rapidly from $\sim 10^{10}$ to $\sim 10^{7}$ poises with increase from 0 to 2% H_2O. Thus, a silicic partial melt containing, say, 2% H_2O at source will possess a much greater potential to segregate from residual mafic source material than another silicic partial melt with only, say, 0.5% H_2O at source. Such differences in water contents and dependent viscosities of silicic partial melts are capable of explaining the relative abundance of mafic inclusions and lack of mineralization in the initially 'dry' Yuat North Batholith, and the relative lack of mafic inclusions and presence of mineralization in the 'wet' Yuat South Batholith. Independent evidence from mineralogy, together with mafic mineral compositional variations (see Chapter 6, sections 6.3.3, 6.4.2), confirms that the rocks of the Yuat South Batholith crystallized under higher P_{O_2} conditions than did

---

*Porphyry-type mineralization in this area is restricted to the Awari Stock, located to the south of the Karawari Batholith.

rocks of the Yuat North Batholith.

Further examples of textural evidence supporting the proposition that P.N.G. granitic rocks contain relic mafic material from basal crustal sources can be given, and two occurrences from different locations will be described:

(i) In the Eastern Highlands, the Mount Michael Stock is located near the northern margin of the Australian continental block. One specimen of plagioclase-hornblende diorite porphyry (DRM011) contains a microxenolith which, in thin section, is observed to contain an identical mineral assemblage to the enclosing diorite porphyry, even down to the presence of abundant angular sphene crystals. Although the microxenolith might be interpreted as a fragment of an earlier-crystallizing portion of the stock, it can equally well be interpreted as a reconstituted fragment of mafic source material which has equilibrated with the enclosing melt and in the course of disintegration has contributed crystalline material to the melt.

(ii) In the Koloula Igneous Complex of Guadalcanal in the Solomon Islands, two intrusive suites of contrasting mineralogy and chemistry have been defined in this work (see Chapter 3, section 3.8.2 , and Chapter 5, section 5.7), and have been named the Mafic Suite and the Felsic Suite. There are also significant textural differences between the two suites. The most silicic member of the Mafic Suite is a two pyroxene-hornblende-biotite-quartz diorite, which displays an hypidiomorphic granular texture with quite uniform distribution of the mafic minerals. In the field, this rock type occurs topographically above gabbroic and mafic dioritic rocks from which it appears to have differentiated *in situ* (A. Chivas, pers. commun.). In contrast, quartz diorites and granodiorites of the later Felsic Suite display hypidiomorphic granular textures in which clots of mafic minerals are quite common. Plagioclase prisms possess mottled cores and strongly zoned rims. Mafic inclusions have been observed infrequently in the granodiorite of the Felsic Suite, and the chemistry of one such inclusion (specimen DRM091) displays a strong coherence with the geochemical variations of the Felsic Suite (see Figs. 36 and 38). It is tempting to postulate a basal crustal source for the later Felsic Suite at Koloula, and perhaps a quite different source (oceanic crust or upper mantle) for the earlier Mafic Suite.

In summary, it is concluded that textures of granitic rocks from the P.N.G. region, as in other regions, can provide clues as to possible source materials for the magmas now seen in batholithic complexes.

Mafic inclusions, microxenoliths, and clots of ferromagnesian minerals are widespread in P.N.G. granitic rocks, and can be interpreted as refractory mafic material from the site of magma generation. Widespread occurrence of mafic inclusions and related textural features in intrusive complexes in a variety of tectonic settings suggests that mafic rocks in basal parts of island arcs, continental margins, and continental blocks may be involved in generation of calc-alkaline batholithic complexes. Distribution of mafic inclusions and related textural features in Western Highlands batholithic rocks are in accord with the proposition based on mineral chemical data that intrusive complexes associated with porphyry copper mineralization crystallized under highly oxidizing conditions resulting from higher water contents in the low-melting liquid at source.

8.4.4 Strontium Isotopic Data

Strontium isotopic data (usually expressed as the ratio 'initial $^{87}Sr/^{86}Sr$') have become useful as indicators of possible source materials for igneous rocks and related ore systems. Because radiogenic ^{87}Rb breaks down to ^{87}Sr with a particular half-life, measurement of present-day ratios of $^{87}Rb/^{86}Sr$ and $^{87}Sr/^{86}Sr$ on groups of cogenetic rocks, or minerals from a rock, can give the time interval since closure of the rock system (i.e. age of rock), and also the initial $^{87}Sr/^{86}Sr$ ratio which was presumably inherited from the rock's source material. The technique has achieved considerable success in confirming the primitive character of mantle-derived oceanic basaltic rocks (initial $^{87}Sr/^{86}Sr \simeq 0.702$; Faure & Hurley, 1963), and the evolved character of Phanerozoic sedimentary rocks and some continental granitic rocks (initial $^{87}Sr/^{86}Sr > 0.708$, as high as 0.71 - 0.72; Moorbath & Bell, 1965).

Rocks yielding initial $^{87}Sr/^{86}Sr$ ratios between the known extreme values have been attributed to sources at intermediate stages of fractionation. However, many difficulties often prevent precise evaluation of strontium isotopic data, and this has lead to a recent tendency toward moderation in the interpretation of initial $^{87}Sr/^{86}Sr$ data (Gill & Compston, 1973; Carmichael et al., 1974).

Limited strontium isotopic data are available for some intrusive rocks from the Papua New Guinea region. Page (1971) showed that many of the Middle Miocene intrusive rocks of the New Guinea Mobile Belt possess initial $^{87}Sr/^{86}Sr$ ratios of 0.7036 - 0.7054. These values are appropriate to a source or sources which has or have been only marginally enriched in

radiogenic strontium, and could variously be attributed to somewhat enriched upper mantle compositions, ocean floor basaltic rocks, or mafic to intermediate igneous rocks at the base of the crust.

The uniform, quite low values of initial $^{87}Sr/^{86}Sr$ are of considerable interest, but are insufficient in themselves to establish a completely uniform source. Although Page (1971, p. 191) concluded that the strontium isotope data indicated derivation from a uniform upper mantle source, it is not at all clear that this was the case. Tilling (1973) has documented the example of the Boulder Batholith, Montana, in which geochemically district intrusive suites possess uniform initial $^{87}Sr/^{86}Sr$ ratios, but quite different lead isotope ratios. Similarly, major and trace element data presented in this study have revealed the presence of geochemically distinct intrusive suites in the New Guinea Mobile Belt, and lead isotope data might well establish differences in source compositions where strontium isotopes have failed to do this.

In summary, the available limited strontium isotope data for Middle Miocene intrusive rocks of the New Guinea Mobile Belt indicate derivation of those rocks from a source (or sources) which was (or were) marginally but uniformly enriched in radiogenic strontium. Such sources could be found in mafic igneous material at the base of the crust. This is compatible with the presence of mafic inclusions described above. The presence of geochemically distinct intrusive suites in the Mobile Belt suggests derivation from geochemically distinct sources, and this might be confirmed by collection of further isotopic data, such as lead isotopes.

8.4.5 Geophysical Evidence

Geochemical, textural, and isotopic data from granitic rocks of the Papua New Guinea region have been interpreted here to indicate derivation mainly from mafic igneous material in the base of the crust. Surface geological information leads us to believe that mafic igneous material is present in oceanic crust of the ocean floor, in basal parts of island arcs, in oceanic crust immediately beneath island arcs, and possibly in subducted oceanic crust beneath island arcs and continental margins. It is pertinent to briefly examine the geophysical evidence for the presence of mafic material near the base of the crust in the different tectonic environments of the P.N.G. region.

There is good seismic evidence for the presence of a layer of mafic material in the basal parts of island arcs (Raitt et al., 1955, on

Tonga; Rikitake et al., 1968, on Japan). Seismically, the layer is equivalent to the basaltic layer of the oceanic crust. If intra-oceanic island arcs have been built directly upon oceanic crust, then the mafic material beneath them will have the composition of ocean-floor basalts (dominantly low-K tholeiites). In the P.N.G. region, recent seismic work (Finlayson & Ryburn, 1973; Finlayson & Cull, 1973) reveals that the Moho lies at depths of 30-40 km beneath the New Britain and New Ireland arcs. Measured seismic velocities indicate that the crustal structure in these arcs is dominated by a lower basaltic horizon ($V_p \geq 7.0$ km/sec) up to 20 km thick, and an overlying horizon ($V_p = 6.1$ km/sec) which can be correlated with the early volcanic rocks of the arcs. The thickened lower basaltic layer (compare Rikitake et al., 1968, p. 1109 and figures) might be ascribed to simple down-warping of the previously existing oceanic crust, or it might be accounted for by addition to the oceanic crust of island arc magmas which failed to erupt at surface. In the latter case, the thickened basaltic layer would reflect any geochemical diversity which might be contained in the arc magmas.

Early seismic data for continents and continental margins (Gutenberg, 1955; Ewing & Press, 1955) supported even earlier geological theories that mafic igneous material occurs at the base of continental crust. More recent syntheses of geophysical data (Worzel, 1968) confirm the presence of mafic material ($\rho \simeq 2.8$ gm/cc; $V_p = 6.8 - 7.0$ km/sec) in the lower parts of continents and their margins. However, the precise nature of the change (the 'Conrad Discontinuity', Richards & Walker, 1959) from dominantly 'sialic' material of the upper continental blocks to dominantly 'basaltic' material in the base of the crust remains in some doubt. Christensen & Fountain (1975) have demonstrated the great variability in seismic velocities in basal parts of the continents ($V_p = 6.0 - 8.0$ km/sec; maxima at 6.7 and 7.1 km/sec) corresponding with an equally wide range of compositions, but with basic compositions dominant.

Little published seismic data is available to enable evaluation of crustal structure in the continental part of P.N.G. Brooks (1969a, 1969b) concluded that "... Shear velocities in the crust in southern New Guinea seem to increase gradually with depth from about 3 - 3.5 km/sec at 4 km ... to values around 4.5 - 4.6 km/sec in the depth range 50 - 100 km." This conclusion is compatible with the possibility of mafic igneous material occurring toward the base of the crust ($\sim$35 km, Brooks, 1969b, figure 12). Similar shear velocities were reported for the New Mexico-Oklahoma part of continental North America by Mitchell & Landisman (1970), who concluded that such velocities "... correspond to that which is commonly

used to characterize basic rock materials."

From the geophysical data available, it is concluded that mafic rocks are present in the lower parts of the crust in a wide variety of tectonic environments in the P.N.G. region. In the intra-oceanic island arcs, such materials are present at depths of 20-40 km and quite possibly reflect the geochemical diversity of oceanic and island arc rocks. In the continental part of P.N.G., mafic and other materials are likely to occur at similar depths, but their composition and distribution are problematic (compare Ringwood & Green, 1966).

8.4.6 Chemical Constraints

Some generalizations in regard to certain geochemical features of the intrusive calc-alkaline rocks place severe constraints upon possible source materials:

(i) Dioritic and granodioritic rocks with SiO_2 in the range 60-65% are by far the most abundant rock types among the Tertiary and younger intrusive rocks of the P.N.G. region (see Table 8). The predominance of silicic rocks and relative scarcity of mafic rocks from which they might have fractionated requires that the former be derived by partial melting of a source which has already been fractionated at least to the stage of silica-saturation. This implies that immediate source regions other than the upper mantle were involved, and most likely were located in the lower crust.

(ii) The abundances of the light rare earth elements (as exemplified by lanthanum and cerium) and the heavy rare earths (as exemplified by yttrium) all increase progressively from low-K, through normal-K to high-K suites (see Fig. 60). The progressive variation and the level of abundance of yttrium ($\sim$15-30 ppm) discount the possibility that these rocks were in equilibrium with garnet at source. This eliminates direct derivation from subducted oceanic crust which must suffer the basalt-eclogite transformation (Green & Ringwood, 1967), and also eliminates derivation from garnet-rich material in the upper mantle or lower crust. The rare earth data suggest source materials in which pyroxene, amphibole and plagioclase were dominant phases. Such phases are stable in mafic and intermediate compositions in the lower crust.

(iii) The high levels of vanadium preclude derivation by fractionation of magnetite, pyroxene, or amphibole from a basaltic parental melt. Relatively low levels of nickel and cobalt are not compatible with derivation from an ultramafic source.

There are major problems in attempting to derive the intrusive rocks by fractionation of a basaltic parental melt, or by partial melting of garnet-rich materials. The chemical features are compatible with derivation by partial melting of basal crustal material which has already been fractionated to variable degrees.

8.5 MAGMA GENERATION FOR INTRUSIVE ROCKS, P.N.G. REGION

8.5.1 Magma Generation from Igneous Source Material

Various lines of evidence have brought this discussion to the point where we can consider the derivation of many of the Tertiary calc-alkaline intrusive rocks of the P.N.G. region in terms of partial melting of igneous material of mafic, intermediate, or even felsic composition. A largely sedimentary, chemically fractionated source is rejected as inappropriate because of low initial strontium ratios for the granitic rocks (compare Kistler & Peterman, 1973, especially their data for the western Sierra Nevada granitic rocks), and because of whole-rock chemical and mineralogical considerations (Chappell & White, 1974, on S- and I-type granitic rocks of southeastern Australia).

It was concluded in section 8.4 that likely source materials lie in basal crustal regions at depths of 20-40 km (equivalent load pressures of 6-11 kb). The prohibitively high liquidus temperatures of granodioritic and dioritic melts at these lower crustal depths, even under the most favourable (and unlikely) conditions of $P_{H_2O}=P_{load}$, have been used as arguments against the generation of such melts in the crustal environment. However, recognition of textural features implying origin of the granitic rocks through mixing ('hybridism') of a silicic melt and relic refractory source material leads to the more readily accommodated requirement of generation of silicic, low-melting liquids.

Basic to the ensuing discussion is the assumption that bulk source composition controls derivative intrusive rock suite composition. The bases for this assumption are to be found in:

(i) observations of chemical coherence between granitic rocks and their mafic inclusions (Chappell, 1966; Piwinskii, 1968; White et al., 1974; Chappell & White, 1974).

and (ii) experimental partial melting results upon materials of differing composition (Winkler, 1967; T. Green & Ringwood, 1968; Brown & Fyfe, 1970; Whitney, 1975a).

Prior to a discussion of generation of intrusion magmas in the different tectonic settings, it is necessary to establish what compositional

variations might exist in the base of the crust, how these variations arise, and the means by which partial melting might be achieved.

8.5.2 Effects of Prolonged Magmatism Upon the Base of the Crust

Prolonged volcanism is a feature of all currently active island arcs, and of some continental margins. While great volumes of volcanogenic rocks are observed at the surface, it is reasonable to expect that some magmas fail to reach the surface (e.g. Sugimura, 1968, p. 554). These magmas are likely to accrete at structurally weak interfaces, such as the base of the developing volcanic pile or the base of any pre-existing crust. This process of accretion of magmas beneath regions of intense volcanic activity will be referred to here as *'crustal subcretion'*.* The reality of the process receives support from seismic studies, which reveal considerable crustal thickening beneath active island arcs and continental margins (e.g. Hasebe et al., 1970).

In island arc environments, crustal subcretion will result in the development of lower crustal compositions comparable with the observed time-space sequence of island arc tholeiite, calc-alkaline, and alkalic magmas (Kuno, 1959; Jakes & Gill, 1970). Whilst a static trench location will produce a well-defined spatial distribution of volcanic rocks and related subcreted material (see Fig. 62a), movement of the trench in time will result in stratification of compositionally different materials (see Fig. 62b). It is important to note than an 'inverse stratigraphy' develops at the base of the crust when compositional stratification occurs.

In continental margin settings, crustal subcretion would be expected to occur as in island arcs if Benioff zones had controlled volcanism (e.g. western Americas). In the northern Australian continental margin (New Guinea Mobile Belt), volcanogenic rocks dominate the successions throughout the stratigraphic record from Upper Triassic to Upper Miocene times (Dow et al., 1972). However, it is difficult to

---

*This term is preferred to such terms as 'subcrustal accretion' and 'underplating' because of certain connotations surrounding the words 'accretion' and 'plates'. The proposed word 'subcretion' has its roots in the Latin *sub*=under and *crescere*=to grow.

FIG. 62 : SCHEMATIC REPRESENTATION OF CRUSTAL SUBCRETION IN ISLAND ARC SETTINGS.

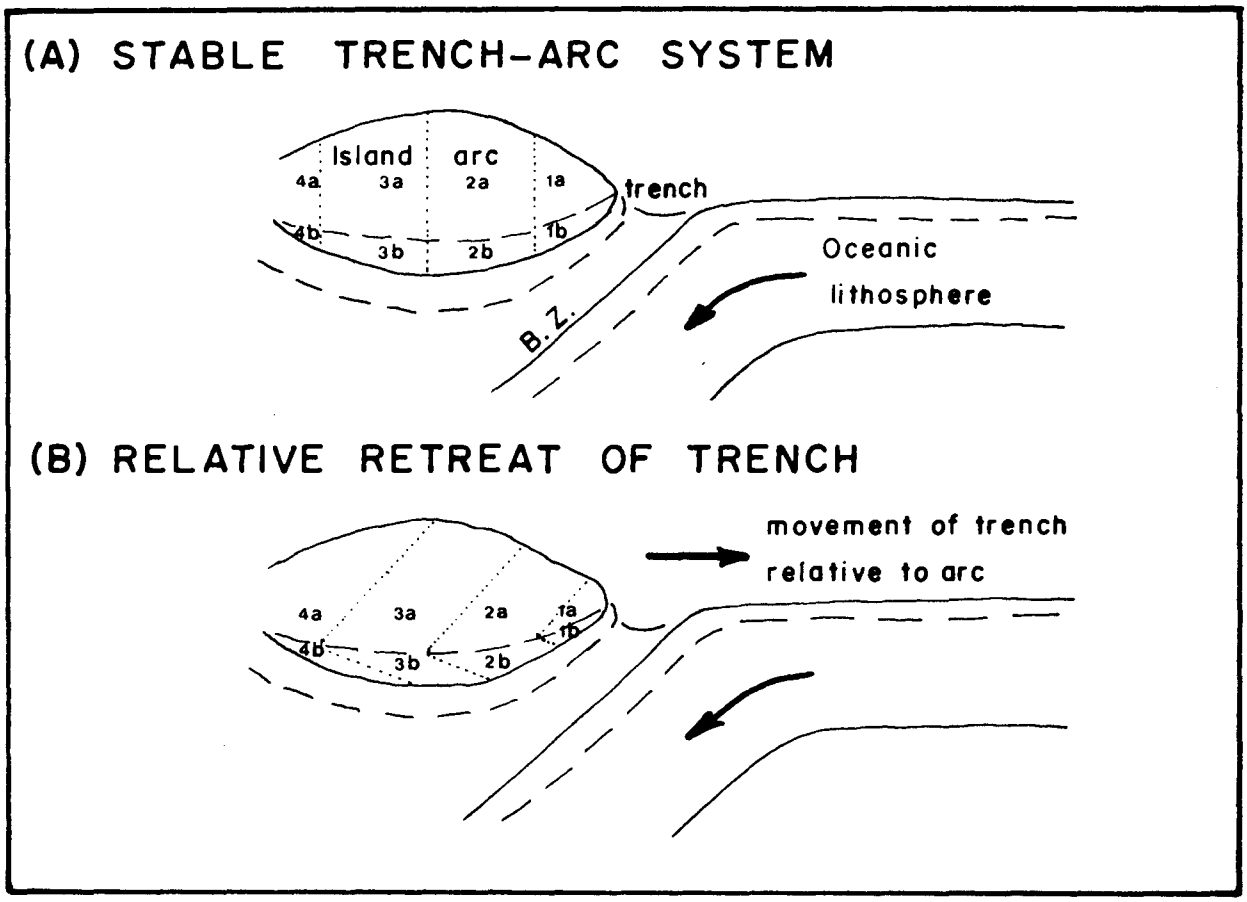

KEY : 1a = island arc tholeiite volcanics
1b = subcreted equivalents
2a = normal-K calc-alkaline volcanics
2b = subcreted equivalents
3a = high-K calc-alkaline volcanics
3b = subcreted equivalents
4a = alkaline volcanics
4b = subcreted equivalents

B.Z. = Benioff Zone

establish the function of Benioff zone activity (see sections 8.3.2 and 8.4.1). In fact, an extensional stress regime is indicated by:

(i) fault-controlled sedimentation (Dow & Dekker, 1964; Dow et al., 1972)

(ii) bimodal volcanism, with early silicic volcanism and later basaltic volcanism (Dow et al., 1972)

(iii) presence of alkali basaltic rocks in the Mesozoic volcanics (specimen DRM026, a doleritic alkali basalt, this study), and in the April Ultramafics (R. Ryburn, pers. commun.).

(iv) pre-Eocene rifting of the southeastern portion of the Mobile Belt (Owen Stanley Metamorphics) away from the Australian continent (Davies & Smith, 1971).

Under these conditions, volcanism in the Mobile Belt would have resulted in crustal subcretion of silicic and basaltic material. Compositional distribution would not have been as regular as that expected in Benioff zone-controlled settings. Compositional variation would simply reflect depth of partial melting in the upper mantle (Green, 1969) or heterogeneous distribution of upper mantle accessory minerals (Wyllie, 1971a; Kesson, 1973). In any case, the present composition of Middle Miocene intrusive rocks is believed to reflect the composition of the source rocks. The relationships are illustrated in Fig. 63.

Apart from causing crustal subcretion, prolonged volcanism can also be expected to raise the isotherms in the subcreted material and overlying volcanic pile. This would result in a greater degree of dehydration of materials in the deeper parts compared with higher crustal levels (compare Ringwood & Green, 1966). The distribution of materials with differing water contents in the base of the crust will have the profound effect of production of partial melts with differing water contents.

8.5.3 Mechanisms for Initiation of Partial Melting in the Base of the Crust.

The simplest mechanism for initiation of partial melting in the base of the crust is by rise of isotherms during prolonged volcanism and crustal subcretion. It is difficult to judge whether this mechanism alone is sufficient to cause widespread partial melting and produce the

FIG. 63 : SCHEMATIC DISTRIBUTION OF COMPOSITIONS OF IGNEOUS ROCKS WITH DEPTH ACROSS THE NEW GUINEA MOBILE BELT, using geochemical data for intrusive rocks, and applying the concept of crustal subcretion.

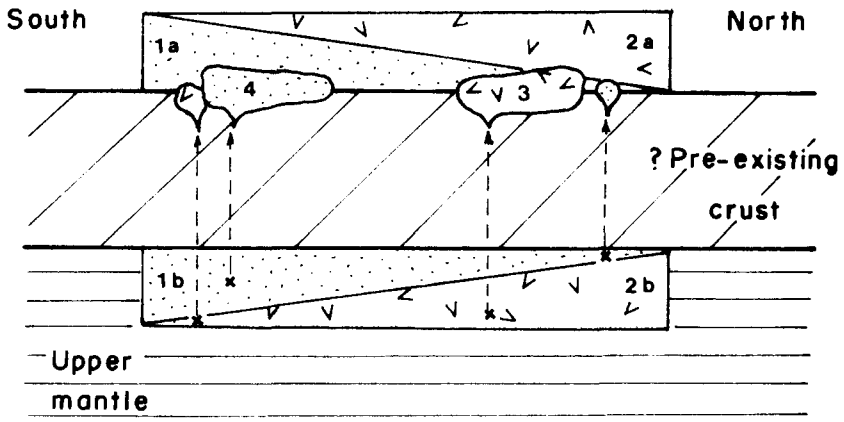

KEY : 1a = early volcanic rocks (low- and normal-K)
1b = subcreted equivalents
2a = later volcanic rocks (high-K)
2b = subcreted equivalents

3 = Yuat North Batholith
4 = Yuat South Batholith
x = partial melting site

abundant granitic rocks of orogenic belts. Estimates of temperatures in lower crustal regions vary widely. Beneath island arcs, temperatures in the range 600-800°C have been estimated (Hasebe et al., 1970; Toksöz et al., 1971). Cermak (1975) has estimated Moho temperatures of 500-700°C beneath the Bohemian Massif and 800-1000°C beneath parts of the Carpathian system. These temperatures approach those required for partial melting in the base of the crust.

Another mechanism which would assist in the initiation of partial melting is relatively sudden decrease in load pressure. In section 8.4.1, attention was drawn to the widespread emplacement of Middle Miocene intrusive rocks in the Mobile Belt after rapid uplift and erosion in Upper Oligocene to Lower Miocene times. The deformation of the Mobile Belt appears to have been a result of collision of the Australian continental block and continental margin with the New Britain-north New Guinea island arc system (Dewey & Bird, 1970; Karig, 1972).

The geothermal consequences of rapid uplift and erosion are depicted in Fig. 64. The horst block represents the large Yuat block containing the Yuat North and Yuat South batholiths. If the block is assumed to be infinitely long compared to its width (∿20 km), and if it is assumed that uplift is rapid compared with thermal readjustment, then the cooling of the block can be treated in the same fashion as a cooling dyke, sill, or other tabular body. Jaeger (1968) has provided appropriate simplified cooling models. The simplified model (Jaeger, 1968, p. 508) of a "sheet of thickness 2a intruded beneath deep cover" makes the further assumptions that termination effects of the body (e.g., termination at surface) extend to depths no greater than the thickness of the body (in our case, ∿20 km), and also that thermal conductivities of most rocks are very similar (Jaeger, p. 505). From graphs of temperature distribution provided by Jaeger (p. 508 and figure) one can determine the cooling history of a particular body. In Fig. 64(b), two likely block-faulting situations are depicted in which uplifts of 5 and 8 km are shown (Dow & Dekker, 1964, and Dow et al., 1972, report common throws of 4-6 km in the Mobile Belt). In both situations, a geothermal gradient of 25° C/km is assumed, although it may have been higher because of the prior history of volcanism. Thus, isotherms will be raised initially by 125 and 200°C respectively for 5 and 8 km of uplift. Subsequent temperatures after a time interval of 2 million years are shown in the accompanying table (Fig.64(c)). Even after 2 m.y., isotherms are of the order of 100°C higher in central parts of the horst block and only slightly less at distances halfway toward the fault margin. Thus temperatures remain

FIG. 64 : TEMPERATURE DISTRIBUTION IN BASAL PARTS OF HORST BLOCKS (using cooling theory of Jaeger, 1968).

(A) HORST BLOCK PRIOR TO UPFAULTING:

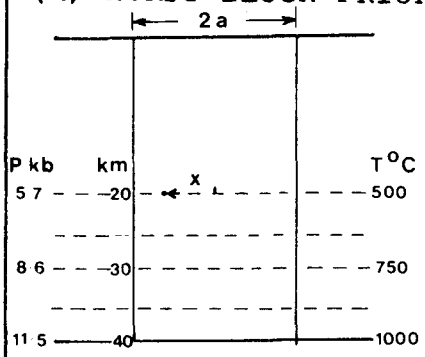

Assume: geobaric gradient 1 kb/3.5 km
geothermal gradient 25°C/ km
uniform conductivity

(B) RAPID UPLIFT:

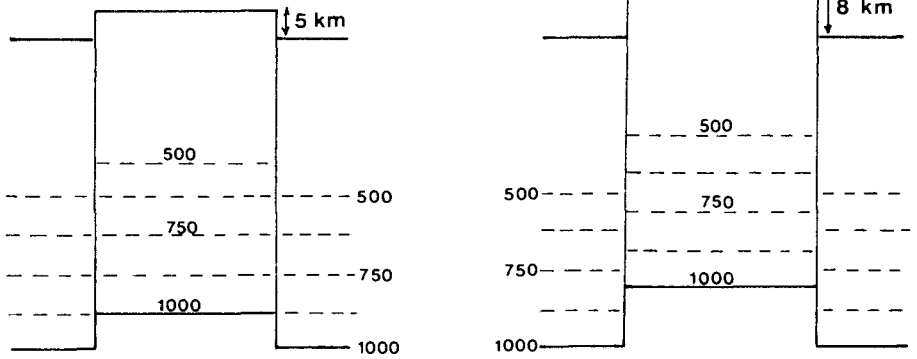

(C) TEMPERATURES AFTER 2 M.Y. IN YUAT HORST BLOCK:

UPLIFT ΔT_{max} (°C)		5km 125	8km 200
TEMPERATURE	T/T_0	ΔT^0C	ΔT^0C
x/a = 0.0	0.7	+ 87	+ 140
0.5	0.6	+ 75	+ 120
1.0	0.5	+ 62	+ 100
1.5	0.3	+ 38	+ 60

Fixed parameters:

a = 10 km

t = 2 million years

$\tau = 31.5t/(a_m)^2 = 0.63$

(D) TEMPERATURE DISTRIBUTION AFTER 2 M.Y:

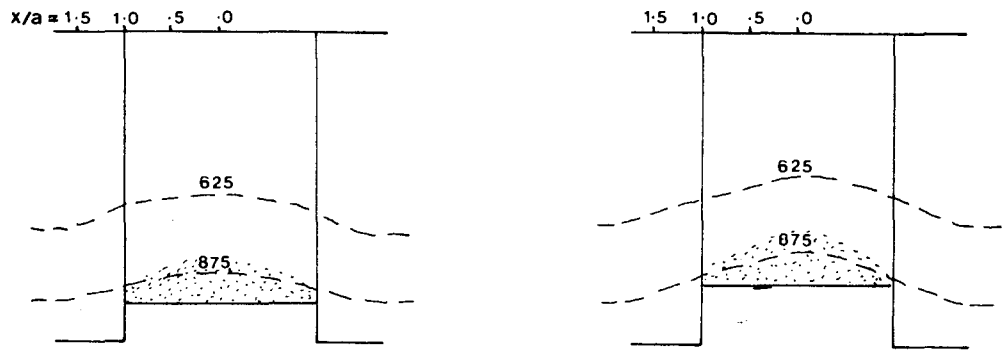

zone of partial melting stipled

high within the block for several million years after uplift.

During this time, however, erosion can be expected to vigorously attack the horst block. Dow et al. (1972, p. 69-70) have estimated 1.5 - 3 km of erosion in the very short (∿2 m.y.) time interval between emplacement and exposure of the Karawari Batholith. If these rapid erosion rates applied in the immediately preceeding Lower to Middle Miocene period, then there is every likelihood that approximately 5 km of material were eroded from horst blocks in the Mobile Belt between late Oligocene and early Miocene times. Rapid erosion of the upper portion of the horst block effectively decreases the load pressure at depth, where, as we have seen, temperatures remain elevated for considerable periods of time after uplift. This combination of elevated isotherms and decreased load pressure could well be the trigger-mechanism for partial melting in basal parts of horst blocks in the Mobile Belt.

The consequence of a sudden decrease in load pressure at elevated temperatures is illustrated in Fig. 65. Because water-undersaturated conditions yield positive dP/dT slopes for solidus and mineral dehydration curves at basal crustal pressures (Burnham, 1967; Brown & Fyfe, 1970; Wyllie, 1971b), it follows that a decrease in load pressure in material which is just below its solidus will move the material above its solidus and necessarily cause partial melting. Additional heating due to renewed basaltic volcanism in Lower Miocene times would further enhance the degree of partial melting. A constraint on the temperature of the melt is provided by the interpretation in this study that, although some amphibole might represent refractory source material, at least the outer portions of euhedral amphibole crystals have crystallized from a melt. Thus the melt must have been at temperatures above the amphibole melting curve. Such temperatures are more likely to be achieved in the base of the crust for geothermal gradients $\geqslant 25^{o}$ C/km (see Fig. 65).

It is doubtful that the partial melting of lower crustal sources by processes outlined above could yield mafic rocks because of the very high temperatures required. Hence similar processes in upper mantle sources are likely for generation of the mafic intrusive suites of the P.N.G. region. Such suites include the mafic stocks of the Gazelle Peninsula (Macnab, 1970) and the Mafic Suite of the Koloula Igneous Complex (this study).

8.5.4 Magma Generation in the Island Arcs

The combined processes of volcanism and crustal subcretion have been building island arcs in the P.N.G. region since late Mesozoic

FIG. 65 : P - T DIAGRAM SHOWING EFFECT OF DECREASED LOAD PRESSURE IN BASE OF CRUST.

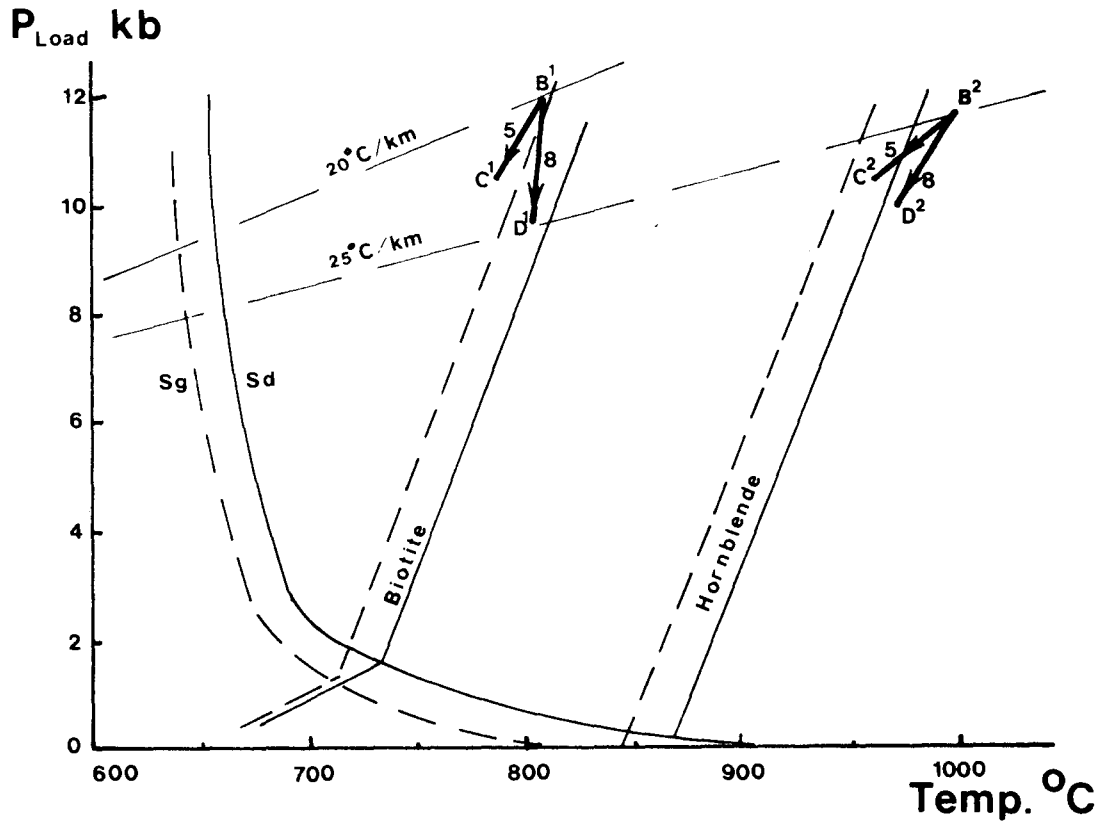

Stability fields after Brown & Fyfe(1970).
Sg, Sd are water-saturated liquidus for granitic (dashed line) and dioritic (full line) quartzo-feldspathic compositions respectively. Biotite and hornblende dehydration curves for water-undersaturated conditions are depicted for both granitic and dioritic compositions.
B represents conditions at base of crust 40 km thick.
C represents conditions at base of crust after 5 km uplift and complete erosion after 2 m.y.
D represents conditions at base of crust after 8 km uplift and complete erosion after 2 m.y.

B^1, C^1, D^1 -- conditions for geotherm of 20°C/km

B^2, C^2, D^2 -- conditions for geotherm of 25°C/km

and early Tertiary times. Presumably, isotherms have been rising as magmatism continued and the arc structures thickened. At a critical time in the evolution of arcs when isotherms intersect the solidus of lower crustal material, partial melting will commence. The time interval between commencement of arc volcanism and intrusion of granitic rocks is probably related to the time required for build-up of crustal thickness and rise of isotherms, and has been noted in section 8.4.1.

Experimental work relevant to this environment has been reported by T. Green & Ringwood (1968), who demonstrated that 'rhyodacitic' and 'dacitic' liquids are derived from partial melting of high-alumina quartz tholeiite at 900°C and 10 kb ($P_{H_2O} < P_{load}$), leaving a residuum of amphibole, pyroxenes, and plagioclase. The precise composition of the partial melts is not of direct concern. It is sufficient to note that silicic partial melts may be derived from basaltic compositions at temperatures and pressures believed to be appropriate for basal parts of island arcs. Andesitic source compositions will provide greater quantities of silicic melts at slightly lower temperatures.

As isotherms rise higher into the base of the arc, partial melting at different levels will produce partial melts and refractory residua at different times. If crustal subcretion has formed a compositionally stratified crust as described in section 8.5.2, early partial melts deep in the arc will be enriched in potassium and depleted in water relative to later melts derived from higher levels. In this way the intrusive sequence as described in section 7.4.1 will be developed.

In the above model, intrusive suites of differing chemistry are generated from compositionally distinct source materials at different loci in the base of the crust. However, the possibility of repeated partial melting of the same source region cannot be discounted at this stage. Qualitatively, initial partial melting of mafic and intermediate compositions will involve quartz, orthoclase, and sodic plagioclase. At higher temperatures, calcic plagioclase and amphibole will begin to melt. Separate extraction from the source region of the silicic, alkalic, water-poor early melt (with some refractory residue) and a later, less-alkalic, water-rich melt (with necessarily different refractory residue) might produce the observed intrusional relationships. The theoretical distinction in intrusive suites of fractional fusion and equilibrium fusion products of different source rocks have been discussed by Presnall (1969) and Presnall & Bateman (1973). The difficulties involved in the practical application of these theories are highlighted in the experimental

work of Steiner et al. (1975). These workers have necessarily restricted their initial investigations to the relatively simple 'granodiorite' system (Qz-Or-Ab-An-H_2O). Repeated partial melting of a single source remains unevaluated for more complex geochemical systems. Until such data become available, it is reasonable to pursue the concept of partial melting of compositionally distinct source rocks in different parts of the base of the crust.

8.5.5 Magma Generation in the Continental Margin (New Guinea Mobile Belt)

Applying the processes of crustal subcretion as described in section 8.5.2 and appropriate mechanisms for initiation of partial melting described in section 8.5.3, the following sequence of events can be traced leading to the generation of the Middle Miocene intrusive complexes in the Mobile Belt:

(i) Prolonged volcanism and crustal subcretion in an extensional stress field built a considerable thickness of essentially volcanogenic material on the northern margin of the Australian continental block (see Fig. 66).

(ii) Consequent upon collision with the New Britain-north New Guinea arc system in (?)late Oligocene times, the Mobile Belt suffered deformation and metamorphism.

(iii) Rapid uplift and erosion in (?)late Oligocene to early Miocene times resulted in raised isotherms and decreased load pressure, especially in horst blocks. Consequent partial melting in basal crustal regions (T. Green & Ringwood, 1968) resulted in emplacement of calc-alkaline intrusive complexes in many parts of the Mobile Belt during the Middle Miocene. Partial melting of compositionally stratified basal crustal material (see section 8.5.2) yielded the compositional-time differences between intrusive suites discussed in section 7.4.1 and 8.3.2.

8.5.6 Magma Generation in the Continental Block

Because of the structural continuity of the Mobile Belt and the Australian continental block (at least on the northern continental margin), uplift of the Mobile Belt has resulted in somewhat later and less pronounced uplift of the adjacent parts of the continental block. The uplift caused sufficient decrease in load pressure to result in partial melting at the base of the crust. Emplacement of intrusive stocks of dioritic and more silicic composition began in late Miocene times and continued into the Pleistocene (Page, 1971; 1975).

FIG. 66 : TECTONIC AND MAGMATIC HISTORY OF PART OF THE NORTHERN AUSTRALIAN CONTINENTAL MARGIN

(A) MESOZOIC:

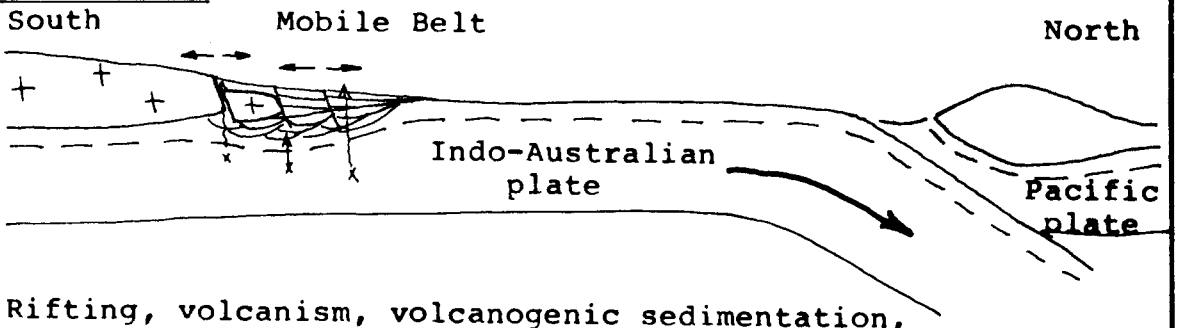

Rifting, volcanism, volcanogenic sedimentation, crustal subcretion.

(B) EOCENE - OLIGOCENE:

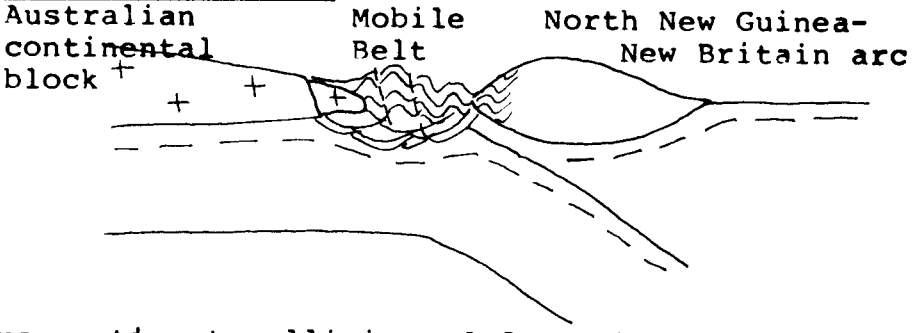

Arc-continent collision; deformation, metamorphism, incipient partial melting in base of Mobile Belt.

(C) MIOCENE - RECENT:

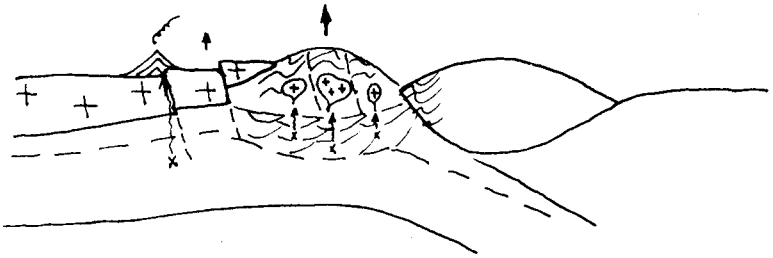

Rapid uplift and erosion; intrusive rocks in Mobile Belt and continental block derived from base of crust; upper mantle sources for Miocene and Quaternary volcanic rocks.

The composition of the base of the crust in continental regions is not known. Estimates vary from mafic to intermediate compositions (e.g. Ringwood & Green, 1966). The chemistry of the Mount Michael and Ok Tedi intrusive complexes, together with other data from the region (Ayres & Bamford, in press), imply derivation by partial melting from a basal crustal source enriched in the 'incompatible' elements (compare Moore, 1962; Bateman & Eaton, 1967; Kistler & Peterman, 1973).

8.6 GENESIS OF PORPHYRY COPPER SYSTEMS

8.6.1 Introduction

The most persistent theme among hypotheses for genesis of ore deposits of the porphyry copper class is the relation between mineralization and calc-alkaline intrusive igneous rocks. It is in the nature of the relationship that hypotheses differ. Some maintain that intrusive activity merely provides a heat source to encourage circulation of meteoric and/or connate solutions, which become metal-rich and capable of forming ore systems. Many workers, however, maintain that the ore-forming fluids and metals (at least in large part) are genetically related to associated intrusive rocks, and are in some way related to the final stages of crystallization of the intrusive rocks (Bowen, 1933; Lindgren, 1937; Burnham, 1967; Krauskopf, 1971). The data presented in this study of certain southwest Pacific porphyry-type occurrences and associated intrusive rocks support the latter view.

8.6.2 Constraints on Porphyry Copper Genesis

Models for the genesis of porphyry-type copper mineralization and associated intrusive rocks in the P.N.G. region must accommodate the following relationships observed during the course of this work:

(i) Porphyry-type mineralization is invariably located within, or near the contact of, an intrusive igneous complex.

(ii) A wide range of chemistry is represented by those intrusive suites associated with mineralization. High-K, normal-K, and low- to normal-K calc-alkaline suites are equally likely to be associated with mineralization (compare Ishihara, 1971). Level of enrichment of potassium in zones of pervasive potassic alteration can be correlated with the level of potassium in the suite as a whole.

(iii) In any single intrusive complex, it is often observed that an early, higher-K, non-mineralized intrusive suite is intruded by a later, lower-K, mineralized intrusive suite. In this study, these

intrusive relationships have been described in the island arc and continental margin settings. Similar intrusive relationships are suspected but not confirmed in the continental setting, where only limited data are presently available (this study; Ayres & Bamford, in press).

(iv) Textural and geochemical criteria permit the conclusion that many intrusive rock suites, including those with associated mineralization, have been generated by partial melting at the base of the crust. Whilst Benioff zones appear to have participated in the evolution of island arcs, this element of plate tectonics theory appears not to have controlled Tertiary and younger magma generation in the New Guinea Mobile Belt or adjacent Australian continental block.

(v) Data from the intrusive suites of the Western Highlands indicate that mineralized suites are characterized by mineralogy and mineral chemistry which have crystallized under high P_{O_2} conditions. These data confirm that suites associated with mineralization contained a water-rich silicate melt during crystallization, and hence were capable of exsolving a metal-rich hydrothermal phase in final stages of crystallization.

Consideration of these constraints on porphyry copper genesis leads one to the conclusion that development of porphyry copper systems depends not upon bulk composition of the associated intrusive rock suite, but rather upon water content of the intrusive suite (and, by implication, the source) and subsequent emplacement and crystallization history of the igneous complex.

In Table 28, the characteristics of mineralized and non-mineralized intrusive rock suites are summarized. The differences are particularly well developed in the Yuat North and Yuat South batholiths of the Western Highlands, and might not be so apparent in other regions due to source composition variability and variable efficiency of the processes involved. Based upon the observed characteristics, a model is constructed for the genesis of porphyry copper systems.

8.6.3 Model for Genesis of Porphyry Copper Systems

Most of the currently popular models for genesis of porphyry copper systems are very closely related to a major feature of plate tectonics theory, i.e. 'subduction' (e.g. Mitchell & Garson, 1972; Sillitoe, 1972a, 1972b; Wright & McCurrey, 1973; Strong, 1974). These models recognize the close genetic relationship between intrusive

TABLE 28: CHARACTERISTICS OF MINERALIZED AND NON-MINERALIZED INTRUSIVE ROCK SUITES WITHIN A SINGLE INTRUSIVE COMPLEX

Characteristic	INTRUSIVE SUITE 1	INTRUSIVE SUITE 2
Porphyry-type mineralization	absent	present
Relative age	early	late
Suite chemistry	higher-K calc-alkaline	lower-K calc-alkaline
Mafic inclusions	abundant; variable stages of disaggregation	scarce; those present have sharp contacts with host rock
Water content	lower	higher
Mineralogy	amphibole $\pm$ pyroxene + Ti-magnetite $\pm$ ilmenite; plagioclase zoning less extreme; amphibole zoned to Fe-rich compositions	amphibole + magnetite + sphene; strongly zoned plagioclase; amphibole ($\pm$ biotite) zoned to Mg-rich compositions at rims

rocks and ore-forming hydrothermal solutions, but appeal to generation of batholithic calc-alkaline magmas from upper parts of subducted oceanic lithosphere, with or without contribution of metallic and volatile components from overlying upper mantle. It has been argued above that many of the calc-alkaline intrusive complexes in the P.N.G. region had their source in mafic and more felsic igneous rocks near the base of the crust, at depths of 20-40 km. Similar sources have been proposed for batholithic masses elsewhere (Piwinskii, 1968; Bateman & Dodge, 1970; Presnall & Bateman, 1973; Chappell & White, 1974). It must be recognized, however, that the igneous source material ultimately had its source in the upper mantle.

Having concluded that calc-alkaline intrusve complexes and associated porphyry-type systems have their immediate source largely in basal crustal regions, it remains to evaluate the extent to which upper crustal processes might contribute to the magmatic system. There is little or no evidence for this in geochemical data. The main evidence for suggesting that meteoric hydrothermal solutions might contribute to porphyry-type systems comes from stable isotopic data in outer alteration zones (Sheppard et al., 1969, 1971; Taylor, 1973). However, Burnham (1967) and Whitney (1975b) have discussed the difficulties involved in circulation of meteoric groundwaters into cooling igneous systems, especially during evolution of a water-rich vapour phase. It seems that there is minimal entry of meteoric hydrothermal solutions into core regions of porphyry systems, but it is likely that such solutions will invade upper and marginal, already-crystallized parts of cooling stocks (Whitney, 1975b, p. 354).

The means of concentration and deposition of metallic, sulfurous, and other constituents of porphyry systems are to be found in prolonged crystallization histories of 'wet' magmas resulting in efficient fractionation of volatile and metallic constituents into residual silicate melts (Ringwood, 1955a, 1955b); in the expulsion of metal-rich hydrothermal solutions into shattered and otherwise structurally-prepared host rocks (Schmitt, 1966; Hodder & Hollister, 1972; Titley, 1972b), and in the changing physico-chemical conditions in pregnant hydrothermal solutions (Helgeson, 1970; Holland, 1972). Combining the results of these workers for post-emplacement development of mineralization with the results of this study in regard to magma generation, one can outline the development of porphyry-type systems in a number of stages.

Porphyry copper model - Stage 1: Formation of Igneous Basement

Various styles of magmatic activity are responsible for crustal thickening in different tectonic settings. In continental blocks, the processes of volcanism, deformation, metamorphism, plutonism, uplift and erosion have resulted in modification of the composition and mineralogy of the base of the crust.

In continental margin regions, volcanism related to rifting or subduction will yield products chemically characteristic of each setting. The basal parts of the crust will be appropriately modified in composition. The basal parts of the northern Australian continental margin (later to become the New Guinea Mobile Belt) were modified by magmatism related to rifting.

In island arcs, volcanism yields magmas characteristic of the environment, and these magmas can also be expected to thicken and chemically modify basal parts of the developing arc.

Porphyry copper model - Stage 2: Partial Melting of Base of Crust.

Partial melting of the material constituting the basal parts of the crust will yield silicic liquids and refractory residue.

The initiation of partial melting might be caused by simple rising of isotherms beneath active volcanic regions. Rapid uplift and erosion of horst blocks will also tend to encourage partial melting through the combined effects of raising the isotherms and decreasing the load pressure. This latter mechanism is believed to have been responsible for partial melting beneath the Mobile Belt in Lower to Middle Miocene times, and somewhat later beneath the adjacent Australian continental crust.

The composition of the partial melt and residue is essentially governed by the composition of the source material and the degree of partial melting. It is to be expected that amounts of water in different sources will vary, not only with the abundance of water-bearing minerals but also with the tendency for increasing dehydration at depth. In the situation where water content decreases downward through accreted, chemically-stratified igneous material near the base of the crust, the earlier melts at depth will be K-rich and water-poor relative to later melts generated higher in the crust. Early water-poor melts might ascend

to sufficiently shallow crustal levels to form extrusive strato-volcanoes (Hutchinson & Hodder, 1972; Sillitoe, 1973; Gustafson & Hunt, 1975). Such relationships between depth, source composition, and water content explain the relationships between distribution, composition and presence of mineralization in batholithic complexes of the Mobile Belt and various island arc intrusive complexes.

Porphyry copper model - Stage 3: Separation from Source and Emplacement

When sufficient silicic melt has formed at depth, it will begin to rise by virtue of its gravitational instability, taking with it some of the refractory source material. Those melts which are slightly more water-rich (2-4% H_2O; Burnham, 1967; Whitney, 1975b) and hence less viscous, will separate much more efficiently from their residual mafic material than will water-poor, more viscous melts. Modest amounts of water in the rising diapiric mush of liquid plus solid components permit ascent to high levels in the crust before saturation of the liquid portion in a vapour phase caused rapid crystallization. During ascent and emplacement, mixing ('hybridism') of the silicic liquid and disaggregated solid refractory material in various proportions results in the range of rock types observed in a single plutonic body or group of related bodies, and yields the linear geochemical relationships characteristic of such bodies.

Porphyry copper model - Stage 4: Final Crystallization and Deposition of Mineralization

The evolution of a water-rich fluid phase from a cooling intrusive body has been discussed in detail by Burnham (1967) and Whitney (1975b). These authors demonstrate the manner in which the process is controlled by composition of the melt, initial water content of the melt, the distribution of temperature and stable mineral species in the body, and depth of emplacement. The efficiency of metal fractionation into the water-rich fluid phase will be greater in the slower-cooling portions of the intrusive body. Final locus of mineralization will be controlled by the ease of access of metal-rich hydrothermal solutions into early-crystallized, fractured outer parts of the intrusive body and adjacent wall rocks, and the temperature gradients, meteoric fluids or other perturbations encountered during expulsion. Favoured sites for mineralization include core, margin, and upper cupola regions of stocks, as well as adjacent wall rocks.

8.7 SUMMARY OF CONCLUSIONS

1. In the Papua New Guinea-Solomon Islands region of the southwest Pacific, calc-alkaline intrusive rock suites of Tertiary and younger age occur in three contrasted tectonic settings: intra-oceanic island arcs, the Australian continental margin (New Guinea Mobile Belt), and the Australian continental block. Porphyry-type copper mineralization is associated with intrusive complexes in all three settings.

2. Intrusive suites of each tectonic setting display a wide range of calc-alkaline chemistry. The least potassic suite lies in an island arc setting and the most potassic suite lies in the continental setting.

3. Regional geochemical variations between intrusive rock suites are of three kinds:

(i) increasing abundance of 'incompatible' elements (K, Rb, Ba, Zr, Nb, La, Ce, Y, Th, U, Pb) from the island arcs, through the continental margin to the continental setting. Copper is erratic in distribution.

(ii) northwards increase in potassium and related trace elements across the Mobile Belt.

(iii) abundance of certain elements in particular regions.

The geochemistry of intrusive suites reflects the composition of their source materials at depth.

4. Genesis of the majority of the Tertiary and younger calc-alkaline intrusive complexes involves hybridism of silicic partial melts and refractory material from mafic and more felsic igneous source rocks in the base of the crust (20-40 km). A smaller number of mafic intrusive complexes had their source in the upper mantle. Partial melting is caused by rise of isotherms due to prolonged magmatism, and is aided by decrease in load pressure due to rapid uplift and erosion. Beneath the Mobile Belt, partial melting in Lower to Middle Miocene times was achieved by such means without the participation of a Benioff zone.

5. There are certain consistencies in the relationship between porphyry-type mineralization and intrusive rock suites:

(i) Mineralization is associated with suites spanning the entire low-to high-K calc-alkaline range.

(ii) Where geochemically distinct suites can be recognized in a

mineralized multiphase intrusive complex, the mineralization is associated with a later lower-K suite. The earlier high-K suite is barren.

(iii) The degree of potassium enrichment in zones of pervasive potassic alteration is dependent on the abundance of potassium in the intrusive suite.

(iv) Mineralized suites were slightly more water-rich than barren suites. They contain primary mineral assemblages indicative of high P_{O_2} (i.e. hornblende + magnetite + sphene), appropriate changes in mafic mineral chemistry (i.e. stability of increasingly Mg-rich compositions),and few mafic inclusions (i.e. enhanced ability to segregate from refractory source material because of lower viscosity of water-rich melt.)

(v) Intrusive suites and associated mineralization in the continental setting possess Ag/Au<1. In the continental margin and island arc settings, Ag/Au>1.

6. The genesis of porphyry-type mineralization is intimately related to phenomena attending final crystallization of relatively water-rich intrusive suites.

BIBLIOGRAPHY

Australian Bureau of Mineral Resources (1972), Geological map of Papua New Guinea, 1:1000,000. Canberra.

Ayres, D. & Bamford, R.W. (in press): The Mount Fubilan (Ok Tedi) porphyry copper deposit - geology, geochemistry, and origin. A.I.M.E. Ann. Mtg., Las Vegas, February, 1976.

Ayres, L.D., Averill, S.A., & Wolfe, W.J. (1973): The early Precambrian Setting Net Lake porphyry molybdenum deposit. C.I.M. Ann. Mtg. April, 1973.

Bain, J.H.C. (1973): A summary of the main structural elements of Papua New Guinea. in The Western Pacific: Island arcs, marginal areas, geochemistry. Coleman, ed. University of Western Australia Press.

_____ & Mackenzie, D.E. (1974): Karimui Papua New Guinea. 1:250,000 Geological Series, Bur. Miner. Resour. Aust. Explan. Notes, SB 55-9.

Bamford, R.W. (1972): The Mount Fubilan (Ok Tedi) porphyry copper deposit, Territory of Papua New Guinea. Econ. Geol. 67, 1019-1033.

Banks, N.G. & Stuckless, J.S. (1973): Chronology of intrusion and ore deposition at Ray, Arizona: Part 2, Fission-track ages, Econ. Geol 68, 657-664.

Bateman, P.C., Clark, L.D., Huber, N.K., Moore, J.G. & Rinehart, C.D. (1963): The Sierra Nevada Batholith, a synthesis of recent work across the central part, Prof. Pap. U.S. geol. Surv. 414-D, 46p.

_____ & Dodge, F.C.W. (1970): Variations of major chemical constituents across the central Sierra Nevada Batholith. Bull. geol. Soc. Am. 81, 409-420.

_____ & Eaton, J.P. (1967): The Sierra Nevada Batholith. Science 158, 1407-1417.

Beaty, R.D. & Manuel, O.K. (1973): Tellurium in rocks. Chemical Geology 12, 155-159.

Blake, D.H. & Miezitis, Y. (1967): The geology of Bougainville and Buka islands, New Guinea. Bull. Bur. Miner. Resour. Aust. 93, 56 p.

Bowen, N.L. (1928): The evolution of the igneous rocks. Princeton University Press.

_____ (1933): The broader story of magmatic differentiation, briefly told. in Ore deposits of the Western States (Lindgren vol.). p. 106-128, A.I.M.E., New York.

Brooks, J.A. (!969a): Rayleigh waves in southern New Guinea 1: Higher mode group velocities. Bull. Seis. Soc. Am. 59, 945-958.

_____ (1969b): Rayleigh waves in southern New Guinea 2: A shear wave profile. Bull. Seis. Soc. Am. 59, 2017-2038.

Brown, G.C. & Fyfe, W.S. (1970): The production of granitic melts during ultrametamorphism. Contr. Mineral. and Petrol. 28, 310-318.

Buddington, A.F. (1959): Granite emplacement with special reference to North America. Bull. geol. Soc. Am. 70, 671-747.

_____ & Lindsley, D.H. (1964): Fe-Ti oxide minerals and their synthetic equivalents. J. Petrology 5, 310-357.

Burnham, C.W. (1967): Hydrothermal fluids at the magmatic stage. in Geochemistry of hydrothermal ore deposits. Barnes, ed. Holt, Rinehart & Winston, Inc., New York.

Carey, S.W. (1938): Tectonic evolution of New Guinea and Melanesia. Ph.D. thesis, University of Sydney.

Carmichael, I.S.E. (1967): The iron-titanium oxides of salic volcanic rocks and their associated ferromagnesian silicates. Contr. Mineral. and Petrol. 14, 36-64.

_____, Turner, F.J., & Verhoogen, J. (1974): Igneous Petrology. McGraw-Hill, New York.

Cermak, V. (1975): Temperature-depth profiles in Czechoslovakia and some adjacent areas derived from heat-flow measurements, deep seismic sounding and other geophysical data. Tectonophysics 26, 103-119.

Chappell, B.W. (1966): Petrogenesis of the granites at Moonbi, New South Wales. Ph.D. Thesis, Australian National University.

_____ (1973): Evaluation of use of calculated mass absorption coefficients in determining Rb and Sr by X-ray spectrometry (unpub. manuscript).

_____ & White, A.J.R. (1974): Two contrasting granite types. Pacific Geology 8, 173-174.

Chivas, A.R. (1975): Geochemistry of the Koloula Igneous Complex, Guadalcanal. Bull. Aust. Soc. Explor. Geophys. 6, 64-65.

Christensen, N.I. & Fountain, D.M. (1975): Constitution of the lower continental crust based on experimental studies of seismic velocities in granulite. Bull. geol. Soc. Am. 86, 227-236.

Clark, K.F. (1972): Stockwork molybdenum deposits in the Western Cordillera of North America. Econ. Geol. 67, 731-748.

Coleman, P.J. (1957): Geology of western Guadalcanal. in Geological reconnaissance of parts of the central islands of the British Solomon Islands Portectorate, by the University of Sydney, Department of Geology and Geophysics, Colon. Geol. Miner. Resour. 6, 267-306.

_____ (1965): Stratigraphic and structural notes on the British Solomon Islands with reference to the First Geological Map, 1962. Geol. Rec. Br. Solomon Isl. 2, 17-31.

_____ (1967): A possible resolution of the Melanesian Re-entrant. Upper Mantle Project, 2nd Aust. Prog. Rept. (1965-67), 192-194. (Ed. A.E. Ringwood). Aust. Acac. Sci., Canberra.

_____ (1970): Geology of the Solomon and New Hebrides Islands, as part of the Melanesian Re-entrant, southwest Pacific. Pacif. Sci. 24, 289-314.

Cooley, W.W. & Lohnes, P.R. (1962): Multivariate procedures for the behavioural sciences. John Wiley & Sons, New York.

Curtis, J.W. (1973a): The spatial seismicity of Papua New Guinea and the Solomon Islands. Jour. geol. Soc. Aust. 20, 1-20.

_____ (1973b): Plate tectonics and the Papua New Guinea-Solomon Islands region. Jour. geol. Soc. Aust. 20, 21-36.

Czamanske, G.K. & Wones, D.R. (1973): Oxidation during magmatic differentiation, Finnmarka Complex, Oslo area, Norway. Part 2: The mafic silicates. J. Petrology. 14, 349-380.

Davies, H.L. & Smith, I.E. (1971): Geology of eastern Papua. Bull. geol. Soc. Am. 82, 3299-3312.

Deer, W.A. (1935): The Cairnsmore of Carsphairn igneous complex. Mineralog. Mag. 24, 495-502.

_____ (1938): The composition and paragenesis of the hornblendes of the Glen Tilt complex, Perthshire. Mineralog. Mag. 25, 56-74.

_____ , Howie, R.A., & Zussman, J. (1963): Rock-forming minerals. Vol. 3: Chain silicates. Longmans, London.

Denham, D. (1969): Distribution of earthquakes in the New Guinea-Solomon Islands region. J. Geophys. Res. 74, 4290-4299.

Dewey, J.F. & Bird, J.M. (1970): Mountain belts and the New Global Tectonics. J. Geophys. Res. 75, 2625-2647.

Dickinson, W.R. (1968): Circum-Pacific andesite types. J. Geophys. Res. 73, 2261-2269.

_____ (1975): Potash-depth (K-h) relations in continental margin and intra-oceanic magmatic arcs. Geology 3, 53-56.

Dodge, F.C.W., Papike, J.J., & Mays, R.E. (1968): Hornblendes from granitic rocks of the central Sierra Nevada Batholith, California. J. Petrology 9, 378-410.

Dow, D.B. (1973): Geology of Papua New Guinea. Bur. Miner. Resour. Aust. Rec. 1973/117.

_____ & Davies, H.L. (1964): The geology of the Bowutu Mountains, New Guinea. Bur. Miner. Resour. Aust. Rep. 1964/75.

_____ & Dekker, F.E. (1964): The geology of the Bismarck Mountains, New Guinea. Bur. Miner. Resour. Aust. Rep. 1964/76.

_____ , Smit , J.A.M., Bain, J.H.C., & Ryburn, R.J. (1967): The geology of the South Sepik region, progress report for 1966. Bur. Miner. Resour. Aust. Rec. 1967/26.

_____ , _____ , _____ , _____ (1968): The geology of the South Sepik region, New Guinea. Bur. Miner. Resour. Aust. Rec. 1968/80.

_____ . _____ , _____ , _____ (1972): Geology of the South Sepik region, New Guinea. Bull. Bur. Miner. Resour. Aust. 133 , 88p.

Ewing, M. & Press, F. (1955): Geophysical contrasts between continents and ocean basins. Spec. Pap. geol. Soc. Am. 62, 1-6.

Faure, G. & Hurley, P.M. (1963): The isotopic composition of strontium in oceanic and continental basalts: application to the origin of igneous rocks. J. Petrology 4, 31-50.

Finlayson, D.M. & Cull, J.P. (1973): Structural profiles in the New Britain/New Ireland region. J. geol. Soc. Aust. 20, 37-48.

_____ & Ryburn, R.J. (1973): Crustal structure at the Bismarck-Solomon-Pacific triple junction. Abs. 2nd Int. Conf. Geophys. Earth and Ocean Basins, Sydney.

Fisher, F.S. (1972): Tertiary mineralization and hydrothermal alteration in the Stinkingwater mining region, Park County, Wyoming. Bull. U.S. geol. Surv. 1332-C, C1-C33.

Fisher, N.H. (1935): Geological report Day Dawn South. Terr. N. Guin. rep. (unpubl).

_____ (1936): Geological report Kupei goldfield, Bougainville, T.N.G. Terr. N. Guin, rep. (unpub.).

_____ (1937): Geological report on the gold-bearing area of the Wewak district. Terr. N. Guin. rep. (unpub.).

Flanagan, F.J. (1973): 1972 values for international geochemical reference samples. Geochim. cosmochim. Acta 37, 1189-1200.

Flint, D.E. (1972): Geology of the Ertsberg copper deposit, Irian Barat, Indonesia. Abs. Reg. Conf. Geol. Southeast Asia: Annex to Newsletter No. 34, Geol. Soc. Malaysia, 10-11.

Foster, M.D. (1960): Interpretation of the composition of trioctahedral micas. Prof. Pap. U.S. geol. Surv. 354-B, 11-48.

Fountain, R.J. (1972): Geological relationships in the Panguna porphyry copper deposit, Bougainville Island, New Guinea. Econ. Geol. 67, 1049-1064.

Gill, J.B. (1970): Geochemistry of Viti Levu, Fiji, and its evolution as an island arc. Contr. Mineral. and Petrol. 27, 179-203.

_____ & Compston, W. (1973): Strontium isotopes in island arc volcanic rocks. in The Western Pacific: Island arcs, marginal seas, geochemistry. Coleman, ed. University of Western Australia Press.

Glaessner, M.F. (1950): Geotectonic position of New Guinea. Bull. Am. Ass. Petrol. Geol. 34, 856-881.

Goldschmidt, V.M. (1954): Geochemistry. Clarendon Press, Oxford.

Grapes, R.H. (1975): Actinolite-hornblende pairs in metamorphosed gabbros, Hidaka Mountains, Hokkaido. Contr. Mineral. and Petrol. 49, 125-140.

Graybeal, F.T. (1973): Copper, manganese, and zinc in coexisting mafic minerals from Laramide intrusive rocks in Arizona. Econ. Geol. 68, 785-798.

Green, D.H. (1969): The origin of basaltic and nephelinitic magmas in the Earth's mantle. Tectonophysics 7, 409-422.

_____, Green, T.H., & Ringwood, A.E. (1967): The origin of high alumina basalts and their relationships to quartz tholeiites and alkali basalts. Earth & planet. Sci. Lett. 2, 41-51.

_____ & Ringwood, A.E. (1967): An experimental investigation of the gabbro to eclogite transformation and its petrological applications. Geochim. cosmochim. Acta 31, 767-833.

Green, T.H. & Ringwood, A.E. (1968): Genesis of the calc-alkaline igneous rock suite. Contr. Mineral. and Petrol. 18, 105-162.

Gulson, B.L., Lovering, J.F., Taylor, S.R., & White, A.J.R. (1972): High-K diorites, their place in the calc-alkaline association and relationship to andesites. Lithos 5, 269-279.

Gustafson, L.B. & Hunt, J.P. (1975): The prophyry copper deposit at El Salvador, Chile. Econ. Geol. 70, 857-912.

Gutenberg, B. (1955): Wave velocities in the Earth's crust. Spec. Pap. geol. Soc. Am. 62, 19-34.

Hackman, B.D. (1968): The geology of east and central Guadalcanal: a preliminary statement, 1966. Geol. Rec. Br. Solomon Isl. 3, 16-25.

_____ (1971): The regional geology of Guadalcanal: a contribution to the geology of fractured island arcs. Ph.D. thesis, University of Western Australia.

_____ (1973): The Solomon Islands fractured arc. in The Western Pacific: Island arcs, marginal seas, geochemistry. Coleman, ed. University of Western Australia Press.

Hall, R.J. & Simpson, P.G. (in press): The Frieda porphyry copper prospect, New Guinea. in Economic geology of Australia and New Guinea. A.I.M.M.

Hamilton, W. (1969): The volcanic central Andes - a modern model for the Cretaceous bathyliths and tectonics of western North America. in Proceedings of the Andesite Conference. McBirney, ed. Oregon Dep. Geol. Mineral Ind. Bull. 65.

_____ & Myers, W.B. (1967): The nature of bathyliths. Prof. Pap. U.S. geol. Surv. 554-C, C1-C30.

Hart, S.R., Glassley, W.E. & Karig, D.E. (1972): Basalts and sea floor spreading behind the Mariana arc. Earth & planet. Sci. Lett. 15, 12-18.

Harebe, K., Fujii, N., & Uyeda, S. (1970): Thermal processes under island arcs. Tectonophysics 10, 335-355.

Hazen, R.M. & Wones, D.R. (1972): The effect of cation substitutions on the physical properties of trioctahedral micas. Am. Mineral. 57, 103-129.

Helgeson, H.C. (1970): A chemical and thermodynamic model of ore deposition in hydrothermal systems. Spec. Pap. Mineralog. Soc. Am. 3, 155-186.

Hodder, R.W. & Hollister, V.F. (1972): Structural features of porphyry copper deposits and the tectonic evolution of continents. C.I.M. Trans. 75, 23-27.

Hohnen, P.D. (1970): Geology of New Ireland. Bur. Miner. Resour. Aust. Rec. 1970/49.

Holland, H.D. (1972): Granites, solutions and base metal deposits. Econ. Geol. 67, 281-301.

Hollister, V.F., Anzalone, S.A., & Richter, D.H. (1975): Porphyry copper deposits of southern Alaska and contiguous Yukon Territory. C.I.M. Bull. 68, 104-112.

Hutchinson, R.W. & Hodder, R.W. (1972): Possible tectonic and metallogenic relationships between porphyry copper and massive sulfide deposits. C.I.M. Bull. 65, 34-40.

Hutchison, D. (1974): Volcanic and tectonic history of the North Sepik region. Bur. Miner. Resour. Aust. Rec. 1974/35. Abstracts of Symposium, April-May, Canberra.

International Union of Geological Sciences (1973): Plutonic rocks - classification and nomenclature by the IUGS Subcommission on the systematics of igneous rocks. Geotimes 18, 26-30.

Ishihara, S. (1971): Some chemical characteristics of the intrusive rocks of the Bethlehem porphyry copper deposits, B.C., Canada. Bull. geol. Soc. Japan 22, 535-546.

Jaeger, J.C. (1968): Cooling and solidification of igneous rocks. in Basalts. Hess & Poldevaart, eds. John Wiley & Sons, New York.

Jakes, P. & Gill, J.B. (1970): Rare earth elements and the island arc tholeiitic series. Earth & planet. Sci. Lett. 9, 17-28.

_____ & Smith, I.E. (1970): High potassium calc-alkaline rocks from Cape Nelson, Eastern Papua. Contr. Mineral. and Petrol. 28, 259-271.

_____ & White, A.J.R. (1969): Structure of the Melanesian arcs and correlation with distribution of magma types. Tectonophysics 8, 223-236.

_____ & _____ (1970): K/Rb ratios of rocks from island arcs. Geochim. cosmochim. Acta 34, 849-856.

_____ & _____(1972): Hornblendes from calc-alkaline volcanic rocks of island arcs and continental margins. Am. Mineral. 57, 887-902.

Jambor, J.L. (1974): Trace element variations in porphyry copper deposits, Babine Lake area, B.C. Geol. Surv. Pap. Can. 74-9, 30 p.

James, A.H. (1971): Hypothetical diagrams of several porphyry copper deposits. Econ. Geol. 66, 43-47.

Jenkins, D.A.L. (1974): Detachment tectonics in western Papua New Guinea. Bull. geol. Soc. Am. 83, 601-618.

Johnson, R.W., Mackenzie, D.E., & Smith, I.E. (1971): Seismicity and late Cenozoic volcanism in parts of Papua New Guinea. Tectonophysics 12, 15-22.

Joplin, G.A. (1959): On the origin and occurrence of basic bodies associated with discordant batholiths. Geol. Mag. 96, 361-373.

_____ (1965): The problem of the potash-rich basaltic rocks. Mineralog. Mag. 34, 266-275.

_____ (1968): The shoshonite association: a review. J. geol. Soc. Aust. 15, 275-294.

Joyce, A.S. (1970): Geochemistry of the Murrumbidgee Batholith. Ph.D. thesis, Australian National University.

_____ (1973): Petrogenesis of the Murrumbidgee Batholith, A.C.T. J. geol. Soc. Aust. 20, 179-197.

Karig, D.E. (1971): Origin and development of marginal basins in the Western Pacific. J. Geophys. Res. 76, 2542-2561.

_____ (1972): Remnant arcs. Bull. geol. Soc. Am. 83, 1057-1068.

Kesler, S.E., Jones, L.M., & Walker, R.L. (1975a): Intrusive rocks associated with porphyry copper mineralization in island arc areas. Econ. Geol. 70, 515-526.

Kesler, S.E., Issigonis, J.M., Brownlow, A.H., Damon, P.E., Moore, W.J., Northcote, K.E., & Preto, V.A. (1975b): Geochemistry of biotites from mineralized and barren intrusive systems. Econ. Geol. 70, 559-567.

Kesson, S.E. (1973): The primary geochemistry of the Monaro alkaline volcanics, southern Australia - evidence for upper mantle heterogeneity. Contr. Mineral. and Petrol. 42, 93-108.

_____ & Smith, I.E. (1972): TiO_2 content and the shoshonite and alkaline associations. Nature Physical Science 236, 110-111.

Kistler, R.W. & Peterman, Z.E. (1973): Variations in Sr, Rb, K, Na, and initial $^{87}Sr/^{86}Sr$ in Mesozoic granitic rocks and intruded wall rocks in central California. Bull. geol. Soc. Am. 84, 3489-3512.

Krauskopf, K.B. (1971): The source of ore metals. Geochim. cosmochim. Acta 35, 643-659.

Kuno, H. (1959): Origin of Cenozoic petrographic provinces of Japan and surrounding areas. Bull. volcan. 20, 37-76.

_____ (1966): Lateral variation of basalt magma type across continental margins and island arcs. Bull. volcan. 29, 195-222.

Larsen, E.S., Jr. (1948): Batholith and associated rocks of the Corona, Elsinore, and San Luis Rey quadrangles, southern California. Mem. geol. Soc. Am. 29, 182 p.

Larsen, E.S., & Draisin, W.M. (1950): Composition of the minerals from rocks of the Southern California Batholith. Rep. 18th Int. Geol. Congr. 2, 66-79. Great Britain.

Leake, B.E. (1968): A catalog of analyzed calciferous and subcaliferous amphiboles together with their nomenclature and associated minerals. Spec. Pap. geol. Soc. Am. 98, 210 p.

Linder, H. (1975): Geology of the Shaft Creek porphyry copper-molybdenum deposit, northwestern B.C. C.I.M. Bull. 68, 49-63.

Lindgren, W. (1937): Succession of minerals and temperatures of formation in ore deposits of magmatic affiliation. A.I.M.E. Trans. 126, 356-376.

Lohnes, P.R. (1961): Test space and discriminant space classification models and related significance tests. Ed. and Psych. Meas. 21, 559.

Lowder, G.G., & Carmichael, I.S.E. (1970): The volcanoes and caldera of Talasea, New Britain. Bull. geol. Soc. Am. 81, 17-38.

Lowell, J.D., & Guilbert, J.M. (1970): Lateral and vertical alteration-mineralization zoning in porphyry copper ore deposits. Econ. Geol. 65, 373-408.

Mackenzie, D.E. (1971): Intrusive rocks of New Britain. Bur. Miner. Resour. Aust. Rec. 1971/70.

_____ & Chappell, B.W. (1972): Shoshonitic and calc-alkaline lavas from the Highlands of Papua New Guinea. Contr. Mineral. and Petrol. 35, 50-62.

Macnab, R.P. (1970): Geology of the Gazelle Peninsula, Territory of Papua and New Guinea. Bur. Miner. Resour. Aust. Rec. 1970/63.

Macnamara, P.M. (1968): Rock types and mineralization at Panguna Porphyry Copper Prospect, Upper Kaverong Valley, Bougainville Island. A.I.M.M. Procs. 228, 71-79.

Mason, B. (1966): Principles of geochemistry. Third edition, Wiley, New York.

Mason, D.R. (1975): Subdivision and geochemistry of Tertiary intrusive complexes from part of the New Guinea Mobile Belt. Bull. Aust. Soc. Explor. Geophys. 6, 69-71.

_____ & Belbin, L. (in prep.): A sequential technique for objective analysis of geochemical data.

Mitchell, A.H.G., & Garson, M.S. (1972): Relationship of porphyry copper and circum-Pacific tin deposits to palaeo-Benioff zones. Trans. Instn. Min. Metall. 81, B10-B25.

Mitchell, B. & Landisman, M. (1970): Interpretation of a crustal section across Oklahoma. Bull. geol. Soc. Am. 81, 2647-2656.

Moorbath, S. & Bell, J.D. (1965): Strontium isotope abundance studies and rubidium-strontium age determinations on Tertiary igneous rocks from the Isle of Skye. J. Petrology 6, 37-66.

Moore, J.G. (1962): K/Na ratio of Cenozoic igneous rocks of the western United States. Geochim. cosmochim. Acta 26, 101-130.

_____, Grantz, A. & Blake, M.C. (1962): The quartz diorite line in northwestern North America. Prof. Pap. U.S. geol. Surv. 450-E, E89-E93.

Moore, W.J. (1973): A summary of radiometric ages of igneous rocks in the Oquirrh Mountains, north-central Utah. Econ. Geol. 68, 97-101.

_____ & Czamanske, G.K. (1973): Compositions of biotites from unaltered and altered monzonitic rocks in the Bingham mining district, Utah. Econ. Geol. 68, 269-280.

_____ & Lanphere, M.A. (1971): The age of porphyry-type copper mineralization in the Bingham mining district, Utah - a refined estimate. Econ. Geol. 66, 331-334.

Netzel, R.K. (1974): Petrography and geochemistry of the Koloula River Igneous Complex, Gaudalcanal, British Solomon Islands. M.Sc. thesis, James Cook University, Townsville, Queensland.

Nicholls, I.A. (1974): A direct fusion method of preparing silicate rock glasses for energy-dispersive electron microprobe analysis. Chemical Geology 14, 151-157.

Noakes, L.C. (1938): Report on the Black Cat-Bitoi River area. Terr. N. Guin. Rep. (unpub).

_____ (1941): Report on Edie Creek Mine. Terr. N. Guin. Rep. (unpub).

Nockolds, S.R. (1934): The production of normal rock types by contamination and their bearing on petrogenesis. Geol. Mag. 71, 31-39.

_____ (1941): The Garrabal Hill-Glen Fyne Igneous Complex. Q.Jl. geol. Soc. Lond. 96, 451-510.

_____ & Allen, R. (1953): The geochemistry of some igneous rock series. Geochim. cosmochim. Acta 4, 105-142.

Norrish, K. & Hutton, J.T. (1969): An accurate X-ray spectrographic method for the analysis of a wide range of geological samples. Geochim. cosmochim. Acta 33, 431-453.

Osborn, E.F. (1969): Genetic significance of V and Ni content of andesites: comments on a paper by Taylor, Kaye, White, Duncan, & Ewart. Geochim. cosmochim. Acta 33, 1553-1554.

Owen, H.B. (1954): Bauxite on Manus Island, Territory of Papua New Guinea. (Appendix 3 in Buaxite in Australia. Bur. Miner. Resour. Aust. Bull. 24, 222-234).

Packham, G.H. (1973): A speculative Phanerozoic history of the southwest Pacific. in The Western Pacific: Island arcs, marginal seas, geochemistry. Coleman, ed. University of Western Australia Press.

Page, R.W. (1971): The geochronology of igneous rocks in the New Guinea region. Ph.D. thesis, Australian National University.

_____ (1975): Geochronology of late Tertiary and Quaternary mineralized intrusive porphyries in the Star Mountains of Papua New Guinea and Irian Jaya. Econ. Geol. 70, 928-936.

_____ (in press): Geochronology of igneous and metamorphic rocks in the New Guinea Highlands. Bur. Miner. Resour. Aust. Bull. 162.

_____ & McDougall, I. (1970): K-Ar dating of the Tertiary f_{1-2} stage in New Guinea and its bearing on the Geological Time Scale. Am. J. Sci. 269, 321-342.

_____ & _____ (1972a): Ages of mineralization of gold and porphyry copper deposits in the New Guinea Highlands. Econ. Geol. 67, 1034-1048.

_____ & _____ (1972b): Geochronology of the Panguna porphyry copper deposit, Bougainville Island, New Guinea, Econ. Geol. 67, 1065-1074.

_____ & Ryburn, R.J. (1973): K-Ar ages and geological relations of plutonic rocks of New Britain. Bur. Miner. Resour. Aust. Rec. 1973/191.

Parsons, A.B. (1933): The porphyry coppers. A.I.M.E. Rocky Mtn. Fund. New York, 580 p.

_____ (1957): The porphyry coppers in 1956. A.I.M.E. Rocky Mtn. Fund. New York, 270 p.

Pearce, J.A. & Cann, J.R. (1971): Ophiolite origin investigated by discriminant analysis using Ti, Zr, and Y. Earth & planet. Sci. Lett. 12, 339-349.

Piwinski, A.J. (1968): Studies of batholithic feldspars: Sierra Nevada, California. Contr. Mineral. and Petrol. 17, 204-223.

Presnall, D.C. (1969): The geometrical analysis of partial fusion. Am. J. Sci. 167, 1178-1194.

Presnall, D.C. & Bateman, P.C. (1973): Fusion relations in the system $NaAlSi_3O_8$-$CaAl_2Si_2O_8$-$KAlSi_3O_8$-SiO_2-H_2O and generation of granitic magmas in the Sierra Nevada Batholith. Bull. geol. Soc. Am. 84, 3181-3202.

Putnam, G.W. (1972): Base metal distribution in granitic rocks; data from the Rocky Hill and Lights Creek Stocks, California. Econ. Geol. 67, 511-527.

Ragland, P.C. & Butler, J.R. (1972): Crystallization of the West Farrington Pluton, north Carolina, U.S.A. J. Petrology 13, 381-404.

Raitt, R.W., Fisher, R.L., & Mason, R.G. (1955): Tonga Trench. Spec. Pap. geol. Soc. Am. 62, 237-254.

Read,H.H. (1949): A contemplation of time in plutonism. Q. Jl. geol. Soc. Lond. 105, 101-156.

_____ (1955): Granite series in mobile belts. Spec. Pap. geol. Soc. Am. 62, 409-430.

Reed, S.J. B. & Ware, N.G. (1973): Quantitative electron microprobe analysis using a lithium drifted silicon detector. X-ray Spectrometry 2, 69-74.

Richards, T.C. & Walker, D.J. (1959): Measurement of the Earth's crustal thickness in Alberta. Geophys. 24, 262-284.

Rickwood, F.K. (1955): The geology of the Western Highlands of New Guinea. J. geol. Soc. Aust. 2, 63-82.

Rikitake, T., Miyamura, S., Tsubokawa, I., Murauchi, S., Uyeda, S., Kuno, H., & Gorai, M. (1968): Geophysical and geological data in and around the Japan arc. Can. J. Earth Sci. 5, 1101-1118.

Ringwood, A.E. (1955a): The principles governing trace element distribution during magmatic crystallization. Part 1: The influence of electronegativity. Geochim. cosmochim. Acta 7, 189-202.

_____ (1955b): The principles governing trace element behaviour during magmatic crystallization. Part 2: The role of complex formation. Geochim. cosmochim. Acta 7, 242-254.

_____ & Green, D.H. (1966): The petrological nature of stable continental crust. in The Earth Beneath the Continents. Rinehart & Smith, eds. Geophysics Monograph 10, A.G.U., Washington, D.C.

Robinson, G.P. (1974): Huon-Sag Sag. Papua New Guinea 1:250,000 Geological Series. Bur. Miner. Resour. Aust. Explan. Notes SB 55-11.

Rose, A.W. (1970): Zonal relationships of wallrock alteration and sulfide distribution at porphyry copper depsoits. Econ. Geol. 65, 920-936.

St. John V.P. (1970): The gravity field and structure of Papua and New Guinea. A.P.E.A. J1., p. 41-55.

Schmitt, H.A. (1966): The porphyry copper deposits in their regional setting. in Geology of the porphyry copper deposits. Titley, ed. University of Arizona Press.

Sheppard, S.M.F., Nielsen, R.L., & Taylor, H.P., Jr. (1969): O and H isotope ratios of clay minerals from porphyry copper deposits. Econ. Geol. 64, 755-777.

_____, _____ , & _____ (1971): H and O isotope ratios in minerals from porphyry copper deposits. Econ. Geol. 66, 515-542.

Sillitoe, R.H. (1972a): A plate tectonic model for the origin of porphyry copper deposits. Econ. Geol. 67, 184-197.

_____ (1972b): Relation of metal provinces in western America to subduction of oceanic lithosphere. Bull. geol. Soc. Am. 83, 813-818.

_____ (1973): The tops and bottoms of porphyry copper deposits. Econ. Geol. 68, 799-815.

Sindeeva, N.D. (1964): Mineralogy and types of deposits of selenium and tellurium. Interscience Publishers Inc., New York.

Smith, I.E., (1971): High-potassium intrusives from southeastern Papua. Contr. Mineral. and Petrol. 34, 167-176.

Soregaroli, A.E. (1974): Geology of the Brenda copper-molybdenum deposit in British Columbia. C.I.M. Bull. 67, 76-83.

Stanely, E.R. (1916): Report on the geology of Cape Vogel Peninsula - mineral indications. Terr. Pap. Rep.(Unpub).

_____ (1923): Report on the salient geological features and natural resources of the New Guinea Territory. Parl. Paper 18 of 1923. Government Printer, Melbourne.

Stanton, R.L. (1972): Ore petrology. McGraw-Hill, New York.

_____ & Bell, J.D. (1969): Volcanic and associated rocks of the New Georgia Group, British Solomon Islands Protectorate. Overseas Geol. Miner. Resour. 10, 113-145.

Steiner, J.C., Jahns, R.H., & Luth, W.C. (1975): Crystallization of alkali feldspar and quartz in the haplogranite system $NaAlSi_3O_8$-$KAlSi_3O_8$-SiO_2-H_2O at 4 kb. Bull. geol. Soc. Am. 86, 83-98.

Streckeisen, A.L. (1967): Classification and nomenclature of igneous rocks. N. Jb. Miner. Abh. 107, 144-214.

Stringham, B. (1960: Differences between barren and productive intrusive porphyry. Econ. Geol. 55, 1622-1630.

Strong, D.F. (1974): Plate tectonic setting of Newfoundland mineral deposits. Geoscience Canada 1, 20-30.

Sugimura, A. (1968): Spatial relations of basaltic magmas in island arcs. in Basalts. Hess & Poldevaart, eds. John Wiley & Sons, New York.

Sutherland Brown, A. (1969): Mineralization in British Columbia and the copper and molybdenum deposits. C.I.M. Trans. 72, 1-15.

Taylor, H.P. (1973): $^{18}O/^{16}O$ evidence for meteoric ore deposition in the Tonopah, Comstock Lode, and Goldfield mining districts, Nevada. Econ. Geol. 68, 747-764.

Taylor, S.R. (1969): Trace element chemistry of andesites and associated calc-alkaline rocks, in Proceedings of the Andesite Conference. McBirney, ed. Oregon Dep. Geol. Mineral Ind. Bull. 65.

_____ Capp, A.C., & Graham, A.L. (1969a): Trace element abundances in andesites 2: Saipan, Bougainville and Fiji. Contr. Mineral. and Petrol. 23, 1-26.

_____ Kaye, M., White, A.J.R., Duncan, A.R., & Ewart, A. (1969b): Genetic significance of vanadium and nickel content of andesites: reply to Prof. E.F. Osborn. Geochim. cosmochim. Acta 33, 1555-1557.

Thompson, J.E. (1952): Report on the geology of Manus Island, Territory of Papua and New Guinea, with reference to the occurrence of bauxite. Bur. Miner. Resour. Aust. Rec. 1952/82.

_____ & Fisher, N.H. (1965): Mineral deposits of New Guinea and Papua and their tectonic setting. 8th Comm. Min. Met. Congress Procs. 6, 115-148.

Tilling, R.I. (1973): Boulder Batholith, Montana: a product of two contemporaneous but chemically distinct magma series. Bull. geol. Soc. Am. 84, 3879-3900.

Titley, S.R. (1966): Preface in Geology of the porphyry copper deposits, southwestern North America. Titley & Hicks, eds. Tucson, University of Arizona Press.

_____ (1972a): Intrusion, and wall rock, porphyry copper deposits. Econ. Geol. 67, 122-123.

_____ (1972b): Pre-ore environment of southwestern North America porphyry copper deposits. in 24th I.G.C., Montreal. Section 4, Mineral Deposits, 252-260.

Titley, S.R. (1973): Geological environment and characteristics of some porphyry copper deposits in the southwestern Pacific. Reprint, A.I.M.E. Ann. Mtg., March 1973.

_____ (1975): Geological characteristics and environment of some porphyry copper occurrences in the southwestern Pacific. Econ. Geol. 70, 499-514.

_____ (1975): Geological characteristics and environment of some porphyry copper occurrences in the southwestern Pacific. Econ. Geol. 70, 499-514.

Toksöz, M.N., Minear, J.W., & Julian, B.R. (1971): Temperature field and geophysical effects of a downgoing slab. J. Geophys. Res. 76, 1113-1138.

Ustiyev, E.K. (1970): Relations between volcanism and plutonism at different stages of the tectonomagmatic cycle. in Mechanism of Igneous Intrusion. Newall & Rast, eds. Geol. Jour. Spec. Issue 2, 1-22.

Vejnar, Z. (1975): Hornblendes and problems of recrystallization of gabbroic rocks. Lithos 8, 59-68.

Ware, N.G. (1973): Annotated computer programs for electron probe microanalysis using a lithium drifted silicon detector. Rep. Res. School Earth Sci., Australian Nat. Univ., Canberra.

Waterman, G.C. & Hamilton, R.L. (1975): The Sar Cheshmeh porphyry copper deposit. Econ. Geol. 70, 568-576.

White, A.J.R., Chappell, B.W., & Branch, C.D. (1964): Classification of granite types according to associated rocks. Abst. Aust. N.Z. Ass. Advnt. Sci. 37, Congr. Canberra.

_____ , _____, & Cleary, J.R. (1974): Geologic setting and emplacement of some Australian Palaeozoic batholiths and implications for intrusive mechanisms. Pacific Geology 8, 159-171.

White, D.E. (1968): Environments of generation of some base metal ore deposits. Econ. Geol. 63, 301-335.

Whitney, J.A. (1975a): The effects of temperature, pressure, and X_{H_2O} on the phase assemblage in four synthetic rock compositions. J. Geol. 83, 1-31.

_____ (1975b): Vapour generation in a quartz monzonite magma: a synthetic model with application to porphyry copper deposits. Econ. Geol. 70, 346-358.

Wilkinson, J.F.G. (1966): Some aspects of calc-alkali rock genesis. J. Proc. Roy. Soc. N.S.W. 99, 69-77.

_____, Vernon, R.H., & Shaw, S.E. (1964): The petrology of

an adamellite-porphyrite from the New England Batholith (N.S.W.). J. Petrology 5, 461-488.

Winkler, H.G.F. (1967): Petrogenesis of metamorphic rocks. Springer-Verlag, New York.

Wones, D.R. (1966): Mineralogical indicators of relative oxidation states of magmatic systems. Trans. Am. geophys. Un. 47, 216.

Wright, J.B. & McCurrey, P. (1973): Magmas, mineralization and sea-floor spreading. Geol. Rndsh. 62, 116-126.

Wright, P.C. (1968a): The pyroxene diorite intrusion of Mt. Kanekolo, central east New Georgia. Geol. Rec. Br. Solomon Isl. 3, 41-46.

_____ (1968b): Central Guadalcanal - the geology of the Ngalimbiu and Tangareso River systems. Geol. Rec. Br. Solomon Isl. 3, 37-39.

Wyllie, P.J. (1971a): The dynamic Earth: textbook in geosciences. John Wiley & Sons, New York.

_____ (1971b): Experimental limits for melting in the Earth's crust and upper mantle. in The Structure and Physical Properties of the Earth's Crust, Geophys. Monogr. Series 14, 279-300, A.G.U. Washington, D.C.

APPENDIX 1 : LIST OF ANALYZED SPECIMENS.

Laboratory number.	Field number.	Location.	Rock Name.	Source.	Nature of specimen.
DRM.001	72-549	Reconnaissance, Manus Is.	Pyroxene Andesite.	Courtesy Dr. R.W. Page	Outcrop
DRM.002	72-550	ditto	Dacite.	ditto	Outcrop
DRM.003	OMPD.	Frieda River prospect Western Highlands.	Plag.-h'b.(bio.) diorite porphyry.	Carpentaria Exploration Co.	Drill core
DRM.004	QQD.	ditto	K-altered plag.(-h'b.)diorite porphyry.	ditto	Drill core
DRM.005	SCD.	ditto	Plag.-h'b,(-bio.) diorite porphyry.	ditto	Drill core
DRM.006	QDP.	ditto	K-altered plag.-bio. diorite porphyry.	ditto	Drill core
DRM.007	SD.	ditto	K-altered h'b.-plag.(-qtz) diorite porphyry.	ditto	Drill core
DRM.008	21NG.0775	Mt.Michael Stock, Eastern Highlands.	Plag.-h'b. diorite porphyry.	Aust. Bureau Min.Resources	Float
DRM.009	21NG.0779	ditto	Plag.-h'b. diorite porphyry.	ditto	Float
DRM.010	21NG.0780	ditto	Plag.-h'b. diorite porphyry.	ditto	Float
DRM.011	21NG.0781	ditto	Plag.-h'b. diorite porphyry.	ditto	Float
DRM.012	Ab.526	Yuat North Batholith South Sepic/W.H.	High-K h'b.-bio.-qtz diorite.	ditto	Outcrop
DRM.013	Ab.535	ditto	High-K h'b.-bio.-qtz diorite.	ditto	Outcrop
DRM.014	Ab.537	ditto	High-K h'b.-bio.-qtz diorite.	ditto	Outcrop
DRM.015	E768406	Kunduron prospect, Yuat South Batholith, W.H.	Orbicular microgranodiorite.	Author	Outcrop
DRM.016	E768412	ditto	Biotite microgranodiorite.	ditto	Outcrop
DRM.017	E768413	ditto	Biotite granodiorite.	ditto	Outcrop
DRM.018	E768430	ditto	Plag.-h'b.(-qtz) diorite porphyry	ditto	Outcrop
DRM.019	E768456	ditto	H'b.-bio.-qtz granodiorite.	ditto	Outcrop
DRM.020	E768459	ditto	Plag.-h'b.diorite porphyry.	ditto	Outcrop
DRM.021	E778066	Lumoro prospect, Yuat South Batholith, W.H.	Hornblende gabbro	ditto	Outcrop
DRM.022	E778067	ditto	Plag.(-h'b-qtz) granodiorite porphyry.	ditto	Outcrop
DRM.023	E778070	ditto	Hornblende (-clinopyroxene)diorite.	ditto	Float
DRM.024	E778072	ditto	Hornblende (-qtz) diorite.	ditto	Float
DRM.025	E778076	ditto	Hornblende-biotite-qtz granodiorite.	ditto	Outcrop
DRM.026	E778077	ditto	Dolerite.	ditto	Outcrop
DRM.027	E778036	Awari prospect, Karawari Batholith, W.H.	K-altered plag.-"h'b" diorite porphyry.	ditto	Outcrop
DRM.028	E778037	ditto	Hornblende leucogabbro	ditto	Outcrop
DRM.029	E778038	ditto	Uralite gabbro	ditto	Outcrop
DRM.030	E778095	ditto	Low-Si h'b.-plag.(-qtz) diorite porphyry.	ditto	Outcrop
DRM.031	E778098	ditto	Qtz-plag.(h'b.)granodiorite porphyry	ditto	Float
DRM.032	E778115	Onong Ck., Karawari Batholith, W.H.	Aplite porphyry.	ditto	Float
DRM.033	E778118	ditto	Basaltic dyke-rock.	ditto	Outcrop
DRM.034	E778120	ditto	Hornblende(-biotite) tonalite	ditto	Float
DRM.035	E778121	ditto	Hornblende(-clinopyroxene)-qtz diorite.	ditto	Float
DRM.036	MDH2/#7	Awari prospect, Karawari Batholith, W.H.	Plag.-"h'b"(-qtz) diorite porphyry.	ditto	Drill core
DRM.037	MDH2/#12	ditto	Plag.-"h'b"(-qtz) diorite porphyry.	ditto	Drill core
DRM.038	E768030	Mount Pugent Stock, W.H.	Pyroxene Gabbro.	ditto	Float
DRM.039	E768047	ditto	Pyroxene Microsyenite.	ditto	Float
DRM.040	E768057	ditto	Pyroxene-biotite microsyenite	ditto	Float
DRM.041	E781195	Yuat North Batholith South Sepic/W.H.	Tremolitised h'b.(-bio.) grano-diorite.	International Nickel (Aust.) Ltd.	Float
DRM.042	E781712	ditto	Hornblende-qtz granodiorite.	ditto	Float
DRM.043	No specimen.	--	--	--	--
DRM.044	E781769	Baeambo Ck., Yuat South Batholith, W.H.	H'b.-bio.-qtz granodiorite.	Author	Float
DRM.045	E781797	ditto	H'b.-bio.-qtz granodiorite.	ditto	Float
DRM.046	E781831	Lamant Stock, W.H.	Porphyritic (h'b.-cpx.) gabbro.	ditto	Outcrop
DRM.047	E781863	ditto	Porphyritic (h'b.-cpx.) gabbro.	ditto	Float
DRM.048	E781887	Wale Stock, W.H.	Hornblende-clinopyroxene leucogabbro	ditto	Float
DRM.049	E781898	ditto	Hornblende microgabbro.	ditto	Float
DRM.050	E781915	ditto	Clinopyroxene-olivine ultramafic cumulate.	ditto	Float

APPENDIX 1: LIST OF ANALYZED SPECIMENS. cont.

Laboratory number.	Field number.	Location.	Rock Name.	Source.	Nature of specimen.
DRM.051	E782268	Yuat Sth Batholith, Western Highlands.	High-K h'b.-bio.-qtz diorite.	Author	Outcrop
DRM.052	E782287	ditto	Hornblende(-cpx.-qtz) gabbro.	ditto	Outcrop
DRM.053	E782291	ditto	Plag.-h'b. diorite porphyry.	ditto	Float
DRM.054	E782315	ditto	Hornblende(-cpx.-qtz) gabbro.	ditto	Float
DRM.055	E782395	ditto	Pegmatitic hornblende gabbro.	ditto	Float
DRM.056	E782648	Yuat North Batholith, South Sepik/ W.H.	Biotite-hornblende microadamellite	ditto	Float
DRM.057	E782926	Sekau Stock,Sth Sepic/ Western Highlands.	Hornblende gabbro.	ditto	Float
DRM.058	E782935	ditto	High-K h'b.-bio.-qtz diorite.	ditto	Float
DRM.059	E782939	ditto	Low-Si. h'b. diorite.	ditto	Float
DRM.060	E782966	ditto	Serpentinized peridotite (lherzolite).	ditto	Float
DRM.061	E782974	ditto	Hornblendite.	ditto	Outcrop
DRM.062	E782993	ditto	Hornblende gabbro.	ditto	Outcrop
DRM.063	Ab.520(A)	Yuat North Batholith South Sepik/ W.H.	Orthoclase gabbro	Aust.Bureau Min. Resources	Outcrop?
DRM.064	Ab.520(B)	ditto	High-K hornblende microdiorite.	ditto	Outcrop?
DRM.065	Ab.558	Karawari Batholith, Western Highlands.	Hornblende (-cpx.) gabbro.	ditto	Float?
DRM.066	Ab.559	ditto	High-K cpx.-h'b.-orthoclase diorite.	ditto	Float?
DRM.067	65-49-0511	Reconnaissance, Panguna region, Bougainville Island.	Plag.-h'b. diorite porphyry.	ditto	Float?
DRM.068	65-49-1064	Reconnaissance,Puspa, Bougainville Island.	Cpx.-bio.-qtz syenite	ditto	Float?
DRM.069	65-49-1212 (A)	S.E. of Mt.Takuan, Bougainville Island.	Low-Si 2px.-h'b.-bio. microdiorite	ditto	Outcrop
DRM.070	70/5980	Panguna region, Bougainville Island.	K-altered "Biotite Diorite".	Courtesy Dr.R.W. Page.	Core
DRM.071	70/5982	ditto	K-altered,porphyritic "Biotite Diorite"	ditto	Core
DRM.072	70/5983	ditto	Sericite, chlor.-alt'd "Biotite Granodiorite".	ditto	Core
DRM.073	70/5984	ditto	Sericite,chlor.-alt'd "Biotite Granodiorite".	ditto	Core
DRM.074	70/5988	ditto	Chlor.-alt'd "Biuro Granodiorite".	ditto	Core
DRM.075	70/5990	ditto	"Panguna Andesite".	ditto	Outcrop?
DRM.076	70/5993	ditto	Altered "Panguna Andesite".	ditto	Core
DRM.077	70/6002	ditto	"Nautango Andesite".	ditto	Outcrop
DRM.078	70/6003	ditto	"Kaverong Quartz Diorite".	ditto	Outcrop
DRM.079	70/6005	ditto	Porphyritic "Kaverong Qtz. Diorite".	ditto	Outcrop
DRM.080	7152-1862	Frieda Prospect (11km. NW.), W.H.	"Quartz diorite porphyry".	Aust.Bureau Min.Resources.	Outcrop
DRM.081	7152-2514	ditto	"Nena Diorite".	ditto	Outcrop
DRM.082	70/6009	Ok Tedi prospect W.H.	K-altered plag.--K-felds latite porphyry.	Courtesy Dr.R.W. Page.	Core
DRM.083	70/6010	ditto	K-altered plag.--K-felds latite porphyry.	ditto	Core
DRM.084	70/6011	ditto	High-K H'b.(-bio) diorite.	ditto	Core
DRM.085	70/6012	ditto	K-altered plag.--K-felds latite porphyry.	ditto	Core
DRM.086	70/6013	ditto	K-altered K-felds-plag. latite porphyry.	ditto	Core
DRM.087	DDH.29	ditto	High-K Cpx.-h'b. diorite.	Kennecott Expor.(Aust.) Ltd.	Drill core
DRM.088	CHIK.1	Chikora prospect, Koloula Complex, Guadalcanal Is., B.S.I.P.	Hornblende-biotite granodiorite.	Author	Outcrop
DRM.089	CHIK.2	ditto	Aplite dyke.	ditto	Outcrop
DRM.090	CHIK.3	ditto	Hornblende-biotite granodiorite.	ditto	Outcrop
DRM.091	CHIK.4	ditto	Plag.-h'b.-qtz diorite porphyry. (Xenolith in CHIK.5).	ditto	Outcrop
DRM.092	CHIK.5	ditto	Hornblende-biotite granodiorite.	ditto	Outcrop
DRM.093	CHIK.7	ditto	2 pyroxene gabbro.	ditto	Outcrop
DRM.094	CHIK.8	ditto	2 pyroxene (-h'b) gabbro	ditto	Outcrop
DRM.095	CHIK.10	ditto	Aplite dyke.	ditto	Outcrop
DRM.096	CHIK.11	ditto	Porphyritic plag.-cpx(-h'b) microdiorite.	ditto	Outcrop

APPENDIX 1 : LIST OF ANALYZED SPECIMENS. cont.

Laboratory number.	Field number.	Location.	Rock name.	Source.	Nature of specimen.
DRM.097	CHIK.12	Chikora prospect, Koloula Complex, Guadalcanal IS. B.S.I.P.	Porphyritic plag.-2px-ox. microdiorite.	Author.	Outcrop
DRM.098	CHIK.14	ditto	Hornblende-biotite-qtz diorite	ditto	Outcrop
DRM.099	CHIK.15	ditto	2 pyroxene microgabbro.	ditto	Outcrop
DRM.100	CHIK.16	ditto	Hornblende-2pyroxene gabbro.	ditto	Outcrop
DRM.101	CHIK.17	ditto	Clinopyroxene (-"h'b") microgabbro.	ditto	Outcrop
DRM.102	CHIK.18	ditto	Porphyritic plag.-h'b. microdiorite.	ditto	Float
DRM.103	CHIK.19	ditto	Porphyritic plag.-h'b-cpx-qtz microdiorite.	ditto	Float
DRM.104	CHIK.20	ditto	Feldspathic olivine pyroxenite.	ditto	Float
DRM.105	CHIK.21	ditto	Feldspathic olivine pyroxenite.	ditto	Float
DRM.106	CHIK.22	ditto	Hornblende-biotite granodiorite.	ditto	Float
DRM.107	CHIK.23	ditto	2 pyroxene-h'b.-bio.-qtz.diorite.	ditto	Float
DRM.108	CHIK.25	ditto	2 pyroxene-h'b.-bio. gabbro	ditto	Float
DRM.109	CHIK.26	ditto	Clinopyroxene-h'b.(-bio) gabbro	ditto	Float
DRM.110	WIL.1	Willie ck., Mt.Kren Complex, Manus Is.	High-K h'b.(-bio.-cpx.) diorite.	ditto	Outcrop
DRM.111	WIL.5	ditto	High-K h'b.(-bio.) diorite.	ditto	Outcrop
DRM.112	WIL.6	ditto	Hornblende-quartz diorite.	ditto	Outcrop
DRM.113	WIL.10	ditto	High-K porphyritic cpx.-plag.-h'b. microdiorite.	ditto	Outcrop
DRM.114	RH.3A	Road hole 3A,250', Mt.Kren Complex, Manus Is.	High-K h'b.-bio. diorite.	ditto	Drill core
DRM.115	RH.3A	Road hole 3A,342', Mt.Kren Complex, Manus Is.	High-K h'b.(-bio.) diorite.	ditto	Drill core
DRM.116	RH.9	Road hole 9,260', Mt.Kren Complex, Manus Is.	Hornblende microgabbro (?xenolith).	ditto	Drill core
DRM.117	RH.9	Road hole 9, 280', Mt.Kren Complex, Manus Is.	High-K h'b (-bio) diorite.	Author	Drill core
DRM.118	WAM.3	Wamuick ck., Mt.Kren Complex, Manus Is.	High-K h'b-cpx. diorite.	ditto	Outcrop
DRM.119	WAM.4	ditto	High-K h'b. diorite.	ditto	Outcrop
DRM.120	P1	Mount Kren Complex, Manus Is.	Low-Si Porphyritic plag.-h'b-qtz microdiorite.	ditto	Outcrop
DRM.121	P2	ditto	High-K h'b. diorite.	ditto	Outcrop
DRM.122	J196	ditto	Clinopyroxene (-"h'b".) microdiorite.	ditto	Outcrop
DRM.125	PAN.1(B)	Panguna,Bougainville Is.	"Nautango Andesite". (Porphyritic h'b-plag.-cpx low-Si andesite.)	ditto	Outcrop
DRM.124	PAN.3	ditto	"Kaverong Quartz Diorite". (H'b-cpx diorite.)	ditto	Outcrop
DRM 125	PAN.8	ditto	"Leucocratic Quartz Diorite". (Altered quartz diorite).	ditto	Outcrop
DRM.126	PAN.11	ditto	Porphyritic plag.-h'b. microdiorite.	ditto	Float
DRM.127	PAN.12	ditto	Hornblende-clinopyroxene microdiorite.	ditto	Float
DRM.128	LEM.7	Lemau Intrusives, S.E. of Lemau Village, New Ireland.	Uralite gabbro.	ditto	Float
DRM.129	LEM.9	ditto	2 pyroxene-bio.(-h'b)-qtz. diorite.	ditto	Float
DRM.130	LEM.10	ditto	Clinopyroxene (-bio.)-qtz diorite.	ditto	Float
DRM.131	LEM.12	ditto	Plagioclase-hornblende diorite porphyry.	ditto	Float
DRM.132	LEM.15	ditto	2 pyroxene (-h'b) granodiorite.	ditto	Float?
DRM.133	MET.4	Metelen Intrusives, Plesyumi prospect, Upper Metelen River, New Britain.	Propylitic-altered "h'b"-qtz granodiorite.	ditto	Outcrop
DRM.134	MET.6	ditto	Hornblende-biotite granodiorite.	ditto	Outcrop
DRM.135	MET.7	ditto	Hornblende-biotite-quartz diorite.	ditto	Float
DRM.136	MET.8	ditto	Hornblende-biotite granodiorite.	ditto	Float
DRM.137	MET.9	ditto	High-K biotite-clinopyroxene(-h'b) diorite.	ditto	Float
DRM.138	MET.10	ditto	2 pyroxene-h'b(-bio) diorite.	ditto	Float
DRM.139	MET.11	ditto	HighK h'b.-bio.-qtz(-cpx) diorite	ditto	Float
DRM.140	MET.12	ditto	Clinopyroxene-h'b-qtz gabbro	ditto	Float
DRM.141	MET.13	ditto	Porphyritic olivine-cpx. gabbro.	ditto	Float
DRM.142	MET.16	ditto	Plag.-"h'b"-qtz dacite porphyry.	ditto	Outcrop
DRM.143	5647	Limbo River Diorite, New Georgia Is., B.S.I.P.	"H'b."-bio.(-cpx) microdiorite	H.M.Geological Survey, B.S.I.P.	Not known

APPENDIX 1: LIST OF ANALYZED SPECIMENS. cont.

Laboratory number.	Field number	Location.	Rock name.	Source.	Nature of specimen.
DRM.144	5661	Limbo River Diorite, New Georgia Is., B.S.I.P.	H'b-cpx.-bio. microdiorite	H.M. Geological Survey, B.S.I.P.	Not known
DRM.145	5663	ditto	2 Pyroxene-bio.(-h'b) gabbro	ditto	Not known
DRM.146	9306	Poha River Diorite, Guadalcanal Is. B.S.I.P.	H'b.-qtz-"bio". diorite	ditto	Not known
DRM.147	9429	ditto	Hornblende leucogabbro	ditto	Not known
DRM.148	E778010	Awari prospect, Karawari Batholith, Western Highlands.	Tremolitised basaltic lava.	Author	Outcrop
DRM.149	E778024	ditto	Tremolitised basaltic lava.	ditto	Outcrop
DRM.150	E778061	ditto	Tremolitised basaltic tuffaceous volcanic.	ditto	Outcrop
DRM.151	E778020	ditto	Partially serpentinised dunite.	ditto	Outcrop
DRM.152	E778047	ditto	Serpentinised harzburgite.	ditto	Outcrop
DRM.153	E778050	ditto	Partially serpentinised harzburgite.	ditto	Outcrop
DRM.154	E778057	ditto	Partially serpentinised harzburgite.	ditto	Outcrop
DRM.155	E778060	ditto	Partially serpentinised dunite.	ditto	Outcrop
DRM.156	E778004	Lumoro prospect, Yuat Sth Batholith, W.H.	K-altered granodiorite.	ditto	Outcrop
DRM.157	E778003	ditto	Propylitic-altered granodiorite.	ditto	Outcrop
DRM.158	DDH.28(B)	Ok Tedi prospect, Western Highlands.	K-altered plag.-K-spar latite porphyry.	Kennecott Explor.(Aust.)Ltd.	Drill core
DRM.159	DDH.33	ditto	K-altered alaskite.	ditto	Drill core
DRM.160	DDH.34	ditto	K-altered plag.-Kspar latite porphyry.	ditto	Drill core
DRM.161	DDH.38	ditto	K-altered plag.-Kspar latite porphyry.	ditto	Drill core

APPENDIX 2 - ANALYTICAL TECHNIQUES

Sample Preparation

Hand specimens were trimmed of any weathered portions, and saw marks were removed on a diamond lap. After splitting to 1 cm cubes in a hydraulic jaw splitter, 300-500 gm of specimen material were fine-ground for 2 minutes in a tungsten carbide Siebtechnic mill. Small amounts (50-60 gm) of each sample were ground in a chrome-steel mill for use in cobalt analysis.

Samples were stored in zip-top plastic bags.

Whole-rock Major Element Analysis

For specimens DRM001 - 042, 044 - 147, major element oxides of Fe (as Fe_2O_3), Mn, Ti, Ga, P, S, Si, Al and Mg were determined by X-ray fluorescence spectrometry on duplicate glass discs following the method of Norrish & Hutton (1969). The conditions for analysis are set down in Table 1(A). Values obtained for standard rocks are compared with the recommended values of Flanagan (1973) in Table 2.

Na_2O was determined in duplicate using a Baird Atomic flame photometer, with Li as an internal standard.

FeO was determined in duplicate by dissolution in HF and H_2SO_4, and titration against $K_2Cr_2O_7$. The laboratory standard was an analyzed hornblende. Ferric iron was calculated by difference.

H_2O- is the percentage loss of a sample after heating for 90 minutes at 110^oC.

H_2O^+ and CO_2 were measured by heating a sample for 30 minutes in a tube furnace at 1000-1050^oC in a stream of dry nitrogen. The H_2O and CO_2 were collected in microabsorption tubes containing a mixture of P_2O_5 and pumice, and soda asbestos.

For specimens DRM148-161, major element oxides of Fe (as FeO), Cr, Mn, Ti, Ca, K, P, Si, Al, Mg and Na were determined by microprobe analysis of whole-rock glasses, using the method described by Nicholls (1974). A comparison of XRF and microprobe analyses of six selected specimens (see Table 3) indicates the close agreement of the two methods. For this group of specimens, total loss on ignition was determined by mass difference after tube furnace heating for 30 minutes.

Whole-rock Trace Element Analysis

Duplicate analyses of samples prepared as pelletised powder discs were made employing X-ray fluorescence techniques (Norrish & Chappell,

APPENDIX 2, TABLE 1: OPERATING CONDITIONS FOR X-RAY FLUORESCENCE SPECTROMETRY

(A) MAJOR ELEMENTS

Machine: Philips PW1220, Research School of Earth Sciences, A.N.U., Canberra

Analysts: P.H. Beasley, D.R. Mason

ELEMENTS	LINE	TIME ON PEAK(secs)	TIME ON BKG(secs)	CRYSTAL	COLLIMATOR	DETECTOR	X-RAY TUBE Target	kV	mA	VACUUM
Fe	Fe Kα	40	-	LiF(200)	Coarse	Flow	Cr	50	32	Yes
Ti	Ti Kα	40	-	LiF(200)	"	"	"	40	20	"
Ca	Ca Kα	40	-	LiF(200)	"	"	"	40	16	"
K	K Kα	40	-	LiF(200)	"	"	"	40	16	"
S	S Kα	100	-	Ge	"	"	"	50	32	"
P	P Kα	100	-	Ge	"	"	"	50	32	"
Si	Si Kα	100	-	PE	"	"	"	50	32	"
Al	Al Kα	100	-	PE	"	"	"	50	32	"
Mn	Mn Kα	20	-	LiF(200)	"	Scint	W	50	30	No
Mg	Mg Kα	200	-	ADP	"	Flow	Cr	50	36	Yes

(B) TRACE ELEMENTS

Machine: Philips PW1220, Geology Department, A.N.U., Canberra

Analysts: R.S. Freeman, D.R. Mason

ELEMENTS	LINE	BKG 2θ (±degrees)	TIME ON PEAK(secs)	TIME ON BKG(secs)	CRYSTAL	COLLIMATOR	DETECTOR	X-RAY TUBE Type	kV	mA	Kα MASS ABSORPTION	VACUUM	NOTES
Rb	Rb Kα	.38	100/40	40/20	LiF(220)	Coarse	Scint	Mo	85/80	35/35	Rb	No	Two runs (Sept. 1973/June 1974)
Sr	Sr Kα	.35	100/40	40/20	LiF(200)	"	"	"	" / "	" / "	Sr	"	ditto
Y	Y Kα	.40	100/40	40/20	"	"	"	"	" / "	" / "	Sr	"	ditto
Pb	Pb Lβ	.23	100/100	40/40	"	Fine	"	"	" / "	" / "	Rb	"	ditto
Th	Th Lα	.23	100	40	"	"	"	"	85	35	Rb	"	One run (June 1974)
U	U Lα	.25	200	100	LiF(220)	"	"	"	"	"	Rb	"	ditto
Zr	Zr Kα	.40	100/100	40/40	LiF(200)	Coarse	"	Au	67/75	30/30	Sr	"	Two runs (Sept. 1973/June 1974)
Nb	Nb Kα	.35	100/200	40/100	"	Fine	"	"	" / "	" / "	Sr	"	ditto
Ti*	Ti Kα	.60	20	10	"	"	Flow	W	55	36	-	Yes	*determined only for interference effects; one run (Oct. 1974)
V	V Kα	1.75	100	40	LiF(220)	"	"	"	"	"	Fe	"	One run (Oct. 1974)
Cr*	Cr Kα	.90	200	100	LiF(200)	"	"	"	"	"	-	"	*determined only for interference effects
Ba	Ba Lβ	1.20	100	40	LiF(220)	Coarse	"	"	"	"	Fe	"	Assymetrical window
La	La Lα	1.25	200	100	"	"	"	"	"	"	Fe	"	
Ce	Ce Lβ	1.20	200	100	LiF(200)	Fine	"	"	"	"	Fe	"	
Fe*	Fe Kα	.45	20	10	LiF(220)	Coarse	Scint	Au	55	50	-	"	*determined only for interference efffects. One run (July-Aug., 1974)
Co	Co Kα	.40	100	100	"	"	"	"	"	"	Fe	"	Measured on sample ground in Co-free mill.
Ni	Ni Kα	.40	100	40	"	"	"	"	"	"	Zn	"	
Cu	Cu Kα	.40	100	40	"	"	"	"	"	"	Zn	"	
Zn	Zn Kα	.40	100	40	"	"	"	"	"	"	Zn	"	

APPENDIX 2, TABLE 2: XRF MAJOR ELEMENT ANALYSES OF STANDARD ROCKS

	USGS-W-1		USGS-AGV-1		USGS-BCR-1		USGS-GSP-1		USGS-PCC-1	
	XRF	Flanagan (1973)	XRF	Flanagan (1973)	XRF	Flanagan (1973)	XRF	Flanagan (1973)	XRF	Flanagan (1973)
% SiO_2	52.35	52.64	59.22	59.00	54.66	54.50	67.38	67.38	40.75	41.90
TiO_2	1.08	1.07	1.05	1.04	2.24	2.20	.66	.66	.005	.015
Al_2O_3	14.93	15.00	17.05	17.25	13.50	13.61	15.13	15.25	.61	.74
sum Fe_2O_3	11.05	11.09	6.69	6.76	13.40	13.40	4.25	4.33	8.33	8.35
CaO	10.90	10.96	4.95	4.90	6.99	6.92	2.03	2.02	.53	.51
K_2O	.65	.64	2.95	2.89	1.73	1.70	5.52	5.53	-.004	.004
P_2O_5	.14	.14	.52	.49	.39	.36	.30	.28	.001	.002
SO_3	.024	.036	.008	<.003	.08	.12	.20	.049	-.032	<.003

APPENDIX 2, TABLE 3: COMPARISON OF XRF AND PROBE MAJOR ELEMENT ANALYSES FOR SELECTED ROCKS

	DRM.013			DRM.029			DRM.042			DRM.114			DRM.120			DRM.146		
	XRF	PROBE		XRF	PROBE		XRF	PROBE		XRF	PROBE		XRF	PROBE		XRF	PROBE	
		2/3*	± 1s.d.		2/5	± 1 s.d.		1/2	± 1 s.d.		2/5	± 1 s.d.		2/6	± 1 s.d.		1/2	± 1 s.d.
$\%SiO_2$	63.99**	63.3	.6	52.29	52.50	.2	65.27	63.6	.4	63.17	63.4	1.1	52.92	52.6	.2	63.92	63.4	.8
TiO_2	0.69	0.7	.1	0.25	0.13	.05	0.66	0.55	.06	0.51	0.46	.02	0.72	0.64	.02	0.43	0.39	.02
Al_2O_3	16.30	16.7	.2	10.64	10.48	.06	17.26	18.3	.2	17.37	17.3	.5	17.03	17.1	.1	16.71	16.9	.3
ΣFeO	5.10	5.27	.07	6.97	7.3	.1	3.10	3.28	.01	4.42	4.4	.2	8.92	9.3	.1	5.65	5.86	.06
MnO	0.10	0.00		0.14	0.00		0.06	0.00		0.04	0.00		0.09	0.00		0.03	0.00	
MgO	2.17	2.49	.07	15.58	15.47	.06	2.09	2.65	.01	2.59	2.7	.1	6.57	6.7	.1	2.80	3.00	.01
CaO	4.86	4.72	.06	12.13	12.25	.02	7.36	7.44	.08	5.26	5.1	.2	10.37	10.22	.02	5.66	5.5	.1
Na_2O#	3.77	3.8	.2	0.94	0.86	.08	3.80	3.8	.1	4.54	4.3	.2	3.12	3.1	.1	3.63	3.5	.1
K_2O	3.11	3.06	.07	0.90	0.81	.05	0.46	0.42	.03	2.13	2.42	.1	0.36	0.40	.01	1.21	1.40	.01

All Na_2O values determined by flame photometry

* Number of glasses/Number of spot analyses

**XRF analyses recalculated 100% anhydrous.

APPENDIX 2, TABLE 4: MICROPROBE MAJOR ELEMENT ANALYSES OF STANDARD ROCK GLASSES

	USGS-AGV-1			USGS-W-1		
	Flanagan (1973)	Probe (av. of 13)	$\pm$ 1s.d.	Flanagan (1973)	Probe (av. of 15)	$\pm$ 1s.d.
$\%SiO_2$	60.84*	60.91	.07	53.14*	52.81	.3
TiO_2	1.07	1.06	.03	1.08	1.00	.05
Al_2O_3	17.79	17.70	.04	15.14	15.48	.1
ΣFeO	6.29	6.33	.06	10.07	10.11	.1
MgO	1.58	1.75	.03	6.68	6.71	.07
CaO	5.05	4.99	.04	11.07	10.93	.03
Na_2O	4.39	4.31	.08	2.17	2.23	.07
K_2O	2.98	2.94	.03	.65	.67	.02
	99.99	99.99		100.00	99.94	

* Recommended values of Flanagan (1973) re-calculated to 100% anhydrous.

APPENDIX 2, TABLE 5: MICROPROBE ANALYSES OF CLINOPYROXENE STANDARD (DELEGATE CLINOPYROXENE)

	AVE. of 5	± 1 s.d.	Recommended (Reed & Ware 1973)
$\%SiO_2$	52.0	.1	51.00
TiO_2	0.43	.02	0.35
Al_2O_3	5.07	.04	5.42
Cr_2O_3	0.80	.04	0.82
sum FeO	4.13	.05	3.94
MnO	0.00		<0.12
MgO	15.81	.06	15.85
CaO	21.1	.2	21.42
Na_2O	0.68	.04	0.89
K_2O	0.00		<0.06
total	100.02		99.87

1967). Machine operating conditions for those elements sought are presented in Table 1(B). All intensities were corrected for detector dead time, and instrument drift was checked against an internal standard. A correction for inter-element interferences was applied, and background intensities were corrected for non-linearity.

For each sample, the attenuated-beam method (Chappell, unpub. manuscript) was used to measure mass absorption coefficients for Sr Kα, Rb Kα, Zn Kα, and Fe Kα wavelengths

Concurrent analysis of standard rocks gave trace element abundances in good agreement with values determined previously in the Geology Department laboratory.

Mineral Major Element Analyais

Mineral major element analyses were made using a TPD electron microprobe in the Research School of Earth Sciences, A.N.U. Specimens were prepared as carbon-coated polished sections or polished thin sections.

Analytical conditions were: accelerating voltage 15 kV, beam current 3 nA, beam diameter 2 μm, counting period 100 sec, at a total count rate of ∿4000 cps. Up to 10 elements were determined simultaneously. The application of instrumental corrections (dead time, background, overlap of analytical lines) and matrix corrections have been summarized by Reed & Ware (1973). Data reduction was applied at the time of analysis using computer programs of Ware (1973).

Analyses of standard rock glasses and a standard pyroxene are compared with preferred analyses in Tables 4 and 5.

APPENDIX 3 OPTICALLY ESTIMATED MODES FOR ANALYZED INTRUSIVE ROCKS

Optically estimated modal compositions are given here for all analyzed intrusive rock specimens. Because many of the specimens used in this study were small in size, point counting on rock slabs was precluded. All modes are given in 'volume percent', and the error is estimated to be approximately ±3% for a mineral abundance of 20%.

The modes have been arranged in locality groups, ordered according to their treatment in Chapters 2 and 3. Within each group, rocks are ordered according to increasing specimen number.

The following abbreviations apply throughout the mode tables:

QTZ	quartz
PLAG	plagioclase
KF	alkali feldspar
HB	hornblende
BIO	biotite
CPX	clinopyroxene
OPX	orthopyroxene
OX	opaque (Fe, Ti) oxides
SULFS	sulfides (as observed in hand specimen)
tr	trace
-	not observed
trem./act.	tremolite/actinolite
Py	pyrite
Cpy	chalcopyrite
Mo	molybdenite
Po	pyrrhotite
mal	malachite
Born	bornite

APPENDIX 3-1 : MODES FOR YUAT NORTH BATHOLITH.

(all figures are volume percent)

Specimen Number.	Rock Name.	QTZ.	PLAG.	KF.	HB.	BIO.	CPX.	OPX.	OX.	SULFS.	Remarks.
DRM.012	High-K hornblende-biotite-Quartz diorite.	20	35	20	10	10	2	tr.	3	tr.	Accessories zircon,apatite;chlorite in biotite; trace Cpy.
DRM.013	ditto	15	40	25	6	9	1	-	2	tr.	Accessory apatite; chlorite in biotite with trace sphene; cpy.
DRM.014	ditto	15	40	25	9	6	2	-	2	-	Accessory zircon, apatite; chlorite in biotite.
DRM.041	Tremolitised hornblende (-biotite) granodiorite.	12	60	8	15	tr.	-	-	3	tr.	Accessory apatite; hornblende replaced by trem./act., chlorite, epidote.
DRM.042	Hornblende-quartz granodiorite.	20	60	8	10	-	-	-	3	tr.	Accessory zircon, chlorite.
DRM.056	Biotite-hornblende micro adamellite.	25	35	25	5	8	-	-	2	-	Trace sericite in feldspar; chlorite in biotite.
DRM.063	Orthoclase gabbro.	-	10	15	5	15	50	-	3	-	Trace sericite in plagioclase; accessory apatite, sphene.
DRM.064	High-K hornblende microdiorite.	15	45	15	25	-	-	-			Trace chlorite, epidote, carbonate.

APPENDIX 3-2: MODES FOR YUAT SOUTH BATHOLITH.

DRM.015	Orbicular microgranodiorite	20	55	-	-	5	-	-	-	3	Altered orbs (+20% white mica).
		20	70	tr.	-	10	-	-	tr.	2	Ground mass (+tr.white mica).Py,Cpy,Mo
DRM.016	Biotite microgranodiorite.	25	50	12	-	8	-	-	2	2	Tr. chlorite, white mica in biotite. Accessory apatite.
DRM.017	Hornblende-biotite granodiorite.	No thin section available.									
DRM.018	Plagioclase-hornblende (quartz) diorite porphyry.	8	10	-	8	1	-	-	2	-	Phenocrysts.
		----48------			15	-	-	-	2	tr.	Ground mass: Accessory sphene, zircon, Cpy.
DRM.019	Hornblende-biotite-quartz granodiorite.	25	40	15	8	7	-	-	2	tr.	Trace chlorite, sericite. Accessory apatite; sphene (1%).
DRM.020	Plagioclase-hornblende(-quartz) diorite porphyry.	1	10	-	20	1	-	-	3	-	Phenocrysts.
		----60-----			5	-	-	-	2	2	Ground mass: Py, Cpy.
DRM.021	Hornblende gabbro	-	50	-	43	-	-	-	7	-	Trace tre./act.
DRM.022	Plagioclase (-hornblende-quartz) granadiorite porphyry.	3	20	-	6	-	-	-	3	-	Phenocrysts: Trace chlorite, epidote.
		----68------			-	-	-	-	tr.	1	Ground mass: Py.
DRM.023	Hornblende(-clinopyroxene) diorite.	5	60	-	25	-	3	-	6	-	
DRM.024	Hornblende(-quartz) diorite.	8	64	3	20	-	-	-	4	tr.	Accessory sphene, Py.
DRM.025	Hornblende-biotite-quartz granodiorite.	25	43	15	8	5	-	-	2	tr.	Accessory sphene, apatite, zircon. Tr. Py, Cpy.
DRM.026	Dolerite (country rock).	-	50	-	40	-	-	-	8	-	Pyroxene altered to trem./act. Accessory apatite.
DRM.044	Hornblende-biotite-quartz granodiorite.	20	50	8	10	10	-	-	1	1	Accessory zircon. Py, Cpy.
DRM.045	ditto	25	50	5	10	8	-	-	2	1	10% chlorite in hb, bio. Accessory apatite, sphene. Py.
DRM.051	High-K hornblende-biotite-quartz diorite.	20	28	15	15	15	2	-	3	1	Accessory apatite, Py, Cpy.
DRM.052	Hornblende (clinopyroxene-quartz) gabbro.	1	67	-	25	-	2	-	3	-	Accessory sphene, Trace calcite, chlorite.
DRM.053	Plagioclase-hornblende diorite porphyry.	-	25	-	15	-	-	-	1	-	Phenocrysts:Tr.chlorite,trem/act,sphene
		5	---40---		15	-	-	-	4	tr.	Groundmass: Po. Accessory sphene.
DRM.054	Hornblende(-clinopyroxene-quartz) gabbro.	5	47	-	40	-	tr.	-	5	2	Trace chlorite, epidote. Accessory apatite, Cpy, Py.
DRM.055	Pegmatitic hornblende gabbro.	-	30	-	70	-	-	-	tr.	-	Trace chlorite, epidote.
DRM.156	K-altered granodiorite.	No thin section available.									cf. DRM.025;abundant clay alteration of feldspars; quartz-Kfelds.veins;Cpy.
DRM.157	Propylitic-altered granodiorite.	15	40	15	10	-	-	-	2	tr.	cf. DRM.025; 20% chlorite, epidote. Accessory apatite, sphene; Cpy.

APPENDIX 3-3 : MODES FOR KARAWARI BATHOLITH.

Specimen Number.	Rock Name.	QTZ.	PLAG.	KF.	HB.	BIO.	CPX.	OPX.	OX.	SULFS.	Remarks.
DRM.027	K-altered plagioclase-hornblende diorite porphyry.	- 8	30 ---40---	-	- -	15 5	- -	- -	- 2	- 4	Phenocrysts: Tr. sericite in plag. Groundmass: H'b replaced by biotite flakes. Py, Cpy.
DRM.028	Hornblende leucogabbro.	-	65	-	35	-	-	-	-	2	Abundant sericite in plag; trem./act. in h'b; Py.
DRM.029	Uralite gabbro.	-	30	-	-	-	65	-	5	tr.	Trem./act. replaces cpx. tr. Py, Cpy. Mode variable.
DRM.030	Low-Si hornblende-plagioclase (-quartz) diorite porphyry.	2 tr.	10 45	- tr.	20 20	-	-	-	2 1	- 2	Phenocrysts: Tr.sericite in plag; Trem/act. in h'b. Groundmass: Accessory zircon; Py.
DRM.031	Quartz-plagioclase(-h'b.) granodiorite porphyry.	15 -----53------	20	-	10 tr.	- -	- -	- -	- 2	- 1	Phenocrysts: Trem./act. and sphene in h'b. Groundmass: Accessory sphene; apatite. Py.
DRM.032	Quartz-plagioclase aplite porphyry.	30 -----40------	25	-	1 -	2 -	- -	- -	- 1	- -	Phenocrysts. Groundmass: Accessory zircon.
DRM.033	Basaltic dyke rock.	- -	- 40	-	- 40	-	15 -	- -	- 2	- -	Phenocrysts: Trem./act. in cpx;tr. chlorite. Groundmass.
DRM.034	Hornblende(-biotite) tonalite.	12	70	5	8	1	-	-	2	-	Accessory zircon, sphene; tr.chlorite.
DRM.035	Hornblende(-clinopyroxene) -quartz diorite.	15	60	5	15	-	2	-	2	-	Accessory sphene, apatite. Trace trem./act. in cpx.
DRM.036	Plagioclase-hornblende(-quartz)diorite porphyry.	1 ----45-----	35	-	15 tr.	- -	- -	- -	- 2	- 2	Phenocrysts: Trem./act., chlorite, sphene in h'b. Groundmass: Accessory apatite, zircon.
DRM.037	ditto	2 ----55-----	30	-	10 tr.	- -	- -	- -	- 1	- 2	Phenocrysts: Trem./act., chlorite, epidote, sphene in h'b.Groundmass: Accessory sphene.
DRM.065	Hornblende(-clinopyroxene) gabbro.	-	60	-	35	-	2	-	3	-	Tr.epidote. Accessory apatite.
DRM.066	High-K clinopyroxene-hornblende diorite.	5	48	20	5	-	10	-	4	-	5%chlor. in cpx; 2% ox.in cpx. Accessory apatite.

APPENDIX 3-4 : MODES FOR WALE AND LAMANT STOCKS.

DRM.046	Porphyritic hornblende-clinopyroxene gabbro.	- 5	- 52	-	30 -	-	10 -	-	3 -	- 3	Phenocrysts: Cpx cores in h'b. Groundmass: Accessory sphene, Py.
DRM.047	ditto	- 3	- 55	-	- 30	- tr.	10 -	- -	- 2	- tr.	Phenocrysts: H'b rims on cpx. Groundmass: Accessory sphene, Py.
DRM.048	Hornblende-clinopyroxene leucogabbro.	-	68	-	12	-	10	-	5	tr.	Trace epidote, Py, Cpy
DRM.049	Hornblende microgabbro	-	40	-	58	-	-	-	2	3	Trem./act. in h'b. Accessory Py,Cpy.
DRM.050	Olivine pyroxenite.	-	1	-	tr.	-	82	-	2	-	Bowlingite in olivine (8%). Trace chlorite, sericite.

APPENDIX 3-5 : MODES FOR SEKAU STOCK.

DRM.057	Hornblende gabbro	-	42	-	55	-	-	-	2	tr.	Sericite in plagioclase; Accessory sphene, Py, Cpy.
DRM.058	High-K hornblende-biotite-quartz diorite.	12	46	15	15	5	3	-	2	-	Trace chlorite in biotite. Accessory apatite, sphene.
DRM.059	Low-Si hornblende diorite.	5	60	10	20	-	-	-	tr.	tr.	3% chlorite, epidote in h'b. Accessory sphene.
DRM.061	Hornblendite.	-	8	-	90	-	-	-	tr.	-	Sericite in plag; tr.epidote in h'b. Accessory sphene, apatite; chlorite.
DRM.062	Hornblende gabbro.	-	37	-	60	-	-	-	1	-	Accessory sphene (2%).

APPENDIX 3-6 : MODES FOR MOUNT MICHAEL STOCK.

DRM.008	Plagioclase-hornblende diorite porphyry	- 2	35 ---30---	-	30 -	-	-	-	4 -	- -	Phenocrysts. Groundmass: Traces chlorite, calcite.
DRM.009	ditto	- ---	30 40 -----	-	25 -	-	-	-	4 -	- -	Phenocrysts: Trem./act. in h'b. Groundmass: Traces calcite, apatite.
DRM.010	ditto	- 5	40 ----25---	-	25 -	-	-	-	2 -	- -	Phenocrysts: Trace sericite.Groundmass: Apatite, sphene,zircon,calcite,chlor.
DRM.011	ditto	- 4	30 ----42---	-	20 -	-	-	-	1 -	- 2	Phenocrysts: Large sphene, apatite.; sericite. Groundmass: Traces calcite, chlorite.

APPENDIX 3-7 : MODES FOR MOUNT PUGENT STOCK.

Specimen Number	Rock Name	QTZ.	PLAG.	KF.	HB.	BIO.	CPX.	OPX.	OX.	SULFS.	Remarks.
DRM.039	Pyroxene (-biotite) microsyenite.	-	----90--		-	2	6	-	2	-	Sericite in plag. Green sodic pyroxene.
DRM.040	Pyroxene-biotite microsyenite.	-	----80--		-	7	8	-	5	-	Clouded feldspars.

APPENDIX 3-8 : MODES FOR FRIEDA RIVER COMPLEX.

DRM.003	Plagioclase-hornblende (-biotite) diorite porphyry.	-	30	-	15	2	-	-	-	-	Phenocrysts; Trace biotite in h'b
		----32------			20	-	-	-	tr.	1	Groundmass: Py,Cpy. Accessory apatite.
DRM.004	K-altered plag.(-h'b.) diorite porphyry.	-	25	-	-	15	-	-	-	-	Phenocrysts: Sericite in plag;15%bio,
		8	----45--		-	-	-	-	1	1	5% chlor. in h'b. Groundmass: Accessory large apatite; Py, Cpy.
DRM.005	Plagioclase-hornblende (-biotite) diorite porphyry.	-	50	-	10	2	-	-	-	-	Phenocrysts: Trace biotite in h'b.
		-----37------			-	-	-	-	tr.	-	Groundmass: Accessory apatite.
DRM.006	K-altered Plagioclase-biotite diorite porphyry.	-	50	-	-	2	-	-	-	-	Phenocrysts: Sericite in plag.Ground-
		-----33------			-	15	-	-	tr.	2	mass; Secondary biotite; Accessory apatite; Py, Cpy.
DRM.007	K-altered hornblende-plagioclase (-quartz) diorite porphyry.	2	40	-	-	12	-	-	-	-	Phenocrysts: 12% secondary bio,
		----40------			-	-	-	-	2	1	3% chlor. in h'b.; sericite. Ground- mass: Accessory apatite; Py, Cpy.
DRM.080	Plagioclase-hornblende-biotite diorite porphyry.	-	45	-	12	2	-	-	2	-	Phenocrysts: Trace chlorite in biotite
		12	5	13	8	-	-	-	-	-	Groundmass: Accessory apatite.
DRM.081	Hornblende diorite ('Nena Diorite').	8	53	15	18	-	-	-	4	-	Poikilitic Kf. Rare h'b phenocrysts. Accessory large sphene (1%), apatite, zircon.

APPENDIX 3-9 : MODES FOR OK TEDI COMPLEX.

DRM.082	K-altered plagioclase-K-feldspar latite porphyry.	-	20	15	-	10	-	-	-	-	Phenocrysts:Secondary biotite.
		----40------			-	10	-	-	2	3	Groundmass; Secondary biotite; Cpy. (Py).
DRM.083	ditto	-	20	10	-	-	-	-	-	-	Phenocrysts.
		----54------			-	12	-	-	1	3	Groundmass: Secondary biotite; access. apatite. Traces epidote, chlorite.
DRM.084	High-K hornblende-biotite diorite.	8	40	30	15	3	-	-	1	2	Traces epidote, chlorite. Accessory zircon, apatite; Py,Cpy.
DRM.085	K-altered plagioclase-K feldspar latite porphyry.	-	40	15	-	-	-	-	-	-	Phenocrysts.
		----32------			-	10	-	-	3	1	Groundmass: Secondary bio., access. apt.,sph.,zirc.
DRM.086	ditto	-	30	25	-	-	-	-	-	-	Phenocrysts.
		15	10	10	-	8	-	-	1	2	Groundmass: Secondary bio., access. apt.,sph.,Cpy.
DRM.087	High-K clinopyroxene-hornblende diorite.	5	45	30	8	1	7	-	3	1	Subporphyritic. Accessory large sphene, apatite.
DRM.158	K-altered plagioclase-K feldspar latite porphyry.	-	25	15	-	-	-	-	-	-	Phenocrysts.
		----52------			-	6	-	-	1	tr.	Groundmass; Secondary bio.;access. apt, zircon.; Cpy.
DRM.159	K-altered alaskite.	20	---65---		-	12	-	-	2	tr.	Secondary biotite. Accessory zircon.
DRM.160	K-altered plagioclase-K feldspar latite porphyry.	-	30	10	-	-	-	-	-	-	Phenocrysts.
		15	---36---		-	5	-	-	2	1	Groundmass: Accessory large apt; ox. after sph.
DRM.161	ditto	-	20	20	-	-	-	-	-	-	Phenocrysts.
		----45------			-	12	-	-	1	1	Groundmass: Cpy. Accessory apatite.

APPENDIX 3-10 : MODES FOR PLESYUMI INTRUSIVE COMPLEX, NEW BRITAIN.

Specimen Number.	Rock Name.	QTZ.	PLAG.	KF.	HB.	BIO.	CPX.	OPX.	OX.	SULFS.	Remarks.
DRM.133	Propylitic-altered hornblende-quartz granodiorite.	25	52	5	15	-	-	-	2	1	Traces trem./act.,chlor. in h'b. Accessory large sphene, apatite, zircon. Py(Cpy).
DRM.134	Hornblende-biotite granodiorite.	20	58	2	12	5	-	-	1	tr.	Traces sericite, chlorite, epidote. Accessory sphene, apatite, zircon. tr. Py.
DRM.135	Hornblende-biotite-quartz diorite.	15	52	15	12	3	tr.	-	2	tr.	Traces sericite, trem./act.Accessory apatite, sphene, zircon. tr.Cpy.
DRM.136	Hornblende-biotite granodiorite.	20	42	10	20	5	-	-	3	tr.	Traces sericite, chlorite. Accessory zircon, apatite, sphene.
DRM.137	High-K biotite-clinopyroxene (-hornblende) diorite.	8	52	10	6	10	10	tr.	3	-	Accessory zircon.
DRM.138	Two pyroxene-hornblende (-biotite) diorite.	5	58	-	15	3	10	5	3	tr.	Accessory apatite. Tr.Cpy.
DRM.139	High-K hornblende-biotite-quartz (-clinopyroxene)diorite.	15	45	20	10	5	2	-	2	-	Trace trem./act. in h'b. Accessory sphene, apatite,zircon.
DRM.140	Clinopyroxene-hornblende-quartz gabbro.	4	60	-	10	-	20	-	5	tr.	Graphic interstices; schiller textured cpx.; trace chlorite in h'b. Tr. Cpy.
DRM.141	Porphyritic olivine-clinopyroxene gabbro.	-	52	-	15	tr.	20	-	1	tr.	12% olivine, talc, oxides. H'b is trem./act.
DRM.142	Propylitic-altered plagioclase hornblende-quartz dacite porphyry.	10	35	-	10	-	-	-	-	-	Sericite,carbonate,epidote in plag;
		----45------			-	-	-	-	1	1	trem./act.,chlor,ox.in h'b. Accessory sphene. Trace Cpy.

APPENDIX 3-11 : MODES FOR MOUNT KREN INTRUSIVE COMPLEX, MANUS ISLAND.

DRM.110	High-K hornblende (-biotite-clinopyroxene) diorite	10	45	20	20	1	1	-	2	-	Accessory large angular sphene, small apatite prisms.
DRM.111	High-K hornblende-biotite diorite.	8	45	30	12	2	-	-	2	-	Accessory sphene, apatite, zircon.
DRM.112	Hornblende-quartz diorite.	12	53	10	20	-	-	-	3	-	Traces chlorite, ox., sphene in h'b. Accessory apatite, zircon.
DRM.113	High-K porphyritic clinopyroxene-plagioclase-hornblende microdiorite.	-	10	-	3	-	12	-	-	-	Phenocrysts: Chlorite in h'b.
		----53------			-	-	15	-	2	-	Groundmass; calcite patches, veinlets.
DRM.114	High-K hornblende-biotite diorite.	12	44	15	15	10	1	-	2	tr.	Trace chlorite in biotite. Accessory apatite, sphene; trace Cpy.
DRM.115	ditto	8	45	30	15	2	-	-	1	-	Trem/act. in h'b. Accessory apatite.
DRM.116	Hornblende microgabbro.	3	42	tr.	45	-	-	-	10	-	H'b is fibrous trem./act. Abundant ox. stringers.
DRM.117	High-K hornblende(-biotite) diorite.	10	40	30	15	1	-	-	2	-	Trace chlorite in biotite. Accessory large sphene, apatite.
DRM.118	High-K hornblende (-biotite) clinopyroxene diorite.	10	42	20	20	1	5	-	2	-	H'b after cpx.
DRM.119	High-K hornblende diorite.	8	49	20	20	-	-	-	3	-	Trace trem./act. in h'b.
DRM.120	Low-Si porphyritic plagioclase-hornblende-quartz microdiorite.	2	10	-	5	-	-	-	-	-	Phenocrysts: Coarse quartz patches.
		----50------			30	-	-	-	3	-	Groundmass.
DRM.121	High-K hornblende diorite.	8	50	20	20	-	-	-	2	-	Accessory large sphene.
DRM.122	Clinopyroxene-hornblende microdiorite.	5	60	12	5	tr.	15	-	3	-	Trem/act. replaces h'b.

APPENDIX 3-12 : MODES FOR LEMAU INTRUSIVE COMPLEX, NEW IRELAND.

DRM.128	Uralite gabbro.	-	60	-	27	-	5	-	1	tr.	Abundant trem./act. replaces cpx,with ox. granules(8%). Trace Py.
DRM.129	Two pyroxene-biotite-hornblende-quartz diorite.	20	38	5	5	5	15	10	1	-	H'b, ox. rims on px. Trace zircon, apatite.
DRM.130	Clinopyroxene (-biotite)-quartz diorite.	25	36	10	tr.	1	25	-	3	tr.	Incipient trem./act. in cpx. Trace Py. 15% qtz as large polycrystalline patches.
DRM.131	Porphyritic plagioclase-hornblende microdiorite.	-	30	-	8	-	-	-	-	-	Phenocrysts.
		3	---57---		-	-	-	-	2	-	Groundmass.
DRM.132	Two pyroxene-hornblende granodiorite.	25	40	20	10	tr.	1	1	3	-	H'b is fibrous trem./act., with px. cores. Also discrete px.

APPENDIX 3-13 : MODES FOR PANGUNA INTRUSIVE COMPLEX, BOUGAINVILLE ISLAND. (*=Reconnaissance)

Specimen Number.	Rock Name	QTZ.	PLAG.	KF.	HB.	BIO.	CPX.	OPX.	OX.	SULFS.	REMARKS.
DRM.067	Plagioclase-hornblende diorite porphyry.	- 12	30 22	- 16	10 5	- -	- -	- -	1 2	- -	Phenocrysts:Traces trem./act,chlor.in h'b. Groundmass: Saccharoidal. Accessory apatite.
DRM.068*	Clinopyroxene-biotite-quartz syenite.	5	35	47	4	2	4	-	2	-	Fibrous trem./act. after px?; trace chlor. in biotite; accessory apatite, sphene.
DRM.069*	Low-Si two pyroxene-hornblende-biotite micro-diorite.	- 2	2 42	- 10	- 12	- 5	10 10	3 -	1 2	- -	Phenocrysts: Trem./act. in pxs. Groundmass: Accessory apatite.
DRM.070	K-altered 'Biotite Diorite'.	20	55	15	-	8	-	-	2	2	Sericite in plag, Kf. Hydrothermal biotite. Cpy.
DRM.071	ditto	cf. DRM.070									Slightly porphyritic in plagioclase.
DRM.072	Propylitic-altered 'Biotite Granodiorite.'	5 ----46-----	35	-	-	- 12	-	- -	- 2	- 2	Secondary biotite; sericite;Py,Cpy. Accessory apatite.
DRM.073	ditto	cf. DRM.072									Slightly coarser groundmass.
DRM,074	Chlorite-altered 'Biuro Granodiorite'.	5 ----48-----	35	-	10 -	tr. -	- -	- -	1 1	- -	Phenocrysts: Trace bio. in h'b. Groundmass: Accessory apatite, sphene.
DRM.075	'Panguna Andesite'.	- -	30 35	- tr.	15 -	- -	15 tr,	- -	3 2	- -	Phenocrysts: Trace trem./act.,chlor.in h'b. Groundmass.
DRM.076	Altered 'Panguna Andesite'.	-	55	-	35	5	-	-	5	-	Hydrothermal biotite; h'b and cpx replaced by trem./act.
DRM.077	'Nautango Andesite'.	- -----37-----	25	-	10 -	- -	10 15	- -	2 1	- -	Phenocrysts: Ox.rims on h'b., also large subhedra. Groundmass.
DRM.078	'Kaverong Quartz Diorite'.	20	40	20	20	tr.	-	-	2	tr.	Traces epidote,biotite,chlorite;Py,Cpy Accessory sphene, apatite.
DRM.079	Porphyritic 'Kaverong Quartz Diorite'.	- 15	15 27	- 10	12 18	tr. -	- -	- -	2 1	- -	Trace bio. in h'b. Accessory apatite.
DRM.123	'Nautango Andesite'.	- - ---35---	25	-	20 -	- -	5 10	- -	- 5	- -	Phenocrysts:Ox.rims on h'b.Fragmented plag. Groundmass: Very fine grained.
DRM.124	'Kaverong Quartz Diorite'.	5	54	8	15	-	15	-	3	-	Trace fibrous trem./act.in h'b. Accessory apatite, sphene.
DRM.125	'Leucocratic Quartz Diorite'.	20	58	15	-	5	-	-	2	4	Traces sericite,epidote in plag.;trace chlor. in biotite;Cpy,Born;accessory apat
DRM.126	Porphyritic plagioclase-hornblende microdiorite.	- ----57------	30	-	10 -	- -	- -	- -	2 1	- -	Phenocrysts. Groundmass.
DRM.127	Hornblende-clinopyroxene microdiorite.	6	60	10	12	-	8	-	3	-	H'b replaces cpx.

APPENDIX 3-14: MODES FOR LIMBO RIVER DIORITE, NEW GEORGIA ISLAND.

DRM.143	Hornblende-biotite-clinopyroxene microdiorite.	8	70	tr.	8	6	1	-	4	-	Cpx replaced by trem./act.,sphene. Trace sericite in plag.
DRM.144	Hornblende-clinopyroxene-biotite microdiorite.	3	68	-	12	5	8	-	4	-	Sericite in plag.
DRM.145	Two pyroxene-biotite(-hornblende) gabbro.	-	44	-	3	5	40	2	8	-	H'b and biotite replace cpx.

APPENDIX 3-15: MODES FOR POHA RIVER DIORITE, GUADALCANAL.

DRM.146	Hornblende-quartz-biotite diorite.	20	54	5	12	6	-	-	3	tr.	5%chlorite, epidote in biotite. Trace Py.
DRM.147	Hornblende leucogabbro.	5	73	-	20	-	-	-	2	-	Trace sericite in plag.; trace sphene in h'b.

APPENDIX 3-16: MODES FOR KOLOULA INTRUSIVE COMPLEX, GUADALCANAL.

Specimen Number.	Rock Name.	QTZ.	PLAG.	KF.	HB.	BIO.	CPX.	OPX.	OX	SULFS.	Remarks.
DRM.088	Hornblende-biotite granodiorite.	15	56	5	12	8	-	-	2	-	Accessory apatite prisms.
DRM.089	Aplite.	35	10	50	-	3	-	-	1	tr.	Trace sericite in plag.; Cpy.
DRM.090	Hornblende-biotite granodiorite.	20	45	15	10	7	-	-	2	-	Traces sericite, chlorite. Accessory zircon, apatite.
DRM.091	Plagioclase-hornblende-quartz diorite porphyry.	8 10	15 ---37---	-	5 25	-	-	-	tr. 1	-	Phenocrysts: Large quartz patches; trace chlor. Groundmass.
DRM.092	Hornblende-biotite granodiorite.	22	43	12	12	8	-	-	3	tr.	Trace trem./act. in h'b; Cpy.
DRM.093	Two pyroxene gabbro.	-	60	-	-	-	35	tr.	4	-	Small cpx granules in plag.
DRM.094	Two pyroxene(-hornblende) gabbro.	-	60	-	10	-	5	20	5	tr.	Fibrous h'b. after cpx. Tr.Py.
DRM.095	Aplite.	35	30	28	-	5	-	-	1	tr.	Trace chlor. in bio.; sericite in plag. Accessory apatite,zircon, sphene; Cpy.
DRM.096	Porphyritic plagioclase-clinopyroxene-hornblende microdiorite.	-	20 ----40------	-	15 tr.	- 12	10 -	- -	- 3	-	Phenocrysts:H'b is trem/act.after cpx. Groundmass.
DRM.097	Porphyritic two pyroxene-plagioclase microdiorite.	- 5	3 39	-	-	- 8	5 35	tr. -	1 4	- tr.	Phenocrysts:Trace trem/act. in cpx. Groundmass: Trace Py.
DRM.098	Hornblende-biotite-quartz diorite.	20	45	5	15	10	-	-	3	tr.	Trace chlor. in biotite;trace epidote. Accessory apatite. Trace Py.
DRM.099	Two pyroxene microgabbro.	-	52	-	1	-	40	2	5	-	Trace h'b.after cpx.
DRM.100	Hornblende-two pyroxene gabbro.	-	54	-	25	5	10	2	4	tr.	Chlorite,sericite,oxides in cpx. Veinlets of quartz.
DRM.101	Clinopyroxene(hornblende) microgabbro.	tr.	54	-	22	-	18	-	6	tr.	H'b is trem/act.after cpx. Trace Py.
DRM.102	Porphyritic plagioclase-hornblende microdiorite.	-	20 ----53------	-	12 12	-	-	-	-	-	Phenocrysts: Trace trem./act.in h'b. Groundmass.
DRM.103	Porphyritic plagioclase-hornblende-clinopyroxene-quartz microdiorite.	3 tr.	20 ---40---	-	15 tr.	- -	5 10	- -	2 2	- -	Phenocrysts: Trace sericite;cpx rims on qtz. Groundmass.
DRM.104	Feldspathic olivine pyroxenite.	-	20	-	-	-	65	-	tr.	-	15% olivine (3%ox. in olivine).
DRM.105	Feldspathic olivine pyroxenite.	-	20	-	tr.	-	50	5	tr.	-	Trem./act. in cpx, opx.Secondary ox. in olivine; 20% olivine.
DRM.106	Hornblende-biotite granodiorite.	25	42	15	8	7	-	-	3	tr.	Trace chlorite in biotite. Trace Cpy.
DRM.107	Two pyroxene-hornblende-biotite-quartz diorite.	12	44	8	15	12	5	1	2	-	Trace chlorite in biotite. Accessory apatite.
DRM.108	Two pyroxene-hornblende-biotite gabbro	8	45	tr.	5	5	25	5	5	-	Trace chlorite in biotite.
DRM.109	Clinopyroxene-hornblende (-biotite) gabbro.	5	39	-	25	2	25	-	4	-	Chlorite in biotite; trace carbonate in h'b.

APPENDIX 4

TABLE 1 : WHOLE-ROCK ANALYSES

TABLE 2 : AMPHIBOLE ANALYSES

TABLE 3 : BIOTITE ANALYSES

TABLE 4 : MAJOR ELEMENT CORRELATION COEFFICIENTS FOR INTRUSIVE ROCK SUITES, P.N.G. REGION.

APPENDIX 4, TABLE 1 : WHOLE-ROCK ANALYSES

Key for GROUP location numbers:

GROUP no.	Location
	Western Highlands:
10	Yuat North Batholith
	Yuat South Batholith
11	Kunduron
12	Lumoro
13	Reconnaissance
14	Awari Stock
15	Karawari Batholith
16	Lamant Stock
17	Wale Stock
18	Sekau Stock
19	Mount Pugent Stock
20	Frieda River Intrusive Complex
21	Ok Tedi Intrusive Complex
	Eastern Highlands:
22	Mount Michael Stock
	Manus Island:
31	Reconnaissance
32	Mount Kren Intrusive Complex
	New Ireland:
41	Lemau Intrusive Complex
	New Britain:
51	Plesyumi Intrusive Complex
	Bougainville Island:
61	Panguna Intrusive Complex
62	Reconnaissance
	Gaudalcanal Island:
71	Koloula Igneous Complex
72	Poha River Diorite
	New Georgia Island:
73	Limbo River Diorite

APPENDIX 4, TABLE 1: WHOLE-ROCK ANALYSES

GROUP	10.	10.	10.	10.	10.	10.	10.	10.	11.	11.	11.	11.	11.	11.	12.	12.	12.	12.	12.	12.	12.	12.	13.	13.	13.	13.
NO.	DRM063	DRM091	DRM012	DRM019	DRM013	DRM092	DRM064	DRM056	DRM018	DRM020	DRM019	DRM015	DRM016	DRM017	DRM021	DRM026	DRM023	DRM024	DRM157	DRM156	DRM125	DRM022	DRM055	DRM054	DRM052	DRM053
SIO2	45.69	54.30	61.51	61.77	62.90	63.66	63.78	68.13	57.77	59.62	65.17	68.48	70.91	70.97	72.67	46.84	49.77	54.55	63.05	63.75	65.57	65.62	72.50	74.81	78.07	57.92
TIO2	1.13	.85	.75	.71	.68	.85	.52	.47	.66	.99	.56	.34	.26	.26	.80	2.04	1.17	.73	.50	.50	.52	.45	1.20	1.54	.07	.85
AL203	13.45	20.80	16.55	16.58	16.02	16.83	15.90	15.20	16.65	17.74	16.14	15.74	15.06	15.30	19.02	16.33	18.11	18.98	17.58	16.77	15.62	15.74	24.89	17.75	20.00	16.18
FE203	4.46	2.30	3.51	3.91	3.31	1.58	.76	1.28	3.75	3.35	2.35	1.91	1.08	1.26	2.93	5.72	5.31	4.08	.00	.00	2.26	2.15	3.39	4.73	4.01	2.81
FEO	6.96	3.83	3.25	2.93	2.93	1.20	2.41	2.08	3.44	2.88	2.20	.42	1.06	1.13	4.04	8.03	5.73	3.56	4.54	4.48	1.90	1.74	4.13	6.86	5.15	4.19
MNO	.20	.12	.10	.10	.10	.06	.07	.06	.12	.15	.10	.03	.04	.10	.15	.18	.19	.13	.00	.00	.10	.11	.08	.17	.17	.13
MGO	8.37	2.43	2.44	2.26	2.13	2.04	2.62	1.01	4.99	2.99	1.71	.89	.72	.95	7.78	4.94	5.08	2.73	2.06	2.04	1.68	1.39	4.25	5.76	4.84	4.91
CAO	12.30	9.06	5.37	5.22	4.78	7.18	3.51	3.16	7.32	6.89	4.92	3.08	2.95	2.89	12.51	10.17	9.79	8.14	4.20	3.27	4.63	4.25	13.54	10.51	9.37	7.25
NA20	1.81	2.85	3.72	3.80	3.71	3.71	4.66	3.43	3.62	3.68	3.83	3.54	3.92	3.92	1.55	3.71	2.49	3.66	3.99	2.78	3.76	3.93	1.58	2.33	3.26	3.42
K20	2.35	1.54	2.92	2.92	3.06	.45	3.39	4.11	1.17	1.20	2.27	2.56	2.58	2.45	.39	.76	.65	.58	2.99	4.61	2.79	1.98	.39	.97	.75	1.23
P205	1.26	.46	.29	.22	.22	.16	.34	.15	.28	.29	.25	.18	.13	.13	.09	.03	.05	.09	.00	.00	.23	.17	.07	.93	.09	.45
S	.09	.13	.07	.07	.07	.99	.03	.04	.10	.19	.08	1.02	.14	.52	1.95	1.93	1.18	.94	1.07	1.82	.48	1.69	1.73	1.69	1.83	1.59
H20+	1.54	1.47	.82	.71	.61	.60	1.60	.63	1.37	1.12	.62	1.05	.48	.13	.16	.26	.10	.22	.00	.00	.16	.34	.45	.20	.12	.11
H20-	.19	.23	.30	.21	.20	.31	.14	.25	.37	.70	.14	.43	.14	.02	.09	.16	.06	.14	.00	.00	.19	.17	.05	.15	.61	.09
CO2	.20	.10	.00	.04	.52	.10	.14	.17	.05	.22	.12	.00	.09	.02	.00	.14	.00	.00	.00	.00	.00	.00	.00	.00	.00	.00
TOTAL	99.11	100.46	100.87	99.99	99.91	100.33	100.21	100.11	100.64	101.79	100.36	100.73	99.66	100.12	99.28	99.50	100.13	100.86	99.98	100.01	99.90	100.08	99.99	98.37	99.69	100.29
TRACE ELEMENTS (P.P.M.)														NTS (P.P.M.)												
RB	83.	52.	91.	87.	99.	7.	110.	170.	50.	43.	74.	59.	69.	74.	6.	14.	11.	15.	77.	149.	77.	96.	5.	29.	22.	45.
BA	696.	256.	925.	934.	940.	74.	1072.	970.	229.	246.	462.	558.	592.	611.	23.	900.	68.	129.	503.	638.	505.	358.	41.	154.	66.	239.
SR	1150.	631.	398.	358.	373.	332.	1159.	269.	434.	475.	463.	472.	418.	417.	452.	1042.	466.	520.	451.	386.	463.	378.	554.	529.	694.	590.
LA	17.	16.	19.	22.	21.	8.	29.	16.	10.	13.	21.	19.	17.	18.	2.	42.	4.	9.	17.	18.	19.	14.	1.	15.	21.	24.
CE	39.	36.	43.	44.	45.	20.	54.	41.	23.	31.	30.	32.	33.	24.	3.	88.	11.	8.	32.	35.	45.	26.	2.	34.	21.	52.
TH	24.	23.	27.	26.	29.	22.	22.	34.	17.	19.	18.	14.	13.	13.	12.	27.	15.	17.	14.	13.	18.	16.	9.	26.	12.	24.
TM	5.	9.	11.	13.	14.	3.	14.	21.	7.	9.	10.	10.	14.	12.	2.	6.	3.	2.	11.	18.	10.	7.	1.	3.	2.	9.
U	2.	2.	3.	4.	4.	0.	3.	5.	2.	2.	2.	2.	2.	2.	0.	2.	1.	0.	3.	5.	2.	2.	1.	1.	0.	2.
ZR	79.	122.	193.	178.	200.	128.	171.	197.	95.	123.	109.	118.	105.	99.	29.	218.	54.	89.	119.	128.	114.	133.	24.	84.	29.	175.
NB	5.	4.	7.	9.	9.	0.	9.	7.	8.	10.	12.	11.	11.	11.	2.	46.	3.	3.	13.	19.	13.	6.	1.	7.	3.	17.
ZN	91.	82.	52.	56.	66.	34.	57.	38.	47.	99.	48.	13.	19.	21.	83.	156.	81.	60.	47.	63.	40.	97.	49.	104.	75.	84.
CU	112.	48.	40.	92.	70.	373.	12.	44.	110.	20.	8.	95.	2.	4.	7.	21.	11.	12.	645.	4384.	7.	20.	1.	3844.	6.	4.
CO	46.	18.	19.	17.	16.	10.	16.	8.	25.	24.	14.	10.	5.	4.	4.	45.	37.	39.	18.	0.	0.	12.	10.	35.	31.	23.
NI	28.	4.	5.	6.	5.	8.	25.	1.	59.	7.	9.	1.	0.	1.	0.	64.	7.	1.	4.	2.	2.	1.	12.	27.	6.	39.
V	352.	156.	146.	139.	120.	101.	82.	62.	158.	150.	97.	44.	32.	34.	539.	298.	329.	130.	88.	103.	91.	68.	3446.	421.	247.	165.
CR	120.	0.	0.	0.	0.	0.	0.	0.	232.	2.	0.	0.	0.	0.	0.	0.	0.	0.	0.	0.	0.	0.	0.	0.	0.	138.
GA	16.	23.	21.	19.	20.	19.	18.	19.	20.	21.	20.	17.	18.	17.	20.	29.	23.	20.	0.	0.	0.	18.	20.	29.	22.	22.
PB	17.	63.	11.	16.	14.	2.	34.	15.	1.	4.	6.	6.	9.	8.	3.	8.	3.	5.	12.	37.	6.	7.	2.	4.	3.	7.

GROUP	13.	13.	13.	14.	14.	14.	14.	14.	14.	14.	14.	14.	14.	14.	14.	14.	15.	15.	15.	15.	15.	15.	16.	16.
NO.	DRM051	DRM044	DRM045	DRM152	DRM153	DRM154	DRM151	DRM155	DRM149	DRM148	DRM028	DRM029	DRM030	DRM150	DRM036	DRM027	DRM037	DRM031	DRM065	DRM033	DRM066	DRM035	DRM039	DRM032	DRM097	DRM096
SIO2	57.97	64.83	65.36	39.40	39.95	42.21	42.22	42.78	46.08	48.86	49.33	50.61	55.99	56.51	60.52	62.18	62.46	68.05	41.61	45.49	56.00	59.67	69.06	74.90	47.38	49.38
TIO2	1.00	.96	.47	.00	.00	.00	.00	.00	1.95	.76	.46	.29	.71	.99	.53	.96	1.30	.38	.48	.99	.77	.72	.48	.18	1.56	1.19
AL203	16.88	14.13	16.08	.33	1.08	2.20	1.61	.77	14.00	14.85	19.71	10.29	16.27	16.97	14.63	17.37	16.58	16.98	21.79	15.70	18.38	17.51	17.26	13.67	13.37	17.97
FE203	2.88	1.67	1.96	.00	.00	.00	.00	.00	1.77	2.53	3.30	3.04	1.77	1.36	3.04	1.79	.76	5.98	3.43	2.52	3.29	2.40	.97	2.88	9.74
FEO	3.86	2.42	2.05	6.89	7.01	7.28	7.61	8.98	10.46	7.61	3.14	4.62	3.40	7.49	3.31	1.01	2.11	1.03	5.69	5.89	4.67	2.75	2.03	.56	6.88	9.93
MNO	.14	.07	.08	.18	.09	.00	.14	.00	.10	.11	.08	.14	.13	.00	.06	.01	.05	.21	.18	.13	.16	.12	.03	.20	.20	.15
MGO	3.09	3.01	1.65	36.89	38.37	34.00	37.43	42.05	5.42	13.17	8.44	14.99	5.73	5.69	2.33	4.78	2.19	4.50	1.80	10.12	4.90	4.90	1.89	2.28	12.07	5.46
CAO	4.16	5.42	5.33	1.70	.00	2.19	.44	.00	9.13	9.27	10.42	11.67	7.76	5.26	4.36	3.85	3.89	9.84	1.91	2.32	3.59	4.32	4.59	3.42	2.07	10.06
NA20	3.48	3.84	3.85	.00	.00	.00	.00	.00	3.06	1.43	2.32	.90	3.20	1.02	.99	1.33	1.20	.25	.36	.98	2.49	1.16	.90	3.49	.82	3.90
K20	2.64	1.20	1.55	.00	.17	.00	.00	.00	.29	1.28	.78	.87	.91	.00	.21	.22	.21	.19	.59	.20	.93	.26	.22	.08	.38	.74
P205	.38	.15	.24	.00	.00	.00	.00	.00	.00	.00	.08	.06	.21	.20	.22	.21	.19	.08	.09	.07	.06	.06	.06	.06	.60	.57
S	.25	.15	.39	.00	.00	.00	.00	.00	.00	.00	.34	.74	1.07	.00	.55	2.08	.91	.08	.09	.07	.06	.06	.06	.06	.60	.90
H20+	.89	.99	.82	14.10	12.89	11.45	10.47	9.48	1.44	2.69	2.50	2.06	1.36	.95	1.78	1.19	1.90	.48	1.10	3.02	1.60	.59	.98	.23	1.66	1.99
H20-	.09	.17	.23	.00	.00	.00	.00	.00	.00	.00	.49	.11	.18	.00	.31	.21	.21	.10	.12	.31	.18	.06	.03	.07	.10	.17
CO2	.21	.26	.00	.00	.00	.00	.00	.00	.00	.00	.21	.36	.66	.00	.00	.00	.21	.10	.07	.21	.18	.00	.00	.07	.64	.51
TOTAL	99.87	100.41	100.55	99.52	99.56	99.33	99.62	99.04	99.93	100.11	100.07	99.96	100.88	100.01	99.89	101.83	100.73	100.65	100.00	100.04	100.27	99.92	100.47	100.51	100.24	100.70
TRACE ELEMENTS (P.P.M.)														ENTS (P.P.M.)												
RB	92.	33.	35.	0.	9.	0.	0.	0.	6.	46.	22.	26.	33.	22.	39.	36.	39.	2.	2.	7.	65.	18.	12.	59.	16.	8.
BA	384.	267.	270.	0.	0.	0.	0.	0.	0.	29.	0.	0.	39.	5.	476.	82.	62.	60.	15.	91.	508.	188.	185.	568.	12.	134.
SR	492.	462.	393.	0.	0.	12.	0.	0.	169.	237.	360.	75.	329.	229.	5.	390.	333.	936.	926.	347.	578.	450.	490.	211.	378.	528.
LA	34.	15.	8.	0.	0.	0.	0.	0.	0.	7.	0.	2.	19.	7.	31.	19.	13.	27.	19.	7.	47.	31.	23.	18.	22.	29.
CE	73.	21.	22.	0.	0.	0.	0.	0.	0.	17.	0.	9.	21.	26.	20.	22.	21.	19.	20.	14.	29.	24.	14.	10.	26.	19.
TH	40.	11.	20.	0.	0.	0.	0.	0.	42.	17.	8.	9.	21.	26.	20.	22.	21.	19.	20.	14.	29.	24.	14.	10.	26.	19.
TM	17.	4.	6.	2.	1.	1.	0.	0.	1.	1.	1.	0.	3.	0.	3.	3.	3.	1.	2.	2.	4.	2.	2.	1.	1.	3.
U	3.	1.	1.	0.	0.	0.	0.	0.	1.	0.	0.	0.	0.	0.	1.	0.	0.	1.	0.	0.	2.	1.	0.	1.	1.	0.
ZR	195.	111.	146.	1.	0.	0.	0.	0.	98.	62.	17.	12.	96.	83.	137.	108.	118.	155.	19.	64.	177.	124.	118.	70.	65.	91.
NB	17.	6.	9.	0.	0.	0.	0.	0.	2.	5.	0.	0.	6.	3.	8.	6.	5.	10.	4.	8.	9.	7.	7.	8.	7.	8.
ZN	80.	33.	49.	15.	39.	46.	49.	39.	67.	73.	28.	42.	34.	23.	69.	13.	23.	19.	98.	110.	60.	71.	41.	27.	0.	63.
CU	52.	350.	79.	41.	197.	10.	7.	48.	350.	7.	79.	428.	202.	13.	1827.	1049.	784.	9.	33.	852.	119.	63.	16.	17.	271.	49.
CO	17.	17.	11.	143.	102.	105.	106.	138.	19.	33.	34.	38.	28.	19.	16.	13.	0.	5.	35.	52.	19.	18.	12.	4.	50.	30.
NI	6.	34.	4.	264.	1576.	20.	1994.	2295.	32.	299.	103.	204.	56.	9.	25.	15.	26.	8.	8.	211.	8.	0.	0.	0.	79.	22.
V	173.	93.	72.	21.	65.	59.	95.	29.	320.	241.	156.	229.	207.	276.	136.	116.	116.	60.	345.	311.	187.	149.	82.	0.	338.	305.
CR	5.	102.	0.	1401.	1077.	2338.	2243.	2381.	52.	613.	1491.	1749.	196.	0.	66.	53.	59.	12.	0.	588.	0.	0.	4.	0.	308.	36.
GA	22.	18.	19.	0.	0.	0.	0.	0.	0.	0.	15.	10.	20.	0.	19.	21.	19.	19.	25.	17.	22.	21.	21.	14.	19.	20.
PB	10.	2.	8.	13.	1.	3.	1.	3.	10.	6.	1.	1.	1.	3.	1.	1.	0.	2.	0.	0.	9.	4.	2.	4.	8.	1.

APPENDIX 4, TABLE 1: WHOLE-ROCK ANALYSES (CONTIN.)

GROUP	17.	17.	17.	18.	18.	18.	18.	18.	18.	19.	19.	19.	20.	20.	20.	20.	20.	20.	20.	21.	21.	21.	21.	21.	21.	21.
NO.	DRM048	DRM049	DRM050	DRM057	DRM060	DRM061	DRM062	DRM059	DRM058	DRM038	DRM039	DRM040	DRM004	DRM003	DRM081	DRM007	DRM006	DRM080	DRM005	DRM084	DRM087	DRM101	DRM083	DRM082	DRM100	DRM085
SIO2	49.15	49.67	49.81	40.28	41.60	44.80	49.39	53.56	55.22	46.95	61.75	61.88	56.68	59.03	59.03	59.42	63.00	63.22	64.44	57.74	59.61	62.16	64.63	65.13	67.12	68.87
TIO2	1.23	1.19	.46	1.90	1.06	1.71	1.22	1.00	.97	3.46	.37	.37	.72	.63	.76	.56	.51	.50	.49	.63	.68	.29	.31	.38	.34	.30
AL203	18.66	15.67	3.98	16.79	6.99	14.00	16.67	18.12	17.86	14.29	17.94	17.80	17.84	16.54	17.99	17.25	17.31	16.73	17.23	17.56	18.12	16.75	16.89	17.29	17.88	14.51
FE203	5.24	2.20	2.88	5.77	1.41	3.81	1.16	1.94	3.02	5.88	2.34	2.33	3.17	2.29	3.12	3.48	1.92	2.18	2.10	2.44	3.06	.00	.80	1.86	.00	.39
FEO	4.08	9.43	5.28	6.45	10.55	6.81	6.40	4.41	3.80	8.06	2.91	2.76	3.25	3.34	2.06	2.08	2.63	1.69	1.86	2.59	1.74	2.32	.36	.94	.84	.15
MNO	.12	.26	.16	.19	.16	.13	.20	.19	.18	.30	.17	.18	.03	.09	.11	.07	.03	.04	.07	.07	.09	.00	.00	.00	.00	.00
MGO	3.34	4.51	17.36	7.92	23.65	12.06	7.41	3.76	2.79	4.97	.33	.30	3.65	5.47	2.13	2.57	2.35	2.56	2.15	1.54	1.46	2.95	.99	.95	.85	.95
CAO	9.74	8.19	15.96	11.19	3.68	9.96	10.44	7.01	6.32	8.58	1.97	1.98	5.08	6.01	6.54	4.79	3.93	4.44	4.48	7.03	5.11	1.25	.13	1.11	1.50	.98
NA2O	3.76	3.43	.46	2.29	.17	2.18	3.19	5.21	5.44	3.04	6.66	6.65	3.29	4.54	4.50	4.15	4.94	4.81	4.80	3.11	4.83	1.77	3.15	5.39	3.48	3.74
K2O	1.43	.92	.09	1.65	.30	1.29	.72	1.16	2.18	.48	5.11	5.09	2.30	1.16	1.67	.97	1.84	2.20	1.90	3.11	3.15	11.46	9.77	4.92	7.26	6.40
P2O5	.38	.35	.03	.90	.17	.14	.27	.41	.66	.51	.20	.19	.40	.22	.31	.34	.26	.26	.21	.37	.37	.00	.15	.18	.00	.15
S	.03	.64	.00	.48	.20	.03	.47	.36	.09	.26	.05	.05	1.79	.06	2.02	2.08	.18	.04	.04	.57	.19	.00	.65	.34	.00	.08
H2O+	2.38	2.00	.61	2.50	7.40	2.77	2.30	1.77	.90	2.45	.72	.68	1.48	1.32	.68	1.41	1.50	.80	.78	.94	.56	1.13	.36	.59	.74	.33
H2O-	.20	.26	.09	.20	.43	.21	.14	.17	.16	.40	.29	.29	.27	.35	.12	.30	.00	.12	.27	.14	.33	.00	.15	.15	.00	.12
CO2	.18	.42	1.12	.21	.11	.09	.10	.35	.08	1.06	.10	.18	1.15	.22	.11	.86	.60	.08	.09	2.17	.82	.60	1.41	.82	.00	.34
TOTAL	99.86	99.48	98.49	98.27	97.88	99.79	100.08	99.31	99.67	100.74	100.81	100.79	101.10	101.27	99.63	100.33	99.80	99.92	100.91	100.01	100.12	100.03	99.75	100.05	99.99	99.61
TRACE ELEMENTS (P.P.M.)																										
RB	26.	14.	2.	36.	15.	16.	12.	20.	40.	6.	130.	134.	51.	22.	35.	13.	33.	27.	27.	100.	106.	333.	218.	115.	131.	139.
BA	261.	179.	0.	273.	7.	224.	137.	554.	1303.	36.	572.	542.	297.	200.	325.	146.	369.	387.	426.	842.	787.	301.	400.	864.	836.	768.
SR	698.	547.	75.	868.	43.	449.	348.	1474.	1029.	225.	195.	192.	579.	669.	663.	724.	771.	738.	749.	1129.	1517.	237.	873.	873.	890.	739.
LA	12.	17.	0.	6.	6.	5.	7.	25.	48.	6.	94.	98.	23.	13.	17.	16.	17.	15.	18.	32.	38.	32.	42.	28.	15.	10.
CE	31.	42.	0.	22.	12.	0.	15.	48.	93.	25.	178.	182.	42.	27.	33.	35.	28.	35.	34.	63.	68.	86.	68.	49.	29.	24.
Y	18.	19.	6.	20.	33.	17.	18.	20.	23.	52.	47.	50.	21.	19.	25.	15.	13.	15.	14.	25.	26.	87.	6.	12.	13.	10.
TH	5.	4.	1.	3.	2.	3.	5.	7.	11.	1.	20.	21.	8.	5.	5.	6.	8.	7.	7.	8.	11.	2.	8.	9.	8.	8.
U	0.	1.	0.	1.	0.	1.	1.	2.	3.	1.	4.	4.	1.	0.	1.	1.	1.	1.	1.	1.	1.	3.	1.	1.	1.	1.
ZR	93.	102.	15.	54.	65.	77.	81.	161.	185.	222.	738.	869.	133.	80.	149.	113.	146.	108.	115.	184.	199.	150.	129.	155.	149.	131.
NB	5.	7.	1.	5.	3.	6.	5.	17.	33.	6.	125.	149.	12.	7.	11.	9.	8.	8.	8.	10.	12.	5.	8.	9.	10.	8.
ZN	32.	202.	56.	89.	150.	78.	136.	84.	100.	149.	145.	169.	38.	46.	70.	38.	23.	28.	29.	68.	51.	6.	4.	13.	8.	11.
CU	239.	911.	2u.	207.	88.	62.	36.	141.	43.	29.	5.	3.	928.	421.	122.	457.	1292.	301.	21.	738.	1373.	8818.	2616.	588.	2016.	554.
CO	25.	133.	67.	49.	145.	72.	38.	23.	18.	45.	3.	0.	20.	22.	14.	12.	16.	11.	12.	8.	9.	0.	6.	0.	0.	0.
NI	10.	30.	121.	39.	974.	60.	23.	28.	9.	21.	0.	0.	7.	59.	3.	9.	4.	10.	11.	0.	10.	8.	4.	2.	2.	2.
V	165.	330.	158.	464.	87.	440.	345.	230.	215.	450.	6.	5.	219.	208.	132.	144.	160.	130.	112.	110.	161.	418.	210.	109.	218.	168.
CR	0.	48.	666.	11.	855.	18.	0.	34.	0.	0.	0.	0.	12.	156.	0.	26.	10.	10.	12.	0.	0.	0.	0.	0.	0.	0.
GA	20.	20.	6.	19.	9.	24.	21.	22.	24.	25.	31.	34.	23.	21.	0.	22.	0.	0.	20.	0.	0.	0.	0.	0.	0.	0.
PB	5.	8.	2.	4.	1.	2.	11.	10.	16.	2.	9.	10.	2.	0.	6.	3.	1.	2.	1.	10.	8.	9.	1.	5.	15.	6.

GROUP	21.	21.	21.	22.	22.	22.	22.	31.	31.	32.	32.	32.	32.	32.	32.	32.	32.	32.	32.	32.	41.	41.	41.	41.
NO.	DRM086	DRM158	DRM159	DRM011	DRM008	DRM010	DRM009	DRM001	DRM002	DRM116	DRM120	DRM113	DRM122	DRM115	DRM118	DRM112	DRM121	DRM119	DRM114	DRM110	DRM111	DRM117	DRM128	DRM130	DRM129	DRM131
SIO2	69.32	70.92	78.40	56.02	59.77	60.10	60.42	56.04	60.05	50.41	51.56	53.05	56.88	59.08	59.68	59.91	60.68	60.70	61.35	61.58	61.96	62.20	47.16	55.97	59.23	61.90
TIO2	.30	.27	.35	.78	.66	.85	.84	.68	.73	.72	.70	.96	.84	.54	.55	.53	.51	.51	.50	.48	.47	.47	.34	.77	.78	.39
AL203	15.80	15.67	10.53	17.68	17.66	17.80	17.84	17.68	16.73	13.32	14.79	14.96	16.84	17.47	17.09	17.31	17.03	17.12	16.87	16.92	17.01	16.66	21.38	14.94	15.53	17.55
FE203	.28	.00	.00	1.69	.97	1.66	2.22	4.50	2.52	3.32	4.77	3.57	3.62	2.55	3.18	2.99	2.74	3.04	2.36	2.51	2.55	2.44	3.72	6.17	2.81	1.76
FEO	.44	.82	.40	3.95	2.06	3.48	3.02	2.71	2.41	4.80	4.40	3.34	2.26	2.46	2.00	2.10	2.08	1.64	2.17	1.81	1.76	1.74	4.00	4.92	4.84	1.08
MNO	.00	.00	.00	.15	.19	.14	.13	.14	.19	.13	.09	.10	.07	.07	.05	.05	.07	.04	.04	.04	.03	.04	.15	.12	.12	.02
MGO	.81	.97	2.17	2.16	1.98	1.81	1.77	4.03	2.94	10.57	6.40	7.29	3.40	3.23	3.41	2.99	3.60	2.64	2.52	2.72	2.54	2.51	6.57	3.48	3.63	1.82
CAO	1.16	1.01	.27	6.99	6.67	6.43	5.71	7.64	4.67	8.36	10.10	6.83	6.20	5.84	5.76	6.62	6.61	5.15	5.41	5.18	5.05	5.04	13.90	6.77	7.48	6.15
NA2O	3.28	3.12	.98	5.11	4.28	4.46	4.36	3.67	4.42	3.15	3.04	3.69	4.35	4.63	4.39	4.75	4.28	4.68	4.57	4.40	4.57	4.33	1.15	3.74	2.78	3.54
K2O	6.22	6.78	6.34	1.81	1.36	1.27	1.94	2.08	2.98	.14	.35	3.35	1.86	2.29	2.69	.88	2.46	2.65	2.07	2.49	2.65	2.64	.16	1.69	1.39	1.00
P2O5	.13	.00	.00	.48	.38	.33	.34	.24	.28	.36	.32	.24	.33	.37	.31	.29	.33	.29	.29	.29	.29	.26	.09	.15	.21	.20
S	.21	.00	.00	.39	.10	.11	.23	.04	.04	.05	.09	.05	.05	.05	.02	.03	.02	.03	.02	.03	.01	.03	.16	.01	.06	.02
H2O+	.35	.46	.56	1.46	1.42	1.26	1.19	1.10	1.27	3.30	1.29	1.96	.98	.88	.80	.95	.72	.85	1.01	.83	.79	.71	1.10	.57	.66	2.47
H2O-	.09	.00	.00	.21	.30	.24	.31	.52	.71	1.15	.17	.47	.27	.30	.26	.19	.31	.35	.27	.20	.18	.22	.17	.18	.15	.66
CO2	.68	.00	.00	2.06	.84	.81	.79	.04	.31	.17	.16	.46	.49	.17	.15	.09	.22	.15	.26	.10	.10	.15	.43	.14	.19	.23
TOTAL	99.06	100.02	100.06	100.13	98.84	100.26	100.49	100.99	100.05	100.14	100.03	99.83	98.41	99.93	99.90	99.69	99.86	99.87	99.25	99.78	99.96	99.44	100.48	99.62	99.83	98.99
TRACE ELEMENTS (P.P.M.)																										
RB	123.	151.	193.	44.	28.	25.	38.	31.	40.	7.	2.	69.	46.	34.	45.	12.	27.	45.	43.	38.	43.	44.	3.	38.	32.	19.
BA	920.	597.	124.	664.	352.	368.	384.	187.	394.	37.	21.	236.	241.	284.	273.	154.	376.	268.	282.	469.	270.	288.	1.	103.	174.	112.
SR	795.	720.	62.	975.	699.	701.	763.	737.	724.	598.	91.	511.	796.	1034.	843.	1002.	967.	902.	763.	830.	861.	847.	164.	163.	238.	763.
LA	8.	13.	8.	41.	17.	21.	17.	19.	21.	15.	12.	15.	20.	26.	21.	19.	21.	21.	21.	22.	21.	18.	0.	4.	7.	7.
CE	24.	30.	18.	73.	28.	41.	38.	31.	46.	40.	28.	33.	47.	57.	52.	44.	50.	49.	48.	50.	45.	41.	0.	10.	18.	14.
Y	9.	13.	13.	22.	20.	21.	22.	16.	18.	18.	19.	17.	18.	20.	19.	18.	21.	19.	18.	17.	17.	14.	5.	24.	23.	9.
TH	7.	10.	4.	12.	8.	7.	7.	4.	7.	3.	2.	4.	5.	4.	6.	5.	5.	5.	5.	5.	5.	4.	0.	2.	2.	2.
U	1.	2.	1.	3.	2.	1.	2.	1.	2.	1.	1.	2.	2.	2.	2.	2.	2.	2.	2.	2.	2.	1.	0.	0.	0.	0.
ZR	126.	157.	168.	204.	134.	139.	134.	125.	179.	143.	111.	129.	167.	193.	188.	188.	166.	183.	193.	177.	182.	186.	1.	71.	113.	86.
NB	8.	10.	5.	18.	10.	10.	9.	1.	3.	2.	2.	2.	3.	3.	3.	3.	3.	3.	3.	3.	3.	3.	0.	2.	2.	1.
ZN	10.	12.	10.	84.	244.	71.	71.	67.	87.	109.	53.	57.	75.	47.	39.	43.	51.	50.	51.	39.	33.	39.	66.	49.	83.	51.
CU	2163.	617.	470.	27.	2.	3.	1.	88.	128.	72.	32.	126.	641.	96.	277.	64.	25.	225.	265.	54.	87.	66.	52.	94.	96.	22.
CO	0.	0.	0.	14.	13.	12.	16.	26.	17.	43.	34.	34.	19.	17.	19.	19.	17.	15.	15.	15.	15.	15.	46.	28.	46.	11.
NI	3.	8.	20.	5.	6.	6.	1.	14.	17.	166.	56.	73.	10.	15.	15.	13.	11.	12.	8.	14.	13.	12.	30.	1.	10.	8.
V	218.	208.	404.	162.	120.	117.	103.	251.	155.	263.	264.	216.	183.	163.	149.	157.	166.	138.	140.	141.	124.	124.	209.	292.	208.	64.
CR	0.	0.	49.	0.	0.	0.	0.	3.	19.	462.	126.	210.	4.	20.	14.	19.	14.	16.	6.	14.	13.	15.	62.	0.	14.	2.
GA	0.	0.	0.	25.	18.	23.	21.	21.	23.	0.	0.	0.	0.	0.	0.	0.	0.	0.	0.	0.	0.	0.	0.	0.	0.	0.
PB	9.	11.	4.	7.	4.	5.	4.	5.	9.	5.	4.	4.	13.	5.	5.	5.	5.	6.	5.	4.	5.	5.	2.	5.	6.	2.

APPENDIX 4, TABLE 1: WHOLE-ROCK ANALYSES (CONTIN.)

GROUP	41.	51.	51.	51.	51.	51.	51.	51.	51.	51.	51.	51.	61.	61.	61.	61.	61.	61.	61.	61.	61.	61.	61.	61.	61.
NO.	DRM132	DRM141	DRM140	DRM138	DRM137	DRM139	DRM135	DRM136	DRM133	DRM134	DRM142	DRM123	DRM071	DRM124	DRM079	DRM075	DRM076	DRM077	DRM078	DRM127	DRM070	DRM126	DRM073	DRM125	DRM074	DRM072
SIO2	67.08	45.85	49.70	52.97	57.67	59.38	60.82	63.07	65.40	65.50	67.64	54.35	55.52	55.56	55.97	56.67	57.28	57.43	59.89	60.33	62.18	63.27	65.34	65.96	66.99	67.66
TIO2	.62	.38	.44	.93	1.07	.90	.82	.74	.41	.57	.37	.78	.60	.78	.67	.84	.63	.49	.63	.49	.37	.46	.40	.32	.33	.33
AL2O3	14.54	16.07	14.01	17.78	16.90	17.33	17.09	16.66	16.65	16.05	14.44	17.59	19.17	17.59	17.23	16.68	13.81	17.47	17.06	17.98	14.41	17.11	16.05	14.49	16.53	16.10
FE2O3	2.54	3.80	4.35	4.80	2.80	2.72	2.81	2.21	1.35	1.82	1.49	5.10	2.02	4.44	4.64	3.60	3.91	3.82	3.35	3.29	1.78	2.49	2.40	3.09	1.77	1.09
FEO	2.15	5.20	5.83	4.70	4.19	3.02	2.62	2.23	1.63	1.83	1.28	3.41	3.08	3.16	3.32	3.38	4.29	2.77	2.76	1.86	1.66	1.88	2.17	2.54	1.37	1.48
MNO	.05	.11	.11	.12	.11	.07	.03	.02	.06	.02	.00	.17	.00	.13	.16	.12	.08	.14	.04	.05	.00	.08	.00	.00	.02	.00
MGO	1.28	11.81	3.85	4.56	2.76	2.51	2.50	2.21	2.03	1.85	1.04	4.06	3.05	3.22	3.52	3.62	5.89	2.84	2.41	1.82	1.35	1.92	1.38	1.84	1.11	1.19
CAO	4.36	13.41	11.39	9.03	5.19	5.36	5.38	4.97	4.86	4.20	3.01	8.86	5.87	7.86	7.53	7.98	7.27	7.99	6.12	6.73	4.33	5.34	4.15	4.21	4.26	2.95
NA2O	3.58	1.08	2.46	3.36	4.18	4.56	4.42	4.65	5.19	4.30	5.19	2.96	3.93	3.89	3.57	3.68	3.67	3.24	4.09	4.30	4.15	4.21	4.68	4.27	4.69	4.97
K2O	2.13	.11	.30	.40	3.59	2.73	1.83	1.46	.20	1.63	.72	1.28	2.09	1.71	1.41	1.33	.79	1.15	2.13	1.79	3.08	1.55	1.93	2.25	1.50	2.01
P2O5	.20	.11	.19	.40	.37	.35	.30	.26	.24	.23	.17	.31	.25	.33	.32	.33	.21	.34	.29	.32	.19	.20	.22	.20	.19	.18
S	.02	.09	.03	.03	.04	.04	.01	.01	.02	.01	.06	.05	1.84	.02	.00	.13	.06	.01	.01	.03	1.33	.02	.44	.22	.00	.17
H2O+	.54	1.93	1.22	.68	.67	.71	.84	.74	.84	.93	1.41	.71	1.17	.88	.96	1.50	1.07	.80	2.32	.54	.89	.87	1.26	.93	.52	.82
H2O-	.18	.19	.22	.16	.23	.21	.32	.24	.28	.26	.46	.37	1.35	.33	.18	.19	.15	.39	.06	.25	.83	.25	.29	.29	.29	.10
CO2	.31	.24	.09	.21	.18	.10	.29	.24	.41	.16	.86	.07	4.08	.18	.13	.66	.35	.42	.11	.11	2.93	.27	.01	.53	.15	.85
TOTAL	99.58	100.18	100.19	100.11	99.18	99.95	99.83	99.71	99.77	99.36	99.83	100.08	99.02	100.08	99.61	95.54	99.57	99.48	101.27	99.79	99.48	99.92	99.67	98.27	99.72	99.90
TRACE ELEMENTS (P.P.M.)																										
RB	38.	2.	4.	8.	137.	90.	67.	54.	3.	46.	16.	21.	50.	26.	24.	91.	18.	24.	36.	22.	44.	28.	41.	34.	17.	39.
BA	258.	0.	9.	39.	220.	181.	148.	162.	59.	176.	131.	159.	204.	222.	284.	577.	118.	215.	290.	318.	204.	264.	201.	190.	348.	250.
SR	213.	314.	295.	458.	524.	729.	717.	745.	724.	671.	834.	640.	484.	686.	784.	937.	310.	705.	664.	968.	571.	690.	508.	498.	707.	568.
LA	9.	0.	2.	2.	19.	17.	14.	12.	7.	8.	8.	9.	10.	10.	10.	14.	8.	11.	11.	11.	6.	8.	8.	3.	8.	9.
CE	24.	3.	8.	4.	42.	34.	31.	24.	22.	15.	21.	19.	10.	20.	20.	30.	10.	21.	10.	22.	25.	18.	10.	6.	13.	14.
Y	34.	8.	22.	17.	26.	18.	14.	12.	13.	10.	8.	24.	15.	24.	22.	21.	17.	22.	20.	21.	11.	15.	12.	9.	12.	12.
TH	3.	0.	1.	1.	5.	3.	3.	3.	4.	5.	2.	0.	2.	1.	2.	2.	2.	2.	2.	3.	2.	2.	2.	2.	2.	2.
U	1.	0.	0.	0.	1.	1.	1.	1.	1.	1.	0.	0.	1.	0.	0.	1.	0.	0.	1.	0.	0.	0.	0.	0.	0.	0.
ZR	186.	15.	62.	49.	455.	214.	159.	109.	119.	124.	89.	83.	83.	99.	80.	105.	58.	98.	101.	106.	82.	101.	89.	85.	94.	88.
NB	4.	1.	1.	1.	9.	6.	4.	3.	3.	3.	1.	5.	5.	3.	4.	5.	4.	5.	4.	5.	4.	5.	5.	2.	5.	4.
ZN	57.	72.	79.	102.	101.	91.	56.	55.	74.	71.	79.	86.	52.	43.	103.	70.	74.	77.	41.	35.	77.	53.	48.	38.	33.	30.
CU	38.	42.	125.	106.	71.	51.	38.	61.	36.	75.	913.	87.	308.	150.	125.	95.	437.	64.	232.	42.	2849.	21.	4438.	4778.	20.	1909.
CO	11.	65.	36.	34.	23.	21.	18.	17.	8.	9.	5.	28.	0.	23.	0.	32.	0.	0.	0.	11.	0.	12.	0.	9.	0.	0.
NI	2.	121.	17.	30.	8.	10.	15.	15.	12.	13.	2.	6.	9.	3.	5.	11.	30.	3.	4.	2.	3.	2.	2.	2.	3.	4.
V	80.	167.	483.	244.	154.	132.	125.	107.	86.	83.	52.	229.	170.	201.	178.	216.	257.	155.	156.	98.	76.	97.	84.	84.	58.	72.
CR	0.	311.	0.	17.	0.	0.	0.	0.	3.	0.	0.	0.	84.	0.	0.	23.	88.	0.	70.	0.	89.	0.	99.	0.	95.	106.
GA	0.	0.	0.	0.	0.	0.	0.	0.	0.	0.	0.	0.	0.	0.	0.	0.	0.	0.	0.	0.	0.	0.	0.	0.	0.	0.
PB	7.	4.	4.	4.	6.	5.	4.	3.	1.	2.	2.	6.	3.	5.	7.	7.	4.	4.	3.	3.	3.	3.	4.	3.	1.	3.

GROUP	62.	62.	62.	71.	71.	71.	71.	71.	71.	71.	71.	71.	71.	71.	71.	71.	71.	71.	71.	71.	71.	71.	71.	71.	72.
NO.	DRM069	DRM068	DRM067	DRM093	DRM099	DRM101	DRM094	DRM104	DRM105	DRM100	DRM109	DRM108	DRM102	DRM097	DRM096	DRM103	DRM091	DRM107	DRM098	DRM088	DRM090	DRM092	DRM106	DRM095	DRM089	DRM147
SIO2	53.97	60.61	63.17	45.59	46.01	47.37	48.21	48.39	49.52	49.53	49.88	51.30	53.91	55.65	55.66	56.96	57.50	59.29	61.02	62.47	63.55	63.86	65.40	71.05	77.55	52.06
TIO2	.76	.52	.37	.81	.79	.58	.67	.22	.27	.78	.73	.47	.62	.68	.68	.42	.55	.59	.38	.37	.33	.33	.39	.20	.12	.55
AL2O3	16.34	18.30	16.80	18.86	18.29	19.94	18.20	19.71	19.73	16.95	13.49	20.33	19.00	16.55	15.90	15.01	18.28	17.09	17.82	17.11	16.80	17.30	16.97	14.80	12.30	17.45
FE2O3	4.16	2.17	2.94	6.33	5.77	4.42	5.27	4.59	3.39	4.05	2.96	3.13	4.21	3.35	3.13	2.27	2.32	2.65	2.90	2.44	2.34	2.40	2.23	1.00	.19	3.85
FEO	4.62	1.82	1.77	5.81	5.97	5.02	5.95	5.32	6.25	5.31	5.98	5.24	3.78	4.25	4.39	3.54	2.96	3.82	2.66	2.27	2.01	2.02	1.83	1.06	.29	3.54
MNO	.13	.12	.06	.21	.20	.16	.26	.19	.19	.12	.18	.11	.09	.11	.12	.11	.17	.10	.06	.08	.08	.07	.04	.00	.00	.07
MGO	4.59	1.28	1.93	6.40	7.61	7.33	6.90	19.51	18.81	7.58	8.91	3.50	4.29	5.17	5.30	6.84	4.32	3.80	2.78	2.53	2.31	2.30	1.89	.98	.38	5.23
CAO	7.90	1.27	4.99	12.43	12.87	12.62	11.69	15.91	16.67	10.97	12.02	11.14	9.13	8.64	8.54	7.26	7.82	7.39	6.91	6.31	5.76	5.99	5.28	3.36	1.11	9.15
NA2O	3.61	5.01	4.14	2.03	1.78	1.60	2.29	.29	.32	2.54	1.86	2.38	2.76	2.85	2.79	2.62	4.20	3.03	3.24	3.66	3.63	3.69	3.73	3.21	3.14	3.03
K2O	1.79	5.74	1.71	.06	.05	.03	.10	.00	.01	.32	.25	.79	.43	1.03	1.24	1.66	.72	1.34	.95	1.29	1.42	1.43	.88	2.65	3.64	.68
P2O5	.34	.31	.25	.27	.34	.09	.10	.07	.08	.21	.16	.15	.17	.22	.20	.19	.21	.21	.19	.17	.17	.19	.17	.11	.08	.27
S	.03	.04	.04	.08	.19	.07	.09	.05	.02	.07	.35	.12	.05	.02	.09	.03	.03	.02	.01	.02	.02	.02	.18	.01	.03	.03
H2O+	1.03	1.08	.99	.58	.46	1.15	.75	1.30	.92	1.19	1.74	.67	1.24	.98	1.01	2.16	1.09	.92	1.00	1.11	1.00	.73	.84	.65	.54	1.63
H2O-	.16	.08	.31	.45	.10	1.11	.14	.15	.12	.40	.21	.08	.15	.09	.14	.25	.01	.11	.08	.05	.03	.40	.09	.10	.30
CO2	.02	.02	.04	.18	.18	.24	.33	.13	.10	.40	.99	.17	.18	.13	.36	.49	.09	.14	.24	.99	.44	.15	.52	.30	.67	.20
TOTAL	99.45	100.37	99.61	99.87	100.56	100.53	100.89	99.79	100.40	100.16	100.72	99.78	99.91	99.72	99.54	99.32	100.09	100.50	100.27	100.85	99.91	100.51	100.66	99.47	100.11	100.00
TRACE ELEMENTS (P.P.M.)																										
RB	34.	126.	22.	1.	0.	0.	2.	0.	0.	5.	2.	15.	6.	22.	27.	35.	18.	26.	16.	22.	29.	29.	21.	38.	56.	17.
BA	248.	386.	299.	13.	13.	13.	21.	0.	0.	78.	49.	103.	85.	202.	218.	214.	154.	223.	240.	264.	287.	309.	302.	482.	593.	114.
SR	763.	660.	678.	569.	639.	634.	499.	55.	57.	498.	422.	588.	483.	494.	474.	620.	669.	513.	563.	593.	593.	587.	609.	395.	175.	778.
LA	11.	18.	9.	0.	1.	0.	0.	0.	0.	4.	1.	4.	3.	6.	7.	8.	5.	5.	6.	6.	6.	5.	5.	4.	9.	16.
CE	27.	37.	20.	0.	0.	0.	0.	0.	0.	11.	5.	11.	6.	13.	15.	16.	13.	16.	12.	6.	15.	10.	11.	6.	22.	42.
Y	19.	21.	17.	12.	14.	10.	11.	4.	3.	23.	19.	16.	14.	19.	20.	12.	15.	19.	15.	13.	13.	13.	11.	7.	5.	16.
TH	2.	8.	1.	1.	2.	1.	1.	1.	0.	1.	2.	2.	1.	1.	4.	3.	2.	2.	3.	2.	2.	2.	1.	2.	6.	3.
U	0.	3.	0.	1.	0.	0.	0.	0.	0.	0.	1.	0.	0.	0.	1.	1.	0.	0.	1.	0.	1.	1.	0.	1.	2.	1.
ZR	91.	189.	103.	6.	9.	7.	6.	6.	3.	33.	26.	34.	45.	79.	89.	59.	47.	77.	52.	61.	64.	64.	59.	73.	78.	72.
NB	3.	20.	4.	0.	1.	1.	1.	1.	1.	1.	0.	1.	0.	3.	3.	2.	1.	3.	2.	2.	1.	2.	2.	2.	2.	2.
ZN	103.	74.	61.	84.	83.	73.	99.	65.	66.	78.	97.	79.	32.	139.	85.	115.	75.	68.	48.	49.	41.	50.	34.	15.	14.	37.
CU	234.	64.	226.	41.	104.	105.	21.	2.	2.	171.	222.	158.	124.	129.	161.	55.	31.	68.	54.	12.	5.	185.	30.	39.	157.	13.
CO	33.	9.	11.	39.	38.	39.	38.	74.	68.	43.	42.	23.	22.	31.	31.	30.	20.	22.	17.	14.	13.	14.	11.	7.	3.	28.
NI	13.	0.	2.	12.	24.	29.	15.	108.	150.	69.	58.	9.	10.	20.	26.	145.	15.	19.	4.	14.	9.	5.	4.	1.	0.	30.
V	256.	69.	103.	413.	293.	314.	367.	154.	191.	294.	341.	294.	216.	262.	245.	136.	104.	192.	134.	128.	99.	107.	83.	36.	9.	231.
CR	3.	0.	0.	23.	53.	41.	5.	801.	793.	201.	202.	0.	0.	36.	61.	306.	13.	14.	0.	5.	2.	0.	0.	0.	0.	51.
GA	0.	0.	0.	0.	0.	0.	0.	0.	0.	0.	0.	0.	0.	0.	0.	0.	0.	0.	0.	0.	0.	0.	0.	0.	0.	0.
PB	7.	12.	3.	4.	4.	4.	5.	4.	5.	5.	6.	5.	2.	13.	6.	4.	2.	5.	3.	3.	3.	2.	3.	3.	3.	3.

APPENDIX 4, TABLE 1: WHOLE-ROCK ANALYSES (CONTIN.)

GROUP	72.	73.	73.	73.
NO.	DRM146	DRM145	DRM144	DRM143
SIO2	62.38	44.06	55.47	60.74
TIO2	.42	.80	.63	.69
AL2O3	16.31	15.52	17.74	17.48
FE2O3	2.80	8.79	3.76	2.85
FEO	2.99	6.27	3.03	1.87
MNO	.03	.20	.15	.03
MGO	2.73	7.93	3.32	2.13
CAO	5.52	13.77	6.54	4.53
NA2O	3.54	1.35	4.31	4.81
K2O	1.18	.25	2.15	2.53
P2O5	.18	.28	.44	.43
S	.04	.03	.07	.02
H2O+	1.32	.42	1.41	1.11
H2O-	.21	.16	.42	.35
CO2	.17	.08	.47	.25
TOTAL	99.82	100.11	99.91	99.82
TRACE ELEMENTS (P.P.M.)				
RB	22.	5.	41.	38.
BA	326.	19.	253.	342.
SR	472.	750.	642.	596.
LA	13.	1.	12.	12.
CE	27.	3.	24.	27.
Y	17.	15.	21.	20.
TH	4.	1.	2.	3.
U	2.	0.	1.	0.
ZR	98.	20.	84.	90.
NB	6.	1.	5.	8.
ZN	33.	80.	47.	42.
CU	212.	24.	212.	26.
CO	24.	43.	21.	14.
NI	3.	52.	6.	9.
V	153.	498.	170.	145.
CR	0.	0.	0.	0.
GA	0.	0.	0.	0.
PB	2.	7.	4.	1.

APPENDIX 4, TABLE 2 : AMPHIBOLE ANALYSES

and

APPENDIX 4, TABLE 3 : BIOTITE ANALYSES

Traverses across mineral grains are denoted thus:

——————→ single traverse across one crystal, core to rim.

——→– – ——→ separate traverses across one crystal, core to rim.

——→ ——→ separate traverses across different crystals.

APPENDIX 4, TABLE 2: AMPHIBOLE ANALYSES (OXIDES, WT. PERCENT), AND STRUCTURAL FORMULAE (ATOMS, O=23)

DRH.NO	.006	.006	.006	.006	.012	.012	.012	.012	.013	.013	.013	.013	.013	.013	.013	.019	.019	.019	.019	.019	.019	.019	.019	.019
ANALNO	1	2	3	4	1	2	3	4	1	3	4	5	6	7	8	1	2	7	3	8	9	5	4	10	6	11
SIO2	46.98	50.64	48.15	50.22	50.30	50.37	50.93	50.22	53.85	49.63	49.49	48.89	47.92	48.36	49.10	49.13	47.92	52.96	48.80	51.42	51.31	49.15	48.58	53.18	47.45	51.46
TIO2	1.10	.79	.95	.86	.63	.44	.79	.59	.18	1.27	1.22	1.41	1.43	1.46	1.44	1.18	1.24	.28	1.17	.62	.54	1.31	1.20	.25	1.51	.55
AL2O3	7.86	5.74	7.18	6.16	4.42	3.96	4.38	3.76	1.16	5.37	5.40	5.82	5.97	5.99	5.70	6.61	7.57	3.12	6.87	4.34	3.45	6.91	6.81	2.94	7.84	4.23
TOTFEO	13.52	12.28	13.26	12.50	15.81	15.36	14.93	14.02	17.24	15.16	14.89	14.62	14.47	14.61	14.90	12.89	12.92	11.83	13.67	12.51	11.85	12.51	12.91	11.75	13.35	11.89
MNO	.46	.40	.28	.28	.61	.53	.43	.58	.48	.51	.46	.41	.43	.36	.42	.77	.63	.67	.53	.76	.67	.51	.50	.78	.50	.75
MGO	14.09	15.98	14.60	15.90	14.03	14.90	14.58	15.06	13.73	14.55	14.64	14.44	14.15	14.26	14.59	14.86	14.32	16.39	14.62	15.40	15.39	14.98	14.89	16.68	14.05	16.24
CAO	11.12	11.22	11.18	11.08	11.69	11.36	11.34	11.57	12.08	11.34	11.47	11.20	11.27	11.11	11.24	11.13	11.16	11.89	11.08	11.46	11.64	11.31	11.06	11.77	11.10	11.37
NA2O	1.31	1.00	1.13	1.07	1.01	.79	.70	.90	.00	1.31	1.23	1.19	1.22	1.36	1.06	1.22	1.19	.37	1.29	.97	.40	1.07	1.14	.31	1.40	.53
K2O	.43	.28	.38	.32	.44	.37	.48	.40	.13	.53	.53	.55	.51	.63	.57	.42	.44	.19	.42	.31	.26	1.43	.18	1.42	.18	.27
TOTAL	96.87	98.34	97.11	98.59	98.94	98.28	97.64	98.11	98.85	99.66	99.33	98.53	97.38	98.09	99.04	98.01	97.19	97.41	97.45	97.48	95.71	98.18	97.25	97.85	97.82	97.30
SI	6.941	7.270	7.061	7.106	7.331	7.375	7.393	7.366	7.822	7.169	7.166	7.126	7.079	7.093	7.127	7.129	7.021	7.626	7.116	7.454	7.549	7.103	7.095	7.630	6.939	7.449
AL(4)	1.059	.730	.939	.794	.669	.625	.657	.634	.178	.831	.834	.874	.921	.907	.873	.871	.979	.374	.884	.546	.451	.897	.905	.370	1.061	.551
AL(6)	.310	.241	.302	.247	.091	.059	.100	.016	.021	.083	.087	.126	.119	.119	.103	.259	.328	.156	.296	.196	.182	.280	.268	.127	.290	.171
TI	.122	.085	.105	.093	.069	.048	.087	.065	.020	.138	.133	.155	.159	.161	.157	.129	.137	.030	.128	.068	.060	.132	.132	.027	.166	.080
TOTFE	1.671	1.474	1.626	1.500	1.927	1.881	1.833	1.720	2.094	1.831	1.803	1.782	1.788	1.792	1.809	1.540	1.559	1.389	1.545	1.517	1.458	1.512	1.528	1.410	1.633	1.439
MN	.058	.049	.035	.058	.075	.066	.053	.072	.059	.062	.056	.051	.054	.045	.052	.095	.078	.082	.065	.093	.083	.062	.062	.095	.062	.092
MG	3.103	3.420	3.192	3.401	3.049	3.252	3.190	3.274	2.973	3.133	3.160	3.138	3.116	3.118	3.128	3.214	3.128	3.519	3.178	3.328	3.375	3.228	3.242	3.568	3.063	3.505
NA	.375	.278	.321	.298	.285	.228	.199	.256	.000	.367	.345	.336	.349	.387	.329	.343	.338	.103	.365	.132	.114	.300	.379	.086	.454	.149
CA	1.760	1.726	1.757	1.703	1.826	1.782	1.782	1.732	1.888	1.755	1.779	1.749	1.784	1.746	1.748	1.730	1.750	1.834	1.731	1.811	1.835	1.751	1.741	1.809	1.739	1.763
K	.081	.051	.071	.059	.082	.069	.090	.075	.024	.098	.098	.102	.096	.118	.106	.078	.082	.035	.078	.057	.049	.079	.069	.033	.078	.050
TOTZ	8.00	8.00	8.00	8.00	8.00	8.00	8.00	8.00	8.00	8.00	8.00	8.00	8.00	8.00	8.00	8.00	8.00	8.00	8.00	8.00	8.00	8.00	8.00	8.00	8.00	8.00
TOTY	5.26	5.27	5.26	5.30	5.21	5.31	5.26	4.95	5.17	5.25	5.24	5.25	5.24	5.23	5.28	5.24	5.23	5.18	5.21	5.20	5.16	5.22	5.23	5.23	5.21	5.27
TOTX	2.22	2.05	2.15	2.06	2.19	2.07	2.07	2.46	1.90	2.22	2.22	2.19	2.23	2.25	2.15	2.15	2.17	1.97	2.17	2.00	2.00	2.13	2.18	1.93	2.27	1.96

DRH.NO	.019	.019	.019	.025	.025	.025	.025	.025	.025	.025	.025	.025	.025	.025	.025	.025	.025	.025	.025	.025	.025	.025	.025	.025	.025
ANALNO	12	13	14	1	2	3	4	5	6	7	8	9	10	11	12	13	14	15	17	18	19	20	21	22	23	24
SIO2	51.53	51.51	51.95	47.83	47.00	47.58	47.30	47.07	47.08	47.77	48.75	53.64	47.60	47.44	46.10	48.41	46.92	47.10	47.73	47.06	48.24	52.40	47.42	46.92	47.40	47.40
TIO2	.61	.63	.63	1.21	1.37	1.26	1.45	1.82	1.21	1.76	1.21	.26	1.46	1.36	1.68	1.23	1.83	.63	1.18	1.57	1.35	.50	1.34	1.50	1.39	1.40
AL203	4.06	4.28	4.23	7.21	7.59	7.12	7.76	8.59	7.61	7.76	7.10	3.29	7.56	7.42	8.21	7.92	8.53	7.68	7.92	7.83	7.60	4.55	7.35	7.58	7.53	7.70
TOTFEO	12.02	11.88	12.12	13.31	13.74	13.43	13.73	13.96	14.00	13.99	12.89	11.53	13.98	14.10	14.73	13.25	14.32	14.05	13.87	13.89	13.18	12.16	14.01	14.12	14.13	13.73
MNO	.72	.77	.72	.96	.44	.41	.62	.70	.58	.52	.53	.61	.42	.41	.47	.71	.44	.86	.63	.44	.71	.61	.41	.61	.46	.55
MGO	15.79	15.54	15.68	14.12	13.79	14.05	13.56	13.36	13.66	13.82	14.51	16.47	13.85	13.81	13.53	14.04	13.59	13.57	13.87	13.75	14.05	15.97	14.03	13.63	14.08	14.03
CAO	11.65	11.49	11.74	11.31	11.39	11.32	11.67	11.43	11.43	11.46	11.44	12.11	11.63	11.52	11.76	11.32	11.46	11.52	11.76	11.48	11.41	12.19	11.54	11.56	11.48	11.57
NA2O	.69	.89	.72	1.30	1.31	1.22	1.17	1.06	1.25	1.39	1.30	.53	1.34	1.33	1.37	1.08	1.25	1.32	.88	1.34	1.15	.38	1.19	1.39	1.39	1.17
K2O	.30	.30	.32	.61	.62	.56	.49	.65	.45	.96	.54	.23	.59	.53	.59	.59	.59	.20	.55	.54	.54	.16	.55	.57	.56	.50
TOTAL	97.36	97.49	98.21	97.36	97.24	96.96	97.95	98.97	97.50	98.77	98.28	98.66	98.42	97.83	97.56	97.44	98.06	98.04	97.60	97.74	97.61	97.99	97.85	97.90	98.39	97.75
SI	7.468	7.457	7.471	7.026	6.940	7.022	6.938	6.840	6.946	6.944	7.070	7.623	6.949	6.961	6.814	7.092	6.894	6.914	7.013	6.915	7.061	7.537	6.978	6.906	6.927	6.957
AL(4)	.532	.543	.529	.974	1.060	.978	1.062	1.160	1.054	.930	.377	1.051	1.039	1.106	.908	1.106	.987	1.086	.987	1.085	.939	.463	1.022	1.094	1.073	1.043
AL(6)	.162	.188	.188	.275	.261	.280	.312	.269	.276	.284	.174	.246	.245	.294	.287	.244	.264	.242	.264	.248	.268	.139	.244	.223	.224	.237
TI	.066	.069	.068	.134	.152	.140	.160	.199	.138	.155	.132	.028	.160	.150	.187	.136	.179	.180	.130	.173	.149	.054	.147	.166	.153	.155
TOTFE	1.457	1.438	1.458	1.635	1.697	1.658	1.684	1.697	1.727	1.701	1.563	1.370	1.707	1.730	1.748	1.620	1.760	1.725	1.692	1.704	1.613	1.463	1.713	1.738	1.727	1.685
MN	.088	.094	.088	.057	.055	.051	.077	.086	.072	.064	.065	.073	.052	.051	.059	.088	.055	.070	.078	.055	.088	.074	.058	.076	.057	.068
MG	3.412	3.354	3.362	3.092	3.035	3.091	2.965	2.894	3.009	2.996	3.137	3.489	3.014	3.021	2.981	3.066	2.977	2.970	3.038	3.012	3.066	3.425	3.058	2.991	3.068	3.070
NA	.196	.250	.201	.376	.375	.349	.333	.394	.355	.362	.366	.146	.379	.378	.373	.307	.367	.376	.251	.382	.326	.106	.323	.397	.394	.333
CA	1.809	1.813	1.804	1.780	1.802	1.790	1.834	1.780	1.807	1.785	1.778	1.844	1.819	1.811	1.815	1.777	1.804	1.812	1.851	1.802	1.789	1.879	1.808	1.823	1.798	1.819
K	.055	.055	.059	.114	.117	.105	.129	.120	.122	.122	.100	.042	.110	.099	.111	.095	.124	.112	.103	.107	.101	.042	.103	.107	.097	.094
TOTZ	8.00	8.00	8.00	8.00	8.00	8.00	8.00	8.00	8.00	8.00	8.00	8.00	8.00	8.00	8.00	8.00	8.00	8.00	8.00	8.00	8.00	8.00	8.00	8.00	8.00	8.00
TOTY	5.19	5.19	5.16	5.19	5.20	5.20	5.17	5.19	5.21	5.18	5.13	5.18	5.21	5.20	5.22	5.20	5.22	5.20	5.19	5.20	5.18	5.15	5.22	5.19	5.23	5.21
TOTX	2.06	2.12	2.07	2.26	2.29	2.29	2.30	2.29	2.28	2.30	2.24	2.03	2.31	2.29	2.32	2.18	2.29	2.30	2.20	2.30	2.22	2.03	2.23	2.33	2.29	2.25

DRH.NO	.025	.025	.025	.025	.025	.025	.025	.025	.025	.025	.025	.025	.025	.025	.025	.034	.034	.035	.035	.035	.036	.036	.036	.036
ANALNO	25	26	27	28	29	30	31	32	33	34	35	36	37	38	39	40	41	1	2	1	2	3	1	2	3	4
SIO2	46.39	46.99	47.67	47.46	47.86	47.75	52.76	47.79	47.61	48.62	53.13	53.78	53.92	47.54	48.11	47.26	47.40	48.77	50.03	49.59	49.06	49.24	47.67	46.81	48.76	47.72
TIO2	1.64	1.68	1.33	1.37	1.29	1.45	.20	1.30	1.07	1.27	.29	.16	.21	1.47	1.39	1.32	1.21	1.40	1.38	1.81	1.42	1.18	.96	.83	.94	.94
AL203	8.17	8.06	7.22	7.49	7.44	7.40	3.88	7.24	6.80	6.66	3.03	2.61	2.90	7.41	7.18	7.24	7.06	6.10	6.21	6.22	6.23	6.14	7.59	7.71	6.71	8.05
TOTFEO	14.36	14.36	14.33	13.77	13.91	13.66	11.94	14.29	14.08	13.68	12.06	11.48	11.57	13.98	13.79	14.04	13.33	12.32	12.93	13.19	13.13	13.04	13.75	13.49	13.30	13.82
MNO	.36	.53	.68	.39	.62	.57	.56	.59	.67	.79	.81	.75	.61	.47	.53	.44	.41	.79	.74	.72	.76	.63	.48	.56	.60	.60
MGO	13.45	13.56	13.53	13.95	14.29	13.55	16.20	13.54	13.41	14.18	16.13	16.55	16.76	14.04	14.42	14.02	14.41	14.94	15.03	14.68	14.61	14.87	14.08	14.07	14.86	14.39
CAO	11.46	11.56	11.46	11.75	11.57	11.67	12.22	11.52	11.40	11.65	12.25	12.06	12.14	11.69	11.55	11.72	11.59	10.82	11.03	11.97	11.28	11.70	10.83	10.94	10.89	10.79
NA2O	1.46	1.59	1.25	1.38	1.22	1.01	.48	1.23	.96	1.07	.29	.17	.25	1.53	1.26	1.20	.99	1.31	1.26	1.29	1.12	1.19	1.07	1.19	1.05	1.10
K2O	.69	.64	.52	.58	.59	.55	.20	.62	.55	.49	.21	.16	.21	.59	.56	.53	.53	.24	.18	.32	.27	.44	.16	.18	.15	.18
TOTAL	97.98	98.97	97.99	98.34	98.78	97.63	98.44	98.12	96.56	98.41	98.21	97.73	98.66	98.69	98.72	97.59	97.20	96.95	98.80	99.30	97.88	98.43	96.60	95.32	97.27	97.61
SI	6.831	6.851	6.999	6.930	6.957	7.008	7.538	7.006	7.079	7.077	7.618	7.706	7.658	6.927	6.987	6.961	6.984	7.157	7.187	7.125	7.141	7.137	7.035	7.004	7.127	6.975
AL(4)	1.169	1.149	1.001	1.070	1.043	.992	.462	.994	.921	.923	.382	.294	.342	1.073	1.013	1.039	1.016	.843	.813	.875	.859	.863	.965	.996	.873	1.025
AL(6)	.249	.235	.248	.253	.231	.289	.192	.256	.271	.220	.130	.147	.144	.201	.216	.218	.210	.212	.238	.178	.210	.186	.356	.363	.283	.362
TI	.182	.184	.147	.150	.141	.160	.021	.143	.120	.139	.031	.017	.022	.161	.152	.146	.134	.154	.149	.174	.155	.129	.107	.093	.103	.103
TOTFE	1.768	1.751	1.759	1.682	1.691	1.677	1.427	1.752	1.751	1.665	1.446	1.376	1.374	1.705	1.675	1.729	1.643	1.512	1.553	1.585	1.598	1.581	1.697	1.688	1.626	1.689
MN	.045	.046	.085	.048	.076	.071	.068	.073	.084	.097	.098	.091	.073	.058	.065	.055	.051	.098	.090	.088	.094	.077	.060	.071	.074	.074
MG	2.953	2.947	2.961	3.037	3.097	2.965	3.451	2.959	2.973	3.077	3.448	3.535	3.549	3.052	3.122	3.077	3.178	3.268	3.219	3.144	3.170	3.213	3.098	3.138	3.238	3.136
NA	.417	.449	.356	.391	.394	.287	.133	.350	.277	.302	.081	.042	.096	.433	.338	.283	.346	.387	.351	.359	.341	.314	.306	.345	.298	.312
CA	1.808	1.806	1.803	1.838	1.802	1.835	1.871	1.809	1.816	1.817	1.882	1.852	1.846	1.827	1.797	1.849	1.830	1.701	1.698	1.796	1.759	1.817	1.713	1.680	1.705	1.690
K	.130	.119	.097	.108	.109	.103	.036	.116	.104	.091	.038	.029	.038	.110	.104	.100	.100	.045	.033	.059	.050	.081	.030	.034	.028	.035
TOTZ	8.00	8.00	8.00	8.00	8.00	8.00	8.00	8.00	8.00	8.00	8.00	8.00	8.00	8.00	8.00	8.00	8.00	8.00	8.00	8.00	8.00	8.00	8.00	8.00	8.00	8.00
TOTY	5.20	5.18	5.20	5.17	5.24	5.16	5.16	5.18	5.20	5.20	5.16	5.17	5.16	5.18	5.23	5.22	5.22	5.24	5.25	5.17	5.23	5.19	5.32	5.35	5.32	5.36
TOTX	2.35	2.37	2.26	2.34	2.25	2.22	2.04	2.27	2.20	2.21	2.00	1.93	1.98	2.37	2.24	2.23	2.28	2.13	2.08	2.21	2.12	2.23	2.05	2.06	2.03	2.04

APPENDIX 4, TABLE 2: AMPHIBOLE ANALYSES (CONTINU)

DRM.NO	.036	.036	.036	.044	.044	.044	.044	.044	.044	.044	.051	.051	.052	.052	.052	.052	.052	.052	.052	.052	.052	.054	.054	.054
ANAL.NO	5	6	7	1	2	3	4	5	6	7	8	1	2	1	2	3	4	5	6	7	8	9	10	1	2	3
SIO2	48.47	54.62	53.91	50.86	52.63	54.47	52.89	52.12	53.09	50.40	50.52	44.90	45.57	50.84	51.35	49.32	48.37	49.73	50.29	49.37	48.20	47.67	51.08	43.33	43.21	43.92
TIO2	.96	.00	.00	.71	.66	.13	.57	.61	.29	1.12	.78	1.20	1.20	.38	.51	1.14	1.49	.62	.66	1.14	1.85	1.66	.62	3.08	3.16	2.70
AL2O3	7.68	1.66	2.18	4.19	3.75	1.95	3.78	3.68	3.10	5.19	4.75	7.25	7.08	5.58	5.73	6.91	6.82	6.47	6.03	6.52	7.83	8.03	4.93	10.11	10.38	9.51
TOTFEO	13.79	11.35	11.72	11.69	11.52	9.66	11.35	11.29	10.91	12.14	12.06	17.59	17.88	14.11	13.90	15.03	15.07	14.42	14.44	14.74	14.87	15.47	12.79	14.31	14.33	14.66
MNO	.49	.00	.00	.43	.47	.49	.57	.57	.46	.54	.58	.40	.49	.38	.36	.42	.44	.44	.47	.47	.42	.36	.40	.33	.44	.34
MGO	14.59	16.90	16.40	16.09	17.13	18.03	16.91	16.75	17.18	15.66	15.60	10.68	11.05	15.01	15.01	14.54	14.02	14.76	15.17	14.76	13.76	13.72	15.25	12.21	12.39	12.44
CAO	10.90	12.56	12.55	11.33	11.40	11.96	11.85	11.94	11.75	11.54	11.56	11.36	11.22	11.42	11.50	11.12	11.31	11.66	11.10	11.05	11.48	11.64	12.06	11.45	11.48	11.35
NA2O	1.25	.00	.00	.35	.52	.00	.42	.39	.35	.86	.55	.90	.99	.55	.61	.77	.87	.79	.70	.66	1.03	.95	.35	1.49	1.54	1.35
K2O	.18	.00	.00	.29	.28	.00	.23	.24	.21	.38	.33	.83	.76	.14	.16	.36	.42	.23	.20	.33	.45	.51	.22	.63	.63	.49
TOTAL	98.31	97.09	96.75	95.89	98.27	96.75	98.55	97.59	97.35	98.03	96.73	95.11	96.05	98.39	99.13	99.10	98.81	98.80	99.06	98.93	99.90	100.03	97.70	96.93	97.59	97.03
SI	7.026	7.836	7.780	7.455	7.502	7.791	7.521	7.498	7.618	7.272	7.374	6.932	6.960	7.332	7.339	7.126	7.035	7.187	7.228	7.127	6.932	6.876	7.390	6.483	6.429	6.569
AL(4)	.974	.164	.220	.545	.498	.209	.479	.502	.382	.728	.626	1.068	1.040	.668	.661	.874	.965	.813	.772	.873	1.068	1.124	.610	1.517	1.571	1.431
AL(6)	.338	.117	.151	.179	.132	.119	.154	.122	.142	.188	.191	.252	.234	.281	.305	.218	.209	.238	.250	.237	.260	.242	.231	.265	.249	.246
TI	.105	.000	.000	.078	.071	.014	.061	.066	.031	.122	.086	.139	.138	.041	.055	.124	.163	.067	.071	.124	.200	.180	.067	.347	.357	.304
TOTFE	1.672	1.362	1.415	1.433	1.373	1.155	1.350	1.358	1.309	1.465	1.472	2.271	2.258	1.702	1.661	1.816	1.833	1.743	1.736	1.780	1.789	1.866	1.547	1.790	1.783	1.834
MN	.060	.000	.000	.053	.057	.059	.069	.069	.056	.066	.072	.052	.063	.046	.044	.051	.054	.054	.057	.045	.051	.094	.067	.042	.057	.043
MG	3.153	3.614	3.528	3.505	3.640	3.844	3.585	3.592	3.675	3.368	3.395	2.458	2.516	3.227	3.198	3.132	3.040	3.181	3.250	3.177	2.956	2.950	3.289	2.723	2.748	2.774
NA	.351	.000	.000	.099	.144	.000	.116	.109	.097	.241	.156	.269	.293	.154	.169	.216	.245	.221	.195	.185	.187	.166	.098	.432	.444	.392
CA	1.693	1.931	1.898	1.779	1.741	1.833	1.805	1.840	1.806	1.784	1.808	1.879	1.836	1.765	1.761	1.722	1.962	1.806	1.709	1.709	1.769	1.766	1.849	1.835	1.830	1.819
K	.033	.006	.000	.054	.051	.011	.042	.044	.038	.070	.061	.163	.146	.026	.029	.066	.078	.042	.037	.061	.083	.094	.041	.120	.120	.147
TOTZ	8.00	8.00	8.00	8.00	8.00	8.00	8.00	8.00	8.00	8.00	8.00	8.00	8.00	8.00	8.00	8.00	8.00	8.00	8.00	8.00	8.00	8.00	8.00	8.00	8.00	8.00
TOTY	5.33	5.09	5.09	5.25	5.27	5.19	5.22	5.21	5.21	5.21	5.22	5.17	5.21	5.30	5.26	5.34	5.29	5.28	5.36	5.36	5.25	5.28	5.18	5.17	5.19	5.20
TOTX	2.08	1.93	1.94	1.93	1.94	1.84	1.96	1.99	1.94	2.09	2.02	2.31	2.27	1.94	1.96	2.00	2.08	2.08	1.94	1.95	2.14	2.16	2.01	2.39	2.39	2.36

DRM.NO	.054	.054	.054	.054	.054	.054	.054	.054	.054	.054	.054	.054	.056	.056	.056	.056	.056	.056	.056	.065	.065	.065	.065	.065	.065
ANAL.NO	4	5	6	7	8	9	10	11	12	13	14	15	16	1	2	3	4	5	6	7	1	2	3	4	5	6
SIO2	44.33	44.64	46.88	48.29	48.27	45.25	45.80	45.39	46.89	45.53	45.65	49.90	50.16	49.46	51.29	45.24	53.76	46.86	52.64	54.77	41.57	41.17	42.67	41.47	42.38	43.51
TIO2	2.42	2.06	1.16	1.81	1.67	2.59	2.42	2.34	1.97	2.27	2.24	.90	.90	.96	.77	1.02	.33	1.75	.55	.34	2.57	2.40	2.31	2.46	2.27	2.06
AL2O3	9.13	8.31	7.20	7.29	6.91	9.18	8.82	9.09	7.97	9.53	8.71	5.31	5.43	5.07	3.78	8.93	2.43	7.14	2.95	1.88	12.99	12.63	12.39	12.95	12.53	11.40
TOTFEO	15.68	15.73	17.09	14.64	13.86	15.00	14.82	14.24	13.80	13.83	14.72	14.10	14.08	16.80	15.97	20.78	15.56	17.86	14.99	14.04	14.10	13.59	13.46	14.34	13.99	13.71
MNO	.20	.39	.22	.32	.33	.43	.41	.36	.41	.21	.29	.29	.27	.42	.42	.42	.46	.21	.29	.00	.18	.29	.26	.26	.30	.34
MGO	12.23	12.24	12.73	13.95	14.28	13.01	13.02	13.21	13.61	12.91	12.87	14.20	14.10	12.95	13.96	12.10	12.87	11.84	15.09	16.39	12.45	12.26	12.08	12.14	12.53	13.06
CAO	11.98	11.66	12.06	11.98	11.76	11.62	11.41	11.51	11.90	11.51	11.62	12.18	12.17	11.10	11.60	9.28	10.95	11.23	11.25	11.26	12.04	12.03	12.07	12.11	12.37	12.29
NA2O	1.34	.95	.56	1.10	1.09	1.29	1.39	1.36	1.08	1.01	1.33	.53	.45	1.06	.71	1.08	.51	1.45	.64	.43	2.23	2.17	2.02	2.01	1.99	1.65
K2O	1.23	.78	.74	.72	.67	.99	.95	.89	.83	.93	.82	.41	.48	.55	.42	.52	.22	.71	.29	.31	.78	.76	.95	.83	.78	.71
TOTAL	98.53	96.76	98.67	100.03	98.74	99.17	99.03	98.33	98.45	97.73	98.25	97.81	98.05	98.37	98.32	98.36	99.44	99.04	98.62	99.72	99.13	97.29	99.01	98.56	99.15	98.78
SI	6.588	6.723	6.927	6.960	7.011	6.631	6.703	6.673	6.855	6.703	6.727	7.284	7.298	7.278	7.481	6.796	7.691	6.925	7.596	7.752	6.121	6.163	6.255	6.142	6.223	6.383
AL(4)	1.412	1.277	1.073	1.040	.989	1.369	1.297	1.327	1.145	1.297	1.273	.716	.702	.722	.519	1.204	.309	1.075	.404	.248	1.879	1.837	1.745	1.858	1.777	1.617
AL(6)	.187	.198	.181	.199	.193	.216	.224	.249	.228	.357	.240	.197	.229	.157	.131	.200	.100	.169	.098	.065	.375	.391	.396	.402	.402	.354
TI	.270	.233	.129	.175	.171	.263	.266	.259	.217	.251	.248	.098	.098	.106	.084	.115	.038	.194	.060	.036	.285	.270	.255	.274	.251	.231
TOTFE	1.949	1.981	2.112	1.765	1.683	1.838	1.814	1.751	1.687	1.703	1.814	1.721	1.713	2.067	1.948	2.608	1.662	2.207	1.799	1.662	1.736	1.701	1.650	1.776	1.718	1.682
MN	.088	.050	.028	.040	.041	.053	.051	.045	.051	.026	.036	.033	.033	.052	.052	.053	.056	.026	.035	.048	.047	.037	.026	.033	.037	.042
MG	2.710	2.748	2.804	2.998	3.092	2.842	2.841	2.895	2.966	2.834	2.827	3.090	3.058	2.841	3.036	2.710	3.246	2.609	3.246	3.458	2.733	2.736	2.815	2.680	2.743	2.856
NA	.928	.877	.660	.807	.867	.807	.769	.813	.864	.816	.835	.905	.897	.750	.779	.741	.678	.778	.739	.708	.637	.630	.574	.577	.567	.469
CA	1.928	1.882	1.913	1.850	1.830	1.824	1.789	1.813	1.864	1.816	1.835	1.905	1.897	1.703	1.778	1.444	1.678	1.778	1.739	1.708	1.899	1.929	1.896	1.922	1.946	1.932
K	.233	.150	.139	.132	.124	.185	.177	.167	.155	.175	.154	.076	.089	.103	.078	.100	.042	.134	.053	.038	.147	.145	.178	.157	.146	.137
TOTZ	8.00	8.00	8.00	8.00	8.00	8.00	8.00	8.00	8.00	8.00	8.00	8.00	8.00	8.00	8.00	8.00	8.00	8.00	8.00	8.00	8.00	8.00	8.00	8.00	8.00	8.00
TOTY	5.20	5.21	5.25	5.18	5.18	5.21	5.20	5.20	5.15	5.17	5.16	5.19	5.13	5.22	5.25	5.69	5.30	5.20	5.24	5.27	5.18	5.13	5.15	5.16	5.14	5.16
TOTX	2.45	2.31	2.21	2.29	2.26	2.38	2.36	2.35	2.32	2.28	2.37	2.13	2.11	2.15	2.00	1.91	1.86	2.33	1.97	1.86	2.68	2.70	2.65	2.66	2.66	2.54

DRM.NO	.080	.080	.080	.080	.080	.080	.080	.080	.080	.080	.080	.080	.080	.080	.080	.080	.080	.080	.080	.080	.080	.080	.080	.080	.080	.081
ANAL.NO	1	2	3	4	5	6	7	8	9	10	11	12	13	14	15	16	17	18	19	21	20	23	22	24	25	1
SIO2	48.35	48.50	47.80	47.73	48.20	47.62	46.67	48.21	52.99	47.39	45.86	42.81	51.96	47.10	48.25	46.81	46.50	48.09	49.68	47.18	50.41	49.91	51.28	48.42	50.42	46.43
TIO2	1.21	1.18	1.18	1.28	1.16	1.13	1.33	1.15	.51	1.02	1.42	2.03	.70	1.11	1.10	1.25	1.05	.92	.94	1.36	.96	.95	.76	1.37	.94	1.85
AL2O3	7.45	7.46	7.46	7.42	7.10	7.57	8.31	7.04	2.79	7.24	8.75	11.06	4.08	6.56	6.74	7.59	7.72	7.97	6.17	6.85	5.91	6.46	5.64	8.09	6.24	9.91
TOTFEO	13.56	13.53	13.15	13.09	12.46	13.17	13.73	12.99	9.16	12.94	13.89	15.02	10.59	13.25	12.30	12.39	13.35	13.82	12.53	13.37	11.65	12.70	11.99	12.98	12.52	15.13
MNO	.47	.53	.51	.46	.50	.45	.43	.49	.56	.50	.49	.40	.49	.53	.43	.59	.51	.48	.47	.51	.42	.39	.57	.54	.52	.65
MGO	14.74	15.13	14.68	14.80	15.13	14.77	14.28	14.98	17.85	14.67	13.87	12.37	16.88	14.91	15.13	14.54	14.31	14.88	15.44	14.49	16.26	15.41	16.27	15.15	15.48	12.77
CAO	11.21	11.32	11.21	11.06	11.16	11.29	11.22	11.25	11.50	11.08	11.12	11.42	11.45	11.10	10.90	11.12	11.14	11.19	11.26	11.33	11.41	11.37	11.46	11.55	11.52	11.59
NA2O	1.51	1.52	1.47	1.49	1.49	1.44	1.59	1.52	.64	1.41	1.80	2.23	.95	1.48	1.34	1.55	1.77	1.51	1.30	1.66	1.16	1.38	1.17	1.82	1.25	1.26
K2O	.43	.41	.43	.45	.42	.42	.54	.38	.23	.36	.49	.92	.28	.42	.37	.49	.73	.32	.29	.48	.34	.35	.32	.48	.55	.56
TOTAL	98.92	99.58	97.88	97.79	97.59	97.86	98.10	97.96	96.23	96.62	97.69	98.07	96.80	97.50	96.76	96.31	96.77	99.17	98.07	98.25	98.59	98.91	99.47	100.39	99.58	98.15
SI	6.987	6.966	6.976	6.971	7.028	6.954	6.834	7.021	7.641	7.001	6.761	6.376	7.448	6.916	7.078	6.938	6.897	6.936	7.183	6.887	7.221	7.160	7.278	6.894	7.195	6.851
AL(4)	1.013	1.034	1.024	1.029	.972	1.046	1.166	.979	.359	.999	1.239	1.624	.552	1.084	.922	1.062	1.103	1.064	.817	1.113	.779	.840	.722	1.106	.805	1.149
AL(6)	.256	.228	.260	.248	.248	.257	.268	.229	.115	.261	.282	.317	.144	.225	.243	.264	.246	.291	.234	.238	.218	.252	.221	.252	.244	.227
TI	.132	.127	.130	.141	.127	.124	.146	.126	.055	.113	.157	.227	.076	.123	.121	.139	.117	.100	.102	.149	.107	.102	.081	.147	.101	.205
TOTFE	1.639	1.625	1.603	1.590	1.522	1.608	1.681	1.576	1.105	1.599	1.711	1.871	1.282	1.627	1.509	1.536	1.654	1.667	1.515	1.632	1.396	1.524	1.423	1.546	1.494	1.867
MN	.058	.064	.063	.057	.062	.056	.053	.060	.068	.063	.061	.050	.050	.066	.053	.074	.069	.059	.058	.063	.051	.047	.069	.065	.063	.081
MG	3.176	3.239	3.199	3.222	3.289	3.216	3.117	3.252	3.837	3.231	3.098	2.746	3.642	3.270	3.353	3.213	3.164	3.200	3.328	3.153	3.459	3.295	3.442	3.216	3.293	2.809
NA	.423	.423	.416	.422	.407	.408	.451	.429	.179	.404	.515	.644	.267	.421	.381	.445	.509	.422	.364	.470	.322	.384	.322	.502	.346	.432
CA	1.736	1.742	1.753	1.731	1.744	1.766	1.760	1.755	1.777	1.754	1.757	1.822	1.775	1.746	1.713	1.766	1.776	1.729	1.744	1.772	1.751	1.747	1.743	1.780	1.761	1.832
K	.079	.075	.080	.084	.078	.078	.101	.071	.042	.068	.092	.139	.052	.079	.069	.091	.079	.059	.053	.091	.062	.064	.058	.087	.100	.105
TOTZ	8.00	8.00	8.00	8.00	8.00	8.00	8.00	8.00	8.00	8.00	8.00	8.00	8.00	8.00	8.00	8.00	8.00	8.00	8.00	8.00	8.00	8.00	8.00	8.00	8.00	8.00
TOTY	5.26	5.28	5.25	5.27	5.25	5.26	5.26	5.24	5.18	5.27	5.26	5.21	5.19	5.31	5.28	5.23	5.25	5.32	5.29	5.23	5.23	5.20	5.24	5.32	5.19	5.19
TOTX	2.24	2.24	2.25	2.24	2.23	2.25	2.31	2.25	2.00	2.23	2.36	2.60	2.09	2.25	2.16	2.30	2.36	2.21	2.16	2.33	2.13	2.19	2.12	2.25	2.21	2.30

APPENDIX 4, TABLE 2: AMPHIBOLE ANALYSES (CONTIN)

DRM.NO	.081	.081	.081	.081	.081	.081	.081	.081	.081	.081	.081	.143	.144	.144	.144	.144	.144	.144	.149	.149	.149	.149
ANALNO	2	3	4	5	6	7	8	9	10	11	12	1	1	2	3	4	5	6	1	2	3	4
SIO2	47.30	45.47	47.80	48.00	47.23	45.99	50.33	46.01	44.88	46.35	49.77	45.14	44.05	44.26	44.05	44.37	44.01	44.52	50.11	48.47	46.41	48.54
TIO2	1.30	1.90	1.18	1.17	1.58	2.17	.81	2.08	2.02	1.75	.77	1.66	2.87	2.87	2.80	2.95	2.87	2.59	.23	.23	.15	.17
AL203	6.96	8.12	6.89	6.80	7.79	8.48	5.20	8.47	7.89	7.74	5.41	11.21	9.93	9.86	10.25	10.23	10.46	10.10	3.88	3.91	7.39	4.39
TOTFEO	14.76	15.64	15.39	15.07	15.09	14.75	13.93	14.92	16.40	15.07	14.56	12.27	12.05	11.70	12.26	12.09	12.07	13.12	15.51	16.93	16.57	18.83
MNO	.69	.64	.74	.81	.66	.52	.72	.50	.61	.86	.68	.21	.29	.26	.32	.22	.22	.29	.72	.58	.65	.79
MGO	12.82	11.78	12.63	12.92	12.96	12.86	14.12	12.82	12.54	12.67	14.22	14.03	14.51	14.64	14.43	14.25	14.33	13.73	12.77	11.90	10.53	10.54
CAO	11.77	11.56	11.69	11.65	11.67	11.50	11.95	11.59	11.18	11.45	11.89	12.16	11.23	11.13	11.37	11.31	11.47	11.34	11.95	11.98	10.59	11.75
NA2O	.82	1.35	.83	.91	1.39	1.40	.63	1.55	1.40	1.19	.75	2.03	2.20	2.22	2.31	2.23	2.25	2.11	.20	.26	.40	.23
K2O	.71	.54	.69	.72	.69	.56	.44	.66	.59	.58	.48	.80	.78	.81	.80	.86	.80	.79	.10	.11	.32	.09
TOTAL	97.14	96.98	97.84	98.05	99.06	98.22	98.14	98.59	97.51	97.66	98.52	99.51	97.90	97.78	98.59	98.51	98.49	98.60	95.47	94.38	93.22	95.34
SI	7.030	6.819	7.063	7.070	6.902	6.771	7.323	6.763	6.730	6.877	7.246	6.511	6.470	6.497	6.437	6.474	6.429	6.515	7.528	7.445	7.195	7.438
AL(4)	.970	1.181	.937	.930	1.098	1.229	.677	1.237	1.270	1.123	.754	1.489	1.530	1.503	1.563	1.526	1.571	1.485	.472	.555	.805	.562
AL(6)	.249	.254	.263	.250	.243	.243	.215	.230	.124	.230	.174	.417	.189	.202	.202	.233	.230	.257	.215	.152	.546	.231
TI	.145	.214	.131	.130	.174	.240	.089	.230	.228	.195	.084	.180	.317	.317	.308	.324	.315	.285	.026	.027	.017	.020
TOTFE	1.835	1.961	1.902	1.856	1.844	1.816	1.695	1.834	2.057	1.870	1.773	1.480	1.480	1.436	1.498	1.475	1.475	1.606	1.949	2.175	2.148	2.413
MN	.087	.081	.093	.101	.082	.065	.089	.062	.077	.108	.084	.026	.036	.032	.040	.027	.027	.036	.092	.075	.085	.103
MG	2.840	2.633	2.782	2.837	2.823	2.823	3.063	2.809	2.803	2.802	3.086	3.017	3.177	3.204	3.143	3.100	3.121	2.995	2.860	2.725	2.434	2.408
NA	.236	.393	.238	.260	.394	.400	.178	.442	.407	.342	.212	.568	.627	.632	.654	.631	.637	.599	.058	.077	.180	.068
CA	1.874	1.857	1.851	1.838	1.827	1.814	1.863	1.825	1.796	1.820	1.855	1.879	1.767	1.750	1.780	1.768	1.795	1.778	1.923	1.971	1.759	1.929
K	.135	.103	.130	.135	.129	.105	.082	.124	.113	.110	.089	.147	.146	.152	.149	.160	.149	.147	.019	.022	.063	.018
TOTZ	8.00	8.00	8.00	8.00	8.00	8.00	8.00	8.00	8.00	8.00	8.00	8.00	8.00	8.00	8.00	8.00	8.00	8.00	8.00	8.00	8.00	8.00
TOTY	5.16	5.14	5.17	5.17	5.17	5.19	5.15	5.16	5.29	5.20	5.20	5.12	5.20	5.19	5.19	5.16	5.17	5.18	5.14	5.16	5.23	5.17
TOTX	2.24	2.35	2.22	2.23	2.35	2.32	2.12	2.39	2.32	2.27	2.16	2.59	2.54	2.53	2.58	2.56	2.58	2.52	2.00	2.07	2.00	2.01

APPENDIX 4, TABLE 3: BIOTITE ANALYSES(OXIDES, WT.PERCENT), AND STRUCTURAL FORMULAE(ATOMS,O=22;CA OMMITTED)

DRM.NO	.004	.004	.004	.004	.004	.012	.012	.012	.012	.012	.013	.013	.013	.013	.013	.019	.019	.019	.019	.019	.019	.019	.019
ANALNO	1	2	6	7	8	1	2	3	4	5	1	2	3	4	5	1	2	3	4	5	6	7	8	9	10	11
SIO2	37.43	36.30	36.74	35.22	35.78	42.75	41.77	44.51	42.53	38.58	37.16	37.17	37.14	37.36	36.82	37.03	37.76	37.70	38.00	36.93	37.30	37.15	37.08	43.23	37.69	37.36
TIO2	2.56	2.89	3.84	3.55	3.72	4.07	4.19	4.39	5.11	5.01	5.55	5.51	5.15	4.88	5.44	3.17	4.48	4.54	4.51	4.50	4.36	4.51	4.59	1.50	4.04	4.10
AL203	16.78	16.03	16.21	15.89	15.92	11.84	13.96	12.22	15.02	13.52	13.08	13.05	13.00	12.99	13.18	14.45	14.34	14.01	14.38	14.23	14.02	14.20	14.10	18.47	13.80	13.97
TOTFEO	17.52	17.06	16.42	17.16	16.69	16.47	17.90	16.22	15.70	19.65	20.45	20.56	20.68	20.82	20.51	17.77	19.07	18.89	18.35	18.38	18.15	18.25	18.26	14.37	18.27	17.75
MNO	.00	.00	.22	.00	.14	.00	.00	.00	.00	.00	.16	.00	.00	.00	.18	.50	.42	.37	.46	.40	.47	.39	.45	.31	.42	.32
MGO	12.68	12.30	17.76	17.76	17.75	12.53	12.61	11.30	9.80	13.26	12.03	11.86	12.08	12.21	12.17	12.72	12.52	12.46	12.54	12.85	13.22	13.03	12.93	10.69	12.99	13.15
CAO	.00	.97	.26	.27	.19	3.49	1.24	.36	1.02	.18	.00	.00	.00	.00	.00	.00	.00	.09	.00	.00	.16	.23	.17	.52	.17	.14
NA2O	.00	.00	.17	.00	.00	.00	.00	.10	.07	.00	.00	.00	.00	.00	.00	1.12	.00	.00	.00	.00	.00	.00	.00	.00	.00	.00
K2O	9.58	9.57	5.48	4.55	5.24	5.36	7.50	7.67	8.22	8.98	9.06	8.94	9.02	9.10	9.01	8.10	9.30	9.32	9.43	9.20	9.26	8.97	9.03	6.58	9.13	8.98
TOTAL	96.55	95.12	97.10	94.29	95.43	96.31	99.17	98.88	98.47	98.87	97.90	97.13	97.08	97.25	97.32	94.85	98.08	97.36	97.68	96.49	96.93	96.75	96.56	95.68	96.50	95.66
SI	5.605	5.546	5.321	5.255	5.277	6.352	6.003	6.543	6.103	5.659	5.571	5.589	5.594	5.618	5.536	5.666	5.582	5.619	5.624	5.545	5.577	5.562	5.564	6.184	5.655	5.635
AL(4)	2.938	2.454	2.679	2.745	2.723	1.648	1.997	1.457	1.897	2.285	2.311	2.313	2.308	2.362	2.336	2.334	2.418	2.381	2.376	2.455	2.423	2.438	2.436	1.816	2.347	2.365
AL(6)	.501	.433	.086	.050	.044	.390	.368	.569	.643	.000	.000	.000	.000	.000	.000	.271	.081	.080	.132	.063	.048	.068	.058	1.299	.093	.101
TI	.286	.332	.418	.413	.413	.455	.453	.551	.553	.465	.426	.426	.583	.552	.615	.365	.520	.509	.502	.508	.490	.508	.512	.181	.456	.465
TOTFE	2.177	2.180	1.988	2.141	2.058	2.046	2.151	1.908	1.802	2.410	2.564	2.585	2.605	2.618	2.579	2.274	2.358	2.352	2.271	2.308	2.270	2.288	2.292	1.719	2.292	2.239
MN	.000	.000	.027	.000	.017	.000	.000	.000	.000	.000	.020	.000	.000	.000	.023	.065	.053	.047	.058	.051	.060	.049	.057	.038	.053	.041
MG	2.809	2.802	3.832	3.951	3.902	2.775	2.702	2.370	2.096	2.899	2.689	2.658	2.712	2.715	2.728	2.901	2.759	2.768	2.767	2.876	2.947	2.908	2.893	2.280	2.905	2.957
NA	.000	.000	.048	.000	.000	.000	.000	.000	.298	.000	.000	.000	.000	.000	.000	.000	.000	.000	.000	.000	.000	.000	.000	.000	.000	.000
CA	.000	.000	.000	.000	.000	.000	.000	.000	.000	.000	.000	.000	.000	.000	.000	.000	.000	.000	.000	.000	.000	.000	.000	.000	.000	.000
K	1.816	1.865	1.008	.866	.986	1.016	1.375	1.376	1.505	1.680	1.733	1.715	1.733	1.746	1.728	1.581	1.754	1.772	1.780	1.762	1.766	1.713	1.729	1.201	1.747	1.728
TOTZ	7.44	8.00	8.00	8.00	8.00	8.00	8.00	8.00	8.00	7.94	7.88	7.90	7.90	7.92	7.87	8.00	8.00	8.00	8.00	8.00	8.00	8.00	8.00	8.00	8.00	8.00
TOTY	5.77	5.75	6.35	6.53	6.43	5.67	5.67	5.36	5.17	5.86	5.90	5.87	5.90	5.88	5.94	5.88	5.77	5.76	5.73	5.81	5.81	5.82	5.81	5.50	5.80	5.80
TOTX	1.82	1.86	1.06	.87	.99	1.02	1.37	1.38	1.80	1.68	1.73	1.72	1.73	1.75	1.73	1.58	1.75	1.77	1.78	1.76	1.77	1.71	1.73	1.20	1.75	1.73

DRM.NO	.019	.019	.019	.019	.019	.019	.019	.019	.019	.019	.025	.025	.025	.025	.025	.025	.025	.025	.025	.025	.025	.025	.025	.025	.025
ANALNO	12	13	14	15	16	17	18	19	20	21	22	1	2	3	4	5	6	7	8	9	10	11	12	13	14	15
SIO2	37.41	37.01	37.05	36.02	35.90	36.59	37.48	37.30	36.86	37.11	36.97	36.93	37.90	38.01	38.14	35.69	37.52	37.70	37.79	37.36	36.77	37.43	37.44	36.77	37.09	36.93
TIO2	3.92	3.87	3.93	3.56	2.97	4.56	4.75	4.68	4.57	4.80	4.57	4.56	4.45	4.35	4.57	3.92	4.54	4.49	4.62	4.51	4.48	4.38	4.50	4.35	4.92	4.51
AL203	14.19	14.38	14.27	14.77	15.00	13.95	14.04	14.33	13.99	14.51	15.33	13.76	13.86	14.22	14.17	14.45	14.10	13.96	13.99	13.74	13.75	13.87	13.94	13.64	14.03	13.95
TOTFEO	17.41	17.05	18.93	18.69	18.50	17.86	18.30	18.11	18.33	18.65	17.64	17.82	17.93	18.43	17.80	18.44	18.04	18.54	18.55	18.25	18.08	18.49	18.42	18.66	18.46	18.45
MNO	.43	.36	.44	.58	.50	.33	.39	.39	.44	.38	.44	.56	.25	.48	.38	.67	.35	.27	.20	.24	.26	.35	.31	.23	.35	.36
MGO	13.02	13.12	13.70	14.35	13.21	12.82	13.01	12.70	12.99	13.01	12.72	13.09	13.25	13.64	13.42	15.04	13.39	13.19	13.56	13.16	12.85	13.45	13.10	12.74	13.22	13.16
CAO	.13	.26	.24	.27	.31	.13	.19	.22	.17	.18	.47	.00	.00	.00	.12	.00	.10	.00	.00	.00	.00	.00	.00	.00	.10	.00
NA2O	.00	.00	.00	.00	.00	.00	.00	.00	.00	.00	.00	.00	.00	.00	.00	.00	.00	.00	.00	.00	.00	.00	.00	.00	.00	.00
K2O	8.95	8.60	8.15	7.26	8.08	8.88	9.22	9.10	9.16	9.26	8.90	9.03	9.31	9.03	9.13	7.28	9.44	9.49	9.53	9.27	9.23	9.20	9.32	9.24	9.35	9.41
TOTAL	95.43	94.65	96.70	95.60	94.80	95.10	97.42	96.75	96.48	98.08	96.93	95.49	96.94	98.15	97.74	95.70	97.48	97.64	98.25	96.53	95.43	97.17	97.02	95.64	97.54	96.77
SI	5.644	5.620	5.542	5.438	5.493	5.565	5.576	5.578	5.546	5.499	5.515	5.585	5.638	5.590	5.622	5.376	5.571	5.593	5.571	5.599	5.580	5.577	5.587	5.582	5.521	5.540
AL(4)	2.356	2.380	2.458	2.562	2.507	2.435	2.424	2.422	2.454	2.501	2.485	2.415	2.362	2.410	2.378	2.565	2.429	2.407	2.429	2.401	2.420	2.423	2.413	2.418	2.461	2.460
AL(6)	.167	.194	.058	.067	.198	.065	.038	.103	.027	.033	.210	.037	.068	.054	.084	.000	.039	.034	.002	.026	.039	.013	.038	.046	.000	.006
TI	.445	.442	.442	.404	.342	.519	.531	.526	.517	.535	.513	.519	.498	.481	.507	.444	.501	.501	.512	.508	.511	.491	.505	.497	.551	.509
TOTFE	2.197	2.166	2.366	2.360	2.406	2.271	2.272	2.265	2.307	2.311	2.201	2.254	2.231	2.267	2.247	2.378	2.278	2.300	2.287	2.287	2.295	2.304	2.299	2.369	2.298	2.315
MN	.055	.048	.056	.074	.065	.043	.049	.039	.052	.070	.054	.038	.031	.057	.047	.085	.044	.034	.025	.030	.033	.044	.039	.030	.044	.046
MG	2.928	2.970	3.055	3.230	3.013	2.906	2.886	2.831	2.914	2.874	2.829	2.951	2.938	2.990	2.949	3.378	2.964	2.917	2.980	2.940	2.907	2.988	2.914	2.883	2.934	2.943
NA	.000	.000	.000	.000	.000	.000	.000	.000	.000	.000	.000	.000	.000	.000	.000	.000	.000	.000	.000	.000	.000	.000	.000	.000	.000	.000
CA	.000	.000	.000	.000	.000	.000	.000	.000	.000	.000	.000	.000	.000	.000	.000	.000	.000	.000	.000	.000	.000	.000	.000	.000	.000	.000
K	1.717	1.666	1.555	1.418	1.579	1.723	1.759	1.736	1.758	1.750	1.636	1.742	1.767	1.694	1.717	1.399	1.788	1.796	1.792	1.772	1.787	1.749	1.774	1.784	1.775	1.801
TOTZ	8.00	8.00	8.00	8.00	8.00	8.00	8.00	8.00	8.00	8.00	8.00	8.00	8.00	8.00	8.00	7.94	8.00	8.00	8.00	8.00	8.00	8.00	8.00	8.00	7.98	8.00
TOTY	5.79	5.82	5.98	6.13	6.02	5.80	5.78	5.76	5.82	5.82	5.81	5.80	5.79	5.85	5.78	6.25	5.79	5.79	5.81	5.79	5.78	5.84	5.79	5.80	5.83	5.82
TOTX	1.72	1.67	1.56	1.42	1.58	1.72	1.76	1.74	1.76	1.75	1.64	1.74	1.77	1.69	1.72	1.40	1.79	1.80	1.79	1.77	1.79	1.75	1.77	1.79	1.78	1.80

DRM.NO	.025	.025	.025	.025	.025	.025	.025	.025	.025	.025	.025	.025	.025	.025	.025	.025	.025	.025	.025	.027	.027	.027	.044	.044	.044	.044
ANALNO	16	17	18	19	20	21	22	23	24	25	26	27	28	29	30	31	32	33	34	1	2	3	1	2	3	4
SIO2	37.07	37.21	37.41	37.21	37.29	36.15	37.39	37.29	36.81	36.99	37.12	37.01	37.45	36.99	37.33	37.87	38.05	37.61	37.94	40.28	40.12	37.42	37.91	37.65	37.74	37.51
TIO2	4.47	4.82	4.58	4.57	4.24	4.02	3.80	4.06	3.67	3.78	3.86	4.48	4.14	4.21	4.18	4.46	4.06	4.76	3.97	1.57	1.82	1.79	3.38	3.51	3.84	3.74
AL203	14.19	13.95	14.14	13.35	14.01	13.92	13.92	13.83	13.85	14.05	13.82	13.92	13.92	13.71	13.77	14.13	14.08	14.02	14.02	15.82	16.91	15.78	12.97	14.21	13.97	13.70
TOTFEO	18.47	18.35	18.19	17.59	18.62	18.39	18.22	18.25	18.13	17.75	17.99	18.91	18.38	18.74	18.46	18.01	17.98	18.46	17.58	10.45	11.71	12.13	15.79	16.07	16.81	16.58
MNO	.30	.27	.40	.33	.38	.38	.43	.36	.34	.45	.31	.35	.39	.30	.37	.18	.38	.26	.31	.00	.00	.00	.00	.00	.18	.00
MGO	13.08	12.98	13.28	13.13	13.07	13.29	13.33	13.09	13.42	13.41	13.29	12.80	13.09	12.70	12.99	13.34	13.97	13.20	13.76	18.36	17.82	17.60	14.82	14.92	14.90	14.96
CAO	.13	.00	.00	.13	.00	.11	.00	.00	.00	.25	.00	.13	.25	.18	.14	.10	.27	.11	.17	.26	.25	.23	.18	.14	.20	.14
NA2O	.00	.00	.00	.00	.00	.00	.00	.00	.00	.06	.00	.00	.00	.00	.00	.00	.00	.00	.00	.00	.00	.00	.00	.00	.00	.00
K2O	9.16	9.33	9.30	8.87	9.13	8.27	9.06	9.31	8.79	8.97	8.94	8.96	8.98	8.61	8.69	9.23	8.96	9.25	9.09	7.57	7.83	5.45	8.80	8.74	8.93	8.95
TOTAL	97.07	96.92	97.18	94.99	96.68	94.52	95.88	96.27	95.05	95.65	95.03	96.62	98.04	95.16	96.34	97.43	97.06	97.73	96.76	94.55	95.11	90.41	94.85	95.23	96.58	95.10
SI	5.537	5.560	5.565	5.646	5.585	5.533	5.634	5.611	5.593	5.596	5.638	5.562	5.631	5.625	5.607	5.610	5.647	5.572	5.646	5.834	5.815	5.666	5.693	5.636	5.607	5.652
AL(4)	2.463	2.440	2.435	2.354	2.415	2.467	2.366	2.389	2.407	2.404	2.362	2.438	2.369	2.375	2.393	2.390	2.353	2.428	2.354	2.166	2.185	2.334	2.307	2.364	2.393	2.348
AL(6)	.035	.017	.044	.033	.058	.044	.106	.063	.082	.099	.112	.039	.098	.083	.080	.078	.076	.030	.104	.512	.464	.482	.165	.194	.054	.085
TI	.525	.543	.512	.521	.478	.463	.408	.459	.419	.430	.407	.506	.468	.481	.472	.497	.453	.530	.444	.171	.198	.204	.382	.395	.429	.424
TOTFE	2.307	2.293	2.263	2.222	2.332	2.354	2.296	2.296	2.304	2.246	2.285	2.377	2.311	2.348	2.345	2.244	2.169	2.287	2.178	1.310	1.425	1.536	1.983	2.012	2.089	2.091
MN	.038	.034	.035	.051	.042	.049	.051	.055	.046	.058	.040	.045	.043	.039	.047	.023	.048	.033	.039	.000	.000	.000	.000	.000	.023	.000
MG	2.912	2.892	2.945	2.970	2.918	3.032	2.994	2.936	3.040	3.029	3.009	2.868	2.934	2.879	2.909	2.946	3.091	2.915	3.052	3.964	3.850	3.973	3.317	3.330	3.300	3.248
NA	.000	.000	.000	.000	.000	.000	.000	.000	.000	.000	.000	.000	.000	.000	.000	.000	.000	.000	.000	.000	.000	.000	.000	.000	.000	.000
CA	.000	.000	.000	.000	.000	.000	.000	.000	.000	.000	.000	.000	.000	.000	.000	.000	.000	.000	.000	.000	.000	.000	.000	.000	.000	.000
K	1.745	1.779	1.765	1.682	1.744	1.615	1.734	1.787	1.704	1.731	1.732	1.718	1.626	1.670	1.665	1.744	1.696	1.748	1.725	1.399	1.448	1.053	1.686	1.669	1.693	1.720
TOTZ	8.00	8.00	8.00	8.00	8.00	8.00	8.00	8.00	8.00	8.00	8.00	8.00	8.00	8.00	8.00	8.00	8.00	8.00	8.00	8.00	8.00	8.00	8.00	8.00	8.00	8.00
TOTY	5.82	5.78	5.80	5.80	5.83	5.94	5.85	5.81	5.89	5.86	5.85	5.83	5.85	5.83	5.85	5.79	5.84	5.79	5.82	5.96	5.94	6.19	5.85	5.88	5.89	5.85
TOTX	1.75	1.78	1.77	1.68	1.74	1.61	1.73	1.79	1.70	1.73	1.73	1.72	1.63	1.67	1.67	1.74	1.70	1.75	1.72	1.40	1.45	1.05	1.69	1.67	1.69	1.72

APPENDIX 4, TABLE 3: BIOTITE ANALYSES (CONTIN.)

DRM.NO	.044	.044	.051	.051	.051	.056	.056	.056	.056	.063	.063	.063	.063	.063	.063	.063	.063	.063	.063	.080	.080	.080	.080	.080	.080
ANAL NO	5	6	1	2	3	1	2	3	4	1	2	3	4	5	6	7	8	9	10	11	1	2	3	4	5	6
SIO2	37.88	37.19	38.26	37.85	37.95	37.20	36.91	36.81	37.47	37.40	37.47	37.16	35.84	36.32	35.98	36.25	36.00	35.81	35.01	35.43	38.32	38.02	37.70	38.82	38.56	37.49
TIO2	3.47	3.35	4.55	4.19	3.95	5.12	5.31	5.26	5.29	4.48	4.74	4.39	6.32	4.34	4.89	4.22	4.89	5.71	6.62	4.60	4.07	4.05	3.90	4.44	4.12	4.19
AL2O3	14.07	13.78	14.25	14.36	14.53	13.53	14.01	14.02	13.99	15.71	15.25	15.30	15.49	15.56	15.13	15.12	14.98	15.64	14.94	14.94	14.14	13.84	13.72	13.96	14.08	13.99
TOTFEO	14.33	14.00	19.05	19.17	19.09	21.14	21.40	21.96	21.83	17.49	17.74	17.15	17.03	16.91	17.54	17.95	18.12	17.35	17.37	17.05	14.75	14.57	14.36	14.77	14.58	14.74
MNO	.14	.00	.17	.15	.24	.00	.00	.00	.00	.00	.14	.25	.00	.00	.00	.00	.00	.00	.00	.00	.25	.00	.00	.00	.00	.00
MGO	15.12	15.09	12.35	12.25	12.57	10.93	10.77	10.43	10.71	14.09	14.10	13.99	13.02	13.89	12.94	13.23	13.48	13.57	12.94	13.32	14.22	14.11	15.80	15.94	15.86	15.71
CAO	.16	.26	.00	.15	.00	.00	.00	.14	.13	.27	.19	.27	.29	.20	.16	.11	.21	.15	.15	.13	.13	.16	.33	.09	.13	.09
NA2O	.00	.00	.00	.00	.00	.00	.00	.25	.00	.00	.00	.00	.00	.00	.00	.00	.00	.00	.00	.00	.00	.00	.19	.00	.20	.00
K2O	8.93	8.79	9.50	9.11	9.43	9.18	9.11	8.93	9.11	9.25	9.15	9.01	8.63	8.76	8.87	9.14	8.96	9.01	8.84	9.03	8.80	8.75	8.26	8.89	8.92	8.92
TOTAL	96.09	94.40	98.12	97.24	97.76	97.10	97.50	97.64	98.49	98.70	98.78	97.52	96.64	97.69	97.08	98.06	96.64	97.27	95.87	94.49	96.68	95.53	94.26	96.41	96.67	95.14
SI	5.636	5.635	5.645	5.641	5.624	5.611	5.549	5.540	5.583	5.454	5.465	5.482	5.339	5.339	5.282	5.345	5.395	5.310	5.281	5.410	5.617	5.639	5.660	5.654	5.651	5.594
AL(IV)	2.364	2.365	2.355	2.359	2.376	2.389	2.451	2.460	2.417	2.546	2.535	2.518	2.661	2.661	2.656	2.628	2.605	2.690	2.656	2.590	2.383	2.361	2.340	2.346	2.349	2.406
AL(VI)	.103	.096	.123	.163	.162	.017	.031	.027	.039	.154	.086	.142	.057	.034	.000	.000	.041	.043	.000	.099	.059	.056	.088	.069	.085	.054
TI	.388	.382	.505	.470	.440	.581	.600	.595	.593	.492	.520	.487	.708	.701	.770	.693	.551	.639	.751	.528	.449	.451	.440	.490	.484	.470
TOTFE	2.032	2.028	2.351	2.389	2.366	2.667	2.691	2.764	2.720	2.133	2.164	2.116	2.120	2.079	2.185	2.214	2.271	2.151	2.191	2.177	1.808	1.806	1.806	1.813	1.811	1.839
MN	.018	.000	.021	.019	.030	.000	.000	.000	.000	.000	.017	.031	.000	.000	.000	.000	.000	.000	.000	.000	.031	.000	.000	.000	.000	.000
MG	3.354	3.397	2.711	2.722	2.777	2.458	2.414	2.340	2.379	3.063	3.066	3.077	2.890	2.978	2.874	2.908	3.012	3.000	2.910	3.032	3.544	3.560	3.536	3.444	3.465	3.494
NA	.000	.000	.000	.000	.000	.000	.000	.073	.000	.000	.000	.000	.000	.000	.000	.000	.000	.000	.000	.000	.000	.000	.055	.000	.067	.000
CA	.000	.000	.000	.000	.000	.000	.000	.000	.000	.000	.000	.000	.000	.000	.000	.000	.000	.000	.000	.000	.000	.000	.000	.000	.000	.000
K	1.695	1.699	1.788	1.732	1.783	1.766	1.747	1.715	1.731	1.721	1.702	1.696	1.639	1.643	1.705	1.719	1.713	1.704	1.701	1.759	1.645	1.654	1.582	1.665	1.668	1.698
TOTZ	8.00	8.00	8.00	8.00	8.00	8.00	8.00	8.00	8.00	8.00	8.00	8.00	8.00	8.00	7.94	7.97	8.00	8.00	7.94	8.00	8.00	8.00	8.00	8.00	8.00	8.00
TOTY	5.89	5.90	5.72	5.76	5.77	5.72	5.74	5.73	5.73	5.84	5.85	5.85	5.77	5.79	5.83	5.81	5.87	5.83	5.85	5.84	5.89	5.87	5.87	5.82	5.81	5.84
TOTX	1.69	1.70	1.79	1.73	1.78	1.77	1.75	1.79	1.73	1.72	1.70	1.70	1.64	1.64	1.70	1.72	1.71	1.70	1.70	1.76	1.64	1.65	1.64	1.67	1.72	1.70

DRM.NO	.080	.080	.080	.080	.080	.143	.143	.143	.143	.144	.144	.144	.145	.145	.145	.145	.160	.160	.160	.160	.160
ANAL NO	7	8	9	10	11	1	2	3	4	1	2	3	1	2	3	4	1	2	3	4	5
SIO2	37.51	38.59	38.31	38.54	37.84	38.86	39.66	38.91	38.98	37.41	37.11	37.13	38.05	37.96	39.07	39.07	42.45	43.09	42.58	42.88	42.27
TIO2	4.69	4.10	4.24	4.83	4.87	5.43	5.19	5.20	5.15	4.28	4.03	4.26	4.45	4.45	4.65	4.36	2.32	2.11	2.26	2.20	2.74
AL2O3	14.84	13.84	14.34	13.69	13.30	13.77	13.97	13.72	13.81	14.59	14.50	13.84	14.33	14.34	14.44	14.17	11.40	11.00	11.98	11.63	11.77
TOTFEO	14.96	14.28	14.35	14.26	14.13	11.78	12.35	13.70	13.16	14.27	13.00	14.19	13.09	12.83	13.09	13.18	8.18	7.87	7.87	7.69	8.73
MNO	.23	.00	.00	.16	.00	.00	.00	.00	.00	.17	.21	.22	.00	.00	.00	.00	.00	.00	.00	.00	.00
MGO	15.03	16.14	16.36	15.82	15.58	16.90	17.39	16.60	16.69	16.57	18.11	16.93	16.52	16.91	17.33	17.27	20.78	21.35	20.77	21.28	20.13
CAO	.21	.00	.13	.09	.19	.10	.00	.00	.00	.43	.35	.41	.29	.34	.00	.09	.15	.12	.13	.18	.00
NA2O	.00	.00	.00	.00	.18	.00	.25	.22	.27	.38	.00	.89	.00	.00	.00	.00	.00	.00	.00	.00	.00
K2O	8.76	8.97	9.15	9.07	9.05	9.24	9.53	9.18	9.31	7.46	6.79	6.84	9.00	8.97	9.30	9.30	9.83	9.68	9.66	9.71	10.02
TOTAL	95.22	95.92	96.82	96.46	95.13	96.07	98.34	97.54	97.37	95.57	94.11	94.79	95.74	95.41	97.90	97.44	95.12	95.21	95.25	95.57	95.65
SI	5.605	5.677	5.603	5.653	5.644	5.655	5.651	5.625	5.634	5.525	5.505	5.532	5.602	5.606	5.606	5.638	6.119	6.180	6.105	6.127	6.071
AL(IV)	2.395	2.323	2.397	2.347	2.338	2.345	2.346	2.338	2.353	2.475	2.495	2.425	2.398	2.394	2.394	2.362	1.881	1.820	1.895	1.873	1.929
AL(VI)	.042	.077	.057	.020	.000	.017	.000	.000	.000	.065	.091	.000	.088	.102	.046	.048	.055	.040	.129	.085	.064
TI	.527	.454	.466	.533	.546	.594	.556	.565	.560	.475	.450	.477	.493	.494	.501	.473	.251	.228	.244	.236	.296
TOTFE	1.869	1.757	1.760	1.749	1.762	1.434	1.472	1.656	1.591	1.763	1.613	1.768	1.612	1.585	1.570	1.591	.986	.944	.944	.919	1.049
MN	.029	.000	.000	.020	.000	.000	.000	.000	.000	.021	.026	.028	.000	.000	.000	.000	.000	.000	.000	.000	.000
MG	3.348	3.540	3.567	3.460	3.484	3.667	3.694	3.578	3.596	3.848	4.005	3.760	3.626	3.602	3.705	3.715	4.465	4.565	4.439	4.533	4.310
NA	.000	.000	.000	.000	.052	.000	.069	.062	.076	.109	.000	.257	.000	.046	.000	.000	.000	.000	.000	.000	.000
CA	.000	.000	.000	.000	.000	.000	.000	.000	.000	.000	.000	.000	.000	.000	.000	.000	.000	.000	.000	.000	.000
K	1.668	1.683	1.707	1.697	1.722	1.715	1.732	1.693	1.717	1.405	1.285	1.319	1.690	1.690	1.701	1.712	1.807	1.771	1.767	1.770	1.836
TOTZ	8.00	8.00	8.00	8.00	7.98	8.00	8.00	7.96	7.99	8.00	8.00	7.96	8.00	8.00	8.00	8.00	8.00	8.00	8.00	8.00	8.00
TOTY	5.81	5.83	5.85	5.78	5.77	5.71	5.72	5.80	5.75	5.97	6.13	6.03	5.82	5.78	5.82	5.83	5.76	5.78	5.76	5.77	5.72
TOTX	1.67	1.68	1.71	1.70	1.77	1.72	1.80	1.75	1.79	1.51	1.28	1.58	1.69	1.74	1.70	1.71	1.81	1.77	1.77	1.77	1.84

APPENDIX 4

TABLE 4 : CORRELATION COEFFICIENTS FOR MAJOR ELEMENT VARIATIONS IN INTRUSIVE ROCK SUITES, PAPUA NEW GUINEA AND SOLOMON ISLANDS

	ISLAND ARC SUITES										CONTINENTAL MARGIN SUITES					
SIO2 VERSUS..	1	2	3A	3B	4	5	6A	6B	7	8	9A	9B	10	11	12	13
TIO2	-.939	-.930	.000	-.935	-.922	-.840	-.957	-.977	-.804	-.995	-.942	.000	-.966	-.986	-.943	-.942
AL2O3	-.937	-.845	.000	-.904	-.816	-.773	-.795	-.777	-.857	-.983	-.979	.000	-.894	-.774	-.485	-.956
SUMFEO	-.989	-.948	.000	-.989	-.943	-.859	-.975	-.834	-.987	-.978	-.992	.000	-.988	-.998	-.997	-.939
MGO	-.984	-.916	.000	-.938	-.973	-.960	-.921	-.946	-.990	-.953	-.997	.000	-.942	-.956	-.665	-.909
CAO	-.985	-.979	.000	-.983	-.929	-.959	-.997	-.951	-.994	-.999	-1.000	.000	-.994	-.990	-.957	-.850
NA2O	.818	.689	.000	.921	.902	.439	.836	.928	.968	-.749	1.000	-.999	.882	.996	.969	.000
K2O	.836	.969	.937	.944	.946	.869	.971	.768	.979	.952	.998	.000	.850	.830	.818	.919
P2O5	-.849	.000	.000	-.981	-.772	.000	-.980	-.868	.807	-.979	-.986	.000	-.940	-.780	-.376	-.943

KEY TO SUITES : ISLAND ARC SUITES
1=NORTH BAININGS NORMAL-K SUITE
2=SOUTH BAININGS HIGH-K SUITE
3A=PLESYUMI HIGH-K SUITE
3B=PLESYUMI NORMAL-K SUITE
4=MOUNT KREN HIGH-K SUITE
5=LEMAU NORMAL-K SUITE
6A=PANGUNA HIGH-K SUITE
6B=PANGUNA NORMAL-K SUITE
7=LIMBO RIVER HIGH-K SUITE
8=KOLOULA LOW- TO NORMAL-K FELSIC SUITE
CONTINENTAL MARGIN SUITES
9=YUAT NORTH HIGH-K SUITE
10=YUAT SOUTH NORMAL-K SUITE
11=KARAWARI LOW- TO NORMAL-K SUITE
12=FRIEDA NORMAL-K SUITE
13=OK TEDI HIGH-K SUITE (CONTINENTAL SUITE)

SUITES 1,2 FROM MACNAB(1970)
SUITES 3-13 THIS THESIS
.000=NOT DETERMINED DUE TO SCATTER OR INSUFFICIENT DATA

APPENDIX 5, TABLE 1 : WHOLE-ROCK NUMBERS AS IN MUSEUM GEOLOGY DEPARTMENT, A.N.U.

NOTE : THERE IS NO SAMPLE DRM.043

DRM.001	34117	DRM.057	34172	DRM.112	34227
DRM.002	34118	DRM.058	34173	DRM.113	34228
DRM.003	34119	DRM.059	34174	DRM.114	34229
DRM.004	34120	DRM.060	34175	DRM.115	34230
DRM.005	34121	DRM.061	34176	DRM.116	34231
DRM.006	34122	DRM.062	34177	DRM.117	34232
DRM.007	34123	DRM.063	34178	DRM.118	34233
DRM.008	34124	DRM.064	34179	DRM.119	34234
DRM.009	34125	DRM.065	34180	DRM.120	34235
DRM.010	34126	DRM.066	34181	DRM.121	34236
DRM.011	34127	DRM.067	34182	DRM.122	34237
DRM.012	34128	DRM.068	34183	DRM.123	34238
DRM.013	34129	DRM.069	34184	DRM.124	34239
DRM.014	34130	DRM.070	34185	DRM.125	34240
DRM.015	34131	DRM.071	34186	DRM.126	34241
DRM.016	34132	DRM.072	34187	DRM.127	34242
DRM.017	34133	DRM.073	34188	DRM.128	34243
DRM.018	34134	DRM.074	34189	DRM.129	34244
DRM.019	34135	DRM.075	34190	DRM.130	34245
DRM.020	34136	DRM.076	34191	DRM.131	34246
DRM.021	34137	DRM.077	34192	DRM.132	34247
DRM.022	34138	DRM.078	34193	DRM.133	34248
DRM.023	34139	DRM.079	34194	DRM.134	34249
DRM.024	34140	DRM.080	34195	DRM.135	34250
DRM.025	34141	DRM.081	34196	DRM.136	34251
DRM.026	34142	DRM.082	34197	DRM.137	34252
DRM.027	34143	DRM.083	34198	DRM.138	34253
DRM.028	34144	DRM.084	34199	DRM.139	34254
DRM.029	34145	DRM.085	34200	DRM.140	34255
DRM.030	34146	DRM.086	34201	DRM.141	34256
DRM.031	34147	DRM.087	34202	DRM.142	34257
DRM.032	34148	DRM.088	34203	DRM.143	34258
DRM.033	34149	DRM.089	34204	DRM.144	34259
DRM.034	34150	DRM.090	34205	DRM.145	34260
DRM.035	34151	DRM.091	34206	DRM.146	34261
DRM.036	34152	DRM.092	34207	DRM.147	34262
DRM.037	34153	DRM.093	34208	DRM.148	34263
DRM.038	34154	DRM.094	34209	DRM.149	34264
DRM.039	34155	DRM.095	34210	DRM.150	34265
DRM.040	34156	DRM.096	34211	DRM.151	34266
DRM.041	34157	DRM.097	34212	DRM.152	34267
DRM.042	34158	DRM.098	34213	DRM.153	34268
DRM.044	34159	DRM.099	34214	DRM.154	34269
DRM.045	34160	DRM.100	34215	DRM.155	34270
DRM.046	34161	DRM.101	34216	DRM.156	34271
DRM.047	34162	DRM.102	34217	DRM.157	34272
DRM.048	34163	DRM.103	34218	DRM.158	34273
DRM.049	34164	DRM.104	34219	DRM.159	34274
DRM.050	34165	DRM.105	34220	DRM.160	34275
DRM.051	34166	DRM.106	34221	DRM.161	34276
DRM.052	34167	DRM.107	34222		
DRM.053	34168	DRM.108	34223		
DRM.054	34169	DRM.109	34224		
DRM.055	34170	DRM.110	34225		
DRM.056	34171	DRM.111	34226		

APPENDIX 6 APRIL ULTRAMAFICS, WESTERN HIGHLANDS, P.N.G.: WHOLE-ROCK AND MINERAL COMPOSITIONS, AND TECTONIC SETTING

1. WHOLE-ROCK AND MINERAL COMPOSITIONS

Dow et al. (1968, 1972) have reported the presence of bodies of Alpine-type ultramafic rocks ('April Ultramafics') in the Western Highlands of Papua New Guinea. Specimens of ultramafic material have been sampled by the author from one such body, located in the vicinity of the Awari Stock, south of the Karawari Batholith (see Fig. 3).

Rock types sampled from this location include tremolitized basaltic lavas, tremolitized basaltic tuffaceous rocks, partially serpentinized harzburgites, and partially serpentinized dunites. Major element analyses for representative specimens are presented in Appendix 6, Table 1, together with analyses for olivine* and chromite from a partially serpentinized dunite (DRM155). The presence of chromite and the olivine composition of Fo(94) are features which are appropriate for an upper mantle origin for these ultramafic rocks. A ternary plot of Ti-Zr-Y (Pearce & Cann, 1971) reveals that the mafic and ultramafic rocks possess abundances of these elements appropriate to an 'oceanic' parentage (see Appendix 6, Fig. 1). Whether that is precisely true or not, the very primitive chemistry of the rocks and constituent olivine serve to distinguish the April Ultramafics from other igneous rocks of the Western Highlands.

2. TECTONIC SETTING

Other work currently in progress indicates that alkali basaltic rocks form part of the April Ultramafics (R. Ryburn, pers. commun.). The presence of such rocks further strengthens the proposition made in the present work and earlier work (e.g., Davies and Smith, 1971) that an extensional stress field operated on the northern Australian continental margin during Mesozoic and early Tertiary times. It is possible that, as a result of extension, an incipient marginal basin(s) (Karig, 1972) developed within, or at the southern margin of, the New Guinea Mobile

---

*Olivine has also been observed in small amounts in mafic cumulate rocks of the Wale Stock (DRM050, this study), and in mafic rocks of the Yuat North and Karawari batholiths (Dow et al., 1972). No analytical data are currently available for these olivine occurrences.

APPENDIX 6, TABLE 1: WHOLE-ROCK AND MINERAL ANALYSES FOR APRIL ULTRAMAFICS, WESTERN HIGHLANDS

	DRM.150	DRM.148	DRM.149	DRM.153	DRM.154	DRM.152	DRM.151	DRM.155	DRM.155 olivine	DRM.155 chromite core	DRM.155 chromite rim
SiO_2(wt.%)	56.51	48.86	46.08	39.95	42.21	39.40	42.22	42.78	41.83	0.00	0.00
TiO_2	0.99	0.76	1.95	0.00	0.00	0.00	0.00	0.00	0.00	0.18	0.38
Al_2O_3	16.97	14.85	14.00	1.08	2.20	0.36	1.61	0.77	0.00	26.11	0.15
								Cr_2O_3	0.00	39.89	14.97
tot. FeO	7.49	7.61	18.46	7.01	7.28	6.89	7.61	8.96	6.02	19.25	75.69
MnO	0.00	0.19	0.10	0.09	0.00	0.18	0.14	0.00	0.37	1.46	1.17
MgO	5.65	13.17	5.42	38.37	34.00	36.89	37.43	42.05	51.86	12.26	3.04
CaO	5.17	9.27	9.13	0.00	2.19	1.70	0.14	0.00	0.00	0.00	0.00
Na_2O	5.26	1.43	3.06	0.00	0.00	0.00	0.00	0.00	0.00	0.36	0.00
K_2O	1.02	1.28	0.29	0.17	0.00	0.00	0.00	0.00	0.00	0.00	0.00
L.O.I.	0.95	2.69	1.44	12.89	11.45	14.10	10.47	4.48	-	-	-
total	100.01	100.11	99.93	99.56	99.33	99.52	99.62	99.04	100.08	99.51	95.40
Ni(ppm)	9	299	32	1576	2013	2614	1994	2295			
Cr	0	613	52	1877	2338	1601	2243	2381			

Note: Whole-rock and mineral major elements by microprobe (whole-rocks on glasses; minerals on polished sections).
Rock trace elements by XRF
DRM.150, tremolitized basaltic tuff
DRM.148 and DRM.149, tremolitized basaltic lavas
DRM.153 and DRM.154, partially serpentinized harzburgites
DRM.152, serpentinized harzburgite
DRM.151 and DRM.155, partially serpentinized dunites

APPENDIX 6:

Fig. 1 : Ti-Zr-Y diagram

Field 1, Ocean floor basalts

" 2, Andesites

after Pearce & Cann, 1971

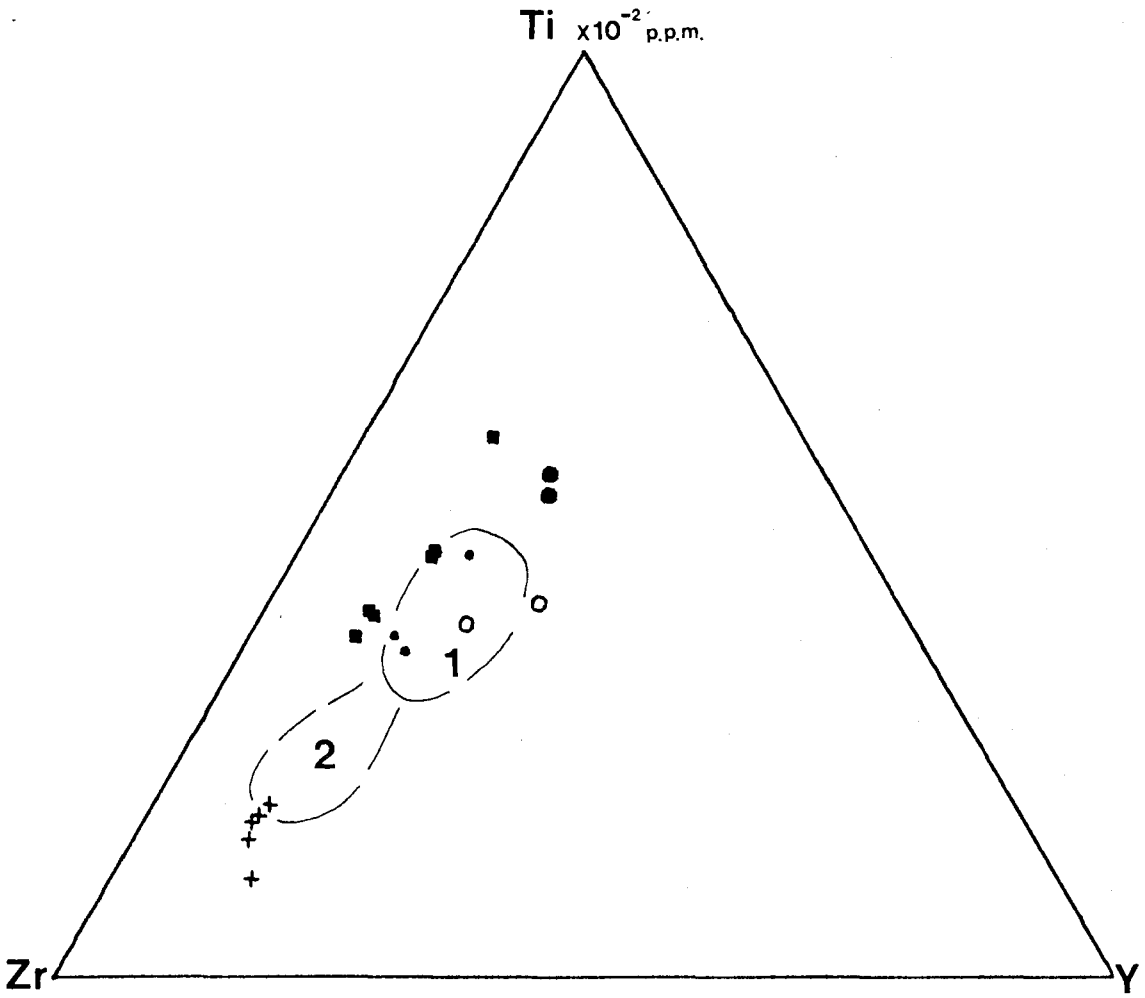

April Ultramafics:

- ● basalts
- O gabbros
- ● ultramafic rocks

Calc-alkaline intrusive rocks:

- \+ diorites, granodiorites
- ■ gabbros

Belt (compare opening of the Coral Sea, Davies & Smith, 1971). The compositions of materials of the newly-generated 'oceanic crust' in such environments may not be strictly comparable with the compositions of oceanic crustal materials as presently known (e.g. Hart et al., 1972). Closure of the incipient marginal basin(s) consequent upon collision with the north New Guinea - New Britain Arc in the early Tertiary resulted in emplacement of the April Ultramafics as tectonic slices.

APPENDIX 7 PUBLISHED WORK

Mason, D.R. (1975): Subdivision and Geochemistry of Tertiary Intrusive Complexes from part of the New Guinea Mobile Belt . Bull. Aust. Soc. Explor. Geophys. 6, 69-71.

This paper was delivered to: First Southwest Pacific Workshop-Symposium

at: University of Sydney

on: 14 February, 1975.

'SUBDIVISION AND GEOCHEMISTRY OF TERTIARY INTRUSIVE COMPLEXES FROM PART OF THE NEW GUINEA MOBILE BELT'.

by D.R. Mason,

Department of Geology,

Australian National University, Canberra, A.C.T.

Within the New Guinea Mobile Belt (Dow et al., 1968), orogeny reached a climax in mid-Miocene times with emplacement of calc-alkaline intrusive complexes and eruption of effusive equivalents (Page, 1971). The intrusive rocks have been collectively termed the 'Maramuni Diorite' (Dow et al., 1967, 1968).

In this paper, intrusions of the 'Maramuni Diorite' in the Western Highlands-South Sepik districts (see Fig. 1) are subdivided on the basis of geographic location, areal extent, and geochemical differences into the following masses:

a) The Karawari Batholith, which is fault-bounded on its northern and southern margins, is greater than 350 km^2 in area, and is composed principally of hornblende-clinopyroxene-quartz diorite and hornblende (-biotite) tonalite.

b) The Lamant and Wale Stocks, which comprise mafic cumulates, low-Si diorites, and hornblende granodiorites.

c) The Yuat South Batholith, which underlies more than 400 km^2,

and is composed principally of hornblende granodiorite in the western part and hornblende-biotite granodiorite in the eastern part.

d) The Yuat North Batholith, which is greater than 375 km^2 in area, and is composed principally of hornblende-biotite-orthoclase-quartz diorite and biotite microadamellite.

Regional variations in mineralogy and chemistry within these dominantly calc-alkaline rock types are apparent. From south to north, a decrease in modal abundance of clinopyroxene and quartz is counterbalanced by an increase in alkali feldspar and biotite. Mineralogical changes are reflected in a regional geochemical polarity that is especially apparent in whole-rock variations of the large alkali and alkaline earth irons, the REE group, and niobium. Fig.2 shows variation of K_2O and Ba with SiO_2. The rate of increase of K_2O with increasing SiO_2 increases from the Karawari Batholith trend (low- to intermediate-K suite), through the Yuat South Batholith trend ('normal' calc-alkaline trend), to the Yuat North Batholith trend (high-K calc-alkaline suite). A similar variation is observed in the plot of Ba against SiO_2. Generally, Ba increases with increasing SiO_2, but for any given SiO_2 content, Ba increases from the lower-K suites through to the high-K suite. Two specimens from a marginal stock of the Yuat North Batholith display very high Ba contents (of the order of 1000 p.p.m.) and are shoshonitic in their affinities. The different calc-alkaline suites can also be distinguished with varying degrees of clarity on plots of Nb, (La+Ce+Y), and Sr against K_2O.

Fig.3 emphasises the regional increase in K_2O across the Mobile Belt. From Harker-type variation diagrams of K_2O versus SiO_2 (cf. Fig.2), K_2O has been determined at the 65% SiO_2 level for the different

calc-alkaline suites, and has been plotted against distance along the line AB in Fig.1. At the 65% SiO_2 level, K_2O increases from 1% in the south to 3.3% in the north.

The geochemical data presented above could have important palaeotectonic implications. The development of the New Guinea Mobile Belt can be envisaged in either of two contrasting tectonic settings. Either it developed as a continental margin feature, or it developed as an island are complex somewhat removed from the Australian continental margin. Dow (1973) has supported the former idea. The data presented here, however, would appear to support the latter proposition. If interpreted in terms of plate tectonics theory, the geochemical polarity northwards across the intrusive rocks of the Mobile Belt implies development of the Belt as an island arc complex above a north-dipping Benioff Zone, necessarily removed from the continental margin. This tectonic regime would have ceased in Oligocene-early Miocene times consequent upon the collision of this arc complex with the Australian continental block. Intervening oceanic (or marginal basin) crust not involved in subduction processes could have been emplaced as Alpine-type ultramafic bodies (April Ultramafics of Dow et al.), or metamorphosed to fault-bounded blocks of glaucophane schist and eclogite (Gufug Gneiss) that occur in this region.

The present expression of the proposed Benioff Zone on the southern margin of the New Guinea Mobile Belt is considered to be the Lagaip Fault Zone. It is a well-defined structural break between the Mobile Belt and the continental shelf-type sediments to the south. It is also the southerly limit of Alpine-type ultramafic bodies, high-pressure metamorphic rocks, and Miocene intrusive complexes.

Regional mapping in the Western Highlands (B.M.R., 1972) has defined the more complex nature of the Lagaip Fault Zone toward the east where the edge of the Australian continental block bends southward. It is suggested that the proposed Benioff Zone differed in this region, as there are no Alpine-type ultramafic bodies or high-pressure metamorphic rocks, and the Miocene volcanic rocks are geochemically different from those in the western part of the New Guinea Mobile Belt (cf. Mackenzie, this volume).

REFERENCES:

AUSTRALIAN BUREAU MINERAL RESOURCES, 1972: Geolocial Map of Papua New Guinea at 1:1,000,000. Australian Bureau Mineral Resources Record 80, pp. 1-31.

DOW, D.B., 1973: 'Geology of Papua New Guinea'. Australian Bureau Mineral Resources Record 1973/117.

DOW, D.B., SMIT, J.A.J., BAIN, J.H.C. and RYBURN, R.J., 1967: The geology of the South Sepik region, progress report for 1966. Australian Bureau Mineral Resources Record 26, pp. 1-35.

DOW, D.B., SMIT, J.A.J., BAIN, J.H.C., and RYBURN, R.J., 1968: The geology of the South Sepik region, New Guinea. Australian Bureau Mineral Resources Record 80, pp. 1-31.

PAGE, R.W., 1971: The geochronology of igneous rocks in the New Guinea region. Ph.D. Thesis, Australian National University.

17th March, 1975

FIG. 1 :

INTRUSIVE MASSES and
SPECIMEN LOCATIONS,
P.A. 124,
Highlands, Papua New Guinea.

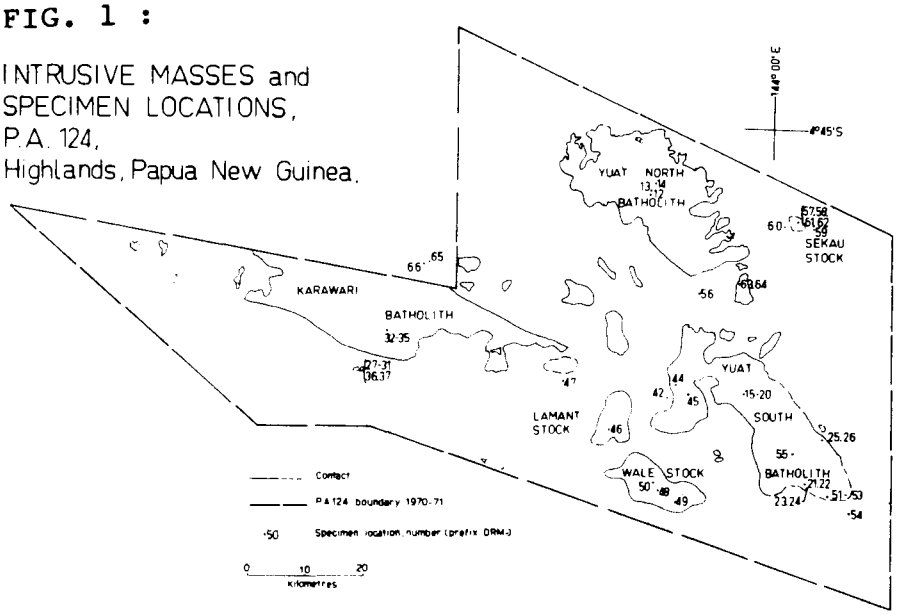

FIG. 2 :

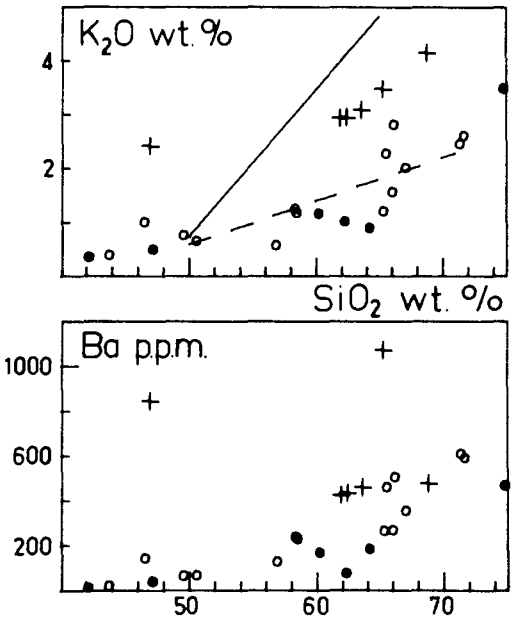

FIG. 3 :

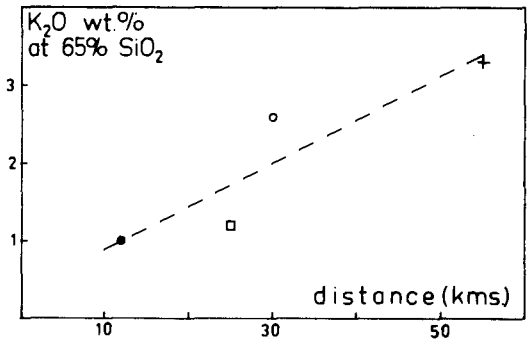

FIGURE CAPTIONS:

Fig. 1 : Nomenclature for intrusive masses, Western Highlands - South Sepik districts, Papua New Guinea.

Fig. 2 : Variation diagrams for K_2O and Ba against SiO_2. Filled circles, Karawari Batholith; open circles, Yuat South Batholith; crosses Yuat North Batholith. For comparison, regression lines have been drawn, in the plot of K_2O against SiO_2, for the Gazelle Peninsula (New Britain) plutonic suites of Macnab (1970) (Full line, South and Central Bainings Mountains high-K calc-alkaline suite; dashed line, North Bainings Mountains 'normal' calc-alkaline suite).

Fig. 3 : K_2O (at 65% SiO_2) against distance along AB in Fig. 1. Full circle, Karawari Batholith; open square, Yuat South Batholith (western region); open circle, Yuat South Batholith (eastern region); cross, Yuat North Batholith.